

ELECTRIC POWER SYSTEM FUNDAMENTALS

SALVADOR ACHA DAZA

Electric Power System Fundamentals

For a listing of recent titles in the
Artech House *Power Engineering and Power Electronics Library*,
turn to the back of this book.

Electric Power System Fundamentals

Salvador Acha Daza



**ARTECH
HOUSE**

BOSTON | LONDON
artechhouse.com

Library of Congress Cataloging-in-Publication Data

A catalog record for this book is available from the U.S. Library of Congress

British Library Cataloguing in Publication Data

A catalog record for this book is available from the British Library.

ISBN-13: 978-1-63081-085-6

Cover design by John Gomes

© 2016 Artech House

685 Canton Street

Norwood, MA

All rights reserved. Printed and bound in the United States of America. No part of this book may be reproduced or utilized in any form or by any means, electronic or mechanical, including photocopying, recording, or by any information storage and retrieval system, without permission in writing from the publisher.

All terms mentioned in this book that are known to be trademarks or service marks have been appropriately capitalized. Artech House cannot attest to the accuracy of this information. Use of a term in this book should not be regarded as affecting the validity of any trademark or service mark.

10 9 8 7 6 5 4 3 2 1

Contents

Acknowledgments	xi
Preface	xiii
CHAPTER 1	
Fundamentals of Energy Systems	1
1.1 Introduction	1
1.2 Work and Energy in Electric Circuits	4
1.2.1 Power and Energy in Constant DC Systems	4
1.2.2 Power and Energy in AC Circuits	6
1.2.3 Instantaneous Power $P(T)$, Real Power P and Reactive Power Q	11
1.2.4 Load Convention for Power Flows	13
1.3 Three-Phase Voltages, Currents and Power	18
Appendix 1A Complex Numbers	23
References	25
CHAPTER 2	
Network Analysis	27
2.1 Introduction	27
2.2 Ohm's Law	29
2.3 Circuits with Lumped Elements	32
2.4 Kirchhoff's Current Law	33
2.5 Nodal Formulation	35
2.6 Kirchhoff Voltage Law (KVL) and the Mesh Method	38
2.7 Linear Equations and Gaussian Elimination	40
2.7.1 Cramer's Rule	42
2.7.2 Partial Inversion	42
2.7.3 Kron's Network Reduction	44
2.8 Matrix Elements for Y_{BUS} and Z_{BUS}	44
2.9 Norton's and Thévenin's Equivalents	47
2.10 Large Scale Network Equivalents	48
2.10.1 Partitioned Networks and Equivalents	49
2.11 Diakoptical Approach	54
2.12 Matrix Inversion Lemma	56
References	57

CHAPTER 3	
POWER TRANSFORMER MODELING	59
3.1 Introduction	59
3.2 Equation's Decoupling and Symmetrical Components	59
3.2.1 Symmetrical Components Transformation	62
3.2.2 Decoupling of State Equations	64
3.3 Single-Phase Transformer Model	67
3.3.1 Per Unit Values	69
3.4 Three-Phase Bank Transformer Model	74
3.4.1 Three-Phase $\Delta\Delta$ Bank	74
3.4.2 Three-Phase $Y\Delta$ Bank	77
3.4.3 Three-Phase YY Bank	79
3.5 Autotransformer Model	85
3.6 Three Winding Transformer	89
3.7 Three-Phase Transformer	92
3.8 Alternate Model for a Single-Phase Transformer	95
3.9 Function for the Partial Inversion Algorithm	97
References	98
CHAPTER 4	
Transmission Line and Cable Modeling	99
4.1 Introduction	99
4.2 Series Inductance	99
4.2.1 Single Conductor	100
4.2.2 Inductance for a Set of Aerial Conductors	102
4.2.3 Set of Bundled Conductors	105
4.2.4 Ground Wire Inclusion	107
4.2.5 Line Transposition	109
4.2.6 Sequence Impedances	111
4.3 Earth Return	112
4.4 Gauss Law and Capacitance	117
4.4.1 Potential at Midpoint Between Two Electric Charges	119
4.4.2 Conductors Parallel to an Ideal Equipotential Plane	119
4.4.3 Capacitance and Shunt Admittance	120
4.5 Calculation of Cable Parameters	122
4.5.1 Cable Series Impedance	123
4.5.2 Cable Shunt Capacitance	126
4.5.3 Three-phase Cables	127
4.5.4 Three-phase Cables, Pipe Type	129
4.6 Geometric Mean Radius	132
4.7 Equivalent Height	133
4.8 Transmission Lines in Parallel	135
References	136

CHAPTER 5

Transmission Line Loadability	137
5.1 Introduction	137
5.2 Approximate Real Power Handling and Losses	137
5.2.1 Number of Circuits Required to Transport Electric Power	139
5.2.2 Reactive Power Required by the AC Transmission Line	141
5.3 $V(x)$ and $I(x)$ Equations for a Long Transmission Line	141
5.3.1 The Flat Line Concept	143
5.3.2 Surge Impedance, Wave Length and Propagation Velocity	143
5.3.3 No-Load Line and General Hyperbolic Form	144
5.3.4 Nominal π and Equivalent Circuit	144
5.3.5 Long Line Equivalent Circuit	145
5.4 $ABCD$ Constants	146
5.4.1 $ABCD$ Equivalent for Series Connection	148
5.4.2 Nodal Admittance Matrix from $ABCD$ Constants	148
5.5 Power Flow Calculations using $ABCD$ Constants	151
5.6 Transmission Limits	154
5.6.1 Thermal Limit	154
5.6.2 Stability's Angle Limit	154
5.6.3 Limit from Voltage Drop	155
5.7 Wave Equation and Time Expressions	156
5.7.1 Product $x\sqrt{LC}$ and Speed v	156
5.7.2 Functions $A_V(t - x/v)$ and $A_I(t - x/v)$	157
5.7.3 Expressions for A_V, B_V, A_I, B_I	158
5.7.4 Reflexion Coefficients	158
5.7.5 Calculation of Coefficients	159
5.7.6 Coefficients for Connection of Various Elements	164
5.7.7 Lattice Diagram	165
5.7.8 Electric Element Connections at Receiving Terminal	166
References	168

CHAPTER 6

Power Flows	169
6.1 Introduction	169
6.2 Solution of Nonlinear Equations	169
6.2.1 Newton's Iterative Process	172
6.3 Newton's Method for Power Flow Solutions	174
6.4 Power Flow Equations	175
6.4.1 Complex Power Transformer and Incremental Power Flows	175
6.4.2 Incremental Power Flow for a Transmission Line	180
6.5 Newton's Power Flow Solution	182
6.6 Power Flow Approximations	186
6.7 DC Network Power Flow Solutions	193
6.7.1 Incremental DC Power Flow Equations	194

6.8	Incremental Power Flow and Control Actions	198
6.9	Unbalanced Three-Phase Power Flow	200
	References	205
CHAPTER 7		
	Optimal Operation of Power Systems	207
7.1	Introduction	207
7.2	Nonlinear Optimization	207
7.3	Optimal Dispatch with No Losses	211
	7.3.1 Inequality Constraints	213
7.4	Real Power Losses	216
7.5	Minimum Losses	218
7.6	Optimal Operation, Transmission Losses Included	222
	7.6.1 Minimum Cost Power Flow Formulation	225
7.7	Hydrothermal Power System Coordination	233
	7.7.1 Objective Function and Constraints	234
7.8	Second-Order Derivatives	242
	Reference	248
CHAPTER 8		
	Real and Reactive Power and Frequency Control	249
8.1	Introduction	249
8.2	Control of Real Power Flows	250
8.3	Control of Real Power Flow, Longitudinal Networks	255
8.4	Control of Reactive Power Flow	258
8.5	Congestion and Minimum Effort Control	262
	8.5.1 Use of Sensitivity Coefficients	262
	8.5.2 Optimal Control of Real Power Flow	265
	8.5.3 Optimal Control for Reactive Power Flow	268
	8.5.4 Optimal Coordinated Control Efforts	270
8.6	Work and Energy	273
	8.6.1 Kinetic Energy and Electrical Frequency	276
	8.6.2 Turbine's Power and System's Frequency	277
	8.6.3 Frequency Control by a Primary Loop	279
8.7	Incremental Power Model to Include a VSC-STATCOM	282
	8.7.1 Power Flows in a Complex Transformer and a Transmission Line	283
	8.7.2 Expressions for Incremental Power Flow	284
8.8	Voltage Source Converter (VSC) and STATCOM	287
	8.8.1 Incremental Model for the VSC	288
8.9	Extensions to the Model	290
	8.9.1 Reactive Power and Voltage Control	290
	8.9.2 DC Load	292
8.10	STATCOM Model	292
	8.10.1 OLTC's Real and Reactive Power Flows	292
8.11	Chapter Summary	295
	References	295

CHAPTER 9

General Fault Studies in Electrical Power Systems	297
9.1 Introduction	297
9.2 Fault Equation in Phase Coordinates abc	297
9.3 Fault Equation in Coordinates 012	298
9.3.1 Three-Phase Fault	300
9.3.2 Other Types of Shunt Faults	307
9.4 Series Faults	309
9.5 Useful Circuit Interpretation for Fault Connections	312
9.5.1 Single-Phase Fault	312
9.5.2 Fault Between Two Phases, No Ground	314
9.5.3 Fault Between Two Phases and Ground	316
9.6 Alternative Equation for Fault Current Calculation	317
9.7 Transient and Subtransient Impedances in Magnetic Circuits	318
9.7.1 Transient Response in a Magnetic Circuit	318
9.7.2 Subtransient Response	319
References	320

CHAPTER 10

Contingency Analysis	321
10.1 Introduction	321
10.2 General System Incremental Linear Network	323
10.3 Sensitivity Matrix for a Linear Circuit	327
10.3.1 Sensitivity Matrix for Incremental Control Changes	328
10.4 Single Contingency Model	329
10.4.1 Thévenin's Equivalent	330
10.4.2 Voltage and Reactive Power Under Contingencies	335
10.5 Participation Factors from System's Lines	340
10.6 Summary	342

CHAPTER 11

State Estimation in Electrical Power Systems	343
11.1 Introduction	343
11.1.1 Centralized Data Acquisition System	344
11.2 Least Squares, Linear Model	345
11.2.1 Power System's Linear State Estimation	348
11.3 Maximum Likelihood and Weighted Least Squares	354
11.3.1 Bad Data Detection	357
11.4 Nonlinear Minimum Squares	361
11.5 Thévenin's Equivalent and Parameter Estimation	364
11.6 Phasor Estimation and Related Problems	366
11.6.1 Wide Area Measurements	371
11.7 Observability	372
References	374
About the Author	375
Index	377

Acknowledgments

This work would not been possible without the loving and kind support of my wife, Eloisa. She made everything possible so that I had the time to undertake this effort. I am very grateful for her contribution. From my daughters and son, I only had words of encouragement, especially when my spirits were not very high. I thank Eloisa, Diana, and Salvador. The little ones—Danny, Ben, and Alex—are a precious joy and when we spend time playing together, learning things that capture their imagination and interest, we certainly have fun, but in that kind of process, I hope to capture some more engineers for the family.

I wish to thank my late mother and father, who always fought hard to give me and my brothers an education. To my brothers, Carlos, Enrique, and Jorge, and my sister, Rosa—I am thankful that we shared the same starting seed and that eventually everyone turned out so well.

I cannot continue without acknowledging the friendship and moral support from Francisco Lemus, the late Professor Gabriel Munoz, and Eduardo Sanchez. I also thank the professors that influenced my thinking about modeling and math applications: Fernando Rodriguez Blanco, Teodoro Avendano, and Leonardo Saenz. Last, but not least, I hold in great regard the support from Enrique Marroquin, of Hunt Co., and his studies and the deployment of DC-DC interties during the last few years.

I am highly in debt for the contribution to my academics to Graduados de ESIME, Politecnico Nacional, in Mexico City and to the University of Texas at Arlington.

Preface

Modern electric power systems are sophisticated ensembles of power plants with diverse primary energy sources, step-up transformers that connect power plants to high-voltage transmission lines, which in turn, make the energy reach long distances up to main load centers where stepdown transformers reduce the voltage to safe values for consumers and equipment. The number of electric elements for a particular power utility might be numerous—in the thousands. The challenge to model, study, and analyze such a system is an enormous task, and is done with the help of numerical algorithms using digital computers.

The operation and control of electrical power systems and the planning of future conditions and system expansion are the main concerns of modern power systems engineers, not to mention security and reliability of supply. This is a large-scale problem that must be solved for the steady state condition using appropriate models, and is here where power system engineers are required to comprehend the basic building blocks used to assemble the power system, namely models for transmission lines and power transformers in various connections. Electrical engineers should be proficient in principles and the assumptions about models and its range of validity to conduct studies of three phase AC networks under balanced or unbalanced conditions or even with today's requirements of a more pervasive interaction between AC and DC networks.

In Chapter 1 of this book, we will stress the fundamental principles used to eventually grasp and handle complexity. This will allow us to solve the steady state of linear and nonlinear networks. In particular, we are interested in what is considered the most basic point of departure (i.e., element's current and voltage at its terminals and currents as nodal balance equations). These allow us to represent interconnection between networks and elements. Fundamental equations for electric circuits come from Ohm's law and nodal current or nodal power balances. These are the stepping stones used as building blocks. Power and energy, phasors, real and reactive power concepts—as well as a brief extension to three-phase circuits—are those principles from which some more elaborated schemes will be later studied.

Chapter 2 is used to establish all the tools for network analysis that we will need later to study large interconnected networks. Starting with Ohm's and Kirchhoff's current law, the use of *Gaussian elimination*, and a particular interpretation of this process known as *partial inversion*, we will show the connection starting from primitive networks up to nodal analysis, as well as Norton's and Thevenin's equivalents and applications. Solutions to large networks and network partition, also known as diakoptics, will be put into a unified perspective.

In Chapter 3, the physical principle of decoupling is motivated and solved so as to have a diagonal matrix that relates state variables and output variables. The symmetrical components transformations is of particular significance for power engineers. We then move into a detailed study of transformers for analysis purposes, starting with a single-phase transformer that can be combined into three-phase configurations, giving us the possibility to model various connections as $\Delta\Delta$, ΔY , YY , and other unbalanced configurations. The calculation of sequence impedances can be carried out as outlined in Chapter 3. Autotransformers and three winding transformers as well as three-phase transformers are discussed.

Transmission lines and cables are discussed in Chapter 4. The importance of series impedance, the Earth return, and capacitive effects are stressed in this chapter. Faraday's and Gauss' laws turn out to be the founding blocks for these important modeling concepts. Earth wires and phase conductors in parallel and neutral connecting points are represented properly and its existence included in the model. The formulas are adequate for transmission lines and cables that work at low frequencies, close to the 60 Hz frequency of operation for the power system. In case the line-cable parameters should need frequency dependent characteristics for other type of problems, then different models should be used.

Chapter 5 studies the very important topic of transmission line load-ability, where the line-distributed parameters are fundamental in order to attain proper values when loading a transmission line. This power system element has various interesting properties that need to be assessed, as the line might work with low power during light morning hours or under heavy load condition at peak hours. A wide range of power required to be shipped might need compensating equipment in order to fully use all the capability of the element and not be limited by the voltage drop criteria. The distributed nature of the series impedance and shunt capacitive susceptance will give a model to characterize the *traveling wave* phenomena, surge impedance and the speed of propagation where tools as the lattice diagrams for *surge* response calculation can be utilized.

In Chapter 6, we derive the real and reactive power flow expressions for a *complex transformer* and a transmission line. We write the incremental expressions, showing that the first and second order derivatives can be obtained in closed form from the calculated values of the real and reactive power that flows through the element itself. First order derivatives are used to write the solution to fundamental network problems, particularly those of the power flows by Newton's iterative process. The second order derivatives are used to solve the nonlinear optimal problem for minimum cost of operation, optimal control, or hydro-thermal coordination. For the iterative process in the load flow problem or in the optimal formulations, we start with reasonable values (*flat start* or a better estimate) for the state variables. The number of equations should be consistent and solved for the incremental corrections to the state variables at each iteration the state variables approach a solution; for a well-posed problem the process, should converge in few iterations. Even though Newton's law is reported to have a good rate of convergence, some problems might show slow convergence or no convergence at all, depending on the nature of the system, topology, and load level. We derive from incremental power flow expressions the decoupled model for power flows that are widely accepted by the power industry for networks the comply with assumptions as r/x ratio and

nodal angles separations. Chapter 6 also includes the nonlinear formulation used to solve an all-DC network; this is presented in a formulation to solve a three-phase unbalanced system.

Optimal power system's operation is discussed in Chapter 7. The nonlinear nature of the problem is maintained in the cost function and the equality and inequality constraints. All functions are incorporated into a Lagrangian and optimal conditions: gradient equal zero are derived. A nonlinear iterative process (Newton's type) is used to solve the gradient equations at the solution point. Minimum operating cost, losses included, or the solution to the minimum loss problem can be written as a solution at one point in time. An extension is made to include time-dependent quantities (such as energy or water to be used in hydro generation in combination with thermal and other energy resources). The interesting problem of energy coordination can be solved within the time horizon of interest and considering appropriate time increments, according to the problem to be solved.

Control of real and reactive power can be viewed from a static point of view in the sense of meeting a balance at every node in the system; dynamics and control are not modeled, and we are only interested in the new equilibrium condition, new nodal angles, voltages, and new power flows. Chapter 8 approaches this problem using linear sensitivity factors for the real power and the reactive power problem to coordinate control actions. Undoubtedly, the dynamics for changes and responses must be considered. As there are different time constants for response at each problem (namely real power frequency and voltage controls), we include a frequency response model in just one electric area, recognizing that the problem is more complex than the one presented. However, we will have a glimpse of what comes when we need to study system's frequency dynamics. In line with the static response, we include an extension of the complex transformer model (introduced previously in Chapter 6) to comprise schemes that work as flexible AC devices, namely a VSC and STATCOM. These arrangements demonstrate versatile ways to compensate reactive power and voltage control and the model discussed can easily be integrated into a regular Newton's power flow program.

Chapter 9 discusses fault studies from a general point of view writing model equations (Thevenin's equivalent) for the network and a set of equations for the *fault connection*. Then, when the fault is ensued, boundary conditions for nodal voltages and nodal currents must be met. The resulting equations will solve for the current feeding the fault. With this value, we then use the network equivalent to calculate the system's response when the fault is present. The process can be applied to both shunt and series faults, giving a natural extension to network equivalents and its properties.

Chapter 10 discusses contingency cases, mainly one element out at a time, starting from a base case. The tools are similar to the ones used in Chapter 9, as network equivalents also play an important role in the simulation of lines/transformers out of service and need to be disconnected from the network to simulate the contingency. Outages of generators or load disconnection are nodal changes and through sensitivity factors the impact can be calculated on nodal angles or voltage magnitudes, as well as the changes in power flows in the network.

Finally, Chapter 11 focuses on state estimation and presents its conceptual link to *minimum squares estimation* when measurements are available, including different

quality of measurements, and the best statistical state is calculated. These concepts are related to network quantities and measurements that can be nodal voltages, nodal magnitudes, power injections, or real and reactive power flow through transmission elements. We stress the need to identify a *measurement matrix* that relates the measured quantity to the state variables, first through linear models and solved by the *least squares principle*, then including nonlinear relations between measurements and state variables. Redundancy as having more measurements than state variables to be determined is key in the process, as some measurements might have gross errors and a step of goodness of fit must be carried out so that spurious measurements are rejected. State estimation is important for monitoring and controlling the modern power system. The process of parameter estimation can be established from the principles described in the *least squares* approach. Natural extensions in the estimation process are phasor measurements that go into phasor measurement units (PMU), and the concept of wide area measurements that will enhance the monitoring, operation, and control of present and future electric power systems.

As the reader can see, the focus is mainly on the steady state of AC and DC networks because the knowledge of state variables is important in its own right, to completely determine the value of derived variables as currents, real and reactive power flows through each element, and losses or the reactive power requirements.

This book is dedicated to slightly advanced students with a background in basic circuits, how to solve a system of linear equations, root finding of nonlinear equations, and the main principles of electric energy conversion. Senior students will benefit from a different approach in building original material, and will learn how fundamental concepts can be put to use in order to generalize the study of electric power networks. Practicing engineers will find a source of reference to refresh material covered in a different order and often through a piecemeal approach, leaving sometimes disconnected fundamental concepts from the system's point of view.

We must recognize that, due to continuously changing conditions in the power network from load requirements, generation supply, or contingencies, there will be a dynamic behavior in state variables (such as voltage magnitudes and nodal angles). Consequently, currents and power changes redistribute the energy until all unbalances are settled (unless the system goes into an unstable condition). Under a dynamic situation, electric elements (such as inductors, capacitors, and the generator's inertia) come to interact. Dynamic modeling and solution require a separate treatment to incorporate the time energy exchange between the generator's inertia, its controls actions, and the electric network. In general, we will need machine dynamics and controls by differential equations and low frequency exchanges through the network, which can be characterized by algebraic equations. Future work can cover this aspect building from the foundations put forth this volume.

Fundamentals of Energy Systems

1.1 Introduction

All human activities rely on some form of energy resource: thermal, mechanical, chemical, and, in some countries, nuclear. Accordingly, progress and development in a country is measured directly by its energy use in transportation, electricity production and agriculture, manufacturing, health services, and banking, as well as in recreational chores. Due to the industrial revolution, the last two hundred years of human history recounts an exponential growth in energy consumption per capita. New developments in technologies and efficient energy use are envisioned to continue exploiting fossil fuels, as well as heavily investing in renewable energy sources, such as solar (which has its origins within the atomic furnace in our nearest star, the sun, the main source of energy for our planet).

Huge amounts of energy are required nowadays in the world. We estimate the quantity used through the average energy utilized in various regions of the world; the numbers are summarized in Figure 1.1. If we add in the growing world population, we can estimate the energy required on a global scale for each region some years into the near future. Figure 1.2 gives a glimpse of the mixture of energy types that were used circa 2000, as new statistics are available the percentages can be updated. The energy mix might change for different countries, but this can give us a sense about the type of primary energy sources. Table 1.3 shows how actual energy requirements are supplied and how they were used by the year 2000, in particular in the case of the United States. This proportion is expected to be modified since renewables, such as solar and wind, are being used more and more even as we write this chapter. Active research and development has come to fruition for wind harnessing as electric power generation and solar capture is also a promising proportion of the total world energy requirements in the near future. Other sources sometimes experience a halt, as is the case for nuclear after the Japanese disaster in Fukushima in March 2011. The portion of fossil fuel for electric energy supply—with respect to renewable resources—is high and will be changing in the near future when we incorporate larger portions of renewables, coupled with efficiency in usage, reduction in losses, and an “intelligent” use of energy. Other small generating plants are emerging in small-scale production. They are connected at the distribution level, but in increased proportion, and are known as dispersed generation appearing throughout the urban and rural distribution networks. This is having a large impact on the generation available in the system and a change in the way that traditional systems are planned, operated, controlled, and protected.

Table 1.1 Yearly Average of Energy Use Per Capita, GJ/yr [1]

<i>Year</i>	<i>North America</i>	<i>Europe</i>	<i>Former USSR</i>	<i>Rest of World</i>	<i>Global</i>
1975	260	120	160	22	60
1980	265	135	175	24	62
1985	250	132	196	26	61
1990	263	135	205	28	63
1995	263	131	140	33	62
2000	272	136	135	35	62
Average	262.2	131.5	168.5	28.0	61.7

The three main sources of primary energy are oil, gas, and coal (Figure 1.2). These fuels experience very high price fluctuations over time, depending on production booms and shortages. This translates to uncertainty in both the cost operation of an actual energy system and plans for future system operations. Other energy resources, such as hydro, geothermal, and wind, are, in a theoretical sense, considered costless fuels, but also there is a high degree of uncertainty to their availability due to seasonal conditions. When the alternative energy sources are interconnected to a thermal system, a coordinated economic study should be done in order to satisfy the criteria of system operation at minimum cost, or some other optimal criteria that is suitable for operation or for planning. The result is a coordinated energy

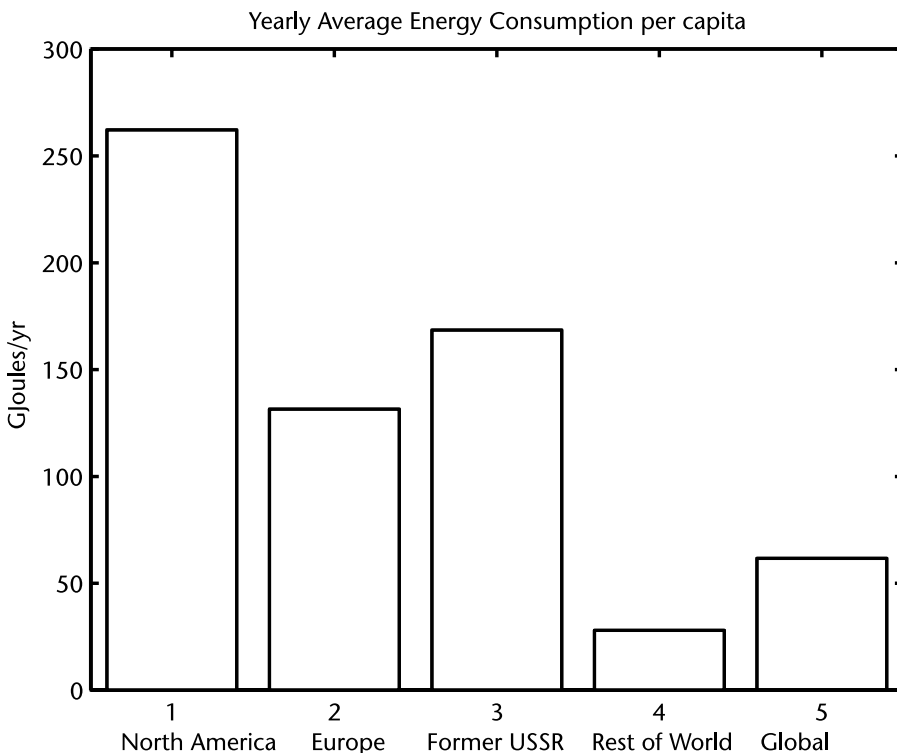
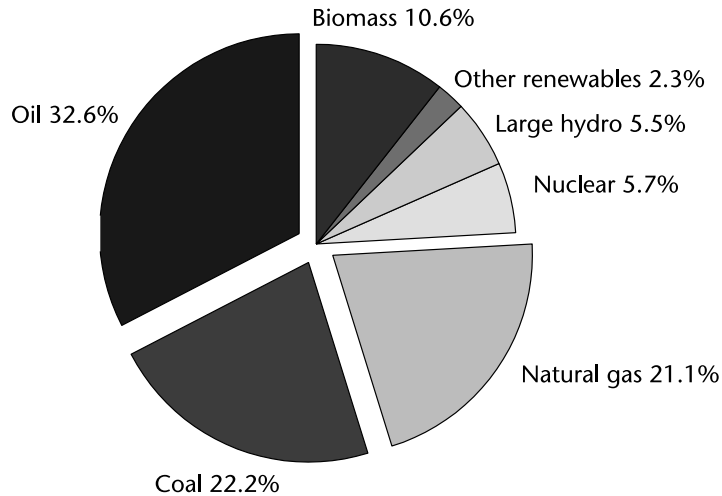
**Figure 1.1** Average use of energy per capita, GJ/yr.

Table 1.2 Energy From Type of Source, in Percentage [1]

<i>Oil</i>	<i>Coal</i>	<i>Natural gas</i>	<i>Nuclear</i>	<i>Large hydro</i>	<i>Other renewables</i>	<i>Biomass</i>
32.6	22.2	21.1	5.7	5.5	2.3	10.6

**Figure 1.2** Percentage of energy according to type of source.

study where we will need to find the minimum of the cost function subjected to physical system's constraints.

The electricity flow during 2011 in the United States was 40.03 quadrillions BTU [1] (quadrillion BTU = $1.05505585 \times 10^{18}$ joules), and a possible breakdown can be as is shown in Table 1.3.

Table 1.3 Energy Consumption USA, 2011

<i>Electric Energy by Type of Fuel</i>	<i>Percentage</i>
Fossil fuels (coal, natural gas, petroleum, other)	66.13
Nuclear and renewables	33.87
<i>Conventional thermal (Fossil fuels and other like nuclear)</i>	
Losses	63.00
Gross generation of electricity	37.00
NOTE: Except for combined cycle schemes where efficiency can go up to 64%	
<i>Electric Power by Power Plant</i>	
Power plant own use	5.47
Net generated power (into the power network)	94.53

For a final balance, we add unaccounted energy and imports to the net use of electricity in the United States (as reported in 2011) through the following numerals:

Transmission and distribution losses	7.32%
Residential use	34.23%
Commercial use	31.69%
Industrial applications	23.45%
Transportation	0.21%
Direct use	3.10%
Total	100.00%

The 40.03 quadrillions of BTU account for an average of 121 GJ/yr per capita. To this average, we must add the use of gasoline, as well as some other energy forms; then we will find the average listed in Figure 1.1 the amount is 262.3 GJ/yr for North America. We should keep in mind various figures; one relates efficiency for the conversion process from raw energy to the electric form. Power plants that work under a combined cycle scheme make a better use of the heat within the process, giving a higher efficiency for whole energy conversion. Electric power plants require energy to service their own motor pumps, fans, lighting, and other services—this might amount to 3% to 4%. The amount of losses in transmission and distribution lines present opportunities to improve the process, and it might have quite an impact in economic and environmental terms, as well as less amounts of required energy from the primary sources.

1.2 Work and Energy in Electric Circuits

We are interested in the energy usage, so let us start with a simple electric circuit as a means to ship energy from an electric source to a consumer; some useful purpose will be accomplished with this arrangement. Energy is required in order to attain motor rotation and then to move a production chain production, lighting loads for illuminating purposes, heating, electric vehicles, and a wide range of industrial applications.

1.2.1 Power and Energy in Constant DC Systems

Even though most generation, transmission, and distribution is done in AC, for a straightforward explanation purposes (and in order to better grasp the basic concepts), it is interesting to begin with an ideal DC source with a fixed voltage V_s (volts) and a supply current I (amperes), as shown in Figure 1.3. The simple configuration has most of the concepts that we will find in more elaborate AC circuits as: a nonlinearity relation when power load is established, multiple solutions, and maximum power transfer and voltage stability margin. At any instant of time, we have a product of voltage and current, the product is the instantaneous power p in watts that the load requires from the source. If this condition lasts for a time Δt (seconds), the supplied energy in joules will be determined.

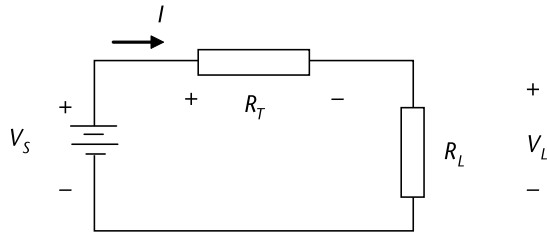


Figure 1.3 Simple DC circuit to illustrate electric power and energy concepts.

Power and energy supplied by a constant DC voltage source is:

$$P_S = V_S I \text{ Watts} \quad (1.1)$$

$$W_S = P_S \Delta t \text{ Joules (W-sec)} \quad (1.2)$$

Power at the load R_L is the power supplied by the source minus transmission losses $R_T I^2$.

$$P_L = V_L I = (V_S - R_T I) I = V_S I - R_T I^2 \text{ Watts} \quad (1.3)$$

$$P_{\text{LOSS}} = R_T I^2 \text{ Watts} \quad (1.4)$$

Energy at the load:

$$W_L = P_S \Delta t - P_{\text{LOSS}} \Delta t \text{ Joules} \quad (1.5)$$

Example 1.1

For the circuit in Figure 1.3 with $V_S = 120 \text{ V}$, $R_T = 1 \Omega$, $R_L = 19 \Omega$. Calculate current I , the voltage at the receiving end V_L , the power supplied by source S , the power received by the load, and the power loss in R_T . Calculate the energy balance when the load R_L is fed for a period of $\Delta t = 2$ seconds.

Voltage source $V_S = 120.0000$		
$R_T = 1.0000 \text{ Ohms}$	$R_L = 19.0000 \text{ Ohms}$	
$I = 6.0000 \text{ A}$	$V_L = 114.0000 \text{ V}$	
$P_S = 720.0000 \text{ W}$	$P_L = 684.0000 \text{ W}$	$P_{\text{LOSS}} = 36.0000 \text{ W}$
$W_S = 1440.0000 \text{ J}$	$W_L = 1368.0000 \text{ J}$	$W_{\text{LOSS}} = 72.0000 \text{ J}$

The current I , the load voltage V_L , the power P_S supplied by the source, power at the load P_L and power losses P_{LOSS} depend on the load resistance R_L . By changing the load resistance, we observe a nonlinear characteristic for the variables involved, as shown in Figure 1.4. The question about the maximum power transfer from the source to the load comes to mind; we will postpone this discussion about this important concept, which has important applications for the real power transfer problem, to Chapter 6.

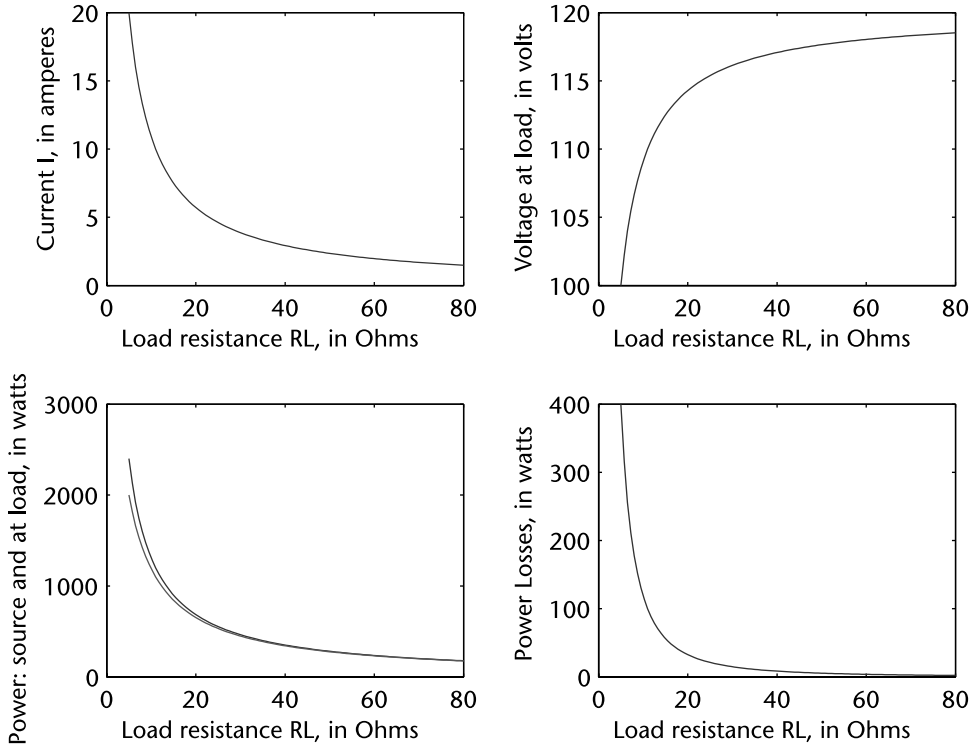


Figure 1.4 Plots for current, voltage at load, power by source, and losses.

1.2.2 Power and Energy in AC Circuits

For alternating current (AC) circuits, we assume that the voltage and the current are perfect sinusoids defined by peak values V_m (volts) and I_m (amperes), a unique frequency f (Hz), and time t in seconds.

$$v(t) = V_m \cos(2\pi f t + \theta_v) \quad \text{Volts} \quad (1.6)$$

$$i(t) = I_m \cos(2\pi f t + \theta_i) \quad \text{Amperes} \quad (1.7)$$

A time varying complex number \hat{V} can be defined as in (1.8) for a sinusoidal voltage and called *complexor*. The real part of the complexor is the cosine time function (1.6).

$$\hat{V} = V_m e^{j(2\pi f t + \theta_v)} \quad \text{Volts} \quad (1.8)$$

For voltage $v(t)$ and current $i(t)$:

$$v(t) = \text{real}\left(V_m e^{j(2\pi f t + \theta_v)}\right) \quad \text{Volts} \quad (1.9)$$

$$i(t) = \text{real}\left(I_m e^{j(2\pi ft + \theta_i)}\right) \text{ Amperes} \quad (1.10)$$

From a voltage complexor, the rms voltage *phasor* is that part of the complexor that does not depend on time t , divided by $\sqrt{2}$. The same definition is applied for the rms current phasor.

$$\tilde{V} = \frac{V_m}{\sqrt{2}} e^{j\theta_v} = |V| \angle \theta_v \text{ Volts} \quad (1.11)$$

$$\tilde{I} = \frac{I_m}{\sqrt{2}} e^{j\theta_i} = |I| \angle \theta_i \text{ Amperes} \quad (1.12)$$

$|V|$ Magnitude of rms voltage phasor, in volts

$|I|$ Magnitude of rms current phasor, in amperes

Example 1.2

A voltage complexor \hat{V} with $V_m = 180$ volts, $\theta_v = 0^\circ = 0$ rad, $f = 60$ Hz is a complex number that rotates counterclockwise; it has a magnitude of 180 volts. For a sampling rate of twelve samples per cycle, the rotating complexor and its real and imaginary components are shown in Figure 1.5.

$$\hat{V} = 180e^{j(2\pi 60t+0)} = V_x + jV_y = 180\cos(2\pi 60t) + j180\sin(2\pi 60t) \quad (1.13)$$

Figure 1.5 shows the 60 Hz complexor for 12 different instants of time for: $t_0 = 0$, $t_1 = 1/720$, $t_2 = 2/720$, $t_3 = 3/720$, ... in seconds, horizontal V_x , and vertical V_y projections versus time, so that a sinusoidal representation is attained.

1.2.2.1 Phasors

RMS phasor is a tool that is used to solve AC steady state problems for electric circuits in single-phase or three-phase configurations. We start our discussion with a simple one phase system configuration by the use of Ohm's law; we relate voltage at terminals and current that flows through a resistor R in ohms, an inductor L in henries, and a capacitor C in farads. We can extend the concepts into three-phase configurations, which are used in power system generation, transmission, and distribution.

Resistor R (ohms) can be seen as a constant of proportionality between voltage (volts) at terminals and current (amperes) that flows through the resistive element; the time equation is:

$$v(t) = Ri(t) \quad (1.14)$$

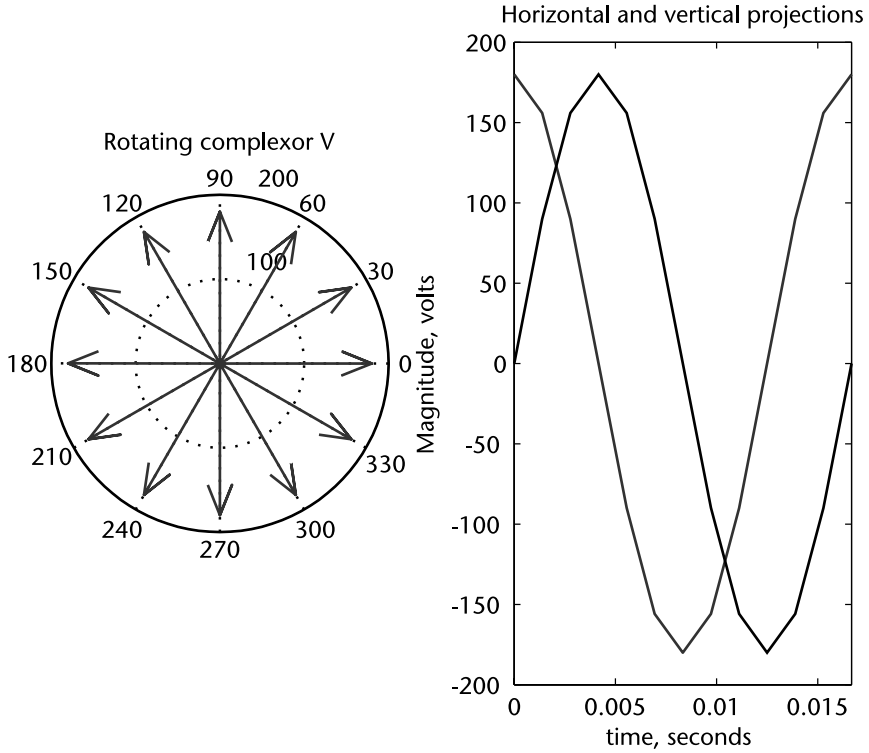


Figure 1.5 Rotating complexor, V_x and V_y projections.

For a sinusoidal voltage, frequency $\omega = 2\pi f$ in rad/sec, (1.14) is:

$$v(t) = \text{real}\left(V_m e^{j(\omega t + \theta_v)}\right) = R \text{ real}\left(I_m e^{j(\omega t + \theta_i)}\right) \tag{1.15}$$

The complexor notation for (1.15) or the phasor notation for Ohm’s Law is as follows in (1.16) and (1.17), respectively (Figures 1.6 and 1.7).

$$\hat{V} = V_m e^{j(\omega t + \theta_v)} = R I_m e^{j(\omega t + \theta_i)} = R \hat{I} \tag{1.16}$$

$$-R \tilde{I} + \tilde{V} = 0 \tag{1.17}$$

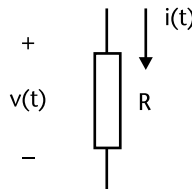


Figure 1.6 Voltage and current through resistance R .

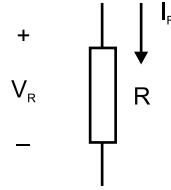


Figure 1.7 Voltage and current phasors in resistance R .

RMS phasors \tilde{V} and \tilde{I} are defined by (1.11) and (1.12), resistance R is a real number then in (1.18) $\theta_V - \theta_I = 0$, so current $i(t)$ through a resistance is in phase with $v(t)$.

$$R = \frac{\tilde{V}}{\tilde{I}} = \frac{V_m e^{j\theta_V} / \sqrt{2}}{I_m e^{j\theta_I} / \sqrt{2}} = \frac{V_m}{I_m e^{j(\theta_V - \theta_I)}} \quad (1.18)$$

In a linear magnetic circuit the *inductor* L is a constant of proportionality between flux linkages λ (Wb-turns) and the current (amperes) that flows through the inductor. By Faraday's law the time equation can be written as

$$v_L(t) = \frac{L di_L(t)}{dt} \quad (1.19)$$

Assuming a sinusoidal current through the inductor, $i_L(t) = I_m \cos(\omega t + \theta_I)$:

$$di_L(t)/dt = -\omega I_m \sin(\omega t + \theta_I) = \omega I_m \cos(\omega t + \theta_I + \pi/2) \quad (1.20)$$

We write the voltage equation for the inductor using complexor notation (1.21), or using rms phasors as in (1.22). Note that the phasor current \tilde{I}_L lags by 90° the phasor voltage \tilde{V}_L . Ohm's Law is written as in (1.23) and shown in Figures 1.8 and 1.9.

$$\hat{V}_L = V_m e^{j(\omega t + \theta_V)} = L \omega I_m e^{j(\omega t + \theta_I + \pi/2)} \quad (1.21)$$

$$\tilde{V}_L = \frac{V_m}{\sqrt{2} e^{j\theta_V}} = \frac{L \omega I_m}{\sqrt{2} e^{j(\theta_I + \pi/2)}} = j \omega L \tilde{I}_L \quad (1.22)$$

$$-j \omega L \tilde{I}_L + \tilde{V}_L = 0 \quad (1.23)$$

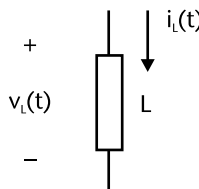


Figure 1.8 Voltage and current through inductance L .

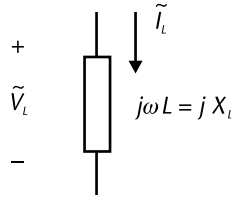


Figure 1.9 Phasor model for inductance L , relation between voltage and current.

A definition is made for the inductive reactance as $X_L = \omega L$ in ohms.

The *capacitor* C (shown in Figure 1.10), given a linear electric field, is a constant of proportionality between the amount of electric charge q (coulombs), $q = Cv_C$, which is accumulated at the device when voltage v_C (in volts) is applied at its terminals. The time equation is:

$$i_C(t) = \frac{Cdv_C(t)}{dt} \quad (1.24)$$

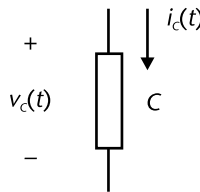


Figure 1.10 Voltage and current through capacitance C .

Assuming a sinusoidal voltage applied at capacitor terminals as $V_C(t) = V_m \cos(\omega t + \theta_V)$:

$$\frac{dv_C(t)}{dt} = -\omega V_m \sin(\omega t + \theta_V) = \omega V_m \cos\left(\omega t + \theta_V + \frac{\pi}{2}\right) \quad (1.25)$$

The current through the capacitor in complexor notation (1.26), or in rms phasors as in (1.27), then Ohm's law is written as in (1.28).

$$\hat{I}_C = I_m e^{j(\omega t + \theta_i)} = C\omega V_m e^{j(\omega t + \theta_V + \pi/2)} \quad (1.26)$$

$$\tilde{I}_C = \frac{I_m}{\sqrt{2}e^{j\theta_i}} = \frac{C\omega V_m}{\sqrt{2}e^{j(\theta_V + \pi/2)}} = j\omega C\tilde{V}_C \quad (1.27)$$

$$-\tilde{I}_C / j\omega C + \tilde{V}_C = 0 \quad (1.28)$$

In (1.27) and Figure 1.11, we see that the rms phasor voltage \tilde{V}_C lags by 90° the rms phasor current \tilde{I}_C ; or the current leads the voltage by 90° .

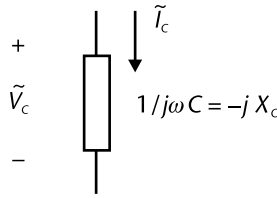


Figure 1.11 Phasor representation for capacitance C , relation between voltage and current.

Example 1.3

A circuit in Figure 1.12 has a voltage source $v_s(t) = V_m \cos(2\pi ft + \theta_V)$, $f = 60$ Hz, $R_s = 2$ ohms, $X_L = \omega L = 12$ ohms, $1/\omega C = 2$ ohms. Solve for current $i(t) = I_m \cos(2\pi ft + \theta_I)$ using $V_m = 180$ volts and $\theta_V = 0$ as a reference. Plot the current and the voltage at nodes 1, 2, and 3 as labeled in Figure 1.13.

Even for simple circuit arrangements, it is convenient to use rms phasors in order to solve for current and voltages phasors and time signals (as shown in Figure 1.14).

1.2.3 Instantaneous Power $p(t)$, Real Power P and Reactive Power Q

For a voltage $v(t)$ and current $i(t)$, in volts and amperes respectively, the product will be an instantaneous power $p(t)$ in volts-ampere (VA) that is supplied to a load. A detailed analysis of instantaneous power $p(t)$ shows imbedded the concept of real

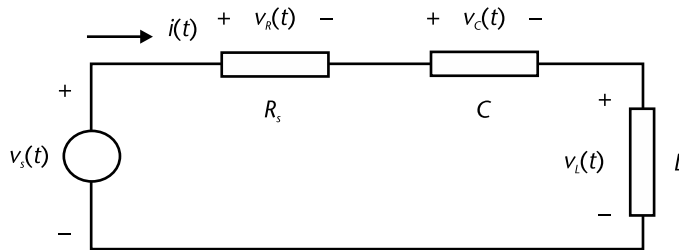


Figure 1.12 Voltages and current through series R, L C circuit.

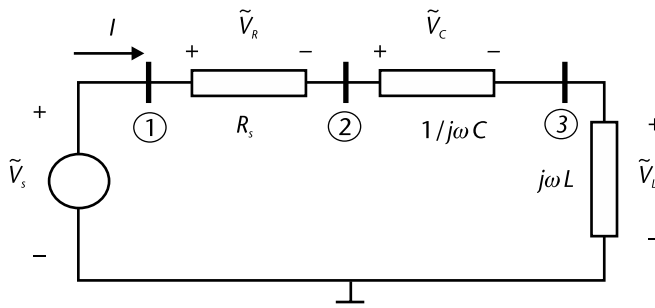


Figure 1.13 Voltages and current rms phasors through R, L C series circuit.

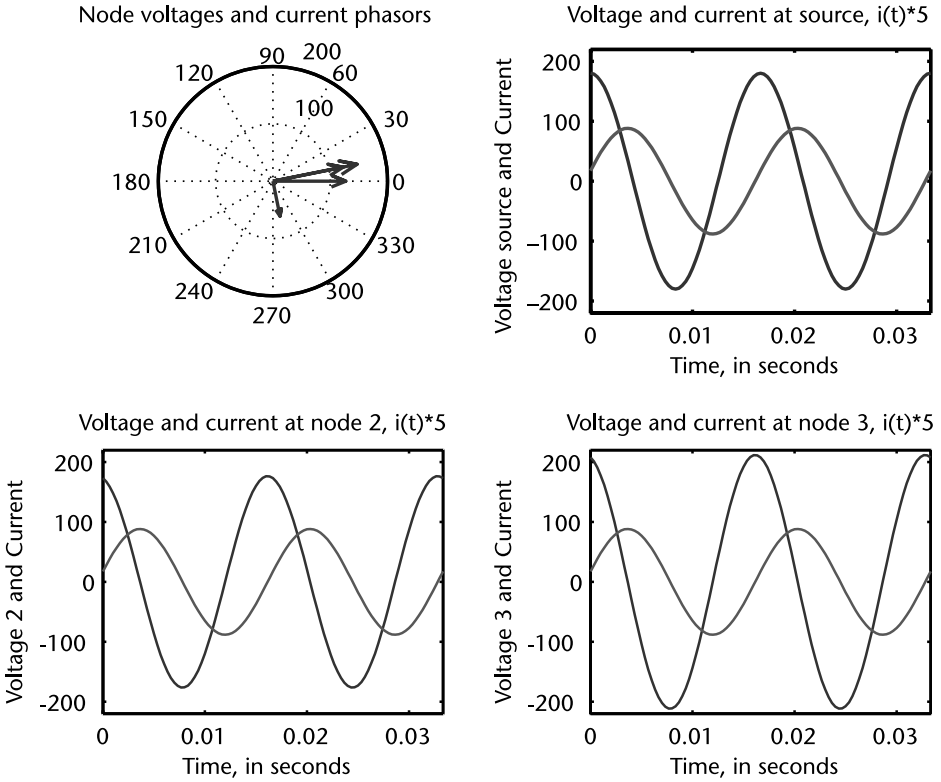


Figure 1.14 Nodal voltages at 1, 2 and 3 and current phasors. Sinusoidal current waves (x5).

power P in watts and the reactive power Q in VARs. For sinusoidal voltage and current, the rms phasors will be used to calculate P and Q .

$$p(t) = v(t)i(t) = V_m \cos(\omega t)I_m \cos(\omega t + \theta) \tag{1.29}$$

$$p(t) = \frac{V_m}{\sqrt{2}} \frac{I_m}{\sqrt{2}} [\cos(2\omega t + \theta) + \cos(\theta)] \tag{1.30}$$

$$p(t) = P[\cos(2\omega t) + 1] + Q\sin(2\omega t) \tag{1.31}$$

The definition for P and Q are part of (1.30) using $\cos\theta$ and $\sin\theta$. Equation (1.35) shows P and Q as those components of a Fourier series expansion for the instantaneous power $p(t)$. P is an average or mean value of $p(t)$ and Q is a peak value of a component of $p(t)$ whose mean value is zero; throughout this explanation voltage is our angular reference.

$$P = |V||I|\cos(\theta) \tag{1.32}$$

$$Q = -|V||I|\sin(\theta) \tag{1.33}$$

$$\text{pf} = \cos(\theta) \tag{1.34}$$

$$p(t) = P + P \cos(2\omega t) + Q \sin(2\omega t) \quad (1.35)$$

1.2.4 Load Convention for Power Flows

It is convenient to work an expression so that our P and Q results are consistent with a load convention (see Figure 1.15) as a preferred reference for power flows. The voltage phasor is our reference and current might be in phase, lagging, or leading the voltage. For power flows, a convenient representation is to picture a load with required values of real power P and reactive power Q . If P and Q are positive, this means that they have the same direction as the current feeding the load, the load requires Q due to its inductive nature and current lags the voltage by an angle θ . For the load connection, a negative Q goes opposite to the current direction, meaning that the load is capacitive and that current leads the voltage by a θ angle. A negative sign for P (coming from a current reversal) will mean that instead of a load we are dealing with a source.

The cosine of the phase angle $\pm\theta$ is positive, the displacement power factor (pf), which is a term that is part of the expression to calculate the real power P (1.32). Once we know that the power factor is lagging ($-\theta$) then in (1.33) $Q = -|V||I|\sin(-\theta) > 0$. For a leading power factor ($+\theta$), then $Q = -|V||I|\sin(\theta) < 0$, which corresponds to the load convention just discussed in the last paragraph.

To analyze the voltage and current phasors, we can use the phasor complex plane, and to work with power relations, we can use the complex power plane, wherein S , P , and Q can be drawn. With the phasor \tilde{V} as reference, $pf = \cos(\theta_V - \theta_I)$.

In summary, for P and Q using the load convention:

- P : Real power is positive and has the same direction as the current going into the load; see Figure 1.16.
- Q : Reactive power is positive, same direction as the current that flows to the load, for inductive load (lagging power factor). Reactive power is negative, opposite to the current direction for a capacitive load (leading power factor).

As can be deduced from Figure 1.16, the complex power calculation is the product of rms phasors: voltage V and the conjugate of current I .

$$S = P + jQ = \tilde{V}\tilde{I}^* \quad (1.36)$$

Example 1.4

Calculate for the circuit in Example 1.3, the complex power in VA supplied by the source to node 1, the complex power sent from node 2 to 3, and the power at

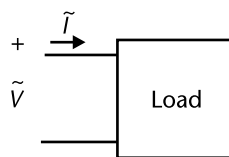


Figure 1.15 Load convention as a reference for power flows.

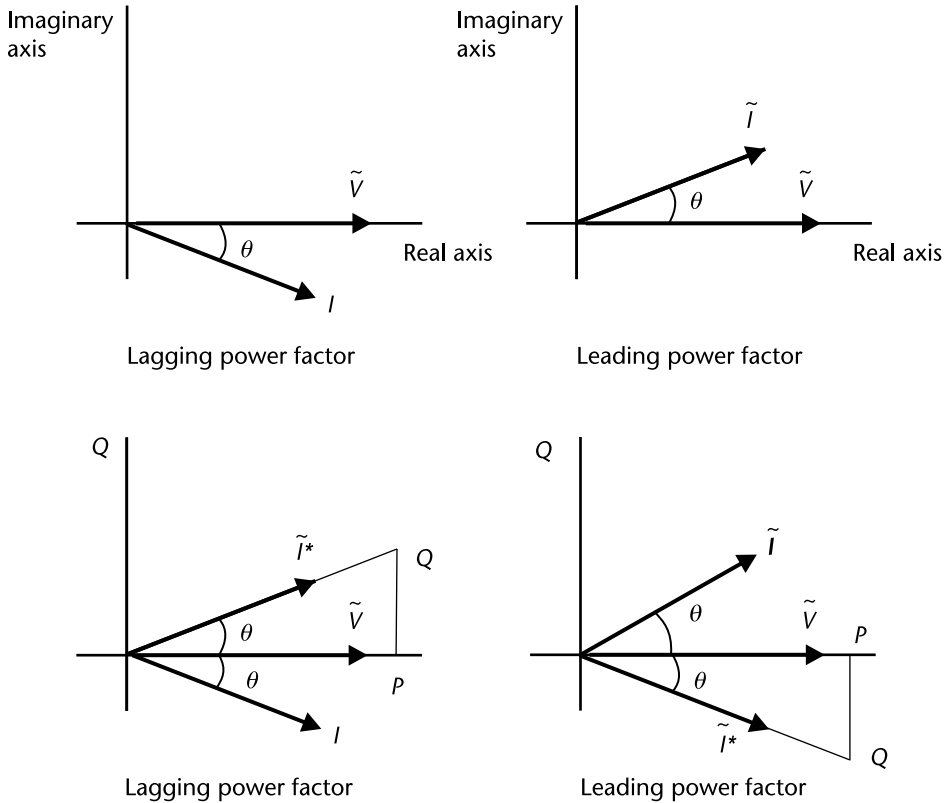


Figure 1.16 Voltage and current phasors. Power triangles show voltage and lagging and leading currents.

node 3. Power P in watts, Q in VARs and angle in degrees. The results are shown in Figure 1.17.

Complex voltages			abs	angle
V1	=	127.279 +0.000j	+127.279	+0.00
V2	=	122.384 +24.477j	+124.808	+11.31
V3	=	146.861 +29.372j	+149.769	+11.31
Current			abs	angle
I12	=	2.448 -12.238j	+12.481	-78.69
Complex power p+jq			abs	angle
S12	=	311.538 +1557.692j	+1588.541	+78.69
S21	=	0.000 -1557.692j	+1557.692	-90.00
S23	=	0.000 +1557.692j	+1557.692	+90.00
S32	=	-0.000 -1869.231j	+1869.231	-90.00
S30	=	0.000 +1869.231j	+1869.231	+90.00

Losses and reactive power
 Plosses = 311.538
 Reactive power (>0 to the system)
 Qtot = 1557.692

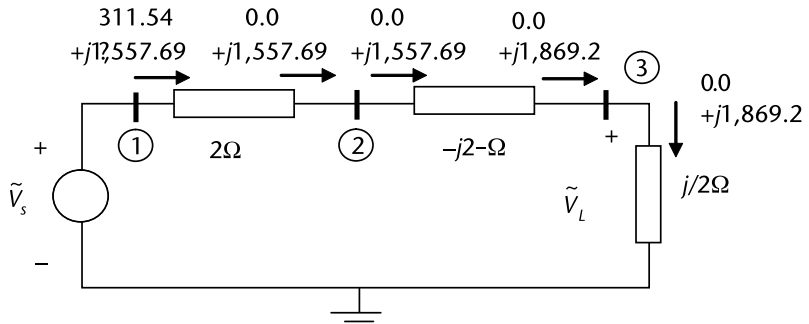


Figure 1.17 Voltages and power flows in Watts and VARs.

Example 1.5

Using voltage and current phasor values and a displaced angle for the current with respect to the voltage, find the voltage, current and instantaneous power. From (1.36) plot the instantaneous power $p(t)$ and the two components $P + P\cos(2\omega t)$ and $Q\sin(2\omega t)$ that make possible to identify P and Q . $V_m = 180$ volts, $I_m = 12.5$ amperes, first for a *lagging power factor* 0.9 (as shown in Figure 1.18) and then for a *leading power factor* of 0.9. Power results are shown in Figures 1.19–1.21.

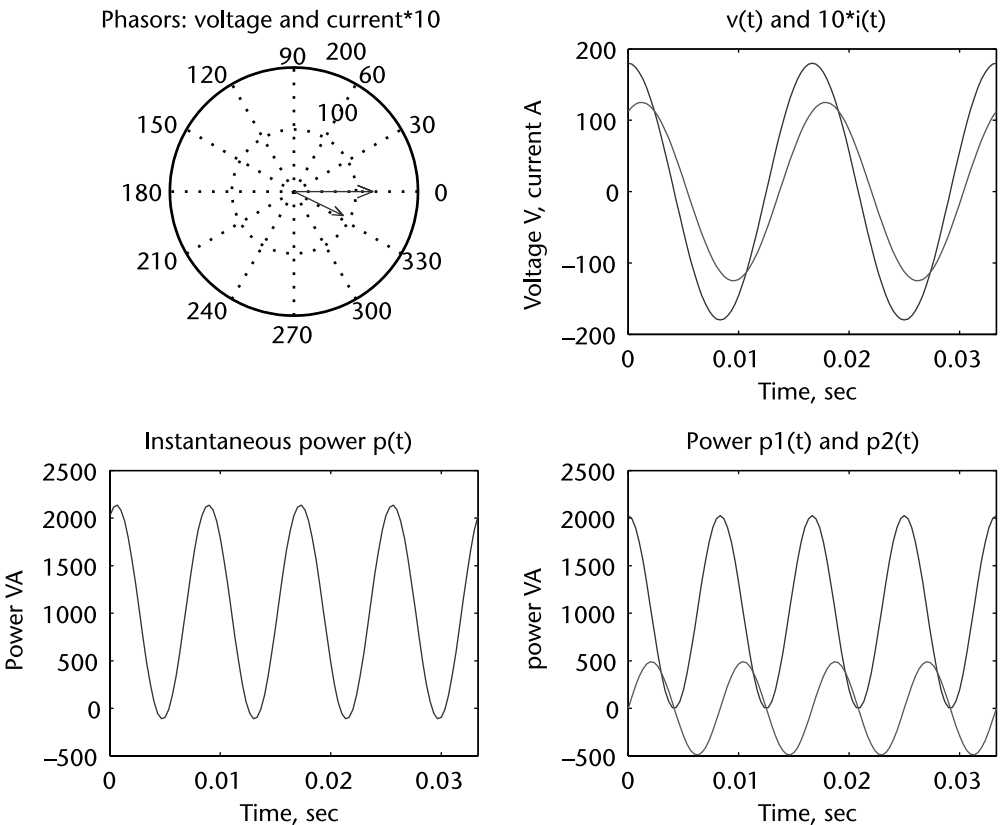


Figure 1.18 $V_m = 180$ volts, $I_m = 12.5$ amperes, power factor = 0.9 (lagging), $\theta = -25.84^\circ$.

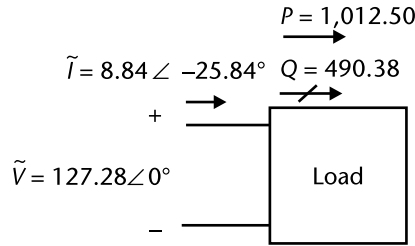


Figure 1.19 Voltage, current and power flows; lagging power factor.

Note: for lagging condition $\theta < 0$ and for leading condition $\theta > 0$.

RMS Voltage and current phasors
 magnitude angle
 $V = 127.279 + j 0.000 \quad 127.279 \quad 0.00$
 $I = 7.955 + j -3.853 \quad 8.839 \quad -25.84$

Power factor = 0.9000 (lagging)
 Real Power = +1012.50 W
 Reactive Power = +490.38 VARs

Voltage and current phasors, $v(t)$ and $i(t)$, instantaneous power $p(t)$ and two components of the instantaneous power.

For the leading power factor condition:

RMS Voltage and current phasors

		magnitude	angle
V	=	127.279 + j 0.000	127.279 0.00
I	=	7.955 + j -3.853	8.839 -25.84

Power factor = 0.9000 (lagging)
 Real Power = +1012.50 W
 Reactive Power = +490.38 VARs

Voltage and current phasors, $v(t)$ and $i(t)$, instantaneous power $p(t)$ and two components of the instantaneous power.

Figures 1.18 and 1.21 show the fundamental concept of power factor, related to the angle phase shift for the current $i(t)$ respect to the voltage $v(t)$; this has consequences on the value of P and Q . An ideal situation would be to have an

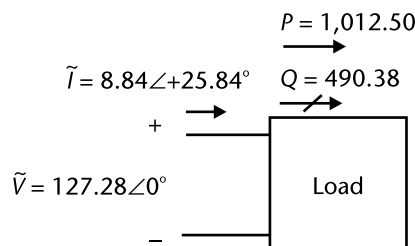


Figure 1.20 Voltage, current, and power flows; leading power factor.

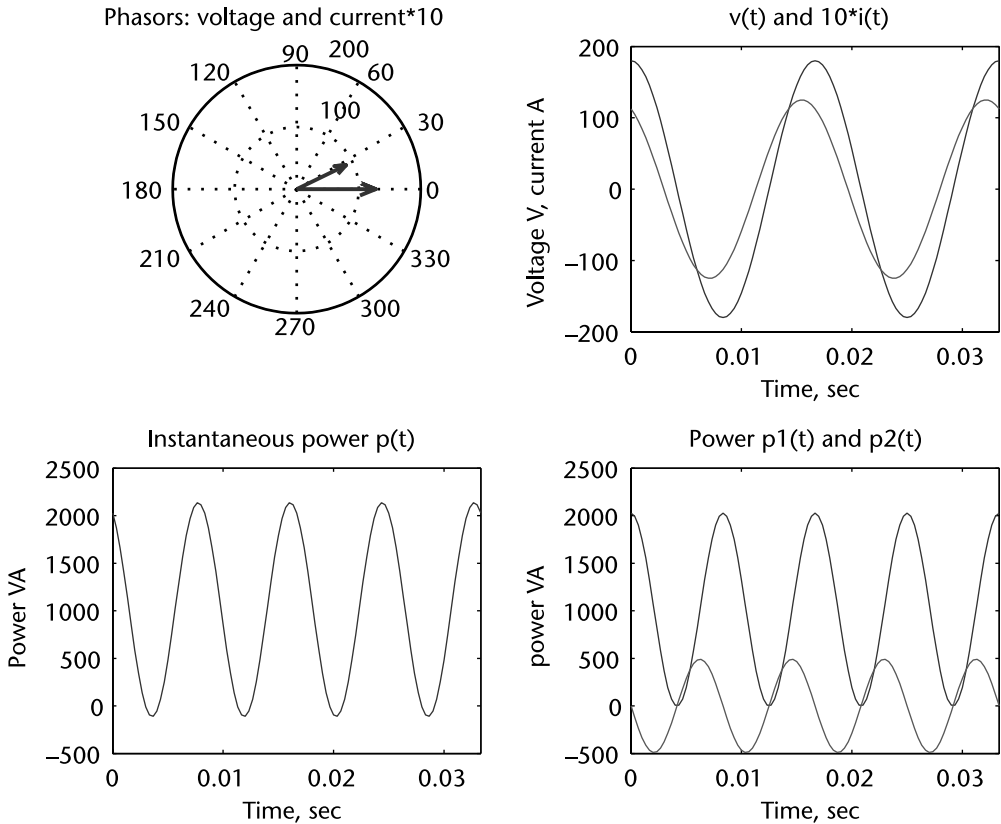


Figure 1.21 $V_m = 180$ volts, $I_m = 12.5$ amperes, power factor = 0.9 (leading), $\theta = 25.84^\circ$.

in-phase current to voltage, so that reactive power Q would be zero. In order to modify the power factor in a lagging or leading situation, current has to be “displaced” to be more closely in phase with the voltage. Such is the nature of *reactive power compensation*.

Example 1.6

The lagging or leading power factor will have an impact on both the nodal voltages and the power system losses. To motivate the attention for this kind of relations let us use a three node system (Figure 1.22(a)) where all values are normalized so that voltage and power are 1 pu (per unit (pu) values are defined later), and analyze the consequences of a change in the power factor at node 3. Pay attention to the voltage magnitude at node 3 and system losses as a function of the power factor at node 3 (for printout assume lagging is – and leading is +). We will study in detail this type of system behavior in Chapter 6 through the use of load flow studies. Table 1.4 summarizes the network solution as pf changes from lagging to leading condition.

Note from Figure 1.22(b) that minimum losses are attained when the power factor is 1.0, current in phase with the applied voltage at the load point, node 3. Losses and nodal voltages change as the power factor has a lagging or leading condition; losses increase under both conditions and node voltage drops from the 1.0

Table 1.4 Power Factor at Node 3, Reactive Power Q_3 , Voltage 3, and System Losses

pf	Q_3	V_3	$Losses$
-0.850	0.6817	0.9139	0.0268
-0.875	0.6086	0.9232	0.0249
-0.900	0.5328	0.9328	0.0233
-0.925	0.4519	0.9427	0.0219
-0.950	0.3616	0.9535	0.0206
-0.975	0.2507	0.9664	0.0195
1.000	0.0000	0.9943	0.0188
0.975	-0.2507	1.0207	0.0202
0.950	-0.3616	1.0319	0.0214
0.925	-0.4519	1.0409	0.0226
0.900	-0.5328	1.0488	0.0238
0.875	-0.6086	1.0562	0.0251
0.850	-0.6817	1.0631	0.0265

pu value when power factor is lagging. The node voltage increases from the 1.0 pu value for the leading power factor values.

1.3 Three-Phase Voltages, Currents and Power

Power system engineers use AC circuits in three-phase arrangements to carry power more efficiently from the generation sites to the demand locations. Load centers are usually located far from the generation plants, so in order to have reasonable transmission losses, step up voltage transformers and high voltage transmission lines are used. Once at the premises of consumers or very close to their location, step down transformers will lower the voltage to distribute energy to individual loads at an appropriately safe voltage level.

To have a glimpse of a three-phase circuit arrangement—even though it is a simplified scheme—we can visualize it through Figure 1.23; an ideal three-phase generator as a voltage source arrangement of a three *balanced complexors* a , b , and c , each one separated by 120 degrees and with the same magnitude. Every single voltage source a , b , and c is connected to the low voltage phases abc of the step-up transformer and ground. The high voltage side of the transformer feeds current into a transmission line, and then at the right side, we reach a step down transformer (not shown). From here, we feed the three-phase loads. The circuit needs to be solved for all node voltages and currents; the principles that we use are Ohm's law and Kirchhoff's current law.

$$\begin{aligned}
 \hat{V}_a &= V_m e^{j(2\pi 60t+0)} \\
 \hat{V}_b &= V_m e^{j(2\pi 60t-2\pi/3)} \\
 \hat{V}_c &= V_m e^{j(2\pi 60t-4\pi/3)}
 \end{aligned}
 \tag{1.37}$$

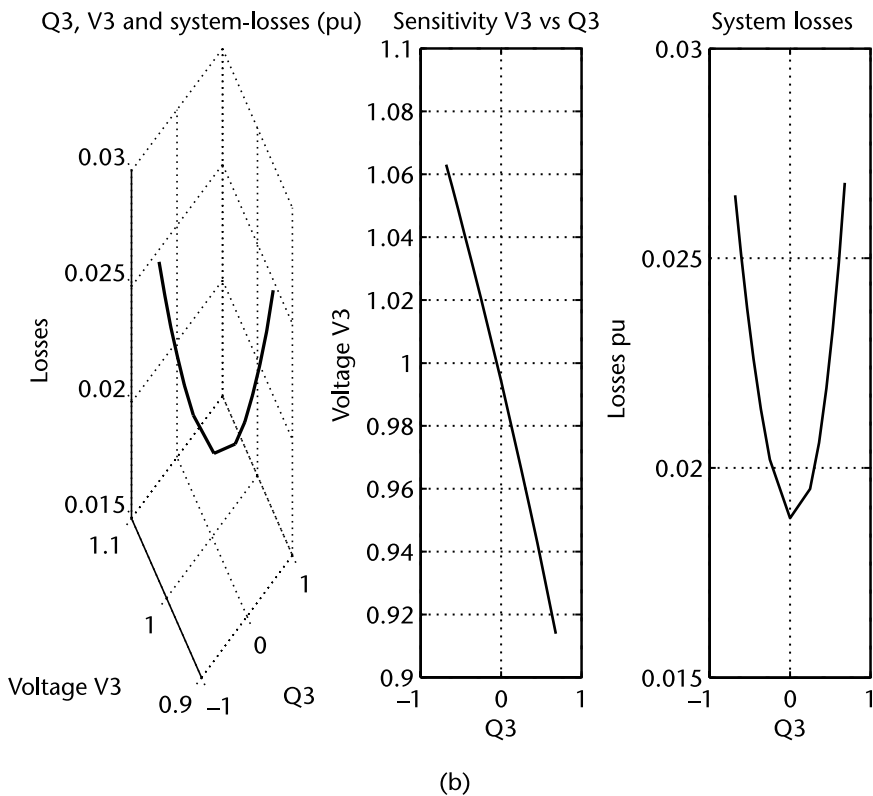
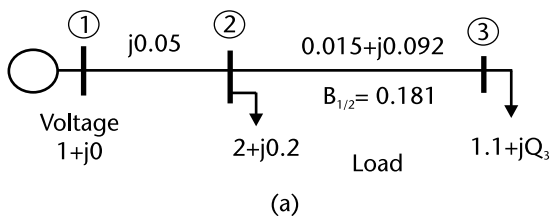


Figure 1.22 Effect of power factor changes on voltage at node 3 and losses; values in per unit.

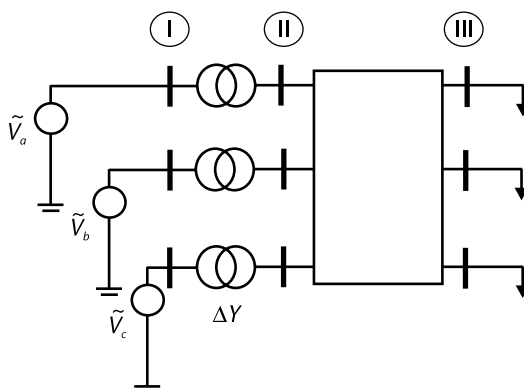


Figure 1.23 Voltages, current and power flows for a three-phase circuit.

We assume the use of RMS phasors as phase voltages at the generator side. An ideal step up transformer with tap $|t|$ applies high voltage values to the sending end of a transmission line, which, in turn, feeds current to the load at each phase at the receiving side. With the main goal of writing current and voltage relations in the three-phase circuit, we use voltages from node to reference or nodal voltages and currents injected to each node. The voltage drops and currents flowing in the windings of the ideal (lossless) transformer, the low voltage side in terms of source voltages, as in Figure 1.24, are (1.38). These voltages are transformed by the ratio $1:|t|$ into voltage values at the high voltage side (1.39). The connection shown for the primary side of the transformer (the left-hand side) is known as a delta Δ configuration, and the high voltage side is in a Y connection; the turns ratio will bust or buck the primary and secondary voltages and currents. The Y Δ connection will shift voltages and currents from the primary to secondary side. Voltages at the receiving end of the line are the voltages at the three-phase node named II, including the voltage drop across the transmission impedances when current flows at each phase. Equation (1.40) is Ohm's law for a three-phase element.

The voltage drop v_k across elements can be expressed in terms of nodal voltages, where nodal voltages are voltages from phase to reference (1.38). Voltages from primary side to secondary side in the transformer are affected by the transformer ratio, t_k as in (1.39). Ohm's law for the three-phase connection that goes from node II to node III is written in (1.40).

$$\begin{bmatrix} v_1 \\ v_3 \\ v_5 \end{bmatrix} = \begin{bmatrix} +1 & -1 & 0 \\ 0 & +1 & -1 \\ -1 & 0 & +1 \end{bmatrix} \begin{bmatrix} V_a \\ V_b \\ V_c \end{bmatrix}^{(I)} \quad (1.38)$$

$$\begin{bmatrix} V_A \\ V_B \\ V_C \end{bmatrix}^{(II)} = \begin{bmatrix} v_2 \\ v_4 \\ v_6 \end{bmatrix} = \begin{bmatrix} t_1 & 0 & 0 \\ 0 & t_2 & 0 \\ 0 & 0 & t_3 \end{bmatrix} \begin{bmatrix} v_1 \\ v_3 \\ v_5 \end{bmatrix} \quad (1.39)$$

$$- \begin{bmatrix} z_{aa} & z_{ab} & z_{ac} \\ z_{ba} & z_{bb} & z_{bc} \\ z_{ca} & z_{cb} & z_{cc} \end{bmatrix} \begin{bmatrix} i_A \\ i_B \\ i_C \end{bmatrix}^{(II,III)} + \begin{bmatrix} V_A \\ V_B \\ V_C \end{bmatrix}^{(II)} - \begin{bmatrix} V_A \\ V_B \\ V_C \end{bmatrix}^{(III)} = \begin{bmatrix} 0 \\ 0 \\ 0 \end{bmatrix} \quad (1.40)$$

Kirchhoff's current law, in Figure 1.23, include current summation at nodes (II) and (III), so we get a set of nodal current equations, assuming that the currents going into a node are positive. Equations (1.40) and (1.41) are our circuit models where U is a 3×3 unit matrix. The three-phase model for our circuit combines (1.40) and (1.41) into (1.42). Solution to the system of equations means calculating nodal voltages and currents that flow through each element. This will allow us to find the Norton equivalent for the Nodal admittance matrix [1, 2], and if we continue the numerical process through Gaussian elimination along the main diagonal, we

will be able to calculate all three-phase nodal voltages and solve for all unknown three-phase currents [3–5].

$$\begin{aligned}
 +i_{ABC}^{II,III} &= I_{ABC}^{II} \\
 -i_{ABC}^{II,III} &= i_{ABC}^{III,II} = I_{ABC}^{III}
 \end{aligned}
 \tag{1.41}$$

$$\begin{bmatrix} -Z_{abc} & +U & -U \\ +U & 0 & 0 \\ -U & 0 & 0 \end{bmatrix} \begin{bmatrix} i_{ABC}^{II,III} \\ V_{ABC}^{II} \\ V_{ABC}^{III} \end{bmatrix} = \begin{bmatrix} 0 \\ I_{ABC}^{II} \\ I_{ABC}^{III} \end{bmatrix}
 \tag{1.42}$$

Example 1.7

For the three-phase arrangement in Figures 1.23 and 1.24—using voltage in Volts, current in amperes, impedance in ohms, and a tap value $t = 20/\sqrt{3}$ —a voltage of 20 kV is applied at the delta side of the step-up ideal transformer; 400 kV will be the voltage at the sending end for the transmission element. With known values for ABC voltages at node II and load currents at ABC node III, a network solution is attained for (1.42), using Z_{abc} impedance values in ohms for the transmission element. In this case, no resistance is considered. Therefore, there will be no power losses at the transmission line. Nodal currents are calculated using (1.41) and complex power can be calculated using (1.36).

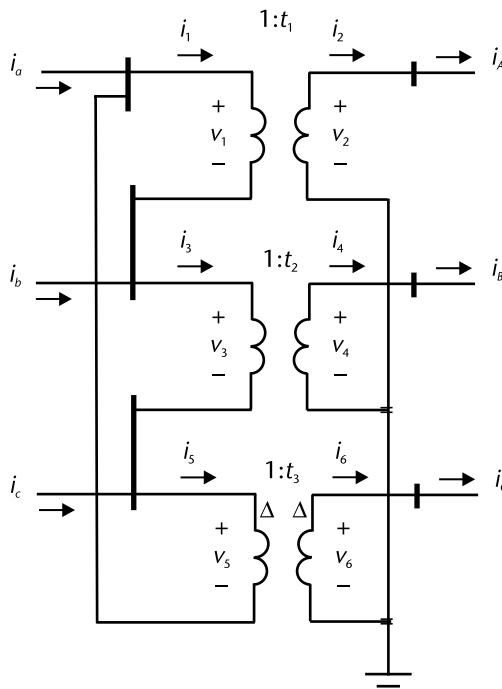


Figure 1.24 Voltages and currents, ideal no-loss transformer, ΔY connection.

Voltages Source (Y connection)

Magnitude kV	angle
+11.55	+0.00
+11.55	-120.00
+11.55	+120.00

Voltages low side transformer (DELTA)

Magnitude kV	angle
+20.00	+30.00
+20.00	-90.00
+20.00	+150.00

Voltages high side transformer (Y connection)

Magnitude kV	angle
+230.94	+30.00
+230.94	-90.00
+230.94	+150.00

zabc =

0 +23.0000i	0 - 2.0000i	0 - 2.0000i
0 - 2.0000i	0 +23.0000i	0 - 2.0000i
0 - 2.0000i	0 - 2.0000i	0 +23.0000i

Load current

Magnitude A	angle
+441.59	+18.69
+441.59	-101.31
+441.59	+138.69

Voltages at load node (Y)

Magnitude kV	angle
+229.03	+27.29
+229.03	-92.71
+229.03	+147.29

Phase currents high side transformer (Y)

Magnitude A	angle
+441.59	+18.69
+441.59	-101.31
+441.59	+138.69

Phase currents, low side transformer (DELTA)

Magnitude A	angle
+5099.02	+18.69
+5099.02	-101.31
+5099.02	+138.69

Phase currents, generators phases (Y)

Magnitude A	angle
+8831.76	-11.31
+8831.76	-131.31
+8831.76	+108.69

Power at load

Power MW	MVARs
+100.00	+15.12

+100.00	+15.13
+100.00	+15.12
Power into transmission element	
Power MW	MVARs
+100.00	+20.00
+100.00	+20.00
+100.00	+20.00
Power from generator	
Power MW	MVARs
+100.00	+20.00
+100.00	+20.00
+100.00	+20.00
Power required by the transmission element	
Power MW	MVARs
-0.00	+4.88
-0.00	+4.88
+0.00	+4.88

To find current values, from the Δ connection to the phase values at the generator side (Figure 1.24) we go from the transformer's currents to the current at each phase of the generator.

$$\begin{bmatrix} I_a \\ I_b \\ I_c \end{bmatrix}^t = \begin{bmatrix} +1 & 0 & -1 \\ -1 & +1 & 0 \\ 0 & -1 & +1 \end{bmatrix} \begin{bmatrix} i_1 \\ i_3 \\ i_5 \end{bmatrix} \quad (1.43)$$

Notice the 30° phase shift due to the ΔY connection of the three-phase bank transformer [5–7]. Resistance values were assumed to be very small when compared to reactance values, and so they were neglected. However, the calculating tool—once we establish the sequence of calculations—should easily handle complex numbers in its calculations.

Appendix 1A Complex Numbers

For electrical power engineers, the complex number tool is basic and widely used. The concept of complexor, as in (1.8), is an example of a complex number; it has magnitude and rotates at angular speed ω in rad/sec.

It is a historic matter that, in order to find a number that is the square root of -1 , the real number line representation has to be extended. Real numbers can be associated to points in a horizontal straight line. By a 90° rotation, the real line has an orthogonal display; to emphasize the rotation a j symbol is associated, we end up with a Cartesian-like plane that has a real and an imaginary axis; the plane is called a *complex plane* (see Figure 1.25). A complex number z has a real x and an imaginary y component, and it can therefore be located in the complex plane.

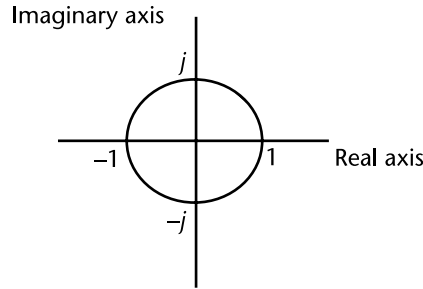


Figure 1.25 Complex plane. We visualize 90° successive rotation for number 1.

Example 1.8

Powers of j imaginary unit

$$1 = e^{j0}$$

$$j = e^{j\pi/2} = \cos(\pi/2) + j \sin(\pi/2)$$

$$j^2 = (e^{j\pi/2})^2 = e^{j\pi} = \cos(\pi) + j \sin(\pi) = -1; \quad j = \sqrt{-1}$$

$$j^3 = -j$$

$$j^4 = 1$$

The algebra of complex numbers can be illustrated assuming two complex numbers, z_1 and z_2 . They can be added, subtracted, multiplied, or divided in a rectangular or polar form. Conjugate in Figure 1.26.

$$z_1 = x_1 + jy_1 = |z_1|e^{j\theta_1} = |z_1|\angle\theta_1$$

$$|z_1| = \sqrt{x_1^2 + y_1^2} \quad \theta_1 = \arctg\left(\frac{y_1}{x_1}\right) \quad (1.44)$$

$$z_2 = x_2 + jy_2 = |z_2|e^{j\theta_2} = |z_2|\angle\theta_2$$

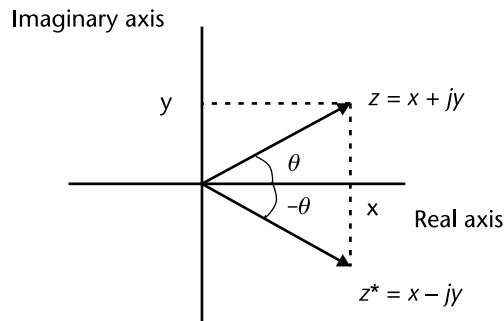


Figure 1.26 Complex number z and conjugate z^* in the complex plane.

$$\begin{aligned}
 z_1 + z_2 &= (x_1 + x_2) + j(y_1 + y_2) \\
 z_1 - z_2 &= (x_1 - x_2) + j(y_1 - y_2) \\
 z_1 z_2 &= (x_1 + jy_1)(x_2 + jy_2) = |z_1|e^{j\theta_1}|z_2|e^{j\theta_2} = |z_1||z_2|e^{j(\theta_1+\theta_2)} \\
 \frac{z_1}{z_2} &= \frac{(x_1 + jy_1)}{(x_2 + jy_2)} = \frac{|z_1|e^{j\theta_1}}{|z_2|e^{j\theta_2}} = \frac{|z_1|}{|z_2|}e^{j(\theta_1-\theta_2)}
 \end{aligned} \tag{1.45}$$

Example 1.9

For two complex numbers, $z_1 = 4 + 3j$ and $z_2 = 3 + 4j$ find $z_1 + z_2$, $z_1 - z_2$, $z_1 z_2$, and z_1/z_2 .

Complex numbers		abs	angle degrees
z1 =	4.000 +j 3.000	5.000	36.87
z2 =	3.000 +j 4.000	5.000	53.13
Algebra of Complex numbers		abs	angle degrees
zsum =	7.000 +j 7.000	9.899	45.00
zdif =	1.000 +j -1.000	1.414	-45.00
zpro =	0.000 +j 25.000	25.000	90.00
zdiv =	0.960 +j -0.280	1.000	-16.26

References

- [1] Shipley, R. B., *Introduction to Matrices and Power Systems*, New York: John Wiley & Sons, Inc., 1976.
- [2] Brown, H. E., *Solution of Large Networks by Matrix Methods*, Second Edition, New York: Wiley-Interscience, 1985.
- [3] Glover, J. D, M. S. Sarma, and T. Overbye, *Power System Analysis and Design*, Fifth Edition, Stamford, CT: Cengage Learning, 2011.
- [4] Grainger, J. J., *Power System Analysis*, New York: McGraw-Hill Science/Engineering, 1994.
- [5] J. Arrillaga, and C. P. Arnold, *Computer Analysis of Power Systems*, Chichester, UK: Wiley, 1990.
- [6] Saadat, H., *Power System Analysis*, Third Edition, Alexandria, VA: PSA Publishing, 2010.
- [7] Elgerd, O. I., *Electric Energy Systems Theory*, New York: McGraw-Hill Science/Engineering/Math, 1982.

Network Analysis

The main purpose in this chapter is to explain various circuit properties and useful algebraic results that can be expanded to study large power networks. We start from the algebraic manipulation of a system of linear equations to be solved for the unknown values. To model and study an electrical power system, which is an intricate ensemble of equipment of various kinds, a high degree of abstraction is required in order to represent the electrical power system as a whole. To conduct this task, we start by describing the physical electrical system by the use of a reduced set of idealized elements with defined properties between variables through them. That is, by Ohm's law we relate the electric current that flows when a voltage difference is applied at its terminals. We write a consistent set of equations for the network, using Kirchhoff's current law at each node, and work out a solution for state variables, which are those electric quantities known as *node voltages* that allow us to calculate currents and voltage drops on all elements in the network.

The analysis of the system enables us to predict its behavior under a range of stimuli with practical applications. From a general network model and its numerical solution, we derive Norton's equivalent, which is a numerical model that relates nodal voltages to nodal currents (those currents injected or extracted from a node by sources/loads) through admittance values or *short circuit* coefficients. The numerical process is conducted by *Gaussian elimination* or its numerical equivalent, *partial inversion*, in a matrix sense [1–3]. If we continue the *partial inversion* process, we eventually get Thévenin's equivalent. Thévenin's circuit relates nodal voltages to nodal currents through impedance values known as *open circuit* coefficients. The importance of network equivalents is that a large network can be reduced to a small equivalent circuit arrangement without losing the effects of connected elements as lines, voltage, or current sources. Using equivalent circuits, we can solve for state variables with less effort, given that we are only interested in the small portion of the original network. The solution to the equivalent can be fed into the complete network equations and the effect of the equivalent's solution can be reflected on the whole network. This approach will be used in fault current calculations and contingency analysis.

2.1 Introduction

A basic electrical power circuit is an interconnection of passive and active elements. Resistors, inductors, and capacitors are passive elements. Other elements

are designed to convert energy from the primary thermal or mechanical sources to electric DC or AC. These current and voltage sources are active components for the power system. Other types of sources with nonlinear characteristics that are based on power electronics are also active elements; through switching devices, they accomplish the useful handling of electric energy for various industrial and large-scale power applications. The electric elements may be series or shunt connected, forming a delta or a star configuration in the case of three-phase AC systems. In more elaborated circuits, the voltage and current sources may be of an independent or a controlled type.

For passive elements, the voltage at their terminals with respect to the current flowing in the resistor, inductor, or capacitor may be through a linear or nonlinear relation, depending on the nature of the element. Furthermore, the response can vary linearly with frequency or in a nonlinear fashion. Among various system elements, the ideal transformer with a real or a complex transformer with tap and phase shifting angle is a very useful device in order to represent voltage and current raises/drops at key sections of the circuit. Depending on the *electrical length* (with respect to the actual size of equipment), its circuit representation may be required to be described by distributed parameters or by lumped parameters—the electrical length is dictated by the actual physical dimension of the device and the voltage’s frequency at which the device is going to work.

Ohm’s law determines the amount of current that flows through a given element (R , L , and C), and it depends on the voltage at terminals for a passive element and the properties that oppose the current to flow. Kirchhoff’s voltage and current laws govern the interaction between the voltages and currents in all passive and active elements within a circuit. We can deduce various voltage-current formulations to study electric circuits; it all depends on the way in which we apply the fundamental laws. Popular outcomes are the *nodal equations* and the *mesh equations*, but other formulations are possible. When dealing with how to find the solution of practical electric power networks—which normally have a very large number of nodes and electric elements—the computational effort may be quite high, even for a digital computer. This is one of the reasons why we have to carefully plan all computational steps in order to keep the numerical burden well under control. It is fortunate that most large physical systems (as in the case of electrical power circuits) are loosely interconnected in a structural sense; not all electrical nodes are connected through elements (transformers, lines, and cables). This characteristic makes the system’s equations sparse and prone to an efficient numerical solution. When we recognize that, for high voltage power systems, up to 80% or more of the numerical coefficients in the nodal model have zero values—and that such coefficients should neither be stored nor processed—then the nodal model is very compact in storage requirements, even for very large power networks. Quite elaborated algorithms called *sparse techniques* will store and process the nonzero essential information. The solution of the sparse system of equations is mainly based on carefully thought Gaussian elimination and are well-developed; these techniques are surely included in all commercial-grade packages that solve electric power networks or for electronic circuits.

2.2 Ohm's Law

To discuss the essence of Ohm's law, which is a fundamental concept, let us use an ideally controllable DC voltage source that feeds an ideal resistive load; the circuit is shown in Figure 2.1(a). Current i through the load and voltage v across its terminals; we assume that both values can be recorded by an ammeter and a voltmeter, respectively. If the voltage applied by the source is increased gradually and the current through R is plotted for a range of values (Figure 2.1(b)), the diagram might reveal a linear relationship between the applied voltage v and the current response i .

From Figure 2.1(a), a linear relationship is readily established from which the slope or gradient is R . The incremental form is in fact Ohm's law, at any given time t it will be true that:

$$-Ri(t) + v(t) = 0 \quad (2.1)$$

The gradient R in ohms is the *resistance* of the resistive element and acts as proportionality constant between the applied voltage and the current as a response. In general, the resistance R is connected between nodes k and m , then at any time t the equation is (2.2) and the circuit is shown in Figure 2.2:

$$-Ri_{km}(t) + V_k(t) - V_m(t) = 0 \quad (2.2)$$

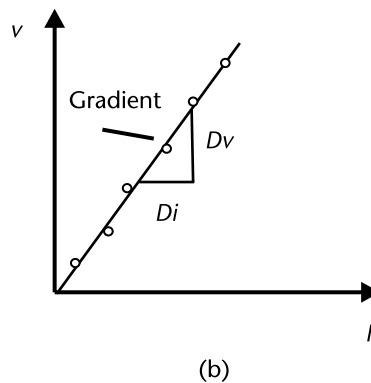
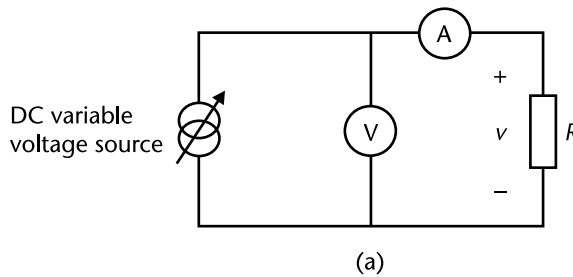


Figure 2.1 (a) Electric circuit, and (b) voltage-current characteristics for a linear resistor.

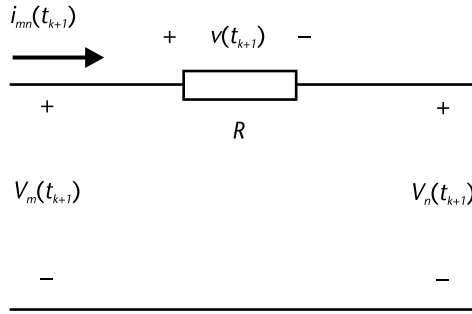


Figure 2.2 Voltage-current relation in circuit with a linear resistor.

V_k and V_m are nodal voltages; R is a linear resistance at time $t = t_{k+1}$

For a different relation between the applied voltage and the output current (as in shown in Figure 2.3), the behavior is not continuously linear. In this case, we should apply Ohm’s law in a piece-wise form, as indicated through (2.3).

$$\begin{cases} v(t) = R_1 i(t) & 0 \leq v(t) \leq V_1 \\ v(t) = R_2 i(t) & V_1 \leq v(t) \leq V_2 \end{cases} \quad (2.3)$$

For the case of an ideal inductance L in henries, an experiment can be conducted. From our background in a physics course on electricity and magnetism, a coil with N number of turns shows that the voltage and current $i(t)$ in amperes are related through flux linkages $\lambda(t)$ in Weber-turn. Flux linkages λ relate the magnetic flux ϕ (Weber) and the coil’s turns N as:

$$\lambda(t) = N\phi(t) = Li(t) \quad (2.4)$$

By Faraday’s law, the rate of change of flux linkages is the induced voltage $v(t)$ in volts at the terminals of the coil, as $\Delta t \rightarrow 0$:

$$v(t) \propto \frac{\Delta\lambda(t)}{\Delta t} \rightarrow \frac{Ldi(t)}{dt} \quad (2.5)$$

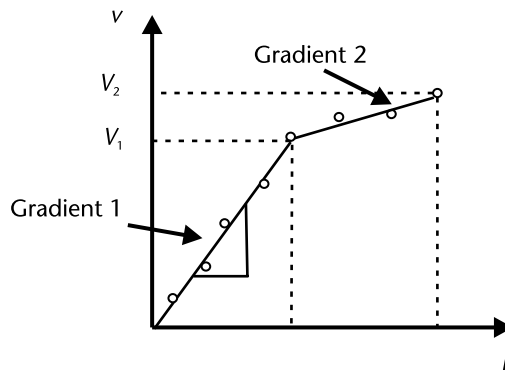


Figure 2.3 Voltage-current characteristics of a piece-wise linear resistor.

A discrete approximation for (2.5) is applied to the incremental form in (2.6). Using the trapezoidal rule of integration, from time t_k to t_{k+1} , as in (2.7) we have the discrete model (2.8).

$$v(t)\Delta t = L\Delta i(t) \tag{2.6}$$

$$\int_k^{k+1} v(\tau)d\tau = \int_k^{k+1} Ldi(\tau) \tag{2.7}$$

$$\left[v(t_{k+1}) + v(t_k) \right] \left(\frac{\Delta t}{2L} \right) = i(t_{k+1}) - i(t_k) \tag{2.8}$$

Ohm's law from (2.8) allows for inductance L to be connected from node k to node m and to have a circuit representation in Figure 2.4.

$$-\left(\frac{2L}{\Delta t} \right) i_{km}(t_{k+1}) + V_k(t_{k+1}) - V_m(t_{k+1}) = -\left(\frac{2L}{\Delta t} \right) i_{km}(t_k) - v(t_k) = -e_{km}(t_k) \tag{2.9}$$

V_k and V_m are nodal voltages, $2L/\Delta t$ is an *equivalent resistance* and e_{km} is an equivalent voltage source. The voltage source e_{km} is calculated using voltage and current values at the previous time t_k .

For a linear capacitor C in farads, the electric charge $q(t)$ coulombs is stored in a dielectric between parallel plates. The stored charge is proportional to the potential difference $v(t)$ in volts applied at capacitor's terminals. The electric current $i(t)$ in amperes that flows is the rate of change of the electric charge $dq(t)/dt$. We again use the trapezoidal rule of integration to the form (2.10). We identify Ohm's equation through (2.13) and its equivalent circuit in Figure 2.5.

$$i(t) = \frac{dq(t)}{dt} = \frac{Cdv_C(t)}{dt} \tag{2.10}$$

$$\int_k^{k+1} i(\tau)d\tau = \int_k^{k+1} Cdv_C(\tau) \tag{2.11}$$

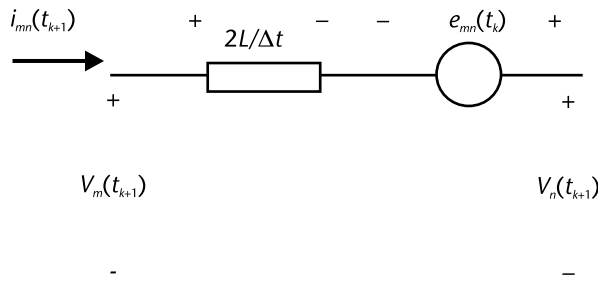


Figure 2.4 Circuit representation for a linear inductor.

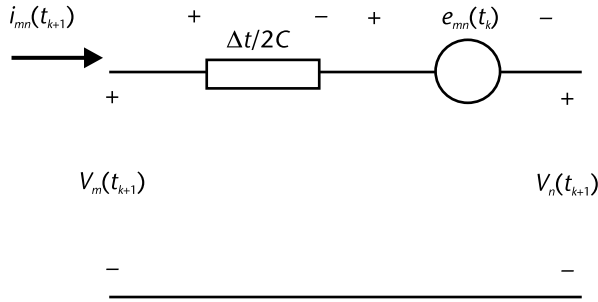


Figure 2.5 Voltage-current characteristics for a capacitor.

$$[i(t_{k+1}) + i(t_k)] \left(\frac{\Delta t}{2C} \right) = v_C(t_{k+1}) - v_C(t_k) \quad (2.12)$$

$$-i_{mn}(t_{k+1}) \left(\frac{\Delta t}{2C} \right) + V_m(t_{k+1}) - V_n(t_{k+1}) = i_{mn}(t_k) \left(\frac{\Delta t}{2C} \right) + v_C(t_k) = e_{mn}(t_k) \quad (2.13)$$

From previous discussions we conclude that R , L , and C are *proportionality constants* that relate fundamental circuit variables as voltage $v(t)$ at the element's terminals and current $i(t)$ flowing through the element.

2.3 Circuits with Lumped Elements

As a starting point to form a network, we interconnect lumped elements. Let us start with two terminal elements: in this case (Figure 2.6), terminals are electrical nodes. We write the basic variables of interest: voltage $v(t)$ at terminals and the current $i(t)$ that flows through the element. We use Ohm's law and, once we solve for voltages, other variables can be calculated as power flows and losses.

We define the voltage $v(t)$ at any time t across terminals k and m , in terms of voltages with respect to reference 0, and call the voltages V_{k0} and V_{m0} nodal voltages, at any time t .

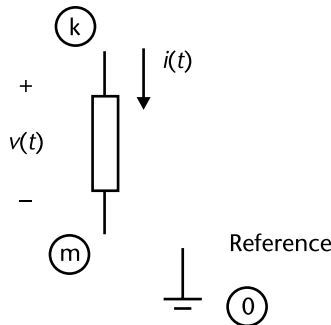


Figure 2.6 voltage-current variables in an electric element.

$$v(t) = V_{k0}(t) - V_{m0}(t) \tag{2.14}$$

Using the *load convention* presented in Chapter 1, the product $v(t)i(t)$ will be the instantaneous power $p(t)$ delivered to the load element.

2.4 Kirchoff's Current Law

In a practical arrangement of lumped elements at any node, the sum of electric currents through connected elements should be zero (for example, for a given node with currents as shown in Figure 2.7). Using a convention that current out of the node is positive, then at any time t , the current summation of $-i_1(t) + i_2(t) - i_3(t)$ should be zero.

We identify the nodal current balance equation as a *node equation*. Let us use a resistive circuit with various nodes, elements and current sources (Figure 2.8). Table 2.1 has the connectivity information for impedances. As we write the node current equation for every node, the information form will be Kirchoff's current

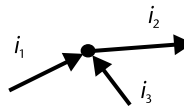


Figure 2.7 Electric currents into an electric node.

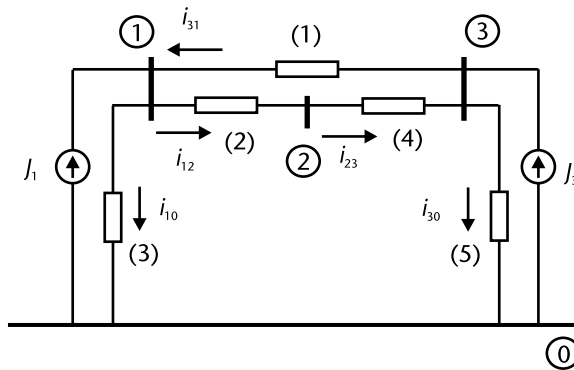


Figure 2.8 Circuit configuration and KCL.

Table 2.1 Connectivity Information, Circuit in Figure 2.8

Element	N_{out}	N_{in}	Impedance Value
1	3	1	z_{31}
2	1	2	z_{12}
3	1	0	z_{10}
4	2	3	z_{23}
5	3	0	z_{30}

law (KCL) in matrix form (2.15) for the circuit in Figure 2.7. The circuit in Figure 2.7 and (2.16) has a compact notation for KCL in matrix form.

$$\begin{bmatrix} -1 & +1 & +1 & 0 & 0 \\ 0 & -1 & 0 & +1 & 0 \\ +1 & 0 & 0 & -1 & +1 \\ 0 & 0 & -1 & 0 & -1 \end{bmatrix} \begin{bmatrix} i_{31} \\ i_{12} \\ i_{10} \\ i_{23} \\ i_{30} \end{bmatrix} = \begin{bmatrix} J_1 \\ 0 \\ J_3 \\ 0 \end{bmatrix} \quad (2.15)$$

$$A^t i = J \quad (2.16)$$

A^t Node to element connection matrix

i vector of currents through each element

J vector of nodal current sources, + into a node and – out from the node

For the set of nodal current equations it can be said that:

- Equation for node 0 is redundant.
- Equations express a linear relation for element's currents.
- KCL is valid for any linear, nonlinear, passive, or active time variant or invariant circuit.
- KCL expresses the conservation of electric charge at every node.
- KCL is not valid for nonlumped (distributed parameters) circuits.

We supplement the node equations with element's voltage drop between nodes k and m (see Figure 2.9 or the currents in Figure 2.10).

A general expression using impedance z_{km} from Ohm's law for element connected at node k and node m is:

$$-z_{km} i_{km} + V_k - V_m = -e_{km} \quad (2.17)$$

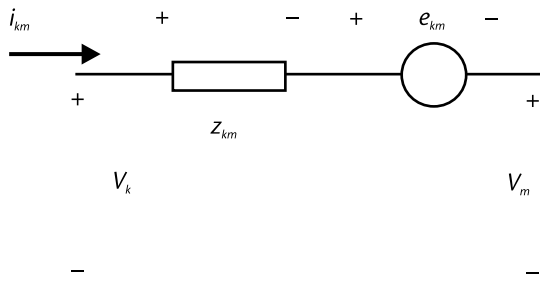


Figure 2.9 Impedance element connected between nodes k and m .

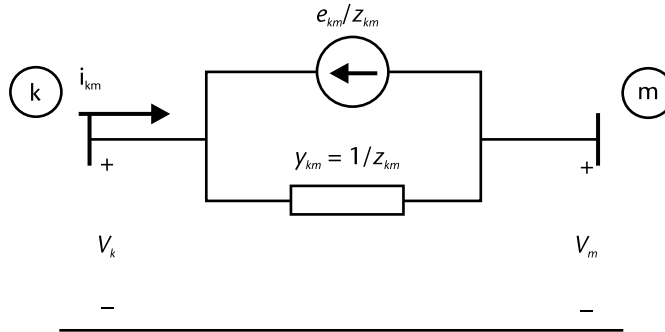


Figure 2.10 Nodal equivalent for element.

We can rewrite Ohm’s Law using the admittance form $y_{km} = 1/z_{km}$.

$$i_{km} = y_{km}(V_k - V_m) + y_{km}e_{km} \tag{2.18}$$

2.5 Nodal Formulation

The voltage drop v_{km} across each element can be written in terms of nodal voltages V_k and V_m ; voltage values are measured from a node with respect to a reference. For the circuit in Figure 2.8, we write (2.19) and (2.20) in a compact matrix notation.

$$\begin{bmatrix} -1 & 0 & +1 & 0 \\ +1 & -1 & 0 & 0 \\ +1 & 0 & 0 & -1 \\ 0 & +1 & -1 & 0 \\ 0 & 0 & +1 & -1 \end{bmatrix} \begin{bmatrix} V_1 \\ V_2 \\ V_3 \\ V_0 \end{bmatrix} = \begin{bmatrix} v_{31} \\ v_{12} \\ v_{10} \\ v_{23} \\ v_{30} \end{bmatrix} \tag{2.19}$$

$$v = AV_{bus} \tag{2.20}$$

- A Element to node connection matrix
- v vector of voltage through each element km
- V vector of nodal voltages, from node to reference

To calculate all nodal voltages as state variables, there is a solution procedure known as *nodal method*. First, we write all voltage-current relation (2.17) for each element km , then for each node, we write the current balance equation or Kirchhoff’s current law; the series voltage source e_{km} is zero if no source is present at element km . Later, this voltage source will be identified as a control, acting in series with the element km .

Example 2.1

For the circuit shown in Figure 2.8, values of impedances in ohms and current sources in amperes are given. Solve for nodal voltages V_{bus} and the set of currents i that flow in every element. Use (2.22) and identify matrices A and Y_{bus} . Solve for V_{bus} using (2.25) and calculate the voltage drop v across elements, determine current i that flows in each element.

Circuit data

Element	Nfrom	Nto	z Value	esource
1	3	1	0.0000+j 2.0000	0.0000+j 0.0000
2	1	2	0.0000+j 1.0000	0.0000+j 0.0000
3	1	0	0.0000+j 5.0000	0.0000+j 0.0000
4	2	3	0.0000+j 3.0000	0.0000+j 0.0000
5	3	0	0.0000+j 10.0000	0.0000+j 0.0000

Nodal conditions, Base Case

Node Num	Js	zshunt
1	20.0000+j 0.0000	
2	0.0000+j 0.0000	
3	10.0000+j 0.0000	
4	0.0000+j 0.0000	

A =

-1	0	1	0
1	-1	0	0
1	0	0	-1
0	1	-1	0
0	0	1	-1

Ybus =

0 - 1.7000i	0 + 1.0000i	0 + 0.5000i	0 + 0.2000i
0 + 1.0000i	0 - 1.3333i	0 + 0.3333i	0
0 + 0.5000i	0 + 0.3333i	0 - 0.9333i	0 + 0.1000i
0 + 0.2000i	0	0 + 0.1000i	0 - 0.3000i

Vbus =

1.0e+002 *

0.0000 + 1.0000i
0.0000 + 1.0000i
0.0000 + 1.0000i
0.0000 - 0.0000i

velem =

1.0e+002 *

0
0 + 0.0000i
0.0000 + 1.0000i
0 - 0.0000i
0.0000 + 1.0000i

ielem =

0
0.0000

$$\begin{array}{l} 20.0000 - 0.0000i \\ -0.0000 \\ 10.0000 - 0.0000i \end{array}$$

2.6 Kirchhoff Voltage Law (KVL) and the Mesh Method

A loop in a circuit is a closed electrical path that initiates and ends at the same node after traveling through various circuit elements. For a circuit with lumped elements, at any given time, t , the algebraic sum of voltage drop/rise on elements that are on a given loop is zero (KVL). An interesting and nontrivial problem is how to find the number of independent loops that exist in a given circuit with ℓ elements and n nodes.

ℓ elements
 n nodes (including reference)

In a network we need $(n - 1)$ elements to connect all nodes; these elements are usually called *branches*. The remaining network elements are *links*. For a circuit with n nodes and e elements: $b = n - 1$ branches and $l = \ell - b = \ell - (n - 1)$ links.

For an oriented graph, a closed trajectory or loop involves only branches and *one link* at a time. The associated link direction assigns direction to the *loop current*. For the circuit in Figure 2.11, we have:

Number of elements	$\ell = 5$
Nodes, including reference	$n = 4$
Branches	$b = n - 1 = 3$
Links	$l = \ell - b = 2$ two loops will be formed, as shown in Figure 2.11

The elements that are part of a given loop have either a voltage drop (loop current coincides with element's assumed direction) or a voltage rise (loop current opposes

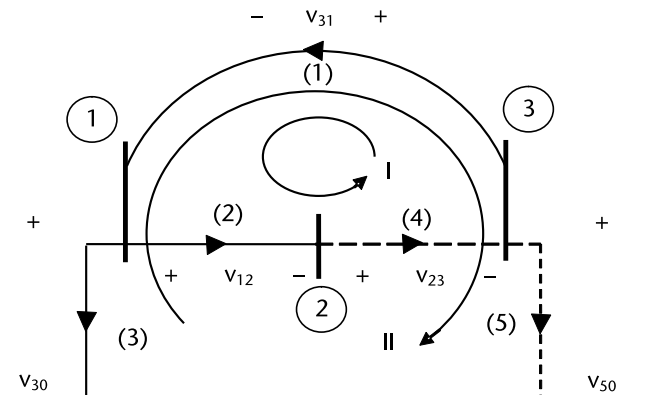


Figure 2.11 Graph of a circuit in terms of branches and links.

the assumed element's direction). By KVL the algebraic sum of voltage, drops will be zero within a loop. From Figure 2.11 in matrix form:

$$\begin{bmatrix} +1 & +1 & 0 & +1 & 0 \\ -1 & 0 & -1 & 0 & +1 \end{bmatrix} \begin{bmatrix} v_{31} \\ v_{12} \\ v_{10} \\ v_{23} \\ v_{30} \end{bmatrix} = \begin{bmatrix} 0 \\ 0 \end{bmatrix} \quad (2.27)$$

With C as a loop-element connection matrix:

$$C^t v = 0 \quad (2.28)$$

For each element km , we use (2.18) and write the current i_{km} in terms of the loop currents:

$$\begin{bmatrix} -y_{31} & & & & +1 & -1 \\ & -y_{12} & & & +1 & \\ & & -y_{10} & & & -1 \\ & & & -y_{23} & +1 & \\ & & & & -y_{30} & +1 \\ +1 & +1 & & +1 & & \\ -1 & & -1 & & +1 & \end{bmatrix} \begin{bmatrix} v_{31} \\ v_{12} \\ v_{10} \\ v_{23} \\ v_{30} \\ I_I \\ I_{II} \end{bmatrix} = \begin{bmatrix} -j_{31} \\ -j_{12} \\ -j_{10} \\ -j_{23} \\ -j_{30} \\ 0 \\ 0 \end{bmatrix} \quad (2.29)$$

$$\begin{bmatrix} -y & C \\ C^t & 0 \end{bmatrix} \begin{bmatrix} v \\ I_{\text{loop}} \end{bmatrix} = \begin{bmatrix} -j \\ 0 \end{bmatrix} \quad (2.30)$$

A solution to the unknown voltages v and loop currents I_{loop} is obtained by writing the first row in matrix (2.30) and then a substitution into the second row of the same matrix equation.

$$Z_{\text{loop}} I_{\text{loop}} = V_{\text{loop}} \quad (2.31)$$

Where: $Z_{\text{loop}} = C^t z C$, $z = y^{-1}$ and $V_{\text{loop}} = -C^t z j$

Solving (2.31) for I_{loop} as state variables in this formulation, assuming Z_{loop} and V_{loop} are known, we then calculate element's current i , and voltage v as follows:

$$i = C I_{\text{loop}} \quad (2.32)$$

$$v = z(i + j) \quad (2.33)$$

2.7 Linear Equations and Gaussian Elimination

A simple set of two linear equations and two unknowns gives useful forms. Solution to unknown values, here V_1 and V_2 , follow basic algebraic steps and with the proper interpretation, the properties of electric circuits emerge as a result.

$$\begin{aligned} Y_{11}V_1 + Y_{12}V_2 &= I_1 \\ Y_{21}V_1 + Y_{22}V_2 &= I_2 \end{aligned} \quad (2.34)$$

Assuming that coefficient $Y_{11} \neq 0$, algebraically V_1 is taken from the first equation in (2.34) as $V_1 = I_1/Y_{11} - Y_{12}V_2/Y_{11}$ and a substitution into the second equation in (2.34) gives:

$$\left[Y_{22} - \frac{Y_{21}Y_{12}}{Y_{11}} \right] V_2 = I_2 - \frac{Y_{21}I_1}{Y_{11}} \quad (2.35)$$

Writing the first row in (2.34) and (2.35), we find a triangular matrix:

$$\begin{bmatrix} Y_{11} & Y_{12} \\ 0 & Y_{22} - \frac{Y_{21}Y_{12}}{Y_{11}} \end{bmatrix} \begin{bmatrix} V_1 \\ V_2 \end{bmatrix} = \begin{bmatrix} I_1 \\ I_2 - \frac{Y_{21}I_1}{Y_{11}} \end{bmatrix} \quad (2.36)$$

Solution for V_2 is a one equation one unknown problem. With V_2 known a *back substitution*, allows V_1 to be determined.

$$V_2 = \left(Y_{22} - Y_{21}Y_{11}^{-1}Y_{12} \right)^{-1} \left(I_2 - Y_{21}Y_{11}^{-1}I_1 \right) \quad (2.37)$$

$$V_1 = Y_{11}^{-1} \left(I_1 - Y_{12}V_2 \right) \quad (2.38)$$

Gaussian elimination and *backward substitution* are the two steps of this process. From the circuit point of view, once we *eliminate* node 1; the numerical process gives a Norton's equivalent (see Figure 2.12). It is important to notice that the current source I_{Norton} depends on current injected into node 1, which is the node that was eliminated. From (2.36), the second row has the equivalent Norton's admittance and the Norton's source.

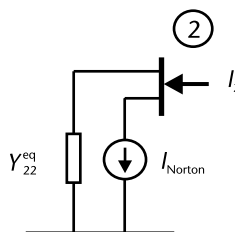


Figure 2.12 Norton equivalent after node elimination.

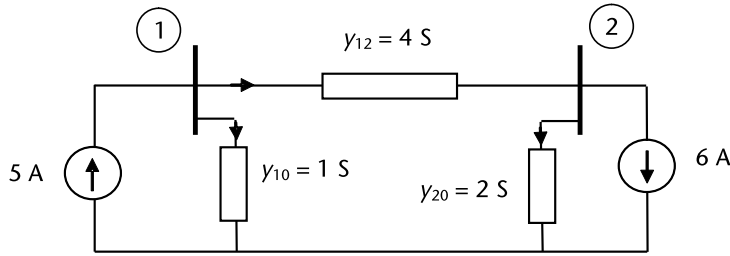


Figure 2.13 Circuit to illustrate node elimination procedure.

$$Y_{22}^{eq} = Y_{22} - Y_{21}Y_{11}^{-1}Y_{12} \quad I_{Norton} = -Y_{21}Y_{11}^{-1}I_1 \quad (2.39)$$

Example 2.2

For the small network and admittances (see Figure 2.13), calculate the equivalent circuit when node 1 is eliminated. Write the nodal matrix Y_{bus} and the element-node incidence matrix A . For a line element out of a node has a value +1, into a node value -1 as values in the A matrix.

$$\begin{bmatrix} +5 & -4 \\ -4 & +6 \end{bmatrix} \begin{bmatrix} V_1 \\ V_2 \end{bmatrix} = \begin{bmatrix} +5 \\ -6 \end{bmatrix} \quad A = \begin{bmatrix} +1 & -1 \\ +1 & 0 \\ 0 & +1 \end{bmatrix} \quad (2.40)$$

With *Gaussian elimination* on node 1 (see Figure 2.14):

$$\begin{bmatrix} +5 & -4 \\ 0 & +6 - \frac{16}{5} \end{bmatrix} \begin{bmatrix} V_1 \\ V_2 \end{bmatrix} = \begin{bmatrix} +5 \\ -6 - \frac{(-4)(5)}{5} \end{bmatrix} \quad (2.41)$$

From (2.41), V_2 is calculated as $V_2 = (-6 + 4)/(14/5) = -10/14$ volts, then with *back substitution* we determine the value of voltage $V_1 = 5^{-1}[5 - (-4)(-10/14)] = 6/14$ volts. Using (2.20) and (2.23), the voltage v across elements and current i flow are $v_{12} = 16/14$ V, $v_{10} = 6/14$ V, $v_{20} = -10/14$ V and $i_{12} = 64/14$ A, $i_{10} = 6/14$ A, $i_{20} = -20/14$ A (see Figure 2.15).

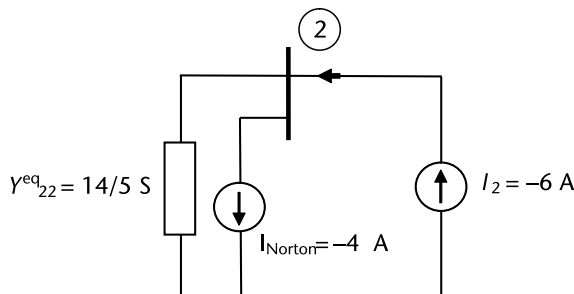


Figure 2.14 Circuit with node 1 eliminated, Norton's equivalent.

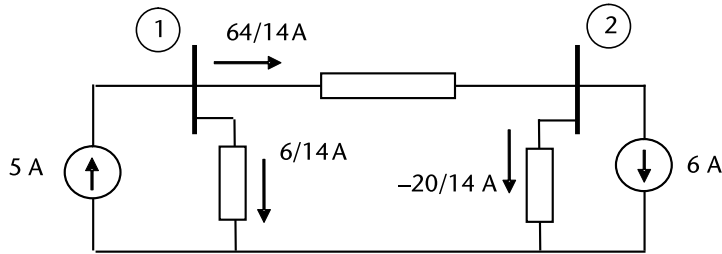


Figure 2.15 Circuit solution with current values.

2.7.1 Cramer's Rule

A procedure called Cramer's is frequently used when solving sets of linear equations. Cramer's rule uses determinants, which we can derive from the last step in the Gaussian elimination algorithm presented in the previous section. A useful circuit interpretation out of these algebraic steps is the Thévenin's equivalent, which requires that all nodes in a circuit be eliminated and that a new *mathematical circuit* be built. For this concept, we start with the nodal admittance matrix and we create the nodal impedance matrix, Z_{bus} , through Gaussian elimination. From expression (2.42):

$$V_2 = \frac{(I_2 - Y_{21}Y_{11}^{-1}I_1)}{(Y_{22} - Y_{21}Y_{11}^{-1}Y_{12})} \quad (2.42)$$

$$V_2 = \frac{\begin{vmatrix} Y_{11} & I_1 \\ Y_{21} & I_2 \end{vmatrix}}{\begin{vmatrix} Y_{11} & Y_{12} \\ Y_{21} & Y_{22} \end{vmatrix}} = \left(\frac{Y_{11}}{\Delta}\right)I_2 - \left(\frac{Y_{21}}{\Delta}\right)I_1$$

In (2.42), we identify the definition of Δ as the system's determinant. The factor Y_{11}/Δ is Thévenin's impedance *open circuit impedance*, as seen from node 2. The term $-(Y_{21}/\Delta)I_1$ is an equivalent voltage source called Thévenin's source; its value depends on I_1 . I_1 is the injected current at node 1 that we eliminated during the process. Equation (2.42) can be written as:

$$V_2 = Z_{\text{Th}}I_2 + E_{\text{Th}} \quad (2.43)$$

Using data from the last example, the values of determinant Δ , Z_{Th} and E_{Th} are shown. The Thévenin's equivalent circuit is presented in Figure 2.16, $\Delta = 14$, $Z_{\text{Th}} = 5/14 \Omega$, and $E_{\text{Th}} = 20/14 \text{ V}$.

2.7.2 Partial Inversion

From the Gaussian elimination process, a different interpretation for the algebraic steps can be done using (2.38) and (2.35). In matrix notation:

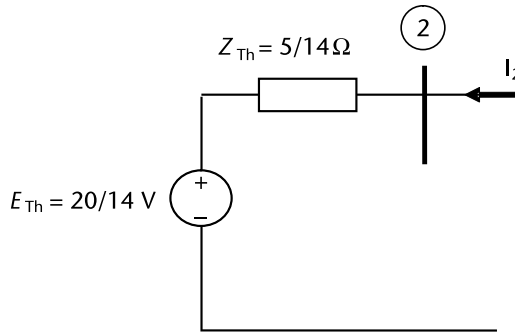


Figure 2.16 Thévenin's equivalent for circuit in Figure 2.15.

$$\begin{bmatrix} \frac{1}{Y_{11}} & \frac{-Y_{12}}{Y_{11}} \\ \frac{+Y_{21}}{Y_{11}} & Y_{22} - \left(\frac{Y_{21}Y_{12}}{Y_{11}}\right) \end{bmatrix} \begin{bmatrix} I_1 \\ V_2 \end{bmatrix} = \begin{bmatrix} V_1 \\ I_2 \end{bmatrix} \quad (2.44)$$

We observe that, with respect to the original problem, an *exchange* in variables takes place between I_1 and V_1 . The sign symmetry can be restored for the off-diagonal elements.

$$\begin{bmatrix} \frac{-1}{Y_{11}} & \frac{-Y_{12}}{Y_{11}} \\ \frac{-Y_{21}}{Y_{11}} & Y_{22} - \left(\frac{Y_{21}Y_{12}}{Y_{11}}\right) \end{bmatrix} \begin{bmatrix} -I_1 \\ V_2 \end{bmatrix} = \begin{bmatrix} V_1 \\ I_2 \end{bmatrix} \quad (2.45)$$

From (2.45) we write the *Partial inversion* rules for a square matrix (k is a *pivot* element that matches the row/column of variables to be exchanged by the process):

1. Pivot k is replaced by $-1/Y_{kk}$.
2. Elements in pivot row k , $m \neq k$ are replaced by $-Y_{km}/Y_{kk}$.
3. Elements in pivot column k , $m \neq k$ are replaced by $-Y_{mk}/Y_{kk}$.
4. Elements outside row and column pivot k will be: $Y_{mn} - Y_{mk}Y_{kn}/Y_{kk}$, $m \neq k$ and $n \neq k$.
5. When solving a set of linear equations the known value I_k is replaced by $-I_k$.

The partial inversion procedure just described is repeated as many times as pivots are required to exchange known values from the right- to the left-hand side of the matrix equation. This needed exchange identifies the pivots to be used. Once the exchange process is done, the solution is found by a matrix multiplication. For dominant matrices (large diagonal elements), it is a common procedure to take the diagonal values in the square matrix as pivots, given that we do not run into a numerical problem as a division by zero. If we use pivots one by one, using diagonal elements of a square matrix, applying the steps given for the *partial inversion*

we end up with the *negative* of the inverse matrix. At every elimination step, new calculated values replace the *old values*; and this procedure can be called *matrix inversion at the same place*.

2.7.3 Kron's Network Reduction

In the technical literature, we find Kron's reduction as a procedure to eliminate nodes. We find that Kron's reduction is a special case of the partial inversion process (discussed in previous sections). If I_1 is zero, the second row of (2.36) has an equivalent admittance as:

$$\left(Y_{22} - \frac{Y_{21}Y_{12}}{Y_{11}} \right) V_2 = Y_{22}^{\text{eq}} V_2 = I_2 \quad (2.46)$$

The equivalent admittance Y_{22}^{eq} is the result of eliminating node 1. We solve for V_2 and after that we can calculate V_1 .

$$V_1 = \left(\frac{-Y_{12}}{Y_{11}} \right) V_2 \quad (2.47)$$

2.8 Matrix Elements for Y_{BUS} and Z_{BUS}

Writing in full the Y_{bus} matrix, there is a useful interpretation for its elements [2, 3]. The same comment applies to the inverse Z_{bus} . To keep a simple explanation, let us consider the matrix for a three-node system.

$$\begin{bmatrix} Y_{11} & Y_{12} & Y_{13} \\ Y_{21} & Y_{22} & Y_{23} \\ Y_{31} & Y_{32} & Y_{33} \end{bmatrix} \begin{bmatrix} V_1 \\ V_2 \\ V_3 \end{bmatrix} = \begin{bmatrix} I_1 \\ I_2 \\ I_3 \end{bmatrix} \quad (2.48)$$

If we assume that node voltages V_2 and V_3 are zero, it means that we connect node 2 and 3 to reference (imagine this procedure is conducted with the use of ideal current meters in a lab environment). If, at the same time, we connect an ideal voltage source of one Volt between node 1 and reference, currents will flow into the circuit and meters will read the nodal currents in or out of the nodes. The described condition in the matrix model numerically gives the first column of Y_{bus} in terms of the ammeter readings.

$$\begin{bmatrix} Y_{11} & Y_{12} & Y_{13} \\ Y_{21} & Y_{22} & Y_{23} \\ Y_{31} & Y_{32} & Y_{33} \end{bmatrix} \begin{bmatrix} 1 \\ 0 \\ 0 \end{bmatrix} = \begin{bmatrix} I_1 \\ I_2 \\ I_3 \end{bmatrix} \quad \begin{matrix} Y_{11} = I_1 \\ Y_{21} = I_2 \\ Y_{31} = I_3 \end{matrix} \quad (2.49)$$

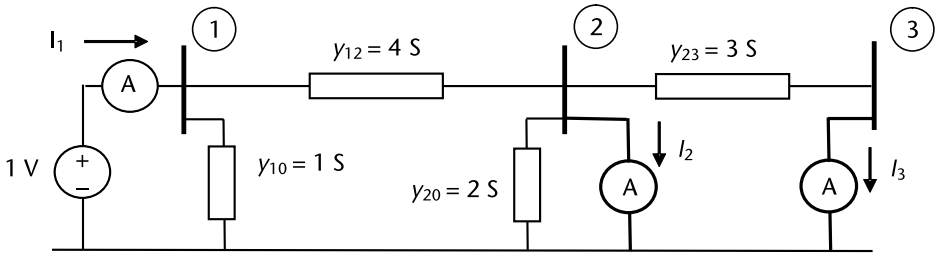


Figure 2.17 Circuit to illustrate interpretation of the Y_{bus} elements.

Results show that measuring will give a direct reading of values of the admittance matrix. This short circuit procedure assigns to the Y_{bus} matrix the name of short circuit matrix. In Figure 2.17, let us connect buses 2 and 3 to reference through ideal current meters and apply a voltage source of 1 V from node 1 to reference. The reading of nodal currents will give the value of elements in the *first column* of Y_{bus} . $Y_{11} = +5$, $Y_{21} = -4$, $Y_{31} = 0$ (see Figure 2.18).

To determine the elements of the *second column* of Y_{bus} , we follow a similar process. We connect the voltage source of 1 V to bus 2 and short node 1 and node 3 to reference by ammeters. Then $Y_{12} = -4$, $Y_{22} = +9$, $Y_{32} = -3$ (see Figure 2.19). We apply the same concept for the *third column* and find that $Y_{13} = 0$, $Y_{23} = -3$, $Y_{33} = +3$.

For the elements of Z_{bus} matrix, let us write the nodal impedance matrix as in (2.50). To obtain the first column, we set the node currents I_2 and I_3 to zero; this

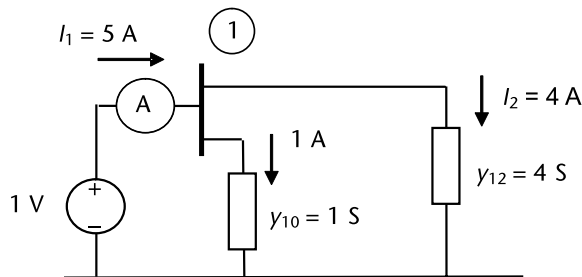


Figure 2.18 Reduced circuit for elements on the first column of Y_{bus} .

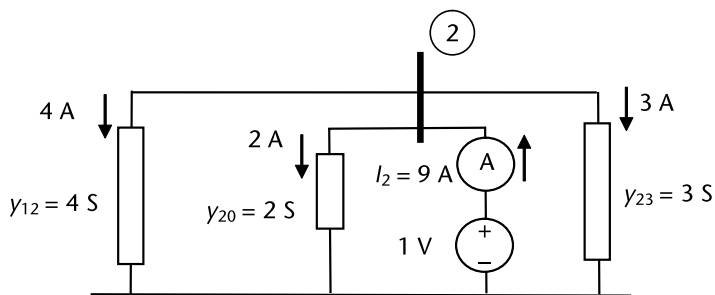


Figure 2.19 Reduced circuit for elements on second column of Y_{bus} .

means that nodes 2 and 3 will be in an *open circuit* condition. If unitary current is injected from reference into node one, voltages can be measured from each node to reference; voltage readings are directly the Z_{bus} elements, as shown in (2.51).

$$\begin{bmatrix} Z_{11} & Z_{12} & Z_{13} \\ Z_{21} & Z_{22} & Z_{23} \\ Z_{31} & Z_{32} & Z_{33} \end{bmatrix} \begin{bmatrix} I_1 \\ I_2 \\ I_3 \end{bmatrix} = \begin{bmatrix} V_1 \\ V_2 \\ V_3 \end{bmatrix} \quad (2.50)$$

$$\begin{bmatrix} Z_{11} & Z_{12} & Z_{13} \\ Z_{21} & Z_{22} & Z_{23} \\ Z_{31} & Z_{32} & Z_{33} \end{bmatrix} \begin{bmatrix} I_1 = 1 \\ 0 \\ 0 \end{bmatrix} = \begin{bmatrix} V_1 \\ V_2 \\ V_3 \end{bmatrix} \quad \begin{bmatrix} Z_{11} \\ Z_{21} \\ Z_{31} \end{bmatrix} = \begin{bmatrix} V_1 \\ V_2 \\ V_3 \end{bmatrix} \quad (2.51)$$

Currents flow and nodal voltages are measured from node to reference (see Figure 2.20(b)). Then, $Z_{11} = 3/7$, $Z_{21} = 2/7$, $Z_{31} = 2/7$. For the second column of Z_{bus} , one-ampere current goes into bus 2; buses 1 and 3 are open, $Z_{12} = 4/14$, $Z_{22} = 5/14$, $Z_{32} = 5/14$ (see Figure 2.21).

For the third column of Z_{bus} (see Figure 2.22); current of one A is injected to bus 3; buses 1 and 2 are “open,” $Z_{13} = 4/14$, $Z_{23} = 5/14$, $Z_{33} = 29/42$. The complete Z_{bus} matrix or *open circuit matrix* is in (2.52).

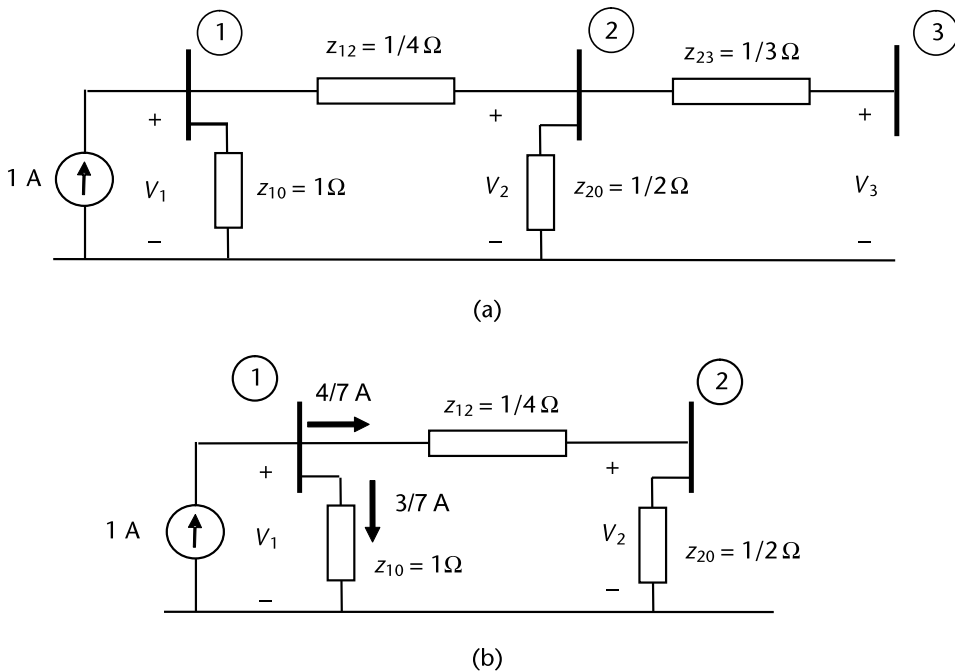


Figure 2.20 Circuit to obtain Z_{bus} elements, first column.

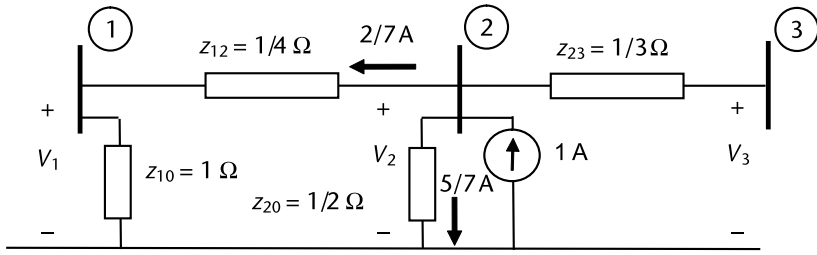


Figure 2.21 Reduced circuit to obtain elements on second column of Z_{bus} .

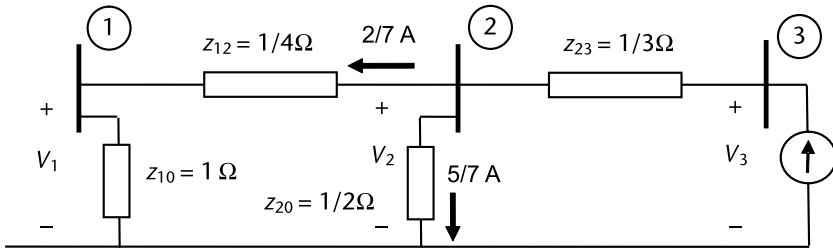


Figure 2.22 Reduced circuit to obtain elements in the third column of Z_{bus} .

$$Z_{bus} = \begin{bmatrix} 6 & 4 & 4 \\ \frac{14}{14} & \frac{4}{14} & \frac{4}{14} \\ 4 & 5 & 5 \\ \frac{14}{14} & \frac{4}{14} & \frac{5}{14} \\ 4 & 5 & \frac{29}{14} \\ \frac{14}{14} & \frac{4}{14} & \frac{5}{14} \end{bmatrix} \Omega \tag{2.52}$$

2.9 Norton's and Thévenin's Equivalents

Important circuit analysis results are related to the Gaussian elimination, these are the Norton's and Thévenin's equivalents. Let us start from (2.37) and explain Norton's equivalent (see Figure 2.23):

$$Y_{22}^{eq} V_2 = I_2 + I_{Norton} \tag{2.53}$$

Where:

$$Y_{22}^{eq} = Y_{22} - Y_{21} Y_{11}^{-1} Y_{12} \tag{2.54}$$

$$I_{Norton} = -Y_{21} Y_{11}^{-1} I_1 \tag{2.55}$$

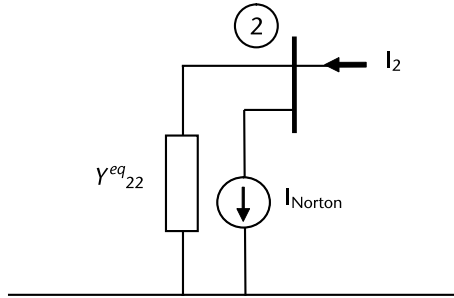


Figure 2.23 Norton's equivalent after node one elimination.

The I_{Norton} equivalent current source will have a value that depends on the injected current by sources that at the eliminated nodes; in our particular case node 1.

One-way to explain Thévenin's equivalent is through the Cramer's rule concept (2.42) and (2.43). We assume that the bus impedance matrix, Z_{bus} , describes the passive network. Let us write the equation for voltage V_2 , and identify Thévenin's impedance and the equivalent voltage source E_{Th} . The equivalent voltage source is in terms of Z_{bus} values and source currents injected at the eliminated node; in our discussion this was node one.

$$\begin{bmatrix} Z_{11} & Z_{12} \\ Z_{21} & Z_{22} \end{bmatrix} \begin{bmatrix} I_1 \\ I_2 \end{bmatrix} = \begin{bmatrix} V_1 \\ V_2 \end{bmatrix} \quad (2.56)$$

$$V_2 = Z_{22}I_2 + Z_{21}I_1 = Z_{22}I_2 + E_{\text{Th}} \quad (2.57)$$

Where $Z_{\text{Th}} = Z_{22}$ and $E_{\text{Th}} = Z_{21}I_1$.

Thévenin's source E_{Th} has a value that is the result of injected current into node 1 and the transfer impedance Z_{21} . If the nodal current into node 1 happens to be zero, then the Thévenin's equivalent voltage source will have a zero value.

2.10 Large Scale Network Equivalents

We will find general and useful results if—instead of writing equations for a two-node network, which helps to discuss basic ideas—we now think about two electric areas: A and B , each with various nodes. For this discussion, we start with the bus admittance matrix and apply Gaussian elimination or partial inversion one step at a time. In this way, the original Y_{bus} matrix is transformed. In the case that all nodes in an electric area A are eliminated, then a network equivalent is constructed for area B by (2.59).

$$\begin{bmatrix} Y_{AA} & Y_{AB} \\ Y_{BA} & Y_{BB} \end{bmatrix} \begin{bmatrix} V_A \\ V_B \end{bmatrix} = \begin{bmatrix} I_A \\ I_B \end{bmatrix} \quad (2.58)$$

$$\begin{bmatrix} Y_{AA} & Y_{AB} \\ 0 & Y_{BB} - Y_{BA}Y_{AA}^{-1}Y_{AB} \end{bmatrix} \begin{bmatrix} V_A \\ V_B \end{bmatrix} = \begin{bmatrix} I_A \\ I_B - Y_{BA}Y_{AA}^{-1}I_A \end{bmatrix} \quad (2.59)$$

The Norton's equivalent for area B can be identified writing the second row of matrix (2.58).

$$(Y_{BB} - Y_{BA}Y_{AA}^{-1}Y_{AB})V_B = I_B - Y_{BA}Y_{AA}^{-1}I_A \quad (2.60)$$

$$Y_{BB}^{eq}V_B = I_B + I_{Norton} \quad (2.61)$$

$$Y_{BB}^{eq} = Y_{BB} - Y_{BA}Y_{AA}^{-1}Y_{AB} \quad (2.62)$$

$$I_{Norton} = -Y_{BA}Y_{AA}^{-1}I_A \quad (2.63)$$

We can apply partial inversion to exchange values from the right to the left hand side, known currents I_A with unknowns V_A in (2.58). When all required exchanges are done with a matrix multiplication, we find the unknown voltages V_A and currents I_B . The product Y_{AB} times V_B in (2.65) is an equivalent injection of nodal currents into nodes in Area A , as a result of voltage sources in area B .

$$\begin{bmatrix} -Y_{AA}^{-1} & -Y_{AA}^{-1}Y_{AB} \\ -Y_{BA}Y_{AA}^{-1} & Y_{BB} - Y_{BA}Y_{AA}^{-1}Y_{AB} \end{bmatrix} \begin{bmatrix} -I_A \\ V_B \end{bmatrix} = \begin{bmatrix} V_A \\ I_B \end{bmatrix} \quad (2.64)$$

$$V_A = +Y_{AA}^{-1}(I_A - Y_{AB}V_B) \quad (2.65)$$

2.10.1 Partitioned Networks and Equivalents

The nodal impedance Z_{bus} is a network model that we can use as a network analysis tool, such as the one required to solve large networks through the concept of a partitioned network. Assume that in Figure 2.24 we connect a line from node 3 to

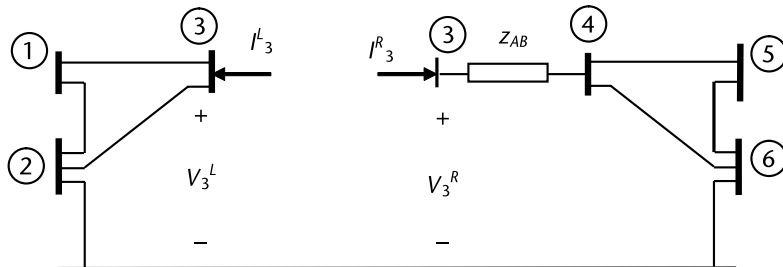


Figure 2.24 Partitioned network configuration.

node 4 through impedance z_{AB} . The line will connect the left side network to the network on the right. The nodal impedance model Z_{bus} for the left-side network, *not including* the line impedance z_{AB} is:

$$\begin{bmatrix} Z_{11} & Z_{12} & Z_{13}^L \\ Z_{21} & Z_{22} & Z_{23}^L \\ Z_{31}^L & Z_{32}^L & Z_{33}^L \end{bmatrix} \begin{bmatrix} I_1 \\ I_2 \\ I_3^L \end{bmatrix} = \begin{bmatrix} V_1 \\ V_2 \\ V_3^L \end{bmatrix} \quad (2.66)$$

Thévenin's equivalent at node 3 for the left side network is:

$$V_3^L = Z_{31}^L I_1 + Z_{32}^L I_2 + Z_{33}^L I_3^L = Z_{33}^L I_3^L + E_{Th,3}^L \quad (2.67)$$

Where $E_{Th,3}$ at the left is the product of nodal currents at node 1 and 2 with impedance values from the Z_{bus} matrix.

The network at the right includes the impedance z_{AB} . Thévenin's equivalent at node 3 is:

$$\begin{bmatrix} Z_{33}^R & Z_{34}^R & Z_{35}^R & Z_{36}^R \\ Z_{43}^R & Z_{44}^R & Z_{45}^R & Z_{46}^R \\ Z_{53}^R & Z_{54}^R & Z_{55}^R & Z_{56}^R \\ Z_{63}^R & Z_{64}^R & Z_{65}^R & Z_{66}^R \end{bmatrix} \begin{bmatrix} I_3^R \\ I_4 \\ I_5 \\ I_6 \end{bmatrix} = \begin{bmatrix} V_3^R \\ V_2 \\ V_5 \\ V_6 \end{bmatrix} \quad (2.68)$$

$$V_3^R = Z_{33}^R I_3^R + Z_{34}^R I_4 + Z_{35}^R I_5 + Z_{36}^R I_6 = Z_{33}^R I_3^R + E_{Th,3}^R \quad (2.69)$$

Where $E_{th,3}$ at the right is the product of nodal currents at nodes 4, 5, and 6 with impedance values from the Z_{bus} matrix.

At a steady state, generation should match load and losses. We calculate voltages for both the left- hand side and the right side.

$$V_0^L = \begin{bmatrix} V_1^L \\ V_2^L \\ V_3^L \end{bmatrix}^0 \quad \text{and} \quad V_0^R = \begin{bmatrix} V_3^R \\ V_4^R \\ V_5^R \\ V_6^R \end{bmatrix}^0 \quad (2.70)$$

When circuits connect at bus 3, the electric boundary conditions (2.71) and (2.72) must be satisfied (see Figure 2.25). We impose the boundary conditions on Thévenin's equations (2.67) and (2.69), we solve for nodal current I_3^R into the right side circuit.

$$V_3^R = V_3^L \quad (2.71)$$

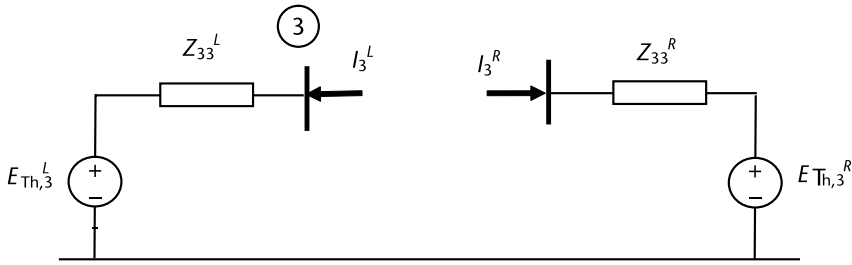


Figure 2.25 Network equivalents from node 3, left and right networks.

$$I_3^R = -I_3^L \tag{2.72}$$

$$V_3^L = Z_{33}^R I_3^R + E_{Th,3}^R = Z_{33}^L I_3^L + E_{Th,3}^L \tag{2.73}$$

$$I_3^R = (Z_{33}^R + Z_{33}^L)^{-1} (E_{Th,3}^L - E_{Th,3}^R) \tag{2.74}$$

As current I_3^R flows into the right-hand side network, nodal voltages change (see Figure 2.26). With a set of voltage corrections are to be added to previous voltage values, we find the new voltage value when the two networks are connected (2.76).

$$\begin{bmatrix} \Delta V_3 \\ \Delta V_4 \\ \Delta V_5 \\ \Delta V_6 \end{bmatrix}^R = \begin{bmatrix} Z_{33}^R & Z_{34}^R & Z_{35}^R & Z_{36}^R \\ Z_{43}^R & Z_{44}^R & Z_{45}^R & Z_{46}^R \\ Z_{53}^R & Z_{54}^R & Z_{55}^R & Z_{56}^R \\ Z_{63}^R & Z_{64}^R & Z_{65}^R & Z_{66}^R \end{bmatrix} \begin{bmatrix} I_3^R \\ 0 \\ 0 \\ 0 \end{bmatrix} = \begin{bmatrix} Z_{33}^R \\ Z_{43}^R \\ Z_{53}^R \\ Z_{63}^R \end{bmatrix} I_3^R \tag{2.75}$$

$$\begin{bmatrix} V_3^R \\ V_4^R \\ V_5^R \\ V_6^R \end{bmatrix}^{\text{New}} = \begin{bmatrix} V_3^R \\ V_4^R \\ V_5^R \\ V_6^R \end{bmatrix}^0 + \begin{bmatrix} \Delta V_3 \\ \Delta V_4 \\ \Delta V_5 \\ \Delta V_6 \end{bmatrix}^R = \begin{bmatrix} V_3^R \\ V_4^R \\ V_5^R \\ V_6^R \end{bmatrix}^0 + \begin{bmatrix} Z_{33}^R \\ Z_{43}^R \\ Z_{53}^R \\ Z_{63}^R \end{bmatrix} I_3^R \tag{2.76}$$

The left-hand side network also experiences voltage changes, current $I_3^L = -I_3^R$ is applied. For the calculation, the information that we need is a column of the left-hand side Z_{bus} matrix.

$$\begin{bmatrix} \Delta V_1 \\ \Delta V_2 \\ \Delta V_3 \end{bmatrix}^L = \begin{bmatrix} Z_{11}^L & Z_{12}^L & Z_{13}^L \\ Z_{21}^L & Z_{22}^L & Z_{23}^L \\ Z_{31}^L & Z_{32}^L & Z_{33}^L \end{bmatrix} \begin{bmatrix} 0 \\ 0 \\ -I_3^R \end{bmatrix} = - \begin{bmatrix} Z_{13}^L \\ Z_{23}^L \\ Z_{33}^L \end{bmatrix} I_3^R \tag{2.77}$$

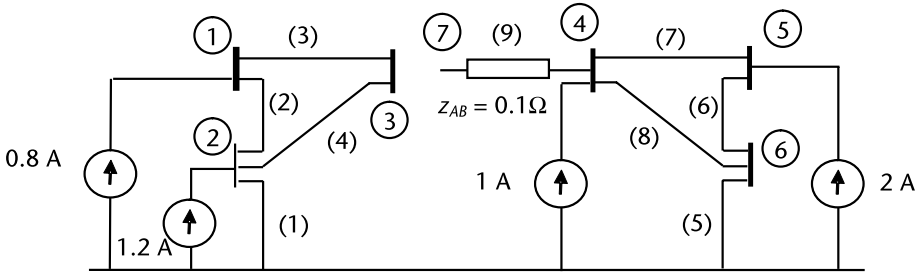


Figure 2.26 Network equivalents form node 3, left side and right side networks.

$$\begin{bmatrix} V_1^L \\ V_2^L \\ V_3^L \end{bmatrix}^{\text{New}} = \begin{bmatrix} V_1^L \\ V_2^L \\ V_3^L \end{bmatrix}^0 + \begin{bmatrix} \Delta V_1 \\ \Delta V_2 \\ \Delta V_3 \end{bmatrix}^L = \begin{bmatrix} V_1^L \\ V_2^L \\ V_3^L \end{bmatrix}^0 - \begin{bmatrix} Z_{13}^L \\ Z_{23}^L \\ Z_{33}^L \end{bmatrix} I_3^R \quad (2.78)$$

Example 2.3

–Note that Node 7 will coalesce to node 3 with the connected network.

$$\begin{aligned}
 Y_{\text{left}} &= \begin{bmatrix} 20. & - 10. & - 10. \\ - 10. & 17. & - 5. \\ - 10. & - 5. & 15. \end{bmatrix} \\
 Z_{\text{left}} &= \begin{bmatrix} 0.575 & 0.5 & 0.55 \\ 0.5 & 0.5 & 0.5 \\ 0.55 & 0.5 & 0.6 \end{bmatrix} \\
 Y_{\text{right}} &= \begin{bmatrix} 22.5 & - 10. & & - 2.5 & - 10. \end{bmatrix}
 \end{aligned}$$

Table 2.2 Connectivity Resistance Elements (Figure 2.26)

Element	Node from	Node to	Value (Ω)
(1)	2	0	0.5
(2)	2	1	0.1
(3)	1	3	0.1
(4)	2	3	0.2
(5)	6	0	0.8
(6)	6	5	0.3
(7)	4	5	0.1
(8)	6	4	0.4
(9)	4	7	0.1

```

- 10.      13.333333  - 3.3333333  0.
- 2.5     - 3.3333333  7.0833333  0.
- 10.      0.          0.          10.
Zright =
  1.      0.95      0.8      1.
  0.95    0.9875    0.8      0.95
  0.8     0.8       0.8      0.8
  1.      0.95      0.8      1.1
V0Left =
  1.06
  1.
  1.04
V0right =
  2.9
  2.925
  2.4
  2.9
Iright = - 1.0941176
DeltaV0Left =
  0.6017647
  0.5470588
  0.6564706

DeltaV0right =
- 1.0941176
- 1.0394118
- 0.8752941
- 1.2035294
VnLeft =
  1.6617647
  1.5470588
  1.6964706
Vnright =
  1.8058824
  1.8855882
  1.5247059
  1.6964706

```

Let us solve the nonseparated network to check results. The nodal admittance matrix Y_{bus} , the impedance matrix Z_{bus} and nodal voltages are values for the completely connected system.

```

Ybus =
  20.  - 10.  - 10.   0.   0.   0.
- 10.   17.  - 5.   0.   0.   0.
- 10.  - 5.   25.  - 10.  0.   0.
  0.   0.  - 10.  22.5 - 10.  - 2.5
  0.   0.   0.  - 10.  13.333333 - 3.3333333
  0.   0.   0.  - 2.5  - 3.3333333  7.0833333

```

$$\begin{aligned}
 Z_{bus} &= \\
 0.3970588 & 0.3382353 & 0.3558824 & 0.3235294 & 0.3073529 & 0.2588235 \\
 0.3382353 & 0.3529412 & 0.3235294 & 0.2941176 & 0.2794118 & 0.2352941 \\
 0.3558824 & 0.3235294 & 0.3882353 & 0.3529412 & 0.3352941 & 0.2823529 \\
 0.3235294 & 0.2941176 & 0.3529412 & 0.4117647 & 0.3911765 & 0.3294118 \\
 0.3073529 & 0.2794118 & 0.3352941 & 0.3911765 & 0.4566176 & 0.3529412 \\
 0.2588235 & 0.2352941 & 0.2823529 & 0.3294118 & 0.3529412 & 0.4235294
 \end{aligned}$$

$$\begin{aligned}
 V_{bus} &= \\
 1.6617647 \\
 1.5470588 \\
 1.6964706 \\
 1.8058824 \\
 1.8855882 \\
 1.5247059
 \end{aligned}$$

2.11 Diakoptical Approach

For a general network, let us start the discussion with a base case and then include a modified solution when changes are made through network elements. Changes modify nodal voltages and currents for the base case as shown by (2.82).

$$Y_{bus} V_{bus}^o = I_{bus}^o \quad (2.79)$$

$$Y_{bus} V_{bus}^n = I_{bus}^o - \Delta I \quad (2.80)$$

$$\Delta I = A^t [\Delta Y] A V_{bus}^n \quad (2.81)$$

$$(Y_{bus} + A^t [\Delta Y] A) V_{bus}^n = I_{bus}^o \quad (2.82)$$

The last expression is useful to calculate the new bus voltages V_{bus} ; at this step, we find it useful to introduce the *partial inversion lemma*. The partial inversion process can explain this result, as shown in the Section 2.12. Solution to (2.82) is written as (2.83).

$$V_{bus}^n = \left[Y_{bus}^{-1} - Y_{bus}^{-1} A^t \left([\Delta Y]^{-1} + A^t Y_{bus}^{-1} A \right)^{-1} A Y_{bus}^{-1} \right] I_{bus}^o \quad (2.83)$$

$$V_{bus}^n = V_{bus} - Z_{bus} A^t \Delta Y (U + A^t Z_{bus} A \Delta Y) A V_{bus} \quad (2.84)$$

Where $Z_{bus} = Y_{bus}^{-1}$ and U is a unitary matrix.

Part of (2.80) is a compensating current ΔI , which contains the effect of network changes. To identify the compensating current, starting with (2.84) and $V_{bus} = V_{bus}^o$, then ΔI is:

$$V_{bus}^n = V_{bus}^0 - Z_{bus} A^t \Delta Y (U + A Z_{bus} A^t \Delta Y)^{-1} A V_{bus}^0 \tag{2.85}$$

$$\Delta I = A^t \Delta Y (U + A Z_{bus} A^t \Delta Y)^{-1} A_{bus}^0 \tag{2.86}$$

Example 2.4

Let us consider, for illustrative purposes, a two-phase network with nodes I, II (see Figure 2.27). The change will be to include a transmission element with impedance value Z_{TL} between nodes I, II.

The condition before we include the Z_{TL} element, with nodal currents going into node I and II; phases a, b respectively, the Y_{bus} matrix for the network is calculated. Current values are in amperes, admittances in siemens, and impedances in ohms.

$$I^o = \begin{bmatrix} +1 \\ +1 \\ +2 \\ +2 \end{bmatrix} \quad Y_{TL} = Z_{TL}^{-1} = \begin{bmatrix} +2 & -1 \\ -1 & +2 \end{bmatrix} \tag{2.87}$$

- Base case (Z_{TL} not included)

$$V_{bus}^o = Y_{bus}^{-1} I_{bus}^o = Z_{bus} I_{bus}^o$$

$$V_{bus}^o = \begin{bmatrix} +2 & -1 & 0 & 0 \\ -1 & +2 & 0 & 0 \\ 0 & 0 & +2 & -1 \\ 0 & 0 & -1 & +2 \end{bmatrix}^{-1} \begin{bmatrix} +1 \\ +1 \\ +2 \\ +2 \end{bmatrix} = \begin{bmatrix} 2/3 & 1/3 & 0 & 0 \\ 1/3 & 2/3 & 0 & 0 \\ 0 & 0 & 2/3 & 1/3 \\ 0 & 0 & 1/3 & 2/3 \end{bmatrix} \begin{bmatrix} +1 \\ +1 \\ +2 \\ +2 \end{bmatrix} = \begin{bmatrix} +1 \\ +1 \\ +2 \\ +2 \end{bmatrix} \tag{2.88}$$

- When Z_{TL} is connected between node I and II we use (2.85) with A and ΔY as:

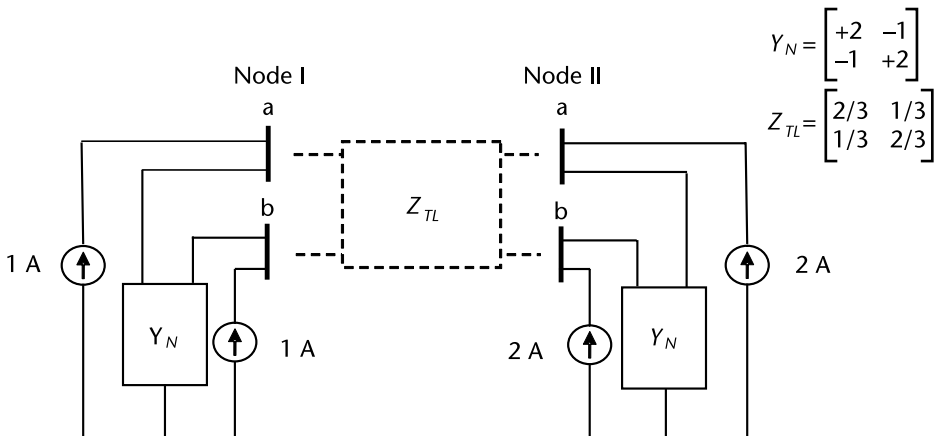


Figure 2.27 Piecewise networks.

$$A = \begin{bmatrix} 1 & 0 & -1 & 0 \\ 0 & 1 & 0 & -1 \end{bmatrix} \quad A^t = \begin{bmatrix} +1 & 0 \\ 0 & +1 \\ -1 & 0 \\ 0 & -1 \end{bmatrix} \quad \Delta Y = \begin{bmatrix} +2 & -1 \\ -1 & +2 \end{bmatrix} \quad (2.89)$$

$$\begin{aligned} Z_{\text{bus}} \Delta I &= Z_{\text{bus}} A^t \Delta Y (U + A Z_{\text{bus}} A^t \Delta Y)^{-1} A V_{\text{bus}}^o \\ &= \begin{bmatrix} 1/3 & 0 \\ 0 & 1/3 \\ -1/3 & 0 \\ 0 & -1/3 \end{bmatrix} \begin{bmatrix} 1 & 0 & -1 & 0 \\ 0 & 1 & 0 & -1 \end{bmatrix} \begin{bmatrix} 1 \\ 1 \\ 2 \\ 2 \end{bmatrix} = \begin{bmatrix} -1/3 \\ -1/3 \\ +1/3 \\ +1/3 \end{bmatrix} \end{aligned} \quad (2.90)$$

The updated voltage values are:

$$\begin{aligned} V_{\text{bus}}^n &= V_{\text{bus}}^o - Z_{\text{bus}} A^t \Delta Y (U + A Z_{\text{bus}} A^t \Delta Y)^{-1} A V_{\text{bus}}^o \\ V_{\text{bus}}^n &= \begin{bmatrix} 1 \\ 1 \\ 2 \\ 2 \end{bmatrix} - \begin{bmatrix} -1/3 \\ -1/3 \\ +1/3 \\ +1/3 \end{bmatrix} = \begin{bmatrix} 4/3 \\ 4/3 \\ 5/3 \\ 5/3 \end{bmatrix} \text{ Volts} \end{aligned} \quad (2.91)$$

- We check the solution given by the partitioned approach, with all elements connected into the $Y_{\text{bus},n}$.

$$V_{\text{bus}}^n = Y_{\text{bus}}^{-1} I_{\text{bus}}^o = \begin{bmatrix} +4 & -2 & -2 & +1 \\ -2 & +4 & +1 & -2 \\ -2 & +1 & +4 & -2 \\ +1 & -2 & -2 & +4 \end{bmatrix}^{-1} \begin{bmatrix} 1 \\ 1 \\ 2 \\ 2 \end{bmatrix} = \begin{bmatrix} 1.3333 \\ 1.3333 \\ 1.6667 \\ 1.6667 \end{bmatrix} \text{ Volts} \quad (2.92)$$

2.12 Matrix Inversion Lemma

The *matrix inversion lemma* will be discussed using a 2×2 impedance matrix, assuming that Z_{11}^{-1} and Z_{22}^{-1} exist.

$$\begin{bmatrix} Z_{11} & Z_{12} \\ Z_{21} & Z_{22} \end{bmatrix} \quad (2.93)$$

With partial inversion using Z_{22} as pivot on the original matrix:

$$\begin{bmatrix} Z_{11} - Z_{12} Z_{22}^{-1} Z_{21} & -Z_{12} Z_{22}^{-1} \\ -Z_{22}^{-1} Z_{21} & -Z_{22}^{-1} \end{bmatrix} \quad (2.94)$$

We apply the partial inversion step again to result (2.94); now we use the element located at 11 as the pivot. The result is the negative of the inverse.

$$\begin{bmatrix} -(Z_{11} - Z_{12}Z_{22}^{-1}Z_{21})^{-1} & +(Z_{11} - Z_{12}Z_{22}^{-1}Z_{21})^{-1}Z_{12}Z_{22}^{-1} \\ +Z_{22}^{-1}Z_{21}(Z_{11} - Z_{12}Z_{22}^{-1}Z_{21})^{-1} & -Z_{22}^{-1} - Z_{22}^{-1}Z_{21}(Z_{11} - Z_{12}Z_{22}^{-1}Z_{21})^{-1}Z_{12}Z_{22}^{-1} \end{bmatrix} \quad (2.95)$$

If we follow a different order, first pivot (1,1), then (2,2) to conduct the partial inversions, and we compare (2.95) to (2.97) for the algebraic result known as the inversion matrix lemma.

$$\begin{bmatrix} -Z_{11}^{-1} & -Z_{11}^{-1}Z_{12} \\ -Z_{21}Z_{11}^{-1} & Z_{22} - Z_{21}Z_{11}^{-1}Z_{12} \end{bmatrix} \quad (2.96)$$

$$\begin{bmatrix} -Z_{11}^{-1} - Z_{11}^{-1}Z_{12}(Z_{22} - Z_{21}Z_{11}^{-1}Z_{12})^{-1}Z_{21}Z_{11}^{-1} & +Z_{11}^{-1}Z_{12}(Z_{22} - Z_{21}Z_{11}^{-1}Z_{12})^{-1} \\ (Z_{22} - Z_{21}Z_{11}^{-1}Z_{12})^{-1}Z_{21}Z_{11}^{-1} & -(Z_{22} - Z_{21}Z_{11}^{-1}Z_{12})^{-1} \end{bmatrix} \quad (2.97)$$

$$(Z_{22} - Z_{21}Z_{11}^{-1}Z_{12})^{-1} = Z_{22}^{-1} + Z_{22}^{-1}Z_{21}(Z_{11} - Z_{12}Z_{22}^{-1}Z_{21})^{-1}Z_{12}Z_{22}^{-1} \quad (2.98)$$

The result has various important applications in network analysis as well as in the signal processing area. For network analysis, in-state estimation and recursive forecasting and control procedures.

References

- [1] Stagg, G., and A. El-Abiad, *Computer Methods in Power System Analysis*, New York: McGraw-Hill Inc., 1968.
- [2] Brown, H. E., *Solution of Large Networks by Matrix Methods*, New York: John Wiley & Sons, 1975.
- [3] Bruce Shipley, R., *Introduction to Matrices and Power Systems*, New York: John Wiley & Sons, 1976.

Power Transformer Modeling

3.1 Introduction

To conduct studies for electrical power systems aiming at planning their expansion or for control and operation, detailed models for the main system's components must be used. Among the important elements are transformers, transmission lines, generators, and electrical loads. To establish models, we start with physical principles, material characteristics, intended use of the device and analytic tools as a solution to a system of equations, and symmetrical components or other mathematical transformations that allow us to establish a manageable problem; variables of interest are nodal voltages, currents through elements, and real and reactive power as well as losses.

A model for each element is derived based on physical laws in order to express the induced voltage, voltage drop, and current flows. The main focus of this chapter is to characterize a single-phase transformer and then to extend it to three-phase bank arrangements. We also review autotransformer voltage current relations, as well as three-phase transformers. Mathematical transformations are used to take the “abc” phase representation into a modal domain that might give computational advantages to solve the problem (i.e., symmetrical components). Once a solution in the modal domain is attained, an inverse transformation can return the solution to the “abc” quantities.

3.2 Equation Decoupling and Symmetrical Components

In many instances, a system of equations can be put into a simpler form. This is accomplished by *decoupling* the variables involved. The concept has many interesting applications in steady state analysis and in the dynamic mode for time changing systems. To present the decoupling concept let us assume a linear system of equations (3.1), where A is a square matrix.

$$y = Ax \tag{3.1}$$

We propose a transformation such that new variables called w and z can be expressed as x and y through the transformation T .

$$x = Tw \tag{3.2}$$

$$y = Tz \quad (3.3)$$

A substitution of (3.2) and (3.3) into (3.1) gives a new system of equations. Assuming T is a square matrix and that its inverse T^{-1} exists.

$$y = Ax = ATw \quad (3.4)$$

$$z = T^{-1}ATw \quad (3.5)$$

Our goal is to find the matrix T and its inverse T^{-1} , such that $T^{-1}AT$ is a diagonal matrix in (3.5). To illustrate the process, let us use a 2×2 general A matrix such that Γ 's in (3.6) are along the diagonal matrix. We write $T^{-1}AT = \Gamma$ in a slightly different form to find the t values.

$$\begin{bmatrix} a_{11} & a_{12} \\ a_{21} & a_{22} \end{bmatrix} \begin{bmatrix} t_{11} & t_{12} \\ t_{21} & t_{22} \end{bmatrix} = \begin{bmatrix} t_{11} & t_{12} \\ t_{21} & t_{22} \end{bmatrix} \begin{bmatrix} \Gamma_{11} & 0 \\ 0 & \Gamma_{22} \end{bmatrix} \quad (3.6)$$

From (3.6) we have two systems of equations. These relations allow for the calculation of values for t_{11} and t_{21} and eventually for t_{12} and t_{22} . Using algebra shows us that certain conditions have to be met through a quadratic equation (3.10) for both Γ_{11} and Γ_{22} . In general, (3.9) describes the *eigenvalue* problem that requires a solution for λ , a polynomial form out of $\det(A - \lambda I) = 0$. First column values for the transformation matrix T .

$$\begin{bmatrix} a_{11} & a_{12} \\ a_{21} & a_{22} \end{bmatrix} \begin{bmatrix} t_{11} \\ t_{21} \end{bmatrix} = \Gamma_{11} \begin{bmatrix} t_{11} \\ t_{21} \end{bmatrix} \quad (3.7)$$

$$\begin{bmatrix} a_{11} - \Gamma_{11} & a_{12} \\ a_{21} & a_{22} - \Gamma_{11} \end{bmatrix} \begin{bmatrix} t_{11} \\ t_{21} \end{bmatrix} = \begin{bmatrix} 0 \\ 0 \end{bmatrix} \quad (3.8)$$

$$\begin{bmatrix} a_{11} - \Gamma_{11} & a_{12} \\ 0 & a_{22} - \Gamma_{11} - a_{21}a_{12}/(a_{11} - \Gamma_{11}) \end{bmatrix} \begin{bmatrix} t_{11} \\ t_{21} \end{bmatrix} = \begin{bmatrix} 0 \\ 0 \end{bmatrix} \quad (3.9)$$

$$\Gamma_{11}^2 - (a_{11} + a_{22})\Gamma_{11} + a_{11}a_{22} - a_{21}a_{12} = 0 \quad (3.10)$$

Example 3.1

$$\text{Given } A = \begin{bmatrix} 5 & 1 \\ 2 & 4 \end{bmatrix} \quad \text{tr}(A) = \sum_{k=1}^n a_{kk} = a_{11} + a_{22} = 5 + 4 = 9 \quad \det(A) = 18$$

Solving $\lambda^2 - 9\lambda + 18 = 0$ or $(\lambda - 6)(\lambda - 3) = 0$, we have two eigenvalues:

$$\lambda_1 = 6$$

$$\lambda_2 = 3$$

Once the eigenvalues are found, the values for the T matrix can be calculated column-wise. These columns are known as *eigenvectors*. From (3.9), any value $t_{21} \neq 0$ will satisfy the equation, and from the first row of (3.9), we find t_{11} . This process establishes the relation between components t_{11} and t_{21} , but does not assign any numerical value directly (i.e., $t_{11} = -a_{12}/(a_{11} - \lambda_1) t_{21} = -1/(5 - 6) t_{21} = t_{21}$). We can choose any convenient values (except zero), depending on the nature of the problem; a simple value for t_{21} is 1, then $t_{11} = 1$. Following a similar procedure with λ_2 , $t_{12} = -a_{12} t_{22}/(a_{11} - \lambda_2) = -t_{22}/(5 - 3) = -t_{22}/2$, if we choose a value for $t_{22} = 1$ and $t_{12} = -1/2$.

The eigenvectors for this example are columns with values as follows: elements for the first column should be equal, and elements for the second column the values are related as $t_{12} = -t_{22}/2$.

The transformation matrix T and its inverse T^{-1} are:

$$T = \begin{bmatrix} 1 & -1/2 \\ 1 & 1 \end{bmatrix} \quad T^{-1} = \frac{2}{3} \begin{bmatrix} 1 & +1/2 \\ -1 & 1 \end{bmatrix} \quad (3.11)$$

If $T^{-1}AT$ is calculated, a diagonal matrix is found, and its elements are the eigenvalues 6 and 3.

The concept can be readily extended and of particular interest is to transform a symmetrical matrix Z as in (3.12) into a diagonal form. The eigenvalues are determined from the characteristic polynomial (3.13).

$$Z = \begin{bmatrix} z & m \\ m & z \end{bmatrix} \quad (3.12)$$

$$\det \begin{bmatrix} z - \lambda & m \\ m & z - \lambda \end{bmatrix} = (z - \lambda)^2 - m^2 = 0 \quad (3.13)$$

$$\lambda_1 = z + m \quad \lambda_2 = z - m \quad (3.14)$$

The elements for the eigenvectors are determined as follows:

$$t_{11} = \frac{-m}{z - (z + m)} t_{21} = +t_{21} \quad t_{12} = \frac{-m}{z - (z - m)} t_{22} = -t_{22} \quad (3.15)$$

First column for T must have equal values and for the second column the summation of its values should be zero. We can select the t 's values, as real or complex numbers and the options are infinite. A constraint is that once T is defined the inverse T^{-1} must exist.

3.2.1 Symmetrical Components Transformation

One matrix structure that has special interest in electrical power systems is the one related to a 3×3 symmetrical matrix, z value along the main diagonal and m values outside. The eigenvalue problem takes the form (3.18). To turn the matrix Z into a diagonal matrix, we said that there are an infinite number of transformations. One of them is the symmetrical components or 012. Clarke's transformation $\alpha\beta\theta$ is another one. Some matrix transformations might include complex numbers and some only real numbers. The solution to the polynomial equation from $\det(Z - \lambda I) = 0$ is simplified if we change to an u variable, given as $u = (z - \lambda)/m$.

$$\det(Z - \lambda I) = \det \begin{bmatrix} z - \lambda & m & m \\ m & z - \lambda & m \\ m & m & z - \lambda \end{bmatrix} = 0 \quad (3.16)$$

$$\left(\frac{z - \lambda}{m} \right)^3 - 3 \left(\frac{z - \lambda}{m} \right) + 2 = 0 \quad (3.17)$$

For (3.17) as $u^3 - 3u + 2 = 0$, one root is $u = 1$, the other solutions will come from the polynomial $u^2 + u - 2 = 0$. The eigenvalues in terms of z and m , for the symmetrical matrix in (3.16) are $\lambda_1 = z + 2m$, $\lambda_2 = z - m$ and $\lambda_3 = z - m$.

The first eigenvector is found when we solve for the first column of the transformation matrix T .

$$\begin{bmatrix} z & m & m \\ m & z & m \\ m & m & z \end{bmatrix} \begin{bmatrix} t_{11} \\ t_{21} \\ t_{31} \end{bmatrix} = \lambda_1 \begin{bmatrix} t_{11} \\ t_{21} \\ t_{31} \end{bmatrix} \quad (3.18)$$

The result for the eigenvector that corresponds to the eigenvalue $z + 2m$, is $t_{11} = t_{21} = t_{31}$. The eigenvectors for the eigenvalues: $\lambda_2 = \lambda_3 = z - m$ require that (3.20) and (3.21) be satisfied.

$$\begin{bmatrix} z - z + m & m & m \\ m & z - z + m & m \\ m & m & z - z + m \end{bmatrix} \begin{bmatrix} t_{12} \\ t_{22} \\ t_{32} \end{bmatrix} = \begin{bmatrix} 0 \\ 0 \\ 0 \end{bmatrix} \quad (3.19)$$

$$t_{12} + t_{22} + t_{32} = 0 \quad (3.20)$$

$$t_{13} + t_{23} + t_{33} = 0 \quad (3.21)$$

In electrical power systems it is common to use the *symmetrical components transformation*, to decouple variables, where T_s and T_s^{-1} , using $\alpha = e^{j2\pi/3}$, $\alpha^2 = (e^{-j2\pi/3})$.

$$T_S = \begin{bmatrix} 1 & 1 & 1 \\ 1 & \alpha^2 & \alpha \\ 1 & \alpha & \alpha^2 \end{bmatrix} \quad T_S^{-1} = \frac{1}{3} \begin{bmatrix} 1 & 1 & 1 \\ 1 & \alpha & \alpha^2 \\ 1 & \alpha^2 & \alpha \end{bmatrix} \quad (3.22)$$

It can be seen that the values in the eigenvectors of T_S satisfy the condition for the first column; all elements are equal. It also satisfies (3.20)–(3.21) where the column's elements should add up to zero.

Example 3.2

Ohm's law for a three-phase balanced impedance element has a voltage drop when currents flow through the series impedance arrangement.

$$\begin{bmatrix} \Delta V_a \\ \Delta V_b \\ \Delta V_c \end{bmatrix} = \begin{bmatrix} z & m & m \\ m & z & m \\ m & m & z \end{bmatrix} \begin{bmatrix} I_a \\ I_b \\ I_c \end{bmatrix} \quad (3.23)$$

Phase currents and voltages drops in reference abc can be changed to the new reference 012, symmetrical components using T_S and T_S^{-1} . By matrix multiplications on the series impedance Z_{abc} , we can find the sequence impedances Z_{012} .

$$T_S \begin{bmatrix} \Delta V_0 \\ \Delta V_1 \\ \Delta V_2 \end{bmatrix} = \begin{bmatrix} z & m & m \\ m & z & m \\ m & m & z \end{bmatrix} T_S \begin{bmatrix} I_0 \\ I_1 \\ I_2 \end{bmatrix} \quad (3.24)$$

$$\begin{bmatrix} \Delta V_0 \\ \Delta V_1 \\ \Delta V_2 \end{bmatrix} = T_S^{-1} \begin{bmatrix} z & m & m \\ m & z & m \\ m & m & z \end{bmatrix} T_S \begin{bmatrix} I_0 \\ I_1 \\ I_2 \end{bmatrix} = \begin{bmatrix} z + 2m & 0 & 0 \\ 0 & z - m & 0 \\ 0 & 0 & z - m \end{bmatrix} \begin{bmatrix} I_0 \\ I_1 \\ I_2 \end{bmatrix} \quad (3.25)$$

The zero sequence impedance is $z + 2m$; positive and negative sequence impedances are equal to $z - m$. Because the resulting impedance matrix in (3.25) has values only along the diagonal, we can say that the sequence networks are decoupled.

Example 3.3

A different type of transformation can be selected using real numbers only: 0, 1, and -1 . The values in the eigenvectors are arranged to satisfy constraint of first column with the same value and constraint (3.20) and (3.21) for the second and third columns of the transformation matrix T_{xyz} .

$$T_{xyz}^{-1} = \frac{1}{3} \begin{bmatrix} +1 & +1 & +1 \\ +1 & -1 & 0 \\ +1 & 0 & -1 \end{bmatrix} \quad T_{xyz} = \begin{bmatrix} +1 & +1 & +1 \\ +1 & -2 & +1 \\ +1 & +1 & -2 \end{bmatrix} \quad (3.26)$$

Example 3.4

For a three-phase impedance matrix, show the transformation of phase impedances abc to sequence components using T_{xyz} and T_{xyz}^{-1} .

$$\begin{aligned}
 z &= 1.0000 + 10.0000i \\
 m &= 0 + 2.0000i \\
 Z_{abc} &= \begin{bmatrix} 1.0000 + 10.0000i & 0 + 2.0000i & 0 + 2.0000i \\ 0 + 2.0000i & 1.0000 + 10.0000i & 0 + 2.0000i \\ 0 + 2.0000i & 0 + 2.0000i & 1.0000 + 10.0000i \end{bmatrix} \\
 Z_{xyz} &= \begin{bmatrix} 1.0000 + 14.0000i & 0 & 0 \\ 0 & 1.0000 + 8.0000i & 0 \\ 0 & 0 & 1.0000 + 8.0000i \end{bmatrix}
 \end{aligned}$$

Example 3.5

For unbalanced currents in the abc domain, find the time xyz components. Phase abc currents are: $i_a(t) = I_{ma} \cos(2\pi ft + \theta_a)$, $i_b(t) = I_{mb} \cos(2\pi ft + \theta_b)$, $i_c(t) = I_{mc} \cos(2\pi ft + \theta_c)$. The transformation (3.26) will change from the abc domain into the xyz sequence domain, use $f = 60$ Hz and the following unbalanced values for the peak currents. Plot currents in the abc domain and then visualize the xyz currents.

$$I_{ma} = 80\sqrt{2}, \quad I_{mb} = 100\sqrt{2}, \quad I_{mc} = 100\sqrt{2}$$

For a balanced condition, the transformed currents xyz have two components of equal magnitude i_x, i_y , one with a phase angle of 30° leading and the other a phase angle of 30° lagging (see Figure 3.31). For the balanced condition, the current component i_z has zero value, similar to the zero sequence current in symmetrical components. We can appreciate some numerical and speed of calculation advantages when using only real numbers in the transformation. Depending on the type of application we might be interested in properties and possible advantages for numerical speed when we need to detect the type of fault in a faulted power system.

3.2.2 Decoupling of State Equations

In the previous section, we presented the decoupling principle for a steady state condition; now, let us try to expand the concept to dynamic equations. We assume a linear dynamic state model (3.27) and a linear transformation by (3.2). The goal is to have the product $T^{-1}AT$ in (3.28) as a diagonal matrix. To illustrate the concept, we use a two variable system. The solution will find the modes of oscillation for the dynamic system and its damping properties. Solving the differential equations (3.29) where $B_k^{(n)}$ are *source participation factors* requires two constants of integration: k_1 and k_2 whose values can be found using the boundary conditions.

$$\frac{dx}{dt} = Ax + Bu \quad (3.27)$$

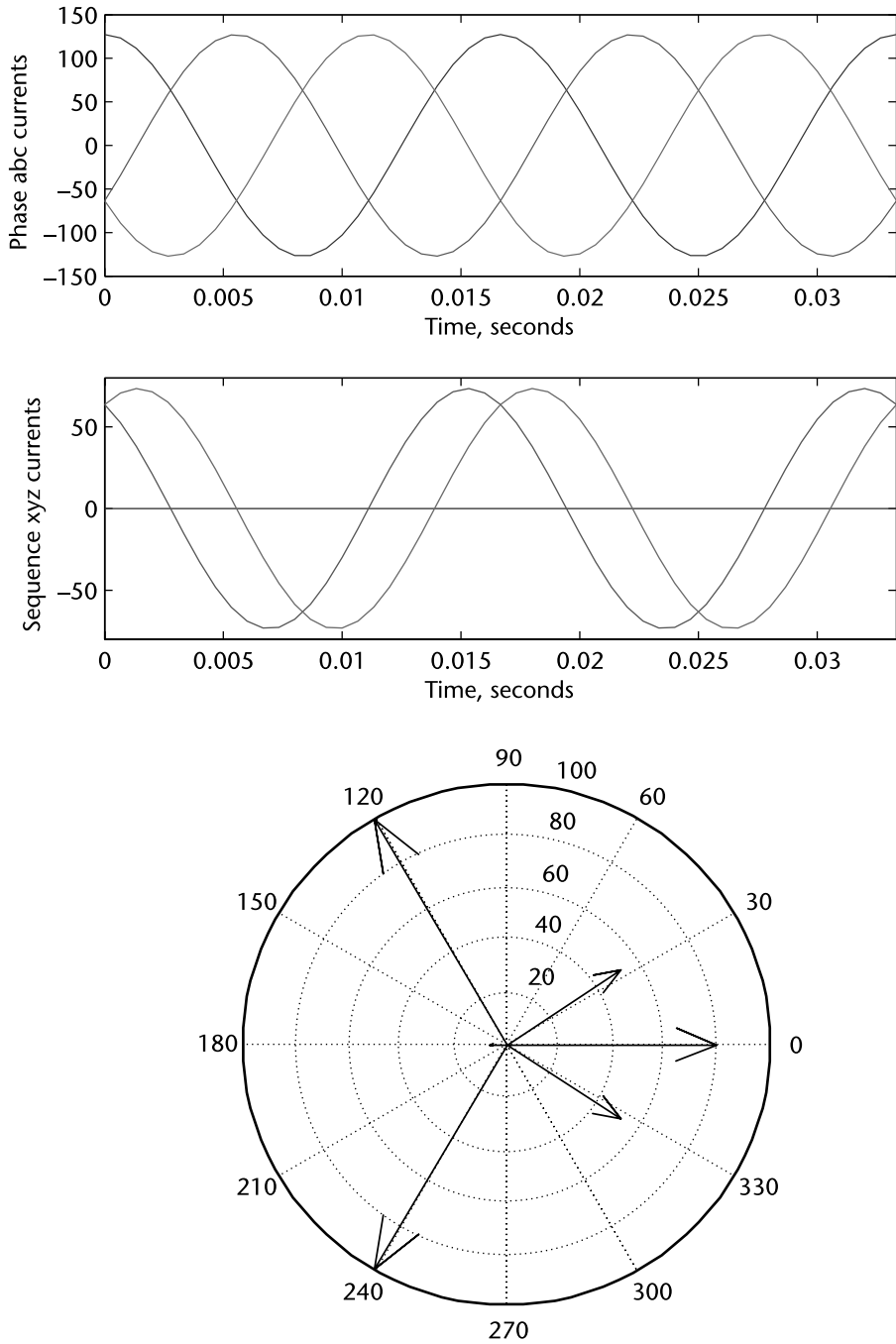


Figure 3.1 Three-phase unbalanced *abc* currents and the *xyz* components.

$$\frac{dw}{dt} = T^{-1}ATw + T^{-1}Bu \quad (3.28)$$

$$\begin{bmatrix} \frac{dw_1}{dt} \\ \frac{dw_2}{dt} \end{bmatrix} = \begin{bmatrix} \Gamma_{11} & 0 \\ 0 & \Gamma_{22} \end{bmatrix} \begin{bmatrix} w_1 \\ w_2 \end{bmatrix} + \begin{bmatrix} B_1^{(n)} \\ B_2^{(n)} \end{bmatrix} u \quad (3.29)$$

Example 3.6

A series *RLC* circuit (shown in Figure 3.2) has values for $R = 4$ ohms, $L = 2$ mH, and $C = 2 \mu\text{F}$ show the transformation process starting with circuit equations and select as state variables current i and voltage drop at capacitor's terminals v_C . Then solve the eigenvalue problem to find the transformation matrix T and T^{-1} .

Using as state variables $x_1 = i$ and $x_2 = v_C$, the system model and the transformed system are:

$$\begin{bmatrix} \dot{x}_1 \\ \dot{x}_2 \end{bmatrix} = \begin{bmatrix} -R/L & -1/L \\ +1/C & 0 \end{bmatrix} \begin{bmatrix} x_1 \\ x_2 \end{bmatrix} + \begin{bmatrix} 1/L \\ 0 \end{bmatrix} v_s \quad (3.30)$$

$$\begin{bmatrix} \dot{w}_1 \\ \dot{w}_2 \end{bmatrix} = T^{-1} \begin{bmatrix} -R/L & -1/L \\ +1/C & 0 \end{bmatrix} T \begin{bmatrix} w_1 \\ w_2 \end{bmatrix} + T^{-1} \begin{bmatrix} 1/L \\ 0 \end{bmatrix} v_s \quad (3.31)$$

```
A =
    -2000    -500
    500000     0
tr = -2000
detA = 250000000
lamda1 = -1.0000e+003 +1.5780e+004i
lamda2 = -1.0000e+003 -1.5780e+004i
T =
    -0.0020 + 0.0316i    -0.0020 - 0.0316i
     1.0000             1.0000
Tinv =
     0    -15.8431i    0.5000 - 0.0317i
```

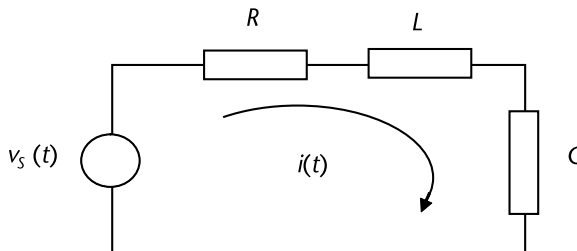


Figure 3.2 Series *RLC* circuit.

```

0 +15.8431i    0.5000 + 0.0317i

Diagonal_matrix =
1.0e+004 *
-0.1000 + 1.5780i    0 - 0.0000i
0 + 0.0000i    -0.1000 - 1.5780i

B =
500
0

Bnew =
1.0e+003 *
0 - 7.9216i
0 + 7.9216i
    
```

The decoupled dynamic equation, in terms of w_1 and w_2 is:

$$\begin{bmatrix} \dot{w}_1 \\ \dot{w}_2 \end{bmatrix} = 10^4 \begin{bmatrix} -0.1 + 1.578i & 0 \\ 0 & -0.1 - 1.578i \end{bmatrix} \begin{bmatrix} w_1 \\ w_2 \end{bmatrix} + 10^3 \begin{bmatrix} -7.9216i \\ +7.9216i \end{bmatrix} v_s \quad (3.32)$$

Initial conditions for the w 's variables are calculated as:

$$\begin{bmatrix} w_1 \\ w_2 \end{bmatrix}^{(0)} = T^{-1} \begin{bmatrix} x_1 \\ x_2 \end{bmatrix}^{(0)} = T^{-1} \begin{bmatrix} i \\ v_C \end{bmatrix}^{(0)} \quad (3.33)$$

3.3 Single-Phase Transformer Model

In order to have a general model for a single-phase transformer component in a power system, let us first consider a complex changing tap arrangement at the primary and also in the secondary sides through ideal transformers.

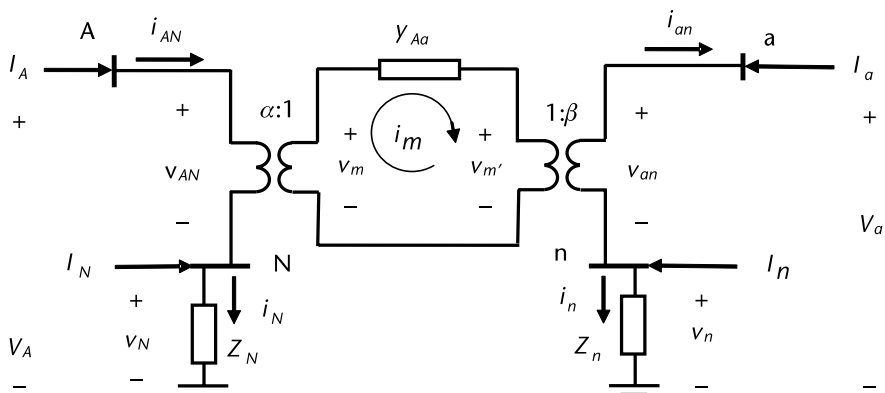


Figure 3.3 Single-phase complex transformer.

$$v_m - v_{m'} = \frac{i_m}{y_{Aa}} = z_{Aa} i_m \quad (3.34)$$

Voltage relations are $v_{AN} = \alpha v_m$ and $v_{an} = \beta v'_m$ and for the ideal transformer, the complex power relation at both sides as $v_{AN} i_{AN}^* = v_m i_m^*$ and $v'_m i_m^* = v_{an} i_{an}^*$. Starting with the v_{AN} voltage, substitution of (3.34) as well as current expressions from the complex power relation, then the equations for the transformer and the shunt impedances are arranged as Ohm's equation:

$$\begin{aligned} -z_{Aa} |\alpha|^2 i_{AN} + V_A - V_N - \frac{\alpha}{\beta} V_a + \frac{\alpha}{\beta} V_n &= 0 \\ -Z_N i_N &= V_N \\ -Z_n i_n &= V_n \end{aligned} \quad (3.35)$$

Writing the nodal currents by KCL and together with the set (3.35) now in matrix form, where i 's are element's currents and I 's are nodal currents.

$$\begin{bmatrix} -z_{Aa} |\alpha|^2 & 0 & 0 & +1 & -\frac{\alpha}{\beta} & -1 & +\frac{\alpha}{\beta} \\ 0 & -z_N & 0 & 0 & 0 & +1 & 0 \\ 0 & 0 & -z_n & 0 & 0 & 0 & +1 \\ +1 & 0 & 0 & 0 & 0 & 0 & 0 \\ -\frac{\alpha^*}{\beta^*} & 0 & 0 & 0 & 0 & 0 & 0 \\ -1 & +1 & 0 & 0 & 0 & 0 & 0 \\ +\frac{\alpha^*}{\beta^*} & 0 & +1 & 0 & 0 & 0 & 0 \end{bmatrix} \begin{bmatrix} i_{AN} \\ i_N \\ i_n \\ V_A \\ V_a \\ V_N \\ V_n \end{bmatrix} = \begin{bmatrix} 0 \\ 0 \\ 0 \\ I_A \\ I_a \\ I_N \\ I_n \end{bmatrix} \quad (3.36)$$

In case both Z_N and Z_n were zero, both nodes N and n are connected to reference. A *partial inversion* on first row-first column will render the nodal matrix equivalent for the single-phase transformer (as seen in Figure 3.4).

$$\begin{bmatrix} \frac{+y_{Aa}}{|\alpha|^2} & \frac{-y_{Aa}}{|\alpha|^2} & \frac{+y_{Aa}}{\alpha^* \beta} & \frac{+y_{Aa}}{|\alpha|^2} & \frac{-y_{Aa}}{\alpha^* \beta} \\ \frac{-y_{Aa}}{|\alpha|^2} & \frac{+y_{Aa}}{|\alpha|^2} & \frac{-y_{Aa}}{\alpha^* \beta} & \frac{-y_{Aa}}{|\alpha|^2} & \frac{+y_{Aa}}{\alpha^* \beta} \\ \frac{+y_{Aa}}{\alpha \beta^*} & \frac{-y_{Aa}}{\alpha \beta^*} & \frac{+y_{Aa}}{|\beta|^2} & \frac{+y_{Aa}}{\alpha \beta^*} & \frac{-y_{Aa}}{|\beta|^2} \\ \frac{+y_{Aa}}{|\alpha|^2} & \frac{-y_{Aa}}{|\alpha|^2} & \frac{+y_{Aa}}{\alpha^* \beta} & \frac{+y_{Aa}}{|\alpha|^2} & \frac{-y_{Aa}}{\alpha^* \beta} \\ \frac{-y_{Aa}}{\alpha \beta^*} & \frac{+y_{Aa}}{\alpha \beta^*} & \frac{-y_{Aa}}{|\beta|^2} & \frac{-y_{Aa}}{\alpha \beta^*} & \frac{+y_{Aa}}{|\beta|^2} \end{bmatrix} \begin{bmatrix} 0 \\ V_A \\ V_a \\ V_N \\ V_n \end{bmatrix} = \begin{bmatrix} i_{AN} \\ I_A \\ I_a \\ I_N \\ I_n \end{bmatrix} \quad (3.37)$$

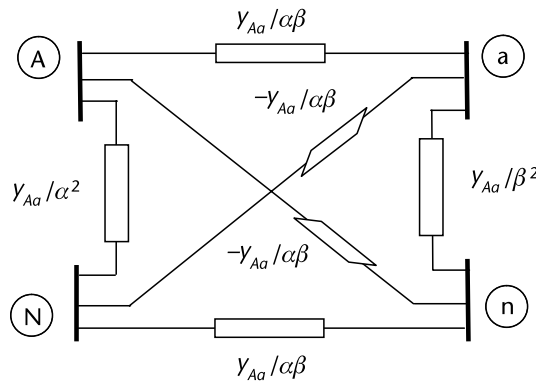


Figure 3.4 Equivalent circuit for a single-phase transformer.

When α and β are real numbers, Norton’s equivalent circuit is visualized as in Figure 3.5.

3.3.1 Per Unit Values

The voltages, currents, and power describe how a power circuit works. Various voltage levels are used to link efficiently generation, transmission, and loads. To this intricacy, it must be added the rating of generators, transformers power rating, and the power handling capacity of the transmission line.

To have a manageable network for analysis, we write its equations in a common base (voltage, current, power, and impedance) to render what is known as per-unit values. With this approach, an easier handling of information can be conducted between different voltage levels, as happens in the primary and secondary of a power transformer. To apply the per unit values, it is customary to choose two base values (usually power and voltage). The derived quantities will then be current, impedance, and admittance; these values will depend on the selected power and voltage bases. Suggested steps to follow for pu base value determination.

1. For the entire network a common power base is selected; $100 \text{ MVA}_{\text{base}}$ commonly used.

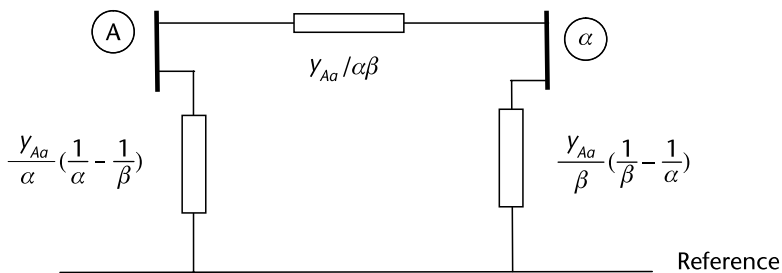


Figure 3.5 Equivalent circuit for a single-phase transformer, grounded neutrals.

2. Base voltage kV_{base} is selected at one side of the voltage transformer; the transformer relation is used to find the corresponding base voltage at the other side.
3. Current base I_{base} and impedance base Z_{base} at each portion of the network can be calculated using the power and voltage bases selected at steps 1 and 2.
4. With the chosen bases and the derived base quantities, the per unit values are calculated as $(V \text{ in kV})/V_{\text{base}}$ in kV, $(S \text{ in MVA})/S_{\text{base}}$ MVA, $Z \text{ in } \Omega/Z_{\text{base}}$ Ω

Example 3.6

For a single-phase transformer (see Figure 3.6), the steps to selecting base quantities are as follows:

- Select a power base for the entire system (a common value is 100 MVA).
- Select the primary and then the secondary base voltage (kV), considering the transformation ratio $|t|$.
- Derive the primary and secondary base currents (kA), then the impedance (Ω) and admittance base (S).

$$\left. \begin{array}{l} S_B \\ \frac{V_B^P}{V_B^S} = \frac{1}{|t|} \end{array} \right\} \quad \text{Common power and voltage relations} \quad (3.38)$$

$$\begin{array}{l} I_B^P = \frac{S_B}{V_B^P} \quad I_B^S = \frac{S_B}{V_B^S} \quad \text{Primary and secondary current base} \\ Z_B^P = \frac{(V_B^P)^2}{S_B} \quad Z_B^S = \frac{(V_B^S)^2}{S_B} \quad \text{Primary and secondary impedance base} \end{array} \quad (3.39)$$

Per unit values

Power base = 100 MVAs

Primary Voltage base = 230.94 kV Secondary Voltage base = 132.79 kV

Primary Current base = 0.4330 kA Secondary Current base = 0.7531 kA

Primary Z base = 533.3333 Ohms Secondary Z base = 176.3333 Ohms

Primary Y base = 0.001875 S Secondary Y base = 0.005671 S

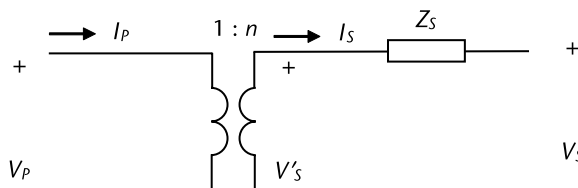


Figure 3.6 Single-phase transformer, voltages, and currents for the primary and secondary.

For three-phase arrangements, the per unit values are calculated using three-phase power $S_{B,3}$ (MVA) and the line-to-line voltage kV_{LL} (kV), then Z_B (Ω) and I_B (kA) are

$$Z_B = \frac{(kV_{LL})^2}{S_{B,3}} \quad (3.40)$$

$$I_B = \frac{S_{B,3}}{\sqrt{3}kV_{LL}}$$

Example 3.7

From Figure 3.6, the impedance Z_s can be transferred from the right side to the left side using voltage relations in an ideal transformer (Figure 3.7, where $n = |t|$), using $I_p = |t|I_s$, starting with V_p .

$$V_p = \frac{1}{|t|}V'_s = \frac{1}{|t|}(Z_s I_s + V_s) \quad (3.41)$$

$$V_p = \frac{1}{|t|}\left(Z_s \frac{1}{|t|}I_p + V_s\right) = \frac{Z_s}{|t|^2}I_p + \frac{1}{|t|}V_s \quad (3.42)$$

Example 3.8

In mutually coupled circuits (see Figure 3.8) operating at different voltage levels V_p and V_s , select the same power base for both systems, then the mutual impedance base can be deduced, starting with $\Delta V_p = Z_p I_p + M I_s$, M is the complex mutual impedance, then the per unit $\Delta V_p/V'_B$ will be

$$\frac{\Delta V_p}{V_B^p} = \frac{Z_p I_p}{Z_B^p I_B^p} + \frac{M I_s}{\frac{V_B^p V_B^s}{S_B} I_B^s} \quad (3.43)$$

$$\Delta V_p^{pu} = Z_p^{pu} I_p^{pu} + \frac{M}{\frac{V_B^p V_B^s}{S_B}} I_s^{pu} \quad (3.44)$$

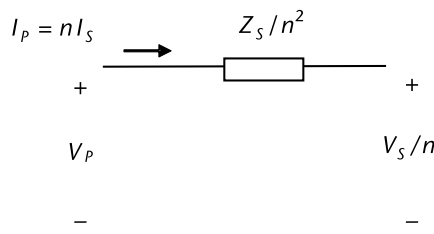


Figure 3.7 Single-phase transformer voltage, current, and impedance at the primary side.

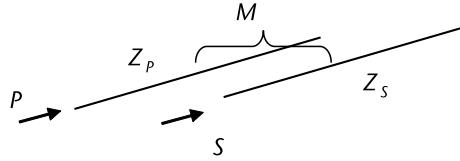


Figure 3.8 Mutually coupled circuits and pu values.

The mutual impedance base, with voltages in kV and power in MVA values, is the denominator of M in (3.44).

Mutual impedance in pu			
Voltage circuit 1 =	169.00 kV phase-phase		
Voltage circuit 2 =	220.00 kV phase-phase		
Power Base =	100.00 MVA-3phase		
Z Base circuit 1 =	285.61 Ohms	I Base circuit 1 =	0.341627 kA
Z Base circuit 2 =	484.00 Ohms	I Base circuit 2 =	0.262432 kA
Z Base mutual =	371.80 Ohms		
Z circuit 1 =	10.00 +j 150.00 Ohms		0.035013 +j0.525192 pu
Z circuit 2 =	12.00 +j 350.00 Ohms		0.024793 +j0.723140 pu
Z mutual =	0.00 +j 20.00 Ohms		0.000000 +j0.053792 pu

Example 3.9

To illustrate an application for the model we have just derived, let us assume a single-phase complex transformer in an *open circuit condition*. Node N and n shorted to ground. Values in pu for $z_{Aa} = j0.1$, $V_A = 1$, $\alpha = 1 \angle 0$ and $\beta = 1 \angle 0$.

The matrix is obtained as in (3.36); known values are identified for the left and for the right hand sides. The information is exchanged by *partial inversion* from the right to left side when pivots 1, 2, and 3 are used; if we stop the partial inversion numerical process, we can read the Y_{bus} matrix. If we continue to use pivots 5, 6, and 7, we will prepare the matrix that is needed to solve the numerical problem. Finally, a multiplication of the *partial inverted matrix* with the vector of known values is used to calculate currents and voltages: i_{AN} , i_N , i_n , I_A , V_a , V_N , and V_n .

Ybus Matrix, after partial inversion process for elements, previous to solving for nodal conditions:

Ybus =

0 -10.0000i	0 +10.0000i	0 +10.0000i	0 -10.0000i
0 +10.0000i	0 -10.0000i	0 -10.0000i	0 +10.0000i
0 +10.0000i	0 -10.0000i	10.0000 -10.0000i	0 +10.0000i
0 -10.0000i	0 +10.0000i	0 +10.0000i	10.0000 -10.0000i

Solution

i(1) =	+0.000000	+0.000000i
i(2) =	+0.000000	+0.000000i
i(3) =	+0.000000	+0.000000i
I(4) =	+0.000000	+0.000000i
V(5) =	+1.000000	+0.000000i
V(6) =	+0.000000	+0.000000i
V(7) =	+0.000000	+0.000000i

In case of feeding a load of $I_a = -0.5$ pu and $Z_N = 0.1$ pu, $V_n = 0$ (is taken to reference).

```

i( 1) = +0.500000 +0.000000i
i( 2) = +0.500000 +0.000000i
i( 3) = -0.000000 +0.000000i
I( 4) = +0.500000 +0.000000i
V( 5) = +0.950000 -0.050000i
V( 6) = +0.050000 +0.000000i
V( 7) = -0.000000 +0.000000i
    
```

The values of all nodal voltages, voltage drops on every element, and internal currents are shown in Figure 3.9:

```

Vbus =
 1.0000
 0.9500 - 0.0500i
 0.0000 - 0.0000i
-0.0500
velem =
 1.0000 + 0.0000i
 1.0000 - 0.0500i
-0.0500
-0.0500
 1.0000 + 0.0000i
 1.0000 - 0.0500i
iAN = 0.5000
ian = 0.5000
im = 0.5000
    
```

A different form to incorporate shunt elements is to recognize that the current through shunt element is $i_N = y_N V_N$ and $i_n = y_n V_n$. The equations for node N and n are modified accordingly.

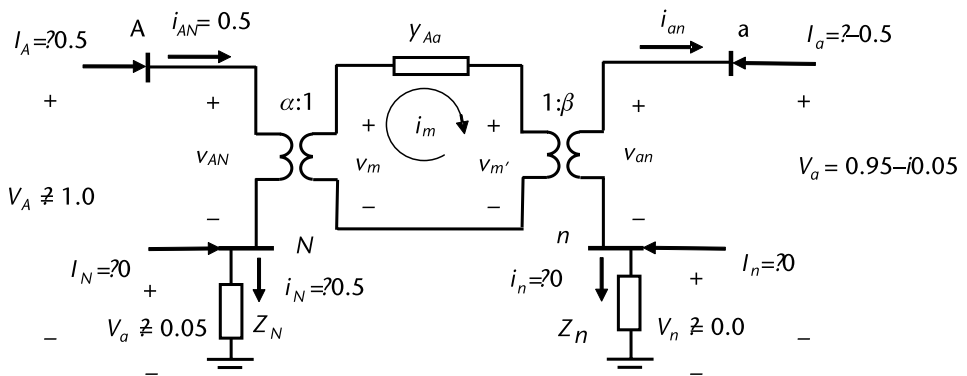


Figure 3.9 Solution for a single-phase transformer, grounded neutrals.

$$\begin{aligned}
 +y_N V_N - i_{AN} &= I_N \\
 +y_n V_n + \left(\frac{\alpha}{\beta}\right)^* i_{AN} &= I_n
 \end{aligned}
 \tag{3.45}$$

As i_N and i_n are incorporated to the node current balance, we have a reduced matrix as compared to the one in (3.36).

$$\begin{bmatrix}
 -z_{Ad}|\alpha|^2 & +1 & -\frac{\alpha}{\beta} & -1 & +\frac{\alpha}{\beta} \\
 +1 & 0 & 0 & 0 & 0 \\
 -\frac{\alpha^*}{\beta^*} & 0 & 0 & 0 & 0 \\
 -1 & 0 & 0 & +y_N & 0 \\
 +\frac{\alpha^*}{\beta^*} & 0 & 0 & 0 & +y_n
 \end{bmatrix}
 \begin{bmatrix}
 i_{AN} \\
 V_A \\
 V_a \\
 V_N \\
 V_n
 \end{bmatrix}
 =
 \begin{bmatrix}
 0 \\
 I_A \\
 I_a \\
 I_N \\
 I_n
 \end{bmatrix}
 \tag{3.46}$$

Usually I_N and I_n are zero, as no source injects or drains current from these nodes. With this model, various cases can be studied: $y_N = 1/z_N$ where $y_N \rightarrow \infty$ as $z_N = 0$ (short circuit) and $y_N = 0$ as $z_N \rightarrow \infty$ (open circuit).

3.4 Three-Phase Bank Transformer Model

When a three-phase unit is required to handle power transfer from different voltage levels, three single-phase units can be connected in Y or in a Δ arrangement. One operating advantage can be to have some flexibility when one of the single-phase units has a malfunction, so that a short-term unbalanced situation can be tolerated; only the failed component needs to be replaced. We start with the single-phase model shown in Figure 3.3; the node connection reflects the Y or the Δ configuration for the high voltage and the low voltage sides.

3.4.1 Three-Phase $\Delta\Delta$ Bank

Assuming relations for voltages and currents in the single-phase units, the element's equation for the connection in Figure 3.10 can be arranged in a three-phase scheme. A compact matrix equation is Ohm's law (3.48).

$$\begin{bmatrix}
 v_1 \\
 v_2 \\
 v_3 \\
 v_4 \\
 v_5 \\
 v_6
 \end{bmatrix}
 =
 \begin{bmatrix}
 z & m & & & & \\
 m & z & & & & \\
 & & z & m & & \\
 & & m & z & & \\
 & & & & z & m \\
 & & & & m & z
 \end{bmatrix}
 \begin{bmatrix}
 i_1 \\
 i_2 \\
 i_3 \\
 i_4 \\
 i_5 \\
 i_6
 \end{bmatrix}
 \tag{3.47}$$

$$-[Z]i + v = 0 \tag{3.48}$$

In terms of nodal voltages, the voltage drop v for each element is

$$\begin{bmatrix} v_1 \\ v_2 \\ v_3 \\ v_4 \\ v_5 \\ v_6 \end{bmatrix} = \begin{bmatrix} +1 & -1 & 0 & 0 & 0 & 0 \\ 0 & 0 & 0 & +1 & 0 & -1 \\ 0 & +1 & -1 & 0 & 0 & 0 \\ 0 & 0 & 0 & 0 & +1 & -1 \\ -1 & 0 & +1 & 0 & 0 & 0 \\ 0 & 0 & 0 & -1 & 0 & +1 \end{bmatrix} \begin{bmatrix} V_A \\ V_B \\ V_C \\ V_a \\ V_b \\ V_c \end{bmatrix} = A_{\Delta\Delta} V_{bus}^{ABC,abc} \tag{3.49}$$

Ohm's equivalent for the three-phase bank is attained using a shorthand notation with $A_{\Delta\Delta}$ as the connectivity matrix. Using (3.48) the model is:

$$-[Z]i + A_{\Delta\Delta} V_{bus}^{ABC,abc} = 0 \tag{3.50}$$

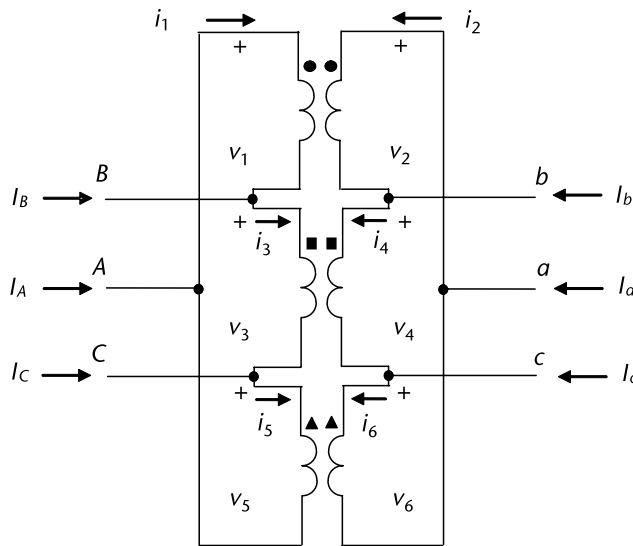


Figure 3.10 A three-phase complex transformer, $\Delta\Delta$ connection.

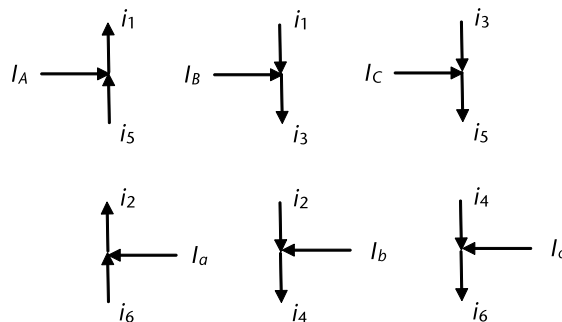


Figure 3.11 A three-phase complex transformer, node currents.

From current information at each node, as given in Figure 3.11, we write the nodal currents.

$$\begin{bmatrix} I_A \\ I_B \\ I_C \\ I_a \\ I_b \\ I_c \end{bmatrix} = \begin{bmatrix} +1 & 0 & 0 & 0 & -1 & 0 \\ -1 & 0 & +1 & 0 & 0 & 0 \\ 0 & 0 & -1 & 0 & +1 & 0 \\ 0 & +1 & 0 & 0 & 0 & -1 \\ 0 & -1 & 0 & +1 & 0 & 0 \\ 0 & 0 & 0 & -1 & 0 & +1 \end{bmatrix} \begin{bmatrix} i_1 \\ i_2 \\ i_3 \\ i_4 \\ i_5 \\ i_6 \end{bmatrix} \quad (3.51)$$

$$I_{\text{bus}} = A_{\Delta\Delta}^t i \quad (3.52)$$

Results (3.50) and (3.52) are combined as a model that relates nodal voltages to nodal currents and currents through each winding with *partial inversion* applied to (3.53), exchanging known and unknown values; with $y = Z^{-1}$ it results as (3.54). We find a three-phase model for a transformer bank connected as $\Delta\Delta$ at the right lower portion of the matrix. The model is a Norton's equivalent, a 6×6 admittance matrix.

$$\begin{bmatrix} -Z & A_{\Delta\Delta} \\ A_{\Delta\Delta}^t & 0 \end{bmatrix} \begin{bmatrix} i \\ V_{\text{bus}} \end{bmatrix} = \begin{bmatrix} 0 \\ I_{\text{bus}} \end{bmatrix} \quad (3.53)$$

$$\begin{bmatrix} y & yA_{\Delta\Delta} \\ -A_{\Delta\Delta}^t y & A_{\Delta\Delta}^t y A_{\Delta\Delta} \end{bmatrix} \begin{bmatrix} 0 \\ V_{\text{bus}} \end{bmatrix} = \begin{bmatrix} i \\ I_{\text{bus}} \end{bmatrix} \quad (3.54)$$

The 6×6 reduced matrix (3.55) can be solved for nodal voltages or currents in the abc domain. The problem can include balanced or unbalanced conditions.

$$\begin{bmatrix} Y_{ABC} & Y_{ABC,abc} \\ Y_{abc,ABC} & Y_{abc} \end{bmatrix} \begin{bmatrix} V_{\text{bus}}^{ABC} \\ V_{\text{bus}}^{abc} \end{bmatrix} = \begin{bmatrix} I_{\text{bus}}^{ABC} \\ I_{\text{bus}}^{abc} \end{bmatrix} \quad (3.55)$$

Using the symmetrical components transformation, we obtain sequence admittances from the primary side P and the secondary side S . Matrix T_s is a 3×3 symmetrical transformation, as in (3.22). The symmetrical component model is given by (3.57), where the nodal admittance matrix, currents, and voltages are in the symmetrical components domain. Sequence admittance values can be read from the admittance matrix and, in the case of a symmetrical matrix, a circuit representation can be drawn.

$$\begin{bmatrix} T_s & 0 \\ 0 & T_s \end{bmatrix}^{-1} \begin{bmatrix} Y_{ABC} & Y_{ABC,abc} \\ Y_{abc,ABC} & Y_{abc} \end{bmatrix} \begin{bmatrix} T_s & 0 \\ 0 & T_s \end{bmatrix} \begin{bmatrix} V_{012}^P \\ V_{012}^S \end{bmatrix} = \begin{bmatrix} I_{012}^P \\ I_{012}^S \end{bmatrix} \quad (3.56)$$

$$\begin{bmatrix} Y_{012}^P & Y_{012}^{PS} \\ Y_{012}^{SP} & Y_{012}^S \end{bmatrix} \begin{bmatrix} V_{012}^P \\ V_{012}^S \end{bmatrix} = \begin{bmatrix} I_{012}^P \\ I_{012}^S \end{bmatrix} \tag{3.57}$$

3.4.2 Three-Phase $Y\Delta$ Bank

To calculate voltages v across elements and currents i that flow at every transformer, the matrix equation for the connection of three single-phase units (as shown at Figure 3.12) use is made of (3.47) and (3.48). Voltage relations are now (3.58) and (3.59), and neutral node N is included. From voltage relations, we write the connectivity matrix. Node current equations in matrix form are obtained from Figure 3.13, and (3.60) and (3.61) are formed.

$$\begin{bmatrix} v_1 \\ v_2 \\ v_3 \\ v_4 \\ v_5 \\ v_6 \\ v_7 \end{bmatrix} = \begin{bmatrix} +1 & 0 & 0 & 0 & 0 & 0 & -1 \\ 0 & 0 & 0 & +1 & -1 & 0 & 0 \\ 0 & +1 & 0 & 0 & 0 & 0 & -1 \\ 0 & 0 & 0 & 0 & +1 & -1 & 0 \\ 0 & 0 & +1 & 0 & 0 & 0 & -1 \\ 0 & 0 & 0 & -1 & 0 & +1 & 0 \\ 0 & 0 & 0 & 0 & 0 & 0 & +1 \end{bmatrix} \begin{bmatrix} V_A \\ V_B \\ V_C \\ V_a \\ V_b \\ V_c \\ V_N \end{bmatrix} \tag{3.58}$$

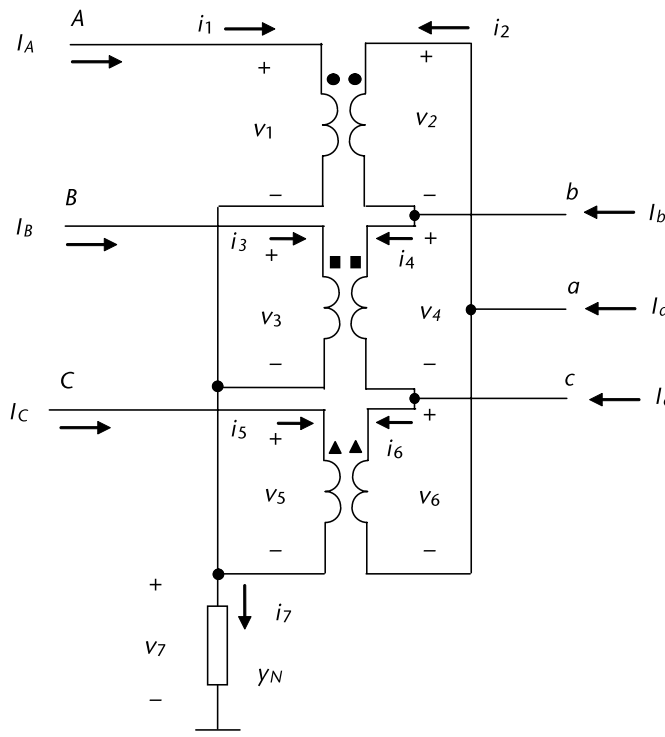


Figure 3.12 A three-phase complex transformer, $Y\Delta$ connection.

$$v = A_{Y\Delta} V_{\text{bus}}^{ABC,abc,N} \quad (3.59)$$

Now the node current relations are used to write the following set for i and I_{bus} .

$$\begin{bmatrix} I_A \\ I_B \\ I_C \\ I_a \\ I_b \\ I_c \\ I_N \end{bmatrix} = \begin{bmatrix} +1 & 0 & 0 & 0 & 0 & 0 & 0 \\ 0 & 0 & +1 & 0 & 0 & 0 & 0 \\ 0 & 0 & 0 & 0 & +1 & 0 & 0 \\ 0 & +1 & 0 & 0 & 0 & -1 & 0 \\ 0 & -1 & 0 & +1 & 0 & 0 & 0 \\ 0 & 0 & 0 & -1 & 0 & +1 & 0 \\ -1 & 0 & -1 & 0 & -1 & 0 & +1 \end{bmatrix} \begin{bmatrix} i_1 \\ i_2 \\ i_3 \\ i_4 \\ i_5 \\ i_6 \\ i_7 \end{bmatrix} \quad (3.60)$$

$$I_{\text{bus}} = A_{Y\Delta}^t i \quad (3.61)$$

With (3.59) including node N into (3.48), the model for this $Y\Delta$ connection is complete when we include (3.61) to get (3.62).

$$\begin{bmatrix} -Z & A_{Y\Delta} \\ A_{Y\Delta}^t & 0 \end{bmatrix} \begin{bmatrix} i \\ V_{\text{bus}}^{ABC,abc,N} \end{bmatrix} = \begin{bmatrix} 0 \\ I_{\text{bus}} \end{bmatrix} \quad (3.62)$$

Using partial inversion on (3.62) and exchanging the current vector i from the left with the vector of zeros at the right, Norton's equivalent is located in the bottom right of the matrix in (3.63), including node N .

$$\begin{bmatrix} +y & -yA_{Y\Delta} \\ -A_{Y\Delta}^t y & A_{Y\Delta}^t y A_{Y\Delta} \end{bmatrix} \begin{bmatrix} 0 \\ V_{\text{bus}}^{ABC,abc,N} \end{bmatrix} = \begin{bmatrix} i \\ I_{\text{bus}} \end{bmatrix} \quad (3.63)$$

If we are only interested in the three-phase terminals ABC and abc, node N must be eliminated. Often I_N has a zero value, and one step of the partial inversion will do the job and compute the Norton's equivalent (as seen from the three-phase nodes on the high and on the low voltage side of the transformer). After node N elimination, the Norton's equivalent—as seen from the nodes ABC and abc of the transformer—is (3.65).

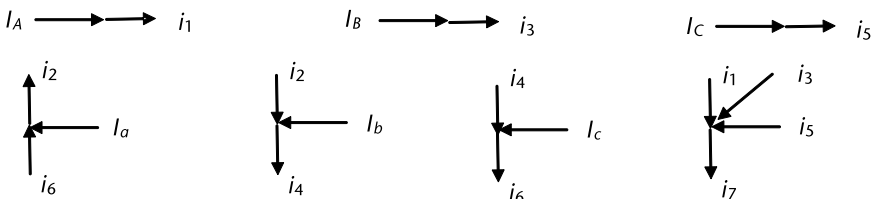


Figure 3.13 A three-phase complex transformer, node currents.

$$\begin{bmatrix} Y_{bus}^{ABC,abc} & Y_{bus}^{ABC,abc,N} \\ Y_{bus}^{N,ABC,abc} & Y_{NN} \end{bmatrix} \begin{bmatrix} V_{bus}^{ABC,abc} \\ V_N \end{bmatrix} = \begin{bmatrix} I_{bus}^{ABC,abc} \\ 0 \end{bmatrix} \tag{3.64}$$

$$\left[Y_{bus}^{ABC,abc} \right]^{eq} \left[V_{bus}^{ABC,abc} \right] = \left[I_{bus}^{ABC,abc} \right] \tag{3.65}$$

3.4.3 Three-Phase YY Bank

Connections for both sides of the single-phase transformer are arranged as in Figure 3.14. Assuming element relations for voltages and currents, then the matrix element equations use (3.47) and (3.48).

In matrix notation, voltage v relations allow us to get a connectivity matrix, including nodes n and N .

$$\begin{bmatrix} v_1 \\ v_2 \\ v_3 \\ v_4 \\ v_5 \\ v_6 \\ v_7 \\ v_8 \end{bmatrix} = \begin{bmatrix} +1 & 0 & 0 & 0 & 0 & 0 & -1 & 0 \\ 0 & 0 & 0 & +1 & 0 & 0 & 0 & -1 \\ 0 & +1 & 0 & 0 & 0 & 0 & -1 & 0 \\ 0 & 0 & 0 & 0 & +1 & 0 & 0 & -1 \\ 0 & 0 & +1 & 0 & 0 & 0 & -1 & 0 \\ 0 & 0 & 0 & 0 & 0 & +1 & 0 & -1 \\ 0 & 0 & 0 & 0 & 0 & 0 & +1 & 0 \\ 0 & 0 & 0 & 0 & 0 & 0 & 0 & +1 \end{bmatrix} \begin{bmatrix} V_A \\ V_B \\ V_C \\ V_a \\ V_b \\ V_c \\ V_N \\ V_n \end{bmatrix} \tag{3.66}$$

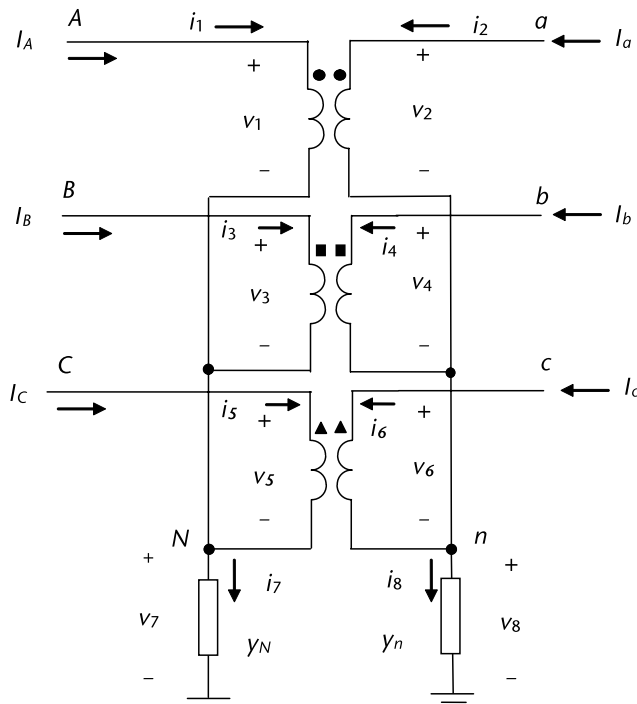


Figure 3.14 A three-phase complex transformer, YY connection.

$$v = A_{YY} V_{bus}^{ABC,abc,N,n} \tag{3.67}$$

Node current relations in matrix form are obtained from Figure 3.15. Substitution of (3.67) into the general Ohm’s equation (3.48)—together with nodal current equation (3.69)—will give us a model for the YY connection that is described in (3.70).

$$\begin{bmatrix} I_A \\ I_B \\ I_C \\ I_a \\ I_b \\ I_c \\ I_N \\ I_n \end{bmatrix} = \begin{bmatrix} +1 & 0 & 0 & 0 & 0 & 0 & 0 & 0 \\ 0 & 0 & +1 & 0 & 0 & 0 & 0 & 0 \\ 0 & 0 & 0 & 0 & +1 & 0 & 0 & 0 \\ 0 & +1 & 0 & 0 & 0 & 0 & 0 & 0 \\ 0 & 0 & 0 & +1 & 0 & 0 & 0 & 0 \\ 0 & 0 & 0 & 0 & 0 & +1 & 0 & 0 \\ -1 & 0 & -1 & 0 & -1 & 0 & +1 & 0 \\ 0 & -1 & 0 & -1 & 0 & -1 & 0 & +1 \end{bmatrix} \begin{bmatrix} i_1 \\ i_2 \\ i_3 \\ i_4 \\ i_5 \\ i_6 \\ i_7 \\ i_8 \end{bmatrix} \tag{3.68}$$

$$I_{bus} = A_{YY}^t i \tag{3.69}$$

$$\begin{bmatrix} -Z & A_{YY} \\ A_{YY}^t & 0 \end{bmatrix} \begin{bmatrix} i \\ V_{bus}^{ABC,abc,N,n} \end{bmatrix} = \begin{bmatrix} 0 \\ I_{bus} \end{bmatrix} \tag{3.70}$$

With partial inversion work on (3.70), we get a Norton’s equivalent, which includes both neutral nodes N and n . Norton’s equivalent appears at the lower right side of the coefficient matrix.

$$\begin{bmatrix} +y & -yA_{YY} \\ -A_{YY}^t y & A_{YY}^t y A_{YY} \end{bmatrix} \begin{bmatrix} 0 \\ V_{bus}^{ABC,abc,N,n} \end{bmatrix} = \begin{bmatrix} i \\ I_{bus} \end{bmatrix} \tag{3.71}$$

If we are only interested in three-phase terminals ABC and abc, nodes N and n must be eliminated through partial inversion. Most of the time, I_N and I_n are of zero value. After the partial inversion, we get the Norton’s equivalent, as seen from

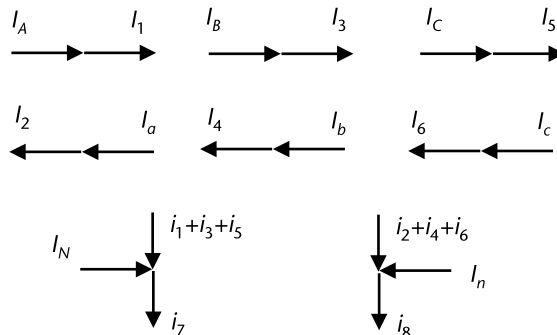


Figure 3.15 A three-phase complex transformer, node currents.

the three-phase nodes on the high side and from the three-phase nodes on the low voltage side of the transformer.

$$\begin{bmatrix} Y_{bus}^{ABC,abc} & Y_{bus}^{ABC,abc,N,n} \\ Y_{bus}^{N,n,ABC,abc} & Y_{NN,nn} \end{bmatrix} \begin{bmatrix} V_{bus}^{ABC,abc} \\ V_{N,n} \end{bmatrix} = \begin{bmatrix} I_{bus}^{ABC,abc} \\ 0 \end{bmatrix} \quad (3.72)$$

$$\begin{bmatrix} Y_{bus}^{ABC,abc} \end{bmatrix}^{eq} \begin{bmatrix} V_{bus}^{ABC,abc} \end{bmatrix} = \begin{bmatrix} I_{bus}^{ABC,abc} \end{bmatrix} \quad (3.73)$$

Example 3.10

Open Δ or V connection with single-phase transformers (see Figure 3.16).

Assuming the following element relation for voltages v and currents i as (3.74), then Ohm’s law as expressed by (3.48) is $-zi + v = 0$.

$$-\begin{bmatrix} z & m & 0 & 0 \\ m & z & 0 & 0 \\ 0 & 0 & z & m \\ 0 & 0 & m & z \end{bmatrix} \begin{bmatrix} i_1 \\ i_2 \\ i_3 \\ i_4 \end{bmatrix} + \begin{bmatrix} v_1 \\ v_2 \\ v_3 \\ v_4 \end{bmatrix} = \begin{bmatrix} 0 \\ 0 \\ 0 \\ 0 \end{bmatrix} \quad (3.74)$$

Voltages across elements v and nodal voltages are related as:

$$\begin{bmatrix} v_1 \\ v_2 \\ v_3 \\ v_4 \end{bmatrix} = \begin{bmatrix} +1 & -1 & 0 & 0 & 0 & 0 \\ 0 & 0 & 0 & +1 & -1 & 0 \\ 0 & +1 & -1 & 0 & 0 & 0 \\ 0 & 0 & 0 & 0 & +1 & -1 \end{bmatrix} \begin{bmatrix} V_A \\ V_B \\ V_C \\ V_a \\ V_b \\ V_c \end{bmatrix} \quad v = A_{VV} V_{bus} \quad (3.75)$$

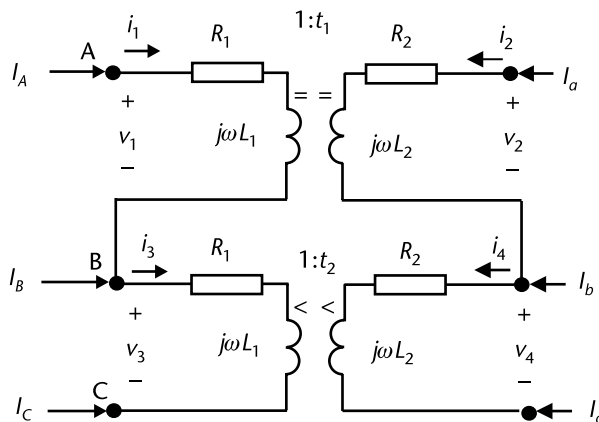


Figure 3.16 Complex transformer, open Δ or V connection.

The node current relations in matrix form are obtained from Figure 3.17. In shorthand notation, we write (3.77).

$$\begin{bmatrix} I_A \\ I_B \\ I_C \\ I_a \\ I_b \\ I_c \end{bmatrix} = \begin{bmatrix} +1 & 0 & 0 & 0 \\ -1 & 0 & +1 & 0 \\ 0 & 0 & -1 & 0 \\ 0 & +1 & 0 & 0 \\ 0 & -1 & 0 & +1 \\ 0 & 0 & 0 & -1 \end{bmatrix} \begin{bmatrix} i_1 \\ i_2 \\ i_3 \\ i_4 \end{bmatrix} \tag{3.76}$$

$$I_{\text{bus}} = A_{VV}^t i \tag{3.77}$$

Equation (3.74), with reference to the reduced transformer connection, and (3.77) into (3.48), the model for open Δ or V is:

$$\begin{bmatrix} -Z & A_{VV} \\ A_{VV}^t & 0 \end{bmatrix} \begin{bmatrix} i \\ V_{\text{bus}}^{ABC,abc} \end{bmatrix} = \begin{bmatrix} 0 \\ I_{\text{bus}} \end{bmatrix} \tag{3.78}$$

Using partial inversion, we find the reduced equivalent, as seen from the three phases ABC and abc . The symmetrical component transformation on the Y_{bus} equivalent matrix can be applied to calculate the sequence admittances, as shown in the following example where $y = Z^{-1}$.

$$\begin{bmatrix} y & -YA_{VV} \\ -A_{VV}^t Y & A_{VV}^t YA_{VV} \end{bmatrix} \begin{bmatrix} 0 \\ V_{\text{bus}}^{ABC,abc} \end{bmatrix} = \begin{bmatrix} i \\ I_{\text{bus}} \end{bmatrix} \tag{3.79}$$

Example 3.11

Consider that for single-phase transformers with a very good magnetic coupling $k \approx 1.0$

$$m = \sqrt{L_1 L_2} = \sqrt{L_1 \left(\frac{N_2}{N_1} \right)^2 L_1} = \frac{N_2}{N_1} L_1 \quad m = \frac{N_1}{N_2} L_2 \tag{3.80}$$

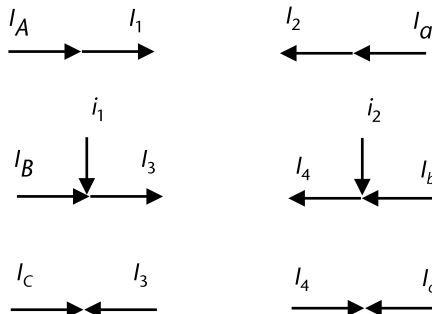


Figure 3.17 A three-phase complex transformer, node currents.

Assuming that $R_1 \ll \omega L_1$ and $R_2 \ll \omega L_2$, the inverse matrix y

$$y = \begin{bmatrix} z_1 & m \\ m & z_2 \end{bmatrix}^{-1} = \frac{1}{z_1 z_2 - m^2} \begin{bmatrix} z_2 & -m \\ -m & z_1 \end{bmatrix} \quad (3.81)$$

Using the following notation:

$$\frac{z_2}{z_1 z_2 - m^2} = y_t \quad (3.82)$$

$$\frac{m}{z_1 z_2 - m^2} = \frac{N_1}{N_2} \frac{L_2}{z_1 z_2 - m^2} = \frac{N_1}{N_2} y_t \quad (3.83)$$

$$\frac{z_1}{z_1 z_2 - m^2} = \frac{N_1}{N_2} \frac{m}{z_1 z_2 - m^2} = \left(\frac{N_1}{N_2} \right)^2 y_t \quad (3.84)$$

The result for the nodal admittance matrix from (3.79) is

$$Y_{\text{bus}} = A_{VV}^t Z A_{VV} \quad (3.85)$$

$$Y_{\text{bus}} = \begin{bmatrix} +z_2 & -z_2 & 0 & -m & +m & 0 \\ -z_2 & +2z_2 & -z_2 & +m & -2m & m \\ 0 & -z_2 & +z_2 & 0 & +m & -m \\ -m & +m & 0 & +z_1 & -z_1 & 0 \\ +m & -2m & +m & -z_1 & +2z_1 & -z_1 \\ 0 & +m & -m & 0 & -z_1 & +z_1 \end{bmatrix} \frac{1}{z_1 z_2 - m^2} \quad (3.86)$$

We write the three-phase nodal matrix using (3.80) to (3.84).

$$Y_{\text{bus}} = \begin{bmatrix} +y_t & -y_t & 0 & -\frac{N_1}{N_2} y_t & +\frac{N_1}{N_2} y_t & 0 \\ -y_t & +2y_t & -y_t & +\frac{N_1}{N_2} y_t & -2\frac{N_1}{N_2} y_t & \frac{N_1}{N_2} y_t \\ 0 & -y_t & +y_t & 0 & +m & -m \\ -\frac{N_1}{N_2} y_t & +\frac{N_1}{N_2} y_t & 0 & +\left(\frac{N_1}{N_2}\right)^2 y_t & -\left(\frac{N_1}{N_2}\right)^2 y_t & 0 \\ +\frac{N_1}{N_2} y_t & -2\frac{N_1}{N_2} y_t & +\frac{N_1}{N_2} y_t & -\left(\frac{N_1}{N_2}\right)^2 y_t & +2\left(\frac{N_1}{N_2}\right)^2 y_t & -\left(\frac{N_1}{N_2}\right)^2 y_t \\ 0 & +\frac{N_1}{N_2} y_t & -\frac{N_1}{N_2} y_t & 0 & -\left(\frac{N_1}{N_2}\right)^2 y_t & +\left(\frac{N_1}{N_2}\right)^2 y_t \end{bmatrix} \quad (3.87)$$

The Y_{bus} matrix in (3.87) can be partitioned into ABC and abc portions, then the symmetrical component transformations can be applied. A P - S notation is used for primary and secondary sides of the VV transformer connection.

$$Y_{\text{bus},012}^{PS} = \begin{bmatrix} T^{-1}Y_I T & T^{-1}Y_{II} T \\ T^{-1}Y_{III} T & T^{-1}Y_{IV} T \end{bmatrix} \quad (3.88)$$

Results for product matrices in (3.88) follow:

$$T^{-1}Y_I T = y_t T^{-1} \begin{bmatrix} +1 & -1 & 0 \\ -1 & +2 & -1 \\ 0 & -1 & +1 \end{bmatrix} \begin{bmatrix} 1 & 1 & 1 \\ 1 & \alpha^2 & \alpha \\ 1 & \alpha & \alpha^2 \end{bmatrix} = y_t \begin{bmatrix} 0 & 0 & 0 \\ 0 & +2 & 1\angle -120^\circ \\ 0 & 1\angle +120^\circ & +2 \end{bmatrix} \quad (3.89)$$

$$T^{-1}Y_{II} T = -\frac{N_1}{N_2} y_t T^{-1} \begin{bmatrix} +1 & -1 & 0 \\ -1 & +2 & -1 \\ 0 & -1 & +1 \end{bmatrix} T = \frac{N_1}{N_2} y_t \begin{bmatrix} 0 & 0 & 0 \\ 0 & -2 & 1\angle +60^\circ \\ 0 & 1\angle -60^\circ & -2 \end{bmatrix} \quad (3.90)$$

$$T^{-1}Y_{III} T = -\frac{N_1}{N_2} y_t T^{-1} \begin{bmatrix} +1 & -1 & 0 \\ -1 & +2 & -1 \\ 0 & -1 & +1 \end{bmatrix} T = \frac{N_1}{N_2} y_t \begin{bmatrix} 0 & 0 & 0 \\ 0 & -2 & 1\angle +60^\circ \\ 0 & 1\angle -60^\circ & -2 \end{bmatrix} \quad (3.91)$$

$$T^{-1}Y_{IV} T = \left(\frac{N_1}{N_2}\right)^2 y_t T^{-1} \begin{bmatrix} +1 & -1 & 0 \\ -1 & +2 & -1 \\ 0 & -1 & +1 \end{bmatrix} T = \left(\frac{N_1}{N_2}\right)^2 y_t \begin{bmatrix} 0 & 0 & 0 \\ 0 & +2 & 1\angle -120^\circ \\ 0 & 1\angle +120^\circ & -+2 \end{bmatrix} \quad (3.92)$$

The nodal matrix written in sequence quantities—as seen from the high voltage side P to the low voltage side S —is:

$$Y_{\text{bus},012}^{PS} = y_t \begin{bmatrix} 0 & 0 & 0 & 0 & 0 & 0 \\ 0 & +2 & 1\angle -120^\circ & 0 & -2\frac{N_1}{N_2} & +\frac{N_1}{N_2}\angle +60^\circ \\ 0 & 1\angle +120^\circ & +2 & 0 & -\frac{N_1}{N_2}\angle -60^\circ & -2\frac{N_1}{N_2} \\ 0 & 0 & 0 & 0 & 0 & 0 \\ 0 & -2\frac{N_1}{N_2} & +\frac{N_1}{N_2}\angle +60^\circ & 0 & +2\left(\frac{N_1}{N_2}\right)^2 & +\left(\frac{N_1}{N_2}\right)^2\angle -120^\circ \\ 0 & +\frac{N_1}{N_2}\angle -60^\circ & -2\frac{N_1}{N_2} & 0 & +\left(\frac{N_1}{N_2}\right)^2\angle +120^\circ & +2\left(\frac{N_1}{N_2}\right)^2 \end{bmatrix} \quad (3.93)$$

The equivalent nodal matrix in sequence quantities is asymmetrical; this means that no equivalent circuit can be drawn. Nodal equation (3.94) will solve for unknowns

that depend on nodal operating conditions. When all sequence nodal voltages are determined, the transformation T_s will take the values back to ABC and abc quantities. Then the phase currents i , power flows, and losses are calculated.

$$Y_{bus,012}^{PS} V_{bus,012}^{PS} = I_{bus,012} \tag{3.94}$$

$$V_{bus}^{ABC,abc} = \begin{bmatrix} T & 0 \\ 0 & T \end{bmatrix} \begin{bmatrix} V_{bus,012}^P \\ V_{bus,012}^S \end{bmatrix} \tag{3.95}$$

$$i = Z^{-1} A_{VV} V_{bus}^{ABC,abc} \tag{3.96}$$

An equivalent three-phase circuit for VV transformer is given by (3.93).

3.5 Autotransformer Model

An autotransformer is a device with N_1 turns in a common winding arrangement and N_2 turns in what is considered a series winding. The arrangement will be in three phases (see Figure 3.18), but in order to obtain an equivalent model, let's start with a single-phase unit (see Figure 3.19).

The voltage relation from high to low voltage can be defined by an overall turn's ratio N . Our goal is to obtain an equivalent as in Figure 3.20.

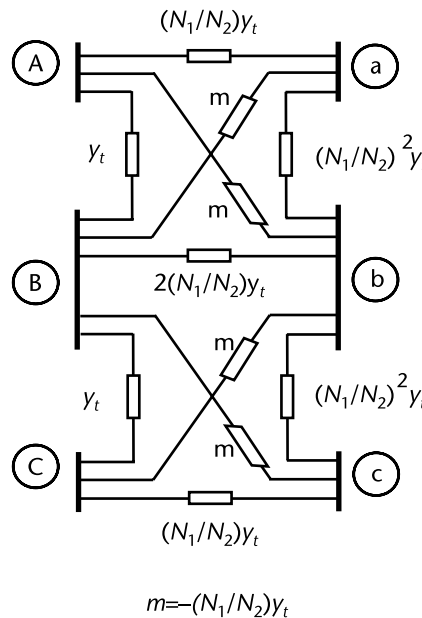


Figure 3.18 Circuit of a three-phase VV bank transformer.

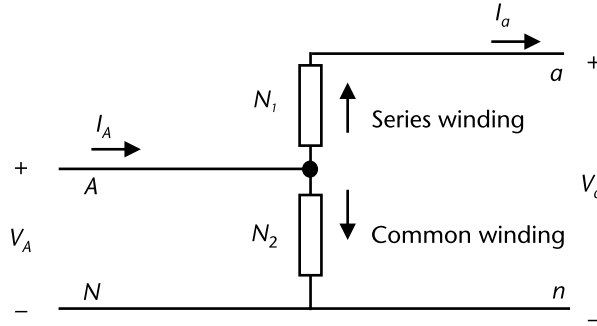


Figure 3.19 Single-phase autotransformer.

$$\frac{V_a}{V_A} = \frac{N_1 + N_2}{N_1} = 1 + \frac{N_2}{N_1} = N \tag{3.97}$$

Two short circuit impedances can be measured in the real autotransformer:

1. Z_{eH} impedance at the high voltage side with N_1 shorted; A is shorted to N.
2. Z_{eL} impedance at the low voltage side with N_2 shorted; A is shorted to a.

When A is shorted to N, in Figure 3.20 we have that the Z_{at} impedance will be reflected to the high voltage side as

$$Z_{eH} = Z_{at}N^2 \tag{3.98}$$

For the second condition, when A is shorted to a, from Figure 3.21 various relations are: $V_A = V_a$, $I_A + I_a = I_L$, $V_L = V_a/N = V_A/N$ and I_L as in (3.99).

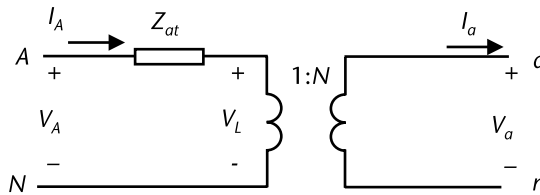


Figure 3.20 Equivalent for an autotransformer.

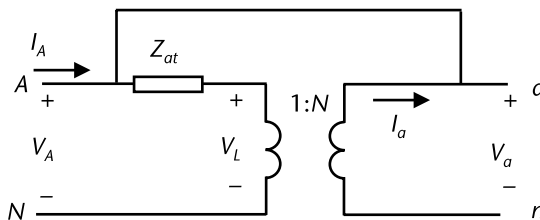


Figure 3.21 Equivalent for an autotransformer.

$$I_L = \frac{V_A - V_L}{Z_{at}} = \frac{V_A - \frac{V_a}{N}}{Z_{at}} = \frac{V_A}{Z_{at}} \left(1 - \frac{1}{N}\right) \quad (3.99)$$

For an ideal transformer (no losses) $V_L I_L = V_a I_a$ and $I_A = (1 - 1/N)I$, then:

$$Z_{eL} = \frac{V_A}{I_A} = \frac{V_A}{I_L \left(1 - \frac{1}{N}\right)} = \frac{V_A}{\frac{V_a}{Z_{at}} \left(1 - \frac{1}{N}\right) \left(1 - \frac{1}{N}\right)} = \frac{Z_{at}}{\left(1 - \frac{1}{N}\right)^2} \quad (3.100)$$

$$Z_{at} = Z_{eL} \frac{(N - 1)^2}{N^2} \quad (3.101)$$

From (3.99)

$$Z_{eH} = Z_{eL} (N - 1)^2 = Z_{at} N^2 \quad (3.102)$$

Example 3.13

For a two winding transformer rated 30 kVA, voltage ratio 220V to 125V, and operating at 60 Hz, obtain an equivalent circuit for the auto-transformer connection (see Figure 3.23). The A side is the 220V with impedance $(0.20 + j0.38) \Omega$, the transformer side a works at 125V with impedance $(0.04 + j0.08) \Omega$. The transformer is going to be used as autotransformer, as shown in Figure 3.22, to feed a load at 125V and connected at the high voltage side to a 345V source.

The equivalent impedances referred to the high-voltage side (see Figure 3.24) or to the low-voltage side, including the transformation ratio are:

$$Z_{eqH} = Z_A + Z_a \left(\frac{N_2}{N_1}\right)^2$$

$$Z_{eqL} = Z_a + \frac{Z_A}{\left(\frac{N_2}{N_1}\right)^2} \quad (3.103)$$

Using (3.97) as $V_a/V_A = (N_1 + N_2)/N_1 = N$, the calculation of the impedance for the equivalent autotransformer, from (3.102) is:

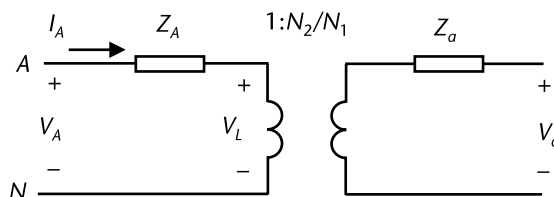


Figure 3.22 Equivalent for an autotransformer.

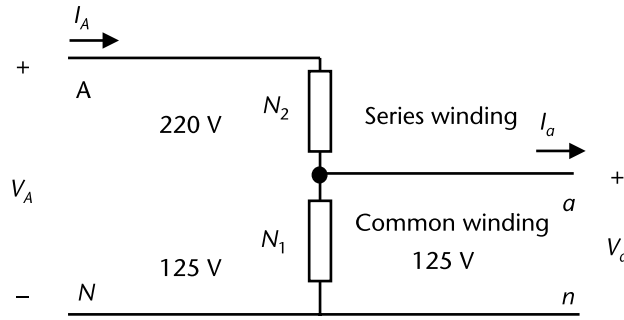


Figure 3.23 Autotransformer connections.

$$Z_{at} = \frac{Z_{eH}}{N^2} = Z_{eL} \frac{(N-1)^2}{N^2} \tag{3.104}$$

Data for one phase transformer

Primary Voltage	Secondary Voltage	Transf. ratio
220.00	125.00	1.760000
Primary Impedance	Secondary Impedance	
ZA = 0.2000+j 0.3800	Za = 0.0400+j 0.0800	

Total Transformer Impedance referred to High Voltage side
 ZeqH = 0.3239+j 0.6278

Total Transformer Impedance referred to Low Voltage side
 ZeqL = 0.1046+j 0.2027

Auto Transformer

Primary Voltage = 345.0000
 Secondary Voltage = 125.0000
 Equivalent relation N = 2.7600

Equivalent Impedance for auto
 Zat = 0.0425+j 0.0824

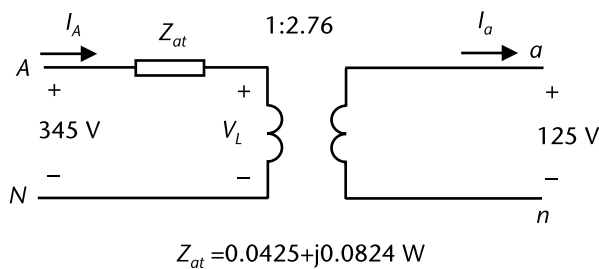


Figure 3.24 Equivalent values for the autotransformer.

3.6 Three Winding Transformer

A three winding transformer is a magnetic arrangement that has one primary, one secondary, and a tertiary winding in the three-phase configuration. It is assumed to be a balanced device and infinite shunt impedance. The primary winding is connected to the source side, the secondary winding might feed a transmission line or a load, and the tertiary winding can feed a load, but it is more commonly used to connect shunt compensating equipment or filter equipment. To include this device in a system's study, an equivalent is derived.

The three impedance values can be obtained by measurements (see Figure 3.25), and then all the impedances are referred to the primary side.

Z_{PS} impedance measured at the primary winding, with secondary shorted, tertiary open.

Z_{PT} impedance measured at the primary winding, with secondary open, tertiary shorted.

Z'_{ST} impedance measured at the secondary winding, with primary open, tertiary shorted.

$$Z_{ST} = Z'_{ST} \left(\frac{N_P}{N_S} \right)^2 \quad (3.105)$$

In matrix form and solving for equivalent impedances:

$$\begin{bmatrix} 1 & 1 & 0 \\ 1 & 0 & 1 \\ 0 & 1 & 1 \end{bmatrix} \begin{bmatrix} Z_P \\ Z_S \\ Z_T \end{bmatrix} = \begin{bmatrix} Z_{PS} \\ Z_{PT} \\ Z_{TS} \end{bmatrix} \quad (3.106)$$

Example 3.13

For a three winding transformer, 60 Hz, with voltages primary 169 kV, secondary 66 kV, and tertiary 33 kV, there are measured values for impedances, all referred

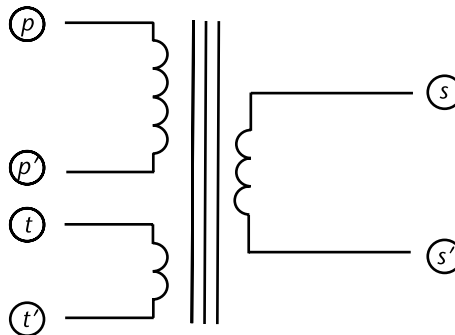


Figure 3.25 Three winding transformer circuit representation.

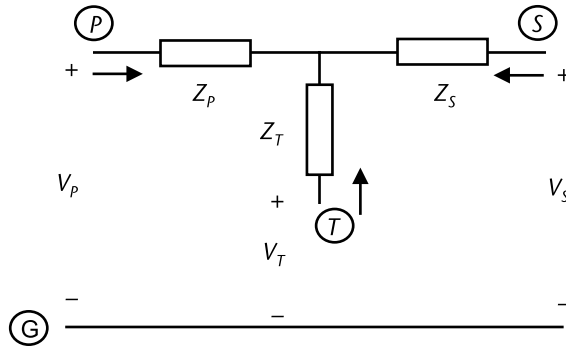


Figure 3.26 Equivalent circuit for a three winding transformer.

to by the primary winding (see Figure 3.26). The transformer unit has a 30 MVA rating. Find the base current and base impedance at each winding. For a reactor of $j50$ ohms/phase connected to the tertiary winding and a load current of 200A and 0.8 lagging power factor at the secondary, calculate the primary voltage when the secondary voltage has a 1.0 pu value and is considered to be the angular reference. Results in Figures 3.27 and 3.28 are for a Y-delta transformation.

Measured impedances, Three winding transformer

$$Z_{PS} = 0.0000 + j 0.1700 \text{ pu}$$

$$Z_{PT} = 0.0000 + j 0.1100 \text{ pu}$$

$$Z_{ST} = 0.0000 + j 0.1000 \text{ pu}$$

Per unit Equivalent impedances

$$Z_P = 0.0000 + j 0.0900$$

$$Z_S = 0.0000 + j 0.0800$$

$$Z_T = 0.0000 + j 0.0200$$

Base MVA, KV, Currents and Impedances

$$MVA_B = 30.0000 \quad KVP = 169.0000 \quad KVS = 66.0000 \quad KVT = 33.0000$$

$$IPB = 102.4882 \text{ A}$$

$$ISB = 262.4319 \text{ A}$$

$$ITB = 524.8639 \text{ A}$$

$$Z_{PB} = 952.0333 \text{ Ohms}$$

$$Z_{SB} = 145.2000 \text{ Ohms}$$

$$Z_{TB} = 36.3000 \text{ Ohms}$$

Impedance in tertiary

$$Z_{Ohmster} = 0.0000 + j 50.0000 \text{ Ohms} \quad Z_{terpu} = 0.0000 + j 1.3774 \text{ pu}$$

Secondary current (magnitude pu and angle)

$$I_{secondary} = 0.7621 \quad -36.87$$

Currents(magnitude pu and angle)

$$I_{tertiary} = 0.7426 \quad -87.31$$

$$I_{primary} = 1.3613 \quad -61.74$$

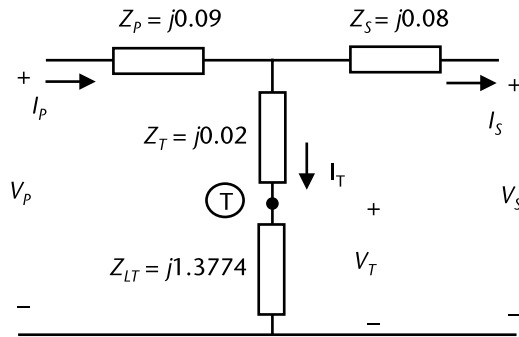
Voltages(magnitude pu and angle)

V_{primary} = 1.1495 5.33
 V_{secondary} = 1.0000 0.00
 V_{tertiary} = 1.0229 2.69

Delta Equivalent Impedances(pu)

Z_{Pri_Sec} = 0.0000 +j 0.5300
 Z_{Pri_Ter} = 0.0000 +j 0.1325
 Z_{Sec_Ter} = 0.0000 +j 0.1178

In three winding transformers, the tertiary winding can be used to supply load, to connect a reactive compensating device (as in the Example 3.13), or to connect filter arrangements for harmonic suppression.



$$I_P = 1.3613 \angle -61.74^\circ \quad V_P = 1.1495 \angle 5.33^\circ$$

$$I_S = 0.7621 \angle -36.87^\circ \quad V_S = 1.0 \angle 0^\circ$$

$$I_T = 0.7426 \angle -87.31^\circ \quad V_T = 1.0229 \angle 2.69^\circ$$

Figure 3.27 Currents and voltage for a three-winding transformer.

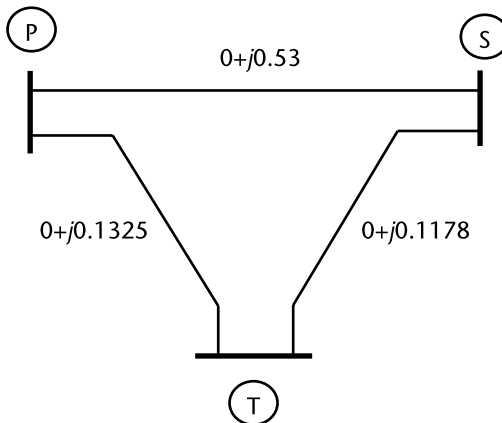


Figure 3.28 Delta equivalent of a three winding transformer; impedances in pu.

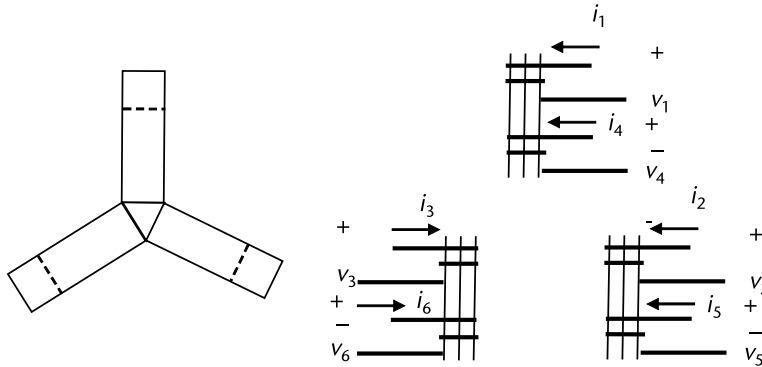


Figure 3.29 Three-phase transformer; core and windings.

3.7 Three-Phase Transformer

A three-phase transformer is a magnetic arrangement in which all windings are located and are magnetically coupled (see Figure 3.29); in this case, the primitive matrix that relates voltage at windings and currents is a full matrix. The self and the mutual impedances depend on the common magnetic flux that each winding shares with all the other windings in the structure. With no loss in generality, let us consider a configuration in which three windings will be connected in Y and the other three windings will be connected as Δ.

In matrix notation voltage v , relations to nodal voltages allow us to get the connectivity matrix.

$$\begin{bmatrix} v_1 \\ v_2 \\ v_3 \\ v_4 \\ v_5 \\ v_6 \\ v_7 \end{bmatrix} = \begin{bmatrix} +1 & 0 & 0 & 0 & 0 & 0 & -1 \\ 0 & +1 & 0 & 0 & 0 & 0 & -1 \\ 0 & 0 & +1 & 0 & 0 & 0 & -1 \\ 0 & 0 & 0 & +1 & -1 & 0 & 0 \\ 0 & 0 & 0 & 0 & +1 & -1 & 0 \\ 0 & 0 & 0 & -1 & 0 & +1 & 0 \\ 0 & 0 & 0 & 0 & 0 & 0 & +1 \end{bmatrix} \begin{bmatrix} V_A \\ V_B \\ V_C \\ V_a \\ V_b \\ V_c \\ V_N \end{bmatrix} \tag{3.107}$$

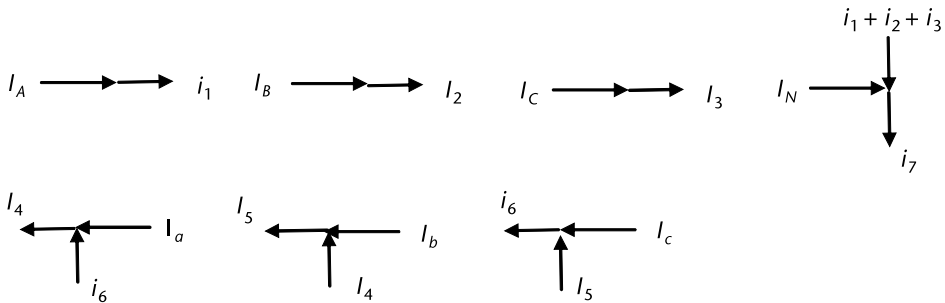


Figure 3.30 A three-phase complex transformer, node currents.

$$v = A_{YY} V_{\text{bus}}^{ABC,abc,N} \quad (3.108)$$

Node current relations in matrix form are obtained from Figure 3.30 and are:

$$\begin{bmatrix} I_A \\ I_B \\ I_C \\ I_a \\ I_b \\ I_c \\ I_N \end{bmatrix} = \begin{bmatrix} +1 & 0 & 0 & 0 & 0 & 0 & 0 \\ 0 & +1 & 0 & 0 & 0 & 0 & 0 \\ 0 & 0 & +1 & 0 & 0 & 0 & 0 \\ 0 & 0 & 0 & +1 & 0 & -1 & 0 \\ 0 & 0 & 0 & -1 & +1 & 0 & 0 \\ 0 & 0 & 0 & 0 & -1 & +1 & 0 \\ -1 & -1 & -1 & 0 & 0 & 0 & +1 \end{bmatrix} \begin{bmatrix} i_1 \\ i_2 \\ i_3 \\ i_4 \\ i_5 \\ i_6 \\ i_7 \end{bmatrix} \quad (3.109)$$

$$I_{\text{bus}} = A_{YY}^t i \quad (3.110)$$

With (3.108) and (3.110) the model is built using (3.48).

$$\begin{bmatrix} -Z & A_{YY} \\ A_{YY}^t & 0 \end{bmatrix} \begin{bmatrix} i \\ V_{\text{bus}}^{ABC,abc,N} \end{bmatrix} = \begin{bmatrix} 0 \\ I_{\text{bus}} \end{bmatrix} \quad (3.111)$$

With partial inversion on (3.111), we exchange the current vector i with the array of 0's in the right hand side. What is left is a Norton's equivalent that includes node N .

$$\begin{bmatrix} +y & -yA_{YY} \\ -A_{YY}^t y & A_{YY}^t y A_{YY} \end{bmatrix} \begin{bmatrix} 0 \\ V_{\text{bus}}^{ABC,abc,N} \end{bmatrix} = \begin{bmatrix} i \\ I_{\text{bus}} \end{bmatrix} \quad (3.112)$$

If we are only interested in terminal nodes ABC and abc , node N must be eliminated. Most times I_N has a value of zero. Additional steps of partial inversion will do the job and leave us with a Norton's equivalent, as seen from the three-phase nodes at the high and low voltage sides of the transformer.

$$\begin{bmatrix} Y_{\text{bus}}^{ABC,abc} & Y_{\text{bus}}^{ABC,abc,N} \\ Y_{\text{bus}}^{N,ABC,abc} & Y_{NN} \end{bmatrix} \begin{bmatrix} V_{\text{bus}}^{ABC,abc} \\ V_N \end{bmatrix} = \begin{bmatrix} I_{\text{bus}}^{ABC,abc} \\ 0 \end{bmatrix} \quad (3.113)$$

$$\left[Y_{\text{bus}}^{ABC,abc} \right]^{eq} \begin{bmatrix} V_{\text{bus}}^{ABC,abc} \end{bmatrix} = \begin{bmatrix} I_{\text{bus}}^{ABC,abc} \end{bmatrix} \quad (3.114)$$

Example 3.14

For a three-phase transformer, the values of primitive impedances are given in the array Z . There is mutual coupling between all windings; given the type of arrangement for the core, values are in pu. The connection is $Y\Delta$ and the connectivity

matrix A has this type of information. Calculate Y_{bus} , including neutral node N at the Y side of the transformer. Eliminate node N to get the $Y_{\text{bus},ABC,abc}$ and then apply symmetrical components transformation to get the sequence admittances.

$Z =$

Columns 1 through 4

0.0100 + 0.1000i	0 + 0.0400i	0 + 0.0400i	0 + 0.0800i
0 + 0.0400i	0.0100 + 0.1000i	0 + 0.0400i	0 + 0.0400i
0 + 0.0400i	0 + 0.0400i	0.0100 + 0.1000i	0 + 0.0400i
0 + 0.0800i	0 + 0.0400i	0 + 0.0400i	0.0100 + 0.1000i
0 + 0.0400i	0 + 0.0800i	0 + 0.0400i	0 + 0.0400i
0 + 0.0400i	0 + 0.0400i	0 + 0.0800i	0 + 0.0400i
0	0	0	0

Columns 5 through 7

0 + 0.0400i	0 + 0.0400i	0
0 + 0.0800i	0 + 0.0400i	0
0 + 0.0400i	0 + 0.0800i	0
0 + 0.0400i	0 + 0.0400i	0
0.0100 + 0.1000i	0 + 0.0400i	0
0 + 0.0400i	0.0100 + 0.1000i	0
0	0	0 + 1.0000i

$A =$

1	0	0	0	0	0	-1
0	1	0	0	0	0	-1
0	0	1	0	0	0	-1
0	0	0	1	-1	0	0
0	0	0	0	1	-1	0
0	0	0	-1	0	1	0
0	0	0	0	0	0	1

$Y_{\text{bus}ABCabc} =$

Columns 1 through 4

0.0100 + 0.1000i	0.0000 + 0.0400i	0.0000 + 0.0400i	0 + 0.0400i
0.0000 + 0.0400i	0.0100 + 0.1000i	0.0000 + 0.0400i	0
0.0000 + 0.0400i	0.0000 + 0.0400i	0.0100 + 0.1000i	0 - 0.0400i
0 + 0.0400i	0	0 - 0.0400i	0.0200 + 0.1200i
0 - 0.0400i	0 + 0.0400i	0	-0.0100 - 0.0600i
0	0 - 0.0400i	0 + 0.0400i	-0.0100 - 0.0600i

Columns 5 through 6

0 - 0.0400i	0
0 + 0.0400i	0 - 0.0400i
0	0 + 0.0400i
-0.0100 - 0.0600i	-0.0100 - 0.0600i
0.0200 + 0.1200i	-0.0100 - 0.0600i
-0.0100 - 0.0600i	0.0200 + 0.1200i

Y_{bus} , symmetrical components =

Columns 1 through 4

0.0100 + 0.1800i	-0.0000 - 0.0000i	-0.0000 + 0.0000i	0
0.0000 + 0.0000i	0.0100 + 0.0600i	0.0000 - 0.0000i	0 - 0.0000i

```

-0.0000 + 0.0000i    0.0000 + 0.0000i    0.0100 + 0.0600i    0 + 0.0000i
      0              0.0000 - 0.0000i    0.0000 + 0.0000i    0.0000
      0              0.0346 + 0.0600i    0.0000              0 + 0.0000i
-0.0000             0.0000 - 0.0000i    -0.0346 + 0.0600i    0 - 0.0000i
Columns 5 through 6
0.0000 + 0.0000i    0.0000 - 0.0000i
-0.0346 + 0.0600i  -0.0000 - 0.0000i
0.0000 + 0.0000i    0.0346 + 0.0600i
0.0000 - 0.0000i    0.0000 + 0.0000i
0.0300 + 0.1800i    0.0000 - 0.0000i
0.0000 - 0.0000i    0.0300 + 0.1800i
    
```

Sequence networks, Y side to D side

Ybus0 =

```

0.0100 + 0.1800i    0
      0              0.0000
    
```

Ybus1 =

```

0.0100 + 0.0600i  -0.0346 + 0.0600i
0.0346 + 0.0600i  0.0300 + 0.1800i
    
```

Ybus2 =

```

0.0100 + 0.0600i  0.0346 + 0.0600i
-0.0346 + 0.0600i  0.0300 + 0.1800i
    
```

Once the model is derived it can be used to study three-phase power transformer voltages, currents, and power flows in either balanced or unbalanced cases. The neutral can be connected to Earth through a neutral impedance, and then studies to determine the transformer electric behavior can be conducted. To account for losses, a circuit component can be connected and easily added to the Y_{bus} circuit just derived.

3.8 Alternate Model for a Single-Phase Transformer

A different analysis for a single-phase transformer is considered if we start from Figure. 3.31.

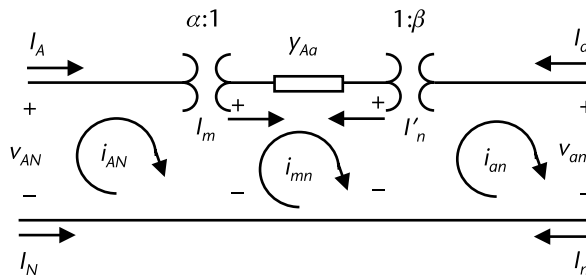


Figure 3.31 Alternative circuit for a single-phase transformer.

$$\begin{bmatrix} -1 & \frac{+y_{Aa}}{|\alpha|^2} & \frac{-y_{Aa}}{\alpha^* \beta} & \frac{-y_{Aa}}{|\alpha|^2} & \frac{+y_{Aa}}{\alpha^* \beta} \\ +1 & 0 & 0 & 0 & 0 \\ -\frac{\alpha^*}{\beta^*} & 0 & 0 & 0 & 0 \\ -1 & 0 & 0 & 0 & 0 \\ +\frac{\alpha^*}{\beta^*} & 0 & 0 & 0 & 0 \end{bmatrix} \begin{bmatrix} i_{AN} \\ V_A \\ V_a \\ V_N \\ V_n \end{bmatrix} = \begin{bmatrix} 0 \\ I_A \\ I_a \\ I_N \\ I_n \end{bmatrix} \quad (3.115)$$

Example 3.13

Assume a single-phase transformer with values in p.u., $y_{Aa} = -j10$, $y_N = 0.1$, $y_n = 0.2$, $V_A = 1 \angle 0^\circ$, $\alpha = 1 \angle 10^\circ$, $\beta = 1 \angle -10^\circ$ to study the no load condition $I_a = 0$, $I_N = 0$, $I_n = 0$

```

Y =
- 1.                - 10.i   - 3.4202014 + 9.3969262i   10.i
  1.                0         0
- 0.9396926 + 0.3420201i  0         0
- 1.                0         0
  0.9396926 - 0.3420201i  0         0

```

```

3.4202014 - 9.3969262i
0
0
0
0.2

```

```

pivots = 1.    3.    4.    5.
V( 1) = 1.00000000 +j 0.00000000
I( 2) = -0.10000000 +j 0.00000000
I( 3) = 0.00000000 +j 0.00000000
I( 4) = 0.00000000 +j 0.00000000

```

```

Y =
- 9.861D-31 + 5.551D-17i   4.441D-16 - 1.776D-15i
- 9.861D-31 + 5.551D-17i   4.441D-16 - 1.776D-15i
  0.0342020 + 0.0939693i   0.9396926 - 0.3420201i
- 9.861D-30 + 5.551D-16i   4.441D-15 - 1.776D-14i
  0                          0

  0.9396926 + 0.3420201i   4.441D-15 - 1.776D-14i   0
  0.9396926 + 0.3420201i   4.441D-15 - 1.776D-14i   0
- 15. - 0.1i              9.3969262 - 3.4202014i   - 5.
  9.3969262 + 3.4202014i  -10. - 1.776D-13i           0
- 5.                        0                          - 5.

```

```

I( 1) = 0.09396926 +j 0.03420201
V( 2) = -0.56030738 +j -0.35202014

```

$$V(3) = 0.93969262 + j 0.34202014$$

$$V(4) = -0.50000000 + j 0.00000000$$

3.9 Function for the Partial Inversion Algorithm

```
function [W]=inverpark(W, k)
// k -- pivot, diagonal element
// n - number of rows
// m - number of columns
// For square matrices: m=n, this will be in most cases
[n, m]=size(W);
pivot=-1/W(k,k);
// Pivot is modified
W(k,k)=pivot;
// Row pivot is modified (except pivot value)
for j9=1:n
    if j9~=k
        W(k,j9)=W(k,j9)*pivot;
    else
        end
end
for i9=1:n // Changes for elements not in pivot row or pivot column
    if i9~=k
        for j9=1:n
            if j9~=k
                W(i9,j9)=W(i9,j9)+W(i9,k)*W(k,j9);
            else
                end
            end
        else
            end
    end
end
// Changes to elements in pivot column (except pivot)
for i9=1:n
    if i9~=k
        W(i9,k)=W(i9,k)*pivot;
    else
        end
    end
end
endfunction

function [W]=pivoteo(W, pivotes)
// Function to conduct partial inversion process
// pivot number is needed and which are those pivots
// results are on matrix W
npiv=length(pivotes);
for k9=1:npiv
    k=pivotes(k9);
    [W]=inverpark(W,k);
end
```

```

end
endfunction

function y=solucpark(W, x, y, pivotes)
// k -- pivot, on the diagonal of the matrix
// n - number of rows
// m - number of columns
// For square matrices m=n, this is assumed as true
// npiv - number of pivots (might go from 1 to n)
// x information vector that might have zeroes in pivot and known
//   values in those that are not pivots
// y is a vector with a known value in the pivots, they might be zero
//   in those that are no pivots
// they will be calculated in the solution process
[n,m]=size(W);
npiv=length(pivotes);
// Information Exchange in the pivot, with the NEGATIVE
// All the known values will stay in the x vector
for j9=1:npiv
    k=pivotes(j9);
    x(k)=-y(k);
end
// By matrix multiplication by the vector of known values we calculate
//   the unknowns
y=W*x;
endfunction

```

References

- [1] Stagg, G., and A. E. El-Abaid, *Computer Methods in Power System Analysis*, New York: McGraw-Hill Inc., 1968.
- [2] Brown, H. E., *Solution of Large Networks by Matrix Methods*, New York: John Wiley & Sons, 1975.
- [3] Shipley, R. B., *Introduction to Matrices and Power Systems*, New York: John Wiley & Sons, 1976.
- [4] Clarke, E., *Circuit Analysis of AC Power Systems, Volume I: Symmetrical and Related Components*, Schenectady, New York: John Wiley & Sons, 1943.
- [5] Elgerd, O. I., *Electric Energy Systems Theory*, New York: McGraw-Hill Book Company, 1971.
- [6] Chen, M. S., and W. E. Dillon, "Power System Modelling," *Proc. IEEE*, Vol. 62, 1974, pp. 901–915.

Transmission Line and Cable Modeling

4.1 Introduction

High-voltage transmission lines mainly operating in AC are required in order to transport energy from electric power plants scattered over a territory where primary energy sources are located in order to reach the consumption places. The principles under which this is possible are based on electromagnetic laws and concepts associated with Ampere's, Faraday's, and Gauss's laws. The value of series impedance that a transmission line presents when power has to flow from the sending to the receiving end is of paramount importance. The shunt admittance is a key component for long distance lines operating at high voltage and cables. Several considerations are applied to derive a useful transmission line model for a three-phase system and the working models to simplify calculations when a balanced condition is met.

4.2 Series Inductance

In this section, we apply Faraday's law of induced voltage and Ampere's law as the departing point to characterize, in various steps and with circuit interpretation, the electromagnetic phenomena of sending current through a conductor, and as a consequence, electric power from the power plants to load centers, usually at various hundreds of kilometers away. The series impedance of transmission lines is present at low frequencies (50 Hz or 60 Hz for most AC electric power systems in the world). This will be characterized through the procedures that are explained in this chapter. Series impedance is composed of resistance R_L and reactance X_L . To obtain the series inductance, we start using Ampere's law with the following assumptions:

- A straight and cylindrical shape conductor with uniform current distribution, and
- Earth as a return path for current that flows in a conducting arrangement.

The initial discussion is for a single conductor and its return path. We then generalize the results to include arrangements of multiple conductors in single-phase or three-phase arrangements.

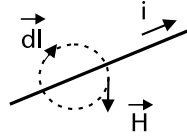


Figure 4.1 Conductor carrying current i .

4.2.1 Single Conductor

The series inductance for a single conductor transmission line can be derived assuming a single-phase conductor and its return path in parallel but at a great distance. In a linear magnetic environment, the magnetic flux linkages λ (webers-turn) and inductance L (henrys) at any instant of time t are related to current i (amperes) by

$$L = \frac{\lambda}{i} \quad (4.1)$$

To relate geometry, magnetic media properties, and circuit representation using current i , voltage v , and magnetic flux ϕ we start with Ampere's law:

$$\oint \vec{H} \cdot d\vec{l} = i_{\text{enclosed}} \quad (4.2)$$

\vec{H} Magnetic field intensity, amperes/m

$d\vec{l}$ Vector of differential distance along the circular trajectory, m

i current in amperes

The intensity of the magnetic field H (A/m) for the conductor in Figure 4.1 has two parts:

H_{int} for a trajectory internal to the conductor and up to radius x (in this case, only a portion of the total current is enclosed; see Figure 4.2), assuming uniform current distribution the proportion of current enclosed has a ratio $\pi x^2 / \pi R^2$, and H_{ext} is for a trajectory external to the conductor's radius $r(m)$. In this case, all of the circulating current i (amperes) flows within the conductor. Distances r and x are in meters.

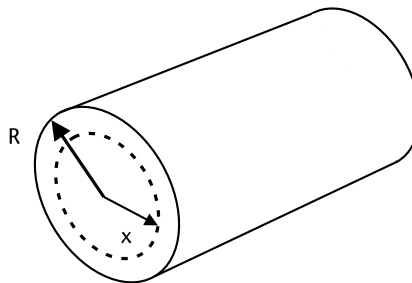


Figure 4.2 Magnetic field intensity outside and inside a round conductor.

$$H_{\text{int}} = \frac{1}{2\pi x} \frac{\pi x^2}{\pi R^2} i \quad (4.3)$$

$$H_{\text{ext}} = \frac{1}{2\pi r} i \quad (4.4)$$

We write the magnetic flux density B (Wb/m²) as μH for each component in (4.3) and (4.4). In what follows, $\mu_0 = 4\pi \times 10^{-7}$ H/m is the magnetic permeability for free space and $\mu = \mu_0 \mu_r$ for any magnetic flux in a magnetic material; μ_r is the relative permeability.

$$B_{\text{int}} = \mu_0 \mu_r \frac{x}{2\pi R^2} i \quad (4.5)$$

$$B_{\text{ext}} = \mu_0 \frac{1}{2\pi r} i \quad (4.6)$$

Flux linkages λ (Wb-turns) to be used in (4.1) are products of the magnetic flux ϕ (Wb) multiplied by the number of turns of the coil structure. To find the total flux ϕ , we write a differential flux $d\phi$ and integrate it over the area with a length of 1 m along the conductor (see Figure 4.3). The equivalent turns N inside the conductor are taken as x^2/R^2 , due to the uniform current distribution assumption. The number of turns for the trajectory outside the conductor is $N = 1$. The internal differential flux linkages (4.7) are integrated inside the conductor with $\mu_r = 1$ for nonmagnetic materials, such as copper and aluminum. For the external differential flux linkages, (4.8) with μ_0 is integrated outside of the conductor from the radial distance R up to a distance S (in meters).

$$d\lambda_{\text{int}} = B_{\text{int}} dA = \frac{\mu_0 \mu_r N i}{2\pi R^2} x dx \quad (4.7)$$

$$d\lambda_{\text{ext}} = B_{\text{ext}} dA = \mu_0 \frac{N i}{2\pi} \frac{dr}{r} \quad (4.8)$$

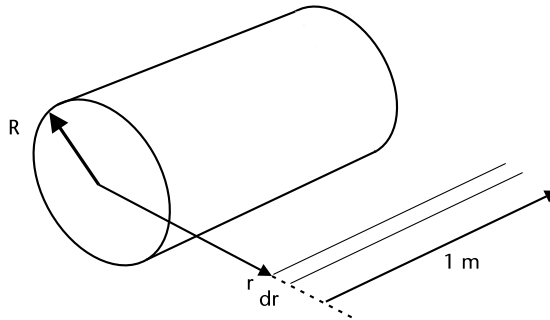


Figure 4.3 Round conductor and its external geometry, 1 m length along the conductor.

$$\lambda_{\text{int}} = \frac{\mu_o i}{2\pi R^4} \int_0^R x^3 dx = \frac{\mu_o i}{8\pi} \quad (4.9)$$

$$\lambda_{\text{ext}} = \mu_o \frac{i}{2\pi} \int_R^S \frac{dr}{r} = \frac{\mu_o i}{2\pi} \ln\left(\frac{S}{R}\right) \quad (4.10)$$

For the single conductor in Figure 4.1

$$L_{\text{tot}} = \frac{\lambda_{\text{ext}}}{i} + \frac{\lambda_{\text{ext}}}{i} = \frac{\mu_o}{8\pi} + \frac{\mu_o}{2\pi} \ln\left(\frac{S}{R}\right) \quad (4.11)$$

$$L_{\text{tot}} = \frac{\mu_o}{2\pi} \left[\frac{1}{4} + \ln\left(\frac{S}{R}\right) \right] = \frac{\mu_o}{2\pi} \ln\left(\frac{S}{R e^{-1/4}}\right) = \frac{\mu_o}{2\pi} \ln\left(\frac{S}{\text{GMR}}\right) \quad (4.12)$$

GMR Equivalent radius of the solid conductor with radius R is
 $R e^{-1/4} = 0.7788 R$

4.2.2 Inductance for a Set of Aerial Conductors

One practical arrangement for a transmission line is a set of parallel conductors carrying a net zero current; some conductors will carry current $+i$ in the forward direction and other conductors will bring back the current, $-i$. Consider three conductors (see Figure 4.4) in the line transmission array so that the combined net flux linkages at a given point (x_p, y_p) is calculated by superposition according to the linear nature of the media where the conductors are located.

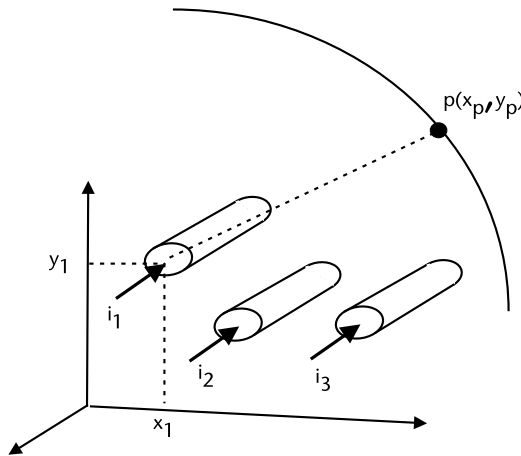


Figure 4.4 Set of three parallel conductors; 1 m length.

The flux linkages due to i_1 , i_2 , and i_3 at point p with coordinates (x_p, y_p) . Distances d_{pk} , x_p , y_p are in meters, then

$$\begin{bmatrix} \lambda_{p1} \\ \lambda_{p2} \\ \lambda_{p3} \end{bmatrix} = \begin{bmatrix} \frac{\mu_o i_1}{2\pi} \ln\left(\frac{S}{d_{p1}}\right) \\ \frac{\mu_o i_2}{2\pi} \ln\left(\frac{S}{d_{p2}}\right) \\ \frac{\mu_o i_3}{2\pi} \ln\left(\frac{S}{d_{p3}}\right) \end{bmatrix} \quad (4.13)$$

$$d_{pk} = \sqrt{(x_p - x_k)^2 + (y_p - y_k)^2} \quad k = 1, 2, 3 \quad (4.14)$$

The total flux linkages at point $p(x_p, y_p)$, $\lambda_{\text{tot},p}$ shows that when $i_1 + i_2 + i_3 = 0$ the flux linkages due to currents i_1 , i_2 , and i_3 will be:

$$\lambda_{\text{tot},p} = \lambda_{p1} + \lambda_{p2} + \lambda_{p3} = \frac{\mu_o}{2\pi} \left[\ln\left(\frac{1}{d_{p1}}\right) \ln\left(\frac{1}{d_{p2}}\right) \ln\left(\frac{1}{d_{p3}}\right) \right] \begin{bmatrix} i_1 \\ i_2 \\ i_3 \end{bmatrix} \quad (4.15)$$

Equation (4.15) can be used to calculate the total flux linkages when the point p is moved to be coincident with the geometrical center of each conductor, one at a time, as point $p = 1, 2$ and 3 . The geometric mean radius (GMR) is the mean geometric distance for each conductor; for more detail, please take a look at Section 4.6.

$$\begin{bmatrix} \lambda_{\text{tot},1} \\ \lambda_{\text{tot},2} \\ \lambda_{\text{tot},3} \end{bmatrix} = \frac{\mu_o}{2\pi} \begin{bmatrix} \ln\left(\frac{1}{d_{11}}\right) & \ln\left(\frac{1}{d_{12}}\right) & \ln\left(\frac{1}{d_{13}}\right) \\ \ln\left(\frac{1}{d_{21}}\right) & \ln\left(\frac{1}{d_{22}}\right) & \ln\left(\frac{1}{d_{23}}\right) \\ \ln\left(\frac{1}{d_{31}}\right) & \ln\left(\frac{1}{d_{32}}\right) & \ln\left(\frac{1}{d_{33}}\right) \end{bmatrix} \begin{bmatrix} i_1 \\ i_2 \\ i_3 \end{bmatrix} \quad (4.16)$$

Equation (4.16) allows us to recognize that along the main diagonal $d_{11} = \text{GMR}_1$, $d_{22} = \text{GMR}_2$, and $d_{33} = \text{GMR}_3$, and that the flux linkages depend on the geometric arrangement of the conductors. The notation \ln means natural logarithms that are to be taken to each element in the matrix. GMR_k must have the same distance units as the distance d_{kj} (meters). The coefficient matrix in (4.16) can be called a *geometric inductance matrix*. The next step is to obtain the series reactance matrix. According to Faraday's law, the induced voltage in phasor form, assuming AC steady state operation, is (4.18).

$$[L] = \frac{\mu_o}{2\pi} \ln \begin{bmatrix} 1/\text{GMR}_1 & 1/d_{12} & 1/d_{13} \\ 1/d_{21} & 1/\text{GMR}_2 & 1/d_{23} \\ 1/d_{31} & 1/d_{32} & 1/\text{GMR}_2 \end{bmatrix} \tag{4.17}$$

$$\Delta V = j\omega[L]i \tag{4.18}$$

When frequency f is 60 Hz and $\mu_o = 4\pi \times 10^{-7}$ H/m, a factor in Ω/km can be used as $\omega\mu_o/2\pi = 0.4 f\pi 10^{-3} = 0.075398$.

Example 4.1

Calculate the reactance matrix in Ω/km for a transmission line that has an arrangement with three conductors (see Figure 4.5). Distance values are shown in meters. Frequency $f = 60$ Hz, reactance in ohms/km. Here, code 0 means a retained conductor, -1, is a ground wire that (in this arrangement) is considered to be a return conductor.

```

Number of conductors = 3   Frequency = 60 Hz
i      x(i)      y(i)      GMR(i)      code(i)
1      0.000      8.000      1.000000e-002    0
2      4.000      8.000      1.000000e-002    0
3      8.000      8.000      5.000000e-003    -1
Inductance matrix L, henrys/km
1.0e-005 *
0.09210340371976 -0.02772588722240 -0.04158883083360
-0.02772588722240 0.09210340371976 -0.02772588722240
-0.04158883083360 -0.02772588722240 0.10596634733096
Xinduc, in  $\Omega/\text{km}$ 
0.34722165179594 -0.10452413233457 -0.15678619850186
-0.10452413233457 0.34722165179594 -0.10452413233457
-0.15678619850186 -0.10452413233457 0.39948371796323
    
```

With a closer look into numerical results, we observe that the reactance matrix is not exactly symmetrical. This is due to the geometry at which the conductors are

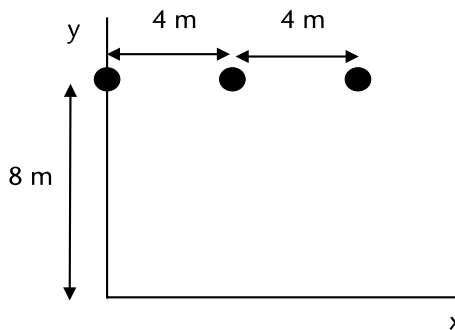


Figure 4.5 Set of three parallel conductors; simple transmission line.

located and not forming an equilateral triangle. More will be said in Section 4.2.5 on how to calculate the total inductance and how to build symmetry in three-phase arrangement of transmission line conductors.

4.2.3 Set of Bundled Conductors

In various situations, two or more conductors make a bundle. In such cases, we might be required to calculate the arrangement's equivalent impedance; the equivalent impedance can replace the arrangement with an equivalent conductor. The physical constraints that must be met are illustrated in Figure 4.6. To explain the constraint that this bundle has, consider that conductors 1 and 3 operate in parallel. There are two constraints listed as (4.19): one for the voltage drop along the line and one for the total current that the bundled conductors must handle. Let us assume that the unreduced series impedance matrix for all three conductors as in (4.20).

$$\begin{aligned}\Delta V_3 &= \Delta V_1 \\ I_1' &= I_1 + I_3\end{aligned}\quad (4.19)$$

$$\begin{bmatrix} z_{11} & z_{12} & z_{13} \\ z_{21} & z_{22} & z_{23} \\ z_{31} & z_{32} & z_{33} \end{bmatrix} \begin{bmatrix} I_1 \\ I_2 \\ I_3 \end{bmatrix} = \begin{bmatrix} \Delta V_1 \\ \Delta V_2 \\ \Delta V_3 \end{bmatrix}\quad (4.20)$$

To comply with the first constraint, voltages should be $\Delta V_3 = \Delta V_1$. To comply with this condition we subtract the first row components to the third row. The modified matrix equation follows.

$$\begin{bmatrix} z_{11} & z_{12} & z_{13} \\ z_{21} & z_{22} & z_{23} \\ z_{31} - z_{11} & z_{32} - z_{12} & z_{33} - z_{13} \end{bmatrix} \begin{bmatrix} I_1 \\ I_2 \\ I_3 \end{bmatrix} = \begin{bmatrix} \Delta V_1 \\ \Delta V_2 \\ \Delta V_3 - \Delta V_1 \end{bmatrix} = \begin{bmatrix} \Delta V_1 \\ \Delta V_2 \\ 0 \end{bmatrix}\quad (4.21)$$

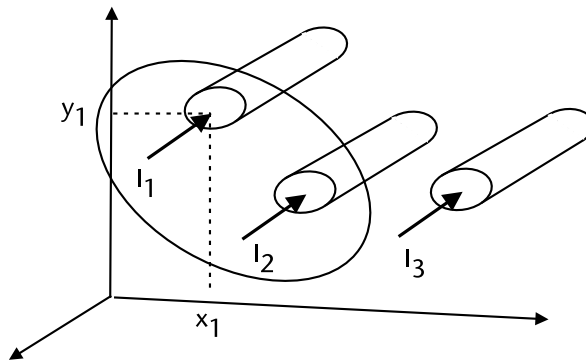


Figure 4.6 Set of parallel conductors, 1 and 3 make up a bundle.

The current constraint in (4.19) requires that the total current I'_1 on the equivalent conductor should be $I_1 + I_3$. This current expression multiplies elements of the first column; in order to keep an unaltered system of equations, we must subtract the appropriate term from the third column. One further step is required—a *partial inversion* procedure to interchange current I_3 and 0 in (4.22). The matrix is modified by the partial inversion to be as in (4.23). The equivalent impedance matrix for the two remaining conductors is a 2×2 array, which we take out of the upper left array in (4.23).

$$\begin{bmatrix} z_{11} & z_{12} & z_{13} - z_{11} \\ z_{21} & z_{22} & z_{23} - z_{21} \\ z_{31} - z_{11} & z_{32} - z_{12} & z_{33} - 2z_{13} + z_{11} \end{bmatrix} \begin{bmatrix} I_1 + I_3 \\ I_2 \\ I_3 \end{bmatrix} = \begin{bmatrix} \Delta V_1 \\ \Delta V_2 \\ 0 \end{bmatrix} \quad (4.22)$$

$$\begin{bmatrix} z'_{11} & z'_{12} & m'_{13} \\ z'_{21} & z'_{22} & m'_{23} \\ m'_{31} & m'_{32} & y_{33} \end{bmatrix} \begin{bmatrix} I'_1 \\ I_2 \\ 0 \end{bmatrix} = \begin{bmatrix} \Delta V_1 \\ \Delta V_2 \\ I_3 \end{bmatrix} \quad (4.23)$$

Example 4.2

An arrangement of conductors is comprised of a single-phase transmission line, three main wires, and a return circuit with two conductors, each with its own GMR (see Figure 4.7). The equivalent reduced impedance matrix is obtained and then the total line impedance in Ω/km is calculated. In our case, a simple code helps us identify which conductors form a bundle; zero is assigned for a retained conductor, and 1 or 2 identifies which main conductor is associated with.

Number of conductors = 5

Frequency = 60

i	x(i)	y(i)	GMR(i)	res(i)	code(i)
1	0.000	12.192	1.978154e-003	0.000000e+000	0
2	9.144	12.192	3.956308e-003	0.000000e+000	0
3	0.000	6.096	1.978154e-003	0.000000e+000	1
4	0.000	0.000	1.978154e-003	0.000000e+000	1
5	9.144	6.096	3.956308e-003	0.000000e+000	2

z =

```

0.4694967i - 0.1668986i - 0.1363208i - 0.1885938i - 0.1807644i
- 0.1668986i 0.4172237i - 0.1807644i - 0.2054220i - 0.1363208i
- 0.1363208i - 0.1807644i 0.4694967i - 0.1363208i - 0.1668986i
- 0.1885938i - 0.2054220i - 0.1363208i 0.4694967i - 0.1807644i
- 0.1807644i - 0.1363208i - 0.1668986i - 0.1807644i 0.4172237i

```

Zreduc =

```

0.0535995i - 0.1804456i
- 0.1804456i 0.1400643i

```

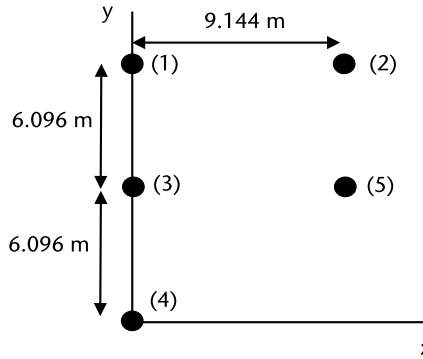


Figure 4.7 Transmission arrangement and geometry for conductors.

The circuit interpretation for the reduced impedance values in ohms/km is given in Figure 4.8.

$$\begin{bmatrix} z_{aa} & z_{ab} \\ z_{ba} & z_{bb} \end{bmatrix} \begin{bmatrix} I_a \\ I_b \end{bmatrix} = \begin{bmatrix} \Delta V_a \\ \Delta V_b \end{bmatrix} \tag{4.24}$$

The current condition is that $I_b = -I_a$, so the total impedance is calculated as:

$$z_{tot} = \frac{\Delta V}{I_a} = \frac{\Delta V_a - \Delta V_b}{I_a} = \frac{(z_{aa} - z_{ab})I_a - (z_{ba} - z_{bb})I_a}{I_a} \tag{4.25}$$

$$z_{tot} = \frac{((0.0535995i + 0.1804456i)I_a - (-0.1804456i - 0.1400643i)I_a)}{I_a}$$

$$z_{tot} = 0.554555i \text{ } \Omega/\text{km}$$

4.2.4 Ground Wire Inclusion

In transmission line models, we start including all of the wires that form the transmission line arrangement. In most studies, we only need the three-phase abc values; therefore, its equivalent series impedance should be obtained. If the ground wires

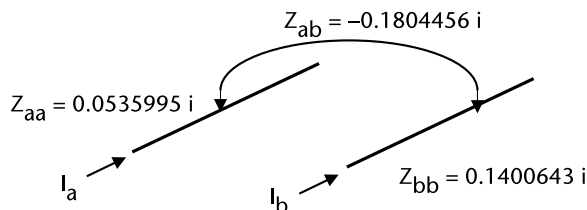


Figure 4.8 Set of parallel conductors, interpretation of the equivalent impedance.

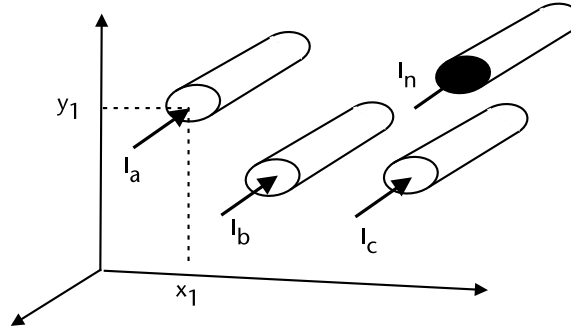


Figure 4.9 Set of conductors abc and a ground wire n .

do exist, they can be eliminated by imposing boundary conditions in terms of voltages and currents and by the use of the Gaussian elimination (partial inversion) process, the reduced model is attained. In Figure 4.9, n is considered a neutral wire, grounded at its extremes; let us assume an arrangement of phase conductors abc and one ground wire n . Boundary conditions for the ground wire are $I_n \neq 0$, $\Delta V_n = 0$.

$$\begin{bmatrix} z_{aa} & z_{ab} & z_{ac} & z_{an} \\ z_{ba} & z_{bb} & z_{bc} & z_{bn} \\ z_{ca} & z_{cb} & z_{cc} & z_{cn} \\ z_{na} & z_{nb} & z_{nc} & z_{nn} \end{bmatrix} \begin{bmatrix} I_a \\ I_b \\ I_c \\ I_n \end{bmatrix} = \begin{bmatrix} \Delta V_a \\ \Delta V_b \\ \Delta V_c \\ 0 \end{bmatrix} \quad (4.26)$$

One step of partial inversion in (4.26) will exchange I_n from the left hand side with the zero value for the voltage drop on the right side of the matrix. The result is:

$$\begin{bmatrix} z'_{aa} & z'_{ab} & z'_{ac} & -z_{an}/z_{nn} \\ z'_{ba} & z'_{bb} & z'_{bc} & -z_{bn}/z_{nn} \\ z'_{ca} & z'_{cb} & z'_{cc} & -z_{cn}/z_{nn} \\ -z_{na}/z_{nn} & -z_{nb}/z_{nn} & -z_{nc}/z_{nn} & -1/z_{nn} \end{bmatrix} \begin{bmatrix} I_a \\ I_b \\ I_c \\ 0 \end{bmatrix} = \begin{bmatrix} \Delta V_a \\ \Delta V_b \\ \Delta V_c \\ I_n \end{bmatrix} \quad (4.27)$$

The primed values are equivalent impedances after the elimination of the ground wire; its new values mathematically reflect this step. The reduced equivalent for the phase conductors abc is:

$$\begin{bmatrix} z'_{aa} & z'_{ab} & z'_{ac} \\ z'_{ba} & z'_{bb} & z'_{bc} \\ z'_{ca} & z'_{cb} & z'_{cc} \end{bmatrix} \begin{bmatrix} I_a \\ I_b \\ I_c \end{bmatrix} = \begin{bmatrix} \Delta V_a \\ \Delta V_b \\ \Delta V_c \end{bmatrix} \quad (4.28)$$

If for any reason the neutral current I_n needs to be calculated, this can be done by an expression out of (4.27) once the phase currents are known.

$$I_n = -\left(\frac{z_{na}}{z_{nn}}\right)I_a - \left(\frac{z_{nb}}{z_{nn}}\right)I_b - \left(\frac{z_{nc}}{z_{nn}}\right)I_c \quad (4.29)$$

When several ground wires are part of the arrangement, the partial inversion procedure is repeated as many times as ground wires are present.

Example 4.3

For Example 4.1 calculate the reduced reactance matrix assuming that the rightmost conductor is a ground wire.

```

Reduced Inductance matrix Ohms/km
Xreduc =
    0.34722165179594   -0.10452413233457
   -0.10452413233457    0.34722165179594

```

4.2.5 Line Transposition

In practice, power system engineers try to design and operate their transmission lines in a balanced condition. To come close to having a balanced condition (from the point of view of the geometric distances), some conductor rearrangement is practiced. If conditions are favorable, a change in *abc* arrangement is conducted at distances 1/3 and 2/3 of the total length of the transmission line.

The first segment can be labeled as *abc* sequence, the second as *cab*, and the third as *bca* (as depicted in Figure. 4.10). Ideal geometrical consideration can be put into practice from the sending to the receiving end; then, the line will be nearly balanced (perfectly balanced only if conductors are at the corners of an equilateral triangle, which hardly happens in a real situation).

The calculation of impedance values start with the first section in order *abc*, followed by a physical arrangement as *cab* for the second section. The *abc* order is rearranged as the second section by a premultiplication by matrix R_2 and a post-multiplication by the transpose of R_2 . The original array *abc* turns to be *cab*.

$$R_2 Z_{abc} R_2^t = \begin{bmatrix} 0 & 0 & 1 \\ 1 & 0 & 0 \\ 0 & 1 & 0 \end{bmatrix} \begin{bmatrix} z_{aa} & z_{ab} & z_{ac} \\ z_{ba} & z_{bb} & z_{bc} \\ z_{ca} & z_{cb} & z_{cc} \end{bmatrix} \begin{bmatrix} 0 & 1 & 0 \\ 0 & 0 & 1 \\ 1 & 0 & 0 \end{bmatrix} = \begin{bmatrix} z_{cc} & z_{ca} & z_{cb} \\ z_{ac} & z_{aa} & z_{ab} \\ z_{bc} & z_{ba} & z_{bb} \end{bmatrix} \quad (4.30)$$

A transformation matrix R_3 and its transpose will change the original *abc* arrangement into third section *bca* in Figure 4.10.

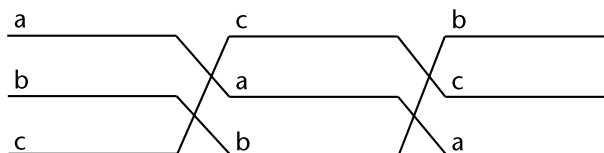


Figure 4.10 Transmission line transposition at every 1/3 of its length.

$$R_3 Z_{abc} R_3^t = \begin{bmatrix} 0 & 1 & 0 \\ 0 & 0 & 1 \\ 1 & 0 & 0 \end{bmatrix} \begin{bmatrix} z_{aa} & z_{ab} & z_{ac} \\ z_{ba} & z_{bb} & z_{bc} \\ z_{ca} & z_{cb} & z_{cc} \end{bmatrix} \begin{bmatrix} 0 & 0 & 1 \\ 1 & 0 & 0 \\ 0 & 1 & 0 \end{bmatrix} = \begin{bmatrix} z_{bb} & z_{bc} & z_{ba} \\ z_{cb} & z_{cc} & z_{ca} \\ z_{ab} & z_{ac} & z_{aa} \end{bmatrix} \quad (4.31)$$

The impedance matrix for the total length of the transposed transmission line will be obtained in general as in (4.32), considering section lengths l_1 , l_2 , and l_3 to make the total line length *long*.

$$Z_{\text{tot}} = \text{long}(l_1 Z_{abc} + l_2 R_2 Z_{abc} R_2^t + l_3 R_3 Z_{abc} R_3^t) \quad (4.32)$$

Example 4.4

Assuming a reactance matrix in ohms for a three-phase conductors and in each section as:

$$Z_{abc} = j \begin{bmatrix} 5.1 & 4 & 2 \\ 4 & 5.2 & 3 \\ 2 & 3 & 5.3 \end{bmatrix}$$

Find the total reactance if the transposed arrangement is done at 1/3 of the total length.

$$Z = j^* \begin{bmatrix} 5.1000 & 4.0000 & 2.0000 \\ 4.0000 & 5.2000 & 3.0000 \\ 2.0000 & 3.0000 & 5.3000 \end{bmatrix}$$

$$R_2 = \begin{bmatrix} 0 & 0 & 1 \\ 1 & 0 & 0 \\ 0 & 1 & 0 \end{bmatrix}$$

$$R_3 = \begin{bmatrix} 0 & 1 & 0 \\ 0 & 0 & 1 \\ 1 & 0 & 0 \end{bmatrix}$$

$$ZT1 = j^* \begin{bmatrix} 5.3000 & 2.0000 & 3.0000 \\ 2.0000 & 5.1000 & 4.0000 \\ 3.0000 & 4.0000 & 5.2000 \end{bmatrix}$$

$$ZT2 = j^* \begin{bmatrix} 5.2000 & 3.0000 & 4.0000 \\ 3.0000 & 5.3000 & 2.0000 \\ 4.0000 & 2.0000 & 5.1000 \end{bmatrix}$$

$$Z_{\text{total}} = j^* \begin{bmatrix} 5.2000 & 3.0000 & 3.0000 \\ 3.0000 & 5.2000 & 3.0000 \\ 3.0000 & 3.0000 & 5.2000 \end{bmatrix}$$

4.2.6 Sequence Impedances

In many instances, after the phase equivalent impedances abc are obtained, one more step is required to find the zero, positive, and negative sequence impedances for the transmission line. The voltage drop on the abc phases can be transformed to the 012 sequence domain. This is done using the symmetrical transformation matrix T_S and T_S^{-1} in (3.22).

$$\begin{bmatrix} \Delta V_a \\ \Delta V_b \\ \Delta V_c \end{bmatrix} = \begin{bmatrix} z'_{aa} & z'_{ab} & z'_{ac} \\ z'_{ba} & z'_{bb} & z'_{bc} \\ z'_{ca} & z'_{cb} & z'_{cc} \end{bmatrix} \begin{bmatrix} I_a \\ I_b \\ I_c \end{bmatrix} \quad (4.33)$$

$$\begin{aligned} I_{abc} &= T_S I_{012} \\ \Delta V_{abc} &= T_S \Delta V_{012} \end{aligned} \quad (4.34)$$

$$\begin{bmatrix} \Delta V_0 \\ \Delta V_1 \\ \Delta V_2 \end{bmatrix} = T_S^{-1} \begin{bmatrix} z'_{aa} & z'_{ab} & z'_{ac} \\ z'_{ba} & z'_{bb} & z'_{bc} \\ z'_{ca} & z'_{cb} & z'_{cc} \end{bmatrix} T_S \begin{bmatrix} I_0 \\ I_1 \\ I_2 \end{bmatrix} \quad (4.35)$$

$$Z_{012} = T_S^{-1} \begin{bmatrix} z'_{aa} & z'_{ab} & z'_{ac} \\ z'_{ba} & z'_{bb} & z'_{bc} \\ z'_{ca} & z'_{cb} & z'_{cc} \end{bmatrix} T_S \quad (4.36)$$

The impedance transformation (4.36) from abc to 012 is a step from which the zero, positive and negative sequence impedances for a transmission line are determined. For the completely transposed line its sequence impedance are decoupled; no mutual impedances among sequences. In the case of three-phase lines with double circuit, ground wires are eliminated, bundled conductors are reduced to an equivalent conductor, and transpositions arrangements are worked out. An equivalent phase impedance matrix 6x6 is then obtained.

$$Z_{abc}^{eq} = \begin{bmatrix} Z_{abc}^I & Z_{abc}^{I,II} \\ Z_{abc}^{II,I} & Z_{abc}^{II,II} \end{bmatrix} \quad (4.37)$$

To find the sequence values of impedances 012 for this type of transmission line, symmetrical component transformation is carried out as shown in (4.38).

$$Z_{012}^{eq} = \begin{bmatrix} T_S^{-1} & 0 \\ 0 & T_S^{-1} \end{bmatrix} \begin{bmatrix} Z_{abc}^I & Z_{abc}^{I,II} \\ Z_{abc}^{II,I} & Z_{abc}^{II,II} \end{bmatrix} \begin{bmatrix} T_S & 0 \\ 0 & T_S \end{bmatrix} \quad (4.38)$$

T_S and T_S^{-1} are the matrix of the symmetrical component transformation and its inverse; each one of the matrices in (4.38) are 3x3 matrices. The importance of this

discussion is that all mutual effects among positive and negative sequence impedances are zero, except the mutual effect between the zero sequence for circuit 1 and the zero sequence for circuit 2. This mutual value is important when zero sequence current flows in one circuit (i.e., due to unbalanced fault, which we will cover in Chapter 9, and induces zero sequence voltage in the neighboring circuit.

4.3 Earth Return

Practical transmission lines are suspended above Earth by insulation arrangements supported by steel or pole structures with a finite height with respect to an ideal flat surface; Earth itself might be used as a current return path. Early in the last century, Carson, Rudenberg, and other researchers studied this operating condition using theoretical considerations and measurements that were conducted on existing communication lines [1, 4–6]. As a result, for unbalanced operating condition, Earth can be represented by an equivalent conductor with resistance, self, and mutual reactance that depends on frequency f in Hz and soil resistivity ρ in $\Omega\cdot\text{m}$. Various expressions were derived and published in the open literature by Rudenberg, Carson, and Clarke [1] as a way to include Earth return correction terms to the *geometric inductance*, which is calculated under the assumptions established in (4.17).

The system's frequency f in Hz and the earth resistivity influence the *equivalent depth* D_e of the equivalent earth conductor. A value of resistance R_d is also present.

$$D_e = 658.37 \sqrt{\frac{\rho}{f}} \text{ m} \quad (4.39)$$

$$R_d = \pi^2 \times 10^{-4} f = 9.869 \times 10^{-4} f \text{ } \Omega/\text{km} \quad (4.40)$$

Carson's result for the field equation was obtained as a series expansion, so the first term in the series is known as first correction [4, 5]. The series impedance matrix for a three-phase arrangement of conductors includes resistance and some correction terms to the resistance and the reactance as in (4.41) (see Figure 4.11).

$$\begin{aligned} \begin{bmatrix} z_{aa} & z_{ab} & z_{ac} \\ z_{ba} & z_{bb} & z_{bc} \\ z_{ca} & z_{cb} & z_{cc} \end{bmatrix} &= \begin{bmatrix} r_{aa} & 0 & 0 \\ 0 & r_{bb} & 0 \\ 0 & 0 & r_{cc} \end{bmatrix} + R_d \begin{bmatrix} 1 & 1 & 1 \\ 1 & 1 & 1 \\ 1 & 1 & 1 \end{bmatrix} \\ &+ j \frac{\mu_o \omega}{2\pi} \text{Ln} \left\{ \begin{bmatrix} 1/\text{GMR}_1 & 1/d_{12} & 1/d_{13} \\ 1/d_{21} & 1/\text{GMR}_2 & 1/d_{23} \\ 1/d_{31} & 1/d_{32} & 1/\text{GMR}_2 \end{bmatrix} + \left\{ D_e \begin{bmatrix} 1 & 1 & 1 \\ 1 & 1 & 1 \\ 1 & 1 & 1 \end{bmatrix} \right\} \right\} \end{aligned} \quad (4.41)$$

To have a sense of the numerical difference in transmission line impedance calculation when no return path is included, assuming a perfectly balanced geometric configuration, and when we recognize the unbalanced nature of the line due to

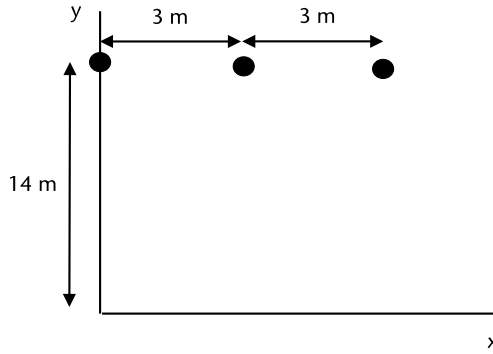


Figure 4.11 Transmission line arrangement to calculate series impedance.

nonsymmetric geometry in the conductors arrangement, we provide the following example.

Example 4.5

For a temperature of 25°C, an arrangement of three copper conductors, 250 MCM, and 12 strands are in a horizontal arrangement (see Figure 4.11). The line length is 65 km, Earth is used as return path, and the transmission line operates at 60 Hz. Conductor’s diameter is 0.6 in (0.01524 m), the GMR as listed by the manufacturer is 0.01902 ft (0.005792 m), resistance at 25°C is 0.257 Ω/mi (0.159727 Ω/km), and current carrying capacity of 540 Amps. Earth resistivity $\rho = 100 \Omega\text{-m}$ and no transposition. Calculate the total series impedance matrix in ohms/km using the geometric inductance only.

In a second step, include the first Carson’s correction (4.41) to include Earth return, which is required when we have an unbalanced condition; this is the case due to the horizontal arrangement of the phase *abc* conductors.

```

Number of conductors = 3
Frequency = 60 Resistivity = 100 long = 65.0
i      x(i)      y(i)      GMR(i)      res(i)      code(i)
1      0.000      14.000      5.797296e-003      1.597265e-001      0
2      3.000      14.000      5.797296e-003      1.597265e-001      0
3      6.000      14.000      5.797296e-003      1.597265e-001      0
De = 849.94943
Rd = 0.059214

Zreduc =
0.2189405 + 0.8970903i      0.059214 + 0.4258300i      0.059214 + 0.3735570i
0.059214 + 0.4258300i      0.2189405 + 0.8970903i      0.059214 + 0.4258300i
0.059214 + 0.3735570i      0.059214 + 0.4258300i      0.2189405 + 0.8970903i
    
```

Example 4.6

Apply the transposition arrangement shown in Figure 4.8 to the conductor’s in Example 4.5 at exactly 1/3 of its total length for the second section and at 2/3 for

the third section. Calculate the 012 sequence impedance values for the transmission line once the transposition is carried out.

```

logtransp = 0.3333333    0.3333333    0.3333333
ZT1 =
 14.2311 +58.3109i    3.8489 +24.2812i    3.8489 +27.6790i
 3.8489 +24.2812i    14.2311 +58.3109i    3.8489 +27.6790i
 3.8489 +27.6790i    3.8489 +27.6790i    14.2311 +58.3109i
ZT2 =
 14.2311 +58.3109i    3.8489 +27.6790i    3.8489 +27.6790i
 3.8489 +27.6790i    14.2311 +58.3109i    3.8489 +24.2812i
 3.8489 +27.6790i    3.8489 +24.2812i    14.2311 +58.3109i
Ztot =
 14.231135 + 58.310869i    3.84891 + 26.54637i    3.84891 + 26.54637i
 3.84891 + 26.54637i    14.231135 + 58.310869i    3.84891 + 26.54637i
 3.84891 + 26.54637i    3.84891 + 26.54637i    14.231135 + 58.310869i
Z012 = 1.0e+002 *
 0.2193 + 1.1140i    -0.0000 - 0.0000i    -0.0000 - 0.0000i
 0 + 0.0000i    0.1038 + 0.3176i    -0.0000 - 0.0000i
 0.0000 + 0.0000i    0.0000 + 0.0000i    0.1038 + 0.3176i
    
```

Carson’s equations were modified by Clarke and gave a more elaborate set of equations [1, 4]. Later, various authors contributed to the formulas that can be consulted in the references [4–6]. Corrections higher than the first order can be included; this step is specifically needed when transmission line studies are to be related to high-order harmonics in the power system and for frequency response studies of the transmission line.

Carson proposed an infinite series solution to the field equations and Clarke modified the expressions [1]. The proposed series converges rather quickly for values of constant k in transmission lines at 60 Hz or less, for $k \leq 1$ when conductors are located at coordinates (x, h) in meters as shown in Figure 4.12. The k values are calculated depending on the self (own conductor) or mutual (between two conductors) and are used in (4.45) and (4.46), respectively.

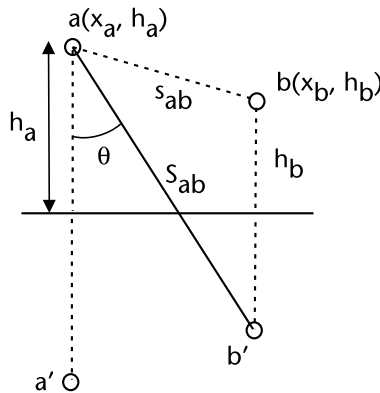


Figure 4.12 Geometric distances of conductors and their images below the Earth plane.

$$k_{\text{self}} = 4\pi h_a \sqrt{\frac{2f}{\rho}} \quad \theta = 0 \quad (4.42)$$

$$k_{\text{mutual}} = 2\pi S_{ab} \sqrt{\frac{2f}{\rho}} \quad \theta = \cos^{-1}\left(\frac{h_a + h_b}{S_{ab}}\right) \quad (4.43)$$

$$S_{ab} = \sqrt{(x_b - x_a)^2 + (h_a + h_b)^2} \quad (4.44)$$

$$\begin{aligned} Z_P = & \frac{\pi}{8} - \frac{1}{3\sqrt{2}} \cos \theta + \frac{k^2}{16} \cos 2\theta \left(0.6728 + \ln\left(\frac{2}{k}\right) \right) + \frac{k^2}{16} \theta \sin 2\theta \\ & + \frac{k^3}{45\sqrt{2}} \cos 3\theta - \frac{\pi k^4}{1,536} \cos 4\theta + \dots \end{aligned} \quad (4.45)$$

$$\begin{aligned} Z_Q = & -0.0386 + \frac{1}{2} \ln\left(\frac{2}{k}\right) + \frac{1}{3\sqrt{2}} k \cos \theta - \frac{\pi k^2}{64} \cos 2\theta + \frac{k^3}{45\sqrt{2}} \cos 3\theta \\ & - \frac{k^4}{384} \theta \sin 4\theta - \frac{k^4}{384} \cos 4\theta \left(1.0895 + \ln\left(\frac{2}{k}\right) \right) + \dots \end{aligned} \quad (4.46)$$

The results (4.45) and (4.46) are to be used in the impedance calculation (4.47) and (4.48).

$$Z_{aa,g} = z_{aa} + j2\omega \ln\left(\frac{4h_a}{d}\right) + 4\omega(Z_P + jZ_Q) \quad (4.47)$$

$$Z_{ab,g} = j2\omega \ln\left(\frac{S_{ab}}{s_{ab}}\right) + 4\omega(Z_P + jZ_Q) \quad (4.48)$$

z_{aa}	Conductor internal impedance, ohms/km
d	Conductor diameter, meters
h_a, h_b	Height above Earth plane, meters
S_{ab}	Distance between conductor a and image of conductor b , meters
s_{ab}	Distance between conductor a and conductor b , meters
ω	Angular frequency, rad/s
f	System frequency, Hz

Example 4.7

Use ground return correction for impedance calculation of a single circuit 400 kV line with two conductors per phase and two ground wires. We use a code to identify the role of the conductor: 0 for a retained conductor, -1 for a ground wire, and a

number to make a bundled conductor. A reduced impedance matrix is calculated by bundling the phase conductors and eliminating the ground wires. A complete transposition is assumed by *abc*, *cab*, and *bac* arrangements. The 012 sequence impedance values are calculated.

400 kV line, FINCH ACSR 1113 MCM (54/19), two ground wires

Imax = 1,110 Amperes

This case has horizontal arrangement a-a, b-b, c-c

Length = 1.000000

Transpositions = 0.000000 1.000000 1.000000

Longnspositions = 0.333333 0.333333 0.333333

Number of conductors = 8

Frequency = 60

Resistivity = 100

i	x(i)	y(i)	GMR(i)	res(i)	code(i)
1	-11.52	26.75	1.107440e-003	6.022370e-002	0
2	-0.23	26.75	1.107440e-003	6.022370e-002	0
3	11.07	26.75	1.107440e-003	6.022370e-002	0
4	-11.07	26.75	1.107440e-003	6.022370e-002	1
5	0.23	26.75	1.107440e-003	6.022370e-002	2
6	11.52	26.75	1.107440e-003	6.022370e-002	3
7	-6.96	35.30	6.334000e-004	4.039770e+000	-1
8	6.96	35.30	6.334000e-004	4.039770e+000	-1

Impedance in Ohms/km

z =

Column 1 to 3

0.1157555 + 1.0258131i	0.0555199 + 0.3299201i	0.0554843 + 0.2776701i
0.0555199 + 0.3299201i	0.1157555 + 1.0258131i	0.0555199 + 0.3299201i
0.0554843 + 0.2776701i	0.0555199 + 0.3299201i	0.1157555 + 1.0258131i
0.0555318 + 0.5728812i	0.0555208 + 0.3329865i	0.0554862 + 0.2791873i
0.0555189 + 0.3269735i	0.0555318 + 0.5728812i	0.0555208 + 0.3329865i
0.0554824 + 0.2761829i	0.0555189 + 0.3269735i	0.0555318 + 0.5728812i
0.0550002 + 0.3420863i	0.0549981 + 0.3333071i	0.0549736 + 0.2876297i
0.0549722 + 0.2861057i	0.0549975 + 0.3313648i	0.0550006 + 0.3436850i

Column 4 to 6

0.0555318 + 0.5728812i	0.0555189 + 0.3269735i	0.0554824 + 0.2761829i
0.0555208 + 0.3329865i	0.0555318 + 0.5728812i	0.0555189 + 0.3269735i
0.0554862 + 0.2791873i	0.0555208 + 0.3329865i	0.0555318 + 0.5728812i
0.1157555 + 1.0258131i	0.0555199 + 0.3299201i	0.0554843 + 0.2776701i
0.0555199 + 0.3299201i	0.1157555 + 1.0258131i	0.0555199 + 0.3299201i
0.0554843 + 0.2776701i	0.0555199 + 0.3299201i	0.1157555 + 1.0258131i
0.0550006 + 0.3436850i	0.0549975 + 0.3313648i	0.0549722 + 0.2861057i
0.0549736 + 0.2876297i	0.0549981 + 0.3333071i	0.0550002 + 0.3420863i

Column 7 to 8

0.0550002 + 0.3420863i	0.0549722 + 0.2861057i
0.0549981 + 0.3333071i	0.0549975 + 0.3313648i
0.0549736 + 0.2876297i	0.0550006 + 0.3436850i
0.0550006 + 0.3436850i	0.0549736 + 0.2876297i
0.0549975 + 0.3313648i	0.0549981 + 0.3333071i

$$\begin{array}{ll} 0.0549722 + 0.2861057i & 0.0550002 + 0.3420863i \\ 4.0942551 + 1.0691910i & 0.0544692 + 0.3153857i \\ 0.0544692 + 0.3153857i & 4.0942551 + 1.0691910i \end{array}$$

Impedance in Ohms/km

Zreduc =

$$\begin{array}{lll} 0.1227019 + 0.7703293i & 0.09444459 + 0.2997967i & 0.0917895 + 0.2488227i \\ 0.09444459 + 0.2997967i & 0.1269475 + 0.7679215i & 0.09444459 + 0.2997967i \\ 0.0917895 + 0.2488227i & 0.09444459 + 0.2997967i & 0.1227019 + 0.7703293i \end{array}$$

ZT1 =

$$\begin{array}{lll} 0.1227 + 0.7703i & 0.0918 + 0.2488i & 0.0944 + 0.2998i \\ 0.0918 + 0.2488i & 0.1227 + 0.7703i & 0.0944 + 0.2998i \\ 0.0944 + 0.2998i & 0.0944 + 0.2998i & 0.1269 + 0.7679i \end{array}$$

ZT2 =

$$\begin{array}{lll} 0.1269 + 0.7679i & 0.0944 + 0.2998i & 0.0944 + 0.2998i \\ 0.0944 + 0.2998i & 0.1227 + 0.7703i & 0.0918 + 0.2488i \\ 0.0944 + 0.2998i & 0.0918 + 0.2488i & 0.1227 + 0.7703i \end{array}$$

Ztotal =

$$\begin{array}{lll} 0.1241 + 0.7695i & 0.0936 + 0.2828i & 0.0936 + 0.2828i \\ 0.0936 + 0.2828i & 0.1241 + 0.7695i & 0.0936 + 0.2828i \\ 0.0936 + 0.2828i & 0.0936 + 0.2828i & 0.1241 + 0.7695i \end{array}$$

Z012 =

$$\begin{array}{lll} 0.3112 + 1.3351i & -0.0000 & 0 + 0.0000i \\ 0 - 0.0000i & 0.0306 + 0.4867i & 0.0000 - 0.0000i \\ 0 - 0.0000i & 0.0000 - 0.0000i & 0.0306 + 0.4867i \end{array}$$

As can be seen from results, a complete transposition restores the balanced condition and helps to get a *decoupled sequence matrix*. An extension to the series impedance calculation might be to have various three-phase circuits running close to each other using the same right of way. Section 4.8 shows the nature of coupling between various circuits one 400 kV line and one 230 kV with a double circuit configuration.

4.4 Gauss Law and Capacitance

At every instant transmission, lines have an electric charge distribution. In a more general sense, a transmission line is subject to electromagnetic phenomena when used as an electric energy waveguide. In Section 4.2, the magnetic field concept was used to characterize the series impedance of the transmission line. Now, an electric line charge arrangement is visualized in free space and by the use of Gauss' Law, the potential with respect to a reference is obtained, the potential coefficients are determined, and the capacitance values for an arrangement of conductors with radius r (meters). Let us start with a single conductor (see Figure 4.13).

$$\iint D \cdot ds = q = \rho l \quad C \quad (4.49)$$

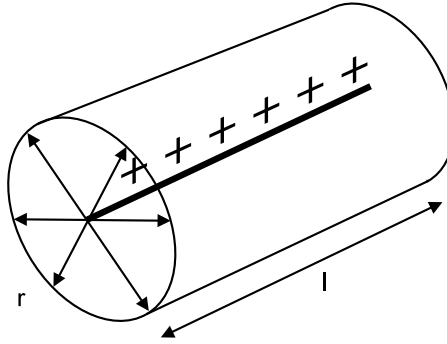


Figure 4.13 Linear density ρ of electric charge, field configuration.

$$D = \frac{q}{2\pi lr} \text{ C/m}^2 \tag{4.50}$$

$$E = \frac{D}{\epsilon_0} = \frac{q}{2\pi\epsilon_0 r} \text{ V/m} \tag{4.51}$$

- D Electric displacement field, coulombs/m²
- Q Electric charge, coulombs
- ρ linear charge density, coulombs/m
- E Intensity of electric field, volts/m
- $\epsilon_0 = 8.854187 \text{ F/m}$ vacuum permittivity

$$V_p = V_{p1} + V_{p2} = \int_{r_1}^{s_{p1}} \vec{E}_1 \cdot d\vec{r} + V_1 + \int_{r_2}^{s_{p2}} \vec{E}_2 \cdot d\vec{r} + V_2 \text{ V} \tag{4.52}$$

$$V_p = \frac{1}{2\pi\epsilon_0} \left[-\ln\left(\frac{s_{p1}}{r_1}\right)q_1 - \ln\left(\frac{s_{p2}}{r_2}\right)q_2 \right] + V_1 + V_2 \tag{4.53}$$

The point p can be located at the surface of conductor 1, with radius r_1 (Figure 4.14):

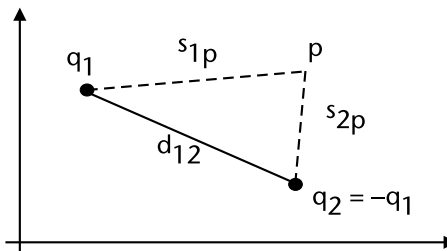


Figure 4.14 Potential at point p due to charges q_1 and q_2 .

$$V_1 = -\frac{1}{2\pi\epsilon_0} \left[\ln\left(\frac{r_1}{r_1}\right)q_1 + \ln\left(\frac{d_{21}}{r_2}\right)q_2 \right] + V_1 + V_2 \quad (4.54)$$

$$V_2 = \frac{1}{2\pi\epsilon_0} \ln\left(\frac{d_{21}}{r_2}\right)q_2$$

In a similar way for the point p at the surface of conductor 2, radius r_2 :

$$V_2 = -\frac{1}{2\pi\epsilon_0} \left[\ln\left(\frac{d_{12}}{r_1}\right)q_1 + \ln\left(\frac{r_2}{r_2}\right)q_2 \right] + V_1 + V_2 \quad (4.55)$$

$$V_1 = +\frac{1}{2\pi\epsilon_0} \ln\left(\frac{d_{12}}{r_1}\right)q_1$$

Results in (4.54) and (4.55) are in matrix from:

$$\begin{bmatrix} V_1 \\ V_2 \end{bmatrix} = \frac{1}{2\pi\epsilon_0} \ln \begin{bmatrix} \frac{1}{r_1} & \frac{1}{d_{12}} \\ \frac{1}{d_{21}} & \frac{1}{r_2} \end{bmatrix} \begin{bmatrix} q_1 \\ q_2 \end{bmatrix} \quad (4.56)$$

One condition that must be satisfied is that the net electric charge $q_1 + q_2 = 0$.

4.4.1 Potential at Midpoint Between Two Electric Charges

When point p is displaced to a point between the two electric charges, as in Figure 4.15, by (4.53), then using (4.54) and (4.55) with $S_{1p} = S_{2p}$ and $r_2 = r_1$:

$$\bar{V}_p = -\frac{1}{2\pi\epsilon_0} \ln\left(\frac{s_{p1}r_2}{r_1s_{p2}}\right)q_1 + V_1 + V_2 = 0 \quad (4.57)$$

4.4.2 Conductors Parallel to an Ideal Equipotential Plane

From results in (4.57), the *image concept* can be used to study the electric charge arrangement on overhead conductors, and to have an opposite charge arrangement

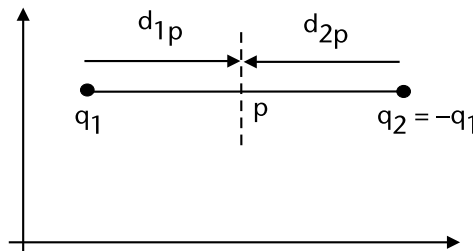


Figure 4.15 If point p is moved to the midpoint between q_1 and q_2 .

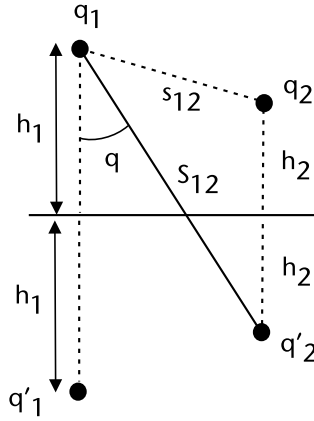


Figure 4.16 Parallel conductors over an ideal plane, charges q_1 and q_2 , images q'_1 and q'_2

underneath an ideal plane. For illustrative purposes, consider in Figure 4.16, two charges q_1 and q_2 at height h_1 and h_2 and corresponding images beneath the ideal plane. For the arrangement of conductors and electric charges imposing physical conditions: $V'_1 = -V_1$, $V'_2 = -V_2$, $q'_1 = -q_1$ and $q'_2 = -q_2$.

$$\begin{bmatrix} V_1 \\ V_2 \end{bmatrix} = \frac{1}{2\pi\epsilon_0} \ln \begin{bmatrix} \frac{2h_1}{r_1} & \frac{S_{12}}{s_{12}} \\ \frac{S_{21}}{s_{21}} & \frac{2h_2}{r_2} \end{bmatrix} \begin{bmatrix} q_1 \\ q_2 \end{bmatrix} \quad (4.58)$$

In a condensed matrix, the expression for (4.58) is:

$$V = [p]q \quad (4.59)$$

$$[p] = \frac{1}{2\pi\epsilon_0} \ln \begin{bmatrix} \frac{2h_1}{r_1} & \frac{S_{12}}{s_{12}} \\ \frac{S_{21}}{s_{21}} & \frac{2h_2}{r_2} \end{bmatrix} \quad (4.60)$$

4.4.3 Capacitance and Shunt Admittance

Matrix $[p, (5.59)]$ is known as the *matrix of potentials* and its inverse is the capacitance matrix $[C]$.

$$q = [C]V \quad (4.61)$$

$$[C] = [p]^{-1} \quad (4.62)$$

The shunt admittance matrix (siemens/km) for AC operation at a frequency f in Hz is:

$$Y_{sh} = j2\pi f[C] \quad (4.63)$$

In summary, the process in (4.56) gives a set of potential coefficients with no consideration to the Earth plane and (4.58) calculates the set of potential coefficients by the *image method*. This last procedure includes the effect of an ideal Earth plane as presented in this section.

Example 4.8

For a set of three conductors arranged in three-phase abc (Figure 4.17), with radius 0.015 m, calculate the potential matrix $[p]$, and the capacitance matrix $[C]$; do not consider the Earth plane. Compare the values obtained if the Earth plane is represented by the *image method*. Calculate the abc shunt admittance matrix and apply a complete transposition assumption to calculate the sequence 012 shunt admittances.

$$\begin{aligned} f &= 60 \\ r &= 0.0150 \\ x &= 0.0 \quad 2.5000 \quad 5.0000 \\ y &= 15.0000 \quad 19.3301 \quad 15.0000 \\ P &= \\ & \quad 66.6667 \quad 0.2000 \quad 0.2000 \\ & \quad 0.2000 \quad 66.6667 \quad 0.2000 \\ & \quad 0.2000 \quad 0.2000 \quad 66.6667 \\ C &= \\ & \quad 0.0253 \quad 0.0157 \quad 0.0157 \\ & \quad 0.0157 \quad 0.0253 \quad 0.0157 \\ & \quad 0.0157 \quad 0.0157 \quad 0.0253 \end{aligned}$$

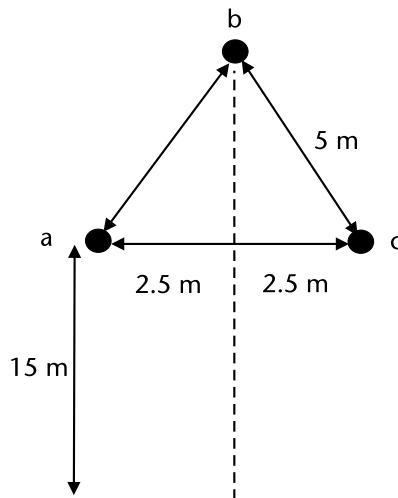


Figure 4.17 Three conductors abc and distances over an ideal plane.

$$\begin{aligned}
 YC = & \\
 & \begin{array}{ccc}
 0 + 9.5213i & 0 + 5.9160i & 0 + 5.9160i \\
 0 + 5.9160i & 0 + 9.5213i & 0 + 5.9160i \\
 0 + 5.9160i & 0 + 5.9160i & 0 + 9.5213i
 \end{array}
 \end{aligned}$$

The results considering images to include Earth plane are:

$$\begin{aligned}
 P_{im} = & \\
 & 1.0e+003 * \\
 & \begin{array}{ccc}
 2.0000 & 0.0069 & 0.0061 \\
 0.0069 & 2.5774 & 0.0069 \\
 0.0061 & 0.0069 & 2.0000
 \end{array} \\
 C_{im} = & \\
 & \begin{array}{ccc}
 0.0081 & -0.0016 & -0.0015 \\
 -0.0016 & 0.0079 & -0.0016 \\
 -0.0015 & -0.0016 & 0.0081
 \end{array} \\
 YC_{im} = & \\
 & \begin{array}{ccc}
 0 + 3.0450i & 0 - 0.6082i & 0 - 0.5689i \\
 0 - 0.6082i & 0 + 2.9652i & 0 - 0.6082i \\
 0 - 0.5689i & 0 - 0.6082i & 0 + 3.0450i
 \end{array} \\
 Y_{T1} = & \\
 & \begin{array}{ccc}
 0 + 3.0450i & 0 - 0.5689i & 0 - 0.6082i \\
 0 - 0.5689i & 0 + 3.0450i & 0 - 0.6082i \\
 0 - 0.6082i & 0 - 0.6082i & 0 + 2.9652i
 \end{array} \\
 Y_{T2} = & \\
 & \begin{array}{ccc}
 0 + 2.9652i & 0 - 0.6082i & 0 - 0.6082i \\
 0 - 0.6082i & 0 + 3.0450i & 0 - 0.5689i \\
 0 - 0.6082i & 0 - 0.5689i & 0 + 3.0450i
 \end{array} \\
 Y_{total} = & \\
 & \begin{array}{ccc}
 0 + 3.0184i & 0 - 0.5951i & 0 - 0.5951i \\
 0 - 0.5951i & 0 + 3.0184i & 0 - 0.5951i \\
 0 - 0.5951i & 0 - 0.5951i & 0 + 3.0184i
 \end{array} \\
 Y_{012} = & \\
 & \begin{array}{ccc}
 0 + 1.8282i & 0 - 0.0000i & 0.0000 + 0.0000i \\
 0 & 0.0000 + 3.6135i & 0.0000 - 0.0000i \\
 0 - 0.0000i & 0.0000 - 0.0000i & -0.0000 + 3.6135i
 \end{array}
 \end{aligned}$$

4.5 Calculation of Cable Parameters

Underground cables are an important part in some electric system configurations where overhead layouts are prohibited or undesirable (i.e., in metropolitan areas, off-shore interconnections, and protected areas). Usually, the distances covered are not very long; contrary to the overhead lines and cables. However, electric and magnetic characteristics are very important, especially for the shunt capacitive admittance. In general, Carson's equations can be applied, considering the constitutive conductors and insulation arrangements. To obtain the equivalent series impedance

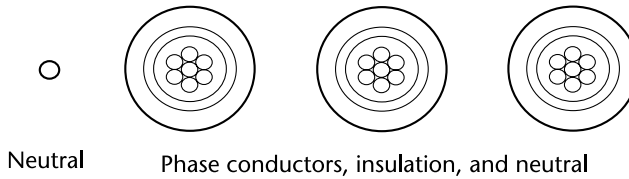


Figure 4.18 Horizontal underground arrangement, including a neutral conductor.

and the shunt admittance, we use the same mathematical procedures as the ones already used for the overhead lines. We can eliminate neutral conductors and shield arrangements (Figure 4.18) applying electrical conditions and the partial inversion process to the set of equations in the model.

4.5.1 Cable Series Impedance

For a concentric cable (Figure 4.19) used as a neutral:

- R Radius of concentric neutral strands, meters
- s_{pb} Phase conductor diameter, meters
- s_{on} Diameter over concentric neutrals, meters
- s_n Diameter of neutral strands, meters
- GMR_{pb} Geometric mean radius of phase conductor, meters
- GMR_n Geometric mean radius of neutral strands, meters
- r_{pb} Resistance of phase conductor, Ω/km
- r_n Resistance of neutral strand, Ω/km
- k Number of neutral strands in the concentric arrangement

A table for conductor’s data has values of GMR_{pb} and for the neutral strand; from here, an equivalent GMR_{dn} is calculated for a concentric neutral.

$$GMR_{cn} = \sqrt[k]{GMR_n k R^{k-1}} \quad R = \frac{(s_{on} - s_n)}{2} \tag{4.64}$$

The resistance (ohms/km) in a concentric neutral as:

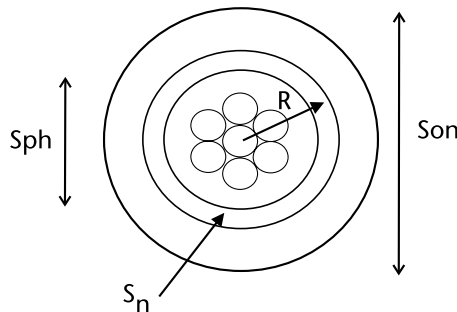


Figure 4.19 Cross section for a concentric cable.

$$r_{cn} = \frac{r_n}{k} \quad (4.65)$$

Let us consider the spacing for concentric neutral and phase conductors as follows:

$$S_{ij} = \begin{cases} R & \text{Concentric neutral conductor to its own phase} \\ S_{ij} & \text{Concentric neutral conductor to adjacent conductor} \end{cases} \quad (4.66)$$

The geometric mean distance between a concentric neutral and an adjacent phase conductor is calculated using the center-to-center distance between phase conductors.

$$S_{ij} = \sqrt[k]{S_{nm}^k - R^k} \approx S_{nm} \quad \text{m} \quad (4.67)$$

$$R = \frac{(s_{on} - s_n)}{2} = \frac{(0.032760 - 0.001628)}{2} = 0.01556$$

Example 4.9

In Figure 4.18, a three-cable arrangement is horizontal. Cables are 250 MCM AA phase conductor, 15 kV, aluminum with 13 strands of #14 annealed copper wires to form a 1/3 neutral, $R = (s_{on} - s_n)/2 = (0.032760 - 0.001628)/2 = 0.01556$.

R	radius of concentric neutral strands, meters
$s_{ph} = 0.0144$ m	phase conductor diameter
$s_{on} = 0.032760$ m	diameter over concentric neutrals
$s_n = 0.001628$ m	diameter of neutral strands
$GMR_{ph} = 0.005212$ m	geometric mean radius of phase conductor
$GMR_n = 0.0006339$ m	geometric mean radius of neutral strand
$r_{ph} = 0.2548$ Ω/km	resistance of phase conductor
$r_n = 9.243$ Ω/km	resistance of neutral strand
$k = 13$	number of neutral strands in the concentric arrangement

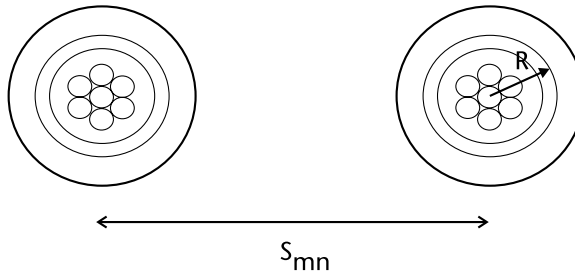


Figure 4.20 Spacing for a concentric neutral and a phase conductor.

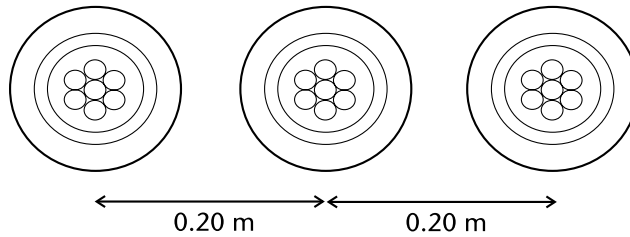


Figure 4.21 Horizontal underground arrangement, concentric neutral.

The GMR for the concentric neutral is $GMR_{cn} = \sqrt[3]{(0.0006339)(13)(0.01556)^{12}} = 0.0148$ m. The equivalent resistance of the concentric neutral in ohm/km is $r_{cn} = r_n/k = 9.243/13 = 0.711$.

Assuming a geometric configuration as in Figure 4.18: the distances in meters are: $S_{ij} = R = 0.01556$ concentric neutral to its own phase and $S_{ij} = 0.20$ concentric neutral to adjacent concentric neutral (see Figures 4.20 and 4.21). Then the series impedance in Ω/km is:

Z =

Columns 1 through 5

0.3140 + 0.9049i	0.0592 + 0.6299i	0.0592 + 0.5776i	0.0592 + 0.8224i	0.0592 + 0.6299i
0.0592 + 0.6299i	0.3140 + 0.9049i	0.0592 + 0.6299i	0.0592 + 0.6299i	0.0592 + 0.8224i
0.0592 + 0.5776i	0.0592 + 0.6299i	0.3140 + 0.9049i	0.0592 + 0.5776i	0.0592 + 0.6299i
0.0592 + 0.8224i	0.0592 + 0.6299i	0.0592 + 0.5776i	0.7702 + 0.8261i	0.0592 + 0.6299i
0.0592 + 0.6299i	0.0592 + 0.8224i	0.0592 + 0.6299i	0.0592 + 0.6299i	0.7702 + 0.8261i
0.0592 + 0.5776i	0.0592 + 0.6299i	0.0592 + 0.8224i	0.0592 + 0.5776i	0.0592 + 0.6299i

Column 6

0.0592 + 0.5776i
0.0592 + 0.6299i
0.0592 + 0.8224i
0.0592 + 0.5776i
0.0592 + 0.6299i
0.7702 + 0.8261i

The Z_{abc} and Z_{012} series impedance matrix for the original phase arrangement are used to calculate, Z_{tot} assuming a complete transposition at 1/3 and 2/3 of the cable length. Finally sequence impedances are calculated. All results in Ω/km .

Zreduc =

0.5019 + 0.2886i	0.1945 + 0.0155i	0.1720 - 0.0124i
0.1945 + 0.0155i	0.4952 + 0.2636i	0.1945 + 0.0155i
0.1720 - 0.0124i	0.1945 + 0.0155i	0.5019 + 0.2886i

Z012ut =

0.8737 + 0.2927i	-0.0018 - 0.0050i	-0.0034 + 0.0041i
-0.0034 + 0.0041i	0.3126 + 0.2741i	-0.0147 + 0.0284i
-0.0018 - 0.0050i	0.0320 - 0.0015i	0.3126 + 0.2741i

$$\begin{aligned}
 Z_{tot} &= \\
 &\begin{matrix} 0.4996 + 0.2803i & 0.1870 + 0.0062i & 0.1870 + 0.0062i \\ 0.1870 + 0.0062i & 0.4996 + 0.2803i & 0.1870 + 0.0062i \\ 0.1870 + 0.0062i & 0.1870 + 0.0062i & 0.4996 + 0.2803i \end{matrix} \\
 \\
 Z_{012} &= \\
 &\begin{matrix} 0.8737 + 0.2927i & -0.0000 + 0.0000i & -0.0000 + 0.0000i \\ -0.0000 + 0.0000i & 0.3126 + 0.2741i & -0.0000 + 0.0000i \\ 0.0000 & -0.0000 - 0.0000i & 0.3126 + 0.2741i \end{matrix}
 \end{aligned}$$

For the tape shielded cables in Figure 4.22.

- s_{ph} phase conductor diameter, meters
- s_{od} outside diameter over jacket, meters
- s_s outside diameter of tape shield, meters
- GMR_{ph} geometric mean radius of phase conductor, meters
- GMR_n geometric mean radius of neutral strand, meters
- r_{sh} resistance of phase conductor, Ω/km
- r_n resistance of neutral strand, Ω/km
- k number of neutral strands in the concentric arrangement

4.5.2 Cable Shunt Capacitance

From Section 4.4 and the geometry shown in Figure 4.23, the capacitance between the conductor's core and its sheath relates the electric charge q and the electric potential V to allow the capacitance C calculation and the capacitive susceptance B_C , $\epsilon_0 = 8.854 \times 10^{-12} \text{ F/m}$, B_C in (4.69) is in $\mu\text{S}/\text{km}$.

$$q_1 = \frac{2\pi\epsilon_0}{\ln\left(\frac{d_{1p}}{r_1}\right)} V = \frac{0.0556325}{\ln\left(\frac{d_{1p}}{r_1}\right)} V \tag{4.68}$$

$$B_C = 2\pi fC = \frac{0.349549f}{\ln\left(\frac{r_{is}}{r_{oc}}\right)} \tag{4.69}$$

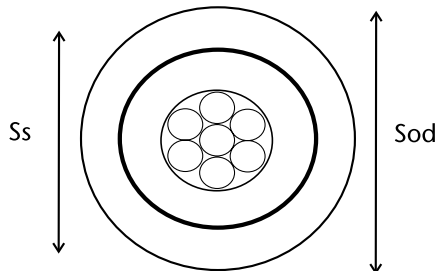


Figure 4.22 Cross section for a tape shielded cable.

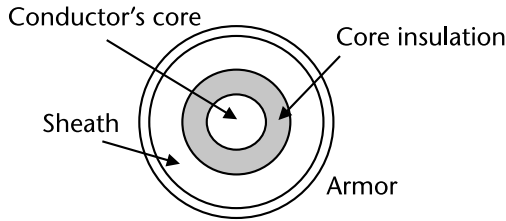


Figure 4.23 Cross section for a one-phase armored cable.

The capacitance in insulation from core to sheath, assuming a known relative permittivity and from sheath to the armor where $\epsilon_{cs} = \epsilon_{cs}^r \epsilon_0$.

$$C_{cs} = \frac{2\pi\epsilon_0\epsilon_{cs}^r}{\ln\left(\frac{r_{is}}{r_{oc}}\right)} = \frac{0.0556325}{\ln\left(\frac{r_{is}}{r_{oc}}\right)} \epsilon_{cs}^r \mu\text{F/km} \quad (4.70)$$

$$C_{sa} = \frac{0.0556325}{\ln\left(\frac{r_{ia}}{r_{os}}\right)} \epsilon_{sa}^r \mu\text{F/km} \quad (4.71)$$

Relative permittivity ϵ_{cs}^r is a complex number with components that depend on frequency. At low frequencies, as is the case in electric power systems, only the real part is significant at a steady state.

4.5.3 Three-phase Cables

For three-phase cable arrangements using single core cables with screen, the phases are laid parallel to each other so that there is no electric coupling between phases. A different layout is the pipe type where phases can be arranged as a triangular arrangement or cradle configuration (see Figure 4.24).

Table 4.1 Real Part of ϵ_{cs}^r

<i>Material</i>	<i>Real part of relative permittivity</i>
Solid impregnated paper	4.0
Oil filled impregnated paper	3.5
Oil pressure pipe type	3.7
Butyl rubber	4.0
EPR	3.0
XLPE	2.5
Polyethylene PE	2.3
Polyvinyl chloride PVC	8.0

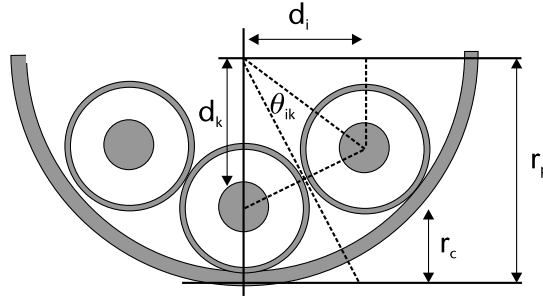


Figure 4.24 Three-phase cable, pipe type cradle arrangement.

The core-to-sheath capacitance is defined by (4.70) and the mutual capacitance between phases and the sheath of each phase and the pipe as:

$$C_{ss} = \frac{0.0556325}{\ln\left(\frac{\text{Radius}}{\sqrt{d_i^2 + d_k^2 - 2d_i d_k \cos\theta_{ik}}}\right)} \epsilon_p^r \mu\text{F/km} \quad (4.72)$$

For pipe type cable, in a three-phase cable and cradle arrangement.

Example 4.10

Values for pipe and cable radius: $r_p = 3.0$ and $r_c = 1.0$. Center of coordinates for cable k is at $(0, 1.0)$ and $d_k = r_p - r_c = 3.0 - 1.0 = 2.0$. First, the center coordinates for cable i , capacitance sheath-armor and capacitance armor-Earth, as in Table 4.2, as $\theta_{ik}/2 = \arcsin(r_c/d_k) = \arcsin(1.0/2.0) = 30^\circ$, $\theta_{ik} = 60^\circ$ (see Figure 4.25).

Table 4.2 Center Coordinates for Cable i and Capacitances

	$d_i = d_k \cos\left(\frac{\pi}{2} - \theta_{ik}\right) = 2.0 \cos\left(\frac{\pi}{2} - 60.0^\circ\right) = 1.732$	
	$r_p - d_k \sin\left(\frac{\pi}{2} - 60.0^\circ\right) = 3.0 - 2.0 \sin\left(\frac{\pi}{2} - 60.0^\circ\right) = 2.0$	
Capacitance core-sheath	$C_{cs} = \frac{0.0556325 \epsilon_{cs}^r}{\ln\left(\frac{r_{is}}{r_{oc}}\right)} \mu\text{F/km}$	$B_{cs} = \frac{0.3495493 f \epsilon_{cs}^r}{\ln\left(\frac{r_{is}}{r_{oc}}\right)} \mu\text{S/km}$
Capacitance sheath-armor	$C_{sa} = \frac{0.0556325 \epsilon_{sa}^r}{\ln\left(\frac{r_{ia}}{r_{os}}\right)} \mu\text{F/km}$	$B_{sa} = \frac{0.3495493 f \epsilon_{sa}^r}{\ln\left(\frac{r_{ia}}{r_{os}}\right)} \mu\text{S/km}$
Capacitance armor-Earth	$C_{ae} = \frac{0.0556325 \epsilon_{ae}^r}{\ln\left(\frac{r_{oa} + t_{ps}}{r_{os}}\right)} \mu\text{F/km}$	$B_{ae} = \frac{0.3495493 f \epsilon_{ae}^r}{\ln\left(\frac{r_{oa} + t_{ps}}{r_{os}}\right)} \mu\text{S/km}$

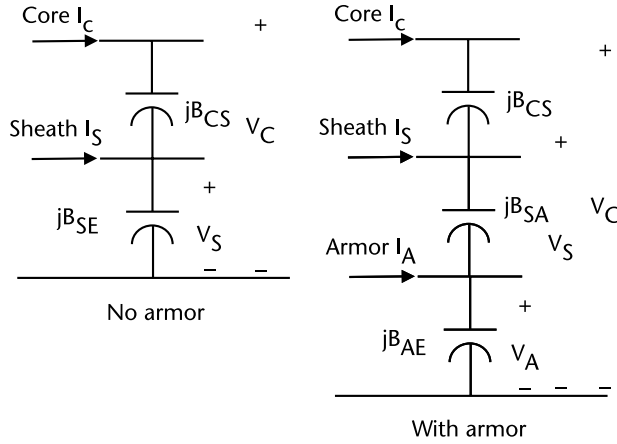


Figure 4.25 Susceptance values among core, sheath, and armor (when present).

The three-phase *abc* shunt admittance matrix for the no-armor case has a 6×6 structure. The sheath *abc* currents are zero; using a *partial inversion*, we find the *abc* equivalent matrix.

$$\begin{bmatrix} Y_{abc}^{cc} & Y_{abc}^{c,s} \\ Y_{abc}^{s,c} & Y_{abc}^{ss} \end{bmatrix} \begin{bmatrix} V_{abc}^c \\ V_{abc}^s \end{bmatrix} = \begin{bmatrix} I_{abc}^c \\ I_{abc}^s \end{bmatrix} \quad I_{abc}^s = 0 \quad (4.73)$$

$$\begin{bmatrix} (Y_{abc}^{cc})^{eq} & - \\ - & - \end{bmatrix} \begin{bmatrix} V_{abc}^c \\ 0 \end{bmatrix} = \begin{bmatrix} I_{abc}^c \\ V_{abc}^s \end{bmatrix} \quad (4.74)$$

4.5.4 Three-phase Cables, Pipe Type

Mutual capacitance in $\mu\text{F}/\text{km}$ between sheaths for each phase and the pipe:

$$C_{ss,ik} \approx \frac{0.0556325\epsilon_p^r}{\ln\left(\frac{r_p}{\sqrt{d_i^2 + d_k^2 - 2d_id_k \cos\theta_{ik}}}\right)} \quad (4.75)$$

$$C_{sp,ii} \approx \frac{0.0556325\epsilon_p^r}{\ln\left(\frac{r_p^2 - r_i^2}{r_p r_i}\right)} \quad (4.76)$$

Self and mutual impedance in ohms/km for underground cables, for the core conductor with Earth return.

$$f(r_{oc}, r_{ic}) = 1.0 - \frac{2r_{ic}^2}{r_{oc}^2 - r_{ic}^2} + \frac{4r_{ic}^4}{(r_{oc}^2 - r_{ic}^2)^2} \ln\left(\frac{r_{oc}}{r_{ic}}\right) \quad (4.77)$$

$$Z_{cc} = R_{c,ca} + \pi^2 10^{-4} f + j4\pi 10^{-4} f \left[\frac{\mu_c^r}{4} f(r_{oc}, r_{ic}) + \ln \left(\frac{D_{erc}}{r_{oc}} \right) \right] \quad (4.78)$$

Depth of equivalent Earth-return conductor in meters is $D_{erc} = 658.37\sqrt{\rho/f}$ and μ_c^r is relative permeability for a core conductor.

For sheath with Earth return, self impedance in ohms/km where μ_s^r is the relative permeability of sheath conductor.

$$f(r_{os}, r_{is}) = 1.0 - \frac{2r_{is}^2}{r_{os}^2 - r_{is}^2} + \frac{4r_{is}^4}{(r_{os}^2 - r_{is}^2)^2} \ln \left(\frac{r_{os}}{r_{is}} \right) \quad (4.79)$$

$$Z_{ss} = R_{s,ca} + \pi^2 10^{-4} f + j4\pi 10^{-4} f \left[\frac{\mu_s^r}{4} f(r_{os}, r_{is}) + \ln \left(\frac{D_{erc}}{r_{os}} \right) \right] \quad (4.80)$$

Self-impedance for armor with Earth return, impedance in ohms/km, and μ_a^r is the relative permeability of armor conductor.

$$f(r_{oa}, r_{ia}) = 1.0 - \frac{2r_{ia}^2}{r_{oa}^2 - r_{ia}^2} + \frac{4r_{ia}^4}{(r_{oa}^2 - r_{ia}^2)^2} \ln \left(\frac{r_{oa}}{r_{ia}} \right) \quad (4.81)$$

$$Z_{aa} = R_{a,ca} + \pi^2 10^{-4} f + j4\pi 10^{-4} f \left[\frac{\mu_a^r}{4} f(r_{oa}, r_{ia}) + \ln \left(\frac{D_{erc}}{r_{oa}} \right) \right] \quad (4.82)$$

The mutual impedance in ohms/km between core or sheath or armor i and core, sheath or armor j including earth return effect, where S_{ij} is the distance between centers of cables i and j from different cables $i \neq j$

$$Z_{ij} = \pi^2 10^{-4} f + j4\pi 10^{-4} f \ln \left(\frac{D_{erc}}{S_{ij}} \right) \quad (4.83)$$

For the same cable, the distance S_{ij} is the GMD between conductors; core and the sheath of cable j as $S_{ij} = (r_{os} + r_{is})/2$.

Example 4.11

For a three-phase cable in a flat arrangement and 275 kV, $f = 50$ Hz, Earth resistivity = 20 Ω -m.

Cu Core inner radius, oil duct = 0.0068 m, outer radius = 0.0219 m, $\mu_r = 1.0$, $R_{ac} = 0.01665 \Omega/\text{km}$.

Core's insulation paper with $\mu_r = 1.0$ and $\epsilon_r = 3.8$.

Lead sheath inner radius = 0.0379 m, outer radius = 0.0409 m, $\mu_r = 1.0$, R_{ac}
= 0.28865 Ω /km.

PVC over-sheath thickness = 0.003 m, $\mu_r = 1.0$, $\epsilon_r = 3.5$.

Capacitance and Shunt admittance for cable arrangements

inner r(m)	core r(m)	relative mu	ac-R (Ohms/km)
0.006800	0.021900	1.000000	0.016655
Core insulation		mu-relative	permittivity
		1.000000	3.800000

Lead sheath

inner r(m)	outer r(m)	mu-relative	ac-R (Ohms/km)
0.037900	0.040900	1.0000	0.288650

PVC over-sheath

thickness(m)	mu-relative	ac-R (Ohms/km)
0.003000	1.0000	3.500000

frequency (Hz)	Capacitance (micro-F/km)	Susceptance (micro-S/km)
50.0000	C_CS = 0.385446	B_CS = + 121.0915
50.0000	C_OS = 2.750806	B_COS = + 864.1911

YshuntC =

1.0e+002 *

Columns 1 through 4

0 + 1.2109i	0	0	0 - 1.2109i
0	0 + 1.2109i	0	0
0	0	0 + 1.2109i	0
0 - 1.2109i	0	0	0 + 9.8528i
0	0 - 1.2109i	0	0
0	0	0 - 1.2109i	0

Columns 5 through 6

0	0
0 - 1.2109i	0
0	0 - 1.2109i
0	0
0 + 9.8528i	0
0	0 + 9.8528i

Solidly bond cable, Vs = 0

Admittances in micro-S/km

YeqABC =

1.0e+002 *

0 + 1.2109i	0	0
0	0 + 1.2109i	0
0	0	0 + 1.2109i

	Phase A	Phase B	Phase C
Voltage =	158.77	-79.39	-79.39 kV
	+j 0.00	+j -137.50	+j +137.50

```

Current =      0.00          16.65          -16.65 A
             +j  +19.23      +j  -9.61      +j  -9.61
Power S =      0.00          -0.00          0.00 MVA/km
             +j  -3.05      +j  -3.05      +j  -3.05

```

Zseries (Ω/km)=

Columns 1 through 4

```

0.0660 + 0.6323i  0.0493 + 0.5087i  0.0493 + 0.4651i  0.0493 + 0.5799i
0.0493 + 0.5087i  0.0660 + 0.6323i  0.0493 + 0.5087i  0.0493 + 0.5087i
0.0493 + 0.4651i  0.0493 + 0.5087i  0.0660 + 0.6323i  0.0493 + 0.4651i
0.0493 + 0.5799i  0.0493 + 0.5087i  0.0493 + 0.4651i  0.3380 + 0.5814i
0.0493 + 0.5087i  0.0493 + 0.5799i  0.0493 + 0.5087i  0.0493 + 0.5087i
0.0493 + 0.4651i  0.0493 + 0.5087i  0.0493 + 0.5799i  0.0493 + 0.4651i

```

Columns 5 through 6

```

0.0493 + 0.5087i  0.0493 + 0.4651i
0.0493 + 0.5799i  0.0493 + 0.5087i
0.0493 + 0.5087i  0.0493 + 0.5799i
0.0493 + 0.5087i  0.0493 + 0.4651i
0.3380 + 0.5814i  0.0493 + 0.5087i
0.0493 + 0.5087i  0.3380 + 0.5814i

```

No armor

Impedances in Ohms/km

ZeqABC =

```

0.1278 + 0.1277i  0.0887 - 0.0011i  0.0719 - 0.0237i
0.0887 - 0.0011i  0.1186 + 0.1058i  0.0887 - 0.0011i
0.0719 - 0.0237i  0.0887 - 0.0011i  0.1278 + 0.1277i

```

Zeq012 =

```

0.2910 + 0.1031i  -0.0011 - 0.0023i  -0.0014 + 0.0021i
-0.0014 + 0.0021i  0.0416 + 0.1290i  -0.0122 + 0.0235i
-0.0011 - 0.0023i  0.0265 - 0.0012i  0.0416 + 0.1290i

```

4.6 Geometric Mean Radius

The concept of geometric mean radius (GMR) can be expanded from the definition (4.12) given for a solid conductor. Let us include various strands that carry a given amount of current I . The procedure is shown for three (see Figure 4.26) and for four (see Figure 4.27) strands arrangement.

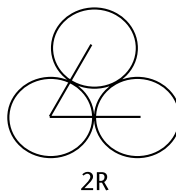


Figure 4.26 Cross section for a three-strand conductor.

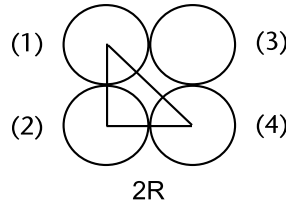


Figure 4.27 Cross section for a four-strand conductor.

Three strands:

$$\text{GMR}_1 = Re^{-1/4} \quad (4.84)$$

For three conductors, the flux linkage equations as in (4.16). with $i_1 = i_2 = i_3 = I/3$ and its GMR as in (4.86).

$$\lambda = \frac{(\lambda_1 + \lambda_2 + \lambda_3)}{3} = \frac{\mu_o I}{2\pi 9} \ln \left(\frac{1}{(\text{GMR}_1)^3 (2R)^6} \right) \quad (4.85)$$

$$\text{RMG} = \sqrt[3]{(Re^{-1/4})^3 (2R)^6} = R(4e^{-1/4})^{1/3} = 1.46048R \quad (4.86)$$

Four strands where distances are: $d_{12} = d_{13} = d_{24} = d_{34} = 2R$ and $d_{14} = d_{23} = 2\sqrt{2}R$. Currents are: $i_1 = i_2 = i_3 = i_4 = I/4$ using (4.16) the flux linkages can be written as in (4.87) and the equivalent GMR as in (4.88).

$$\lambda = \frac{\lambda_1 + \lambda_2 + \lambda_3 + \lambda_4}{4} = \frac{\mu_o I}{2\pi 16} \ln \left(\frac{1}{(\text{GMR}_1)^4 (2R)^8 (2\sqrt{2}R)^4} \right) \quad (4.87)$$

$$\text{RMG} = \sqrt[4]{(Re^{-1/4})^4 (2R)^8 (2\sqrt{2}R)^4} = R(8\sqrt{2}e^{-1/4})^{1/4} = 1.72289R \quad (4.88)$$

4.7 Equivalent Height

Calculate an equivalent height of an overhead transmission line that has a catenary form (assuming that it can be approximated to a parabola; see Figure 4.28). The conductor's sag between supports are: $x = 0, y = y_{sm}, x = d/2, y = y_t$. Constants for (4.89) are: $y_{sm} = b, y_t = k(d/2)^2 + y_{sm}$ and $k = (y_t - y_{sm})/(d/2)^2$.

$$y = kx^2 + b \quad (4.89)$$

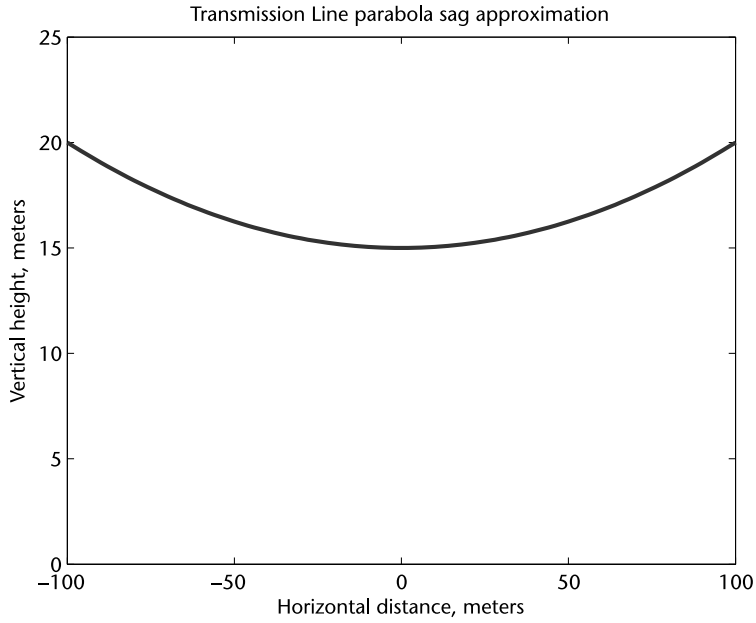


Figure 4.28 Sag estimation by means of approximation to a parabola.

The parabola equation is:

$$y = \frac{y_t - y_{sm}}{(d/2)^2} x^2 + y_{sm} \tag{4.90}$$

The equivalent height y_{eq} times the distance between supports d can be made equal to the area enclosed from $-d/2$ to $+d/2$ by the parabola (4.90) with $sag = y_t - y_{sm}$.

$$y_{eq} = \frac{1}{d} \frac{y_t - y_{sm}}{3(d/2)^2} 2 \left(\frac{d}{2} \right)^3 + y_{sm} = \frac{sag}{3} + y_{sm} \tag{4.91}$$

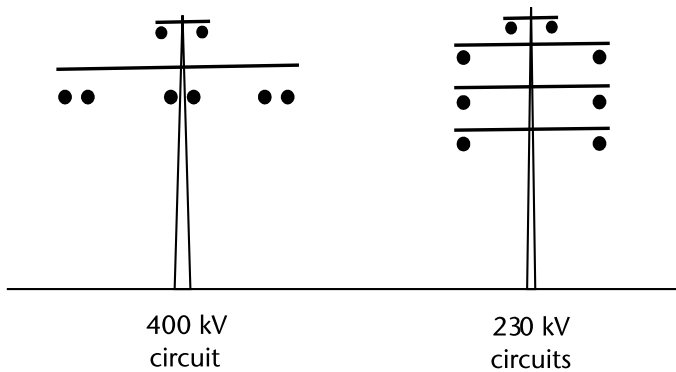


Figure 4.29 400 kV and 230 kV circuits running in parallel (drawing not to scale).

4.8 Transmission Lines in Parallel

Assume one 400 kV line and one 230 kV with double circuit configuration, each arrangement has two *shield wires*. The 400 kV line has two conductors per phase and the 230 kV line has two circuits in a vertical arrangement. Data is given below, distances are in meters, and there is no transposition. Results are shown for series impedance calculation. Shunt capacitive admittance can be calculated through the steps outlined in Section 4.4.2.

Number of conductors = 16
 Frequency = 60
 resistivity = 100 Ohms-m

k	x(k)	y(k)	GMR(k)	res(k)	code(k)
1	-11.5150	26.7500	1.10744e-003	6.02237e-002	0
2	-0.2250	26.7500	1.10744e-003	6.02237e-002	0
3	11.0650	26.7500	1.10744e-003	6.02237e-002	0
4	21.5000	17.6700	9.95680e-004	6.02237e-002	0
5	21.5000	23.1700	9.95680e-004	6.02237e-002	0
6	21.5000	28.6700	9.95680e-004	6.02237e-002	0
7	28.5000	17.6700	9.95680e-004	6.02237e-002	0
8	28.5000	23.1700	9.95680e-004	6.02237e-002	0
9	28.5000	28.6700	9.95680e-004	6.02237e-002	0
10	-11.0650	26.7500	1.10744e-003	6.02237e-002	1
11	0.2250	26.7500	1.10744e-003	6.02237e-002	2
12	11.5150	26.7500	1.10744e-003	6.02237e-002	3
13	-6.9600	35.3000	6.33400e-004	4.03977e+000	-1
14	6.9600	35.3000	6.33400e-004	4.03977e+000	-1
15	22.6400	32.9200	6.33400e-004	4.03977e+000	-1
16	27.3600	32.9200	6.33400e-004	4.03977e+000	-1

Impedance in Ohms/km

Z₀₁₂ =

Columns 1 through 4

0.3609 + 1.2570i	0.0111 - 0.0031i	-0.0219 - 0.0060i	0.3331 + 0.6834i
-0.0219 - 0.0060i	0.0311 + 0.4865i	-0.0297 + 0.0181i	0.0338 - 0.0537i
0.0111 - 0.0031i	0.0303 + 0.0165i	0.0311 + 0.4865i	-0.0480 - 0.0473i
0.3331 + 0.6834i	-0.0480 - 0.0473i	0.0338 - 0.0537i	0.4060 + 1.5880i
-0.0084 - 0.0092i	0.0041 + 0.0037i	-0.0040 + 0.0032i	-0.0264 - 0.0096i
-0.0044 - 0.0001i	0.0044 + 0.0020i	-0.0029 + 0.0036i	0.0108 + 0.0017i
0.3267 + 0.6191i	-0.0361 - 0.0345i	0.0221 - 0.0410i	0.3407 + 0.8670i
-0.0081 - 0.0045i	0.0019 + 0.0013i	-0.0012 + 0.0016i	-0.0187 - 0.0057i
-0.0033 + 0.0037i	0.0016 + 0.0005i	-0.0007 + 0.0013i	0.0044 + 0.0048i

Columns 5 through 8

-0.0044 - 0.0001i	-0.0084 - 0.0092i	0.3267 + 0.6191i	-0.0033 + 0.0037i
-0.0029 + 0.0036i	-0.0040 + 0.0032i	0.0221 - 0.0410i	-0.0007 + 0.0013i
0.0044 + 0.0020i	0.0041 + 0.0037i	-0.0361 - 0.0345i	0.0016 + 0.0005i
0.0108 + 0.0017i	-0.0264 - 0.0096i	0.3407 + 0.8670i	0.0044 + 0.0048i
0.0610 + 0.6668i	-0.0297 + 0.0180i	-0.0194 - 0.0056i	0.0006 + 0.0275i
0.0301 + 0.0166i	0.0610 + 0.6668i	0.0041 + 0.0054i	0.0166 + 0.0089i
0.0041 + 0.0054i	-0.0194 - 0.0056i	0.3966 + 1.5955i	0.0111 + 0.0010i

	0.0006 + 0.0275i	-0.0162 + 0.0101i	-0.0255 - 0.0097i	0.0609 + 0.6669i
	0.0166 + 0.0089i	0.0006 + 0.0275i	0.0111 + 0.0010i	0.0301 + 0.0167i
Column 9				
	-0.0081 - 0.0045i			
	-0.0012 + 0.0016i			
	0.0019 + 0.0013i			
	-0.0187 - 0.0057i			
	-0.0162 + 0.0101i			
	0.0006 + 0.0275i			
	-0.0255 - 0.0097i			
	-0.0298 + 0.0180i			
	0.0609 + 0.6669i			

The code for each conductor helps us in classifying a conductor as a *retained* versus one conductor that is part of a *bundle* or a conductor that works as a shield wire. The reduced sequence 012 impedance matrices have information for the zero, positive, and negative sequences. Mutual effects between zero sequence impedances to neighboring circuits are not negligible, as highlighted in the first column of the printout results.

References

- [1] Clarke, E., *Circuit Analysis of AC Power Systems, Volume I: Symmetrical and Related Components*, New York: John Wiley & Sons, 1943.
- [2] Elgerd, O. I., *Electric Energy Systems Theory*, New York: McGraw-Hill Book Company, 1971.
- [3] Bruce Shipley, R., *Introduction to Matrices and Power Systems*, New York: John Wiley & Sons, 1976.
- [4] Sakis Meliopoulos, A. P., *Power System Grounding and Transients*, New York: Marcel Dekker, Inc., 1988.
- [5] Kersting, W. H., *Distribution System Modeling and Analysis*, Boca Raton, FL: CRC Press, 2002.
- [6] Tleis, N., *Power Systems Modelling and Fault Analysis*, Burlington, MA: Elsevier, 2008.

Transmission Line Loadability

5.1 Introduction

To plan and properly operate a large electric power system, planning engineers need to know with reasonable accuracy how much power the new transmission lines can carry given the changing seasonal demand conditions. Operating engineers in the control center need to monitor how much power various important lines are carrying. The load that a transmission line will carry depends on various parameter values, as well as weather conditions (i.e., heat, wind, and rain). Load ability studies determine how a given transmission line can use its power carrying capacities, especially under market rules and conditions. The maximum safe limit is to be determined based on the voltage level, conductor current capacity, length of the line, and electrical parameters (i.e., series impedance and shunt capacitance per unit length), as well as the existing reactive power compensation. To discuss the loadability concept, we assume a balanced transmission line; only positive sequence values will be used, and the maximum power and losses incurred can be estimated. Various tools can be applied to establish current and power handling capability (namely constants written as ABCD or nodal analysis). However, the distributed parameters model must be used so that the nature of the transmission line is better reflected through this modeling.

5.2 Approximate Real Power Handling and Losses

In steady state for an AC transmission line, the power transfer on a balanced line follows a general model; with $\tilde{V}_k = |V_k| \angle \theta_k$, $\tilde{V}_m = |V_m| \angle \theta_m$ and $y_{sh/2} = -1/jX_{C/2} = jB_{sh/2}$ notation as in Figure 5.1.

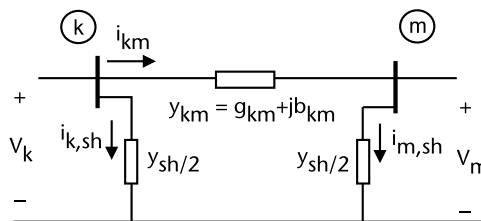


Figure 5.1 Transmission line model, nodes k and m .

The complex power flow, from node k to node m , using $\theta_{km} = \theta_k - \theta_m$:

$$s_{km} = \tilde{V}_k (i_{km} + i_{k,sh})^* = \tilde{V}_k \left[(\tilde{V}_k - \tilde{V}_m) y_{km} + \tilde{V}_k y_{sb/2} \right]^* \quad (5.1)$$

From here, we have the real and imaginary parts for the real and reactive power:

$$p_{km} = |V_k|^2 g_{km} - |V_k||V_m| g_{km} \cos \theta_{km} - |V_k||V_m| b_{km} \sin \theta_{km} \quad (5.2)$$

$$q_{km} = -|V_k|^2 (b_{km} + B_{sb/2}) - |V_k||V_m| g_{km} \sin \theta_{km} + |V_k||V_m| b_{km} \cos \theta_{km} \quad (5.3)$$

Some approximations for high voltage transmission lines are $g_{km} \ll b_{km}$ and $b_{km} \approx -1/x_{km}$, then:

$$p_{km} \approx \sin \theta_{km} \frac{|V_k||V_m|}{x_{km}} \quad (5.4)$$

The three-phase power in megawatts can be estimated using phase-to-phase voltage magnitudes $|V_k|$, $|V_m|$ and $x_{km} = xl$, where x is the inductive series reactance in ohms/km and l is the line's length in km. We use the line's positive sequence series impedance as listed in Table 5.1. Angle θ_{km} , by a stability criteria sets a limit to 30° and terminal voltages magnitudes with similar values $|V|$.

$$p_{km}^{\max} \approx \sin \left(\frac{\pi}{6} \right) \frac{|V|^2}{xl} = \frac{|V|^2}{2xl} \quad (5.5)$$

In order to have an estimation about the amount of power losses, we can assume that current is in phase with the voltage at the receiving end m ; this amounts to having unity power factor. This will give an approximate figure that is close enough for our evaluation purposes.

Table 5.1 Transmission Line Parameter Values

System voltage, kV	400	750
Mean conductor height, m	15	18
Phase to phase distance, m	12	15
Phase conductors, 954 MCM	2	4
Conductor diameter, m	0.03037	0.03037
Subconductor distance, m	0.46	0.46
r (25°C) ohms/km	0.03048	0.01524
x (50 Hz), ohms/km	0.3330	0.2857
x/r ratio	10.92	18.74

$$I = \frac{p_{km}}{3|V|/\sqrt{3}} = |V| \frac{\sin \theta_{km}}{\sqrt{3}xl} \quad (5.6)$$

$$P_{\text{Loss}} = 3rI^2 = rl \left(\frac{|V| \sin \theta_{km}}{xl} \right)^2 \quad (5.7)$$

$$\frac{P_{\text{Loss}}}{p_{km}} \% = 100 \frac{\sin \theta_{km}}{(x/r)} \quad (5.8)$$

From numbers on Table 5.2, it can be said that:

- Approximate values can be used as a preliminary guideline. Detailed models will give power and losses when variable load conditions and shunt capacitive effects are included; early morning load and the peak demand values are usually very different in any electrical system.
- The 750 kV transmission line, over the same distance, can carry up to four times ($4,900/1,200 \approx 4.1$ or $3,281/800 \approx 4.1$) as much power as the 400 kV line.
- Losses depend on the x/r ratio and angle θ_{km} (phase difference in sending and receiving voltages). To calculate line losses, the positive sequence reactance and phase resistance are required.
- For a given real power P , the amount of losses on the 750 kV line as compared to the 400 kV line, are $2.5/4.57 = 0.547$ times.

5.2.1 Number of Circuits Required to Transport Electric Power

A problem often faced by planning engineers is how to send a given amount of power from a generation site to the load center (see Figure 5.2). For a known distance, the question is: how many three-phase transmission circuits will be required and at what voltage? The planning engineers must also study to see if there are other technologies, such as DC transmission, that can be technical and economically attractive.

For the following discussion on how to handle 5,000 MW in a distance of 300 km, it is assumed that options are AC, operating either at 400 kV or 750 kV, with nodal angle separation of 30° , which gives a reasonable steady state stability margin. With this value under severe contingencies, the power generation plants

Table 5.2 Maximum Power and Losses in %, $\theta_{km} = 30^\circ$ (Data from Table 5.1)

System voltage kV	400	750
r (25°C) ohms/km	0.03048	0.01524
x (50 Hz), ohms/km	0.3330	0.2857
x/r ratio	10.92	18.74
Max P (MW), $\ell = 200$ km	1,200	4,922
Max P (MW), $\ell = 300$ km	800	3,281
Losses %	4.57	2.66

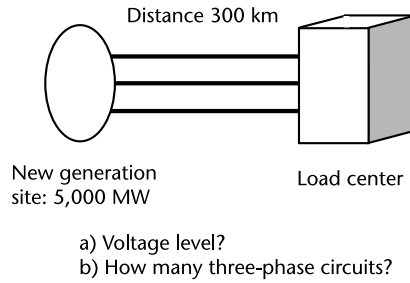


Figure 5.2 Generation site remote from a load center.

on both sides of the transmission line will remain in synchronous operating condition. The number of three-phase circuits needed, current per phase, and losses are given by the voltage level.

With 400 kV lines:

$$\text{Number of circuits} = 5,000 \text{ MW}/800 \text{ MW} = 6.25$$

$$\text{Current} = (5,000 \text{ MW}/3)/(400 \text{ kV}/\sqrt{3}) = 7.22 \text{ kA}$$

$$\text{Losses in \%} = 4.57$$

$$\text{Total losses} = 228.5 \text{ MW}$$

With 750 kV lines:

$$\text{Number of circuits} = 5,000 \text{ MW}/3,281 \text{ MW} = 1.52$$

$$\text{Current} = (5,000 \text{ MW}/3)/(750 \text{ kV}/\sqrt{3}) = 3.85 \text{ kA}$$

$$\text{Losses in \%} = 2.66$$

$$\text{Total losses} = 133 \text{ MW}$$

The preliminary answer—using this approximate model—suggests the use of seven circuits of 400 kV or two circuits working at 750 kV. An economic evaluation should follow this step. A related situation is the *right of way*; the 400 kV lines needs around 40m each, and 80m are required for every 750 kV circuit lines. A simple comparison with a DC transmission line (not including the converter stations) and considering a ± 400 kV bipolar scheme, using four conductors carrying 1,000 amperes each; then the DC power transfer capacity is 1,600 MW. For a DC bipolar voltage ± 500 kV, the power handling capacity goes up to 2,000 MW.

To handle 5,000 MW for the bipolar ± 400 kV, the number of circuits is estimated as $5,000 \text{ MW}/1,600 \text{ MW} = 3.12$ with a current of $(5,000 \text{ MW})/(400 \text{ kV}) = 15.5 \text{ kA}$. If a bipolar ± 500 kV DC is considered, the estimated number of circuits are $5,000 \text{ MW}/2,000 \text{ MW} = 2.5$, and current as $(5,000 \text{ MW})/(500 \text{ kV}) = 10.0 \text{ kA}$. The numbers point to solving by using four DC circuits working at ± 400 kV or three DC circuits at ± 500 kV. An economic evaluation should follow in which the right of way required has a high economic impact on the options. One alternative would be to increase the number of conductors per pole (i.e., four conductors per pole will handle 4,000A and 2,000 MW). Mechanical stress and structure design should follow more detailed studies.

5.2.2 Reactive Power Required by the AC Transmission Line

The approximate real power transfer and the maximum real power were obtained by (5.4)–(5.5), and losses were obtained by (5.8). In the case of AC transmission lines, reactive power is required to support sending and receiving voltages within the 5% limit. Therefore, if we assume 400 kV and 400(0.95) kV. With $g_{km} \ll b_{km}$ and $b_{km} \approx -1/x_{km}$,

$$q_{km} \approx \left(-|V|^2 + |V|^2 \cos\theta_{km} \right) b_{km} = \frac{|V|^2 (1 - \cos\theta_{km})}{xl} \tag{5.9}$$

Example 5.1

For a 200 km, 400 kV line, 50 Hz, in order to supply a three-phase load of 600 MW at unity power factor, by (5.9) angle θ_{km} is required. The angle is calculated and then the reactive power from sending side q_{km} is obtained. $\sin \theta_{km} \approx p_{km}xl/|V_k||V_m|$, with value of 0.2628 rad or 15.23°. The reactive power is calculated by (5.9), as $q_{km} \approx 400^2 (0.95)(1 - \cos(15.23^\circ))/(0.333)(200)$, as 80.2 MVARs. Sending voltage 400 kV and receiving end at 400 (0.95) kV by the 5% voltage drop limit.

For a maximum power transfer of 1,200 MW, the reactive power required is 305.7 MVARs, calculated by $q_{km} \approx 400^2 (0.95)(1 - \cos(30^\circ))/(0.333)(200)$.

A series of detailed analysis must be carried out using load flow studies; this method of study will be presented in Chapter 6. One thing stands out from the approximated values: the transmission line needs reactive power support in order to fulfill its duties of real power transfer, in order to keep its operating variables within limits, and to include both light and heavy load conditions. More comprehensive studies need increased detailed models as the ones presented in Section 5.5.

5.3 $V(x)$ and $I(x)$ Equations for a Long Transmission Line

As transmission lines of increased length are required, a more detailed model is needed to correctly represent the electromagnetic behavior. The model needs to relate steady state conditions as voltage phasor V and current phasor I with distance x . One common assumption is to start with a balanced transmission line and to write

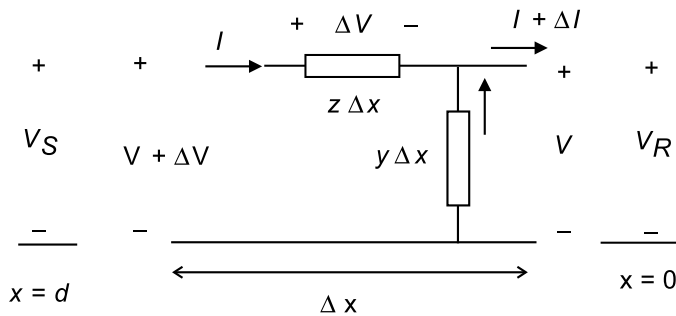


Figure 5.3 Incremental distance in a long transmission line, phasor relations.

the incremental distance Δx relations for the voltage series drop ΔV and the incremental current ΔI through the shunt component; z is the impedance in ohms per unit of length and y is the admittance in siemens per unit of length (see Figure 5.3).

$$\Delta V = z\Delta x I \quad \Delta I = y\Delta x V \quad (5.10)$$

The incremental voltage and current relations as $\Delta x \rightarrow 0$

$$\frac{dV}{dx} = zI \quad \frac{dI}{dx} = yV \quad (5.11)$$

The differential equations in (5.10) are related through their derivatives:

$$\frac{d^2V}{dx^2} = z \frac{dI}{dx} = zyV \quad (5.12)$$

Expression (5.12) has a characteristic polynomial $(p^2 - zy)V = 0$ with two roots, which are written as $\gamma = \pm\sqrt{zy} = \alpha + j\beta$. One general solution for phasor voltage V has the following form:

$$V(x) = A_1 e^{+\gamma x} + A_2 e^{-\gamma x} \quad (5.13)$$

- α Attenuation constant, pu/unit of distance
- β phase shift, radians/unit of distance

To prove that (5.13) is a solution to (5.12), we derive $V(x)$ twice with respect to x , so:

$$\frac{d^2V}{dx^2} = \frac{d}{dx} \left(\frac{dV}{dx} \right) = \frac{d}{dx} (pA_1 e^{+\gamma x} - pA_2 e^{-\gamma x}) = \gamma^2 (A_1 e^{+\gamma x} + A_2 e^{-\gamma x}) = zyV \quad (5.14)$$

Now, we focus on using voltage and current conditions at the boundaries as a means to find constants A_1 and A_2 . We use boundary values known at terminal ($x = 0$, $V(0) = V_R$). For current I , let us use (5.11) and define the characteristic impedance:

$$Z_c = \sqrt{\frac{z}{y}} \quad (5.15)$$

$$I = \frac{1}{z} \frac{dV}{dx} = \frac{\gamma}{z} A_1 e^{+\gamma x} - \frac{\gamma}{z} A_2 e^{-\gamma x} = \frac{A_1}{\sqrt{z/y}} e^{+\gamma x} - \frac{A_2}{\sqrt{z/y}} e^{-\gamma x} \quad (5.16)$$

A system of equations from (5.13) and (5.16), using the receiving end conditions at $x = 0$, will help us solve for A_1 and A_2 .

$$\begin{aligned} V(0) &= V_R = A_1 + A_2 \\ I(0) &= I_R = \frac{A_1}{Z_c} - \frac{A_2}{Z_c} \end{aligned} \quad (5.17)$$

$$\begin{bmatrix} A_1 \\ A_2 \end{bmatrix} = \begin{bmatrix} \frac{V_R + Z_c I_R}{2} \\ \frac{V_R - Z_c I_R}{2} \end{bmatrix} \quad (5.18)$$

The solution for voltage $V(x)$ and current $I(x)$ is given by (5.19). The first part of these equations is called an *incident wave* and the second part a *reflected wave*.

$$\begin{bmatrix} V(x) \\ I(x) \end{bmatrix} = \begin{bmatrix} \frac{V_R + Z_c I_R}{2} + \frac{V_R - Z_c I_R}{2} \\ \frac{V_R/Z_c + I_R}{2} - \frac{V_R/Z_c - I_R}{2} \end{bmatrix} \begin{bmatrix} e^{+\gamma x} \\ e^{-\gamma x} \end{bmatrix} \quad (5.19)$$

5.3.1 The Flat Line Concept

In case that, at the receiving end (where $V(x=0) = V_R$ and $I(x=0) = I_R$), the impedance load happens to be equal to the characteristic impedance Z_c , then by (5.19) there will not be *reflected wave* and $V_R = Z_c I_R$ (see Figure 5.4).

5.3.2 Surge Impedance, Wave Length and Propagation Velocity

In general, the characteristic impedance Z_c is a complex number. For a lossless line ($r=0, g=0$) it has a particular real value in ohms and is known as *surge impedance*.

$$Z_c = \sqrt{\frac{L}{C}} \quad (5.20)$$

The *wavelength* λ is a distance at which the wave is shifted by 2π radians. As $\gamma = \alpha + j\beta$ in the exponential $e^{\gamma x} = e^{(\alpha+j\beta)x} = e^{\alpha x} e^{+j\beta x}$ the term $e^{+j\beta x}$ is a phase shift that increases as x gets larger. When $\beta x = 2\pi$, we have the distance $2\pi/\beta$ as:

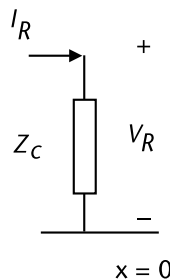


Figure 5.4 Characteristic impedance Z_c as load at receiving end.

$$\lambda = \frac{2\pi}{\beta} \quad (5.21)$$

The speed of propagation (m/s) relates distance λ and period T at a given frequency f in Hz:

$$v = \frac{\lambda}{T} = f\lambda \quad (5.22)$$

5.3.3 No-Load Line and General Hyperbolic Form

For an *open circuit* or no load condition at $x = 0$, the receiving end has current as $I_R = 0$. Therefore, (5.19) will give the voltage value $V(x = 0) = V_R$ and current $I(x = 0) = I_R = 0$. The incident wave and the reflected wave cancel each other out, giving the condition $I_R = 0$.

Writing in (5.19) an arrangement with V_R and I_R will give hyperbolic expressions for a long transmission line. If we let $x = d$ (the total line distance), we can write sending end conditions in terms of the receiving end, as in (5.23).

$$\begin{bmatrix} V_S \\ I_S \end{bmatrix} = \begin{bmatrix} \cosh(\gamma d) & Z_c \sinh(\gamma d) \\ \frac{1}{Z_c} \sinh(\gamma d) & \cosh(\gamma d) \end{bmatrix} \begin{bmatrix} V_R \\ I_R \end{bmatrix} \quad (5.23)$$

For the no-load case, $I_R = 0$ in (5.23) gives voltage the $V_S = \cosh(\gamma d)V_R$. From this no-load condition, (5.24) shows the case known as *Ferranti effect*, which explains why we have a higher voltage value at the receiving end; even when the line is working at an *open circuit* condition. The value for the sending current I_S , under the same no-load condition is (5.25).

$$V_R = \frac{V_S}{\cosh(\gamma d)} \quad (5.24)$$

$$I_S = \frac{1}{Z_c} \sinh(\gamma d)V_R = \frac{1}{Z_c} \tanh(\gamma d)V_S \quad (5.25)$$

5.3.4 Nominal π and Equivalent Circuit

Equivalent circuits for a transmission line relate sending and receiving voltage and current V_S, I_S, V_R, I_R through various parameters. Total impedance Z (ohms) and total admittance Y (siemens) are used in a nominal π circuit for a transmission line with distance d units of distance, z ohms/unit of distance, and y S/unit of distance, as shown in Figure 5.5.

$$Z = zd \quad Y = yd \quad (5.26)$$

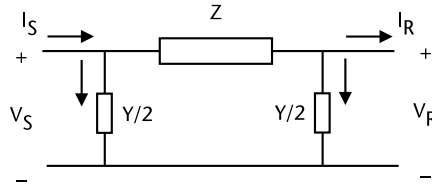


Figure 5.5 Nominal π circuit, total impedance Z and total admittance Y for a transmission line.

- Z Total line impedance, ohms
- Y Total line admittance, siemens
- z impedance per unit of distance, ohms/km
- y admittance per unit of distance, siemens/km
- d distance, km

Voltage and current equations for the sending end, as seen in Figure 5.5, are:

$$V_S = V_R + Z \left(I_R + \frac{Y}{2} V_R \right) = \left(1 + \frac{ZY}{2} \right) V_R + Z I_R \tag{5.27}$$

$$I_S = \frac{Y}{2} V_S + \frac{Y}{2} V_R + I_R = Y \left(1 + \frac{ZY}{4} \right) V_R + \left(1 + \frac{ZY}{2} \right) I_R \tag{5.28}$$

$$\begin{bmatrix} V_S \\ I_S \end{bmatrix} = \begin{bmatrix} \left(1 + \frac{ZY}{2} \right) & Z \\ Y \left(1 + \frac{ZY}{4} \right) & \left(1 + \frac{ZY}{2} \right) \end{bmatrix} \begin{bmatrix} V_R \\ I_R \end{bmatrix} \tag{5.29}$$

5.3.5 Long Line Equivalent Circuit

For the long-distance transmission line, an equivalent circuit similar to (5.23) can be written. If we compare the terms to the hyperbolic form; the equivalent circuit for a long transmission line is shown in Figure 5.6:

$$\begin{bmatrix} V_S \\ I_S \end{bmatrix} = \begin{bmatrix} \left(1 + \frac{Z'Y'}{2} \right) & Z' \\ Y' \left(1 + \frac{Z'Y'}{4} \right) & \left(1 + \frac{Z'Y'}{2} \right) \end{bmatrix} \begin{bmatrix} V_R \\ I_R \end{bmatrix} \tag{5.30}$$

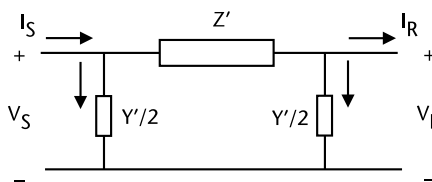


Figure 5.6 Equivalent circuit for a long distance transmission line.

$$Z' = Z_c \sinh(\gamma d) = Z \frac{\sinh(\gamma d)}{\gamma d} \tag{5.31}$$

$$\frac{Y'}{2} = \frac{\cosh(\gamma d) - 1}{Z'} = \frac{\cosh(\gamma d) - 1}{Z_c \sinh(\gamma d)} = \frac{Y \tanh(\gamma d/2)}{2 \gamma d/2} \tag{5.32}$$

From (5.31) by direct comparison of Z' and admittance Y' we identify the *correction factors* for the total impedance Z and admittance Y . The long transmission line impedance Z' and admittance $Y'/2$ are obtained.

5.4 ABCD Constants

One matrix that relates the sending to the receiving voltage and current is written for the two-terminal circuit using nodal voltages and line currents (assuming that positive sequence values are known); see Figure 5.7.

$$\begin{bmatrix} V_S \\ I_S \end{bmatrix} = \begin{bmatrix} A & B \\ C & D \end{bmatrix} \begin{bmatrix} V_R \\ I_R \end{bmatrix} \tag{5.33}$$

In general, the A, B, C, D constants are complex numbers whose values depend on the total parameters $R, L, C,$ and G of the transmission line element. A, D have no dimensions, B is in ohms, and C in Siemens.

For a passive circuit that is linear and bilateral (see Figure 5.8), with r (Ω/km) and ωL (Ω/km), length of ℓ (km). $R = r\ell$ and $X = \omega L \ell$, then $Z = R + jX$. From (5.34) and matrix (5.35) $A = D = 1, B = Z,$ and $C = 0$.

$$V_S = Z I_S + V_R \quad I_S = I_R \tag{5.34}$$

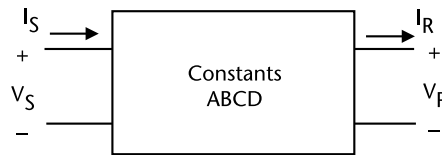


Figure 5.7 Variables in a two-port network.

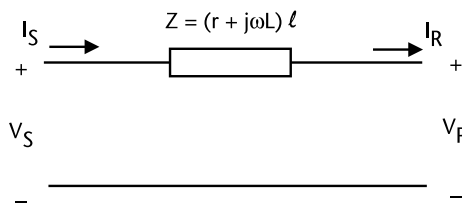


Figure 5.8 Two-port element for series impedance.

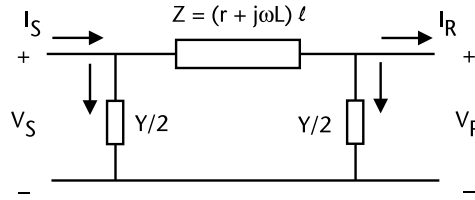


Figure 5.9 ABCD constants for a two-port π network.

$$\begin{bmatrix} V_S \\ I_S \end{bmatrix} = \begin{bmatrix} 1 & Z \\ 0 & 1 \end{bmatrix} \begin{bmatrix} V_R \\ I_R \end{bmatrix} \quad (5.35)$$

For a nominal π circuit (see Figure 5.9), the $ABCD$ constants of a mid-length transmission line (40–100 km) are as in (5.37). We start with (5.36) and V_S is already in terms of V_R and I_R , some algebra is required to get I_S in terms of V_R and I_R . From (5.37), we find directly that $A = D = 1 + YZ/2$, $B = Z$, and $C = Y(1 + YZ/4)$.

$$I_R + \frac{Y}{2}V_R = \frac{V_S - V_R}{Z} \quad V_S = \left(1 + \frac{YZ}{2}\right)V_R + ZI_R \quad (5.36)$$

$$\begin{bmatrix} V_S \\ I_S \end{bmatrix} = \begin{bmatrix} \left(1 + \frac{YZ}{2}\right) & Z \\ Y\left(1 + \frac{YZ}{4}\right) & \left(1 + \frac{YZ}{2}\right) \end{bmatrix} \begin{bmatrix} V_R \\ I_R \end{bmatrix} \quad (5.37)$$

For a shunt admittance element (see Figure 5.10), the $ABCD$ constants are deduced by writing voltages $V_S = V_R$, and the current $I_S = Y_{sb} V_R + I_R$. The constant are $A = D = 1$, $B = 0$, and $C = Y_{sb}$.

$$\begin{bmatrix} V_S \\ I_S \end{bmatrix} = \begin{bmatrix} 1 & 0 \\ Y_{sb} & 1 \end{bmatrix} \begin{bmatrix} V_R \\ I_R \end{bmatrix} \quad (5.38)$$

Where $A = D = 1$, $B = 0$, and $C = Y_{sb}$ (siemens).

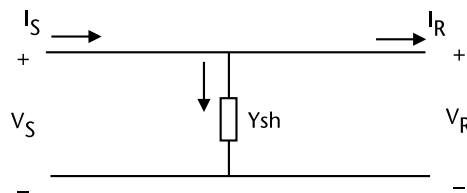


Figure 5.10 Shunt admittance and $ABCD$ constants.

5.4.1 ABCD Equivalent for Series Connection

For circuits with an $ABCD$ representation that need to be connected in series (see Figure 5.11), the boundary voltages and currents are conditions that must be met. In this case, voltages $V_{R1} = V_{S2}$ and $I_{R1} = I_{S2}$. Starting with $ABCD$ expressions for each series component, (5.39) and when connected the final result follows: the $ABCD$ constants for the series equivalent are obtained by matrix multiplication.

$$\begin{bmatrix} V_{S1} \\ I_{S1} \end{bmatrix} = \begin{bmatrix} A_1 & B_1 \\ C_1 & D_1 \end{bmatrix} \begin{bmatrix} V_{R1} \\ I_{R1} \end{bmatrix} \quad \begin{bmatrix} V_{S2} \\ I_{S2} \end{bmatrix} = \begin{bmatrix} A_2 & B_2 \\ C_2 & D_2 \end{bmatrix} \begin{bmatrix} V_{R2} \\ I_{R2} \end{bmatrix} \quad (5.39)$$

$$\begin{bmatrix} V_{S1} \\ I_{S1} \end{bmatrix} = \begin{bmatrix} A_1 & B_1 \\ C_1 & D_1 \end{bmatrix} \begin{bmatrix} A_2 & B_2 \\ C_2 & D_2 \end{bmatrix} \begin{bmatrix} V_{R2} \\ I_{R2} \end{bmatrix} \quad (5.40)$$

5.4.2 Nodal Admittance Matrix from ABCD Constants

Starting with $ABCD$ values for a given circuit, algebra will be used to identify the nodal admittance values. From (5.33) and recognizing the property that $AD - CB = 1$, I_S and I_R are written in terms of V_S and V_R .

$$V_S = AV_R + BI_R \quad I_S = CV_R + DI_R \quad (5.41)$$

Current I_R from (5.41) is substituted into I_S in order to find the elements that go into the first row of (5.42). Nodal current is assumed to be positive when it goes into a node, then nodal current I_R has a negative sign. The nodal admittance matrix is obtained as (5.43).

$$\begin{bmatrix} \frac{+D}{B} & \frac{-1}{B} \\ \frac{-1}{B} & \frac{+A}{B} \end{bmatrix} \begin{bmatrix} V_S \\ V_R \end{bmatrix} = \begin{bmatrix} I_S \\ I_R \end{bmatrix} \quad (5.42)$$

$$Y_{\text{nodal}} = \begin{bmatrix} \frac{+D}{B} & \frac{-1}{B} \\ \frac{-1}{B} & \frac{+A}{B} \end{bmatrix} \quad (5.43)$$

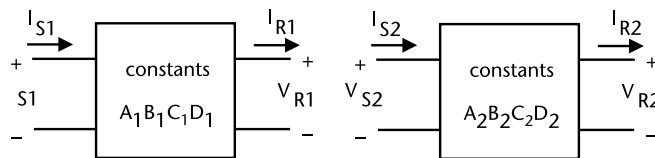


Figure 5.11 Series connection of two $ABCD$ models.

Example 5.2

A 115 kV transmission line has positive sequence parameters, and its operating frequency is 50 Hz. Series reactance $x = 0.4178 \text{ } \Omega/\text{km}$, shunt susceptance $b_{sh} = 2.767 \times 10^{-6} \text{ S/km}$, series resistance $r = 0.1463 \text{ } \Omega/\text{km}$. Assuming that approximations can be carried out, estimate the maximum power transfer, given that 30° is set by the stability limit. Find the surge impedance loading (SIL) value and estimate power losses in percentage all for a length of 140 km. Estimate the reactive power required in order to handle the real power.

$$p_{km}^{\max} \approx \frac{|V|^2}{xl} \sin\left(\frac{\pi}{6}\right) = 0.5 \frac{|V|^2}{xl} \quad (5.44)$$

$$Z_c = \sqrt{\frac{x}{bsh}} \quad (5.45)$$

$$\text{SIL} = \frac{kV^2}{Z_c} \quad (5.46)$$

$$\frac{P_{\text{Loss}}}{p_{km}} \% = 100 \frac{\sin \theta_{km}}{x/r} = \frac{50.0}{x/r} \quad (5.47)$$

```

Transmission line loadability
Voltage = 115 kV      length = 140 km
r        = 0.1463    Ohms/km
x        = 0.4178    Ohms/km
bsh      = 2.7670e-006 S/km
MaxP     = 113.0496 MW (30 degrees limit)
SIL      = 34.0342 MW      Pmax   = 3.3216 pu of SIL
Losses   = 17.51 in percentage
q_req    = 30.29 MVARs     q_req  = 0.8900 pu of SIL
Imax     = 392.00 Amp/conductor
Pthermal= 78.0809 MW      Pmax   = 2.2942 pu of SIL

```

The formulas used to calculate the required values are plotted in Figure 5.12:

$$p_{km} \approx \frac{|V_k||V_m|}{x_{km}} \sin \theta_{km} \approx \frac{|V|^2}{xl} \frac{\sqrt{x/bsh}}{Z_c} \sin \theta_{km} \quad (5.48)$$

$$\frac{p_{km}}{\text{SIL}} \approx \frac{\sin \theta_{km}}{\sqrt{xbshl}} \quad (5.49)$$

$$q_{km}(l) = \frac{|V_k||V_m| \cos(\theta_{km}) - |V_m|^2 \cos(\beta l)}{Z_c \sin(\beta l)} \quad (5.50)$$

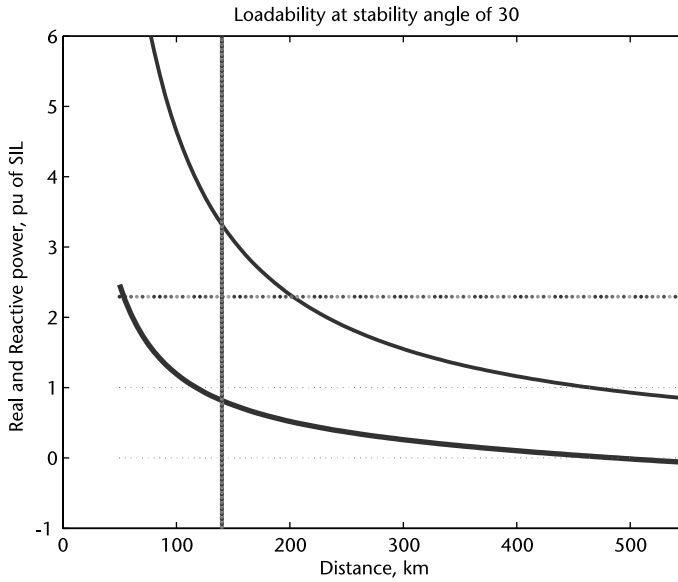


Figure 5.12 Loadability plots for stability limit of 30°.

$$\frac{q_{km}(l)}{SIL} = \frac{1}{\tan(\beta l)} - \frac{\cos(\theta_{km})}{\sin(\beta l)} \tag{5.51}$$

For the transmission line with a length of 140 km and a load variation from 0 to 3.2 pu of SIL within the stability limit, starting with the required power, the angle

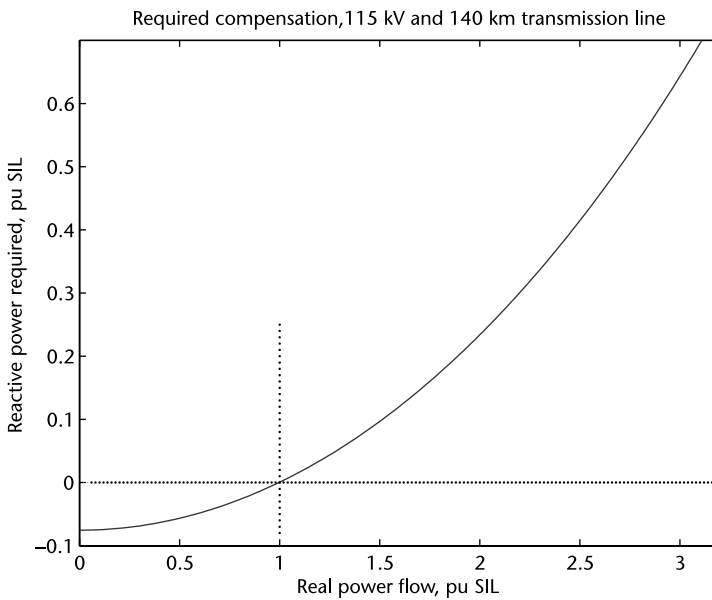


Figure 5.13 Compensation requirements for a 140 km and 115kV transmission line.

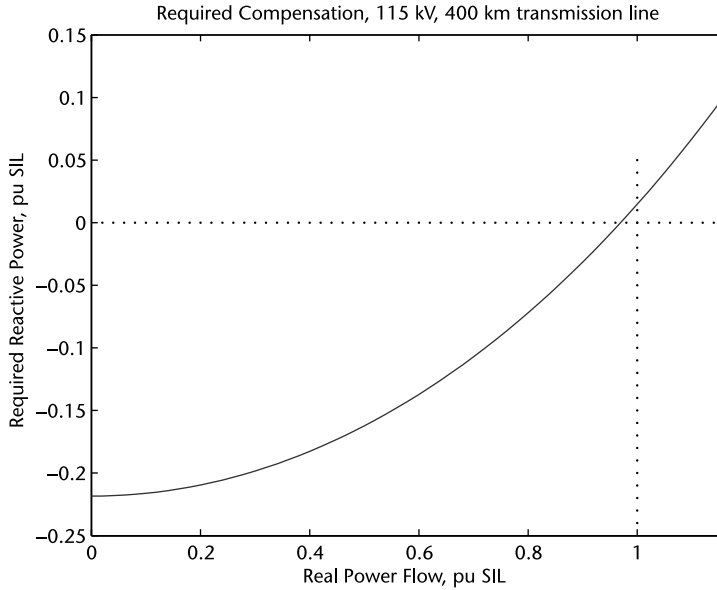


Figure 5.14 Compensation requirements for a 400 km and 115 kV transmission line.

θ_{km} can be determined by (5.49) and the reactive power in pu of SIL is calculated with (5.51). Results in pu of SIL are shown in Figure 5.13. The range of required reactive power to maintain a 1.0 pu voltage at terminals is:

$$q_{reqmin} = -2.57 \text{ MVARs and } q_{reqmax} = 27.81 \text{ MVARs}$$

If the line length is quite large (i.e., 400 km), the real power that can be transmitted and the reactive power needed in pu of SIL are much less than for the case of 140 km line. This is shown in Figure 5.14. Now the reactive power required is:

$$Q_{recmin} = -6.82 \text{ MVARs and } Q_{recmax} = 4.93 \text{ MVARs}$$

5.5 Power Flow Calculations using ABCD Constants

Real and reactive power can be obtained from terminal relations in the ABCD frame of reference. From Figure 5.7 and (5.33), using V_R as reference and $V_S = |V_S| \angle \delta$, $V_R = |V_R| \angle 0^\circ$ and $I_R = |I_R| \angle \theta$, $A = |A| \angle \alpha$, $B = |B| \angle \beta$. Complex power for the receiving end where $V_S = AV_R + BI_R$ is a circle with center and radius as follows.

$$S_R = V_R I_R^* = |V_R| \angle 0^\circ \left(\frac{V_S - AV_R}{B} \right)^* \quad (5.52)$$

$$P_R = \frac{|V_R| |V_S|}{|B|} \cos(\beta - \delta) - \frac{|A| |V_R|^2}{|B|} \cos(\beta - \alpha) \quad (5.53)$$

$$Q_R = \frac{|V_R||V_S|}{|B|} \sin(\beta - \delta) - \frac{|A||V_R|^2}{|B|} \sin(\beta - \alpha) \tag{5.54}$$

$$\text{Center} \left(-\frac{|A||V_R|^2}{|B|} \cos(\beta - \alpha), -\frac{|A||V_R|^2}{|B|} \sin(\beta - \alpha) \right) \tag{5.55}$$

$$\text{Radius} \frac{|V_R||V_S|}{|B|} \tag{5.56}$$

When the receiving voltage has constant magnitude $|V_R|$, the center is fixed and the radius depends on the magnitude of $|V_S|$.

Example 5.3

For a three-phase transmission line and given *ABCD* constants, receiving voltage is 220 kV and the three-phase load is 40 MW with a lagging 0.9 power factor. Find the center of the circle and the per phase current at the receiving end. Calculate the sending end voltage, the δ power angle (load angle), and the radius of the receiving circle (see Figure 5.15).

Constants ABCD, circles for receiving and sending ends

A	B(Ohms)	C(S)	D
9.360000e-001	3.350000e+001	-5.180000e-006	9.360000e-001

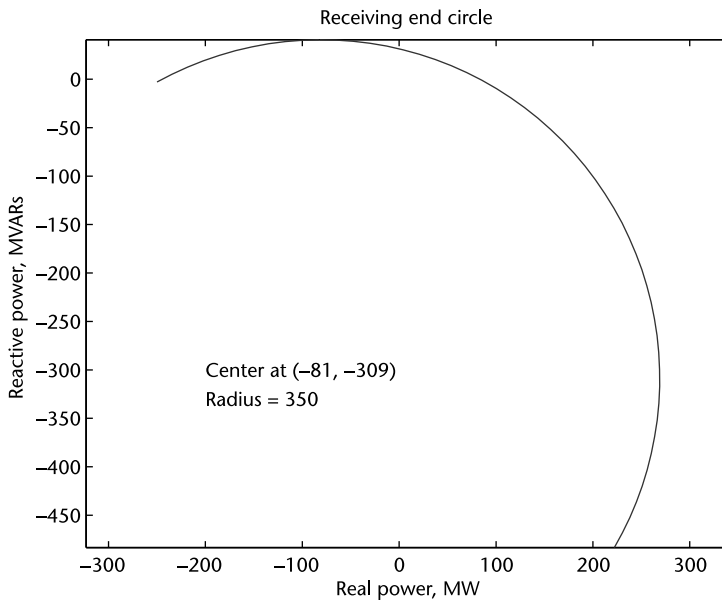


Figure 5.15 Circle diagram at the receiving end.

```

j+1.600000e-002  j+1.380000e+002  j+9.140000e-004  j+1.600000e-002
Voltage VR =      220.00 kV   angle =    0.00 degrees
Power factor =    -0.9000   angle =  -25.84 degrees
SR =      40.00 +j   19.37 MVA total
CenterR at (  -80.56,  -308.72) MVAs
Current IR =      116.64 A   angle =  -25.84 degrees (A/phase)
Voltage VS =      225.63 kV   delta angle =    6.53 degrees
RadiusR      =      349.54 MVAs

```

At the sending terminal, using V_S as a reference and the inverse matrix from (5.33), then $V_R = DV_S - BI_S$, multiplying by $-1/B$ and to apply the complex power definition as *load convention*, we use the conjugated current.

$$-V_S \left(\frac{V_R}{B} \right)^* = -V_S \left(\frac{DV_S}{B} \right)^* + V_S I_S^* \quad (5.57)$$

This is the equation of a circle with center and radius as:

$$\text{Center} \left(+ \frac{|D||V_S|^2}{|B|} \cos(\beta - \Delta), + \frac{|D||V_S|^2}{|B|} \sin(\beta - \Delta) \right) \quad (5.58)$$

$$\text{Radius} \frac{|V_R||V_S|}{|B|} \quad (5.59)$$

For a fixed magnitude $|V_R|$, the radius and the center depend on the magnitude $|V_S|$.

Example 5.4

Using previous data given in Example 5.3, calculate the circle diagram, the complex power, and the net power at the sending end. Calculate the voltage drop in percentage (see Figure 5.16).

```

Current IS =      120.8745 A   angle =   35.50 degrees (A/phase)
CenterS at (   84.73,   324.72) MVAs
RadiusS     =      349.54 MVAs
SS =      41.33 +j  -22.88 MVA total
P Losses   =         1.33 MW
Q required  =     -42.25 MVARs (<0 to the system, >0 to the line)
Vdrop      =         2.49 percentage

```

Circle diagrams are useful when visualizing the range of operation for a transmission line, including its long-line representation through the *ABCD* constants. Inclusion of line series compensations and other arrangements can be accomplished easily through the properties of two-port networks (as previously discussed in Section 5.4).

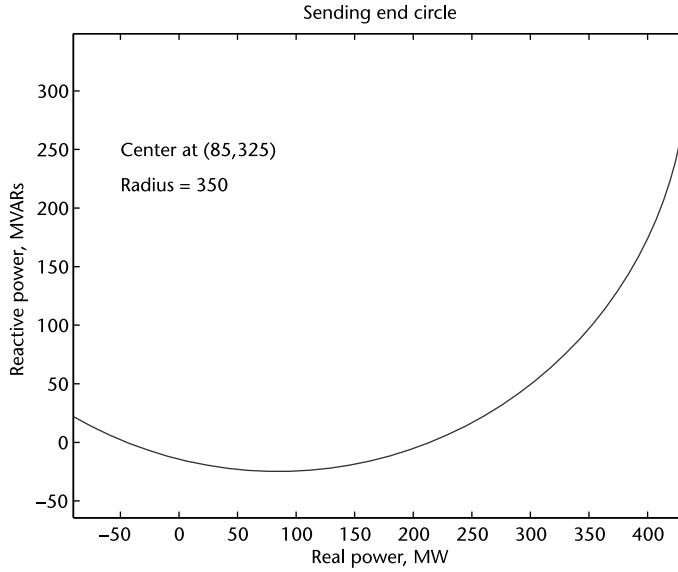


Figure 5.16 Circle diagram at the sending end.

5.6 Transmission Limits

5.6.1 Thermal Limit

Depending on the type and geometry of the phase conductors, a maximum current is recommended by the manufacturer. The ambient temperature, wind, and weather conditions will play an important role in establishing the actual current that phase conductors will carry with no detrimental effects on conductor's properties. In our case, a simplified calculation is carried out with no inclusion of all the factors involved.

$$|S_{\max}| = 3 \frac{|V|}{\sqrt{3}} |I_{\max}| \quad \text{MVA} \quad (5.60)$$

V magnitude of phase-to-phase voltage, kV

I_{\max} kA, maximum recommended current from manufacturer. Temperature, wind, and weather data is not included.

5.6.2 Stability's Angle Limit

To have a reasonable stability margin, an angle of 30° is used to guard against wide power swings during transient oscillations. A maximum power limit can be calculated for a line with length ℓ in km, x in ohms/km, and b_{sh} in S/km.

$$\frac{p_{km}}{\text{SIL}} \approx \frac{\sin \theta_{km}}{\sqrt{x b_{sh} \ell}} \quad (5.61)$$

5.6.3 Limit from Voltage Drop

When power is transmitted, a voltage drop is experienced, especially during heavy load conditions. The allowed voltage drop of 5% during the planning stage is used to determine the maximum power that the line will handle. In an operation setting, a maximum voltage drop of 7% for short periods can be permitted. The power circle equations can be used to establish the value of the voltage drop (see Figure 5.17); this preliminary result can be useful before detailed power load flow studies are conducted.

Example 5.5

Using the data provided in Example 5.4, calculate the transmission limits, assuming one conductor/phase with capacity of 1,000 Amp.

```

Constants ABCD, Max Power. Receiving Circle
      A              B (Ohms)          C(S)
0.936000          33.500000          -0.000005
j+ 0.016000      j+138.000000      j+ 0.000914
ABCD Magnitude and angle (degrees)
0.936137          142.007922          0.000914
0.98              76.36              90.32

Transmission limits
Voltage drop 5 percent
VS   = 220.00 kV   VR = 209.52 kV   Radius = 324.60 MVAs
PS   = 172.14 MW   QS = -3.41 MVAR      172.17 MVAs
PR   = 150.97 MW   QR = -45.13 MVAR    157.57 MVAs
Losses= 21.17 MW   Q = 41.72 MVAR (>0 needed by TL)
    
```

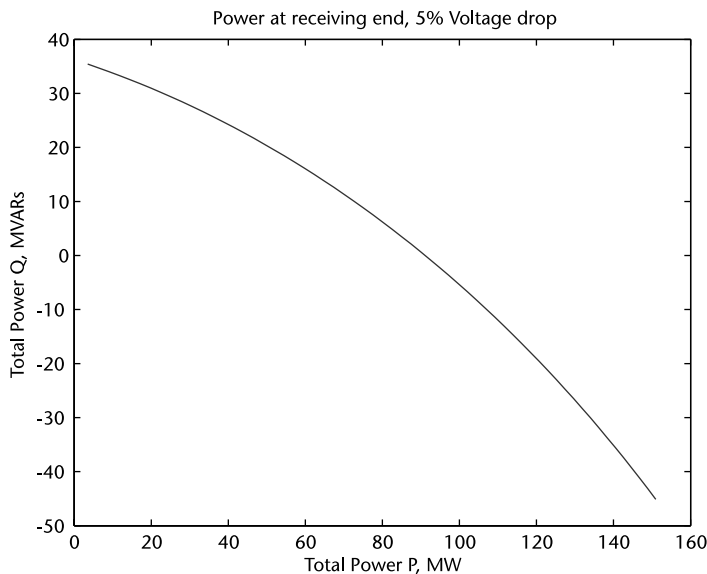


Figure 5.17 Total power at the receiving end, voltage drop 5%.

```

delta = 30.00 degrees
Stability values for delta = 30 degrees
VS = 220.00 kV   VR = 220.00 kV   Radius = 340.83 MVAs
PS = 176.53 MW  QS = -18.31 MVAR      177.48 MVAs
PR = 154.68 MW  QR = -62.09 MVAR      166.67 MVAs
Losses= 21.85 MW  Q = 43.78 MVAR (>0 needed by TL)
Thermal limit
Imax = 1000 Amp   cond/phase = 1      381.05 MVAs

```

Results show that the transmission limit is set by the voltage drop criteria of 5%. Additional information as reactive compensation required and losses incurred at the limiting values is an additional valuable information for the planning design and the operation of this transmission line.

5.7 Wave Equation and Time Expressions

In Section 5.3, phasor equations were used to derive results for the distributed parameters of a long transmission line. From (5.12), its Laplace transform is like (5.62). To include the time variable t we write the Laplace transformed equations for voltage and current. The inverse Laplace Transform will take us back to the time domain t . The exponential function at the Laplace domain represents a time displacement:^{1*}

$$V(x,s) = A_V(s)e^{-sx\sqrt{LC}} + B_V(s)e^{+sx\sqrt{LC}} \quad (5.62)$$

$$v(x,t) = A_V(t - x\sqrt{LC}) + B_V(t + x\sqrt{LC}) \quad (5.63)$$

Similar properties are applied for the current expression.

$$i(x,t) = A_I(t - x\sqrt{LC}) + B_I(t + x\sqrt{LC}) \quad (5.64)$$

The coefficients A_V , B_V , A_I , and B_I are to be determined by the values at the boundary, as well as at the sending and receiving end of the transmission line.

5.7.1 Product $x\sqrt{LC}$ and Speed v

The product of distance x (meters) times \sqrt{LC} must be in time unit of seconds, so v will be the propagation speed in m/s, inductance L in (H) and capacitance C in (F).

$$\tau = x\sqrt{LC} \quad (5.65)$$

$$\frac{\tau}{x} = \sqrt{LC} = \frac{1}{v} \quad (5.66)$$

* $L[f(t - \tau)] = F(s)e^{-s\tau}$

$$v = \frac{1}{\sqrt{LC}} \text{ m/s} \tag{5.67}$$

For a given transmission line, the inductance L is proportional to μ and capacitance C is proportional to ϵ , which means that—at the *vacuum*—the propagation speed is $v \approx 1/\sqrt{\mu_0\epsilon_0}$ with value of $1/\sqrt{(4\pi 10^{-7} \text{ H/m})(8.854 10^{-12} \text{ F/m})} \approx 300,000 \text{ km/s}$. The values ϵ/ϵ_0 that can be found for cables approximates a value of 5, which means that cables $v = 134,000 \text{ km/s}$.

5.7.2 Functions $A_V(t - x/v)$ and $A_I(t - x/v)$

The expression $A_V(t - x/v)$ in (5.63) represents a *traveling voltage* in the positive x direction with speed v . If we assume in Figure 5.18 that $A_V = f^+(u)$, where $u = t - x/v$, at time t_1 the wave is located at u_1 , with $x_1 = v(t_1 - u_1)$. For a different time t_2 , where $t_2 > t_1$, the wave is found now at $x_2 = v(t_2 - u_2)$; and $x_2 > x_1$. The wave has travelled a distance $x_2 - x_1$; the time spent is $t_2 - t_1$ and the speed is $v = (x_2 - x_1)/(t_2 - t_1)$. A similar conclusion can be reached for $A_I(t - x/v)$; these are traveling waves *moving forward*.

The wave $A_V(t + x/v)$ is a voltage that travels in the negative direction of x . The speed is v and we conclude that A_V is a *traveling wave*. Assume that $A_V = f^-(u)$; where $u = t + x/v$, then at time t_1 the wave is situated at position u_1 , or $x_1 = v(u_1 - t_1)$. From Figure 5.19, $t_2 > t_1$, the wave is located at $x_2 = v(u_2 - t_2)$. The wave has traveled the distance $(x_2 - x_1)$ using the time $(t_2 - t_1)$. From these results, we

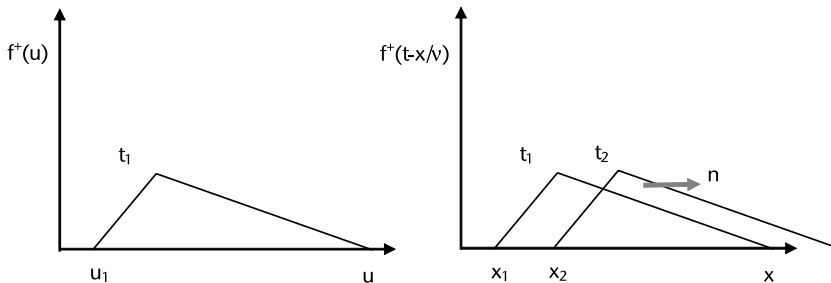


Figure 5.18 Traveling waves in the forward direction, positive x .

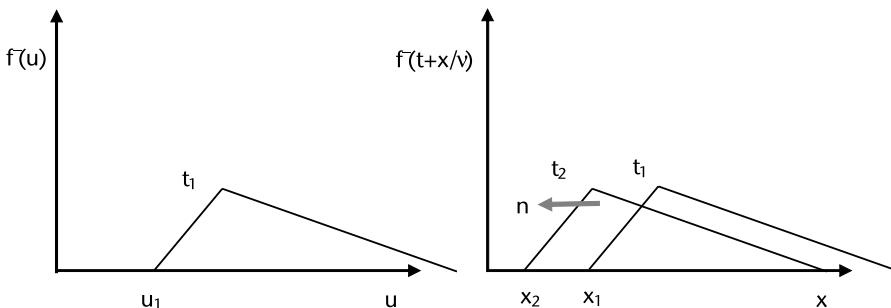


Figure 5.19 Traveling waves in the backward direction, negative x .

conclude that the speed is negative as $v = (x_2 - x_1)/(t_2 - t_1)$. The same reasoning can be applied to $A_I(t + x/v)$; these are waves moving *backward* (shown in Figure 5.19).

5.7.3 Expressions for A_V , B_V , A_I , B_I

With a substitution of voltage and current functions at the transmission line differential equations, we identify the constant term known as the *characteristic impedance* $Z_C = \sqrt{L/C}$ in (5.20). The second derivative of (5.62) with respect to x and the first derivative of current $I(x, s)$ must satisfy (5.14) with $v = 1/\sqrt{LC}$. At the left, we substitute the second derivative of voltage, and at the right, the derivative of the current, equating right and left side components.

$$\frac{d^2V(x, s)}{dx^2} = -sL \frac{dI(x, s)}{dx} \quad (5.68)$$

$$\left(\frac{s}{v}\right)^2 A_V(s)e^{-sx/v} + \left(\frac{s}{v}\right)^2 B_V(s)e^{+sx/v} = -sL \left[-\frac{s}{v} A_I(s)e^{-sx/v} + \frac{s}{v} B_I(s)e^{+sx/v} \right] \quad (5.69)$$

Expressions for the backward waves:

$$B_I(s) = -CvB_V(s) = \sqrt{\frac{C}{L}} A_I(s) = -\frac{B_V(s)}{Z_C} \quad (5.70)$$

For the forward waves:

$$A_I(s) = CvA_V(s) = \sqrt{\frac{C}{L}} A_I(s) = \frac{A_V(s)}{Z_C} \quad (5.71)$$

Expression for $v(t, x)$ and $i(t, x)$, now with coefficients A_V , B_V , A_I , and B_I in (5.70) and (5.71), the Inverse Laplace Transform will give us $v(x, t)$ and $i(x, t)$.

$$V(x, s) = Z_c [A_I(s)e^{-sx/v} - B_V(s)e^{+sx/v}] \quad (5.72)$$

$$v(x, t) = Z_c [a_I(t - x/v) - b_V(t + x/v)] \quad (5.73)$$

$$I(x, s) = A_I(s)e^{-sx/v} + B_I(s)e^{+sx/v} \quad (5.74)$$

$$i(x, t) = \frac{1}{Z_c} [a_V(t - x/v) - b_V(t + x/v)] \quad (5.75)$$

5.7.4 Reflexion Coefficients

A wave that travels to the receiving end located at a distance $x = l$ (Figure 5.20), which represents the total line length; part of the wave is *reflected* and part is *refracted*. To

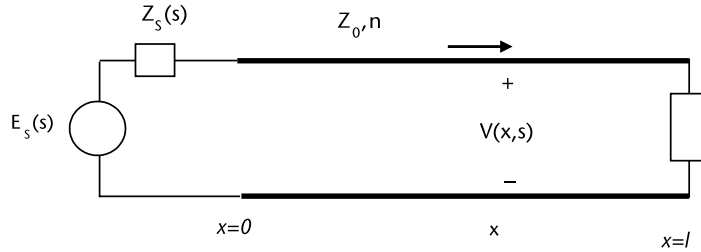


Figure 5.20 Transmission line, characteristic impedance Z_0 , and terminal impedance $Z_R(s)$.

study what happens as time increases, it is a good idea to calculate the coefficients and then express how the incoming wave is split into a wave that is *reflected* and a wave that is *kept* at the receiving end. The boundary conditions must be satisfied for both the current and voltage waves. To determine the reflexion and refraction coefficients, let us start with a voltage wave in the Laplace domain, assuming that there is an impedance $Z_R(s)$ connected at the end of the transmission line.

At $x = l$, the voltage expression using previous results in (5.72) and (5.74).

$$V(l, s) = Z_R(s)I(l, s) \quad (5.76)$$

$$A_V(s)e^{-sl/v} + B_V(s)e^{+sl/v} = Z_R(s)\frac{1}{Z_C} [A_V(s)e^{-sl/v} - B_V(s)e^{+sl/v}] \quad (5.77)$$

$$B_V(s)e^{+sl/v} \left[1 + \frac{Z_R(s)}{Z_C} \right] = \left[\frac{Z_R(s)}{Z_C} - 1 \right] A_V(s)e^{-sl/v} \quad (5.78)$$

Reflection coefficient Γ_R at the receiving end can be defined as the portion of the forward wave that is reflected as a backward wave.

$$\Gamma_R = \frac{[Z_R(s) - Z_C]}{[Z_R(s) + Z_C]} \quad (5.79)$$

Similar reasoning is applied to finding the reflection coefficient at the sending end.

$$\Gamma_S = \frac{[Z_S(s) - Z_C]}{[Z_S(s) + Z_C]} \quad (5.80)$$

5.7.5 Calculation of Coefficients

At a transition point where elements with different characteristic impedances are connected, incident waves have a part of it *reflected* and part *refracted*. For the incident wave, the part that is reflected travels back and the part that is refracted continues to travel to the next element. It is interesting to calculate the refracted portion as this value travels to the next characteristic impedance down the series

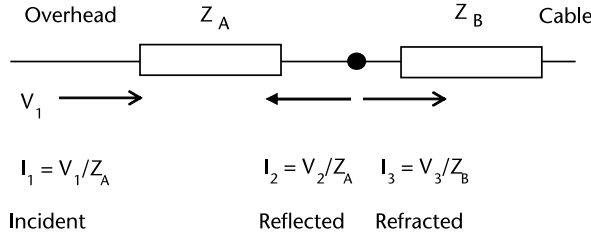


Figure 5.21 Boundary conditions at point of connection, characteristic impedances Z_A and Z_B .

of connections, and the overvoltage needs to be estimated so that the insulation strength level is selected.

Continuity at boundary conditions requires that for the voltage waves $V_1 + V_2 = V_3$ and for currents $I_2 + I_3 = I_1$ (see Figures 5.21 and 5.22). These relations are written in terms of the incoming source voltage V_1 . A matrix array can be written using voltages as and currents through the characteristic impedance.

$$-V_2 + V_3 = V_1 \quad (5.81)$$

$$+\frac{V_2}{Z_A} + \frac{V_3}{Z_B} = \frac{V_1}{Z_A} \quad (5.82)$$

$$\begin{bmatrix} -1 & +1 \\ +1 & +\frac{Z_A}{Z_B} \end{bmatrix} \begin{bmatrix} V_2 \\ V_3 \end{bmatrix} = \begin{bmatrix} 1 \\ 1 \end{bmatrix} V_1 \quad (5.83)$$

Solving for V_2 and V_3 :

$$\begin{bmatrix} V_2 \\ V_3 \end{bmatrix} = \begin{bmatrix} \frac{Z_B - Z_A}{Z_B + Z_A} \\ \frac{2Z_B}{Z_B + Z_A} \end{bmatrix} V_1 \quad (5.84)$$

The inverse matrix from (5.83), together with the identity $V_1 = V_1$, gives a set of coefficients (reflection a and refraction b) for the series arrangement of impedances discussed in this section. Traveling currents I_1 , I_2 , and I_3 are related to traveling voltages through characteristic impedances, so the matrix equation (5.86) can finally express how the transient voltage V_1 will determine currents I_1 , I_2 , and I_3 .

$$\begin{bmatrix} V_1 \\ V_2 \\ V_3 \end{bmatrix} = \begin{bmatrix} 1 \\ \frac{Z_B - Z_A}{Z_B + Z_A} \\ \frac{2Z_B}{Z_B + Z_A} \end{bmatrix} V_1 = \begin{bmatrix} 1 \\ a \\ b \end{bmatrix} V_1 \quad (5.85)$$

$$\begin{bmatrix} I_1 \\ I_2 \\ I_3 \end{bmatrix} = \begin{bmatrix} 1/Z_A & 0 & 0 \\ 0 & 1/Z_A & 0 \\ 0 & 0 & 1/Z_B \end{bmatrix} \begin{bmatrix} V_1 \\ V_2 \\ V_3 \end{bmatrix} \tag{5.86}$$

$$\begin{bmatrix} I_1 \\ I_2 \\ I_3 \end{bmatrix} = \begin{bmatrix} 1/Z_A & 0 & 0 \\ 0 & 1/Z_A & 0 \\ 0 & 0 & 1/Z_B \end{bmatrix} \begin{bmatrix} 1 \\ \frac{Z_B - Z_A}{Z_B + Z_A} \\ \frac{2Z_B}{Z_B + Z_A} \end{bmatrix} V_1 \tag{5.87}$$

Example 5.6

A voltage of $V_1 = 300$ kV is applied at the terminal of the overhead line; a cable is connected in series. The values of the characteristic impedances for the transmission line and the cable are $Z_A = 400 \Omega$, and $Z_B = 50 \Omega$. The connection diagram is shown in Figure 5.21.

Data of Characteristic impedances

Line Characteristic impedance = 400.00(ohms)
 Cable Characteristic impedance = 50.00(ohms)

Reflexion coefficient a = -0.7778 Refraction coefficient b = 0.2222

Voltage(1) = 300000.00(volts) Current(1) = 750.00(Amp)
 Voltage(2) = -233333.33(volts) Current(2) = -583.33(Amp)
 Voltage(3) = 66666.67(volts) Current(3) = 1333.33(Amp)

Example 5.7

Write the algebraic equations for the incident and the reflected waves at a transition point for a series configuration with an overhead line and a cable. Use the diagram in Figure 5.23 to write the set of equations that characterize the boundary conditions at the sending end and at the connecting point A for voltages and currents as traveling waves.

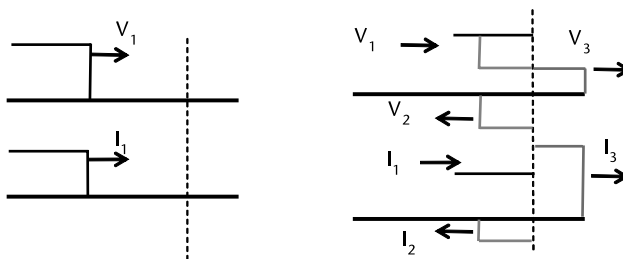


Figure 5.22 Visual image for traveling voltages and currents, before and after reaching the receiving end.

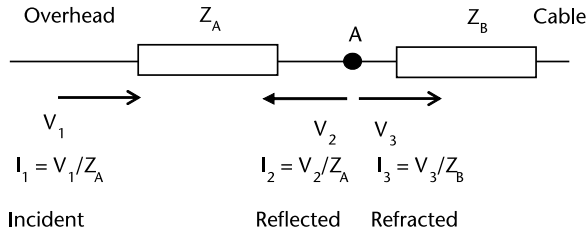


Figure 5.23 Continuity of voltage and current waves, incident end and at node A.

First, we write the equations for the incident wave, then for the reflected and the refracted waves. Follow with those equations for the *continuity* of voltage and current at node A.

$$\begin{aligned}
 (1) \quad & -Z_A I_1 = -V_1 \\
 (2) \quad & -Z_A I_2 + V_2 = 0 \\
 (3) \quad & -Z_B I_3 + V_3 = 0 \\
 A \quad & +I_1 - I_2 - I_3 = 0 \\
 V_A \quad & -V_2 + V_3 = +V_1
 \end{aligned}
 \tag{5.88}$$

The equations in matrix form where Ohm’s law for traveling waves is applied, plus the transition point continuity conditions for currents and voltages.

$$\begin{bmatrix}
 -Z_A & 0 & 0 & 0 & 0 \\
 0 & -Z_A & 0 & +1 & 0 \\
 0 & 0 & -Z_B & 0 & +1 \\
 +1 & -1 & -1 & 0 & 0 \\
 0 & 0 & 0 & -1 & +1
 \end{bmatrix}
 \begin{bmatrix}
 I_1 \\
 I_2 \\
 I_3 \\
 V_2 \\
 V_3
 \end{bmatrix}
 =
 \begin{bmatrix}
 -1 \\
 0 \\
 0 \\
 0 \\
 +1
 \end{bmatrix}
 V_1
 \tag{5.89}$$

For an incoming voltage $V_1 = 300$ kV through impedances $Z_A = 400$ ohms and $Z_B = 50$ ohms, find the reflection coefficient a and refraction b . Calculate the magnitudes of all voltages and currents.

```

V1 =      300000
ZA =      400
ZB =      50
A =
  -400    0    0    0    0
    0   -400    0    1    0
    0    0   -50    0    1
    1   -1   -1    0    0
    0    0    0   -1    1

```

Coefficients
 Reflection a = -0.777778

```

Refraction  b = 0.222222
Values
Current ( 1) = +750.00 A
Current ( 2) = -583.33 A
Current ( 3) = +1333.33 A
Voltage ( 2) = -233333.33 V
Voltage ( 3) = +66666.67 V
    
```

Example 5.8

Calculate the reflection and refraction coefficients for a series connection of an overhead line $Z_A = 500 \Omega$ with a resistance $R = 550 \Omega$ and a cable section with $Z_B = 50 \Omega$ (see Figure 5.24). Note that R is a concentrated parameter element, and that Z_A and Z_B are characteristic impedances associated with distributed parameters elements as L and C for an overhead line and a cable section.

$$\begin{aligned}
 (1) \quad & -Z_A I_1 = -V_1 \\
 (2) \quad & -Z_A I_2 + V_2 = 0 \\
 (3) \quad & -(R + Z_B) I_3 + V_3 = 0 \\
 A \quad & +I_1 - I_2 - I_3 = 0 \\
 V_A \quad & -V_2 + V_3 = +V_1
 \end{aligned} \tag{5.90}$$

$$\begin{bmatrix} -Z_A & 0 & 0 & 0 & 0 \\ 0 & -Z_A & 0 & +1 & 0 \\ 0 & 0 & -(R + Z_B) & 0 & +1 \\ +1 & -1 & -1 & 0 & 0 \\ 0 & 0 & 0 & -1 & +1 \end{bmatrix} \begin{bmatrix} I_1 \\ I_2 \\ I_3 \\ V_2 \\ V_3 \end{bmatrix} = \begin{bmatrix} -1 \\ 0 \\ 0 \\ 0 \\ +1 \end{bmatrix} V_1 \tag{5.91}$$

$$\begin{matrix}
 V_1 = 1 & Z_A = 500 & R = 550 & Z_B = 50 \\
 A = \\
 \begin{matrix} -500 & 0 & 0 & 0 & 0 \\ 0 & -500 & 0 & 1 & 0 \\ 0 & 0 & -600 & 0 & 1 \\ 1 & -1 & -1 & 0 & 0 \end{matrix}
 \end{matrix}$$

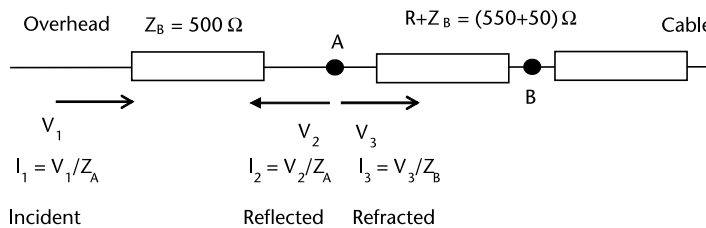


Figure 5.24 Continuity of voltage and current waves, incident end and at node A.

```

      0      0      0      -1      1
Coefficients
Reflection a = 0.090909
Refraction b = 1.090909
Values times V1
Current ( 1) = +2.00000e-003 A
Current ( 2) = +1.81818e-004 A
Current ( 3) = +1.81818e-003 A
Voltage ( 2) = +9.09091e-002 V
Voltage ( 3) = +1.09091e+000 V
    
```

Besides currents and voltages, we might be interested in calculating how much energy is associated with each portion of the circuit. Relations that we have in terms of incoming voltage V_1 and current I_1 are: $V_1 = Z_A I_1 = 500 I_1$, $I_B = I_3 = 0.00181818 V_1 = 0.90909 I_1$, $I_{rA} = I_2 = 0.000181818 V_1 = 0.090909 I_1$ and $V_B = V_3 - I_3 R = 0.090909 V_1$. From here, the energy in R is $R I_3^2 = 550(0.090909 I_1)^2 = 454.5 I_1^2 = 454.5/500 V_1 I_1 = 0.90909 V_1 I_1$ and the energy in B is $V_B I_B = I_2 = (0.090909 V_1) 0.090909 I_1 = 0.08264 V_1 I_1$. The reflected energy is $V_2 I_2 = (0.090909 V_1) 0.090909 I_1 = 0.08264 V_1 I_1$.

```

V1 = 1      ZA = 500      R = 550      ZB = 50
A =
  -500      0      0      0      0
    0     -500      0      1      0
    0      0     -600      0      1
    1     -1     -1      0      0
    0      0      0     -1      1
Coefficients
Reflection a = 0.090909
Refraction b = 1.090909
Values times V1
Current ( 1) = +2.00000e-003 A
Current ( 2) = +1.81818e-004 A
Current ( 3) = +1.81818e-003 A
Voltage ( 2) = +9.09091e-002 V
Voltage ( 3) = +1.09091e+000 V
    
```

5.7.6 Coefficients for Connection of Various Elements

In order to solve for various configurations (see Figure 5.25) there are, as we have presented, a few conditions that must be met: 1) incident wave conditions, 2) reflected waves, and 3) refracted waves, which in general must satisfy the continuity condition for currents and voltages.

$$\begin{aligned}
 I_{1A} &= I_{2A} + I_{3B} + I_{3C} \\
 V_{1A} + V_{2A} &= V_{3B} \\
 V_{1A} + V_{2A} &= V_{3C}
 \end{aligned}
 \tag{5.92}$$

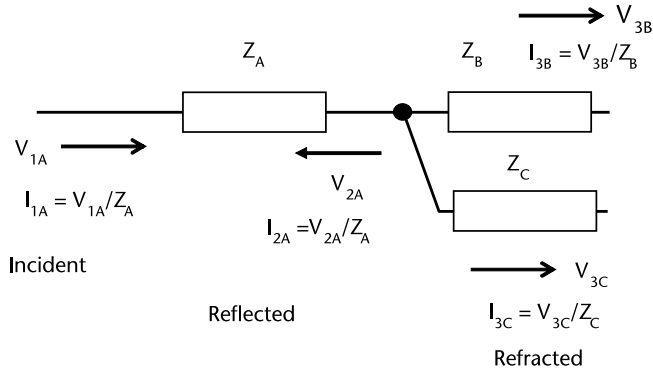


Figure 5.25 Configuration of various elements and its characteristic impedances.

The equation in matrix form, including Ohm’s law for each element:

$$\begin{bmatrix}
 -Z_A & 0 & 0 & 0 & 0 & 0 & 0 \\
 0 & -Z_A & 0 & 0 & +1 & 0 & 0 \\
 0 & 0 & -Z_B & 0 & 0 & +1 & 0 \\
 0 & 0 & 0 & -Z_C & 0 & 0 & +1 \\
 +1 & -1 & -1 & -1 & 0 & 0 & 0 \\
 0 & 0 & 0 & 0 & -1 & +1 & 0 \\
 0 & 0 & 0 & 0 & -1 & 0 & +1
 \end{bmatrix}
 \begin{bmatrix}
 I_{1A} \\
 I_{2A} \\
 I_{3B} \\
 I_{3C} \\
 V_{2A} \\
 V_{3B} \\
 V_{3C}
 \end{bmatrix}
 =
 \begin{bmatrix}
 -1 \\
 0 \\
 0 \\
 0 \\
 0 \\
 +1 \\
 +1
 \end{bmatrix}
 V_{1A}
 \tag{5.93}$$

5.7.7 Lattice Diagram

With the information about reflecting and refracting coefficients at the sending end and the receiving end a *lattice diagram* for Figure 5.26 can be constructed to show, as time advances, how the transient voltage and the current evolve at either side, sending or receiving.

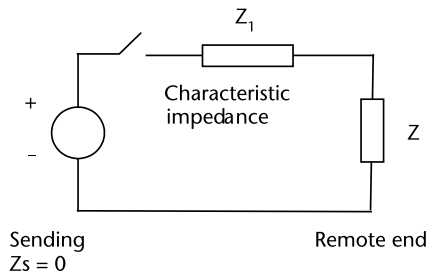


Figure 5.26 Simple arrangement of a transmission line, its characteristic impedance and load Z.

$$\begin{bmatrix} 1 \\ a_s \\ b_s \end{bmatrix} = \begin{bmatrix} 1 \\ \frac{Z_s - Z_1}{Z_s + Z_1} \\ \frac{2Z_s}{Z_s + Z_1} \end{bmatrix} \quad \begin{bmatrix} 1 \\ a_r \\ b_r \end{bmatrix} = \begin{bmatrix} 1 \\ \frac{Z - Z_1}{Z + Z_1} \\ \frac{2Z}{Z + Z_1} \end{bmatrix} \quad (5.94)$$

The following steps summarize the way in which the lattice diagram is constructed (see Figure 5.27):

1. Select a vertical scale in ms or in pu, selecting the time to travel as $\tau = \sqrt{LC}$
2. Choose a horizontal scale to represent the line length x .
3. Calculate values for reflection and refraction coefficients at both extremes of the transmission line.

5.7.8 Electric Element Connections at Receiving Terminal

One interesting question is: What is the circuit’s time response for the traveling wave’s voltage and current when a unit step voltage is applied at the sending end? What is the voltage as time progresses from initial time, up to the final time t seconds? What is the transient for various line termininations (see Figure 5.28): open circuit, shorted circuit, or an impedance value? In Figure 5.30, the transient equations for an inductor at the end of the line are written.

The receiving reflection and refraction coefficients are calculated as in (5.94).

1. We need an equivalent, as seen from nodes A and B , looking into the power source (see Figure 5.29).
2. Connect element L or C in the Laplace domain, and solve for voltage as function of time.

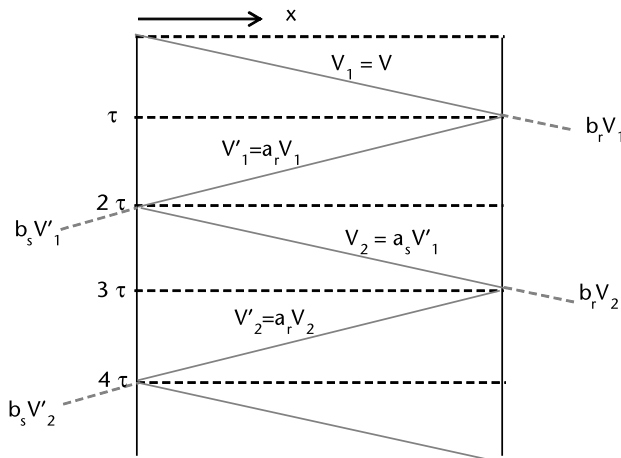


Figure 5.27 Lattice diagram, distance x at the horizontal axis, vertical scale τ time travel.

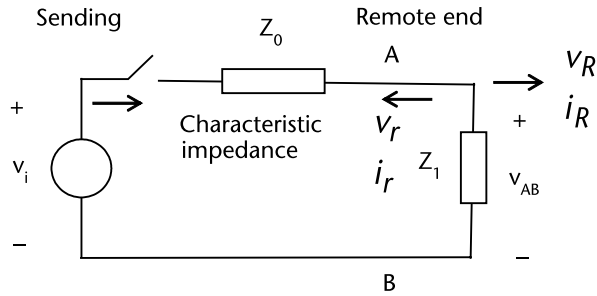


Figure 5.28 Circuit configuration with voltage source, transmission line's characteristic impedance Z_0 , and impedance Z_{AB} at receiving end.

3. Calculate the reflected voltage at the remote extreme.

$$v_R = v_{AB} = v_i + v_r \tag{5.95}$$

$$v_{AB} = v_i + \left(\frac{Z_1 - Z_0}{Z_1 + Z_0} \right) v_i = \frac{Z_1}{Z_1 + Z_0} 2v_i \tag{5.96}$$

$$i_R = \frac{v_{AB}}{Z_1} = \frac{2v_i}{Z_1 + Z_0} \tag{5.97}$$

5.7.8.1 Reactor L at the Receiving End

When element L is connected, we use the Laplace domain to find the time solution. The reflected voltage at the remote terminal is also calculated.

First, solve for the equivalent circuit in the Laplace domain, then use the inverse Laplace transform to find the solution at the time domain.

$$V_{AB}(s) = \frac{2v_i/s}{(Z_0 + sL)} sL = \frac{2v_i}{(Z_0/L + s)} \tag{5.98}$$

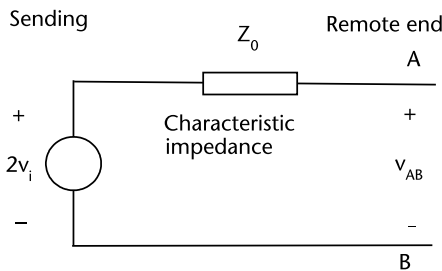


Figure 5.29 Thévenin's equivalent circuit.

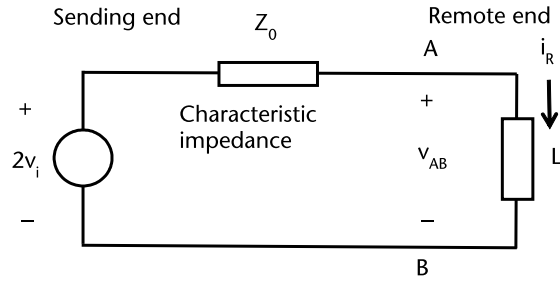


Figure 5.30 Thévenin's equivalent, impedance, and load connection.

$$v_{AB}(t) = 2v_i e^{-(Z_0/L)t} \quad (5.99)$$

$$v_r = v_{AB}(t) - v_i(t) = v_i \left(2e^{-(Z_0/L)t} - 1 \right) \quad (5.100)$$

For the reflected voltage v_r , there is an open circuit at $t = 0$ for this condition $v_r = v_i$. As $t \rightarrow \infty$, $v_r \rightarrow -v_i$; and it represents a short circuit condition.

References

- [1] Stevenson, W. D., *Elements of Power System Analysis, Second Edition*, Tokyo, Japan: McGraw-Hill Book Company, 1962.
- [2] Edited by Edison Electric Institute, *EHV Transmission Line Reference Book*, 1968.
- [3] Edited by Electric Power Research Institute, *Transmission Line Reference Book: 345 kV and Above, Second Edition*, 2006.
- [4] Greenwood, A., *Electrical Transients in Power Systems, Second Edition*, New York: Wiley-Interscience, 1991.
- [5] Das, J. C., *Transients in Electrical Systems*, Singapore: McGraw-Hill Education, 2010.

Power Flows

6.1 Introduction

Power flow studies are a fundamental tool for power system engineers; they solve the steady state condition of an electrical network. Assuming an AC system as a balanced three-phase network and assuming that the positive sequence parameters are available, we establish the network problem with known topology and impedance values, which include transformers, transmission lines, power injections from generators, and real and reactive power loads that must be satisfied within nodal voltage limits. The crux of this circuit problem is to solve for all nodal voltages for every electrical node. With this information and element impedance we calculate current, real power, reactive power, and losses. Planning engineers use the load flow solution to analyze alternatives and an adequate system expansion; the load flow is the cornerstone for power system operation. When solving the nonlinear set of equations, the Newton-Raphson iterative method generally shows fast convergence. In this chapter, we revise the nature of the convergence process for nonlinear equations; we discuss in detail the power flow equations and their solutions in a general form that encompasses the iterative Newton’s nodal frame of reference.

6.2 Solution of Nonlinear Equations

Let us begin with a discussion of nonlinear equations and convergence using a simple DC power transfer over a transmission element (as shown in Figure 6.1); voltages, current, and resistance are in pu values.

Power from node k to node m with current $i_{km} = (V_k - V_m)/r_{km}$, then power flows and losses are:

$$p_{km} = V_k i_{km} = \frac{(V_k^2 - V_k V_m)}{r_{km}} \tag{6.1}$$

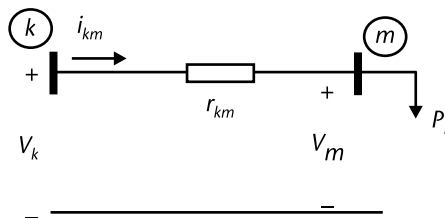


Figure 6.1 Simple DC transmission model, nodes k and m .

$$p_{mk} = -V_m i_{km} = \frac{(V_m^2 - V_m V_k)}{r_{km}} \quad (6.2)$$

$$p_{mk,losses} = p_{km} + p_{mk} = \frac{(V_k^2 + V_m^2 - 2V_m V_k)}{r_{km}} \quad (6.3)$$

A power-voltage relation, from the system point of view, considering an ideal voltage source at node k and m as a load node it is a quadratic equation (6.1). From (6.2) voltage V_m can be calculated using $-p_{km} = P_L$ in (6.2) .

$$V_m^2 - V_m V_k + r_{km} P_L = 0 \quad (6.4)$$

The solution to (6.4) shows a multiple solution problem; such is the nature of the quadratic equation (Figure 6.2). Using (6.4), the maximum power transfer shows that the limiting factor is r_{km} when V_k is fixed and assumed ideal.

$$\frac{dP_L}{dV_m} = \frac{(-2V_m + V_k)}{r_{km}} = 0, \quad V_m = \frac{V_k}{2} \quad (6.5)$$

$$P_L^{\max} = \frac{V_k^2}{4r_{km}} \quad (6.6)$$

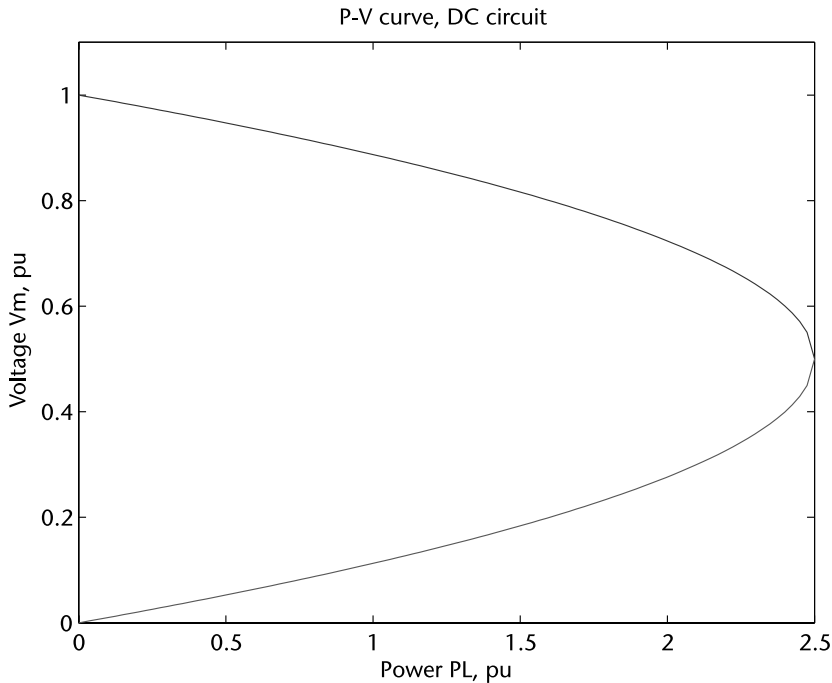


Figure 6.2 PV curve, multiple solutions to a basic power flow; load model constant power P_L .

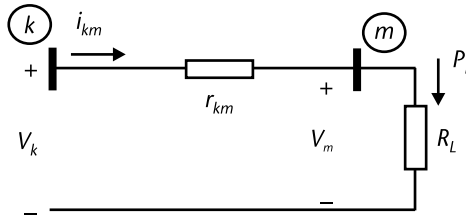


Figure 6.3 Circuit for PV curve and the nature of load R_L .

Example 6.1

For a value of $V_k = 1.0$, $r_{km} = 0.1$ in pu (Figure 6.3). Plot the solution V_m using (6.4) for load values P_L from zero to its maximum value. Use the quadratic form $V_m = (V_k \pm \sqrt{V_k^2 - 4V_m r_{km} P_L})/2$.

Depending on the type of load, we will have various graphical forms on top of the PV curve (see Figure 6.2). Let's consider a resistive type R_L ; the voltage solution is the common point for the PV characteristics and the load (see Figure 6.4).

$$P_L = V_m i_{km} = \frac{V_m^2}{R_L} \tag{6.7}$$

From (6.7), an expression for constant current load is (see Figure 6.5):

$$\frac{P_L}{V_m} = i_{km} = \text{constant} \tag{6.8}$$

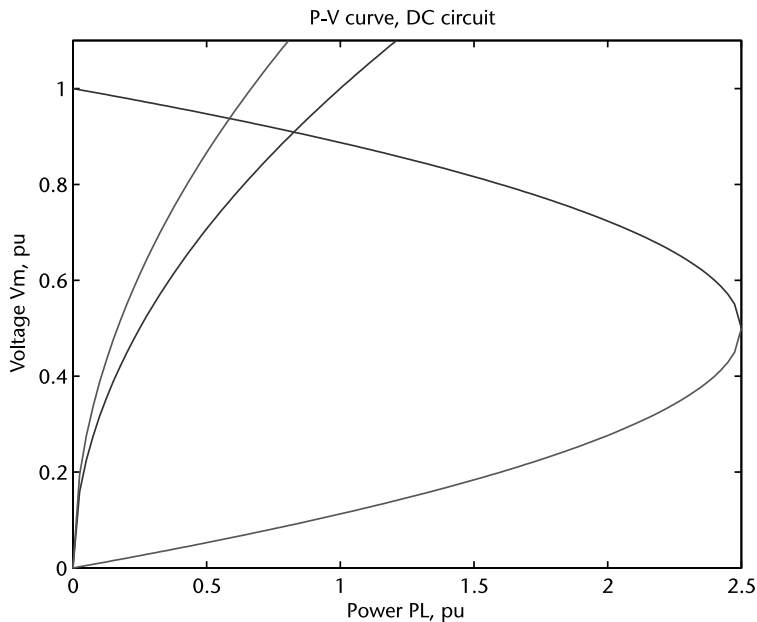


Figure 6.4 The system's PV curve for a resistive load, $R_L = 1.5$, 1.1 pu.

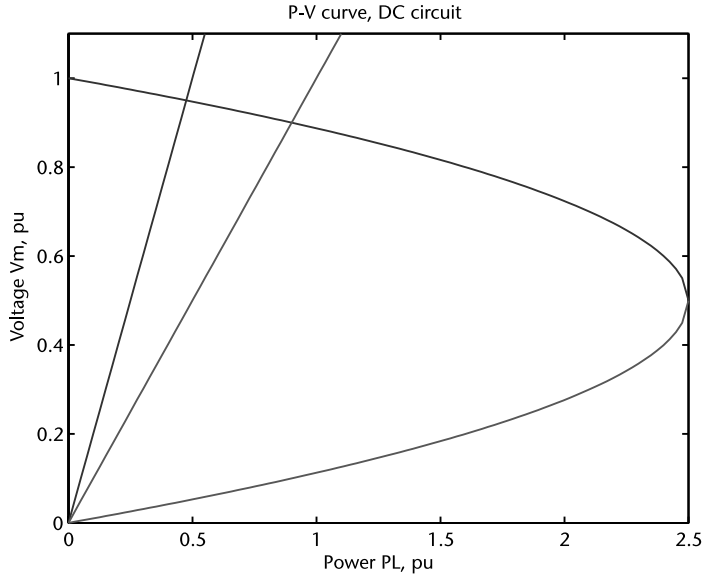


Figure 6.5 The system's PV curve and constant current load characteristics.

6.2.1 Newton's Iterative Process

Nonlinear equations like (6.4) might be present when solving DC real power flow problems. An iterative method with good convergence is Newton's approach. Newton's method is written in incremental form (6.9); this problem is one equation one unknown.

$$f(V_m^1) = f(V_m^0 + \Delta V_m) = f(V_m^0) + \frac{df(V_m^0)}{dV_m} \Delta V_m = 0 \quad (6.9)$$

$$\Delta V_m = - \left(\frac{df(V_m^0)}{dV_m} \right)^{-1} f(V_m^0) \quad (6.10)$$

Once the correction value ΔV_m is calculated, the new V_m value is:

$$V_m^1 = V_m^0 + \Delta V_m \quad (6.11)$$

We repeat the iterative process several times and stop when the absolute value for $f(V_m^k)$, in the k th iteration, is less than a specified tolerance. If the ΔV_m is less than a specified tolerance, it can also be used as convergence criteria.

Example 6.2

For $V_k = 1.0$, $r_{km} = 0.1$ in pu. Solve (6.4) for voltage V_m when $P_L = 0.50$, starting value $V_m^0 = 1.1$. Then start the iterative process with $V_m^0 = 0.1$. The nonlinear equation and its first derivative are $f(V_m) = V_m^2 - V_m + 0.05 = 0$ and $f'(V_m) = 2V_m - 1.0$.

Newton's iterative process

Iteration	Voltage	Mismatch
0	1.10000	1.6000e-001
1	0.96667	1.7778e-002
2	0.94762	3.6281e-004
3	0.94721	1.6424e-007

Newton's iterative process

Iteration	Voltage	Mismatch
0	0.10000	4.0000e-002
1	0.05000	2.5000e-003
2	0.05278	7.7160e-006

We can glimpse into the nature of convergence by plotting the iterative equation (6.12), one set for the left hand side and another for the right side, with values from Example 6.2.

$$V_m^1 = V_m^0 + \Delta V_m = V_m^0 - \frac{(V_m^0)^2 - V_m^0 V_k + r_{km} P_L}{2V_m^0 - V_k} = \frac{(V_m^0)^2 - r_{km} P_L}{2V_m^0 - V_k} \quad (6.12)$$

In Figure 6.6, the upper plot shows the solution for what we call *normal operating voltage*. The bottom plot is a *low voltage solution*, which is not a practical solution because it involves very large currents and extremely low voltages.

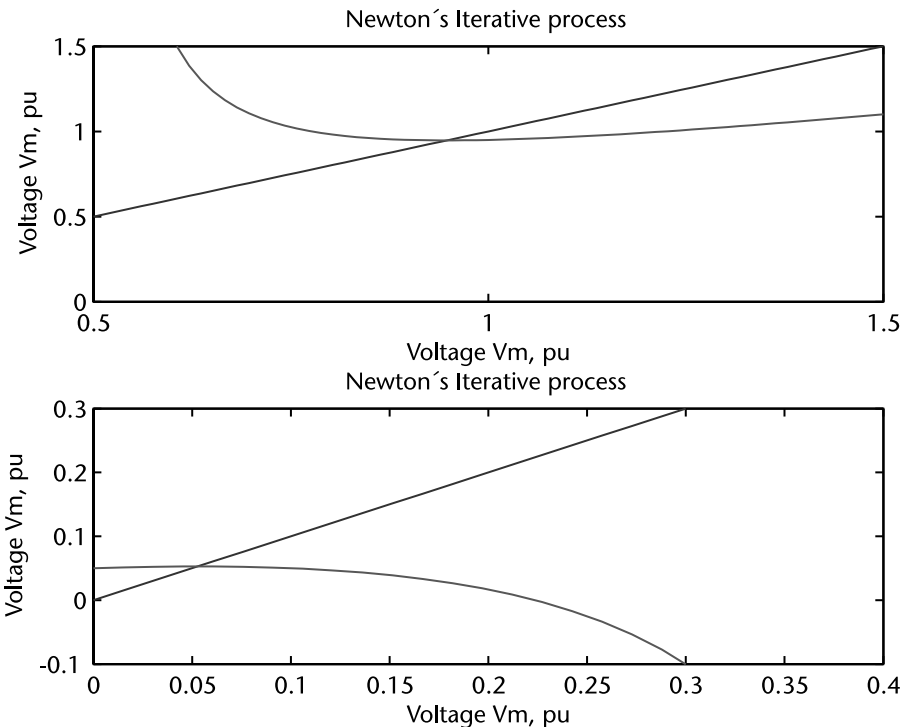


Figure 6.6 Newton's convergence characteristics for its iterative process.

6.3 Newton's Method for Power Flow Solutions

To illustrate the use of Newton's method in solving two nonlinear equations, let's assume a simple two-node system where the transmission can be modeled by a series reactance x_{km} in pu and the power source has a complex voltage V_k in pu (see Figure 6.7).

Equations for the complex power flows, both real and reactive components:

$$p_{mk} + jq_{mk} = V_m i_{mk}^* = V_m \left(\frac{V_m - V_k}{jx_{mk}} \right)^* = -P_L - jQ_L \quad (6.13)$$

$$\begin{bmatrix} f_1(\theta_m, |V_m|) \\ f_2(\theta_m, |V_m|) \end{bmatrix} = \begin{bmatrix} \frac{|V_k||V_m|\sin\theta_m}{x_{mk}} + P_L \\ \frac{(|V_m|^2 - |V_k||V_m|\cos\theta_m)}{x_{mk}} + Q_L \end{bmatrix} = \begin{bmatrix} 0 \\ 0 \end{bmatrix} \quad (6.14)$$

Newton's iterative process requires partial derivatives and a starting point $\theta_m^0, |V_m|^0$. Partial derivatives for this problem are shown in (6.15).

$$\begin{bmatrix} \frac{\partial f_1}{\partial \theta_m} & \frac{\partial f_1}{\partial |V_m|} \\ \frac{\partial f_2}{\partial \theta_m} & \frac{\partial f_2}{\partial |V_m|} \end{bmatrix}_{\theta_m^0, |V_m|^0} \begin{bmatrix} \Delta\theta_m \\ \Delta|V_m| \end{bmatrix} = - \begin{bmatrix} f_1(\theta_m, |V_m|) \\ f_2(\theta_m, |V_m|) \end{bmatrix}_{\theta_m^0, |V_m|^0} \quad (6.15)$$

$$\begin{bmatrix} \frac{\partial f_1}{\partial \theta_m} & \frac{\partial f_1}{\partial |V_m|} \\ \frac{\partial f_2}{\partial \theta_m} & \frac{\partial f_2}{\partial |V_m|} \end{bmatrix} = \begin{bmatrix} \frac{|V_k||V_m|\cos\theta_m}{x_{mk}} & \frac{|V_k|\sin\theta_m}{x_{mk}} \\ \frac{|V_k||V_m|\sin\theta_m}{x_{mk}} & \frac{(2|V_m| - |V_k|\cos\theta_m)}{x_{mk}} \end{bmatrix} \quad (6.16)$$

Example 6.3

Values in pu: $x_{km} = 0.1$, $V_k = 1.0$, $P_L = 0.5$, $Q_L = 0.1$. The iterative process converges after three iterations with a very small mismatch, then the complex power flow is calculated. The iterative process started with $\theta_m^0 = 0$, $|V_m|^0 = 1.0$.

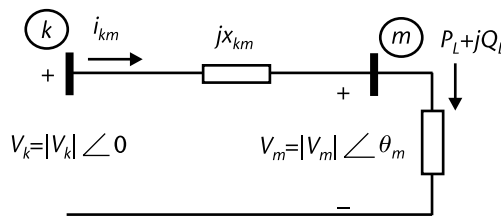


Figure 6.7 A basic two-node AC system.

Newton's iterative process

Iteration	Voltage	Angle, rad	Mismatch
0	1.00000	0.00000	5.0000e-001
1	0.99000	-0.05000	1.3372e-002
2	0.98861	-0.05060	2.0745e-005
3	0.98860	-0.05060	5.0563e-011
Voltage		Angle, degrees	
0.98860		-2.90	
Complex power flows $s_{mk} = -0.50000 + j-0.10000$			

6.4 Power Flow Equations

In Section 6.3.2, we presented an approach to solving a system of equations that would comply with both the real and reactive power requirements at a single node. After some iterative steps, Newton's process works using incremental changes to find the complex voltage solution for the AC power network. Let's present the power flow and losses equations, assuming a complex transformer, then a transmission line; these are the main power transmission elements that we find in the electric network.

6.4.1 Complex Power Transformer and Incremental Power Flows

Figure 6.8 shows an ideal transformer (no losses) with a complex relation, primary and secondary currents, and voltages. For the ideal transformer $s_{\text{primary}} = s_{\text{secondary}}$, which is (6.18), from which current relations are derived as (6.19).

$$\frac{\tilde{V}_k}{\tilde{V}'_k} = \frac{1}{|t| \angle \tau} \tag{6.17}$$

$$\tilde{V}_k i_{km}^* = \tilde{V}'_k (i'_{km})^* \tag{6.18}$$

$$\frac{i_{km}^*}{(i'_{km})^*} = \frac{\tilde{V}'_k}{\tilde{V}_k} = |t| \angle \tau \tag{6.19}$$

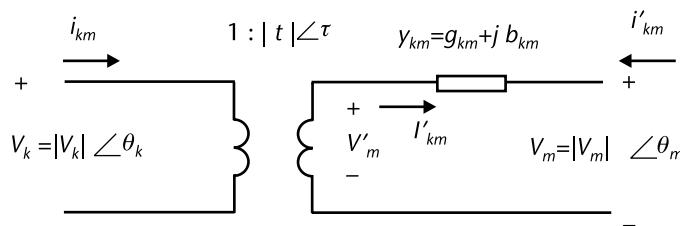


Figure 6.8 Ideal transformer and complex transformation.

The complex power flow from node k to node m is:

$$\begin{aligned} s_{km} &= \tilde{V}_k i_{km}^* = \tilde{V}_k |t| \angle \tau (\tilde{V}_k |t| \angle \tau - \tilde{V}_m)^* y_{km}^* \\ &= \left[|V_k|^2 |t|^2 - |V_k| |V_m| |t| \angle (\theta_k - \theta_m + \tau) \right] (g_{km} - j b_{km}) \end{aligned} \quad (6.20)$$

Separating the real and reactive power expressions:

$$p_{km} = +|V_k|^2 |t|^2 g_{km} - |V_k| |V_m| |t| g_{km} \cos(\theta_k - \theta_m + \tau) - |V_k| |V_m| |t| b_{km} \sin(\theta_k - \theta_m + \tau) \quad (6.21)$$

$$q_{km} = -|V_k|^2 |t|^2 b_{km} - |V_k| |V_m| |t| g_{km} \sin(\theta_k - \theta_m + \tau) + |V_k| |V_m| |t| b_{km} \cos(\theta_k - \theta_m + \tau) \quad (6.22)$$

Now, the complex power from node m to node k and the real and imaginary components are shown.

$$\begin{aligned} s_{mk} &= \tilde{V}_m (i'_{mk})^* = \tilde{V}_m (-i'_{km})^* \\ &= \left[|V_m|^2 - |V_m| |V_k| |t| \angle (\theta_m - \theta_k - \tau) \right] (g_{km} - j b_{km}) \end{aligned} \quad (6.23)$$

$$p_{mk} = +|V_m|^2 g_{km} - |V_m| |V_k| |t| g_{km} \cos(\theta_m - \theta_k - \tau) - |V_m| |V_k| |t| b_{km} \sin(\theta_m - \theta_k - \tau) \quad (6.24)$$

$$q_{mk} = -|V_m|^2 b_{km} - |V_m| |V_k| |t| g_{km} \sin(\theta_m - \theta_k - \tau) + |V_m| |V_k| |t| b_{km} \cos(\theta_m - \theta_k - \tau) \quad (6.25)$$

We add (6.21) and (6.24) to find the expression for power losses in the complex power transformer:

$$p_{L,km} = |V_k|^2 |t|^2 g_{km} + |V_m|^2 g_{km} - 2|V_k| |V_m| |t| \cos(\theta_k - \theta_m + \tau) g_{km} \quad (6.26)$$

In order to reduce transformer losses, looking into (6.26), we observe that two control variables might be available: tap magnitude $|t|$ and phase shift angle τ (assuming that nodal voltages remain fixed).

Note that the reactive power handled by the transformer is calculated by:

$$q_{L,km} = -\left(|V_k|^2 |t|^2 + |V_m|^2 \right) b_{km} + 2|V_k| |V_m| |t| b_{km} \cos(\theta_k - \theta_m + \tau) \quad (6.27)$$

If $q_{L,km} > 0$, reactive power is required by the complex transformer; if $q_{L,km} < 0$ reactive power is supplied to the system.

6.4.1.1 Incremental Real Power Flow Δp_{km} in a Transformer

To study the behavior of real power flow in the steady state condition, the incremental real power expression shows the effect of small changes from every variable

that must be adjusted by control action or variables that adjust themselves to comply with network constraints. Let us assume an expression for a complex relation transformer. The incremental form for Δp_{km} depends on small changes for variables on p_{km} as in (6.21). Partial derivatives are shown.

$$\Delta p_{km} = \frac{\partial p_{km}}{\partial \theta_k} \Delta \theta_k + \frac{\partial p_{km}}{\partial \theta_m} \Delta \theta_m + \frac{\partial p_{km}}{\partial \tau} \Delta \tau + \frac{\partial p_{km}}{\partial |V_k|} |V_k| \frac{\Delta |V_k|}{|V_k|} + \frac{\partial p_{km}}{\partial |V_m|} |V_m| \frac{\Delta |V_m|}{|V_m|} + \frac{\partial p_{km}}{\partial |t|} |t| \frac{\Delta |t|}{|t|} \quad (6.28)$$

$$\frac{\partial p_{km}}{\partial \theta_k} = +|V_k||V_m||t| [g_{km} \sin(\theta_k - \theta_m + \tau) - b_{km} \cos(\theta_k - \theta_m + \tau)] = -|V_k|^2 |t|^2 b_{km} - q_{km} \quad (6.29)$$

$$\frac{\partial p_{km}}{\partial \theta_m} = +|V_k||V_m||t| [-g_{km} \sin(\theta_k - \theta_m + \tau) + b_{km} \cos(\theta_k - \theta_m + \tau)] = +|V_k|^2 |t|^2 b_{km} + q_{km} \quad (6.30)$$

$$\frac{\partial p_{km}}{\partial \tau} = +|V_k||V_m||t| [+g_{km} \sin(\theta_k - \theta_m + \tau) - b_{km} \cos(\theta_k - \theta_m + \tau)] = -|V_k|^2 |t|^2 b_{km} - q_{km} \quad (6.31)$$

$$\frac{\partial p_{km}}{\partial |V_k|} |V_k| = |V_k|^2 |t|^2 g_{km} + p_{km} \quad (6.32)$$

$$\frac{\partial p_{km}}{\partial |V_m|} |V_m| = -|V_k|^2 |t|^2 g_{km} + p_{km} \quad (6.33)$$

$$\frac{\partial p_{km}}{\partial |t|} |t| = +|V_k|^2 |t|^2 g_{km} + p_{km} \quad (6.34)$$

6.4.1.2 Incremental Reactive Power Flow Δq_{km} in a Transformer

The incremental reactive power flow Δq_{km} in a complex power transformer depends on small increments of the nodal variables and control actions on tap or phase shifter.

$$\Delta q_{km} = \frac{\partial q_{km}}{\partial \theta_k} \Delta \theta_k + \frac{\partial q_{km}}{\partial \theta_m} \Delta \theta_m + \frac{\partial q_{km}}{\partial \tau} \Delta \tau + \frac{\partial q_{km}}{\partial |V_k|} |V_k| \frac{\Delta |V_k|}{|V_k|} + \frac{\partial q_{km}}{\partial |V_m|} |V_m| \frac{\Delta |V_m|}{|V_m|} + \frac{\partial q_{km}}{\partial |t|} |t| \frac{\Delta |t|}{|t|} \quad (6.35)$$

The partial derivatives are:

$$\frac{\partial q_{km}}{\partial \theta_k} = |V_k||V_m||t| [-g_{km} \cos(\theta_k - \theta_m + \tau) - b_{km} \sin(\theta_k - \theta_m + \tau)] = -|V_k|^2 |t|^2 g_{km} + p_{km} \quad (6.36)$$

$$\frac{\partial q_{km}}{\partial \theta_m} = |V_k| |V_m| |t| \left[+g_{km} \cos(\theta_k - \theta_m + \tau) + b_{km} \sin(\theta_k - \theta_m + \tau) \right] = +|V_k|^2 |t|^2 g_{km} - p_{km} \quad (6.37)$$

$$\frac{\partial q_{km}}{\partial \tau} = |V_k| |V_m| |t| \left[-g_{km} \cos(\theta_k - \theta_m + \tau) - b_{km} \sin(\theta_k - \theta_m + \tau) \right] = -|V_k|^2 |t|^2 g_{km} + p_{km} \quad (6.38)$$

$$\frac{\partial q_{km}}{\partial |V_k|} |V_k| = -|V_k|^2 |t|^2 b_{km} + q_{km} \quad (6.39)$$

$$\frac{\partial q_{km}}{\partial |V_m|} |V_m| = +|V_k|^2 |t|^2 b_{km} + q_{km} \quad (6.40)$$

$$\frac{\partial q_{km}}{\partial |t|} |t| = -|V_k|^2 |t|^2 b_{km} + q_{km} \quad (6.41)$$

6.4.1.3 Incremental Real Power Flow Δp_{mk} in a Transformer

The real and reactive powers that flow from node m to node k through the complex transformer are different from the ones that flow from node k to node m ; the complex tap affects how these quantities are calculated. This characteristic permeates to the partial derivatives in (6.42) and is not symmetric with partial derivatives in (6.28).

$$\Delta p_{mk} = \frac{\partial p_{mk}}{\partial \theta_m} \Delta \theta_m + \frac{\partial p_{mk}}{\partial \theta_k} \Delta \theta_k + \frac{\partial p_{mk}}{\partial \tau} \Delta \tau + \frac{\partial p_{mk}}{\partial |V_m|} |V_m| \frac{\Delta |V_m|}{|V_m|} + \frac{\partial p_{mk}}{\partial |V_k|} |V_k| \frac{\Delta |V_k|}{|V_k|} + \frac{\partial p_{mk}}{\partial |t|} |t| \frac{\Delta |t|}{|t|} \quad (6.42)$$

$$\begin{aligned} \frac{\partial p_{mk}}{\partial \theta_m} &= +|V_m| |V_k| |t| g_{km} \sin(\theta_m - \theta_k - \tau) - |V_m| |V_k| |t| b_{km} \cos(\theta_m - \theta_k - \tau) \\ &= -|V_m|^2 b_{km} - q_{mk} \end{aligned} \quad (6.43)$$

$$\begin{aligned} \frac{\partial p_{mk}}{\partial \theta_k} &= -|V_m| |V_k| |t| g_{km} \sin(\theta_m - \theta_k - \tau) + |V_m| |V_k| |t| b_{km} \cos(\theta_m - \theta_k - \tau) \\ &= +|V_m|^2 b_{km} + q_{mk} \end{aligned} \quad (6.44)$$

$$\begin{aligned} \frac{\partial p_{mk}}{\partial \tau} &= -|V_m| |V_k| |t| g_{km} \sin(\theta_m - \theta_k - \tau) + |V_m| |V_k| |t| b_{km} \cos(\theta_m - \theta_k - \tau) \\ &= +|V_m|^2 b_{km} + q_{mk} \end{aligned} \quad (6.45)$$

$$\frac{\partial p_{mk}}{\partial |V_m|} |V_m| = +|V_m|^2 g_{km} + p_{mk} \quad (6.46)$$

$$\frac{\partial p_{mk}}{\partial |V_k|} |V_k| = -|V_m|^2 g_{km} + p_{mk} \quad (6.47)$$

$$\frac{\partial p_{mk}}{\partial |t|} |t| = -|V_m|^2 g_{km} + p_{mk} \quad (6.48)$$

6.4.1.4 Incremental Reactive Power Flow Δq_{mk} in a Transformer

The incremental reactive power flow Δq_{km} :

$$\Delta q_{mk} = \frac{\partial q_{mk}}{\partial \theta_m} \Delta \theta_m + \frac{\partial q_{mk}}{\partial \theta_k} \Delta \theta_k + \frac{\partial q_{mk}}{\partial \tau} \Delta \tau + \frac{\partial q_{mk}}{\partial |V_m|} |V_m| \frac{\Delta |V_m|}{|V_m|} + \frac{\partial q_{mk}}{\partial |V_k|} |V_k| \frac{\Delta |V_k|}{|V_k|} + \frac{\partial q_{mk}}{\partial |t|} |t| \frac{\Delta |t|}{|t|} \quad (6.49)$$

The partial derivatives:

$$\begin{aligned} \frac{\partial q_{mk}}{\partial \theta_m} &= -|V_m| |V_k| |t| g_{km} \cos(\theta_m - \theta_k - \tau) - |V_m| |V_k| |t| b_{km} \sin(\theta_m - \theta_k - \tau) \\ &= -|V_m|^2 g_{km} + p_{mk} \end{aligned} \quad (6.50)$$

$$\begin{aligned} \frac{\partial q_{mk}}{\partial \theta_k} &= +|V_m| |V_k| |t| g_{km} \cos(\theta_m - \theta_k - \tau) + |V_m| |V_k| |t| b_{km} \sin(\theta_m - \theta_k - \tau) \\ &= +|V_m|^2 g_{km} - p_{mk} \end{aligned} \quad (6.51)$$

$$\begin{aligned} \frac{\partial q_{mk}}{\partial \tau} &= +|V_m| |V_k| |t| g_{km} \cos(\theta_m - \theta_k - \tau) + |V_m| |V_k| |t| b_{km} \sin(\theta_m - \theta_k - \tau) \\ &= +|V_m|^2 g_{km} - p_{mk} \end{aligned} \quad (6.52)$$

$$\frac{\partial q_{mk}}{\partial |V_m|} |V_m| = -|V_m|^2 b_{km} + q_{mk} \quad (6.53)$$

$$\frac{\partial q_{mk}}{\partial |V_k|} |V_k| = +|V_m|^2 b_{km} + q_{mk} \quad (6.54)$$

$$\frac{\partial q_{mk}}{\partial |t|} |t| = +|V_m|^2 b_{km} + q_{mk} \quad (6.55)$$

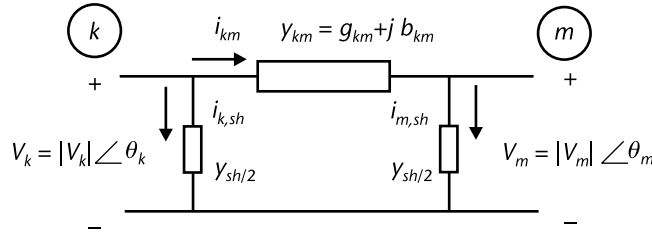


Figure 6.9 Transmission line model, positive sequence series impedance, and shunt admittance.

6.4.2 Incremental Power Flow for a Transmission Line

For a transmission line (see Figure 6.9), the model has nodal voltages $\tilde{V}_k = |V_k| \angle \theta_k$, $\tilde{V}_m = |V_m| \angle \theta_m$, series admittance $y_{km} = g_{km} + j b_{km}$, and charging admittance $y_{sh/2} = 1/(-jX_{C/2}) = jB_{sh/2}$.

The complex power on the transmission line from k to m using $\theta_{km} = \theta_k - \theta_m$ is:

$$s_{km} = \tilde{V}_k (i_{km} + i_{k,sh})^* \quad (6.56)$$

$$\begin{aligned} s_{km} &= \tilde{V}_k \left[(\tilde{V}_k - \tilde{V}_m) y_{km} + \tilde{V}_k y_{sh/2} \right]^* \\ &= |V_k|^2 g_{km} - |V_k| |V_m| g_{km} \cos \theta_{km} - |V_k| |V_m| b_{km} \sin \theta_{km} - j |V_k|^2 b_{km} \\ &\quad - j |V_k|^2 B_{sh/2} + j |V_k| |V_m| b_{km} \cos \theta_{km} - j |V_k| |V_m| g_{km} \sin \theta_{km} \end{aligned} \quad (6.57)$$

$$p_{km} = |V_k|^2 g_{km} - |V_k| |V_m| g_{km} \cos \theta_{km} - |V_k| |V_m| b_{km} \sin \theta_{km} \quad (6.58)$$

$$q_{km} = -|V_k|^2 (b_{km} + B_{sh/2}) - |V_k| |V_m| g_{km} \sin \theta_{km} + |V_k| |V_m| b_{km} \cos \theta_{km} \quad (6.59)$$

Now, the complex power from m to k using $\theta_{mk} = \theta_m - \theta_k$:

$$s_{mk} = (\tilde{V}_m - i_{km} + i_{m,sh})^* \quad (6.60)$$

$$\begin{aligned} s_{mk} &= \tilde{V}_m \left[-(\tilde{V}_k - \tilde{V}_m) y_{km} + \tilde{V}_m y_{sh/2} \right]^* \\ &= |V_m|^2 g_{km} - |V_m| |V_k| g_{km} \cos \theta_{mk} - |V_m| |V_k| b_{km} \sin \theta_{mk} \\ &\quad - j |V_m|^2 b_{km} - j |V_m|^2 B_{sh/2} + j |V_m| |V_k| b_{km} \cos \theta_{mk} - j |V_k| |V_m| g_{km} \sin \theta_{mk} \end{aligned} \quad (6.61)$$

$$p_{mk} = |V_m|^2 g_{km} - |V_m| |V_k| g_{km} \cos \theta_{mk} - |V_m| |V_k| b_{km} \sin \theta_{mk} \quad (6.62)$$

$$q_{mk} = -|V_m|^2 (b_{km} + B_{sh/2}) - |V_m| |V_k| g_{km} \sin \theta_{mk} + |V_m| |V_k| b_{km} \cos \theta_{mk} \quad (6.63)$$

Transmission losses are calculated by adding (6.58) and (6.62).

$$p_{L,km} = p_{km} + p_{mk} = \left(|V_k|^2 + |V_m|^2 \right) g_{km} - 2|V_k||V_m|g_{km} \cos\theta_{km} \quad (6.64)$$

Adding the reactive power (6.59) and (6.63), a positive value ($q_{L,km} > 0$) means that reactive power is required by the transmission element. When ($q_{L,km} < 0$), the reactive power is supplied by the transmission line into the power system.

$$q_{L,km} = -\left(|V_k|^2 + |V_m|^2 \right) (b_{km} + B_{sb/2}) + 2|V_k||V_m|b_{km} \cos\theta_{km} \quad (6.65)$$

Note that that p_{mk} (6.62) and q_{mk} (6.63) can be calculated by (6.58) and (6.59) if an exchange is made for k as m ; this can be carried into the process of its partial derivatives so that only the set to calculate quantities from k to m will be written.

6.4.2.1 Incremental Real Power Flow Δp_{km} for Transmission Line

For a transmission line the power p_{km} is as in (6.58), the incremental real power km , and its partial derivatives are:

$$\Delta p_{km} = \frac{\partial p_{km}}{\partial \theta_k} \Delta \theta_k + \frac{\partial p_{km}}{\partial \theta_m} \Delta \theta_m + \frac{\partial p_{km}}{\partial |V_k|} |V_k| \frac{\Delta |V_k|}{|V_k|} + \frac{\partial p_{km}}{\partial |V_m|} |V_m| \frac{\Delta |V_m|}{|V_m|} \quad (6.66)$$

$$\frac{\partial p_{km}}{\partial \theta_k} = +|\tilde{V}_k||\tilde{V}_m|g_{km} \sin\theta_{km} - |\tilde{V}_k||\tilde{V}_m|b_{km} \cos\theta_{km} = -|\tilde{V}_k|^2 (b_{km} + B_{sb/2}) - q_{km} \quad (6.67)$$

$$\frac{\partial p_{km}}{\partial \theta_m} = -|\tilde{V}_k||\tilde{V}_m|g_{km} \sin\theta_{km} + |\tilde{V}_k||\tilde{V}_m|b_{km} \cos\theta_{km} = +|\tilde{V}_k|^2 (b_{km} + B_{sb/2}) + q_{km} \quad (6.68)$$

$$\frac{\partial p_{km}}{\partial |\tilde{V}_k|} |\tilde{V}_k| = +|\tilde{V}_k|^2 g_{km} + p_{km} \quad (6.69)$$

$$\frac{\partial p_{km}}{\partial |\tilde{V}_m|} |\tilde{V}_m| = -|\tilde{V}_k|^2 g_{km} + p_{km} \quad (6.70)$$

6.4.2.2 Incremental Reactive Power Flow Δq_{km} for a Transmission Line

The incremental reactive power flow from k to m and its partial derivatives are:

$$\Delta q_{km} = \frac{\partial q_{km}}{\partial \theta_k} \Delta \theta_k + \frac{\partial q_{km}}{\partial \theta_m} \Delta \theta_m + \frac{\partial q_{km}}{\partial |V_k|} |V_k| \frac{\Delta |V_k|}{|V_k|} + \frac{\partial q_{km}}{\partial |V_m|} |V_m| \frac{\Delta |V_m|}{|V_m|} \quad (6.71)$$

$$\frac{\partial q_{km}}{\partial \theta_k} = -|\tilde{V}_k||\tilde{V}_m|g_{km} \cos \theta_{km} - |\tilde{V}_k||\tilde{V}_m|b_{km} \sin \theta_{km} = -|\tilde{V}_k|^2 g_{km} + p_{km} \quad (6.72)$$

$$\frac{\partial q_{km}}{\partial \theta_m} = +|\tilde{V}_k||\tilde{V}_m|g_{km} \cos \theta_{km} + |\tilde{V}_k||\tilde{V}_m|b_{km} \sin \theta_{km} = +|\tilde{V}_k|^2 g_{km} - p_{km} \quad (6.73)$$

$$\frac{\partial q_{km}}{\partial |\tilde{V}_k|} |\tilde{V}_k| = -|\tilde{V}_k|^2 (b_{km} + B_{sh/2}) + q_{km} \quad (6.74)$$

$$\frac{\partial q_{km}}{\partial |\tilde{V}_m|} |\tilde{V}_m| = +|\tilde{V}_k|^2 (b_{km} + B_{sh/2}) + q_{km} \quad (6.75)$$

6.4.2.3 Incremental Real Power Flow Δp_{mk} for a Transmission Line

The incremental real power flow from m to k as in (6.76) and partial derivatives in this equation can be calculated by (6.67) to (6.70) if we reverse k and m .

$$\Delta p_{mk} = \frac{\partial p_{mk}}{\partial \theta_m} \Delta \theta_m + \frac{\partial p_{mk}}{\partial \theta_k} \Delta \theta_k + \frac{\partial p_{mk}}{\partial |V_m|} |V_m| \frac{\Delta |V_m|}{|V_m|} + \frac{\partial p_{mk}}{\partial |V_k|} |V_k| \frac{\Delta |V_k|}{|V_k|} \quad (6.76)$$

6.4.2.4 Incremental Reactive Power Flow Δq_{mk} for a Transmission Line

The incremental reactive power flow Δq_{mk} from m to k and partial derivatives are calculated by (6.72) to (6.75) if we interchange k by m .

$$\Delta q_{mk} = \frac{\partial q_{mk}}{\partial \theta_m} \Delta \theta_m + \frac{\partial q_{mk}}{\partial \theta_k} \Delta \theta_k + \frac{\partial q_{mk}}{\partial |V_m|} |V_m| \frac{\Delta |V_m|}{|V_m|} + \frac{\partial q_{mk}}{\partial |V_k|} |V_k| \frac{\Delta |V_k|}{|V_k|} \quad (6.77)$$

6.5 Newton's Power Flow Solution

To solve a load flow problem that will determine all nodal voltages, we write two power balance equations; one for the real power and one for the reactive power at each node.

For a given node k :

$$f_{P,k} = \sum_{\forall m \in k} p_{km} - P_{Gk} + P_{Dk} = 0 \quad (6.78)$$

$$f_{Q,k} = \sum_{\forall m \in k} q_{km} - Q_{Gk} + Q_{Dk} = 0 \quad (6.79)$$

- p_{km} Real power flow from node k to node m
- q_{km} Reactive power flow from node k to node m
- $\forall m \in k$ Every element m connected to node k
- P_{Gk} Real power by generator into node k
- P_{Dk} Real power by load out of node k
- Q_{Gk} Reactive power by generator into node k
- Q_{Dk} Reactive power by load out of node k

We seek the node voltage solution for all nodes in the power system so that both (6.78) and (6.79) are satisfied as being zero. We write an incremental expression for the real and the reactive power mismatches at each node. Newton's method solves the system of equations such that at iteration r , after the correction values are calculated, (6.81) updates nodal voltage angles and node voltages.

$$\begin{bmatrix} \frac{\partial f_{P,k}}{\partial \theta} & |V| \frac{\partial f_{P,k}}{\partial |V|} \\ \frac{\partial f_{Q,k}}{\partial \theta} & |V| \frac{\partial f_{Q,k}}{\partial |V|} \end{bmatrix}^{(r)} \begin{bmatrix} \Delta \theta \\ \frac{\Delta |V|}{|V|} \end{bmatrix} = - \begin{bmatrix} f_{P,k} \\ f_{Q,k} \end{bmatrix}^{(r)} \tag{6.80}$$

$$\begin{bmatrix} \theta \\ |V| \end{bmatrix}^{(r+1)} = \begin{bmatrix} \theta \\ |V| \end{bmatrix}^{(r)} + \begin{bmatrix} \Delta \theta \\ \Delta |V| \end{bmatrix} \tag{6.81}$$

Example 6.4

For an AC simple system (see Figure 6.10), a three-node arrangement writes the complete set of equations for the power balance at every node. In this system, there are two elements (one transformer and one transmission line).

The real and reactive nodal balances are constraint equations that need to be satisfied through the set of nonlinear equations. Newton's method improves the initial values by solving for corrections for nodal angles $\Delta \theta$ and voltage magnitudes $\Delta |V|/|V|$. The iterative process starts with initial values for unknowns $\theta_1 = \theta_2 = \theta_3$

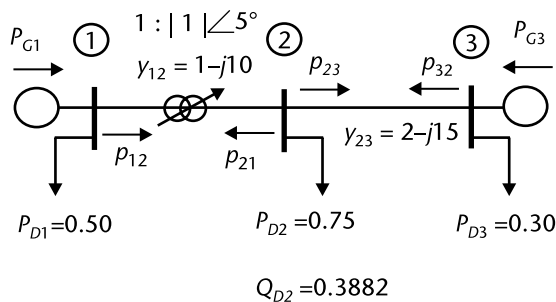


Figure 6.10 Network arrangement to study incremental load flow equations, values in pu.

and nodal voltages $|V|_1 = |V|_2 = |V|_3$. We start with the power mismatch equations for the real and the reactive power at each node. Then we apply the incremental form that uses partial derivatives, which were already presented in Section 6.4.

$$\begin{aligned}
 \text{node 1} \quad g_1 &= p_{12} - P_{G1} + P_{D1} = 0 \\
 \text{node 2} \quad g_2 &= p_{21} + p_{23} + P_{D2} = 0 \\
 \text{node 3} \quad g_3 &= p_{32} - P_{G3} + P_{D3} = 0 \\
 \text{node 1} \quad g_4 &= q_{12} - Q_{G1} + Q_{D1} = 0 \\
 \text{node 2} \quad g_5 &= q_{21} + q_{23} + Q_{D2} = 0 \\
 \text{node 3} \quad g_6 &= q_{32} - Q_{G3} + Q_{D3} = 0
 \end{aligned} \tag{6.82}$$

The numerical values for partial derivatives and g 's (mismatch equations) are calculated with the assumed starting nodal values.

$$\begin{bmatrix}
 \frac{\partial p_{12}}{\partial \theta_1} & \frac{\partial p_{12}}{\partial \theta_2} & 0 & |V|_1 \frac{\partial p_{12}}{\partial |V|_1} & |V|_2 \frac{\partial p_{12}}{\partial |V|_2} & 0 \\
 \frac{\partial p_{21}}{\partial \theta_1} & \frac{\partial p_{21}}{\partial \theta_2} + \frac{\partial p_{23}}{\partial \theta_2} & \frac{\partial p_{23}}{\partial \theta_3} & |V|_1 \frac{\partial p_{21}}{\partial |V|_1} & |V|_2 \frac{\partial p_{21}}{\partial |V|_2} + |V|_2 \frac{\partial p_{23}}{\partial |V|_2} & |V|_3 \frac{\partial p_{23}}{\partial |V|_3} \\
 0 & \frac{\partial p_{32}}{\partial \theta_2} & \frac{\partial p_{32}}{\partial \theta_3} & 0 & |V|_2 \frac{\partial p_{32}}{\partial |V|_2} & |V|_3 \frac{\partial p_{32}}{\partial |V|_3} \\
 \frac{\partial q_{12}}{\partial \theta_1} & \frac{\partial q_{12}}{\partial \theta_2} & 0 & |V|_1 \frac{\partial q_{12}}{\partial |V|_1} & |V|_2 \frac{\partial q_{12}}{\partial |V|_2} & 0 \\
 \frac{\partial q_{21}}{\partial \theta_1} & \frac{\partial q_{21}}{\partial \theta_2} + \frac{\partial q_{23}}{\partial \theta_2} & \frac{\partial q_{23}}{\partial \theta_3} & |V|_1 \frac{\partial q_{21}}{\partial |V|_1} & |V|_2 \frac{\partial q_{21}}{\partial |V|_2} + |V|_2 \frac{\partial q_{23}}{\partial |V|_2} & |V|_3 \frac{\partial q_{23}}{\partial |V|_3} \\
 0 & \frac{\partial q_{32}}{\partial \theta_2} & \frac{\partial q_{32}}{\partial \theta_3} & 0 & |V|_2 \frac{\partial q_{32}}{\partial |V|_2} & |V|_3 \frac{\partial q_{32}}{\partial |V|_3}
 \end{bmatrix}
 \begin{bmatrix}
 \Delta \theta_1 \\
 \Delta \theta_2 \\
 \Delta \theta_3 \\
 \frac{\Delta |V|_1}{|V|_1} \\
 \frac{\Delta |V|_2}{|V|_2} \\
 \frac{\Delta |V|_3}{|V|_3}
 \end{bmatrix}
 = -
 \begin{bmatrix}
 g_1 \\
 g_2 \\
 g_3 \\
 g_4 \\
 g_5 \\
 g_6
 \end{bmatrix} \tag{6.83}$$

Prior to conducting the first iteration, one nodal angle is selected as reference; usually, θ_1 is selected and set to 0 radians. The magnitude of nodal voltages at generation buses will be kept constant because no incremental change is allowed, given that the reactive power limits of the source are not exceeded. To solve (6.83), the reference angle and the constant voltages (at generation nodes) must numerically reflect these fixed conditions. After a few iterations, a converged solution for all nodal voltages is attained and the power flows in lines and transformers can be calculated. In our case for numerical code, node type 0 is the slack node, -1 is a load type PQ , and $+1$ is a PV generation bus. The results are shown in Figure 6.11.

```

Iterative process Newton, Data
Elements = 2
Nodes = 3
Table for elements

```

Elem	N-k	N-m	type1	tap	tau	yelem	Bsh/2
1	1	2	-1	1.00	5.00	1.0000 +j-10.0000	+j 0.0000
2	2	3	1	1.00	0.00	2.0000 +j-15.0000	+j 0.0000

Number of transformers = 1

Table of nodal conditions

Node	type	Voltage	Angle	Pgen	Pload	Qload
1	0	1.0000	0.0000	0.0000	0.5000	0.0000
2	-1	1.0000	0.0000	0.0000	0.7500	0.3882
3	1	1.0000	0.0000	0.6633	0.3000	0.0000

Type of nodes

Generation Nodes = 2 Load Nodes = 1

Iteration = 1 maxdev = 7.071320e-002

Iteration = 2 maxdev = 1.030489e-003

Iteration = 3 maxdev = 1.172099e-006

Nodal Report

Node	type	Voltage	Angle	Pgen	Pload	Qgen	Qload
1	0	1.0000	-0.00	0.8902	0.5000	0.1654	0.0000
2	-1	0.9805	2.84	0.0000	0.7500	0.0000	0.3882
3	1	1.0000	4.10	0.6633	0.3000	0.2535	0.0000

Table for elements (duplicated, -1 transformer, +1 transmission line)

Elem	N-k	N-m	typ-e1	tap	tau	pkm	qkm
1	1	2	-1	1.0000	5.00	0.3902	0.1654
1	2	1	-1	1.0000	5.00	-0.3884	-0.1476
2	2	3	1	1.0000	0.00	-0.3616	-0.2406
2	3	2	1	1.0000	0.00	0.3633	0.2535

PLtot = 0.0035 pu Qltot = 0.0306 pu (>0 required), (<0 to the system)

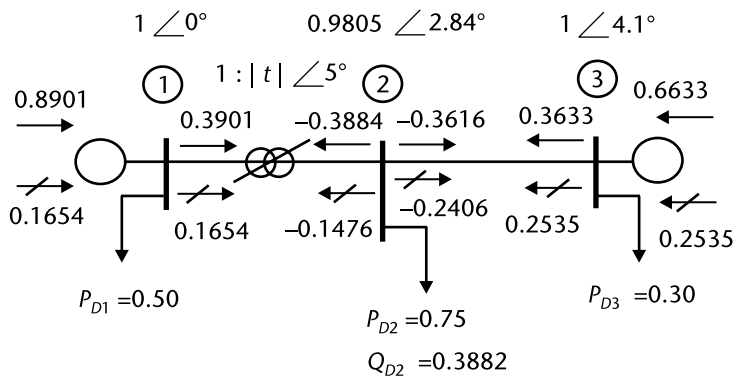


Figure 6.11 Load flow results for Example 6.4.

6.6 Power Flow Approximations

The incremental real power flows (6.28) and (6.42) Δp_{km} , Δp_{mk} and incremental reactive power flow (6.35) and (6.49) Δq_{km} , Δq_{mk} for a complex transformer and in (6.66), (6.71), (6.76), and (6.77) for a transmission line that are the departure for the approximation. For example, in the case of a transmission line, it can be scrutinized closely with particular attention to the relative values observed for the partial derivatives. Using reasonable considerations that are observed in high voltage power circuits, the parameters are of such values that $g_{km} \ll b_{km}$, $\cos(\theta_k - \theta_m + \tau) \cong 1.0$, $|V_m| \cong 1.0$, $|t| \cong 1.0$, and $\sin(\theta_k - \theta_m + \tau) \cong \theta_k - \theta_m + \tau$. These are considered decoupling assumptions.

These values are placed into the partial derivatives (6.29)–(6.34) and (6.67)–(6.70) and we have:

$$\frac{\partial p_{km}}{\partial \theta_k} \cong -|V_k| b_{km} \quad (6.84)$$

$$\frac{\partial p_{km}}{\partial \theta_m} = +|V_k| b_{km} \quad (6.85)$$

$$\frac{\partial p_{km}}{\partial \tau} = -|V_k| b_{km} \quad (6.86)$$

$$\frac{\partial p_{km}}{\partial |V_k|} = -|V_k| b_{km} (\theta_k - \theta_m + \tau) \quad (6.87)$$

$$\frac{\partial p_{km}}{\partial |V_m|} = -|V_k| b_{km} (\theta_k - \theta_m + \tau) \quad (6.88)$$

$$\frac{\partial p_{km}}{\partial |t|} = -|V_k| b_{km} (\theta_k - \theta_m + \tau) \quad (6.89)$$

The substitution of approximated values into Δp_{km} can be written as an Ohm's equivalent (6.91) for the incremental real power flow from node k to node m .

$$\begin{aligned} \Delta p_{km} = & -|V_k| b_{km} \Delta \theta_k + |V_k| b_{km} \Delta \theta_m - |V_k| b_{km} \Delta \tau - |V_k| b_{km} (\theta_k - \theta_m + \tau) \Delta |V_k| \\ & - |V_k| b_{km} (\theta_k - \theta_m + \tau) \Delta |V_m| - |V_k| b_{km} (\theta_k - \theta_m + \tau) \Delta |t| \end{aligned} \quad (6.90)$$

$$-x_{km} \frac{\Delta p_{km}}{|V_k|} + \Delta \theta_k - \Delta \theta_m = -\Delta F_p \approx -\Delta \tau \quad (6.91)$$

The incremental Ohm's equivalent circuit in (6.91) can be drawn (see Figure 6.12).

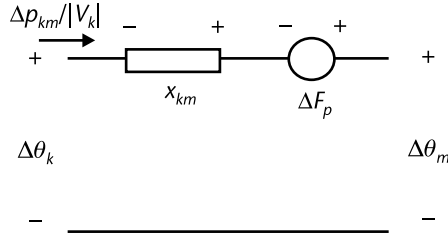


Figure 6.12 Incremental real power flow equivalent circuit; complex transformer.

The equivalent series source ΔF_p in (6.92) includes changes to incremental values in radians for a *phase shifter*, magnitude changes at sending and receiving nodal voltages, and incremental tap change. ΔF_p can be approximated to $\Delta\tau$ (in radians). We propose to use this model to analyze the effects of control actions by phase incremental changes and to study how network flows change and a way to solve for a system's congestion relief.

$$\Delta F_p = +\Delta\tau + \frac{(\theta_k - \theta_m + \tau)}{|V_k|} \Delta|V_k| + (\theta_k - \theta_m + \tau) \Delta|V_m| + (\theta_k - \theta_m + \tau) \Delta|t| \quad (6.92)$$

For the incremental reactive power flow Δq_{km} , the approximate expressions for partial derivatives take the form:

$$\frac{\partial q_{km}}{\partial \theta_k} = -|V_k| b_{km} (\theta_k - \theta_m + \tau) \quad (6.93)$$

$$\frac{\partial q_{km}}{\partial \theta_m} = +|V_k| b_{km} (\theta_k - \theta_m + \tau) \quad (6.94)$$

$$\frac{\partial q_{km}}{\partial \tau} = -|V_k| b_{km} (\theta_k - \theta_m + \tau) \quad (6.95)$$

$$\frac{\partial q_{km}}{\partial |V_k|} = -|V_k| b_{km} \quad (6.96)$$

$$\frac{\partial q_{km}}{\partial |V_m|} = +|V_k| b_{km} \quad (6.97)$$

$$\frac{\partial q_{km}}{\partial |t|} = -|V_k| b_{km} \quad (6.98)$$

Substitution into (6.35) gives an Ohm's equivalent form for reactive power flow and incremental voltages (see Figure 6.13):

$$-x_{km} \frac{\Delta q_{km}}{|V_k|} + \Delta|V_k| - \Delta|V_m| = -\Delta F_q \tag{6.99}$$

$$\Delta F_q = (\theta_k - \theta_m + \tau)\Delta\theta_k - (\theta_k - \theta_m + \tau)\Delta\theta_m + (\theta_k - \theta_m + \tau)\Delta\tau + \Delta|t| \tag{6.100}$$

Further considerations for ΔF_q allow an approximation to $\Delta|t|$.

For transmission lines the incremental real power Δp_{km} (6.66) with partial derivatives in an approximated form; using $-x_{km} = 1/b_{km}$ and $\partial p_{km} / \partial|V_k| \approx 0$, $\partial p_{km} / \partial|V_m| \approx 0$ are:

$$\frac{\partial p_{km}}{\partial\theta_k} \approx -b_{km}|V_k| \tag{6.101}$$

$$\frac{\partial p_{km}}{\partial\theta_m} \approx +b_{km}|V_k| \tag{6.102}$$

$$-x_{km} \frac{\Delta p_{km}}{|V_k|} + (\Delta\theta_k - \Delta\theta_m) = 0 \tag{6.103}$$

The incremental reactive power Δq_{km} (6.71) for the transmission line requires the partial derivatives that are approximated by $\partial q_{km} / \partial\theta_k \approx 0, \partial q_{km} / \partial\theta_m \approx 0$. The Ohm's Law model is now (6.106) and Figure 6.15.

$$\frac{\partial q_{km}}{\partial|V_k|} \approx -2Bsh2|V_k| - b_{km}|V_k| \tag{6.104}$$

$$\frac{\partial q_{km}}{\partial|V_m|} \approx +b_{km}|V_k| \tag{6.105}$$

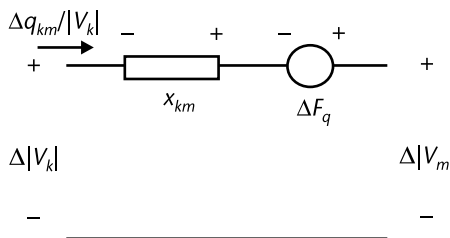


Figure 6.13 Incremental reactive power flow equivalent circuit; complex transformer.

$$\frac{\Delta q_{km}}{|V_k|} = -(2Bsb2)\Delta|V_k| - b_{km}(\Delta|V_k| - \Delta|V_m|) \quad (6.106)$$

Example 6.5

As a small test network, let us solve the load flow problem using *reasonable* approximations (such as the ones used in what is known as the *fast decoupled load flow*). The first derivatives in the Jacobian matrix reflect the approximations. The unknowns are nodal angles θ_2 , θ_3 , and θ_4 and the voltage magnitude for node 4. The constraints to be satisfied are the real and reactive power flows at each element and the nodal real and reactive power balances.

$$|t| \angle \tau = t_\alpha + jt_\beta = 1.05 \angle 5^\circ$$

The incremental real power flow for each element and the nodal real power balance are written using both (6.91) and the real power incremental balances at each node. In matrix form:

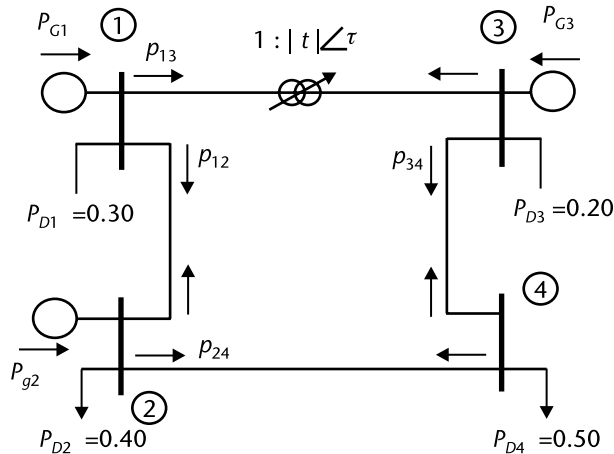


Figure 6.14 A Small network to study the decoupled power flow.

Table 6.1 Data for Small Networks (Figure 6.14)

Element	Node - k	Node - m	y_{km}	tap	$yb_{sh/2}$
1	1	2	$1.0 - j10$	-1	0
2	1	3	$1.0 - j10$	$t_\alpha + jt_\beta$	0
3	3	4	$1.5 - j15$	-1	0
4	2	4	$2.0 - j20$	-1	0

$$\begin{bmatrix}
 -x_{12} & 0 & 0 & 0 & +1 & -1 & 0 & 0 \\
 0 & -x_{13} & 0 & 0 & +1 & 0 & -1 & 0 \\
 0 & 0 & -x_{34} & 0 & 0 & +1 & 0 & -1 \\
 0 & 0 & 0 & -x_{24} & 0 & 0 & +1 & -1 \\
 +1 & -1 & 0 & 0 & 0 & 0 & 0 & 0 \\
 -1 & 0 & +1 & 0 & 0 & 0 & 0 & 0 \\
 0 & -1 & +1 & 0 & 0 & 0 & 0 & 0 \\
 0 & -1 & -1 & 0 & 0 & 0 & 0 & 0
 \end{bmatrix}
 \begin{bmatrix}
 \frac{\Delta p_{12}}{|V_1|} \\
 \frac{\Delta p_{13}}{|V_1|} \\
 \frac{\Delta p_{24}}{|V_2|} \\
 \frac{\Delta p_{34}}{|V_3|} \\
 \Delta\theta_1 \\
 \Delta\theta_2 \\
 \Delta\theta_3 \\
 \Delta\theta_4
 \end{bmatrix}
 =
 \begin{bmatrix}
 -\Delta\tau \\
 0 \\
 0 \\
 0 \\
 \frac{\Delta P_1}{|V_1|} \\
 \frac{\Delta P_2}{|V_2|} \\
 \frac{\Delta P_3}{|V_3|} \\
 \frac{\Delta P_4}{|V_4|}
 \end{bmatrix}
 \quad (6.107)$$

The solution to (6.107) requires one node angle as reference; its value is to remain fixed. Usually $\Delta\tau$, the incremental phase shift control is set to zero under the assumption that the phase shifting angle is not changed within this numerical step. For the reactive power incremental equivalent using (6.108), we must include all series and shunt components. This gives a similar network to the one written for real power—nodal angle power flows. Shunt components add to the incremental reactive power contributions which are added into the nodal reactive power balance, as seen in (6.109).

$$\frac{\Delta q_{km}}{|V_k|} = -(2B_{sh2})\Delta|V_k| - b_{km}(\Delta|V_k| - \Delta|V_m|) \quad (6.108)$$

$$\begin{bmatrix}
 -x_{12} & 0 & 0 & 0 & +1 & -1 & 0 & 0 \\
 0 & -x_{13} & 0 & 0 & +1 & 0 & -1 & 0 \\
 0 & 0 & -x_{34} & 0 & 0 & +1 & 0 & -1 \\
 0 & 0 & 0 & -x_{24} & 0 & 0 & +1 & -1 \\
 +1 & -1 & 0 & 0 & -2B_{sh2}^{12} & 0 & 0 & 0 \\
 -1 & 0 & +1 & 0 & 0 & -2B_{sh2}^{12} - 2B_{sh2}^{24} & 0 & 0 \\
 0 & -1 & +1 & 0 & 0 & 0 & -2B_{sh2}^{34} & 0 \\
 0 & -1 & -1 & 0 & 0 & 0 & 0 & -2B_{sh2}^{24} - 2B_{sh2}^{34}
 \end{bmatrix}
 \begin{bmatrix}
 \frac{\Delta q_{12}}{|V_1|} \\
 \frac{\Delta q_{13}}{|V_1|} \\
 \frac{\Delta q_{24}}{|V_2|} \\
 \frac{\Delta q_{34}}{|V_3|} \\
 \Delta|V_1| \\
 \Delta|V_2| \\
 \Delta|V_3| \\
 \Delta|V_4|
 \end{bmatrix}
 =
 \begin{bmatrix}
 -\Delta|t| \\
 0 \\
 0 \\
 0 \\
 \frac{\Delta Q_1}{|V_1|} \\
 \frac{\Delta Q_2}{|V_2|} \\
 \frac{\Delta Q_3}{|V_3|} \\
 \frac{\Delta Q_4}{|V_4|}
 \end{bmatrix}
 \quad (6.109)$$

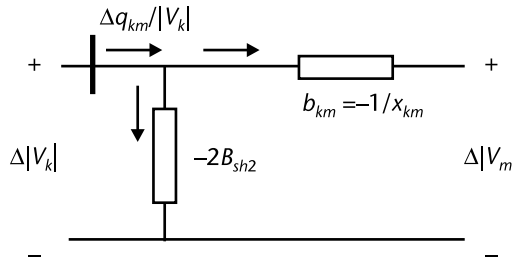


Figure 6.15 Circuit to include shunt reactive compensation.

Given that there is enough reactive power from the reactive sources at that node, the nodal voltage magnitudes for the generation nodes must remain fixed; numerically, we treat the nodal voltage in the same way as the node angle reference. At this stage, $\Delta|t|$ is considered zero because no change for tap position is active. Once the set of variables related to element are *eliminated* in both the incremental real power model (6.107) and the incremental reactive power (6.109), we iteratively solve the two systems of equations in sequence or under other possible schemes, following numerical steps as described by Figure 6.17. A succinct notation for the *fast decoupled* load flow is composed by two set of equations. Results are shown in Figure 6.16.

$$B' \Delta\theta = \frac{\Delta P}{|V|} \tag{6.110}$$

$$B'' \Delta|V| = \frac{\Delta Q}{|V|} \tag{6.111}$$

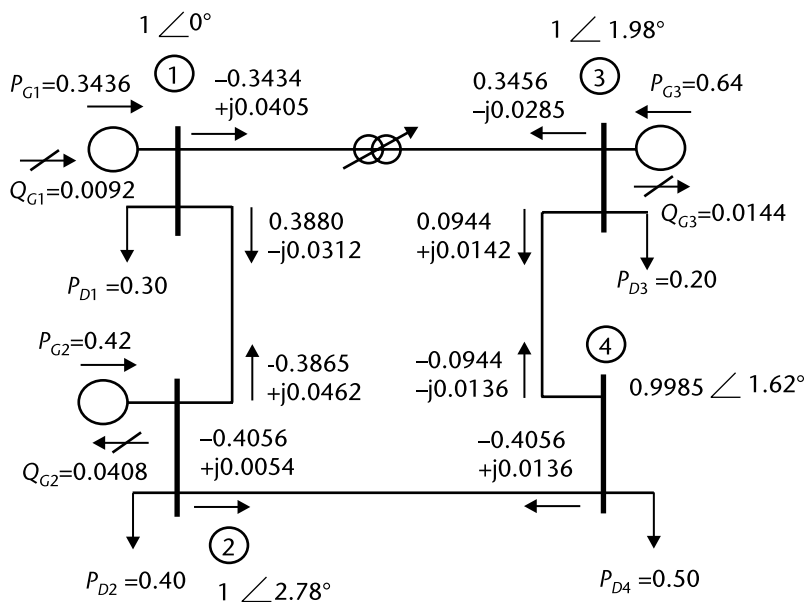


Figure 6.16 Load flow solution diagram for Example 6.5.

Data for an iterative process

Nodes = 4 Element = 4

Element type	From	to	yseries	1/2Ysh (tap)
1	1	2	1.0000 +j-10.0000	0.9962 +j 0.0872
0	1	3	1.0000 +j-10.0000	0.0000 +j 0.0000
0	3	4	1.5000 +j-15.0000	0.0000 +j 0.0000
0	2	4	2.0000 +j-20.0000	0.0000 +j 0.0000
1	2	1	1.0000 +j-10.0000	0.9962 +j 0.0872
0	3	1	1.0000 +j-10.0000	0.0000 +j 0.0000
0	4	3	1.5000 +j-15.0000	0.0000 +j 0.0000
0	4	2	2.0000 +j-20.0000	0.0000 +j 0.0000

Call to line flow calculation and Max mismatch

Convergence in P 1.5 Q 1.0 iterations MaxDQ =3.3251e-006

Node Report

Node type	Vmag(pu)	Angle(deg)	PG	QG	PL	QL
1 +0	1.0000	0.00	0.3436	0.0092	0.3000	0.0000
2 +1	1.0000	2.78	0.4200	0.0408	0.4000	0.0000
3 +1	1.0000	1.98	0.6400	-0.0144	0.2000	0.0000
4 -1	0.9985	1.62	-0.0000	0.0000	0.5000	0.0000

Load flow results

Element	Node from	Node to	spk
1	1	2	0.3880 +j -0.0312
2	1	3	-0.3444 +j 0.0405
3	3	4	0.0944 +j 0.0142
4	2	4	0.4065 +j -0.0054
5	2	1	-0.3865 +j 0.0462
6	3	1	0.3456 +j -0.0285
7	4	3	-0.0944 +j -0.0136
8	4	2	-0.4056 +j 0.0136

Power Losses = 0.0036 pu

Qsystem = 0.0357 pu (>0 required), (<0 to the system)

In practice, when solving large power networks, the experience reported is that the fast-decoupled load flow shows a good type of convergence for systems that have reasonable load condition, not very stressed systems, and for high-voltage networks where the assumptions for the decoupling principle are satisfied. The fast decoupled model in (6.110) and (6.111) where the Jacobian elements have the linear approximation so B' and B'' are kept constant from iteration to iteration. Equations (6.110) and (6.111) are very useful for network control studies, relating control actions to changes in nodal electrical variables and for changes in power flows; we discuss such application in Chapter 8.

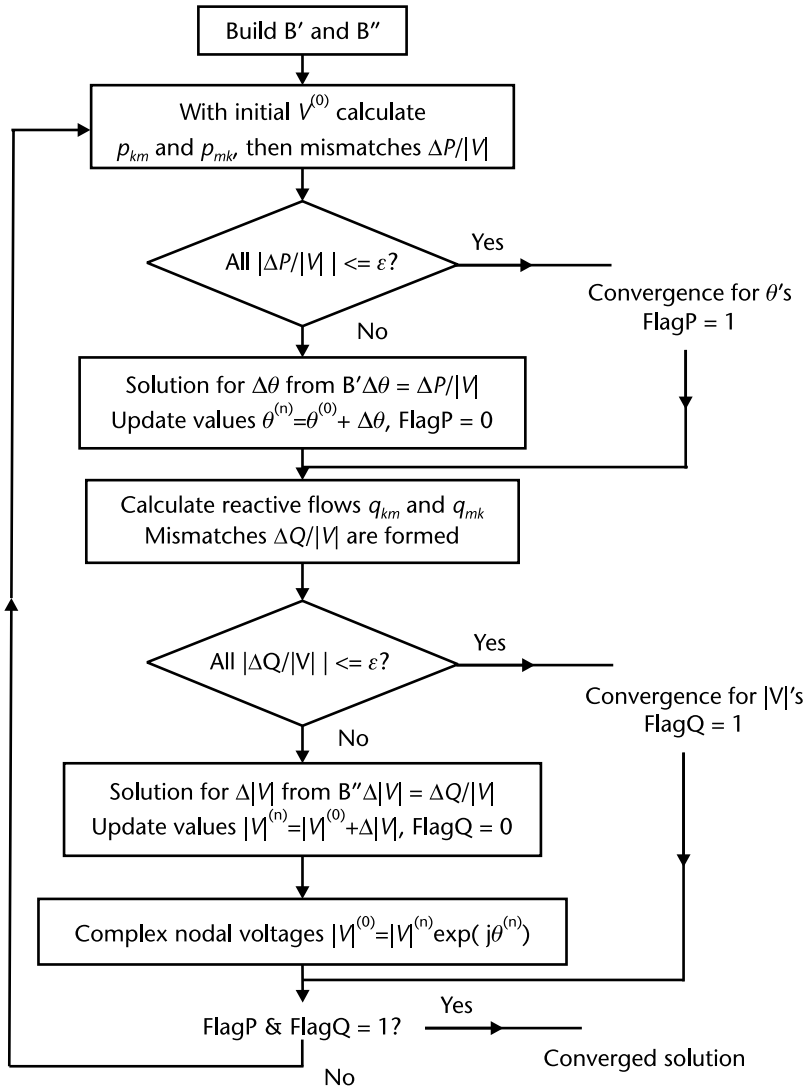


Figure 6.17 Diagram for the decoupled power flow calculations.

6.7 DC Network Power Flow Solutions

Most books that treat power system analysis stress the AC network solution for the load flow problem. We now give attention to a ubiquitous form of use of electric energy, which is the direct current (DC), transmission, and distribution. An increasing use of low DC voltage devices at home and office, coupled to its use in industrial processes, makes this type of electrical energy nonfluctuating in time, no frequency and no reactive power, to reach renewed impetus in its applications. Of course, switching on or off DC electric loads ensues transients and this is a particular area of study and design that we will not be covering. The basic R , L ,

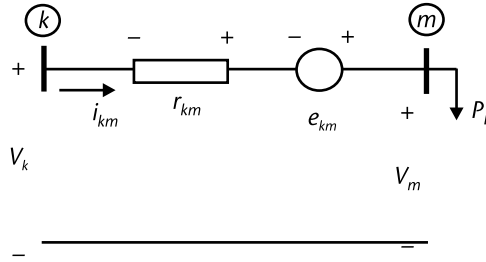


Figure 6.18 DC current transmission element.

and C circuit components are present in the DC networks as part of series or shunt connections, but in the steady state, only the resistance R appears in the current's trajectory. The fundamental relations for load flow analysis in DC networks follow Figure 6.18. Power expressions from node k to node m and from m to k , recognizing the current through element km is $i_{km} = (V_k + e_{km} - V_m)/r_{km}$.

$$p_{km} = V_k i_{km} = \frac{(V_k^2 + V_k e_{km} - V_k V_m)}{r_{mk}} \quad (6.112)$$

$$p_{mk} = -V_m i_{km} = \frac{(-V_m V_k - V_m e_{km} + V_m^2)}{r_{mk}} \quad (6.113)$$

Losses:

$$p_{mk, \text{losses}} = p_{km} + p_{mk} = \frac{(V_k^2 + V_m^2 + e_{km}(V_k - V_m) - 2V_m V_k)}{r_{km}} \quad (6.114)$$

6.7.1 Incremental DC Power Flow Equations

Incremental power Δp_{km} from node k to m , and its partial derivatives are:

$$\Delta p_{km} = \frac{\partial p_{km}}{\partial V_k} \Delta V_k + \frac{\partial p_{km}}{\partial V_m} \Delta V_m + \frac{\partial p_{km}}{\partial e_{km}} \Delta e_{km} \quad (6.115)$$

$$\frac{\partial p_{km}}{\partial V_k} = \frac{(2V_k + e_{km} - V_m)}{r_{km}} = \frac{V_k}{r_{km}} + \frac{p_{km}}{V_k} \quad (6.116)$$

$$\frac{\partial p_{km}}{\partial V_m} = -\frac{V_k}{r_{km}} \quad (6.117)$$

$$\frac{\partial p_{km}}{\partial e_{km}} = + \frac{V_k}{r_{km}} \quad (6.118)$$

Substitution of partial derivatives in (6.115) are:

$$\Delta p_{km} = \frac{(2V_k + e_{km} - V_m)}{r_{km}} \Delta V_k - \frac{V_k}{r_{km}} \Delta V_m + \frac{V_k}{r_{km}} \Delta e_{km} \quad (6.119)$$

$$-r_{km} \frac{\Delta p_{km}}{V_k} + \left(1 + \frac{r_{km} p_{km}}{V_k^2} \right) \Delta V_k - \Delta V_m = -\Delta e_{km} \quad (6.120)$$

Incremental power Δp_{mk} from node m to k , and its partial derivatives are:

$$\Delta p_{mk} = \frac{\partial p_{mk}}{\partial V_m} \Delta V_m + \frac{\partial p_{mk}}{\partial V_k} \Delta V_k + \frac{\partial p_{mk}}{\partial e_{km}} \Delta e_{km} \quad (6.121)$$

$$\frac{\partial p_{mk}}{\partial V_m} = \frac{(-V_k - e_{km} + 2V_m)}{r_{mk}} \quad (6.122)$$

$$\frac{\partial p_{mk}}{\partial V_k} = -\frac{V_m}{r_{mk}} \quad (6.123)$$

$$\frac{\partial p_{mk}}{\partial e_{km}} = -\frac{V_m}{r_{mk}} \quad (6.124)$$

Substitution of partial derivatives in (6.121):

$$\Delta p_{mk} = \frac{(-V_k - e_{km} + V_m)}{r_{mk}} \Delta V_m + \frac{V_m}{r_{mk}} \Delta V_m - \frac{V_m}{r_{mk}} \Delta V_k - \frac{V_m}{r_{mk}} \Delta e_{km} \quad (6.125)$$

$$-r_{mk} \frac{\Delta p_{mk}}{V_m} + \left(1 + \frac{r_{mk} p_{mk}}{V_m^2} \right) \Delta V_m - \Delta V_k = +\Delta e_{km} \quad (6.126)$$

Example 6.6

To illustrate the general nature of the load flow problem for a DC circuit let us consider three nodes with three elements. $V_1 = 20$ V and assume no control elements, as shown in Figure 6.19.

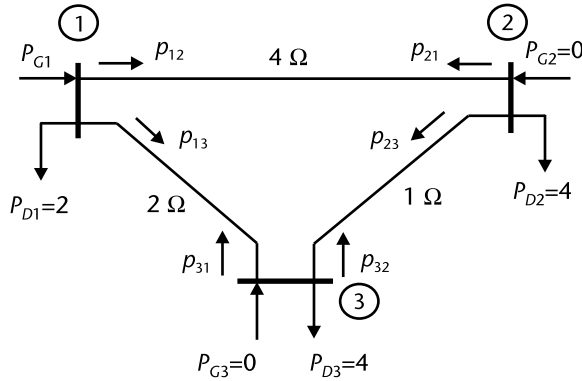


Figure 6.19 Small DC current network.

The incremental model Δp_{km} in (6.120) and Δp_{mk} (6.126) is applied to the three transmission elements. We have six power flow equations and incorporate the three power nodal balances. The system of equations is 9×9 , as in (6.127).

$$\begin{bmatrix}
 -1 & 0 & 0 & 0 & 0 & 0 & \frac{\partial p_{12}}{\partial V_1} & \frac{\partial p_{12}}{\partial V_2} & 0 \\
 0 & -1 & 0 & 0 & 0 & 0 & \frac{\partial p_{13}}{\partial V_1} & 0 & \frac{\partial p_{13}}{\partial V_3} \\
 0 & 0 & -1 & 0 & 0 & 0 & 0 & \frac{\partial p_{23}}{\partial V_2} & \frac{\partial p_{23}}{\partial V_3} \\
 0 & 0 & 0 & -1 & 0 & 0 & \frac{\partial p_{21}}{\partial V_1} & \frac{\partial p_{21}}{\partial V_2} & 0 \\
 0 & 0 & 0 & 0 & -1 & 0 & \frac{\partial p_{31}}{\partial V_1} & 0 & \frac{\partial p_{31}}{\partial V_3} \\
 0 & 0 & 0 & 0 & 0 & -1 & 0 & \frac{\partial p_{32}}{\partial V_2} & \frac{\partial p_{32}}{\partial V_3} \\
 +1 & +1 & 0 & 0 & 0 & 0 & 0 & 0 & 0 \\
 0 & 0 & +1 & +1 & 0 & 0 & 0 & 0 & 0 \\
 0 & 0 & 0 & 0 & +1 & +1 & 0 & 0 & 0
 \end{bmatrix}
 \begin{bmatrix}
 \Delta p_{12} \\
 \Delta p_{13} \\
 \Delta p_{23} \\
 \Delta p_{21} \\
 \Delta p_{31} \\
 \Delta p_{32} \\
 \Delta V_1 \\
 \Delta V_2 \\
 \Delta V_3
 \end{bmatrix}
 = -
 \begin{bmatrix}
 \frac{\partial p_{12}}{\partial e_{12}} \Delta e_{12} \\
 \frac{\partial p_{13}}{\partial e_{13}} \Delta e_{13} \\
 \frac{\partial p_{23}}{\partial e_{23}} \Delta e_{23} \\
 \frac{\partial p_{21}}{\partial e_{12}} \Delta e_{12} \\
 \frac{\partial p_{31}}{\partial e_{13}} \Delta e_{13} \\
 \frac{\partial p_{32}}{\partial e_{23}} \Delta e_{23} \\
 -\Delta P_1 \\
 -\Delta P_2 \\
 -\Delta P_3
 \end{bmatrix}
 \quad (6.127)$$

The partial derivatives are calculated by (6.116)–(6.118) and (6.122)–(6.124). The voltage for nodes with a source will be fixed, and its incremental voltage will be zero; we work this condition numerically in the process (the solution is shown in Figure 6.20).

```

Total nodes = 3      Elements = 3
Element  Node from  Node to  rkm
  1      1         2        4.0000
  2      1         3        2.0000
  3      2         3        1.0000
  4      2         1        4.0000
  5      3         1        2.0000
  6      3         2        1.0000

```

Node Information

Node	type	Vmag(pu)	PG	PL
1	+0	20.0000	0.0000	2.0000
2	-1	20.0000	0.0000	4.0000
3	-1	20.0000	0.0000	4.0000

```

Iteration = 0      Maxdev = 4.00000e+000
Iteration = 1      Maxdev = 1.02857e-001
Iteration = 2      Maxdev = 7.96669e-005
Iteration = 3      Maxdev = 5.11591e-011
Convergence in 3 iterations

```

Node Report

Node	type	Vmag	PG	PL
1	+0	20.0000	10.2298	2.0000
2	-1	19.4120	0.0000	4.0000
3	-1	19.4710	0.0000	4.0000

Load flow results

```

Element  Node from  Node to  pkm
  1      1         2        2.9401
  2      1         3        5.2897
  3      2         3       -1.1463
  4      2         1       -2.8537
  5      3         1       -5.1498
  6      3         2        1.1498

```

Power Generation = 10.2298 Power Load = 10.0000 Power Losses = 0.2298

Sensitivity Matrix =

-1.0000	-0.0000	-0.4535	-0.4535	-0.3035	-0.3035	-0.0000	-0.4535	-0.3035
-0.0000	-1.0000	-0.6089	-0.6089	-0.7524	-0.7524	-0.0000	-0.6089	-0.7524
0.0000	0.0000	-0.4268	0.5732	-0.2857	-0.2857	0.0000	0.5732	-0.2857
-0.0000	-0.0000	0.4268	-0.5732	0.2857	0.2857	-0.0000	0.4268	0.2857
0.0000	0.0000	0.5767	0.5767	-0.2874	0.7126	0.0000	0.5767	0.7126
-0.0000	-0.0000	-0.5767	-0.5767	0.2874	-0.7126	-0.0000	-0.5767	0.2874
0.0000	0.0000	0.0000	0.0000	0.0000	0.0000	0.0000	0.0000	0.0000
0.0000	0.0000	0.0907	0.0907	0.0607	0.0607	0.0000	0.0907	0.0607
0.0000	0.0000	0.0609	0.0609	0.0752	0.0752	0.0000	0.0609	0.0752

For this network, we calculated the sensitivity matrix, whose elements relate column-wise the effect of controls that might be acting in a given element, which might be

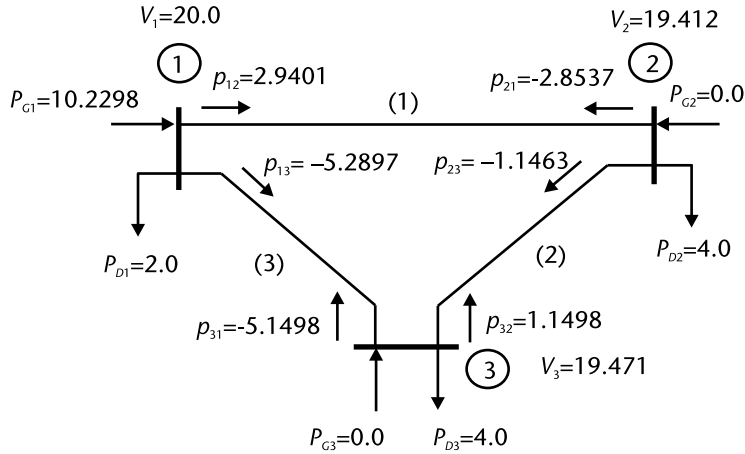


Figure 6.20 Small DC load flow solution.

a series voltage source or changes to the nodal injections by a source or from load requirements. Control actions will modify the system's power flows and nodal voltages at the load nodes. Control action effects on system's elements are of paramount importance to quantify and evaluate both control actions and the controllability of the power flows and nodal voltages in a power system. We can use this concept to analyze the most appropriate control location and to have the most effective action for a given network. The sensitivity information can be used to coordinate a *minimum effort* of existing controls and to solve the congestion problems.

6.8 Incremental Power Flow and Control Actions

The incremental AC load flow formulation has information about incremental real and reactive power flows on each element in the system, as well as incremental voltages and nodal angles. In this sense, we can extend the analysis into the line power flows control; with an explicit model, we can calculate control actions in a given network. We can analyze control devices as taps, phase shifters, and power

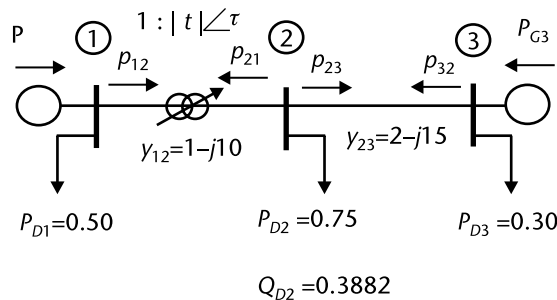


Figure 6.21 Three-node system to illustrate incremental power flow concepts.

$$\beta = \begin{bmatrix} 0 & 0 & 0 & 0 & \frac{\partial q_{12}}{\partial \theta_1} & \frac{\partial q_{12}}{\partial \theta_2} & 0 & -1 & 0 & 0 & 0 & \frac{\partial q_{12}}{\partial |V_1|} |V_1| & \frac{\partial q_{12}}{\partial |V_2|} |V_2| & 0 \\ 0 & 0 & 0 & 0 & \frac{\partial q_{21}}{\partial \theta_1} & \frac{\partial q_{21}}{\partial \theta_2} & 0 & 0 & -1 & 0 & 0 & \frac{\partial q_{21}}{\partial |V_1|} |V_1| & \frac{\partial q_{21}}{\partial |V_2|} |V_2| & 0 \\ 0 & 0 & 0 & 0 & 0 & \frac{\partial q_{23}}{\partial \theta_2} & \frac{\partial q_{23}}{\partial \theta_3} & 0 & 0 & -1 & 0 & 0 & \frac{\partial q_{23}}{\partial |V_2|} |V_2| & \frac{\partial q_{23}}{\partial |V_3|} |V_3| \\ 0 & 0 & 0 & 0 & 0 & \frac{\partial q_{32}}{\partial \theta_2} & \frac{\partial q_{32}}{\partial \theta_3} & 0 & 0 & 0 & -1 & 0 & \frac{\partial q_{32}}{\partial |V_2|} |V_2| & \frac{\partial q_{32}}{\partial |V_3|} |V_3| \\ 0 & 0 & 0 & 0 & 0 & 0 & 0 & +1 & 0 & 0 & 0 & 0 & 0 & 0 \\ 0 & 0 & 0 & 0 & 0 & 0 & 0 & 0 & +1 & +1 & 0 & 0 & 0 & 0 \\ 0 & 0 & 0 & 0 & 0 & 0 & 0 & 0 & 0 & 0 & +1 & 0 & 0 & 0 \end{bmatrix} \quad (6.129)$$

A reference angle must be selected and the generating nodes that must keep a constant voltage should be identified. The inverse of the complete Jacobian matrix will have numerical information about sensitivity factors; these values translate into valuable information when solving control-related problems in electric power networks and are very helpful when solving congestion problems. The problem will be presented in Chapter 8 from an optimal point of view when control coordination can be solved.

6.9 Unbalanced Three-Phase Power Flow

Most studies are conducted assuming a three-phase balanced system; therefore, only the positive sequence impedances are required to conduct load flow studies, fault analysis (except at the fault point which might be an unbalanced connection), and other studies (such as transient stability). In the more general case unbalanced conditions might be at the load, the transmission lines that were not transposed, and other situations such as an *open conductor*. To solve for the unbalanced load flow in the three-phase power system, we need an abc matrix formulation. One way to set up the problem is through the three-phase nodal admittance matrix $Y_{\text{bus},abc}$ in the abc frame of reference.

$$Y_{\text{bus}}^{abc} V_{\text{bus}}^{abc} = I_{\text{bus}}^{abc} \quad (6.130)$$

Nodal voltages, complex power, and currents will be in the *abc* frame of reference; Norton's equivalent for power sources might be used. In order to establish the iterative process, let us use a small three-phase power system (see Figure 6.22): one three-phase power source, a transformer bank in a ΔY connection, and a transmission

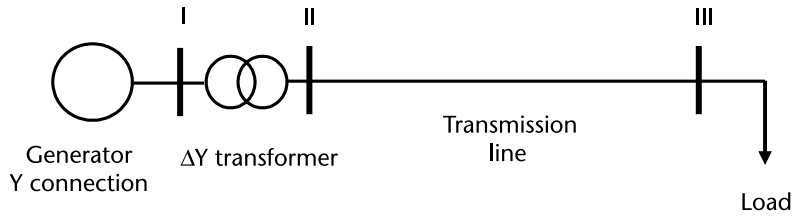


Figure 6.22 Three-node system to illustrate incremental power flow concepts.

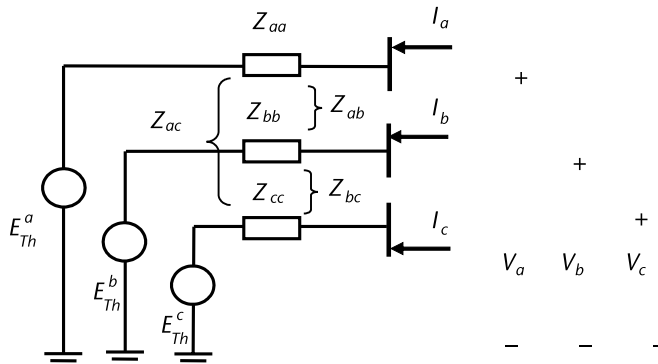


Figure 6.23 Thévenin's equivalent for the synchronous generator.

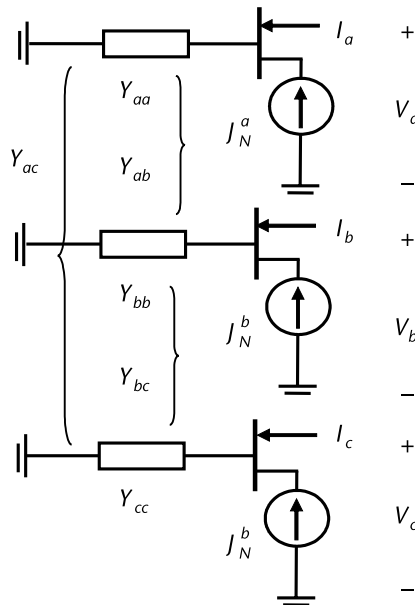


Figure 6.24 Norton's equivalent for synchronous generator.

line. Values of impedances and voltages are in pu and the numerical process starts assuming an *abc flat start*, balanced phase-shift from phase *a*, *b*, and *c*.

To build the $Y_{bus,abc}$ matrix, we assume that the generator is represented by its Thévenin's equivalent (see Figure 6.23). We can then calculate Norton's equivalent for each synchronous generator (see Figure 6.24).

Thévenin's and Norton's model for the generator is written as:

$$V_{bus,g}^{abc} = Z_{bus,g}^{abc} I_{bus}^{abc} + E_{Th}^{abc} \tag{6.131}$$

$$Y_{bus,g}^{abc} V_{bus,g}^{abc} = I_{bus}^{abc} + J_{bus,g}^{abc} \tag{6.132}$$

With the three-phase admittance for the generator for the ΔY transformer and for the transmission line, we build the three-phase admittance matrix for the electric network. Nodes *I*, *II*, and *III* in Figure 6.22 are three-phase *abc* nodes.

$$\begin{bmatrix} Y_{bus,g}^{abc} + Y_{bus,tr}^{abc,\Delta} & -Y_{bus,tr}^{abc,\Delta Y} & 0 \\ -Y_{bus,tr}^{abc,Y\Delta} & Y_{bus,tr}^{abc,Y} + Y_{bus,TL}^{abc} & -Y_{bus,TL}^{abc} \\ 0 & -Y_{bus,TL}^{abc} & Y_{bus,TL}^{abc} \end{bmatrix} \begin{bmatrix} V_{bus,I}^{abc} \\ V_{bus,II}^{abc} \\ V_{bus,III}^{abc} \end{bmatrix} = \begin{bmatrix} I_{bus,I}^{abc} + J_{bus,g}^{abc} \\ I_{bus,II}^{abc} \\ I_{bus,III}^{abc} \end{bmatrix} \tag{6.133}$$

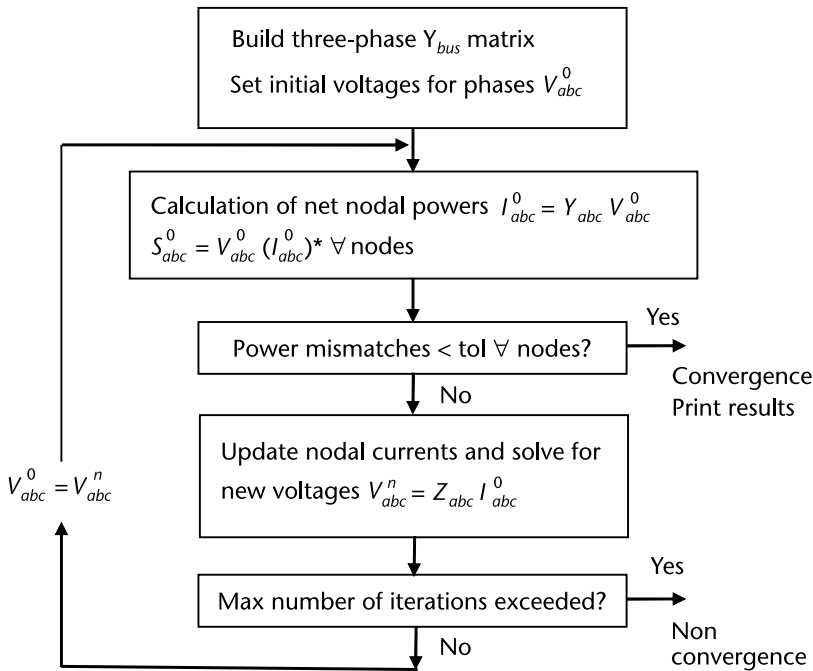


Figure 6.25 Iterative process for three-phase load flows, using Z_{bus} matrix.

Example 6.7

To illustrate the general nature of the three-phase load flow (especially for unbalanced conditions presented by the system's elements or from the load), let us apply the Z_{bus} iterative method to solve the small network in Figure 6.22. We follow the steps in Figure 6.25. All values are in pu.

Unbalanced load power flows, using $Z_{bus,abc}$ matrix

Thevenin impedance matrix for generator, phases abc

0.0000+j 0.1800 0.0000+j -0.0200 0.0000+j -0.0200

0.0000+j -0.0200 0.0000+j 0.1800 0.0000+j -0.0200

0.0000+j -0.0200 0.0000+j -0.0200 0.0000+j 0.1800

Norton equivalent for generator, phases abc

Nodal Admittance matrix

Current source

0.0000+j -5.7143 0.0000+j -0.7143 0.0000+j -0.7143 -0.0000+j -5.0000

0.0000+j -0.7143 0.0000+j -5.7143 0.0000+j -0.7143 -4.3301+j 2.5000

0.0000+j -0.7143 0.0000+j -0.7143 0.0000+j -5.7143 4.3301+j 2.5000

Admittance matrix for transformer bank D-Y

Columns 1 through 3

0.0000+j-13.3333 0.0000+j 6.6667 0.0000+j 6.6667

0.0000+j 6.6667 0.0000+j-13.3333 0.0000+j 6.6667

0.0000+j 6.6667 0.0000+j 6.6667 0.0000+j-13.3333

0.0000+j 11.5470 0.0000+j-11.5470 0.0000+j 0.0000

0.0000+j 0.0000 0.0000+j 11.5470 0.0000+j-11.5470

0.0000+j-11.5470 0.0000+j 0.0000 0.0000+j 11.5470

Columns 4 through 6

0.0000+j 11.5470 0.0000+j 0.0000 0.0000+j-11.5470

0.0000+j-11.5470 0.0000+j 11.5470 0.0000+j 0.0000

0.0000+j 0.0000 0.0000+j-11.5470 0.0000+j 11.5470

0.0000+j-20.0000 0.0000+j 0.0000 0.0000+j 0.0000

0.0000+j 0.0000 0.0000+j-20.0000 0.0000+j 0.0000

0.0000+j 0.0000 0.0000+j 0.0000 0.0000+j-20.0000

Transmission line, series impedance model

0.0000+j 0.1667 0.0000+j 0.0667 0.0000+j 0.0667

0.0000+j 0.0667 0.0000+j 0.1667 0.0000+j 0.0667

0.0000+j 0.0667 0.0000+j 0.0667 0.0000+j 0.1667

$Z_{busabc} =$

Columns 1 through 6

0 + 0.1800i 0 - 0.0200i 0 - 0.0200i 0 + 0.1155i 0 - 0.0000i 0 - 0.1155i

0 - 0.0200i 0 + 0.1800i 0 - 0.0200i 0 - 0.1155i 0 + 0.1155i 0 + 0.0000i

0 - 0.0200i 0 - 0.0200i 0 + 0.1800i 0 - 0.0000i 0 - 0.1155i 0 + 0.1155i

0 + 0.1155i 0 - 0.1155i 0 + 0.0000i 0 + 0.1833i 0 - 0.0667i 0 - 0.0667i

0 + 0.0000i 0 + 0.1155i 0 - 0.1155i 0 - 0.0667i 0 + 0.1833i 0 - 0.0667i

0 - 0.1155i 0 + 0.0000i 0 + 0.1155i 0 - 0.0667i 0 - 0.0667i 0 + 0.1833i

0 + 0.1155i 0 - 0.1155i 0 + 0.0000i 0 + 0.1833i 0 - 0.0667i 0 - 0.0667i

0 + 0.0000i 0 + 0.1155i 0 - 0.1155i 0 - 0.0667i 0 + 0.1833i 0 - 0.0667i

0 - 0.1155i 0 + 0.0000i 0 + 0.1155i 0 - 0.0667i 0 - 0.0667i 0 + 0.1833i
 Columns 7 through 9

0 + 0.1155i 0 - 0.0000i 0 - 0.1155i
 0 - 0.1155i 0 + 0.1155i 0 + 0.0000i
 0 - 0.0000i 0 - 0.1155i 0 + 0.1155i
 0 + 0.1833i 0 - 0.0667i 0 - 0.0667i
 0 - 0.0667i 0 + 0.1833i 0 - 0.0667i
 0 - 0.0667i 0 - 0.0667i 0 + 0.1833i
 0 + 0.3500i 0 + 0.0000i 0 + 0.0000i
 0 + 0.0000i 0 + 0.3500i 0 + 0.0000i
 0 + 0.0000i 0 + 0.0000i 0 + 0.3500i

Nodal initial conditions

Node	Voltage		Load	
1	1.0000+j	0.0000	0.0000+j	0.0000
2	-0.5000+j	-0.8660	0.0000+j	0.0000
3	-0.5000+j	0.8660	0.0000+j	0.0000
4	1.0000+j	0.0000	0.0000+j	0.0000
5	-0.5000+j	-0.8660	0.0000+j	0.0000
6	-0.5000+j	0.8660	0.0000+j	0.0000
7	1.0000+j	0.0000	0.3000+j	0.1000
8	-0.5000+j	-0.8660	0.2000+j	0.0800
9	-0.5000+j	0.8660	0.4000+j	0.0000

Iteration	Max V update
1	7.987551e-002
2	5.394074e-002
3	2.976889e-003
4	1.154804e-003
5	6.144031e-005
6	2.359442e-005
7	1.254336e-006
8	4.816108e-007
9	2.560290e-008

Node	Voltage		Magnitude	angle
1	0.974690+j	-0.074679	0.977547	-4.38
2	-0.526594+j	-0.816807	0.971842	-122.81
3	-0.448096+j	0.891486	0.997766	116.69
4	0.868283+j	0.412023	0.961082	25.39
5	-0.055321+j	-0.981417	0.982975	-93.23
6	-0.808971+j	0.573707	0.991753	144.66
7	0.876640+j	0.384886	0.957411	23.70
8	-0.069998+j	-0.965933	0.968466	-94.14
9	-0.778698+j	0.611244	0.989944	141.87

Generator	Voltage E		Voltage R		Current	
	1.000000	-0.00	0.977547	-4.38	-0.3734+j	0.1266
	1.000000	-120.00	0.971842	-122.81	0.2461+j	0.1330
	1.000000	120.00	0.997766	116.69	0.1273+j	-0.2595
	Power E		Power R			

	0.3734+j	0.1266	-0.3734+j	-0.0955		
	0.2382+j	0.1466	-0.2382+j	-0.1310		
	0.2884+j	0.0195	-0.2884+j	-0.0028		
Transformer	Voltage S		Voltage R		Current	
	0.977547	-4.38	0.961082	25.39	0.3734+j	-0.1266
	0.971842	-122.81	0.982975	-93.23	-0.2461+j	-0.1330
	0.997766	116.69	0.991753	144.66	-0.1273+j	0.2595
	Power E		Power R			
	0.3734+j	0.0955	-0.2981+j	-0.1092		
	0.2382+j	0.1310	-0.2017+j	-0.0844		
	0.2884+j	0.0028	-0.4003+j	-0.0195		
T Line	Voltage S		Voltage R		Current	
	0.961082	25.39	0.957411	23.70	0.3289+j	0.0303
	0.982975	-93.23	0.968466	-94.14	-0.0973+j	-0.2000
	0.991753	144.66	0.989944	141.87	-0.3178+j	0.2495
	Power E		Power R			
	0.2981+j	0.1092	-0.3000+j	-0.1000		
	0.2017+j	0.0844	-0.2000+j	-0.0800		
	0.4003+j	0.0195	-0.4000+j	-0.0000		

The Z_{bus} iterative process takes several iterations to converge to a voltage solution; in this case, nine iterations were needed. The rate of convergence is linear as compared to the quadratic rate of Newton's method used in the balanced power flows. One drawback for the Z_{bus} method is that the impedance matrix is full, and in order to solve large power problems, an *implicit method* should be applied; this requires the use of factors on $Y_{bus,abc}$ to synthetically find the inverse $Z_{bus,abc}$. Sparsity techniques must be used when solving large sets of equations, as is the case of real-world power networks and all of their related problems: fault analysis, load power flows, contingency analysis, state estimation, and transient stability.

References

- [1] Stagg, G. W., and A. H. El-Abiad, *Computer Methods in Power System Analysis*, New York: McGraw-Hill Book Company, 1968.
- [2] Elgerd, O. I., *Electric Energy Systems Theory: An Introduction, Second Edition*, New York: McGraw-Hill Book Company, 1982.
- [3] Gross, C. A., *Power Systems Analysis*, New York: John Wiley & Sons, 1979.
- [4] Grainger, J. D., and W. D. Stevenson, *Power System Analysis*, New York: McGraw-Hill Science/Engineering, 1994.
- [5] Arrillaga, J., *Computer Modelling of Electrical Power Systems*, New York: Wiley, 2001.
- [6] Glover, J. D., S. Sarma, and T. J. Overbye, *Power System Analysis and Design*, Boston: Cengage Learning, 2011.
- [7] Tinney, W. F., and C. E. Hart, "Power Flow Solution by Newton's Method," *IEEE Trans.*, Vol. PAS-86, No. 11, November 1967.

-
- [8] Stott, B., and O. Alsac, "Fast Decoupled Load Flow," *IEEE Trans.*, Vol. PAS-93, pp. 859–869, 1974.
 - [9] Sun, D. I., B. Ashley, B. Brewer, A. Hughes, and W. F. Tinney, "Optimal Power Flow by Newton Approach," *IEEE Trans.*, Vol. PER-4, Issue 10, 1984.

Optimal Operation of Power Systems

When an electric power system is working in a steady state condition, with all its vital indicators: nominal frequency and nodal voltages within a pre-established range, that is, voltages close to 1.0 pu, then a coordinated synchronous operation with an economic goal in mind can be pursued. To attain this general objective, it is important to include the limited transporting nature of transmission links, scarce resources as fuels to the thermal plants, available water in the hydro reservoirs, and other important energy resources (e.g., nuclear, wind, and geothermal). We can establish an appropriate nonlinear frame of reference considering the nonlinear nature of the electric power problem and the constraints listed. Solving an optimal constrained problem in an efficient and useful way for operation, control, and planning stages for system expansion has been the goal of power engineers for more than 50 years. There were many advances during this period, and no doubt the nonlinear formulation is the most interesting as it highlights the nature of the power problem.

7.1 Introduction

In this chapter, we present a systematic development, starting with simplified assumptions for a lossless network, which gives us the opportunity to focus on the main concepts and its physical interpretations. The advantage with this approach is that we do not need complicated relations. Once the first step is covered, the task is to include all relevant variations in power system operation as transmission losses, equality, and inequality constraints. It is important to keep the nonlinear nature of the problem, as this allows for a much better characterization of a realistic electrical power system. We focus the cost or objective function on minimization where the gradient of the cost function equated to zero will give the necessary condition for the optimum. The set of equations that form the gradient is usually nonlinear. Therefore, there is the need for an iterative process like Newton's method. In practice, the large number of variables and the dimension of the problem restrains the proof of the sufficient condition to attain the local optimum. Because it represents a huge numerical burden, this condition is not tested in practice.

7.2 Nonlinear Optimization

To find the best operating point for a set of given condition in a power system, we have to select a *cost criterion*. Minimum operating cost is a sound goal for

the optimum of an electric power system; minimum losses or the least amount of emissions are also valid cost functions. The starting point is to establish a *cost function* and a proper set of constraints that must be satisfied in order to have a feasible solution.

$$\begin{aligned} \min C(x, u) \\ \text{subject to } f(x, u) = 0 \end{aligned} \quad (7.1)$$

C	cost function
x	state variables
u	control variables
$f(x, u)$	set of equality constraints

A solution to (7.1), assuming continuous functions, starts with differential expressions for the cost function $C(x, u)$ and for the equality constraint $f(x, u)$.

$$dC(x, u) = \left[\frac{\partial C}{\partial x} \right]^t dx + \left[\frac{\partial C}{\partial u} \right]^t du \quad df(x, u) = \left[\frac{\partial f}{\partial x} \right] dx + \left[\frac{\partial f}{\partial u} \right] du = 0 \quad (7.2)$$

From (7.2) we write the differential dx and make a substitution, given that we have the same number of equality constraints as state variables x .

$$dx = - \left[\frac{\partial f}{\partial x} \right]^{-1} \left[\frac{\partial f}{\partial u} \right] du \quad (7.3)$$

$$dC(x, u) = \left[\frac{\partial C}{\partial x} \right]^t \left(- \left[\frac{\partial f}{\partial x} \right]^{-1} \left[\frac{\partial f}{\partial u} \right] du \right) + \left[\frac{\partial C}{\partial u} \right]^t du \quad (7.4)$$

We note that (7.4) is a gradient with respect to u . It is a *reduced gradient*.

$$\nabla_u C(x, u) = \frac{dC(x, u)}{du} = - \left[\frac{\partial C}{\partial x} \right]^t \left[\frac{\partial f}{\partial x} \right]^{-1} \left[\frac{\partial f}{\partial u} \right] + \left[\frac{\partial C}{\partial u} \right]^t = 0 \quad (7.5)$$

We define the Lagrange multipliers that later can be identified as *short-term marginal costs* by:

$$\lambda^t = - \left[\frac{\partial C}{\partial x} \right]^t \left[\frac{\partial f}{\partial x} \right]^{-1} \quad \text{or} \quad \lambda^t \left[\frac{\partial f}{\partial x} \right] = - \left[\frac{\partial C}{\partial x} \right]^t \quad (7.6)$$

From (7.6):

$$\lambda^t \left[\frac{\partial f}{\partial u} \right] + \left[\frac{\partial C}{\partial u} \right]^t = 0 \quad (7.7)$$

The last equation (7.7) and the equality constraint $f(x, u) = 0$ are components for the gradient of a cost function $\xi(x, u, \lambda)$ or augmented Lagrangian.

$$\xi(x, u, \lambda) = C(x, u) + \lambda^t f(x, u) \quad (7.8)$$

$$\nabla \xi(x, u, \lambda) = \begin{bmatrix} \frac{\partial \xi(x, u, \lambda)}{\partial x} \\ \frac{\partial \xi(x, u, \lambda)}{\partial u} \\ \frac{\partial \xi(x, u, \lambda)}{\partial \lambda} \end{bmatrix} = \begin{bmatrix} \left[\frac{\partial C}{\partial x} \right] + \left[\frac{\partial f}{\partial x} \right]^t \lambda \\ \left[\frac{\partial C}{\partial u} \right] + \left[\frac{\partial f}{\partial u} \right]^t \lambda \\ f(x, u) \end{bmatrix} = \begin{bmatrix} 0 \\ 0 \\ 0 \end{bmatrix} \quad (7.9)$$

We transformed the original problem into a problem with no constraints; λ variables are to be determined when we solve the gradient equal zero. The resulting system of equations, gradient equal zero, might be nonlinear so an iterative process might be required.

Example 7.1

Surface plot for a two variable cost $C(x, u) = x^2 + 3u^2$ (see Figure 7.1), equality constraint $f(x, u) = 4 - x - u = 0$.

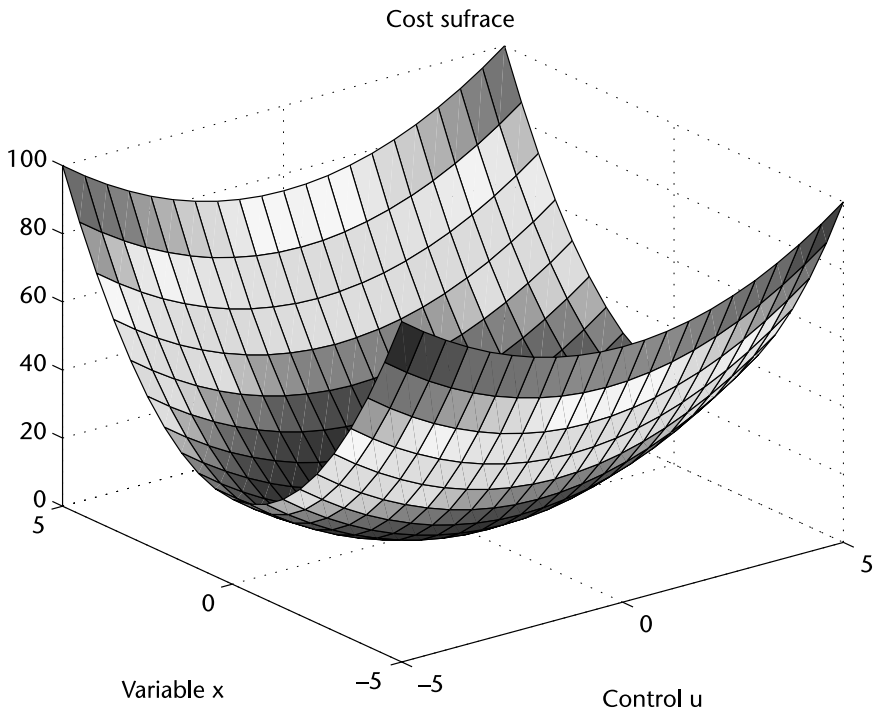


Figure 7.1 Cost function surface, $C(x, u) = x^2 + 3u^2$.

```

% Code to plot a surface
clear
x=-5:0.5:5;
y=x;
[X,Y]=meshgrid(x,y);
C=X.*X+3*Y.*Y;
surf(X,Y,C)
C1=4-X-Y;
surf(X,Y,C1)

```

Example 7.2

- a) Write the augmented Lagrangian function for Example 7.1. The cost function is $C(x, u) = x^2 + 3u^2$ and the equality constraint is $f(x, u) = 4 - x - u = 0$ (see Figure 7.2), then: $\xi(x, u, \lambda) = x^2 + 3u^2 + \lambda^t(4 - x - u)$.
- b) Find the gradient for the Lagrangian in a) and write the solution for x , u , and λ .

$$\nabla \xi(x, u, \lambda) = \begin{bmatrix} \frac{\partial \xi(x, u, \lambda)}{\partial x} \\ \frac{\partial \xi(x, u, \lambda)}{\partial u} \\ \frac{\partial \xi(x, u, \lambda)}{\partial \lambda} \end{bmatrix} = \begin{bmatrix} 2x - \lambda \\ 6u - \lambda \\ 4 - x - u \end{bmatrix} = \begin{bmatrix} 0 \\ 0 \\ 0 \end{bmatrix} \text{ Gradient} \quad (7.10)$$

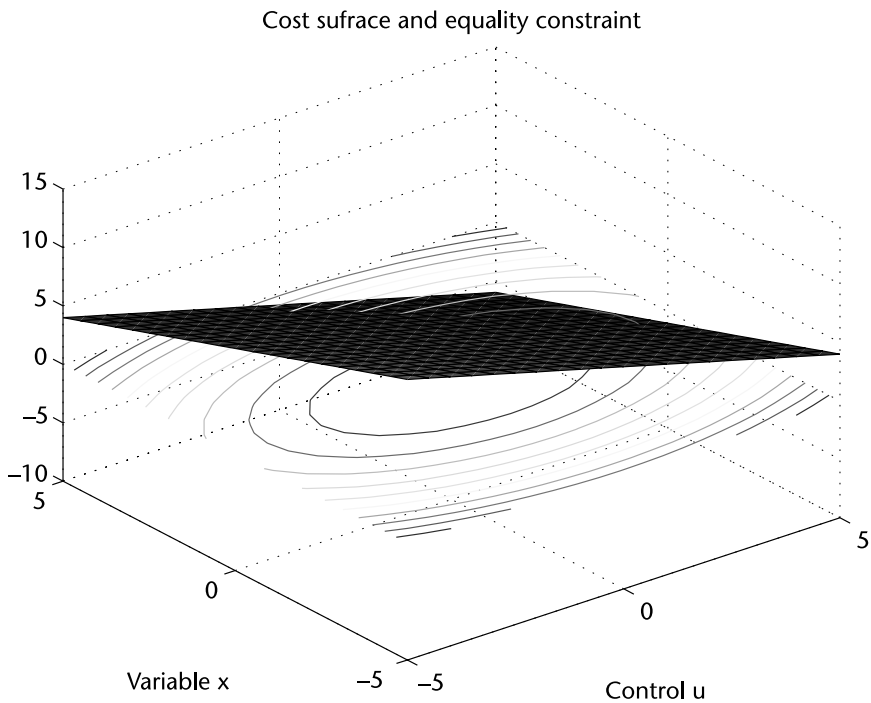


Figure 7.2 Cost function surface and equality constraint, $C_1 = 4 - x - u$.

In this case, the gradient is a linear set of equations, the solution for x , u , and λ are found when the linear system of equations is solved.

$$\begin{bmatrix} 2 & 0 & -1 \\ 0 & 6 & -1 \\ -1 & -1 & 0 \end{bmatrix} \begin{bmatrix} x \\ u \\ \lambda \end{bmatrix} = \begin{bmatrix} 0 \\ 0 \\ -4 \end{bmatrix} \quad \begin{bmatrix} x \\ u \\ \lambda \end{bmatrix} = \begin{bmatrix} 3 \\ 1 \\ 6 \end{bmatrix} \quad (7.11)$$

The cost function has a value of $C(3, 1) = (3)^2 + 3(1)^2 = 12$.

7.3 Optimal Dispatch with No Losses

The material presented so far gives us the opportunity to discuss basic concepts and a useful interpretation from the basic solution. Assume that n thermal units need to be coordinated to supply a total amount of load P_D MW. The assumption is that all the n units are connected, no limits are enforced, and the cost for the generators are nonlinear functions with first and second derivatives with no discontinuities. Let us write the cost function (7.12) and equality constraint (7.13).

$$C_{\text{Total}} = \sum_{k=1}^n C_k(P_{Gk}) \quad \$/\text{h} \quad (7.12)$$

$$P_D - \sum_{k=1}^n P_{Gk} = 0 \quad \text{MW} \quad (7.13)$$

The augmented Lagrangian is a function that includes the cost functions and the equality constraint.

$$\xi(P, \lambda) = \sum_{k=1}^n C_k(P_{Gk}) + \lambda \left[P_D - \sum_{k=1}^n P_{Gk} \right] \quad (7.14)$$

At the optimum the gradient of (7.14) should equal to zero.

$$\nabla \xi(P, \lambda) = \begin{bmatrix} \frac{\partial \xi(P, \lambda)}{\partial P_{G1}} \\ \frac{\partial \xi(P, \lambda)}{\partial P_{G2}} \\ \dots \\ \frac{\partial \xi(P, \lambda)}{\partial \lambda} \end{bmatrix} = \begin{bmatrix} \frac{\partial C_1(P_{G1})}{\partial P_{G1}} - \lambda \\ \frac{\partial C_2(P_{G2})}{\partial P_{G2}} - \lambda \\ \dots \\ P_D - \sum_{k=1}^n P_{Gk} \end{bmatrix} = \begin{bmatrix} 0 \\ 0 \\ \dots \\ 0 \end{bmatrix} \quad (7.15)$$

From (7.15) we readily see that the first component of the gradient gives an *equal incremental cost solution*. From these components, we find system's lambda units

as \$/MWh. A common interpretation is that the *marginal cost* is the cost of the next MWh for the system's demand.

$$\lambda = \frac{\partial C_1(P_{G1})}{\partial P_{G1}} = \frac{\partial C_2(P_{G2})}{\partial P_{G2}} = \dots = \frac{\partial C_n(P_{Gn})}{\partial P_{Gn}} \quad (7.16)$$

Example 7.3

For a no-loss system with two units that have quadratic cost function and the equality constraint representing the balance between load and generation that must be satisfied as in (7.13). Let us solve the economic dispatch and then solve for the real power flows using a DC approximation for the network (see Figure 7.3).

$$\begin{bmatrix} C_1(P_{G1}) \\ C_2(P_{G2}) \\ f(P_{G1}, P_{G2}) \end{bmatrix} = \begin{bmatrix} 4 + 2P_{G1} + \frac{1}{2}P_{G1}^2 \\ 5 + 3P_{G2} + \frac{1}{2}P_{G2}^2 \\ 4 - P_{G1} - P_{G2} \end{bmatrix} \quad (7.17)$$

The Lagrangian equation and its gradient are:

$$\xi(P_{G1}, P_{G2}, \lambda) = C_1(P_{G1}) + C_2(P_{G2}) + \lambda[P_D - P_{G1} - P_{G2}] \quad (7.18)$$

$$\nabla \xi(P_{G1}, P_{G2}, \lambda) = \begin{bmatrix} \frac{\partial \xi(P_{G1}, P_{G2}, \lambda)}{\partial P_{G1}} \\ \frac{\partial \xi(P_{G1}, P_{G2}, \lambda)}{\partial P_{G2}} \\ \frac{\partial \xi(P_{G1}, P_{G2}, \lambda)}{\partial \lambda} \end{bmatrix} = \begin{bmatrix} \frac{\partial C_1(P_{G1})}{\partial P_{G1}} - \lambda \\ \frac{\partial C_2(P_{G2})}{\partial P_{G2}} - \lambda \\ P_D - P_{G1} - P_{G2} \end{bmatrix} = \begin{bmatrix} 0 \\ 0 \\ 0 \end{bmatrix} \quad (7.19)$$

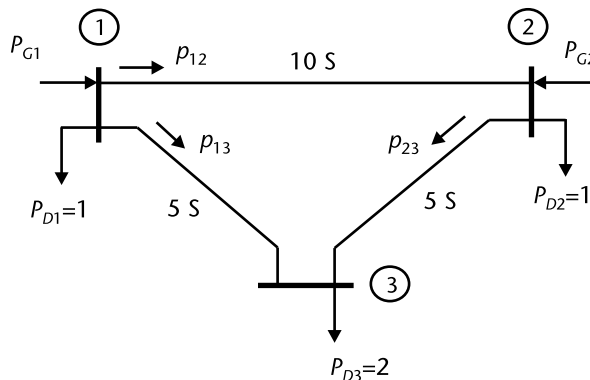


Figure 7.3 System with three nodes, no losses.

The gradient equal zero and the linear system of equations:

$$\begin{bmatrix} 2 + P_{G1} - \lambda \\ 3 + P_{G2} - \lambda \\ 4 - P_{G1} - P_{G2} \end{bmatrix} = \begin{bmatrix} 0 \\ 0 \\ 0 \end{bmatrix} \quad \begin{bmatrix} 1 & 0 & -1 \\ 0 & 1 & -1 \\ -1 & -1 & 0 \end{bmatrix} \begin{bmatrix} P_{G1} \\ P_{G2} \\ \lambda \end{bmatrix} = \begin{bmatrix} -2 \\ -3 \\ -4 \end{bmatrix} \quad (7.20)$$

Solution is $P_{G1} = 2.5$ MW, $P_{G2} = 1.5$ MW, system's $\lambda = 4.5$ \$/MWh, and the total cost is $C_{\text{Total}} = 4 + 2(2.5) + 1/2(2.5)^2 + 5 + 3(1.5) + 1/2(1.5)^2 = 22.75$ \$/h.

Once we find the economic dispatch that assigns the level of generation for each generator, a DC approximation to load flow solution follows. Through the nodal admittance matrix, we relate real power injection and nodal angles in radians. One nodal angle is reference—let's say θ_1 zero.

$$\begin{bmatrix} +15 & -10 & -5 \\ +10 & +15 & -5 \\ -5 & -5 & +10 \end{bmatrix} \begin{bmatrix} 0 \\ \theta_2 \\ \theta_3 \end{bmatrix} = \begin{bmatrix} P_{G1} - 1 \\ 1.5 - 1 \\ -2 \end{bmatrix} \begin{bmatrix} \theta_2 \\ \theta_3 \end{bmatrix} = \begin{bmatrix} \frac{-2}{50} \\ \frac{-11}{50} \end{bmatrix} \text{ rad} \quad (7.21)$$

The line flows are $p_{12} = (\theta_1 - \theta_2)/x_{12} = 4/10$, $p_{13} = (\theta_1 - \theta_3)/x_{13} = 11/10$ and $p_{23} = (\theta_2 - \theta_3)/x_{23} = 9/10$ (see Figure 7.4).

7.3.1 Inequality Constraints

This is a proper place to introduce the inequality constraints among various inequalities that must be satisfied. For example, the output of a generator might be limited. Equations (7.12) and (7.13) establish the problem, and then we add the inequality; for this problem, the total cost in \$/h, equality constraint in MW, and the inequality constraint in MW.

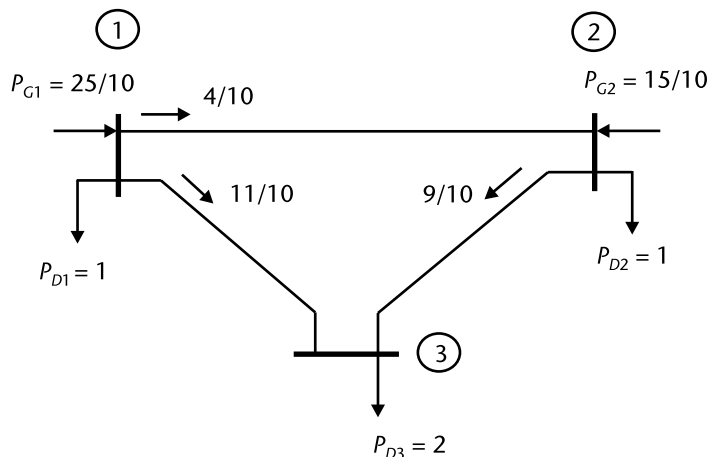


Figure 7.4 Load flow solution for three-node system, no-losses.

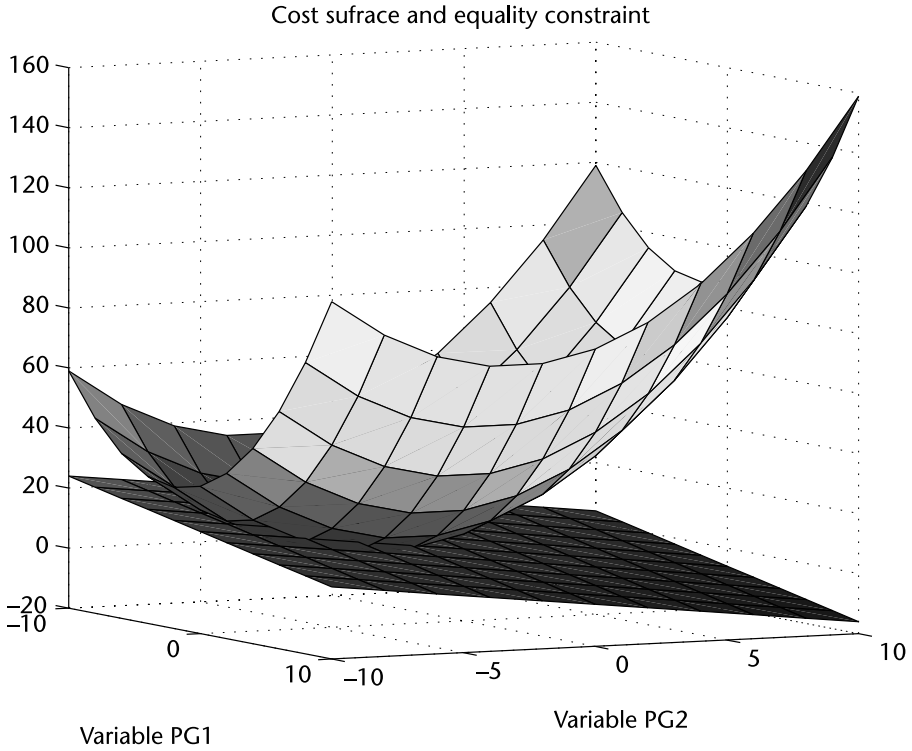


Figure 7.5 Cost surface and equality constraint.

$$\begin{bmatrix} C_{\text{Total}} \\ f(P) \\ h(P) \end{bmatrix} = \begin{bmatrix} \sum_{k=1}^n C_k(P_{Gk}) \\ P_D - \sum_{k=1}^n P_{Gk} = 0 \\ P_k^{\text{max}} - P_{Gk} \leq 0 \end{bmatrix} \quad (7.22)$$

We write the augmented Lagrangian, including a Kuhn-Tucker multiplier μ , to augment the inequality constraint.

$$\xi(P, \lambda, \mu) = \sum_{k=1}^n C_k(P_{Gk}) + \lambda \left[P_D - \sum_{k=1}^n P_{Gk} \right] + \mu (P_{Gk} - P_k^{\text{max}}) \quad (7.23)$$

The necessary condition for an optimal gradient that must be equal to zero, and has the solution at the *same incremental cost* for every generator working within limits, and a μ as an *adjusted incremental cost* for generator k at one of its limits.

$$\nabla \xi(P, \lambda, \mu) = \begin{bmatrix} \vdots \\ \frac{\partial \xi(P, \lambda, \mu)}{\partial P_{Gk}} \\ \vdots \\ \frac{\partial \xi(P, \lambda, \mu)}{\partial \lambda} \\ \frac{\partial \xi(P, \lambda, \mu)}{\partial \mu} \end{bmatrix} = \begin{bmatrix} \vdots \\ \frac{\partial C_k(P_{Gk})}{\partial P_{Gk}} - \lambda + \mu \\ \vdots \\ P_D - \sum_{k=1}^n P_{Gk} \\ P_{Gk} - P_k^{\max} \end{bmatrix} = \begin{bmatrix} 0 \\ 0 \\ \vdots \\ 0 \\ 0 \end{bmatrix} \quad (7.24)$$

$$\lambda = \frac{\partial C_1(P_{G1})}{\partial P_{G1}} = \frac{\partial C_2(P_{G2})}{\partial P_{G2}} = \dots = \frac{\partial C_k(P_{Gk})}{\partial P_{Gk}} + \mu \quad (7.25)$$

Example 7.4

Assume a lossless system with three generators that have lower and upper generating limits as shown in (7.26). Total load demand is $P_D = 1,100$ MW. Solve for the optimal dispatch problem, assuming that the incremental costs and limits are:

$$\begin{bmatrix} \frac{dC_1}{dP_{G1}} \\ \frac{dC_2}{dP_{G2}} \\ \frac{dC_3}{dP_{G3}} \\ 0 \end{bmatrix} = \begin{bmatrix} 7.92 + 0.003124 P_{G1} \\ 7.85 + 0.00388 P_{G2} \\ 7.97 + 0.00964 P_{G3} \\ 1,100 - P_{G1} - P_{G2} - P_{G3} \end{bmatrix} \quad \begin{matrix} 150 \leq P_{G1} \leq 600 \\ 100 \leq P_{G2} \leq 400 \\ 50 \leq P_{G3} \leq 300 \end{matrix} \quad (7.26)$$

- Solution assuming no limit violations:

Economic Dispatch, no losses

Number of dispatchable units = 3 Demand = 1100 MW

Unit	Incremental cost		Limits Min Max	
1	0.003124	7.920000	150.00	600.00
2	0.003880	7.850000	100.00	400.00
3	0.009640	7.970000	50.00	300.00

Solution, Marginal Cost = 9.52 \$/MWh

Unit	PG(k)	Violation (Min Max)		Flag	IC(k)
1	510.58	-----	-----	0	9.52
2	429.14	-----	400.00	1	9.52
3	160.28	-----	-----	0	9.52

Total Generation = 1100 MW

New Marginal Cost = 9.58 \$/MWh mu = 0.18 \$/MWh

Unit	PG(k)	Violation (Min Max)		Flag	IC(k)
1	532.59	-----	-----	0	9.58
2	400.00	-----	-----	0	9.40
3	167.41	-----	-----	0	9.58
Total Generation =		1100 MW			

7.4 Real Power Losses

Transmission losses are present in a real power system; losses must be included in the real power balance equation. One approach is to derive an equation to calculate power losses P_L in the system; the amount of losses depends on the electrical distance that the generator's power has to travel up to the load nodes. A more general approach than a loss formula is required. However, in order to illustrate this process, let us minimize the operating cost to include losses with no inequality constraints in order to concentrate our attention in the meaning of the solution. First, we write the Lagrangian (7.27), where total cost function \$/h, the equality constraints and losses are in MW: $C_{\text{Total}} = \sum_{k=1}^n C_k(P_{Gk})$, $f(P_G) = P_D + P_L - \sum_{k=1}^n P_{Gk} = 0$, $P_L = P_L(P_{G1}, P_{G2}, \dots, P_{Gn})$. The gradient is a set (7.28) where incremental losses $\partial P_L / \partial P_{Gk}$ are required.

$$\xi(P, \lambda) = \sum_{k=1}^n C_k(P_{Gk}) + \lambda \left(P_D + P_L - \sum_{k=1}^n P_{Gk} \right) \quad (7.27)$$

$$\nabla \xi(P, \lambda) = \begin{bmatrix} \vdots \\ \frac{\partial C_k(P_{Gk})}{\partial P_{Gk}} + \lambda \left(\frac{\partial P_L}{\partial P_{Gk}} - 1 \right) \\ \vdots \\ P_D + P_L - \sum_{k=1}^n P_{Gk} \end{bmatrix} = \begin{bmatrix} \vdots \\ 0 \\ \vdots \\ 0 \\ 0 \end{bmatrix} \quad (7.28)$$

From (7.28) the solution at the *same incremental cost* remains valid, and now λ is a *penalized* incremental cost for generator k :

$$\lambda = \frac{\frac{\partial C_k(P_{Gk})}{\partial P_{Gk}}}{\left(1 - \frac{\partial P_L}{\partial P_{Gk}} \right)} \quad (7.29)$$

Power losses are a nonlinear function. Therefore, the gradient components in (7.28) are nonlinear equations. An iterative algorithm as Newton's type is the proper way to solve the nonlinear equation (7.28). Newton's incremental form is:

$$\begin{bmatrix}
 \vdots & \vdots & \vdots \\
 \dots \frac{\partial^2 C_k(P_{Gk})}{\partial P_{Gk}^2} + \lambda \frac{\partial^2 P_L}{\partial P_{Gk}^2} \dots & \lambda \frac{\partial^2 P_L}{\partial P_{Gk} \partial P_{Gm}} & \dots \frac{\partial P_L}{\partial P_{Gk}} - 1 \\
 \vdots & \vdots & \vdots \\
 \dots \lambda \frac{\partial^2 P_L}{\partial P_{Gm} \partial P_{Gk}} & \dots \frac{\partial^2 C_m(P_{Gm})}{\partial P_{Gm}^2} + \lambda \frac{\partial^2 P_L}{\partial P_{Gm}^2} & \dots \frac{\partial P_L}{\partial P_{Gm}} - 1 \\
 \vdots & \vdots & \vdots \\
 \dots \frac{\partial P_L}{\partial P_{Gk}} - 1 & \dots \frac{\partial P_L}{\partial P_{Gm}} - 1 & \dots 0
 \end{bmatrix}
 \begin{bmatrix}
 \vdots \\
 \Delta P_{Gk} \\
 \vdots \\
 \Delta P_{Gm} \\
 \vdots \\
 \Delta \lambda
 \end{bmatrix}
 = -
 \begin{bmatrix}
 \vdots \\
 g_k \\
 \vdots \\
 g_m \\
 \vdots \\
 g_{n+1}
 \end{bmatrix}
 \tag{7.30}$$

Example 7.5

A system with two generators must supply the load P_D and losses P_L . The loss formula is given as $P_L = 0.1 P_{G1}^2 - 0.1 P_{G1} P_{G2} + 0.2 P_{G2}^2$ (see Figure 7.6), and we use it to solve the optimal dispatch problem, assuming incremental costs for the two generators as $\partial C_1/\partial P_{G1} = P_{G1} + 2$, $\partial C_1/\partial P_{G2} = 0$, $\partial C_2/\partial P_{G1} = 0$, and $\partial C_2/\partial P_{G2} = P_{G2} + 1.5$.

The gradient as in (7.28) is equal to zero; Newton’s method is used to solve the nonlinear set of equations from the gradient. The incremental set of equations is (7.32).

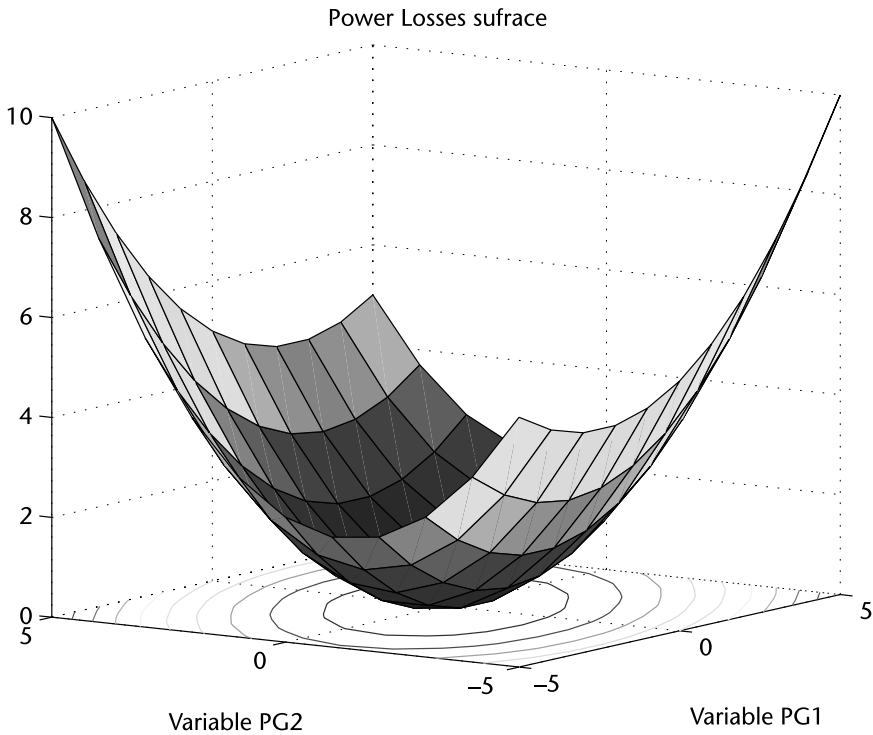


Figure 7.6 Surface for power losses, Example 7.5.

$$\begin{bmatrix} g_1 \\ g_1 \\ g_1 \end{bmatrix} = \begin{bmatrix} \frac{\partial C_1}{\partial P_{G1}} + \lambda \left(\frac{\partial P_L}{\partial P_{G1}} - 1 \right) \\ \frac{\partial C_2}{\partial P_{G2}} + \lambda \left(\frac{\partial P_L}{\partial P_{G2}} - 1 \right) \\ P_D + P_L - P_{G1} - P_{G2} \end{bmatrix} = \begin{bmatrix} P_{G1} + 2 + \lambda(0.2P_{G1} - 0.1P_{G2} - 1) \\ P_{G2} + 1.5 + \lambda(-0.1P_{G1} + 0.4P_{G2} - 1) \\ P_D + P_L - P_{G1} - P_{G2} \end{bmatrix} = \begin{bmatrix} 0 \\ 0 \\ 0 \end{bmatrix} \quad (7.31)$$

$$\begin{bmatrix} 1 + 0.2\lambda & -0.1\lambda & 0.2P_{G1} - 0.1P_{G2} - 1 \\ -0.1\lambda & 1 + 0.4\lambda & -0.1P_{G1} + 0.4P_{G2} - 1 \\ 0.2P_{G1} - 0.1P_{G2} - 1 & -0.1P_{G1} + 0.4P_{G2} - 1 & 0 \end{bmatrix} \begin{bmatrix} \Delta P_{G1} \\ \Delta P_{G2} \\ \Delta \lambda \end{bmatrix} = - \begin{bmatrix} g_1 \\ g_1 \\ g_1 \end{bmatrix} \quad (7.32)$$

Starting with values $P_{G1} = P_{G2} = \lambda = 0$, the iterative process solves the no-loss problem. We found that the solution i in four iterations within a tight tolerance, solution shows *equal incremental costs* when the penalty factor due to the incremental losses is included.

Economic Dispatch, including losses

Iteration	PG values and lamda			Maxdev
0	0.000000	0.000000	0.000000	2.000000e+000
1	0.310550	0.810550	2.310550	6.773724e-001
2	0.557465	0.618537	2.665436	3.601975e-002
3	0.556278	0.642462	2.682422	1.645744e-004
4	0.556404	0.642459	2.682578	3.976804e-009

Convergence in 4 iterations

Solution

PG1	PG2	Pdemand	Plosses	System lamda
0.556404	0.642459	1.121100	0.077763	2.682578

Incremental Costs for generators

2.556404	2.142459
----------	----------

Incremental losses

0.047035	0.201343
----------	----------

Penalty factors

0.952965	0.798657
----------	----------

Penalized Incremental costs

2.682578	2.682578
----------	----------

7.5 Minimum Losses

The *cost* function for the optimal problem can be other than the cost itself, for instance, it might be interesting to solve the minimum loss problem. Let us assume n generators, a loss formula $P_L = f_L(P_{G1}, P_{G2}, \dots, P_{Gn})$ and a system's demand P_D to be satisfied. The Lagrange function is:

$$\min \xi = P_L + \lambda_L (P_D + P_L - P_{G1} - P_{G2} \dots - P_{Gn}) \quad (7.33)$$

λ_L Lagrange multiplier, to include the demand equality constraint

The gradient to minimize losses is written:

$$\nabla \xi = \begin{bmatrix} \frac{\partial \xi}{\partial P_{G1}} \\ \frac{\partial \xi}{\partial P_{G2}} \\ \vdots \\ \frac{\partial \xi}{\partial \lambda_L} \end{bmatrix} = \begin{bmatrix} \frac{\partial P_L}{\partial P_{G1}} + \lambda_L \left(\frac{\partial P_L}{\partial P_{G1}} - 1 \right) \\ \frac{\partial P_L}{\partial P_{G2}} + \lambda_L \left(\frac{\partial P_L}{\partial P_{G2}} - 1 \right) \\ \vdots \\ P_D + P_L - P_{G1} - P_{G2} \dots - P_{Gn} \end{bmatrix} = \begin{bmatrix} 0 \\ 0 \\ \vdots \\ 0 \end{bmatrix} \quad (7.34)$$

Equation (7.34) shows that we will find a solution when the *penalized* incremental losses are the same for every participating generator. Note that in this case, the Lagrange multiplier λ_L has no dimensions and its meaning is very different from the interpretation given to the Lagrange multiplier in the minimum cost solution.

$$\lambda_L = \frac{\frac{\partial P_L}{\partial P_{G1}}}{\left(1 - \frac{\partial P_L}{\partial P_{G1}}\right)} = \dots = \frac{\frac{\partial P_L}{\partial P_{Gn}}}{\left(1 - \frac{\partial P_L}{\partial P_{Gn}}\right)} \quad (7.35)$$

Example 7.6

For a two-generator system to supply load P_D and losses P_L (see Figure 7.7), solve the minimum loss problem, given the loss formula. Find the augmented Lagrangian,

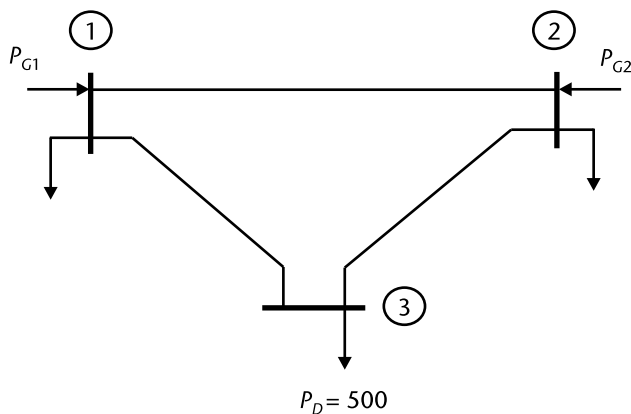


Figure 7.7 A three-node system, the minimum loss solution.

the gradient by (7.34), and the operation cost given cost and loss formula $C_1(P_{G1}) = 7.0 P_{G1} + 0.002 P_{G1}^2$, $C_2(P_{G2}) = 7.0 P_{G2} + 0.002 P_{G2}^2$, and $P_L = 0.0002 P_{G1}^2 + 0.00015 P_{G2}^2$.

$$\min \xi = P_L + \lambda_L (P_D + P_L - P_{G1} - P_{G2}) \quad (7.36)$$

$$\nabla \xi = \begin{bmatrix} \frac{\partial P_L}{\partial P_{G1}} + \lambda_L \left(\frac{\partial P_L}{\partial P_{G1}} - 1 \right) \\ \frac{\partial P_L}{\partial P_{G2}} + \lambda_L \left(\frac{\partial P_L}{\partial P_{G2}} - 1 \right) \\ P_D + P_L - P_{G1} - P_{G2} \end{bmatrix} = \begin{bmatrix} 0.0004P_{G1} + \lambda_L (0.0004P_{G1} - 1) \\ 0.0003P_{G2} + \lambda_L (0.0003P_{G2} - 1) \\ 500 + P_L - P_{G1} - P_{G2} \end{bmatrix} = \begin{bmatrix} 0 \\ 0 \\ 0 \end{bmatrix} \quad (7.37)$$

We propose to solve the nonlinear set by Newton's iterative procedure. Gradient and Newton's incremental form:

$$\begin{bmatrix} g_1 \\ g_2 \\ g_3 \end{bmatrix} = \begin{bmatrix} 0.0004P_{G1} + \lambda_L (0.0004P_{G1} - 1) \\ 0.0003P_{G2} + \lambda_L (0.0003P_{G2} - 1) \\ 500 + P_L - P_{G1} - P_{G2} \end{bmatrix} = \begin{bmatrix} 0 \\ 0 \\ 0 \end{bmatrix} \quad (7.38)$$

$$\begin{bmatrix} 0.0004(1 + \lambda_L) & 0 & 0.0004P_{G1} - 1 \\ 0 & 0.0003(1 + \lambda_L) & 0.0003P_{G2} - 1 \\ 0.0004P_{G1} - 1 & 0.0003P_{G2} - 1 & 0 \end{bmatrix} \begin{bmatrix} \Delta P_{G1} \\ \Delta P_{G2} \\ \Delta \lambda_L \end{bmatrix} = - \begin{bmatrix} g_1 \\ g_2 \\ g_3 \end{bmatrix} \quad (7.39)$$

Minimum losses

Iteration	PG values and lamda			Maxdev
0	0.000000	0.000000	0.000000	5.000000e+002
1	214.285714	285.714286	0.085714	2.142857e+001
2	224.330357	299.107143	0.098521	4.708426e-002
3	224.352525	299.136700	0.098588	2.293329e-007

Convergence in 3 iterations

PG1	PG2	Pdemand	Plosses	lamda	Losses
224.352525	299.136700	500.000000	23.489226	0.098588	

Incremental Costs

7.897410 8.196547

Incremental losses

0.089741 0.089741

Penalty factors

0.910259 0.910259

Penalized Incremental Losses

0.098588 0.098588

Penalized Incremental Costs

8.676003 9.004632

Cost G1 = 1671.14 \$/h Cost G2 = 2272.92 \$/h

Total Operating Cost = 3944.06 \$/h

Let us compare the solution to the minimum cost when the load to be supplied is 500 MW.

$$\nabla \xi = \begin{bmatrix} \frac{\partial C_1}{\partial P_{G1}} + \lambda \left(\frac{\partial P_L}{\partial P_{G1}} - 1 \right) \\ \frac{\partial C_2}{\partial P_{G2}} + \lambda \left(\frac{\partial P_L}{\partial P_{G2}} - 1 \right) \\ P_D + P_L - P_{G1} - P_{G2} \end{bmatrix} = \begin{bmatrix} 0.004P_{G1} + 7 + \lambda(0.0004P_{G1} - 1) \\ 0.004P_{G2} + 7 + \lambda(0.0003P_{G2} - 1) \\ 500 + P_L - P_{G1} - P_{G2} \end{bmatrix} = \begin{bmatrix} 0 \\ 0 \\ 0 \end{bmatrix} \quad (7.40)$$

$$\begin{bmatrix} 0.004 + 0.0004\lambda & 0 & 0.0004P_{G1} - 1 \\ 0 & 0.004 + 0.0003\lambda & 0.0003P_{G2} - 1 \\ 0.0004P_{G1} - 1 & 0.0003P_{G2} - 1 & 0 \end{bmatrix} \begin{bmatrix} \Delta P_{G1} \\ \Delta P_{G2} \\ \Delta \lambda \end{bmatrix} = - \begin{bmatrix} g_1 \\ g_1 \\ g_1 \end{bmatrix} \quad (7.41)$$

Economic Dispatch, including losses

Iteration	PG values		lambda	Maxdev
0	0.000000	0.000000	0.000000	5.000000e+002
1	250.000000	250.000000	8.000000	2.187500e+001
2	244.799242	278.708846	8.847283	1.290393e-001
3	245.504785	278.155131	8.851225	1.455484e-004
4	245.504734	278.155340	8.851226	7.048584e-012

Convergence in 4 iterations

PG1	PG2	Pdemand	Plosses	System lambda
245.504734	278.155340	500.000000	23.660074	8.851226

Incremental Costs

7.982019 8.112621

Incremental losses

0.098202 0.083447

Penalty factors

0.901798 0.916553

Penalized Incremental costs

8.851226 8.851226

Cost G1 = 1839.08 \$/h Cost G2 = 2101.83 \$/h

Total Operating Cost = 3940.91 \$/h

The example shows the minimum loss solution versus the minimum operating cost; it is worth noting that the minimum losses solution has a slightly higher cost. The solution is at the same penalized incremental loss and the same penalized incremental cost, respectively. It is a common practice by power system operators to pursue the minimum cost solution; this is the goal from the economic point of view.

7.6 Optimal Operation, Transmission Losses Included

At this point, we are ready to establish a more general formulation for the power flow problem. One issue is how to include transmission losses. In Sections 7.4 and 7.5 we used a loss formula, but in general, no such formula is readily available, even though much effort went into establishing a procedure to find the loss formula for a given network in the past. Losses at each transmission line are included in the nodal power balance, so there is no need to write a system's loss formula by itself unless some specific application requires that information.

To illustrate the concepts of the minimum loss solution, let us use a three-node system (see Figure 7.8). To concentrate on the solution steps, we assume that nodal voltages are held at 1.0 pu, so no voltages and reactive power flows are written explicitly.

$$\begin{aligned}
 \min P_L &= P_{G1} + P_{G3} - P_D \\
 \text{s.a. } p_{12} - P_{G1} + P_{D1} &= 0 \\
 p_{21} + p_{23} + P_{D2} &= 0 \\
 p_{32} - P_{G3} + P_{D3} &= 0
 \end{aligned}
 \tag{7.42}$$

The Lagrange function has as unknown variables: $P_{G1}, P_{G3}, \theta_1, \theta_2, \theta_3, \lambda_{1L}, \lambda_{2L}, \lambda_{3L}$. At the solution, the gradient of the augmented Lagrangian must be equal to zero, and one nodal angle will be reference.

$$\begin{aligned}
 \min \zeta &= P_{G1} + P_{G3} - P_D + \lambda_{1L}(p_{12} - P_{G1} + P_{D1}) \\
 &+ \lambda_{2L}(p_{21} + p_{23} + P_{D2}) + \lambda_{3L}(p_{32} - P_{G3} + P_{D3})
 \end{aligned}
 \tag{7.43}$$

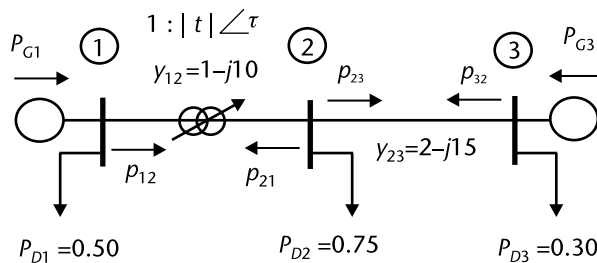


Figure 7.8 System to generalize the minimum loss solution, three-node.

$$\nabla \zeta = \begin{bmatrix} \frac{\partial \zeta}{\partial P_{G1}} \\ \frac{\partial \zeta}{\partial P_{G3}} \\ \frac{\partial \zeta}{\partial \theta_1} \\ \frac{\partial \zeta}{\partial \theta_2} \\ \frac{\partial \zeta}{\partial \theta_3} \\ \frac{\partial \zeta}{\partial \lambda_{1L}} \\ \frac{\partial \zeta}{\partial \lambda_{2L}} \\ \frac{\partial \zeta}{\partial \lambda_{3L}} \end{bmatrix} = \begin{bmatrix} g_1 \\ g_2 \\ g_3 \\ g_4 \\ g_5 \\ g_6 \\ g_7 \\ g_8 \end{bmatrix} = \begin{bmatrix} 1 - \lambda_{1L} \\ 1 - \lambda_{3L} \\ \lambda_{1L} \frac{\partial p_{12}}{\partial \theta_1} + \lambda_{2L} \frac{\partial p_{21}}{\partial \theta_1} \\ \lambda_{1L} \frac{\partial p_{12}}{\partial \theta_2} + \lambda_{2L} \left(\frac{\partial p_{21}}{\partial \theta_2} + \frac{\partial p_{23}}{\partial \theta_2} \right) + \lambda_{3L} \frac{\partial p_{32}}{\partial \theta_2} \\ \lambda_{2L} \frac{\partial p_{23}}{\partial \theta_3} + \lambda_{3L} \frac{\partial p_{32}}{\partial \theta_3} \\ p_{12} - P_{G1} + P_{D1} \\ p_{21} + p_{23} + P_{D2} \\ p_{32} - P_{G3} + P_{D3} \end{bmatrix} = \begin{bmatrix} 0 \\ 0 \\ 0 \\ 0 \\ 0 \\ 0 \\ 0 \\ 0 \end{bmatrix} \quad (7.44)$$

We write Newton's iterative method to solve the nonlinear equations from the gradient (7.44).

$$\begin{bmatrix} 0 & 0 & 0 & 0 & 0 & -1 & 0 & 0 \\ 0 & 0 & 0 & 0 & 0 & 0 & 0 & -1 \\ 0 & 0 & \frac{\partial g_3}{\partial \theta_1} & \frac{\partial g_3}{\partial \theta_2} & 0 & \frac{\partial g_3}{\partial \lambda_{1L}} & \frac{\partial g_3}{\partial \lambda_{2L}} & 0 \\ 0 & 0 & \frac{\partial g_4}{\partial \theta_1} & \frac{\partial g_4}{\partial \theta_2} & \frac{\partial g_4}{\partial \theta_3} & \frac{\partial g_4}{\partial \lambda_{1L}} & \frac{\partial g_4}{\partial \lambda_{2L}} & \frac{\partial g_4}{\partial \lambda_{3L}} \\ 0 & 0 & 0 & \frac{\partial g_5}{\partial \theta_2} & \frac{\partial g_5}{\partial \theta_3} & 0 & \frac{\partial g_5}{\partial \lambda_{2L}} & \frac{\partial g_5}{\partial \lambda_{3L}} \\ -1 & 0 & \frac{\partial g_6}{\partial \theta_1} & \frac{\partial g_6}{\partial \theta_2} & 0 & 0 & 0 & 0 \\ 0 & 0 & \frac{\partial g_7}{\partial \theta_1} & \frac{\partial g_7}{\partial \theta_2} & \frac{\partial g_7}{\partial \theta_3} & 0 & 0 & 0 \\ 0 & -1 & 0 & \frac{\partial g_8}{\partial \theta_2} & \frac{\partial g_8}{\partial \theta_3} & 0 & 0 & 0 \end{bmatrix} \begin{bmatrix} \Delta P_{G1} \\ \Delta P_{G3} \\ \Delta \theta_1 \\ \Delta \theta_2 \\ \Delta \theta_3 \\ \Delta \lambda_{1L} \\ \Delta \lambda_{2L} \\ \Delta \lambda_{3L} \end{bmatrix} = - \begin{bmatrix} g_1 \\ g_2 \\ g_3 \\ g_4 \\ g_5 \\ g_6 \\ g_7 \\ g_8 \end{bmatrix} \quad (7.45)$$

In (7.45) we see that some gradient components already have first partial derivatives, and then some second derivatives are required. Section 7.8 lists the set of derivatives that are required. The incremental real power flows are for transmission lines and transformers with a complex tap changer are basic elements that must be considered. For the problem at hand, we list the partial derivatives required in (7.45) as the set (7.46). Numerical results will follow in Figure 7.9.

$$\begin{aligned}
 \frac{\partial g_3}{\partial \theta_1} &= \lambda_{1L} \frac{\partial^2 p_{12}}{\partial \theta_1^2} + \lambda_{2L} \frac{\partial^2 p_{21}}{\partial \theta_1^2} \\
 \frac{\partial g_3}{\partial \theta_2} &= \lambda_{1L} \frac{\partial^2 p_{12}}{\partial \theta_2 \partial \theta_1} + \lambda_{2L} \frac{\partial^2 p_{21}}{\partial \theta_2 \partial \theta_1} \\
 \frac{\partial g_3}{\partial \lambda_{1L}} &= \frac{\partial p_{12}}{\partial \theta_1} \\
 \frac{\partial g_3}{\partial \lambda_{2L}} &= \frac{\partial p_{21}}{\partial \theta_1} \\
 \frac{\partial g_4}{\partial \theta_1} &= \lambda_{1L} \frac{\partial^2 p_{12}}{\partial \theta_1 \partial \theta_2} + \lambda_{2L} \frac{\partial^2 p_{21}}{\partial \theta_1 \partial \theta_2} \\
 \frac{\partial g_4}{\partial \theta_2} &= \lambda_{1L} \frac{\partial^2 p_{12}}{\partial \theta_2^2} + \lambda_{2L} \left(\frac{\partial^2 p_{21}}{\partial \theta_2^2} + \frac{\partial^2 p_{23}}{\partial \theta_2^2} \right) + \lambda_{3L} \frac{\partial^2 p_{32}}{\partial \theta_2^2} \\
 \frac{\partial g_4}{\partial \theta_3} &= \lambda_{2L} \frac{\partial^2 p_{23}}{\partial \theta_3 \partial \theta_2} + \lambda_{3L} \frac{\partial^2 p_{32}}{\partial \theta_3 \partial \theta_2} \\
 \frac{\partial g_4}{\partial \lambda_{1L}} &= \frac{\partial p_{12}}{\partial \theta_2} \\
 \frac{\partial g_4}{\partial \lambda_{2L}} &= \frac{\partial p_{21}}{\partial \theta_2} + \frac{\partial p_{23}}{\partial \theta_2} \\
 \frac{\partial g_4}{\partial \lambda_{3L}} &= \frac{\partial p_{32}}{\partial \theta_2} \\
 \frac{\partial g_5}{\partial \theta_2} &= \lambda_{2L} \frac{\partial^2 p_{23}}{\partial \theta_2 \partial \theta_3} + \lambda_{3L} \frac{\partial^2 p_{32}}{\partial \theta_2 \partial \theta_3} \\
 \frac{\partial g_5}{\partial \theta_3} &= \lambda_{2L} \frac{\partial^2 p_{23}}{\partial \theta_3^2} + \lambda_{3L} \frac{\partial^2 p_{32}}{\partial \theta_3^2} \\
 \frac{\partial g_5}{\partial \lambda_{2L}} &= \frac{\partial p_{23}}{\partial \theta_3} \\
 \frac{\partial g_5}{\partial \lambda_{3L}} &= \frac{\partial p_{32}}{\partial \theta_3} \\
 \frac{\partial g_6}{\partial \theta_1} &= \frac{\partial p_{12}}{\partial \theta_1} \\
 \frac{\partial g_6}{\partial \theta_2} &= \frac{\partial p_{12}}{\partial \theta_2} \\
 \frac{\partial g_7}{\partial \theta_1} &= \frac{\partial p_{21}}{\partial \theta_1} \\
 \frac{\partial g_7}{\partial \theta_2} &= \frac{\partial p_{21}}{\partial \theta_2} + \frac{\partial p_{23}}{\partial \theta_2} \\
 \frac{\partial g_7}{\partial \theta_3} &= \frac{\partial p_{23}}{\partial \theta_3} \\
 \frac{\partial g_8}{\partial \theta_2} &= \frac{\partial p_{32}}{\partial \theta_2} \\
 \frac{\partial g_8}{\partial \theta_3} &= \frac{\partial p_{32}}{\partial \theta_3}
 \end{aligned} \tag{7.46}$$

```

Elements = 2
Nodes = 3
Array of elements (duplicated)
Elem  N_from  N_to  type_el  tap    tau    yelem          Bsh/2
  1    1      2    -1      1.05  0.09  1.0000 +j-10.0000  +j 0.0000
  2    2      3     1       1.00  0.00  2.0000 +j-15.0000  +j 0.0000
  3    2      1    -1      1.05  0.09  1.0000 +j-10.0000  +j 0.0000
  4    3      2     1       1.00  0.00  2.0000 +j-15.0000  +j 0.0000
Node data
Node   type    Voltage    Angle    Pgen    Pload
  1     0      1.0000    0.0000    0.00    0.50
  2    -1      1.0000    0.0000    0.00    0.75
  3     1      1.0000    0.0000    0.00    0.30
Node type Generation = 2    Load = 1
Iteration = 0    Maxdev = 7.216309e-001
Iteration = 1    Maxdev = 3.342385e-003
Iteration = 2    Maxdev = 1.231484e-007

Node summary
Node   type    Voltage    Angle    Pgen    Pload    Qgen    Qload
  1     0      1.0000    -0.00    0.8915  0.5000    0.4966  0.0000
  2    -1      1.0000     3.15    0.0000  0.7500    0.0000  0.4080
  3     1      1.0000     4.54    0.6633  0.3000   -0.0440  0.0000
Load flows (duplicated)
Elem  N_from  N_to  type_el  tap    tau    pkm          qkm
  1    1      2    -1      1.05  5.00    0.3915    0.4966
  1    2      1    -1      1.05  5.00   -0.3879   -0.4607
  2    2      3     1       1.00  0.00   -0.3621    0.0527
  2    3      2     1       1.00  0.00    0.3633   -0.0440
PLtot = 0.0048    QLtot = 0.0447
Lamda values
k = 1    Lamdap = 1.0000
k = 2    Lamdap = 1.0065
k = 3    Lamdap = 1.0000
    
```

7.6.1 Minimum Cost Power Flow Formulation

If a solution to the minimum operating cost is more general than load power flows, then we use the formulation for optimum power flow; we must represent all nodal

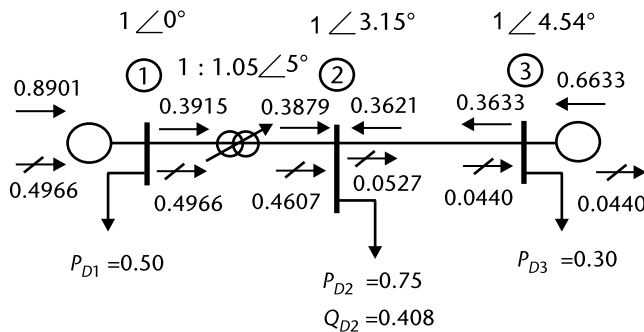


Figure 7.9 Three-node system load flows for a minimum loss solution.

$$\begin{bmatrix} W_{11} & W_{12} \\ W_{21} & W_{22} \end{bmatrix} \begin{bmatrix} \Delta x_P \\ \Delta x_Q \end{bmatrix} = - \begin{bmatrix} g_P \\ g_Q \end{bmatrix} \quad (7.49)$$

$$\begin{aligned} \Delta x_P &= \begin{bmatrix} \Delta P_{G1} & \Delta P_{G3} & \Delta \theta_1 & \Delta \theta_2 & \Delta \theta_3 & \Delta \lambda_{1P} & \Delta \lambda_{2P} & \Delta \lambda_{3P} \end{bmatrix} \\ \Delta x_Q &= \begin{bmatrix} \Delta Q_{G1} & \Delta Q_{G3} & \Delta \frac{|V_1|}{|V_1|} & \Delta \frac{|V_2|}{|V_2|} & \Delta \frac{|V_3|}{|V_3|} & \Delta \lambda_{1Q} & \Delta \lambda_{2Q} & \Delta \lambda_{3Q} \end{bmatrix} \end{aligned} \quad (7.50)$$

$$\begin{aligned} g_P &= \begin{bmatrix} g_1 & \cdots & g_8 \end{bmatrix} \\ g_Q &= \begin{bmatrix} g_9 & \cdots & g_{14} \end{bmatrix} \end{aligned} \quad (7.51)$$

Elements in submatrix W_{11} and W_{22} (assuming that W_{12} and W_{21} have small values compared to the ones at W_{11} and W_{22}) will render a decoupled real-reactive approach.

$$W_{11} = \begin{bmatrix} \frac{d^2 C_1}{dP_{G1}^2} & 0 & 0 & 0 & 0 & -1 & 0 & 0 \\ 0 & \frac{d^2 C_3}{dP_{G3}^2} & 0 & 0 & 0 & 0 & 0 & -1 \\ 0 & 0 & \frac{\partial g_3}{\partial \theta_1} & \frac{\partial g_3}{\partial \theta_2} & 0 & \frac{\partial p_{12}}{\partial \theta_1} & \frac{\partial p_{21}}{\partial \theta_1} & 0 \\ 0 & 0 & \frac{\partial g_4}{\partial \theta_1} & \frac{\partial g_4}{\partial \theta_2} & \frac{\partial g_4}{\partial \theta_3} & \frac{\partial p_{12}}{\partial \theta_2} & \frac{\partial p_{21}}{\partial \theta_2} + \frac{\partial p_{23}}{\partial \theta_2} & \frac{\partial p_{32}}{\partial \theta_2} \\ 0 & 0 & 0 & \frac{\partial g_5}{\partial \theta_2} & \frac{\partial g_5}{\partial \theta_3} & 0 & \frac{\partial p_{23}}{\partial \theta_3} & \frac{\partial p_{32}}{\partial \theta_3} \\ -1 & 0 & \frac{\partial p_{12}}{\partial \theta_1} & \frac{\partial p_{12}}{\partial \theta_2} & 0 & 0 & 0 & 0 \\ 0 & 0 & \frac{\partial p_{21}}{\partial \theta_1} & \frac{\partial p_{21}}{\partial \theta_2} + \frac{\partial p_{23}}{\partial \theta_2} & \frac{\partial p_{23}}{\partial \theta_3} & 0 & 0 & 0 \\ 0 & -1 & 0 & \frac{\partial p_{32}}{\partial \theta_2} & \frac{\partial p_{32}}{\partial \theta_3} & 0 & 0 & 0 \end{bmatrix} \quad (7.52)$$

The required partial derivatives for W_{11} and W_{22} are:

$$\left[\begin{array}{l}
 \frac{\partial g_3}{\partial \theta_1} = \lambda_{1P} \frac{\partial^2 p_{12}}{\partial \theta_1^2} + \lambda_{2P} \frac{\partial^2 p_{21}}{\partial \theta_1^2} + \lambda_{1Q} \frac{\partial^2 q_{12}}{\partial \theta_1^2} + \lambda_{2Q} \frac{\partial^2 q_{21}}{\partial \theta_1^2} \\
 \frac{\partial g_3}{\partial \theta_2} = \lambda_{1P} \frac{\partial^2 p_{12}}{\partial \theta_2 \partial \theta_1} + \lambda_{2P} \frac{\partial^2 p_{21}}{\partial \theta_2 \partial \theta_1} + \lambda_{1Q} \frac{\partial^2 q_{12}}{\partial \theta_2 \partial \theta_1} + \lambda_{2Q} \frac{\partial^2 q_{21}}{\partial \theta_2 \partial \theta_1} \\
 \frac{\partial g_4}{\partial \theta_1} = \lambda_{1P} \frac{\partial^2 p_{12}}{\partial \theta_1 \partial \theta_2} + \lambda_{2P} \frac{\partial^2 p_{21}}{\partial \theta_1 \partial \theta_2} + \lambda_{1Q} \frac{\partial^2 q_{12}}{\partial \theta_1 \partial \theta_2} + \lambda_{2Q} \frac{\partial^2 q_{21}}{\partial \theta_1 \partial \theta_2} = \frac{\partial g_3}{\partial \theta_2} \\
 \frac{\partial g_4}{\partial \theta_2} = \lambda_{1P} \frac{\partial^2 p_{12}}{\partial \theta_2^2} + \lambda_{2P} \left(\frac{\partial^2 p_{21}}{\partial \theta_2^2} + \frac{\partial^2 p_{23}}{\partial \theta_2^2} \right) + \lambda_{3P} \frac{\partial^2 p_{32}}{\partial \theta_2^2} + \lambda_{1Q} \frac{\partial^2 q_{12}}{\partial \theta_2^2} + \lambda_{2Q} \left(\frac{\partial^2 q_{21}}{\partial \theta_2^2} + \frac{\partial^2 q_{23}}{\partial \theta_2^2} \right) + \lambda_{3Q} \frac{\partial^2 q_{32}}{\partial \theta_2^2} \\
 \frac{\partial g_4}{\partial \theta_3} = \lambda_{2P} \frac{\partial^2 p_{23}}{\partial \theta_3 \partial \theta_2} + \lambda_{3P} \frac{\partial^2 p_{32}}{\partial \theta_3 \partial \theta_2} + \lambda_{2Q} \frac{\partial^2 q_{23}}{\partial \theta_3 \partial \theta_2} + \lambda_{3Q} \frac{\partial^2 q_{32}}{\partial \theta_3 \partial \theta_2} \\
 \frac{\partial g_5}{\partial \theta_2} = \lambda_{2P} \frac{\partial^2 p_{23}}{\partial \theta_2 \partial \theta_3} + \lambda_{3P} \frac{\partial^2 p_{32}}{\partial \theta_2 \partial \theta_3} + \lambda_{2Q} \frac{\partial^2 q_{23}}{\partial \theta_2 \partial \theta_3} + \lambda_{3Q} \frac{\partial^2 q_{32}}{\partial \theta_2 \partial \theta_3} = \frac{\partial g_4}{\partial \theta_3} \\
 \frac{\partial g_5}{\partial \theta_3} = \lambda_{2P} \frac{\partial^2 p_{23}}{\partial \theta_3^2} + \lambda_{3P} \frac{\partial^2 p_{32}}{\partial \theta_3^2} + \lambda_{2Q} \frac{\partial^2 q_{23}}{\partial \theta_3^2} + \lambda_{3Q} \frac{\partial^2 q_{32}}{\partial \theta_3^2}
 \end{array} \right] \quad (7.53)$$

$$W_{22} = \left[\begin{array}{cccccccc}
 1 & 0 & 0 & 0 & 0 & -1 & 0 & 0 \\
 0 & 1 & 0 & 0 & 0 & 0 & 0 & -1 \\
 0 & 0 & \frac{\partial g_{11}}{\partial |V_1|} |V_1| & \frac{\partial g_{11}}{\partial |V_2|} |V_2| & 0 & \frac{\partial q_{12}}{\partial |V_1|} |V_1| & \frac{\partial q_{12}}{\partial |V_1|} |V_1| & 0 \\
 0 & 0 & \frac{\partial g_{12}}{\partial |V_1|} |V_1| & \frac{\partial g_{12}}{\partial |V_2|} |V_2| & \frac{\partial g_{12}}{\partial |V_3|} |V_3| & \frac{\partial q_{12}}{\partial |V_2|} |V_2| & \frac{\partial q_{21}}{\partial |V_2|} |V_2| + \frac{\partial q_{23}}{\partial |V_2|} |V_2| & \frac{\partial q_{23}}{\partial |V_2|} |V_2| \\
 0 & 0 & 0 & \frac{\partial g_{13}}{\partial |V_2|} |V_2| & \frac{\partial g_{13}}{\partial |V_3|} |V_3| & 0 & \frac{\partial q_{32}}{\partial |V_3|} |V_3| & \frac{\partial q_{32}}{\partial |V_3|} |V_3| \\
 -1 & 0 & \frac{\partial q_{12}}{\partial |V_1|} |V_1| & \frac{\partial q_{12}}{\partial |V_2|} |V_2| & 0 & 0 & 0 & 0 \\
 0 & 0 & \frac{\partial q_{21}}{\partial |V_1|} |V_1| & \frac{\partial q_{21}}{\partial |V_2|} |V_2| + \frac{\partial q_{23}}{\partial |V_2|} |V_2| & \frac{\partial q_{23}}{\partial |V_3|} |V_3| & 0 & 0 & 0 \\
 0 & -1 & 0 & \frac{\partial q_{32}}{\partial |V_2|} |V_2| & \frac{\partial q_{32}}{\partial |V_3|} |V_3| & 0 & 0 & 0
 \end{array} \right] \quad (7.54)$$

$$\begin{aligned}
 \frac{\partial g_{11}}{\partial |V_1|} |V_1| &= \left(\lambda_{1P} \frac{\partial^2 p_{12}}{\partial |V_1|^2} + \lambda_{2P} \frac{\partial^2 p_{21}}{\partial |V_1|^2} + \lambda_{1Q} \frac{\partial^2 q_{12}}{\partial |V_1|^2} + \lambda_{2Q} \frac{\partial^2 q_{21}}{\partial |V_1|^2} \right) |V_1|^2 \\
 \frac{\partial g_{11}}{\partial |V_2|} |V_2| &= \left(\lambda_{1P} \frac{\partial^2 p_{12}}{\partial |V_2| \partial |V_1|} + \lambda_{2P} \frac{\partial^2 p_{21}}{\partial |V_2| \partial |V_1|} + \lambda_{1Q} \frac{\partial^2 q_{12}}{\partial |V_2| \partial |V_1|} + \lambda_{2Q} \frac{\partial^2 q_{21}}{\partial |V_2| \partial |V_1|} \right) |V_1| |V_2| \\
 \frac{\partial g_{12}}{\partial |V_1|} |V_1| &= \left(\lambda_{1P} \frac{\partial^2 p_{12}}{\partial |V_1| \partial |V_2|} + \lambda_{2P} \frac{\partial^2 p_{21}}{\partial |V_1| \partial |V_2|} + \lambda_{1Q} \frac{\partial^2 q_{12}}{\partial |V_1| \partial |V_2|} + \lambda_{2Q} \frac{\partial^2 q_{21}}{\partial |V_1| \partial |V_2|} \right) |V_2| |V_1| \\
 \frac{\partial g_{12}}{\partial |V_2|} |V_2| &= \left(\lambda_{1P} \frac{\partial^2 p_{12}}{\partial |V_2|^2} + \lambda_{2P} \left(\frac{\partial^2 p_{21}}{\partial |V_2|^2} + \frac{\partial^2 p_{23}}{\partial |V_2|^2} \right) + \lambda_{3P} \frac{\partial^2 p_{32}}{\partial |V_2|^2} \right) |V_2|^2 + \left(\lambda_{1Q} \frac{\partial^2 q_{12}}{\partial |V_2|^2} + \lambda_{2Q} \left(\frac{\partial^2 q_{21}}{\partial |V_2|^2} + \frac{\partial^2 q_{23}}{\partial |V_2|^2} \right) + \lambda_{3Q} \frac{\partial^2 q_{32}}{\partial |V_2|^2} \right) |V_2|^2 \\
 \frac{\partial g_{12}}{\partial |V_3|} |V_3| &= \left(\lambda_{2P} \frac{\partial^2 p_{23}}{\partial |V_3| \partial |V_2|} + \lambda_{3P} \frac{\partial^2 p_{32}}{\partial |V_3| \partial |V_2|} + \lambda_{2Q} \frac{\partial^2 q_{23}}{\partial |V_3| \partial |V_2|} + \lambda_{3Q} \frac{\partial^2 q_{32}}{\partial |V_3| \partial |V_2|} \right) |V_2| |V_3| \\
 \frac{\partial g_{13}}{\partial |V_2|} |V_2| &= \left(\lambda_{2P} \frac{\partial^2 p_{23}}{\partial |V_2| \partial |V_3|} + \lambda_{3P} \frac{\partial^2 p_{32}}{\partial |V_2| \partial |V_3|} + \lambda_{2Q} \frac{\partial^2 q_{23}}{\partial |V_2| \partial |V_3|} + \lambda_{3Q} \frac{\partial^2 q_{32}}{\partial |V_2| \partial |V_3|} \right) |V_3| |V_2| \\
 \frac{\partial g_{13}}{\partial |V_3|} |V_3| &= \left(\lambda_{2P} \frac{\partial^2 p_{23}}{\partial |V_3|^2} + \lambda_{3P} \frac{\partial^2 p_{32}}{\partial |V_3|^2} + \lambda_{2Q} \frac{\partial^2 q_{23}}{\partial |V_3|^2} + \lambda_{3Q} \frac{\partial^2 q_{32}}{\partial |V_3|^2} \right) |V_3|^2
 \end{aligned}
 \tag{7.55}$$

Results are obtained after we apply the *decoupled optimal power flow solution*. Using incremental costs for generator 1 and 3 $dC_1/dP_{G1} = 7.5 P_{G1} + 2$ $dC_3/dP_{G3} = 6.0 P_{G3} + 1$.

To start the iterative process, initial values for P_{G1} , P_{G3} , θ_1 , θ_2 , θ_3 , λ_{1P} , λ_{2P} , λ_{3P} , Q_{G1} , Q_{G3} , V_1 , V_2 , V_3 , λ_{1Q} , λ_{2Q} , λ_{3Q} are $x_0 = [0.80 \ 0.75 \ 0 \ 0 \ 0 \ 1 \ 1 \ 1 \ 0.0 \ 0.0 \ 1 \ 1 \ 1 \ 1 \ 1]$, which seem reasonable to start the numerical process. An estimate might be obtained for these values if we solve a no-loss problem.

```

Elements =      2
Nodes        =      3
Elements (duplicated)
Elem  N_from  N_to  type  tap  tau  yelem  Bsh/2
  1    1      2    -1    1.050  0.087  1.0000 +j-10.0000  +j  0.0000
  2    2      3     1    1.000  0.000  2.0000 +j-15.0000  +j  0.0000
  3    2      1    -1    1.050  0.087  1.0000 +j-10.0000  +j  0.0000
  4    3      2     1    1.000  0.000  2.0000 +j-15.0000  +j  0.0000

```

Node Information

Node	type	Voltage	Angle	Pgen	Pload	Qgen	Qload
1	0	1.0000	0.0000	0.000	0.500	0.000	0.000
2	-1	1.0000	0.0000	0.000	0.750	0.000	0.408
3	1	1.0000	0.0000	0.000	0.300	0.000	0.000

Node Type

Generation = 2 Load = 1

Iteration_P 0.0 Maximum gradient = 7.000000e+000
 Iteration_Q 0.0 Maximum gradient = 1.000000e+000

```

Iteration_P 0.5   Maximum gradient = 9.668531e-001
Iteration_Q 0.5   Maximum gradient = 1.991190e-002
Iteration_P 1.0   Maximum gradient = 2.079699e-004
Iteration_Q 1.0   Maximum gradient = 1.736139e-006

```

Convergence at 3 iterations

Node information

Node	type	Voltage	Angle	Pgen	Pload	Qgen	Qload
1	0	1.0000	0.00	0.6224	0.5000	0.5237	0.0000
2	-1	0.9995	4.62	0.0000	0.7500	0.0000	0.4080
3	1	1.0000	7.04	0.9337	0.3000	-0.0631	0.0000

Element information

Elem	Nsa1	Nlleg	typee1	tap	tau	pkm	qkm
1	1	2	-1	1.050	5.002	0.1224	0.5237
1	2	1	-1	1.050	5.002	-0.1198	-0.4977
2	2	3	1	1.000	0.000	-0.6302	0.0897
2	3	2	1	1.000	0.000	0.6337	-0.0631

PLtot = 0.0061 QLtot = 0.0525

Lamda values

```

k = 1   LamdaP = 6.6681
k = 2   LamdaP = 6.6769
k = 3   LamdaP = 6.6024
k = 1   LamdaQ = 0.5237
k = 2   LamdaQ = 0.1851
k = 3   LamdaQ = -0.0631

```

Example 7.7

For a small four-node network (see Figure 7.11), assume that node voltages are 1.0 pu. Solve the minimum loss problem where control variables are P_{G1} , P_{G2} , P_{G3} , $|t|$ and τ . The equality constraints are the real power balances at each node.

Let us write the augmented Lagrangian to minimize the system's losses and to satisfy the real power balance at each node. First, let us solve the problem of keeping

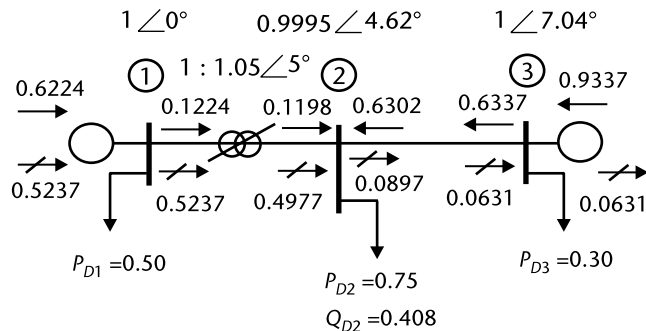


Figure 7.10 Three node system load flows for a minimum cost solution.

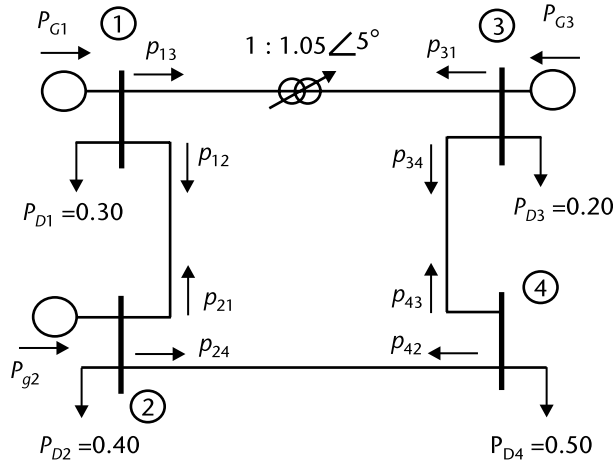


Figure 7.11 Four-node system load flows for optimal solution.

Table 7.1 Line Data System on Figure 7.11

Element	N from - k	N to - m	y_{km}	tap
1	1	2	$1.0 - j10$	-1
2	1	3	$1.0 - j10$	$t_\alpha + jt_\beta$
3	3	4	$1.5 - j15$	-1
4	2	4	$2.0 - j20$	-1

constant values for $|t|$ and τ . Voltage and reactive power flows are not included, assuming voltages are fixed at 1.0 pu and that there are no problems with the reactive power flows. Results are shown in Figure 7.12.

$$\zeta = P_{G1} + P_{G2} + P_{G3} - P_D + \lambda_{1L}(p_{12} + p_{13} - P_{G1} + P_{D1}) + \lambda_{2L}(p_{21} + p_{24} - P_{G2} + P_{D2}) + \lambda_{3L}(p_{31} + p_{34} - P_{G3} + P_{D3}) + \lambda_{4L}(p_{42} + p_{43} + P_{D4}) \quad (7.56)$$

Elements = 4

Nodes = 4

Elements (duplicated)

Elem	N_from	N_to	type	tap	tau	yelem	Bsh/2
1	1	2	-1	1.05	0.09	$1.0000 + j-10.0000$	+j 0.0000
2	1	3	1	1.00	0.00	$1.0000 + j-10.0000$	+j 0.0000
3	3	4	1	1.00	0.00	$1.5000 + j-15.0000$	+j 0.0000
4	2	4	1	1.00	0.00	$2.0000 + j-20.0000$	+j 0.0000
5	2	1	-1	1.05	0.09	$1.0000 + j-10.0000$	+j 0.0000
6	3	1	1	1.00	0.00	$1.0000 + j-10.0000$	+j 0.0000
7	4	3	1	1.00	0.00	$1.5000 + j-15.0000$	+j 0.0000
8	4	2	1	1.00	0.00	$2.0000 + j-20.0000$	+j 0.0000

Node Information

Node	type	Voltage	Angle	Pgen	Pload	Qgen	Qload
1	0	1.0000	0.0000	0.00	0.30	0.00	0.00
2	1	1.0000	0.0000	0.00	0.40	0.00	0.00
3	1	1.0000	0.0000	0.00	0.20	0.00	0.00
4	-1	1.0000	0.0000	0.00	0.50	0.00	0.00

Node Type Generation = 3 Load = 1
 Iteration = 0 Maxdev = 1.361140e+000
 Iteration = 1 Maxdev = 3.950764e-003
 Iteration = 2 Maxdev = 6.617341e-009

Node Information

Node	type	Voltage	Angle	Pgen	Pload	Qgen	Qload	Lamda
1	0	1.0000	0.00	0.3533	0.3000	0.5327	-0.0000	1.0000
2	1	1.0000	3.47	0.6369	0.4000	-0.5168	0.0000	1.0000
3	1	1.0000	1.60	0.4155	0.2000	-0.0174	0.0000	1.0000
4	-1	1.0000	1.85	0.0000	0.5000	0.0000	-0.0582	1.0029

Power flows

Elem	N_from	N_to	type1	tap	tau	pkm	qkm
1	1	2	-1	1.05	5.00	0.3328	0.5007
2	1	3	1	1.00	0.00	-0.2795	0.0319
3	3	4	1	1.00	0.00	-0.0648	0.0066
4	2	4	1	1.00	0.00	0.5665	-0.0486
5	2	1	-1	1.05	5.00	-0.3295	-0.4683
6	3	1	1	1.00	0.00	0.2803	-0.0241
7	4	3	1	1.00	0.00	0.0649	-0.0063
8	4	2	1	1.00	0.00	-0.5649	0.0646

PLtot = 0.0057 QLtot = 0.0566

The iterative solution for automatic adjustment on $|t|$ follows, keeping constant τ .

Transformers = 1
 Node Type
 Generation = 3 Load = 1

Iteration = 0 Maxdev = 1.061140e+000
 Iteration = 1 Maxdev = 3.166379e-002
 Iteration = 2 Maxdev = 3.341148e-005
 Iteration = 3 Maxdev = 3.458872e-011

Node Information

Node	type	Voltage	Angle	Pgen	Pload	Qgen	Qload	Lamda
1	0	1.0000	-0.00	0.3004	0.3000	0.0038	0.0000	1.0000
2	1	1.0000	3.42	0.6873	0.4000	-0.0131	0.0000	1.0000
3	1	1.0000	1.58	0.4155	0.2000	-0.0176	0.0000	1.0000
4	-1	1.0000	1.81	0.0000	0.5000	0.0000	-0.0581	1.0029

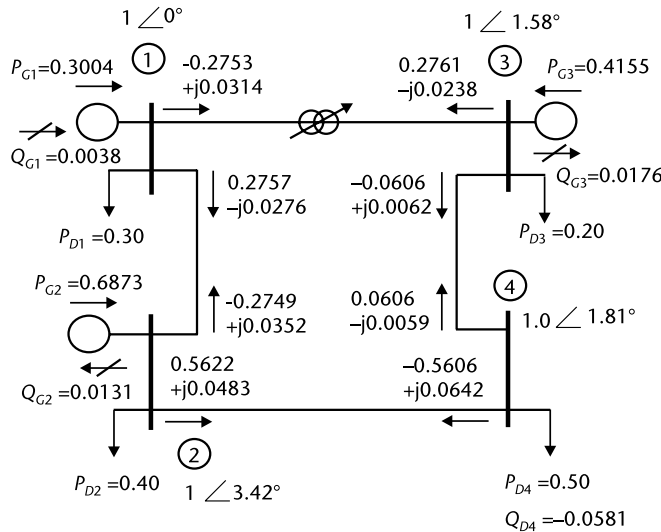


Figure 7.12 Four-node system load flows.

Power flows (from an to)

Elem	N_from	N_to	typeel	tap	tau	pkm	qkm
1	1	2	-1	0.9996	5.00	0.2757	-0.0276
2	1	3	1	1.0000	0.00	-0.2753	0.0314
3	3	4	1	1.0000	0.00	-0.0606	0.0062
4	2	4	1	1.0000	0.00	0.5622	-0.0483
5	2	1	-1	0.9996	5.00	-0.2749	0.0352
6	3	1	1	1.0000	0.00	0.2761	-0.0238
7	4	3	1	1.0000	0.00	0.0606	-0.0059
8	4	2	1	1.0000	0.00	-0.5606	0.0640

PLtot = 0.0031 QLtot = 0.0312

Real power losses decrease from 0.0057 to 0.0031 when we compared to the previous solution where the tap is fixed.

7.7 Hydrothermal Power System Coordination

One more component to control and operate a power system is to include (besides thermal power plants) hydrogeneration, geothermal, wind, or some other generation resources that represent energy contribution at those instances where its primary energy is available. The volume of water that can be generated with a hydroplant might be limited, and we may be required to use it within a given period. The problem is called *hydrothermal coordination*, and can be solved in the following steps:

- Minimize the total operating cost for the hydrothermal system.
- Write the augmented Lagrangian function. The necessary condition to attain the optimum, assuming convexity, is that its gradient should be zero.

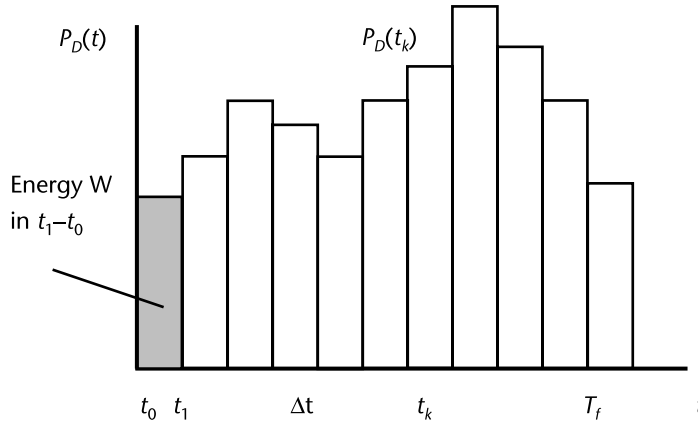


Figure 7.13 Stepwise demands for period $[0, T_f]$.

- In general, the gradient will be a nonlinear set of equations. To solve the problem, we apply Newton’s method.

7.7.1 Objective Function and Constraints

To grasp the details that go into the formulation of the problem, let us use a simple two-power plant problem: one thermal and one hydro. The objective is to minimize the cost of the fuel used by the thermal plant within the optimization period $[0, T_f]$ (see Figures 7.13 and 7.14). An input-output cost function is used for the thermal plant, \$/h is the input and the output is the net power P_T to the network. For the hydroplant, we assume that a water volume per hour is the available input and net power, and that P_H is the output. The equality constraints include:

- Load to be supplied and power transmission losses for each time period t_k .
- An equality constraint that considers the total volume of water available to be used by the hydrogenerator within the optimization period $[0, T_f]$.

$$\begin{aligned}
 & \min \sum_{k=1}^{T_f} C(P_T^k) t_k \\
 \text{subject to} \quad & P_D^k + P_L^k - P_H^k - P_T^k = 0 \\
 & \sum_{k=1}^{T_f} q(P_H^k, b^k) t_k - b = 0
 \end{aligned} \tag{7.57}$$

- b volume available
- $C(P_T^k)$ Cost function for thermal generation plant
- P_T^k Net power output form thermal plant at time t_k
- P_H^k Net power output from hydroplant at time t_k

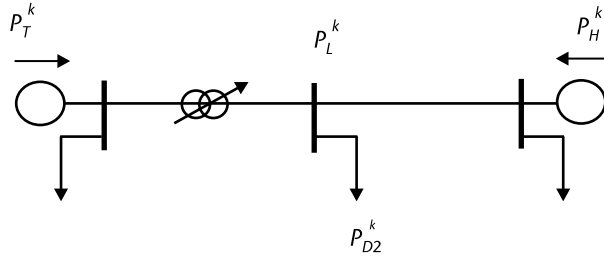


Figure 7.14 Coordination of two power plants, thermal and hydro.

P_L^k	Electrical power losses at time interval t_k
P_D^k	Electrical power demand at time interval t_k
t_k	Time interval k
T_f	Final time for the optimization period

The augmented Lagrangian follows as (7.58). The solution must be the gradient equal to zero at each discrete interval partition t_k for the study period.

$$\zeta = \sum_{k=1}^{T_f} \left[C(P_T^k) t_k + \lambda_p^k (P_D^k + P_L^k - P_T^k - P_H^k) t_k \right] + \lambda_b \left[\sum_{k=1}^{T_f} q(P_H^k, h^k) t_k - b \right] \quad (7.58)$$

$$\nabla \zeta = \begin{bmatrix} \frac{\partial \zeta}{\partial P_T^k} \\ \frac{\partial \zeta}{\partial P_H^k} \\ \frac{\partial \zeta}{\partial \lambda_p^k} \\ \dots \\ \frac{\partial \zeta}{\partial \lambda_b} \end{bmatrix} = \begin{bmatrix} \frac{\partial C(P_T^k)}{\partial P_T^k} t_k + \lambda_p^k \left(\frac{\partial P_L^k}{\partial P_T^k} - 1 \right) t_k \\ \lambda_p^k \left(\frac{\partial P_L^k}{\partial P_H^k} - 1 \right) t_k + \lambda_b \frac{\partial q(P_H^k, h^k)}{\partial P_H^k} t_k \\ (P_D^k + P_L^k - P_T^k - P_H^k) t_k \\ \dots \\ \sum_{k=1}^{T_f} q(P_H^k, h^k) t_k - b \end{bmatrix} = \begin{bmatrix} 0 \\ 0 \\ 0 \\ \dots \\ 0 \end{bmatrix} \quad (7.59)$$

From the first row in the gradient, we find the *short-term marginal cost* λ_p^k at the node of the thermal plant, penalized by an incremental loss factor. From the second row, λ_b is the *value of water*. This expression, combined with the incremental water flow, gives an equivalent *incremental cost* for the hydropower plant.

$$\lambda_p^k = \frac{\partial C(P_T^k)}{\partial P_T^k} \left(1 - \frac{\partial P_L^k}{\partial P_T^k} \right)^{-1} \quad (7.60)$$

$$\lambda_p^k = \lambda_b \frac{\partial q(P_H^k, h^k)}{\partial P_H^k} \left(1 - \frac{\partial P_L^k}{\partial P_H^k} \right)^{-1} \quad (7.61)$$

Where

$\partial P_L^k / \partial P_T^k$	Incremental losses for thermal plant
$\partial q(P_H^k, b^k) / \partial P_H^k$	Incremental flow for hydroplant, Mgal/MW
λ_b	Value of water, \$/Mgal
$\lambda_b (\partial q(P_H^k, b^k) / \partial P_H^k)$	Equivalent incremental cost for the hydroplant, \$/MW

At each electrical node, the power balance constraint appears as a gradient component. The last gradient element from (7.59) represents the total amount of water available within the time interval $[0, T_f]$ for the optimization process.

$$q(P_H^1, b^1)t_1 + q(P_H^2, b^2)t_2 + \dots + q(P_H^{T_f}, b^{T_f})t_{T_f} - b = 0 \tag{7.62}$$

We use (7.59) and solve for each time interval t_k . The solution to (7.62) covers the optimization period T , and it is assured through (7.62).

Example 7.8

Given a cost function for a thermal generator, the amount of water q discharged through the hydraulic turbine, and an expression for electrical losses, the total operating cost must be minimized. The load to be supplied is 450 MW during a period of 10 hours (see Figure 7.15). Solve and point out the economic interpretation for the solution when the total amount of water available is $b = 1,000$ MPC.

$$\left[\begin{array}{l} C(P_T) = 2.7P_T + 0.003(P_T)^2 \\ q(P_H) = 8.568 + 0.216P_H \\ P_L(P_T, P_H) = 0.4 \times 10^{-4}(P_T)^2 + 1.43 \times 10^{-4}(P_H)^2 \end{array} \right] \tag{7.63}$$

Where:

$C(P_T)$	Thermal plant cost in \$/h
$q(P_H)$	Water discharge, MCF/h
$P_L(P_T, P_H)$	Power losses, MW

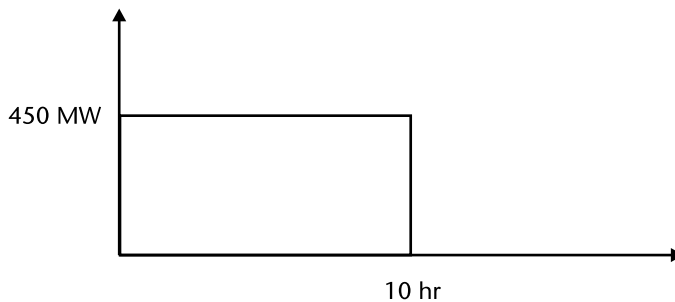


Figure 7.15 Demand required from the two power plants.

The augmented Lagrangian includes the cost function, power balance, and the available water volume as equality constraints. The gradient for one time interval of $t_1 = 10$ hours is a nonlinear set of equations that are solved by Newton's iterative process.

$$\zeta = C(P_T^1)t_1 + \lambda_p^1(P_D^1 + P_L^1 - P_T^1 - P_H^1)t_1 + \lambda_b(q(P_H^1, b^1)t_1 - b) \quad (7.64)$$

$$\nabla\zeta = \begin{bmatrix} \frac{\partial\zeta}{\partial P_T^1} \\ \frac{\partial\zeta}{\partial P_H^1} \\ \frac{\partial\zeta}{\partial \lambda_p^1} \\ \frac{\partial\zeta}{\partial \lambda_b} \end{bmatrix} = \begin{bmatrix} \frac{\partial C(P_T^1)}{\partial P_T^1}t_1 + \lambda_p^1\left(\frac{\partial P_L^1}{\partial P_T^1} - 1\right)t_1 \\ \lambda_p^1\left(\frac{\partial P_L^1}{\partial P_H^1} - 1\right)t_1 + \lambda_b\frac{\partial q(P_H^1, b^1)}{\partial P_H^1}t_1 \\ (P_D^1 + P_L^1 - P_T^1 - P_H^1)t_1 \\ q(P_H^1, b^1)t_1 - b \end{bmatrix} = \begin{bmatrix} 0 \\ 0 \\ 0 \\ 0 \end{bmatrix} \quad (7.65)$$

$$\begin{bmatrix} \frac{dC(P_T^1)}{dP_T^1} = 2.7 + 0.006 P_T^1 \text{ \$/MWh} \\ \frac{\partial P_L^1}{\partial P_T^1} = 0.8 \times 10^{-4} P_T^1 \text{ pu} \\ \frac{\partial P_L^1}{\partial P_H^1} = 2.86 \times 10^{-4} P_H^1 \text{ pu} \\ \frac{\partial q(P_H^1)}{\partial P_H^1} = 0.216 \text{ MCF/MW} \end{bmatrix} \quad (7.66)$$

Using partial derivatives (7.66), the elements of the gradient are in (7.67). To start the iterative process, initial proposed values might be about half the total demand. For the Lagrange multipliers, a value of 2 is selected: $[P_T \ P_H \ \lambda_p \ \lambda_b] = [250 \ 250 \ 2 \ 2]$.

$$\nabla\zeta = \begin{bmatrix} g_1 \\ g_2 \\ g_3 \\ g_4 \end{bmatrix} = \begin{bmatrix} (2.7 + 0.006P_T^1)t_1 + \lambda_p^1(0.8 \times 10^{-4}P_T^1 - 1)t_1 \\ \lambda_p^1(2.86 \times 10^{-4}P_H^1 - 1)t_1 + \lambda_b(0.216)t_1 \\ (450 + 0.4 \times 10^{-4}(P_T^1)^2 + 1.43 \times 10^{-4}(P_H^1)^2 - P_T^1 - P_H^1)t_1 \\ (8.568 + 0.216P_H^1)t_1 - 1,000 \end{bmatrix} = \begin{bmatrix} 0 \\ 0 \\ 0 \\ 0 \end{bmatrix} \quad (7.67)$$

The Hessian matrix of second-order partial derivatives has elements that change at each iteration:

$$\begin{bmatrix} (0.006 + \lambda_p^1 0.8 \times 10^{-4})t_1 & 0 & (0.8 \times 10^{-4} P_T^1 - 1)t_1 & 0 \\ 0 & \lambda_p^1 2.86 \times 10^{-4} t_1 & (2.86 \times 10^{-4} P_H^1 - 1)t_1 & 0.216t_1 \\ (0.8 \times 10^{-4} P_T^1 - 1)t_1 & (2.86 \times 10^{-4} P_H^1 - 1)t_1 & 0 & 0 \\ 0 & 0.216t_1 & 0 & 0 \end{bmatrix} \begin{bmatrix} \Delta P_T^1 \\ \Delta P_H^1 \\ \Delta \lambda_p^1 \\ \Delta \lambda_b \end{bmatrix} = - \begin{bmatrix} g_1 \\ g_2 \\ g_3 \\ g_4 \end{bmatrix} \quad (7.68)$$

Hydro-Thermal Coordination

Total demand 450.00 time period 10.00 hours

Initial values PT = 225.00 PH = 225.00 lamdaP = 2.0000 lamdaH = 2.0000

Converged Solution Iteration = 3 Maxdev = 1.494413e-009

Power 52.44 MW thermal plant 423.30 MW hydro plant

Total Power 475.73 MW

Power Losses 25.73 MW

ILosseST 0.0042 pu ILossesH 0.1211 pu

LamdaP 3.0273 \$/MWh Lamda_h 12.3186 \$/MCF (water equivalent cost)

ICostTer 3.0146 \$/MWh Penalty 1.0042 pu PenalizedCost 3.0273 \$/MWh

ICostHyd 2.6608 \$/MWh Penalty 1.1377 pu PenalizedCost 3.0273 \$/MWh

TotCost 1498.27 \$ Water Used 1000.00 MCF

The solution shown in Figures 7.16 and 7.17 and units for the calculated results are:

$$\lambda = \frac{\partial C}{\partial P_T^1} = 3.0146 \text{ \$/MWh}$$

$$\frac{\partial P_L^1}{\partial P_T^1} = 0.004195 \text{ pu}$$

$$P_D^1 = 450 \text{ MW}$$

$$\frac{dC}{dP_T^1} \left(1 - \frac{\partial P_L^1}{\partial P_T^1} \right)^{-1} = 3.2073 \text{ \$/MWh}$$

$$\lambda_p^1 = 3.0273 \text{ \$/MWh}$$

$$\lambda_b = 12.3186 \text{ \$/MPC}$$

$$\lambda_b \frac{\partial q}{\partial P_H^1} = 2.66082 \text{ \$/MWh}$$

$$\frac{\partial P_L^1}{\partial P_H^1} = 0.121063 \text{ pu}$$

$$\lambda_b \frac{\partial q}{\partial P_H^1} \left(1 - \frac{\partial P_L^1}{\partial P_H^1} \right)^{-1} = 3.2073 \text{ \$/MWh}$$

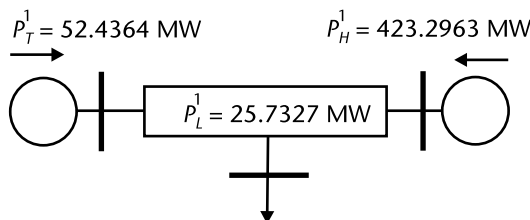


Figure 7.16 Coordinated solution to supply demand by a thermal and a hydro-plant.

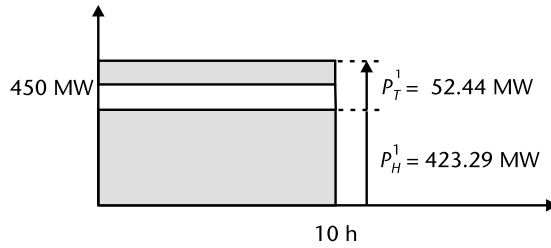


Figure 7.17 Generation blocks for the hydro and the thermal, demand, and losses.

The numerical solution shows an operating point at the *same incremental cost* for the thermal plant the penalized incremental cost as well as the penalized *equivalent incremental cost* for the hydroplant.

Example 7.9

For a thermal equivalent, the water discharge for the hydraulic plant, losses, and a load demand as shown by (7.70), minimize the total operating cost when the amount of available water is $b = 1,000$ MPC.

The problem is similar to Example 7.8. However, we now extend the study time to various periods and coordinate for two periods, $t_1 = 10$ hours and $t_2 = 14$ hours (see Figure 7.18). The augmented Lagrangian has to include the cost function and the power balance equalities for periods one and two. The Lagrangian function must include an equality constraint to coordinate the water usage at each period, and must also comply with the constraint of total water available.

$$\zeta = C(P_T^1)t_1 + \lambda_p^1(P_D^1 + P_L^1 - P_T^1 - P_H^1)t_1 + C(P_T^2)t_2 + \lambda_p^2(P_D^2 + P_L^2 - P_T^2 - P_H^2)t_2 + \lambda_b[q(P_H^1, b^1)t_1 + q(P_H^2, b^2)t_2 - b] \tag{7.69}$$

The thermal cost, water discharge function, and losses are:

$$\left[\begin{array}{l} C(P_T) = 2.7P_T + 0.003(P_T)^2 \text{ \$/h} \\ q(P_H) = 8.568 + 0.216P_H \text{ MCF/h} \\ P_L(P_T, P_H) = 0.4 \times 10^{-4}(P_T)^2 + 1.43 \times 10^{-4}(P_H)^2 \text{ MW} \end{array} \right] \tag{7.70}$$

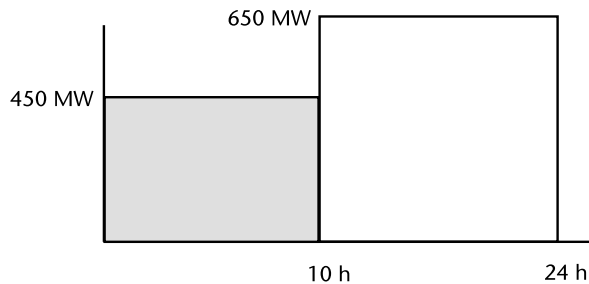


Figure 7.18 Load demand for time changing values.

The augmented Lagrangian (7.69) includes unknowns for each time periods t_1 and t_2 and one water equation to coordinate the total use of water within the whole time period.

$$\nabla \zeta = \begin{bmatrix} \frac{\partial \zeta}{\partial P_T^1} \\ \frac{\partial \zeta}{\partial P_H^1} \\ \frac{\partial \zeta}{\partial \lambda_p^1} \\ \frac{\partial \zeta}{\partial P_T^2} \\ \frac{\partial \zeta}{\partial P_H^2} \\ \frac{\partial \zeta}{\partial \lambda_p^2} \\ \frac{\partial \zeta}{\partial \lambda_b} \end{bmatrix} = \begin{bmatrix} \frac{\partial C(P_T^1)}{\partial P_T^1} t_1 + \lambda_p^1 \left(\frac{\partial P_L^1}{\partial P_T^1} - 1 \right) t_1 \\ \lambda_p^1 \left(\frac{\partial P_L^1}{\partial P_H^1} - 1 \right) t_1 + \lambda_b \frac{\partial q(P_H^1, b^1)}{\partial P_H^1} t_1 \\ (P_D^1 + P_L^1 - P_T^1 - P_H^1) t_1 \\ \frac{\partial C(P_T^2)}{\partial P_T^2} t_2 + \lambda_p^2 \left(\frac{\partial P_L^2}{\partial P_T^2} - 1 \right) t_2 \\ \lambda_p^2 \left(\frac{\partial P_L^2}{\partial P_H^2} - 1 \right) t_2 + \lambda_b \frac{\partial q(P_H^2, b^2)}{\partial P_H^2} t_2 \\ (P_D^2 + P_L^2 - P_T^2 - P_H^2) t_2 \\ q(P_H^1, b^1) t_1 + q(P_H^2, b^2) t_2 - b \end{bmatrix} = \begin{bmatrix} 0 \\ 0 \\ 0 \\ 0 \\ 0 \\ 0 \\ 0 \end{bmatrix} \quad (7.71)$$

$$\nabla \zeta = \begin{bmatrix} g_1 \\ g_2 \\ g_3 \\ g_4 \\ g_5 \\ g_6 \\ g_7 \end{bmatrix} = \begin{bmatrix} (2.7 + 0.006P_T^1) t_1 + \lambda_p^1 (0.8 \times 10^{-4} P_T^1 - 1) t_1 \\ \lambda_p^1 (2.86 \times 10^{-4} P_H^1 - 1) t_1 + \lambda_b (0.216) t_1 \\ (450 + 0.4 \times 10^{-4} (P_T^1)^2 + 1.43 \times 10^{-4} (P_H^1)^2 - P_T^1 - P_H^1) t_1 \\ (2.7 + 0.006P_T^2) t_2 + \lambda_p^2 (0.8 \times 10^{-4} P_T^2 - 1) t_2 \\ \lambda_p^2 (2.86 \times 10^{-4} P_H^2 - 1) t_2 + \lambda_b (0.216) t_2 \\ (650 + 0.4 \times 10^{-4} (P_T^2)^2 + 1.43 \times 10^{-4} (P_H^2)^2 - P_T^2 - P_H^2) t_2 \\ (8.568 + 0.216P_H^1) t_1 + (8.568 + 0.216P_H^2) t_2 - 1,000 \end{bmatrix} = \begin{bmatrix} 0 \\ 0 \\ 0 \\ 0 \\ 0 \\ 0 \\ 0 \end{bmatrix} \quad (7.72)$$

Initial values to start the iterative process $[P_{T1} \ P_{H1} \ \lambda_{p1} \ P_{T2} \ P_{H2} \ \lambda_{p2} \ \lambda_H] = [225 \ 225 \ 2 \ 325 \ 325 \ 2 \ 2]$. The solution is shown in Figure 7.19.

Hydro-Thermal Coordination

Total demand 450.00 time period 10.00 hours

Total demand 650.00 time period 14.00 hours

Initial values PT1 = 225.00 PH1 = 225.00 lamdaP1 = 2.0000

Initial values PT2 = 325.00 PH2 = 325.00 lamdaP2 = 2.0000 lamdaH = 2.0000

Converged Solution Iterations = 3 Maxdev = 8.535247e-007

First interval

Power 401.35 MW thermal plant
 Power 55.54 MW hydro plant
 Total Power 456.88 MW
 Power Losses 6.88 MW

ILossesT 0.0321 pu ILossesH 0.0159 pu
 LamdaP 5.2775 \$/MWh Lamda_h 24.0449 \$/MCF (water equivalent cost)
 ICostTer 5.1081 \$/MWh Penalty F 1.0332 pu PenalizedCost 5.2775 \$/MWh
 ICostHyd 5.1937 \$/MWh Penalty F 1.0161 pu PenalizedCost 5.2775 \$/MWh

Second interval

Power 441.91 MW thermal plant
 Power 223.02 MW hydro plant
 Total Power 664.92 MW
 Power Losses 14.92 MW

ILossesT 0.0354 pu ILossesH 0.0638 pu
 LamdaP 5.5475 \$/MWh Lamda_h 24.0449 \$/MCF (water equivalent cost)
 ICostTer 5.3514 \$/MWh Penalty F 1.0366 pu PenalizedCost 5.5475 \$/MWh
 ICostHyd 5.1937 \$/MWh Penalty F 1.0681 pu PenalizedCost 5.5475 \$/MWh

TotCost 40574.54 \$ Water Used 1000.00 MCF

Other interesting problems include coordination between thermal plants and multiple energy resources (i.e., water resources, solar, and wind contribution to the energy balance). In some cases, the water volume equation is an equality constraint that establishes the amount of energy available instead of volume. Other types of power plants with available energy and of course hydroplants that have a cascade configuration can be included. The cascaded case means that water is used to generate more than once the hydronetwork might be quite involved and the water time travel between hydroplants could be important and must be included in the model.

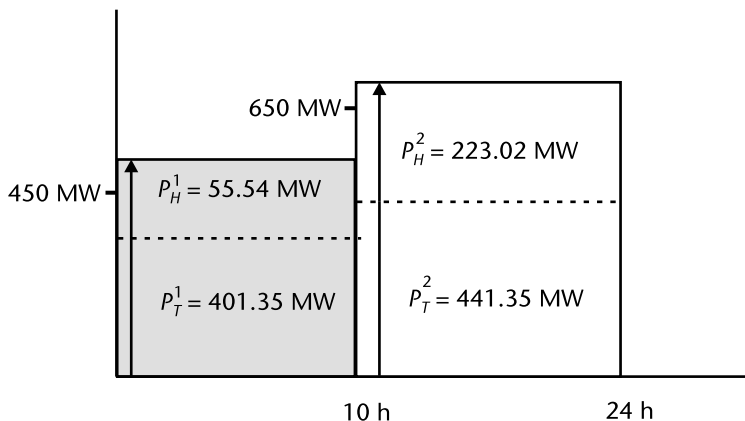


Figure 7.19 Hydro and thermal generation to supply demand and losses.

Variations in a general coordination problem require quite of bit of details to include both equality constraints and inequality constraints. Such material is part of a specialized optimal power system study needed in the planning and operating areas where we face a complex mix of energy power resources with constant output as nuclear and big thermal plants or intermittent contribution as wind and solar.

7.8 Second-Order Derivatives

The partial second-order derivatives for real and reactive power flows are crucial to the proper solution implementation of the optimal power flow as seen in Sections 7.6 and 7.7. The power flows might be through a complex transformer or in transmission lines. The partial derivatives are with respect to state variables, nodal angles, and voltage magnitudes. For a transformer with complex tap, partial derivatives include tap magnitude and the phase-shifting angle.

$$p_{km} = +|V_k|^2 |t|^2 g_{km} - |V_k||V_m||t|g_{km} \cos(\theta_k - \theta_m + \tau) - |V_k||V_m||t|b_{km} \sin(\theta_k - \theta_m + \tau) \quad (7.73)$$

$$q_{km} = -|V_k|^2 |t|^2 b_{km} - |V_k||V_m||t|g_{km} \sin(\theta_k - \theta_m + \tau) + |V_k||V_m||t|b_{km} \cos(\theta_k - \theta_m + \tau) \quad (7.74)$$

The partial second-order derivatives required for p_{km} and q_{km} take advantage of the symmetric nature of the following array where 36 expressions are in (7.75). However, due to the symmetric nature of the results, we will only show 21 expressions.

$$\begin{array}{cccccc}
 \theta_k^2 & \theta_k \theta_m & \theta_k \tau & \theta_k |V_k| & \theta_k |V_m| & \theta_k |t| \\
 \theta_m \theta_k & \theta_m^2 & \theta_m \tau & \theta_m |V_k| & \theta_m |V_m| & \theta_m |t| \\
 \tau \theta_k & \tau \theta_m & \tau^2 & \tau |V_k| & \tau |V_m| & \tau |t| \\
 |V_k| \theta_k & |V_k| \theta_m & |V_k| \tau & |V_k|^2 & |V_k||V_m| & |V_k||t| \\
 |V_m| \theta_k & |V_m| \theta_m & |V_m| \tau & |V_m||V_k| & |V_m|^2 & |V_m||t| \\
 |t| \theta_k & |t| \theta_m & |t| \tau & |t||V_k| & |t||V_m| & |t|^2
 \end{array} \quad (7.75)$$

For a complex transformer, the partial derivatives of real power p_{km} , starting with partial first-order derivatives from (6.29) to (6.34) are

$$\frac{\partial^2 p_{km}}{\partial \theta_k^2} = -\frac{\partial q_{km}}{\partial \theta_k} = +|V_k|^2 |t|^2 g_{km} - p_{km} \quad (7.76)$$

$$\frac{\partial^2 p_{km}}{\partial \theta_k \partial \theta_m} = +\frac{\partial q_{km}}{\partial \theta_k} = -|V_k|^2 |t|^2 g_{km} + p_{km} \quad (7.77)$$

$$\frac{\partial^2 p_{km}}{\partial \theta_k \partial \tau} = -\frac{\partial q_{km}}{\partial \theta_k} = +|V_k|^2 |t|^2 g_{km} - p_{km} \quad (7.78)$$

$$\frac{\partial^2 p_{km}}{\partial \theta_k \partial |V_k|} |V_k| = -|V_k|^2 |t|^2 b_{km} - q_{km} \quad (7.79)$$

$$\frac{\partial^2 p_{km}}{\partial \theta_k \partial |V_m|} |V_m| = -|V_k|^2 |t|^2 b_{km} - q_{km} \quad (7.80)$$

$$\frac{\partial^2 p_{km}}{\partial \theta_k \partial |t|} |t| = -|V_k|^2 |t|^2 b_{km} - q_{km} \quad (7.81)$$

$$\frac{\partial^2 p_{km}}{\partial \theta_m^2} = +\frac{\partial q_{km}}{\partial \theta_m} = +|V_k|^2 |t|^2 g_{km} - p_{km} \quad (7.82)$$

$$\frac{\partial^2 p_{km}}{\partial \theta_m \partial \tau} = -\frac{\partial q_{km}}{\partial \theta_m} = -|V_k|^2 |t|^2 g_{km} + p_{km} \quad (7.83)$$

$$\frac{\partial^2 p_{km}}{\partial \theta_m \partial |V_k|} |V_k| = +|V_k|^2 |t|^2 b_{km} + q_{km} \quad (7.84)$$

$$\frac{\partial^2 p_{km}}{\partial \theta_m \partial |V_m|} |V_m| = +|V_k|^2 |t|^2 b_{km} + q_{km} \quad (7.85)$$

$$\frac{\partial^2 p_{km}}{\partial \theta_m \partial |t|} |t| = +|V_k|^2 |t|^2 b_{km} + q_{km} \quad (7.86)$$

$$\frac{\partial^2 p_{km}}{\partial \tau^2} = -\frac{\partial q_{km}}{\partial \tau} = +|V_k|^2 |t|^2 g_{km} - p_{km} \quad (7.87)$$

$$\frac{\partial^2 p_{km}}{\partial \tau \partial |V_k|} |V_k| = -|V_k|^2 |t|^2 b_{km} - q_{km} \quad (7.88)$$

$$\frac{\partial^2 p_{km}}{\partial \tau \partial |V_m|} |V_m| = -|V_k|^2 |t|^2 b_{km} - q_{km} \quad (7.89)$$

$$\frac{\partial^2 p_{km}}{\partial \tau \partial |t|} |t| = -|V_k|^2 |t|^2 b_{km} - q_{km} \quad (7.90)$$

$$\frac{\partial^2 p_{km}}{\partial |V_k|^2} |V_k|^2 = 2|V_k|^2 |t|^2 g_{km} \quad (7.91)$$

$$\frac{\partial^2 p_{km}}{\partial |V_k| \partial |V_m|} |V_m| |V_k| = -|V_k|^2 |t|^2 g_{km} + p_{km} \quad (7.92)$$

$$\frac{\partial^2 p_{km}}{\partial |V_k| \partial |t|} |t| |V_k| = +3|V_k|^2 |t|^2 g_{km} + p_{km} \quad (7.93)$$

$$\frac{\partial^2 p_{km}}{\partial |V_m|^2} |V_m|^2 = 0 \quad (7.94)$$

$$\frac{\partial^2 p_{km}}{\partial |V_m| \partial |t|} |t| |V_m| = -|V_k|^2 |t|^2 g_{km} + p_{km} \quad (7.95)$$

$$\frac{\partial^2 p_{km}}{\partial |t|^2} |t|^2 = 2|V_k|^2 |t|^2 g_{km} \quad (7.96)$$

For a complex power transformer, the partial derivatives of reactive power q_{km} starting from (6.36) to (6.41) are

$$\frac{\partial^2 q_{km}}{\partial \theta_k^2} = \frac{\partial p_{km}}{\partial \theta_k} = -|V_k|^2 |t|^2 b_{km} - q_{km} \quad (7.97)$$

$$\frac{\partial^2 q_{km}}{\partial \theta_k \partial \theta_m} = -\frac{\partial p_{km}}{\partial \theta_k} = +|V_k|^2 |t|^2 b_{km} + q_{km} \quad (7.98)$$

$$\frac{\partial^2 q_{km}}{\partial \theta_k \partial \tau} = \frac{\partial p_{km}}{\partial \theta_k} = -|V_k|^2 |t|^2 b_{km} - q_{km} \quad (7.99)$$

$$\frac{\partial^2 q_{km}}{\partial \theta_k \partial |V_k|} |V_k| = -|V_k|^2 |t|^2 g_{km} + p_{km} \quad (7.100)$$

$$\frac{\partial^2 q_{km}}{\partial \theta_k \partial |V_m|} |V_m| = -|V_k|^2 |t|^2 g_{km} + p_{km} \quad (7.101)$$

$$\frac{\partial^2 q_{km}}{\partial \theta_k \partial |t|} |t| = -|V_k|^2 |t|^2 g_{km} + p_{km} \quad (7.102)$$

$$\frac{\partial^2 q_{km}}{\partial \theta_m^2} = -\frac{\partial p_{km}}{\partial \theta_m} = -|V_k|^2 |t|^2 b_{km} - q_{km} \quad (7.103)$$

$$\frac{\partial^2 q_{km}}{\partial \theta_m \partial \tau} = \frac{\partial p_{km}}{\partial \theta_m} = +|V_k|^2 |t|^2 b_{km} + q_{km} \quad (7.104)$$

$$\frac{\partial^2 q_{km}}{\partial \theta_m \partial |V_k|} |V_k| = +|V_k|^2 |t|^2 g_{km} - p_{km} \quad (7.105)$$

$$\frac{\partial^2 q_{km}}{\partial \theta_m \partial |V_m|} |V_m| = +|V_k|^2 |t|^2 g_{km} - p_{km} \quad (7.106)$$

$$\frac{\partial^2 q_{km}}{\partial \theta_m \partial |t|} = \frac{1}{|t|} \frac{\partial q_{km}}{\partial \theta_m} = \frac{+|V_k|^2 |t|^2 g_{km} - p_{km}}{|t|} \quad (7.107)$$

$$\frac{\partial^2 q_{km}}{\partial \tau^2} = \frac{\partial p_{km}}{\partial \tau} = -|V_k|^2 |t|^2 b_{km} - q_{km} \quad (7.108)$$

$$\frac{\partial^2 q_{km}}{\partial \tau \partial |V_k|} |V_k| = -|V_k|^2 |t|^2 g_{km} + p_{km} \quad (7.109)$$

$$\frac{\partial^2 q_{km}}{\partial \tau \partial |V_m|} |V_m| = -|V_k|^2 |t|^2 g_{km} + p_{km} \quad (7.110)$$

$$\frac{\partial^2 q_{km}}{\partial \tau \partial |t|} |t| = -|V_k|^2 |t|^2 g_{km} + p_{km} \quad (7.111)$$

$$\frac{\partial^2 q_{km}}{\partial |V_k|^2} |V_k|^2 = -2|V_k|^2 |t|^2 b_{km} \quad (7.112)$$

$$\frac{\partial^2 q_{km}}{\partial |V_k| \partial |V_m|} |V_k| |V_m| = +|V_k|^2 |t|^2 b_{km} + q_{km} \quad (7.113)$$

$$\frac{\partial^2 q_{km}}{\partial |V_k| \partial |t|} |V_k| |t| = -3|V_k|^2 |t|^2 b_{km} + q_{km} \quad (7.114)$$

$$\frac{\partial^2 q_{km}}{\partial |V_m|^2} |V_m|^2 = 0 \quad (7.115)$$

$$\frac{\partial^2 q_{km}}{\partial |V_m| \partial |t|} |V_m| |t| = +|V_k|^2 |t|^2 b_{km} + q_{km} \quad (7.116)$$

$$\frac{\partial^2 q_{km}}{\partial |t|^2} |t|^2 = -2|V_k|^2 |t|^2 b_{km} \tag{7.117}$$

For partial derivatives of second-order in a transmission line (see Figure 7.20), the real and reactive power flows show that compared with the complex transformer equations $|t| = 1$ and $\tau = 0$. Instead, the charging susceptance B_{sb2} must be included in the reactive power flow. The reduced array (7.118) shows that by symmetry only ten expressions are required.

$$\begin{matrix} \theta_k^2 & \theta_k \theta_m & \theta_k |V_k| & \theta_k |V_m| \\ \theta_m \theta_k & \theta_m^2 & \theta_m |V_k| & \theta_m |V_m| \\ |V_k| \theta_k & |V_k| \theta_m & |V_k|^2 & |V_k| |V_m| \\ |V_m| \theta_k & |V_m| \theta_m & |V_m| |V_k| & |V_m|^2 \end{matrix} \tag{7.118}$$

$$p_{km} = |V_k|^2 g_{km} - |V_k| |V_m| g_{km} \cos \theta_{km} - |V_k| |V_m| b_{km} \sin \theta_{km} \tag{7.119}$$

$$q_{km} = -|V_k|^2 (b_{km} + B_{sb/2}) - |V_k| |V_m| g_{km} \sin \theta_{km} + |V_k| |V_m| b_{km} \cos \theta_{km} \tag{7.120}$$

The partial second-order derivatives for real power p_{km} from (6.67) to (6.70):

$$\frac{\partial^2 p_{km}}{\partial \theta_k^2} = -\frac{\partial q_{km}}{\partial \theta_k} = +|\tilde{V}_k|^2 g_{km} - p_{km} \tag{7.121}$$

$$\frac{\partial^2 p_{km}}{\partial \theta_k \partial \theta_m} = +\frac{\partial q_{km}}{\partial \theta_k} = -|\tilde{V}_k|^2 g_{km} + p_{km} \tag{7.122}$$

$$\frac{\partial^2 p_{km}}{\partial \theta_k \partial |\tilde{V}_k|} |\tilde{V}_k| = -|\tilde{V}_k|^2 (b_{km} + B_{sb/2}) - q_{km} \tag{7.123}$$

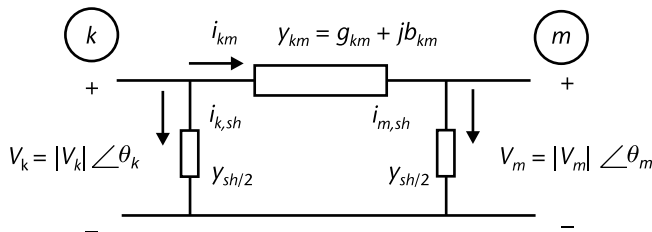


Figure 7.20 Transmission line π model.

$$\frac{\partial^2 p_{km}}{\partial \theta_k \partial |\tilde{V}_m|} |\tilde{V}_m| = -|\tilde{V}_k|^2 (b_{km} + B_{sh/2}) - q_{km} \quad (7.124)$$

$$\frac{\partial^2 p_{km}}{\partial \theta_m^2} = \frac{\partial}{\partial \theta_m} \left[+|\tilde{V}_k|^2 (b_{km} + B_{sh/2}) + q_{km} \right] = \frac{\partial q_{km}}{\partial \theta_m} = +|\tilde{V}_k|^2 g_{km} - p_{km} \quad (7.125)$$

$$\frac{\partial^2 p_{km}}{\partial \theta_m \partial |\tilde{V}_k|} |\tilde{V}_k| = +|\tilde{V}_k|^2 (b_{km} + B_{sh/2}) + q_{km} \quad (7.126)$$

$$\frac{\partial^2 p_{km}}{\partial \theta_m \partial |\tilde{V}_m|} |\tilde{V}_m| = +|\tilde{V}_k|^2 (b_{km} + B_{sh/2}) + q_{km} \quad (7.127)$$

$$\frac{\partial^2 p_{km}}{\partial |\tilde{V}_k|^2} |\tilde{V}_k|^2 = 2|\tilde{V}_k|^2 g_{km} \quad (7.128)$$

$$\frac{\partial^2 p_{km}}{\partial |\tilde{V}_k| \partial |\tilde{V}_m|} |\tilde{V}_m| |\tilde{V}_k| = -|\tilde{V}_k|^2 g_{km} + p_{km} \quad (7.129)$$

$$\frac{\partial^2 p_{km}}{\partial |\tilde{V}_m|^2} |\tilde{V}_m|^2 = 0 \quad (7.130)$$

The partial second-order derivatives for the reactive power q_{km} from (6.72) to (6.75) are:

$$\frac{\partial^2 q_{km}}{\partial \theta_k^2} = \frac{\partial}{\partial \theta_k} \left[-|\tilde{V}_k|^2 g_{km} + p_{km} \right] = \frac{\partial p_{km}}{\partial \theta_k} = -|\tilde{V}_k|^2 (b_{km} + B_{sh/2}) - q_{km} \quad (7.131)$$

$$\frac{\partial^2 q_{km}}{\partial \theta_k \partial \theta_m} = \frac{\partial}{\partial \theta_k} \left[+|\tilde{V}_k|^2 g_{km} - p_{km} \right] = -\frac{\partial p_{km}}{\partial \theta_k} = +|\tilde{V}_k|^2 (b_{km} + B_{sh/2}) + q_{km} \quad (7.132)$$

$$\frac{\partial^2 q_{km}}{\partial \theta_k \partial |\tilde{V}_k|} |\tilde{V}_k| = -|\tilde{V}_k|^2 g_{km} + p_{km} \quad (7.133)$$

$$\frac{\partial^2 q_{km}}{\partial \theta_k \partial |\tilde{V}_m|} |\tilde{V}_m| = -|\tilde{V}_k|^2 g_{km} + p_{km} \quad (7.134)$$

$$\frac{\partial^2 q_{km}}{\partial \theta_m^2} = \frac{\partial}{\partial \theta_m} \left[+|\tilde{V}_k|^2 g_{km} - p_{km} \right] = -\frac{\partial p_{km}}{\partial \theta_m} = -|\tilde{V}_k|^2 (b_{km} + B_{sh/2}) - q_{km} \quad (7.135)$$

$$\frac{\partial^2 q_{km}}{\partial \theta_m \partial |\tilde{V}_k|} |\tilde{V}_k| = + |\tilde{V}_k|^2 g_{km} - p_{km} \quad (7.136)$$

$$\frac{\partial^2 q_{km}}{\partial \theta_m \partial |\tilde{V}_m|} |\tilde{V}_m| = + |\tilde{V}_k|^2 g_{km} - p_{km} \quad (7.137)$$

$$\frac{\partial^2 q_{km}}{\partial |\tilde{V}_k|^2} |\tilde{V}_k|^2 = -2 |\tilde{V}_k|^2 (b_{km} + B_{sb/2}) \quad (7.138)$$

$$\frac{\partial^2 q_{km}}{\partial |\tilde{V}_k| \partial |\tilde{V}_m|} |\tilde{V}_k| |\tilde{V}_m| = + |\tilde{V}_k|^2 (b_{km} + B_{sb/2}) + q_{km} \quad (7.139)$$

$$\frac{\partial^2 q_{km}}{\partial |\tilde{V}_m|^2} |\tilde{V}_m|^2 = 0 \quad (7.140)$$

References

- [1] El-Hawary, M. E., and G. S. Christensen, *Optimal Operation of Electric Power Systems*, New York: Academic Press, 1979.

Real and Reactive Power and Frequency Control

8.1 Introduction

The electrical power system continually experiences changes in its daily operating conditions. A load evolves and is determined by the daily use of electrical energy by industries, households, offices, and services. The changing load pattern requires the commitment of enough generating units in order to satisfy the required power and energy usage. Also, some units must be synchronized in order to have an appropriate operating reserve. The power reserve is determined based on the amount of load and the nature of the electric system, and also because generating units need to be prepared to respond to situations such as possible outages, faults, and line tripping.

One indication that the system meets the real power requirements at every instant is the system's frequency, deviations from a nominal value, and how steep its change gives an indication about the severity of an unmatched power within the system. By appropriate and coordinated control actions in the system, the relief of overloaded elements is accomplished and the voltage profile is kept within prescribed bounds. Control actions are changes in real power injections by generators, phase-shifting by transformers, and tap changing and reactive VARs by compensating devices. To these now-basic controls, electrical power systems have devices based on power electronics that handle energy in a way that its time response is very fast. Flexible AC transmission systems (FACTS) will be briefly discussed in Sections 8.7–8.10.

As important as it is to match the system's load by the appropriate amount of generation and its regulating control characteristics, it is equally important to be able to control the voltage at every electrical node in the system within prescribed limits. The variables that are intrinsically related are nodal voltages and reactive power flows, and the problem is posed as one of reactive power requirements and the supply of reactive power by different sources, such as generators, line charging susceptance, and compensating devices, such as capacitors, reactors, and static VAR compensators (SVCs). Reactive power does not carry out useful work. Therefore, the reactive power should not travel within the network; it has consequences on power losses, transmission overloading, and the deterioration of voltage outside specified quality range. An excess of reactive power, related to high-capacitive effects, increases the nodal voltages, whereas a lack of reactive power associated with a dominant inductive nature in the network degrades the voltage values.

A clear understanding of the control problems of real power flow and the reactive power (voltage) must be established. Appropriate model for transformers, transmission lines, synchronous generators, and reactive power compensating equipment is a must for operation and control of any electrical system—especially for weak longitudinal power systems. Planning activities require an integral solution to this type of control problem so that a comprehensive steady state control solution is advisable. This task is required for system's operation as well, and we can apply concepts already discussed in Chapters 6 and 7 in a systematic way.

8.2 Control of Real Power Flows

We start this section with a model for an ideal (no losses) power transformer with complex tap (shown in Figure 8.1). A detailed presentation of incremental equations for real power flow in a transformer and a set of approximations were already derived in Chapter 6 as (6.99)–(6.107). From the incremental real power flow equation, we recognize an Ohm's equivalent circuit as in (8.1) (see Figure 8.2); the purpose of this is to have a circuit model that can be applied to each element in a network. With this procedure, we are able to build a straightforward relation between control settings and changes, as well as their influence on network variables (nodal angles and voltage magnitudes).

In Section 8.5, we will take a more general approach and include a coordinated effort of available controls to achieve what we might call *minimum control actions*.

$$-x_{km} \frac{\Delta p_{km}}{|V_k|} + \Delta\theta_k - \Delta\theta_m = -\Delta\tau \quad (8.1)$$

For the real power flow problem, (8.1) will be applied to each network element that has a phase shifter for a transmission line $\Delta\tau = 0$. To completely solve the network, we must write the algebraic sum of real power at each node. This step gives complementary equations that allow us to build a consistent set of equations. The set is solved for incremental angles (rad) and incremental real power flows through the represented transmission lines and transformers, given the incremental power by sources and the incremental phase shifting angle control in transformers. One

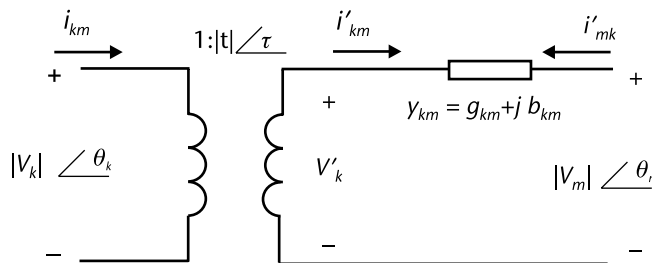


Figure 8.1 Power transformer with complex tap.

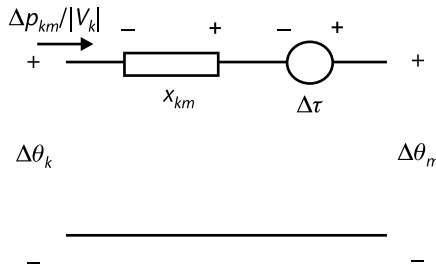


Figure 8.2 Equivalent circuit for the incremental real power flow, complex transformer.

node angle is set as reference. The next question is: how can we coordinate the effort of various available controls so that a real power congestion problem is solved in our network?

Example 8.1

Assuming a network of Figure 8.3 and using data in Table 8.1, write the model for each transmission element and complement with one balance equation for each node and solve the system of equations. Show the sensitivity matrix.

Equation (8.1) is applied to each transmission element and four nodal power balances are added.

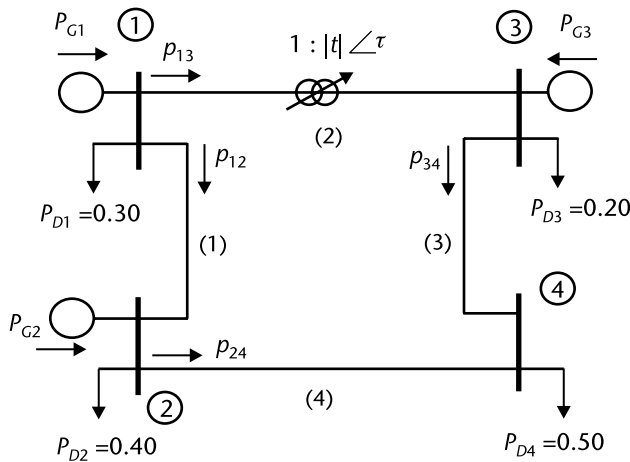


Figure 8.3 Network for the real power control.

Table 8.1 Data for Example 8.1 $|t| \angle \tau = t_\alpha + jt_\beta = 1.05 \angle 5^\circ$

Element	$N_{sat} - k$	$N_{illeg} - m$	$y_{km} pu$	tap	$yb_{sh/2}$
1	1	2	$1.0 - j10$	-1	0
2	1	3	$1.0 - j10$	$t_\alpha + jt_\beta$	0
3	3	4	$1.5 - j15$	-1	0
4	2	4	$2.0 - j20$	-1	0

$$\begin{aligned}
 & \left[\begin{array}{l}
 (1) \quad -x_{12} \frac{\Delta p_{12}}{|V_1|} + \Delta\theta_1 - \Delta\theta_2 = 0 \\
 (2) \quad -x_{13} \frac{\Delta p_{13}}{|V_1|} + \Delta\theta_1 - \Delta\theta_3 = -\Delta\tau \\
 (3) \quad -x_{34} \frac{\Delta p_{34}}{|V_3|} + \Delta\theta_3 - \Delta\theta_4 = 0 \\
 (4) \quad -x_{24} \frac{\Delta p_{24}}{|V_2|} + \Delta\theta_2 - \Delta\theta_4 = 0 \\
 \text{node 1} \quad \frac{+\Delta p_{12}}{|V_1|} + \frac{\Delta p_{13}}{|V_1|} = \frac{\Delta P_1}{|V_1|} \\
 \text{node 2} \quad \frac{-\Delta p_{12}}{|V_1|} + \frac{\Delta p_{24}}{|V_2|} = \frac{\Delta P_2}{|V_2|} \\
 \text{node 3} \quad \frac{+\Delta p_{34}}{|V_2|} - \frac{\Delta p_{13}}{|V_1|} = \frac{\Delta P_3}{|V_3|} \\
 \text{node 4} \quad \frac{-\Delta p_{24}}{|V_2|} - \frac{\Delta p_{34}}{|V_3|} = \frac{\Delta P_4}{|V_4|}
 \end{array} \right] \quad (8.2)
 \end{aligned}$$

The previous equations in matrix form:

$$\begin{aligned}
 & \left[\begin{array}{cccccc}
 -x_{12} & 0 & 0 & 0 & +1 & -1 & 0 & 0 \\
 & & & & & + & & \\
 0 & -x_{13} & 0 & 0 & 1 & 0 & -1 & 0 \\
 0 & 0 & -x_{34} & 0 & 0 & 0 & +1 & -1 \\
 0 & 0 & 0 & -x_{24} & 0 & +1 & 0 & -1 \\
 +1 & +1 & 0 & 0 & 0 & 0 & 0 & 0 \\
 -1 & 0 & 0 & +1 & 0 & 0 & 0 & 0 \\
 0 & -1 & +1 & 0 & 0 & 0 & 0 & 0 \\
 0 & 0 & -1 & -1 & 0 & 0 & 0 & 0
 \end{array} \right] \left[\begin{array}{c}
 \frac{\Delta p_{12}}{|V_1|} \\
 \frac{\Delta p_{13}}{|V_1|} \\
 \frac{\Delta p_{34}}{|V_2|} \\
 \frac{\Delta p_{24}}{|V_3|} \\
 \Delta\theta_1 \\
 \Delta\theta_2 \\
 \Delta\theta_3 \\
 \Delta\theta_4
 \end{array} \right] = \left[\begin{array}{c}
 0 \\
 -\Delta\tau \\
 0 \\
 0 \\
 \frac{\Delta P_1}{|V_1|} \\
 \frac{\Delta P_2}{|V_2|} \\
 \frac{\Delta P_3}{|V_3|} \\
 \frac{\Delta P_4}{|V_4|}
 \end{array} \right] \quad (8.3)
 \end{aligned}$$

$$\left[\begin{array}{cc}
 -x & A \\
 A^t & 0
 \end{array} \right] \left[\begin{array}{c}
 \frac{\Delta p}{|V|} \\
 \Delta\theta
 \end{array} \right] = \left[\begin{array}{c}
 -\Delta\tau \\
 \frac{\Delta P}{|V|}
 \end{array} \right] \quad (8.4)$$

- x Diagonal matrix of element's reactance
- A Incidence matrix, information about element's connectivity between nodes
- $\Delta p/|V|$ Vector of incremental power flow in every element
- $\Delta\tau$ Vector of available phase shifting control in branches
- $\Delta P/|V|$ Vector of net injection of incremental real power into a node

For the reactance values as read from Table 8.1, the sensitivity matrix is:

-3.1895	3.1895	3.1895	-3.1895	0.0000	-0.6842	-0.3158	-0.5263
3.1895	-3.1895	-3.1895	3.1895	0	-0.3158	-0.6842	-0.4737
3.1895	-3.1895	-3.1895	3.1895	-0.0000	-0.3158	0.3158	-0.4737
-3.1895	3.1895	3.1895	-3.1895	0.0000	0.3158	-0.3158	-0.5263
0	0	0	0	0.0000	0.0000	0.0000	0.0000
-0.6842	-0.3158	-0.3158	0.3158	-0.0000	0.0677	0.0313	0.0521
-0.3158	-0.6842	0.3158	-0.3158	0.0000	0.0313	0.0677	0.0469
-0.5263	-0.4737	-0.4737	-0.5263	-0.0000	0.0521	0.0469	0.0782

For a change in angle control $\Delta\tau$, it will affect line flows and nodal angles as:

$$\begin{bmatrix} \frac{\Delta p_{12}}{|V_1|} \\ \frac{\Delta p_{13}}{|V_1|} \\ \frac{\Delta p_{34}}{|V_2|} \\ \frac{\Delta p_{24}}{|V_3|} \\ \Delta\theta_1 \\ \Delta\theta_2 \\ \Delta\theta_3 \\ \Delta\theta_4 \end{bmatrix} = (-\Delta\tau) \begin{bmatrix} +3.1895 \\ -3.1895 \\ -3.1895 \\ +3.1895 \\ 0 \\ -0.3158 \\ +0.6842 \\ -0.4737 \end{bmatrix} \tag{8.5}$$

The column shows values of sensitivity factors, assuming that we have a phase shifting change $\Delta\tau$ in element 2 that connects node 1 to 3. Column 6 of the sensitivity matrix shows factors for a ΔP injection into node two. The sparse nature of the coefficient matrix in (8.3) is also shown in the structure in Figure 8.4.

```

Sensitivity factors, control in element 2
Elem( 1) = +3.189474
Elem( 2) = -3.189474
Elem( 3) = -3.189474
Elem( 4) = +3.189474
node( 1) = +0.000000
    
```

```

node( 2) = -0.315789
node( 3) = -0.684211
node( 4) = -0.473684

Sensitivity factors, control in node    2
Elem( 1) = -0.684211
Elem( 2) = -0.315789
Elem( 3) = -0.315789
Elem( 4) = +0.315789
node( 1) = +0.000000
node( 2) = +0.067744
node( 3) = +0.031266
node( 4) = +0.052110

```

For Example 8.1, node one is selected as our angle reference $\theta_1 = 0$ radians. The matrix inversion for the coefficient array in (8.3) will render column-wise sensitivity constants; the sensitivity factors have information about the impact of control actions on transmission line real power flows. For example, the second column has the effect of an incremental change of the phase shifter, $\Delta\tau$ acting in the second element. For this example, we only solve for real power flows. Nodal voltages are assumed to be 1.0 pu, and we concentrate our attention to the real power flow problem.

A real power system usually has several actions that can be classified as controls. These include phase-shifting devices, power injections by generators, and changes in

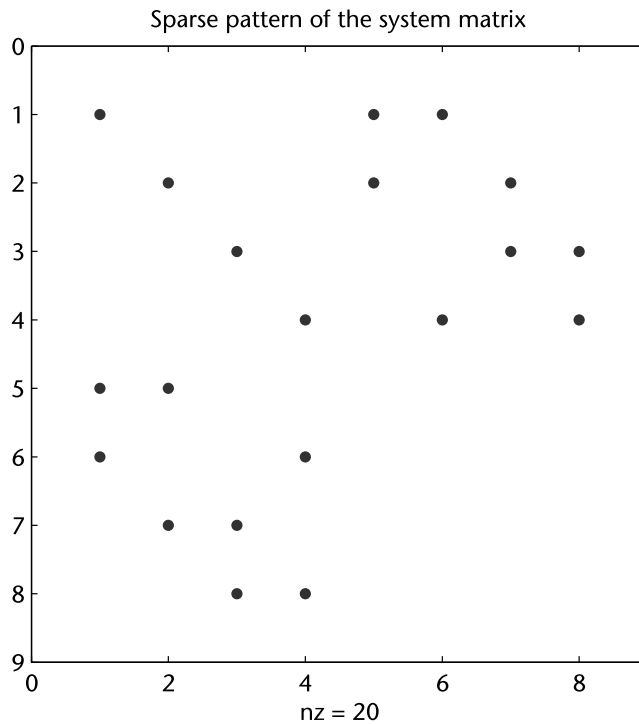


Figure 8.4 Sparse nature of the matrix, previous to sensitivity factors calculation.

load requirements or load shedding schemes, just to mention a few of the controls in the real power control problem. Multiple control options are possible and should be coordinated so that a given objective can be accomplished, as in the case of network congestion relief where moving just one control might not give a complete solution.

8.3 Control of Real Power Flow, Longitudinal Networks

A longitudinal network is one that is not well developed in terms of loops and electrical support as well as one which does not have a robust HV transmission system. A weak network is prone to difficult voltage control problems and is very sensitive to reactive power changes. For dynamic real power imbalances, there are oscillations that do not damp out rapidly; it is a system with a low damping condition. With longitudinal systems, one difficult situation that operating engineers face is how to control the real power flow in networks that are not well-meshed and without a robust electrical condition. Sensitivity factors, such as the calculated in Section 8.2 can pave the way to solving this interesting problem; in particular, we need to visualize how far into the network a control action can reach, how effective it is, and where is more appropriate to locate new control devices so as to develop successful control schemes for a particular network.

Example 8.2

In order to discuss details about weak longitudinal networks, let us use the electric structure in Figure 8.5—15 nodes and 15 elements. We will take a detailed look into the network, the sparse nature of the coefficients matrix as shown in Figure 8.6, and the sensitivity factors for existing or for planned controls to upgrade network performance.

Sensitivity factors, real power control
Longitudinal network
Nodes = 15 Elements = 15

Element	Node from	Node to	z (pu)	
1	2	3	0.0000 +j	0.1189
2	3	4	0.0000 +j	0.0568
3	5	7	0.0000 +j	0.0807
4	7	8	0.0000 +j	0.0451
5	4	10	0.0000 +j	0.1316
6	3	9	0.0000 +j	0.1458
7	10	9	0.0000 +j	0.0449
8	12	15	0.0000 +j	0.1699
9	12	13	0.0000 +j	0.0849
10	1	2	0.0000 +j	0.0930
11	3	5	0.0000 +j	0.1885
12	6	5	0.0000 +j	0.1330
13	11	10	0.0000 +j	0.0930
14	9	12	0.0000 +j	0.1885
15	14	13	0.0000 +j	0.1331

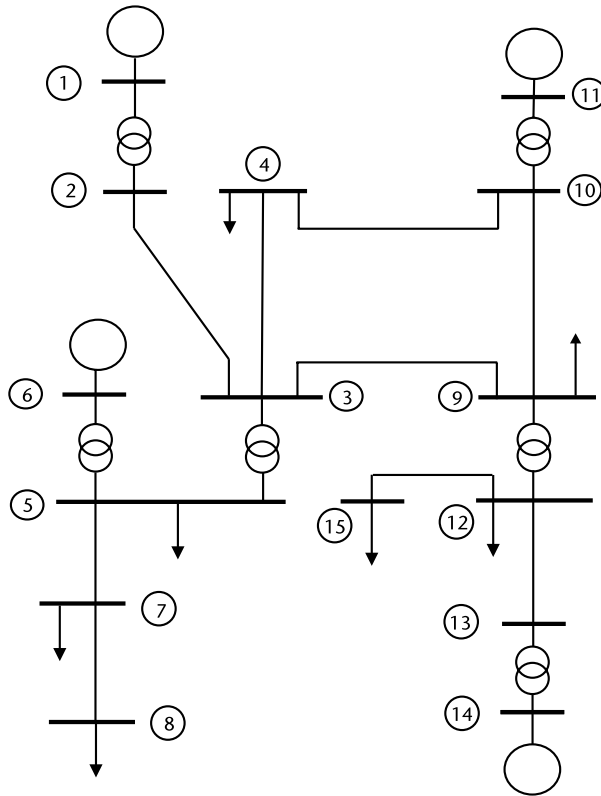


Figure 8.5 A longitudinal system, 15 nodes and 15 elements.

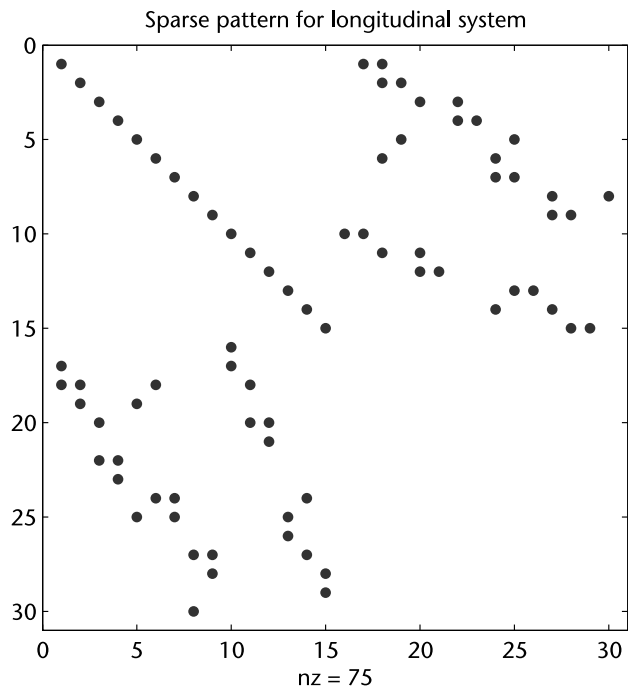


Figure 8.6 Sparse patterns for the matrix of a longitudinal system, Figure 8.5.

For this network, its connectivity and numerical values for reactance, the sensitivity factors numerically show how a control change will affect power flows or nodal angle (radians) for the real power problem. If a transformer located between node 1 and 2 is able to shift a control angle, then the column of factors shows that flows are unaffected; node 1 does not sense a change, all other nodes are affected by coefficient -1 (the nodal value will increase if $\Delta\tau_{12} < 0$).

Sensitivity factors, control in element 10 (transformer from node 1 to 2)

```

Elem( 1) = +0.000000
Elem( 2) = +0.000000
Elem( 3) = +0.000000
Elem( 4) = +0.000000
Elem( 5) = +0.000000
Elem( 6) = +0.000000
Elem( 7) = +0.000000
Elem( 8) = +0.000000
Elem( 9) = +0.000000
Elem(10) = +0.000000
Elem(11) = +0.000000
Elem(12) = +0.000000
Elem(13) = +0.000000
Elem(14) = +0.000000
Elem(15) = +0.000000
node( 1) = +0.000000
node( 2) = -1.000000
node( 3) = -1.000000
node( 4) = -1.000000
node( 5) = -1.000000
node( 6) = -1.000000
node( 7) = -1.000000
node( 8) = -1.000000
node( 9) = -1.000000
node(10) = -1.000000
node(11) = -1.000000
node(12) = -1.000000
node(13) = -1.000000
node(14) = -1.000000
node(15) = -1.000000

```

Now for a real power injection ΔP at node 4, which is a node part of a loop, it will affect several power flows and nodal angles, except for node 1, which is our reference.

```

Sensitivity factors, control in node 4 (injection)
Elem( 1) = -1.000000
Elem( 2) = -0.850171
Elem( 3) = +0.000000

```

```

Elem( 4) = +0.000000
Elem( 5) = +0.149829
Elem( 6) = -0.149829
Elem( 7) = +0.149829
Elem( 8) = +0.000000
Elem( 9) = +0.000000
Elem(10) = -1.000000
Elem(11) = +0.000000
Elem(12) = +0.000000
Elem(13) = +0.000000
Elem(14) = +0.000000
Elem(15) = +0.000000
node( 1) = +0.000000
node( 2) = +0.093030
node( 3) = +0.211930
node( 4) = +0.260220
node( 5) = +0.211930
node( 6) = +0.211930
node( 7) = +0.211930
node( 8) = +0.211930
node( 9) = +0.233775
node(10) = +0.240502
node(11) = +0.240502
node(12) = +0.233775
node(13) = +0.233775
node(14) = +0.233775
node(15) = +0.233775

```

We examine numerical results and find that some control actions might have a zero sensitivity factor. This means that those controls cannot modify the power flow in those elements. A similar conclusion can be drawn for nodal control actions by means of power injections if the sensitivity factors happen to be zero. In order to overcome this situation, new transmission lines have to be planned so that loop structures are formed and control actions can have a wider reach into more elements; the value of the sensitivity factors will show how strong or effective a control action is.

8.4 Control of Reactive Power Flow

To discuss the reactive power control, we again use the power transformer with complex tap, as in Figure 8.1. The approximations used in Chapter 6 for the reactive power flow as (6.107) will give us an incremental reactive power model and an Ohm's representation.

$$-x_{km} \frac{\Delta q_{km}}{|V_k|} + \Delta |V_k| - \Delta |V_m| = -\Delta |t| \quad (8.6)$$

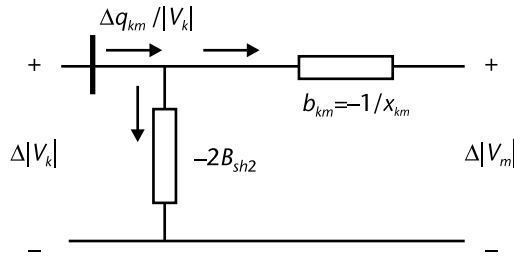


Figure 8.7 Circuit to explain the shunt reactive compensation.

For a π equivalent representation of a transmission line, the incremental reactive power from node k to node m from (6.114) with approximate partial derivatives as in (6.50)–(6.55) and $-x_{km} = 1/b_{km}$ is:

$$\frac{\Delta q_{km}}{|V_k|} = -(2B_{sh2})\Delta |V_k| - b_{km}(\Delta |V_k| - \Delta |V_m|) \tag{8.7}$$

The incremental reactive power flow (8.7) can be split into a series and a shunt component as shown in Figure 8.7. The advantage of this approach is to have a similar type of network for the real incremental real power flow and for the incremental reactive power flow. For the transmission line series, susceptance and a shunt component satisfy the nodal reactive power balance.

Example 8.3

In Figure 8.8, there are two voltage-controlled buses and using (8.6) and (8.7), equations for the elements are written. Balance nodal equations for reactive power complement the required set to solve for unknowns.

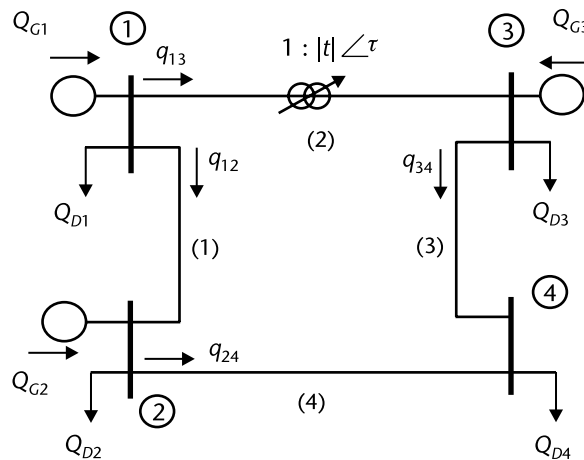


Figure 8.8 Circuit to study the reactive power control.

$$\begin{aligned}
 & \left[\begin{array}{l}
 (1) \quad -x_{12} \frac{\Delta q_{12}}{|V_1|} + (\Delta|V_1| - \Delta|V_2|) = 0 \\
 (2) \quad -x_{13} \frac{\Delta q_{13}}{|V_1|} + (\Delta|V_1| - \Delta|V_3|) = -\Delta|t| \\
 (3) \quad -x_{34} \frac{\Delta q_{34}}{|V_3|} + (\Delta|V_3| - \Delta|V_4|) = 0 \\
 (4) \quad -x_{24} \frac{\Delta q_{24}}{|V_2|} + (\Delta|V_2| - \Delta|V_4|) = 0 \\
 1 \quad \frac{+\Delta q_{12}}{|V_1|} + \frac{\Delta q_{13}}{|V_1|} = \frac{\Delta Q_1}{|V_1|} \\
 2 \quad \frac{-\Delta q_{12}}{|V_1|} + \frac{\Delta q_{24}}{|V_2|} = \frac{\Delta Q_2}{|V_2|} \\
 3 \quad \frac{+\Delta q_{34}}{|V_2|} - \frac{\Delta q_{13}}{|V_1|} = \frac{\Delta Q_3}{|V_3|} \\
 4 \quad \frac{-\Delta q_{24}}{|V_2|} - \frac{\Delta q_{34}}{|V_3|} = \frac{\Delta Q_4}{|V_4|}
 \end{array} \right] \quad (8.8)
 \end{aligned}$$

$$\begin{bmatrix}
 -x_{12} & 0 & 0 & 0 & +1 & -1 & 0 & 0 \\
 0 & -x_{13} & 0 & 0 & +1 & 0 & -1 & 0 \\
 0 & 0 & -x_{34} & 0 & 0 & 0 & +1 & -1 \\
 0 & 0 & 0 & -x_{24} & 0 & +1 & 0 & -1 \\
 +1 & +1 & 0 & 0 & -2B_{sb2}^{12} & 0 & 0 & 0 \\
 -1 & 0 & 0 & +1 & 0 & -2B_{sb2}^{12} - 2B_{sb2}^{24} & 0 & 0 \\
 0 & -1 & +1 & 0 & 0 & 0 & -2B_{sb2}^{34} & 0 \\
 0 & 0 & -1 & -1 & 0 & 0 & 0 & -2B_{sb2}^{24} - 2B_{sb2}^{34}
 \end{bmatrix}
 \begin{bmatrix}
 \Delta q_{12} / |V_1| \\
 \Delta q_{13} / |V_1| \\
 \Delta q_{34} / |V_2| \\
 \Delta q_{24} / |V_3| \\
 \Delta|V_1| \\
 \Delta|V_2| \\
 \Delta|V_3| \\
 \Delta|V_4|
 \end{bmatrix}
 =
 \begin{bmatrix}
 0 \\
 -\Delta|t| \\
 0 \\
 0 \\
 \Delta Q_1 / |V_1| \\
 \Delta Q_2 / |V_2| \\
 \Delta Q_3 / |V_3| \\
 \Delta Q_4 / |V_4|
 \end{bmatrix} \quad (8.9)$$

The previous matrix equation in compact form is:

$$\begin{bmatrix} -x & A \\ A^t & -2B_{sb} \end{bmatrix} \begin{bmatrix} \frac{\Delta q}{|V|} \\ \Delta|V| \end{bmatrix} = \begin{bmatrix} -\Delta|t| \\ \frac{\Delta Q}{|V|} \end{bmatrix} \quad (8.10)$$

- x diagonal matrix of element's reactance in the network
- A incidence matrix that has connectivity information
- $\Delta q/|V|$ vector of incremental reactive power flow in every element in the network

- $\Delta|t|$ vector of tap controls available in the branches
 $\Delta Q/|V|$ vector of net nodal incremental reactive power
 $2 B_{sb}$ array of capacitive effect of transmission lines; might include node reactive shunt compensation.

Once the inverse matrix in (8.10) is calculated, we will find sensitivity coefficients. The coefficients will show the impact of control actions on the incremental reactive power flows and nodal voltages. For example, the second column of the inverse shows the effect of an incremental change $\Delta|t|$ for a tap control located in element 2. In this model, the nodal angles are assumed to have a fixed value from the power flow solution, which is solved prior to the change in control actions. In order to obtain results considering all PV nodes from the regular load flow problem, we assumed that the voltage magnitude has a fixed value. This voltage condition must be included in the model before the matrix inversion process.

Sensitivity factors, Voltage-Reactive Power

Nodes = 4 Elements = 4

Element	Nfrom	Nto	Type	z(pu)	bsh2(pu)
1	1	2	+0	0.00990+j 0.09901	+0.20000
2	1	3	+1	0.00990+j 0.09901	+0.00000
3	3	4	+0	0.00660+j 0.06601	+0.20000
4	2	4	+0	0.00495+j 0.04950	+0.20000

Sensitivity factors for change in control 2

```

Elem( 1) = +0.000000
Elem( 2) = -5.994970
Elem( 3) = -6.157545
Elem( 4) = +0.000000
node( 1) = +0.000000
node( 2) = -0.000000
node( 3) = -0.406439
node( 4) = -0.000000

```

Sensitivity factors for change in node 2

```

Elem( 1) = -0.342373
Elem( 2) = -0.000000
Elem( 3) = -0.000000
Elem( 4) = +0.684746
node( 1) = +0.000000
node( 2) = +0.033898
node( 3) = +0.000000
node( 4) = +0.000000

```

A close look at results for the incremental reactive power model will give us a better understanding of the problem. In Figure 8.8, node 1 and 4 are PV buses; in the incremental network (see Figure 8.9), both nodes are shorted to reference and an electrically split network is obtained. A tap change in element (2) will affect the flow in elements (2) and (3) and the nodal voltage for node 3. A power injection change into node 2 will affect nodal voltage 2 and the incremental reactive power in elements (1) and (4).

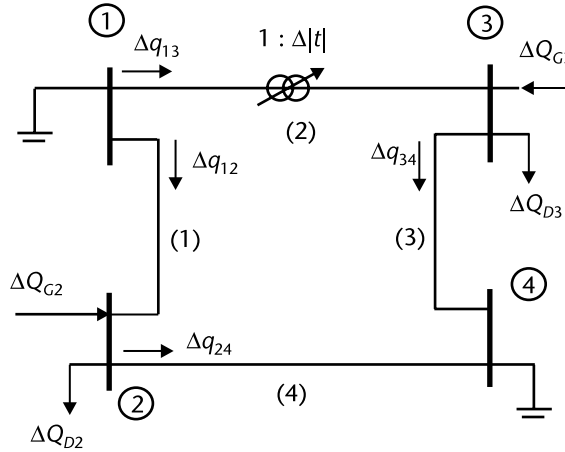


Figure 8.9 Network for the incremental reactive power control.

8.5 Congestion and Minimum Control Effort

A congestion problem in a given network is related to elements and nodes in the system that cannot maintain its operation within preset bounds. For transmission lines and transformers, this means that they are restricted because of thermal limit, stability constraint, or by voltage drop criteria. A congestion problem limits the power transfer capability and makes the network inefficient, leading to higher operating costs.

For example, to solve a congestion problem in reactive power flows and to maintain nodal voltages within limits, there might be several possible actions: tap changes in transformers, by shunt-connected elements to take reactive power, or by nodal injections. A more sophisticated arrangement will be through FACTS devices that allow smooth control within their operating limits. FACTS devices are designed with passive inductance/capacitance arrangements, and are controlled by power electronics that shape current and control switching times for conduction or blocking status. Some aspects will be discussed in Sections 8.7–8.10.

When one or two controls are available, experienced system operators know how to increase/decrease the controls in order to solve a problem. However, when there are various controls with possibly conflicting actions, the operators' actions must be coordinated. One approach can be to establish coordination through optimal control (i.e., we can think about *minimum control effort*). To build the optimal model, we require a cost function and linear or nonlinear equality constraints to be observed, as well as possible inequality constraints.

8.5.1 Use of Sensitivity Coefficients

To design useful applications for the sensitivity factors just discussed, let us establish a base case load flow solution for a set of load and generation conditions in a network. Let us first pay attention to the control of real power flow and solve a real power congestion problem. In Section 8.5.3, we consider the reactive power flow or out of range nodal voltages for a given operating condition.

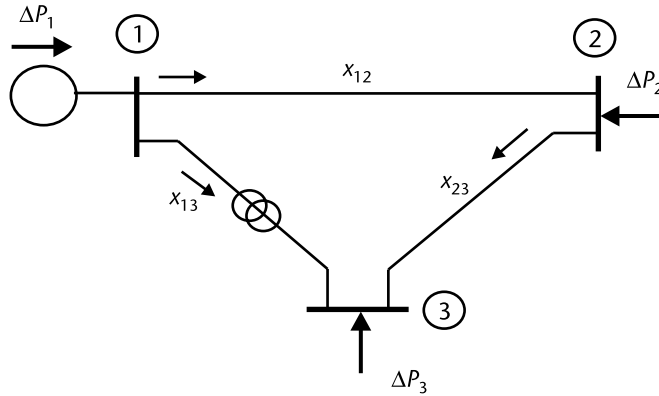


Figure 8.10 Three-node system for real power control.

Example 8.4

For a three-node system (see Figure 8.10), let us first solve for real power flows. Using the incremental model for real power flows and sensitivity coefficients, let's find the incremental change required from a phase shifter control $\Delta\tau_{13}$ to increment in 0.1 pu the flow in line 2 – 3 (i.e., $\Delta p_{23} = +0.1$ pu).

The incremental model is (8.11), assuming unitary voltage magnitudes.

$$\begin{bmatrix} -x_{12} & 0 & 0 & +1 & -1 & 0 \\ 0 & -x_{13} & 0 & +1 & 0 & -1 \\ 0 & 0 & -x_{23} & 0 & +1 & -1 \\ +1 & +1 & 0 & 0 & 0 & 0 \\ -1 & 0 & +1 & 0 & 0 & 0 \\ 0 & -1 & -1 & 0 & 0 & 0 \end{bmatrix} \begin{bmatrix} \Delta p_{12} / |V_1| \\ \Delta p_{13} / |V_1| \\ \Delta p_{23} / |V_2| \\ \Delta\theta_1 \\ \Delta\theta_2 \\ \Delta\theta_3 \end{bmatrix} = \begin{bmatrix} 0 \\ -\Delta\tau_{13} \\ 0 \\ \Delta P_1 / |V_1| \\ \Delta P_2 / |V_2| \\ \Delta P_2 / |V_3| \end{bmatrix} \quad (8.11)$$

DC Load Flows and Sensitivity factors, P-theta

Nodes = 3 Elements = 3

(0 is a transmission line, +1 a phase shifter)

Element	Nfrom	Nto	Type	x(pu)
1	1	2	+0	0.05000
2	1	3	+1	0.10000
3	2	3	+0	0.12500

Node initial conditions (0 slack, +1 PV and -1 PQ node)

Node	Ntype	Voltage	theta(rad)	PG	PL
1	0	1.00000	+0.00000	0.0000	0.0000
2	-1	1.00000	+0.00000	0.0000	0.0000
3	-1	1.00000	+0.00000	0.0000	1.0000

Coefficient matrix

-0.0500	0	0	1.0000	-1.0000	0
0	-0.1000	0	1.0000	0	-1.0000

	0	0	-0.1250	0	1.0000	-1.0000
	1.0000	1.0000	0	0	0	0
	-1.0000	0	1.0000	0	0	0
	0	-1.0000	-1.0000	0	0	0

Sensitivity matrix (node 1 as reference)

	-3.6364	3.6364	-3.6364	0	-0.8182	-0.3636
	3.6364	-3.6364	3.6364	-0.0000	-0.1818	-0.6364
	-3.6364	3.6364	-3.6364	0.0000	0.1818	-0.3636
	0	0	0	0.0000	0.0000	0.0000
	-0.8182	-0.1818	0.1818	-0.0000	0.0409	0.0182
	-0.3636	-0.6364	-0.3636	-0.0000	0.0182	0.0636

Node solution

Node	Ntype	Voltage	theta(deg)	PG	PL
1	0	1.00000	-0.00000	1.0000	0.0000
2	-1	1.00000	-1.04174	0.0000	0.0000
3	-1	1.00000	-3.64610	0.0000	1.0000

Line flows

Element	Nfrom	Nto	Type	p(pu)
1	1	2	+0	0.36364
2	1	3	+1	0.63636
3	2	3	+0	0.36364

From the load flow results $p_{23} = 0.36364$ pu, and this flow changes by a control (phase shifter) in element 2. The second column of the sensitivity matrix has for element 3 the following coefficients $\Delta p_{23} = 3.6364$ ($-\Delta\tau_{13}$), $\Delta\tau_{13} = -\Delta p_{23}/3.6364 = -(+0.1)/3.6364 = -0.0275$ rad.

The incremental changes on network variables are calculated by multiplying the second column of the sensitivity matrix by the phase shift increment we just calculated. The new values are obtained when we add the incremental solution to the base case results.

Dtau = -0.0275

Node adjusted solution

Node	Ntype	Voltage	theta(deg)	PG	PL
1	0	1.00000	-0.00000	1.0000	0.0000
2	-1	1.00000	-1.32822	0.0000	0.0000
3	-1	1.00000	-4.64877	0.0000	1.0000

Line adjusted flows

Element	Nfrom	Nto	Type	p(pu)
1	1	2	+0	0.46364
2	1	3	+1	0.53636
3	2	3	+0	0.46364

Results show the change in nodal angles (radians) and the new power flow values for the lines. The required increase of flow in line 2–3 of 0.1 pu is accomplished by the control action.

8.5.2 Optimal Control of Real Power Flow

In Section 8.5.1, we worked the real power flow control problems by means of a simple example and the use of the sensitivity coefficients; we then found the value of the required control. Once the control action is implemented, the new operating conditions are calculated. The assumption is that we would find an adjusted solution close to the base case so that the assumption of a linear model is valid. One extension that can be made to the previous problem is to include the nodal power injections as additional control actions. Power from generators and loads is an additional means of control for the real power in the system.

With values obtained from the sensitivity matrix, we can determine in what direction to move the available controls, and by a coordinated action, we can determine how much to move each control. Let us focus our effort into establishing a cost function, so that by control actions we can solve a congestion problem. To start the discussion, let us use the simple three-node system from Figure 8.11 modified in generation nodes and load values. Assume that an analysis of the base case requires a decrease in power flows as $\Delta p_{13} = -0.2182$ pu and $\Delta p_{23} = -0.1818$ pu. We use phase shifter $\Delta\tau$ and nodal power injections ΔP_2 and ΔP_3 . From the sensitivity matrix, we write two equality constraints to comply with the required decrease in power flows:

$$\begin{bmatrix} \Delta p_{13} \\ \Delta p_{23} \end{bmatrix} = \begin{bmatrix} -S_{22}\Delta\tau_{13} + S_{25}\Delta P_2 + S_{26}\Delta P_3 \\ -S_{32}\Delta\tau_{13} + S_{35}\Delta P_2 + S_{36}\Delta P_3 \end{bmatrix} = \begin{bmatrix} -0.2128 \\ -0.1818 \end{bmatrix} \quad (8.12)$$

To minimize the control effort, we write a cost function with weighted control variables w_k , according to the relative importance attached to each control. In our case, the equality and inequality constraints are written as follows:

$$\min \sum_{k \in T} w_k \Delta\tau_k^2 + \sum_{k \in PG} w_k \Delta P_k^2 \quad (8.13)$$

$$\begin{aligned} \text{subject to } & [f = 0] \\ & \Delta\tau \leq \Delta\tau^{\max} \\ & \Delta P \leq \Delta P^{\max} \end{aligned} \quad (8.14)$$

Example 8.5 Base Case

DC Load Flows and Optimal factors, P-theta

Nodes = 3 Elements = 3

Element	Nfrom	Nto	Type	x(pu)
1	1	2	+0	0.05000
2	1	3	+1	0.10000
3	2	3	+0	0.12500

Node initial conditions

Node	Ntype	Voltage	theta(rad)	PG	PL
1	+0	1.00000	+0.00000	0.0000	0.0000
2	+1	1.00000	+0.00000	1.5000	0.0000
3	+1	1.00000	+0.00000	0.5000	3.0000

Node solution						
Node	Ntype	Voltage	theta(deg)	PG	PL	
1	0	1.00000	-0.00000	1.0000	0.0000	
2	1	1.00000	+0.91152	1.5000	0.0000	
3	1	1.00000	-7.55263	0.5000	3.0000	

Line flows in Base Case					
Element	Nfrom	Nto	Type	p(pu)	
1	1	2	+0	-0.31818	
2	1	3	+1	1.31818	
3	2	3	+0	1.18182	

Minimize the cost function subject to constraints:

$$\min \frac{1}{2}w_1\Delta\tau_{13}^2 + \frac{1}{2}w_2\Delta P_2^2 + \frac{1}{2}w_3\Delta P_3^2 \tag{8.15}$$

$$\begin{aligned} -S_{22}\Delta\tau_{13} + S_{25}\Delta P_2 + S_{26}\Delta P_3 &= \Delta p_{13} \\ -S_{32}\Delta\tau_{13} + S_{35}\Delta P_2 + S_{36}\Delta P_3 &= \Delta p_{23} \\ \Delta\tau_{13} &\leq 0.0085 \end{aligned} \tag{8.16}$$

The augmented Lagrangian includes the equality and the inequality constraints (8.16), as well as the Lagrange and Kuhn-Tucker multipliers. The problem has six variables: phase shifter, two nodal power injections, two Lagrange multipliers, and one Khun-Tucker multiplier. The solution is attained when the Lagrange gradient is equal to zero.

$$\begin{aligned} \min \zeta = w_1\Delta\tau_{13}^2 + w_2\Delta P_2^2 + w_3\Delta P_3^2 + \lambda_1(-S_{22}\Delta\tau_{13} + S_{25}\Delta P_2 + S_{26}\Delta P_3 - \Delta p_{13}) \\ + \lambda_2(-S_{32}\Delta\tau_{13} + S_{35}\Delta P_2 + S_{36}\Delta P_3 - \Delta p_{23}) + \mu(\Delta\tau_{13} - 0.0085) \end{aligned} \tag{8.17}$$

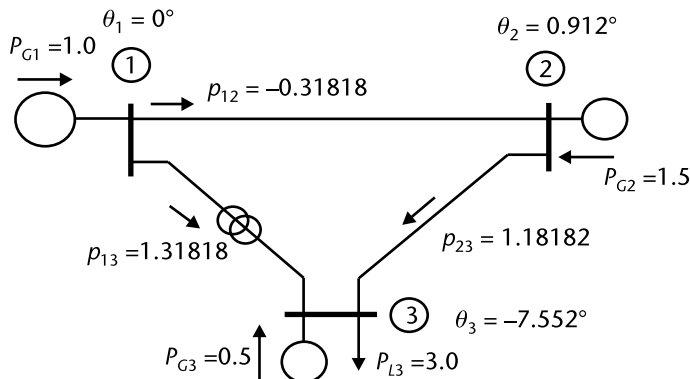


Figure 8.11 Three-node system base case.

$$\left[\begin{array}{l} \frac{\partial \zeta}{\partial \Delta \tau_{13}} = w_1 \Delta \tau_{13} - \lambda_1 S_{22} - \lambda_2 S_{32} + \mu = 0 \\ \frac{\partial \zeta}{\partial \Delta \tau_{13}} = w_1 \Delta \tau_{13} - \lambda_1 S_{22} - \lambda_2 S_{32} + \mu = 0 \\ \frac{\partial \zeta}{\partial \Delta P_2} = w_2 \Delta P_2 + \lambda_1 S_{25} + \lambda_2 S_{35} = 0 \\ \frac{\partial \zeta}{\partial \Delta P_3} = w_3 \Delta P_3 + \lambda_1 S_{26} + \lambda_2 S_{36} = 0 \\ \frac{\partial \zeta}{\partial \lambda_1} = -S_{22} \Delta \tau_{13} + S_{25} \Delta P_2 + S_{26} \Delta P_3 - \Delta p_{13} = 0 \\ \frac{\partial \zeta}{\partial \lambda_2} = -S_{32} \Delta \tau_{13} + S_{35} \Delta P_2 + S_{36} \Delta P_3 - \Delta p_{23} = 0 \\ \frac{\partial \zeta}{\partial \mu} = \Delta \tau_{13} - 0.0085 = 0 \end{array} \right] \quad (8.18)$$

In this case, the gradient is a system of linear equations, an optimal solution that complies with constraints using weights $w_k = 1.0 \forall k$ and flows $\Delta p_{13} = -0.2182$ pu, $\Delta p_{23} = -0.1818$ pu.

$$\left[\begin{array}{cccccc} w_1 & 0 & 0 & -S_{22} & -S_{32} & +1 \\ 0 & w_2 & 0 & +S_{25} & +S_{35} & 0 \\ 0 & 0 & w_3 & +S_{26} & +S_{36} & 0 \\ -S_{22} & +S_{25} & +S_{26} & 0 & 0 & 0 \\ -S_{32} & +S_{35} & +S_{36} & 0 & 0 & 0 \\ +1 & 0 & 0 & 0 & 0 & 0 \end{array} \right] \left[\begin{array}{c} \Delta \tau_{13} \\ \Delta P_2 \\ \Delta P_3 \\ \lambda_1 \\ \lambda_2 \\ \mu \end{array} \right] = \left[\begin{array}{c} 0 \\ 0 \\ 0 \\ -0.2182 \\ -0.1818 \\ +0.0085 \end{array} \right] \quad (8.19)$$

Hess =

$$\begin{array}{cccccc} 1.0000 & 0 & 0 & 3.6364 & -3.6364 & 1.0000 \\ 0 & 1.0000 & 0 & -0.1818 & 0.1818 & 0 \\ 0 & 0 & 1.0000 & -0.6364 & -0.3636 & 0 \\ 3.6364 & -0.1818 & -0.6364 & 0 & 0 & 0 \\ -3.6364 & 0.1818 & -0.3636 & 0 & 0 & 0 \\ 1.0000 & 0 & 0 & 0 & 0 & 0 \end{array}$$

The changes on the control variables $\Delta \tau = 0.0085$ rad, $\Delta P_2 = -0.0299$ pu, and $\Delta P_3 = +0.4$ pu affect the base case. We have changes to the transmission line flows, and the equality and inequality constraints are satisfied (see Figure 8.12).

$$\left[\begin{array}{c} \Delta \tau_{13} \\ \Delta P_2 \\ \Delta P_3 \\ \lambda_1 \\ \lambda_2 \\ \mu \end{array} \right] = \left[\begin{array}{c} +0.0085 \\ -0.0299 \\ +0.4000 \\ +0.3402 \\ +0.5047 \\ +0.5895 \end{array} \right] \quad (8.20)$$

Node solution, optimal changes

Node	Ntype	Voltage	theta(deg)	PG	PL
1	0	1.00000	-0.00000	0.6299	0.0000
2	1	1.00000	+1.34669	1.4701	0.0000
3	1	1.00000	-5.81542	0.9000	3.0000

Line flows

Element	Nfrom	Nto	Type	p(pu)
1	1	2	+0	-0.47008
2	1	3	+1	1.09998
3	2	3	+0	1.00002

8.5.3 Optimal Control for Reactive Power Flow

Now, let us turn our attention to the reactive power—nodal voltage control problem. The assumption is that we have a base case solution that is a converged load

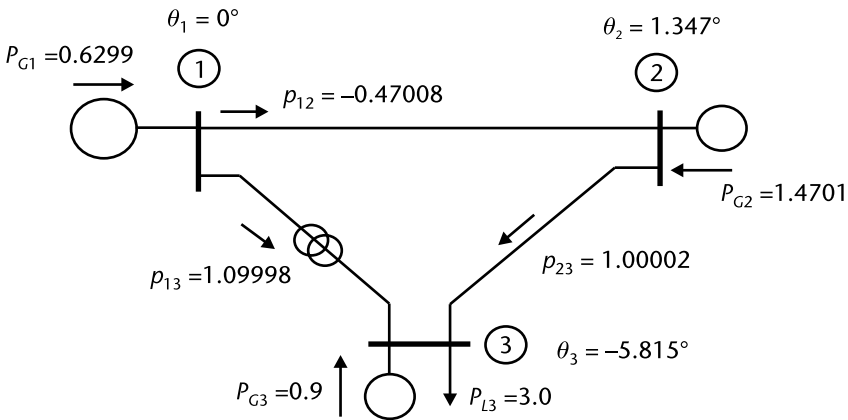


Figure 8.12 Three-node system with *minimum control effort*.

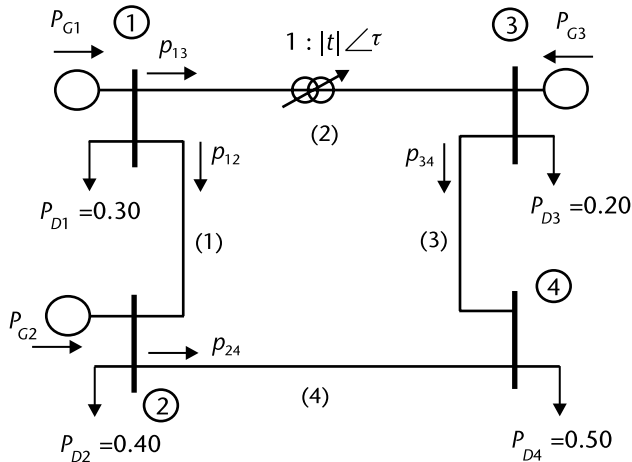


Figure 8.13 Circuit to study reactive power control.

flow for real and reactive power. Then, when a congestion problem is identified, we must solve it. For this problem, the reactive power and nodal voltages will be our main concern. We start with the appropriate model for LTC and transmission line elements, as in (8.6) and (8.7).

Example 8.6 Base Case

In Figure 8.13, the slack bus voltage is 1.0 pu. There are two PV buses whose voltage must also be maintained at 1.0 pu. Nodal generation and load conditions are shown in the printout.

4 Node Model

```
Number of Nodes =      4
Number of Lines =      3
Number of transformers = 1
Number of shunts =     0
```

Line Parameters

Line	Node From	Node To	Resist	React	ysh/2	Smax
1	1	2	0.00990	0.09901	0.04000	1.00000
2	3	4	0.00660	0.06601	0.03000	1.00000
3	2	4	0.00495	0.04950	0.02500	1.00000

Transformer's data

Transf	Node From	Node To	Resist	React	tap	Angle	Smax
1	1	3	0.00990	0.09901	1.00000	0.00000	1.00000

Nodal Values

Node	Type	V	th(rad)	th(degrees)	Sgen	Sload
1	0	1.0000	0.000000	0.00	0.0000 +j 0.0000	0.6000 +j 0.2000
2	1	1.0000	0.000000	0.00	0.6000 +j 0.0000	0.8000 +j 0.3000
3	-1	1.0000	0.000000	0.00	0.0000 +j 0.0000	0.4000 +j 0.1600
4	-1	1.0000	0.000000	0.00	0.0000 +j 0.0000	1.0000 +j 0.4000

CONVERGENCE IN 3 ITERATIONS

Converged Values for Variables

Node	V	th(rad)	th(degrees)
1	1.000000	0.0000	0.0000
2	1.000000	-0.0803	-4.6021
3	0.977823	-0.0805	-4.6111
4	0.977146	-0.1086	-6.2226

Line power flows in 3 lines

Line	Node from	Node To	p+jq	S	overload
1	1	2	0.8056 +j -0.0880	0.8104	
	2	1	-0.7991 +j 0.0725	0.8024	
2	3	4	0.4046 +j -0.0534	0.4081	
	4	3	-0.4035 +j 0.0074	0.4035	
3	2	4	0.5991 +j 0.3846	0.7120	
	4	2	-0.5965 +j -0.4074	0.7224	

Load power flows in 1 transformers

Trans	Node From	Node To	p+jq	S	overload
1	1	3	0.8114 +j 0.1748	0.8300	
	3	1	-0.8046 +j -0.1066	0.8116	

S in generators (>0) and Load

Node	type	PG+jQG	Qmin	Qmax	PL+jQL
1	+0	2.2170 +j 0.2868	-5.0000	5.0000	0.6000 +j 0.2000
2	+1	0.6000 +j 0.7571	-2.0000	2.0000	0.8000 +j 0.3000
3	-1	-0.0000 +j 0.0000			0.4000 +j 0.1600
4	-1	0.0000 +j 0.0000			1.0000 +j 0.4000

Total Generation

2.8170 +j 1.0439

Total Load

2.8000 +j 1.0600

In lines: Losses P and Q (>0 required, <0 supplied)

0.0170 +j -0.0161

8.5.4 Optimal Coordinated Control Efforts

From the base case in Figure 8.14, we notice that nodal voltages 3 and 4 need to be improved. We have various control actions at our disposal: the tap change in element (4) and the reactive power injections at nodes 3 and 4. An *optimal coordinated effort* can be established by means of the sensitivity matrix for the tap control and nodal injections.

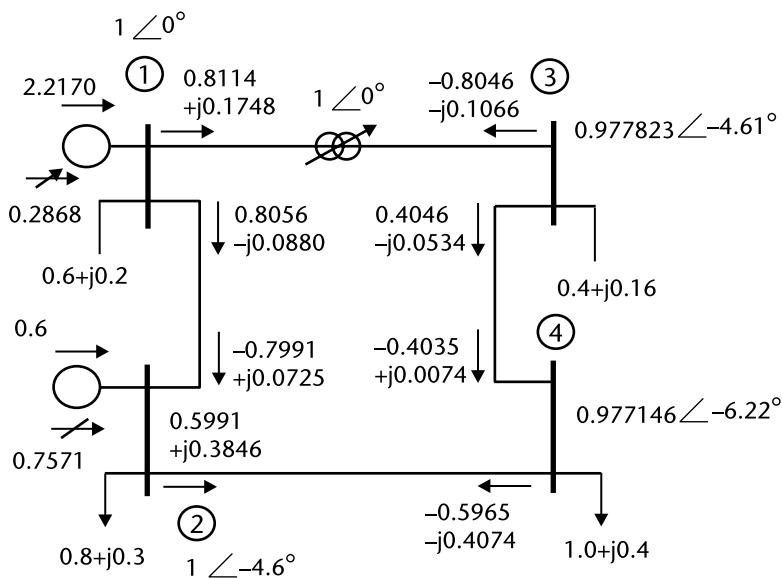


Figure 8.14 Load power flows, base case.

Sensitivity factors for change in control 4 (tap)
 Elem(1) = -0.000000
 Elem(2) = -4.670612
 Elem(3) = +4.696186
 Elem(4) = -4.638166
 node(1) = +0.000000
 node(2) = -0.000000
 node(3) = -0.540776
 node(4) = -0.232484

Sensitivity factors for change in node 3 (injection)
 Elem(1) = -0.000000
 Elem(2) = +0.462437
 Elem(3) = -0.464969
 Elem(4) = -0.540776
 node(1) = +0.000000
 node(2) = +0.000000
 node(3) = +0.053542
 node(4) = +0.023018

Sensitivity factors for change in node 4 (injection)
 Elem(1) = -0.000000
 Elem(2) = -0.231103
 Elem(3) = -0.773107
 Elem(4) = -0.232484
 node(1) = +0.000000
 node(2) = +0.000000
 node(3) = +0.023018
 node(4) = +0.038273

The optimal coordination of three controls—tap change, reactive power at node 3, and into node 4—are solved with the requirement that voltage magnitudes V_3 and V_4 should be as close to 1 pu as possible.

$$\min \frac{1}{2}w_1\Delta t_{13}^2 + \frac{1}{2}w_2\Delta Q_3^2 + \frac{1}{2}w_3\Delta Q_4^2 \quad (8.21)$$

Subject to:

$$\left[\begin{array}{l} -S_{74}\Delta t_{13} + S_{77}\Delta Q_3 + S_{78}\Delta Q_4 = \Delta V_3 \\ -S_{84}\Delta t_{13} + S_{87}\Delta Q_2 + S_{88}\Delta Q_3 = \Delta V_4 \\ \Delta t_{13} \leq 0.05 \end{array} \right] \quad (8.22)$$

The augmented Lagrangian includes equality and inequality constraints such as Lagrange and Kuhn-Tucker multipliers.

$$\begin{aligned} \min \zeta = & \frac{1}{2}w_1\Delta t_{13}^2 + \frac{1}{2}w_2\Delta Q_3^2 + \frac{1}{2}w_3\Delta Q_4^2 + \lambda_1(-S_{74}\Delta t_{13} + S_{77}\Delta Q_3 + S_{78}\Delta Q_4 - \Delta V_3) \\ & + \lambda_2(-S_{84}\Delta t_{13} + S_{87}\Delta Q_3 + S_{88}\Delta Q_4 - \Delta V_4) + \mu(\Delta t_{13} - 0.05) \end{aligned} \quad (8.23)$$

Solution when the gradient is equal to zero:

$$\left[\begin{array}{l} \frac{\partial \zeta}{\partial \Delta t_{13}} = w_1 \Delta t_{13} - \lambda_1 S_{74} - \lambda_2 S_{84} + \mu = 0 \\ \frac{\partial \zeta}{\partial \Delta Q_3} = w_2 \Delta Q_3 + \lambda_1 S_{77} + \lambda_2 S_{87} = 0 \\ \frac{\partial \zeta}{\partial \Delta Q_4} = w_3 \Delta Q_4 + \lambda_1 S_{78} + \lambda_2 S_{88} = 0 \\ \frac{\partial \zeta}{\partial \lambda_1} = -S_{74} \Delta t_{13} + S_{77} \Delta Q_3 + S_{78} \Delta Q_4 - \Delta V_3 = 0 \\ \frac{\partial \zeta}{\partial \lambda_2} = -S_{84} \Delta t_{13} + S_{87} \Delta Q_3 + S_{88} \Delta Q_4 - \Delta V_4 = 0 \\ \frac{\partial \zeta}{\partial \mu} = \Delta t_{13} - 0.05 = 0 \end{array} \right] \quad (8.24)$$

In this case, the gradient is a system of linear equations and the optimal solution complies with the required constraints. We use weights $w_k = 1.0 \forall k$ and the voltage changes $\Delta V_3 = 0.02$ pu and $\Delta V_4 = 0.02$ pu.

$$\left[\begin{array}{cccccc} w_1 & 0 & 0 & -S_{74} & -S_{84} & +1 \\ 0 & w_2 & 0 & +S_{77} & +S_{87} & 0 \\ 0 & 0 & w_3 & +S_{78} & +S_{88} & 0 \\ -S_{74} & +S_{77} & +S_{78} & 0 & 0 & 0 \\ -S_{84} & +S_{87} & +S_{88} & 0 & 0 & 0 \\ +1 & 0 & 0 & 0 & 0 & 0 \end{array} \right] \left[\begin{array}{c} \Delta t_{13} \\ \Delta Q_3 \\ \Delta Q_4 \\ \lambda_1 \\ \lambda_2 \\ \mu \end{array} \right] = \left[\begin{array}{c} 0 \\ 0 \\ 0 \\ +0.02 \\ +0.02 \\ +0.05 \end{array} \right] \quad (8.25)$$

The sensitivity coefficients S are taken from the columns of *sensitivity matrix*: fourth for tap control, seventh and eighth for reactive power injection into nodes 3 and 4, respectively.

The Hessian (8.25) is:

$$\begin{array}{l} \text{Hess} = \\ \begin{array}{cccccc} 1.0000 & 0 & 0 & 0.5408 & 0.2325 & 1.0000 \\ 0 & 1.0000 & 0 & 0.0535 & 0.0230 & 0 \\ 0 & 0 & 1.0000 & 0.0230 & 0.0383 & 0 \\ 0.5408 & 0.0535 & 0.0230 & 0 & 0 & 0 \\ 0.2325 & 0.0230 & 0.0383 & 0 & 0 & 0 \\ 1.0000 & 0 & 0 & 0 & 0 & 0 \end{array} \\ \Delta \text{cont} = \\ \begin{array}{l} 0.0500 \\ -0.3042 \\ 0.4018 \\ 13.7501 \\ -18.7681 \\ -3.1224 \end{array} \end{array}$$

The required controls are $\Delta t_{13} = 0.05$, $\Delta Q_3 = -0.3042$ and $\Delta Q_4 = 0.4018$ where (< 0) is inductive compensation and (> 0) capacitive compensation. Once the control settings are adjusted, the new load flow solution is found.

Transformer's data

Transf	Node From	Node To	Resist	React	tap	Angle	Smax
1	1	3	0.00990	0.09901	1.05000	0.00000	1.00000

Nodal Values

Node	Type	V	th(rad)	th(degrees)	Sgen	Sload
1	0	1.0000	0.000000	0.00	0.0000 +j 0.0000	0.6000 +j 0.2000
2	1	1.0000	0.000000	0.00	0.6000 +j 0.0000	0.8000 +j 0.3000
3	-1	1.0000	0.000000	0.00	0.0000 +j 0.0000	0.4000 +j 0.4642
4	-1	1.0000	0.000000	0.00	0.0000 +j 0.0000	1.0000 +j -0.0180

New Values for Variables

Node	V	th(rad)	th(degrees)
1	1.000000	0.0000	0.0000
2	1.000000	-0.0767	-4.3971
3	0.998697	-0.0755	-4.3253
4	0.998263	-0.1048	-6.0029

With control actions, the voltage magnitudes are—for all practical purposes—very close to 1 pu. A summary of power at generators, total generation, loads, and losses is shown.

S in generators (>0) and Load

Node	type	PG+jQG	Qmin	Qmax	PL+jQL
1	+0	2.2173 +j 0.6022	-5.0000	5.0000	0.6000 +j 0.2000
2	+1	0.6000 +j 0.3277	-2.0000	2.0000	0.8000 +j 0.3000
3	-1	0.0000 +j 0.0000			0.4000 +j 0.4642
4	-1	0.0000 +j 0.0000			1.0000 +j -0.0180

Total Generation

2.8173 +j 0.9300

Total Load

2.8000 +j 0.9462

In lines: Losses P and Q (>0 required, <0 supplied)

0.0173 +j -0.016

8.6 Work and Energy

Even though this book focuses on the steady state for the electrical power system, energy, work, and power are foundational concepts; from the physics point of view, it is fundamental to understand the concept of energy. Work can be associated with a force applied to displace a body of mass M , for a given distance x , with respect

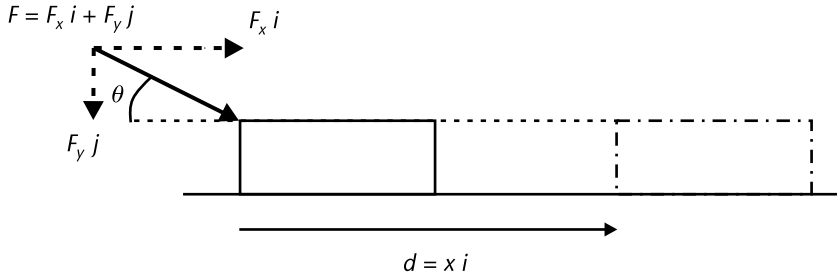


Figure 8.15 Force and distance, vector arrangement.

to a reference. The units for the quantities involved are: mass (M) in kg, force (F) in Newton and displacement (d) in meters. Force and distance can be represented as vectors (i.e., physical quantities that have magnitude and direction). We associate the concept of work to the force F_x that acts along the required displacement x (see Figure 8.15).

The vector force F will have two components in a plane: F_x along a horizontal reference x and F_y , making a 90° angle (in a counterclockwise direction) with respect to the x direction. The vector arrangement is shown in Figure 8.15.

$$F = F_x i + F_y j \quad d = x i \quad (8.26)$$

$$|F| = \sqrt{F_x^2 + F_y^2} \quad (8.27)$$

$$\theta = \arctg\left(\frac{F_y}{F_x}\right) \quad (8.28)$$

$i, j,$ and k Unit vectors that point along the $x, y,$ and z reference direction, respectively.

Using an interior point product for vectors, the work done by vector force F along the vector distance d is calculated using (8.29), units in Newton-meter (N-m), or Jules.

$$W = \vec{F} \cdot \vec{d} = |F||d|\cos\theta \quad (8.29)$$

The amount of incremental work (ΔW) realized in a given time increment of time (Δt) measured in seconds will render the concept of power, expressed in N-m/s or watts (W).

$$p = \frac{\Delta W}{\Delta t} \quad (8.30)$$

In applications where the instantaneous power $p(t)$ is known, for a given time interval $\Delta t = t_1 - t_0$, the amount of energy is calculated using an integral, which is the area underneath the plot $p(t)$ and the time axis t ; from t_0 to t_1 :

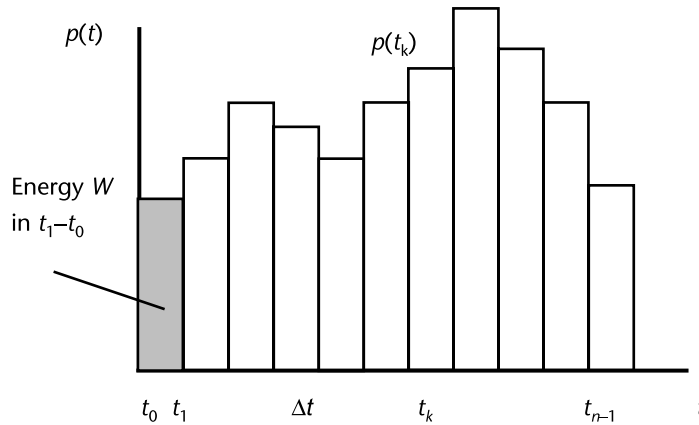


Figure 8.16 Stepwise characteristic for power $p(t)$ versus time.

$$W = \int_{t_0}^{t_1} p(\tau) d\tau \quad (8.31)$$

We find the total energy for a stepwise characteristic of the power $p(t)$ (as depicted in Figure 8.16) through a summation of the energy at each interval.

$$W = \sum_{t_0}^{t_{n-1}} p(t_k) \Delta t \quad (8.32)$$

In the case of a rotational system, assuming a rigid body that rotates in an xy plane with respect to an orthogonal z -axis, a vector force \mathbf{F} applied at a distance vector \mathbf{r} will produce a rotating torque, calculated as in (8.33) (see Figure 8.17).

$$\boldsymbol{\tau} = \mathbf{r} \times \mathbf{F} = \begin{vmatrix} \mathbf{i} & \mathbf{j} & \mathbf{k} \\ x & y & z \\ F_x & F_y & F_z \end{vmatrix} = (yF_z - zF_y)\mathbf{i} - (xF_z - zF_x)\mathbf{j} + (xF_y - yF_x)\mathbf{k} \quad (8.33)$$

For rotational devices (as is the case of rotors in electrical generators), the primary energy source supplies the mechanical torque from a steam turbine or from a hydro turbine (in the case of hydroelectric prime mover). The torque in (N·m) times the rotating speed ω (rad/s) is the amount of power that the turbine-generator set can supply to the electrical power system discounting the power used within

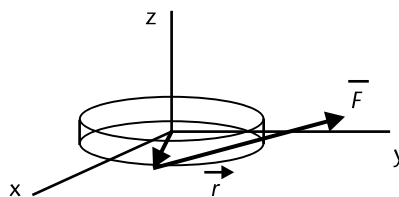


Figure 8.17 Rotating torque produced by force \mathbf{F} at a distance vector \mathbf{r} .

the power plant for its auxiliary services. The dynamics of rotating masses in the synchronous generator is dictated by the difference between the power supplied by the turbine, the electrical power that is delivered to the power system, the inertia, and the number of poles that are included in the design.

8.6.1 Kinetic Energy and Electrical Frequency

The majority of electrical power systems in the world operate with (AC) alternating voltage sources. Power generators make energy conversion possible by taking mechanical energy from high-pressure steam or water flow at hydraulic turbines; these two forms comprise the main source of primary energy nowadays. We are also now finding alternative energy sources, such as wind, solar, geothermal, biogas, and nuclear. This state of affairs is changing rapidly as growing concerns about climate change are setting a definite trend in looking for a larger share of renewable sources for primary energy before transforming it to electric form. The conventional primary energy sources—thermal and hydro—supply mechanical torque from steam or hydro turbines to electrical generators, working through a rotating shaft on which a rotor with appropriate electrical windings is located. The mass of the rotor, shaft, and other masses rotating at a given angular speed imply that kinetic energy is involved in the conversion process from mechanical to electrical energy coupled with electromechanical principles.

AC voltage, electric frequency, and kinetic energy in the rotor of a generator are related. Consider, as a starting point for the discussion, that the system is working at a nominal frequency f_o ; for that instant, it means that the electric power generated by all of the connected power units match the electrical load required by customers and the losses when power flows from generation to the load centers. If the generation exceeds the load and transmission losses, the net effect has a *change in rotating speed*. The rate of frequency increase depends on the amount of excess in kinetic energy into the rotors of the generators and the rotating mass of all the rotating generators that are currently synchronized to the network. The dynamic component of the electrical load responds to higher frequency and an increased mechanical torque is required because of the increased electrical load. The net effect is to attain a generation-load balance at a higher frequency. The power system has a target frequency and a scheme of frequency control that takes action to bring the frequency back to its rated value; this is done by decreasing the power output at all generators that participate in the *regulation* action in the proper amount. This problem is extensive and with various modeling details; now, our purpose is to have a succinct presentation about the dynamics and some analytical and simulation tools that are required for this problem.

As the kinetic energy explains the relation between all the generators connected to the system, the dynamics in a system can start with a generator, inertia I in $\text{Kg}\cdot\text{m}^2$, at a nominal frequency f_o in Hz and ω in rad/sec:

$$\begin{aligned} W_{\text{kin}} &= \frac{I\omega^2}{2} \\ W_{\text{kin}}^o &= \frac{I\omega_o^2}{2} \end{aligned} \tag{8.34}$$

From this expression, a relation of kinetic energy at frequency ω (with respect to the nominal rated value at ω_0) depends on the frequency square.

$$\frac{W_{\text{kin}}}{W_{\text{kin}}^o} = \frac{\omega^2}{\omega_0^2} = \frac{f^2}{f_0^2} \quad (8.35)$$

For an incremental torque ΔT (N-m) or an increment of power ΔP (Watts), the rotor of the synchronous machines will experience an acceleration α (rad/sec²). This is related to its kinetic energy.

$$\Delta T = \frac{\Delta P}{\omega} = I\alpha = \frac{Id\omega}{dt} \quad (8.36)$$

$$\Delta P = \omega I\alpha = \frac{\omega Id\omega}{dt} = \frac{d}{dt} \left(\frac{I\omega^2}{2} \right) = \frac{dW_{\text{kin}}}{dt} \quad (8.37)$$

Using (8.35) in (8.37):

$$\Delta P = d/dt (W_{\text{kin}}^o f^2 / f_0^2) = 2W_{\text{kin}}^o f / f_0^2 df/dt \quad (8.38)$$

Example 8.7

For a given electrical system [1] its total kinetic energy is 1,500 MJ, at a rated frequency of 60 Hz. What will be the rate of frequency increase for a surplus of 5 MW? Use (8.36) to find the change in frequency.

$$\left[\begin{array}{l} 5 \text{ MW} = 2(1,500 \text{ MJ}) \frac{(60 \text{ Hz})}{(60 \text{ Hz})^2} \frac{df}{dt} \\ \frac{df}{dt} = \frac{(5 \text{ MW})(60 \text{ Hz})}{2(1,500 \text{ MJ})} = 0.1 \text{ Hz/sec} \end{array} \right] \quad (8.39)$$

8.6.2 Turbine's Power and System's Frequency

As the load system changes, the generators that are equipped to regulate change the generated power to try to minimize the power imbalance due to load changes. The type of control problem described is a *following* one; in such cases, the system's frequency is the variable that gives a measure of power imbalance, and it is the variable that must be controlled. To have a viable model, some assumptions are required.

- Initially, a system's rated frequency is f_o , with a balance for generation P_G^o and demand P_D^o , as well as losses P_L^o . Kinetic energy for all rotors is P_{kin}^o in MW-sec.

- For a demand increment ΔP_D in the system, the electric generators supply an incremental power output such that $\Delta P_G = \Delta P_D$.
- For a power imbalance $\Delta P_T - \Delta P_D$, measured as turbine output and the required demand increment, a change in frequency is experienced. One initial assumption is that the change is uniform at every part of the electrical area. According to (8.35), the kinetic energy shows a squared dependence on frequency.

$$W_{\text{kin}} = W_{\text{kin}}^o \frac{f^2}{f_0^2} \text{ MW-sec} \quad (8.40)$$

- Load has a component that responds to frequency. One kind of representation is considered through the constant D .

$$D = \frac{\partial P_D}{\partial f} \text{ MW/Hz} \quad (8.41)$$

The power balance in an electrical area requires that the power increment from the turbine ΔP_T should be equal to the load increment ΔP_D , plus the load frequency dependent contribution $\partial P_D / \partial f \Delta f$, plus the power change equal to the rate of change in kinetic energy $\Delta P = dW_{\text{kin}}/dt$; this last term comes from (8.40).

$$\Delta P_T = \Delta P_D + \frac{\partial P_D}{\partial f} \Delta f + \frac{d}{dt} \left(W_{\text{kin}}^o \frac{f^2}{f_0^2} \right) \text{ MW} \quad (8.42)$$

Assuming that the new frequency will be $f = f_0 + \Delta f$ once high order terms are neglected, we come to (8.44).

$$\Delta P_T - \Delta P_D = D\Delta f + \frac{d}{dt} \left(\frac{W_{\text{kin}}^o (f_0 + \Delta f)^2}{f_0^2} \right) = D\Delta f + W_{\text{kin}}^o \frac{d}{dt} \left(1 + \frac{2\Delta f}{f_0} + \frac{\Delta f^2}{f_0^2} \right) \text{ MW} \quad (8.43)$$

$$\Delta P_T - \Delta P_D \approx D\Delta f + \frac{2W_{\text{kin}}^o}{f_0} \frac{d}{dt} (\Delta f) \text{ MW} \quad (8.44)$$

Using the rated nominal power for the generator as base P_r , a pu expression is written:

$$\Delta P_T - \Delta P_D \approx D\Delta f + \frac{2H}{f_0} \frac{d}{dt} (\Delta f) \text{ p.u. MW} \quad (8.45)$$

H is the *inertia constant* in seconds; its typical values are in a range from 2 to 8 seconds. D constant will be as pu MW/Hz.

$$H = \frac{W_{\text{kin}}^o}{P_r} \text{ sec} \quad (8.46)$$

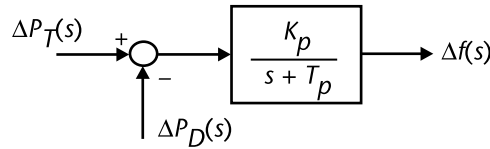


Figure 8.18 Frequency change as a function of disturbance from turbine power and load change.

A Laplace transform on (8.45) gives:

$$\Delta P_T(s) - \Delta P_D(s) = D\Delta f(s) + \frac{2H}{f_o} s\Delta f(s) \tag{8.47}$$

The transfer function in (8.48) and a feedback through the power system closes the power system response that goes to the turbine control. We can use this model to start studying power-frequency dynamics.

$$\frac{\Delta f(s)}{\Delta P_T(s) - \Delta P_D(s)} = \frac{1}{D + 2H/f_o s} = \frac{1/D}{1 + 2H/(Df_o)s} = \frac{K_p}{(1 + T_p s)} \tag{8.48}$$

8.6.3 Frequency Control by a Primary Loop

The change in frequency Δf due to a load disturbance ΔP_D will require *feedback* (as shown in Figure 8.19), generally done through a *droop* characteristic, R . The droop will regulate the turbine output requirement in order to correct for a drop in speed with respect to a reference when the load is increased.

$$\Delta P_g(s) = \Delta P_{ref}(s) - \frac{\Delta f(s)}{R} \tag{8.49}$$

$$\Delta P_T(s) = TF(s)\Delta P_g(s) \tag{8.50}$$

$$\frac{\Delta f(s)}{\Delta P_T(s) - \Delta P_D(s)} = \frac{K_p}{1 + T_p s} \tag{8.51}$$

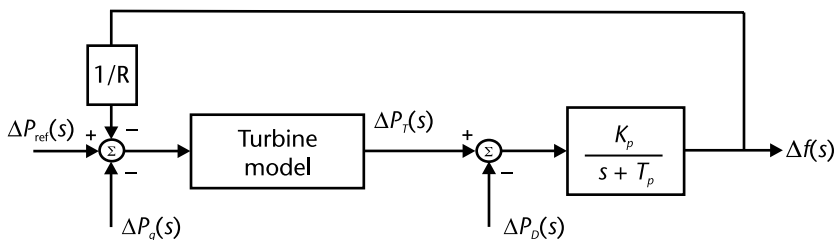


Figure 8.19 Primary loop frequency control.

Example 8.7

The type of response when a load change is experienced, the following values are used in the model: load change $\Delta P_D = +0.01$ pu MW at time 1 sec; $R = 2.4$ Hz/pu MW; $K_p = 1/D = 120$ Hz/pu MW; and $T_p = 2H/(Df_o) = 2(5)(120)/60 = 20$ sec. Reference is set to zero change. The time response (see Figure 8.20) shows a steady state frequency error; therefore, additional control action is required in order to get the system frequency restored to its nominal value.

Estimated time constant $(3.5 - 1.0)/5 = 0.5$ sec.

In this case, the frequency error after 5 seconds is shown in Figure 8.21. To reduce the error in frequency, a secondary control loop with an integral characteristic

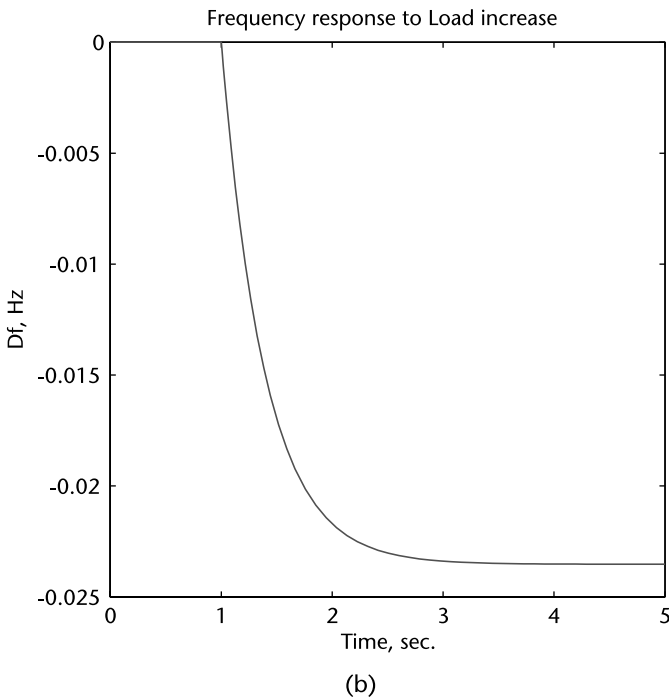
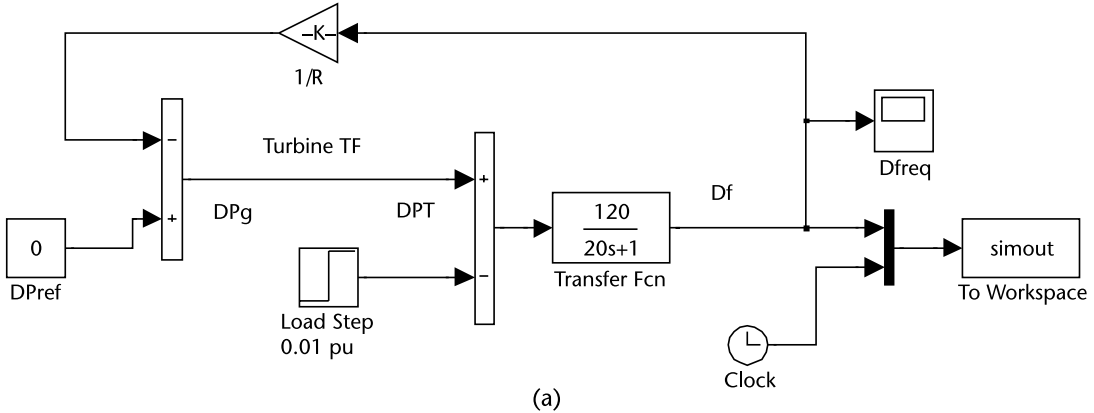


Figure 8.20 Dynamic frequency response for primary loop control, no turbine model is included.

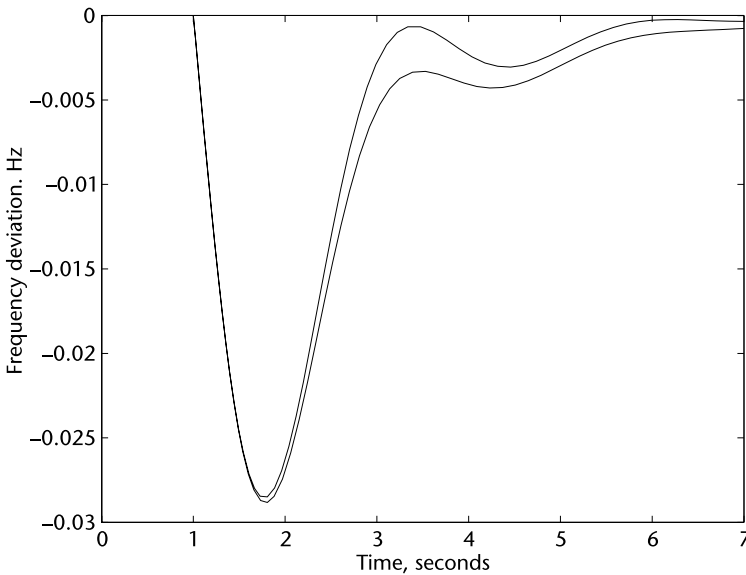
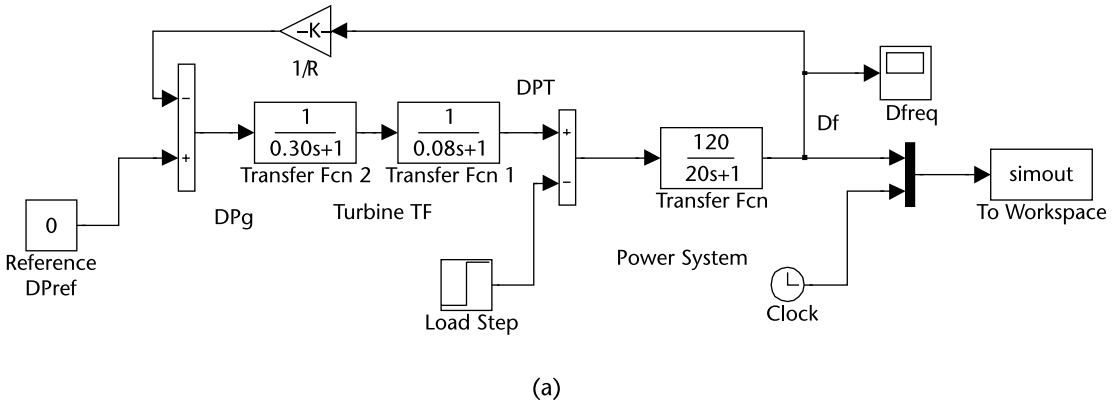


Figure 8.21 Primary loop frequency response, including a turbine model.

is required. This will eventually make the frequency error go to zero (see Figure 8.21); this part is extended through Example 8.8.

Example 8.9

In order to correct the error frequency seen in Example 8.7, an additional control block with an integral function and an appropriate gain K_I will bring the frequency back to normal. We show the effect of using $K_I = -0.5$ and -0.6 (see Figure 8.22).

A great deal of material needs to be extended in order to cover the nature of power-frequency control, such as the tie-line control, areas interchanges, and neighbor assistance characteristics when one area experiences frequency disturbances.

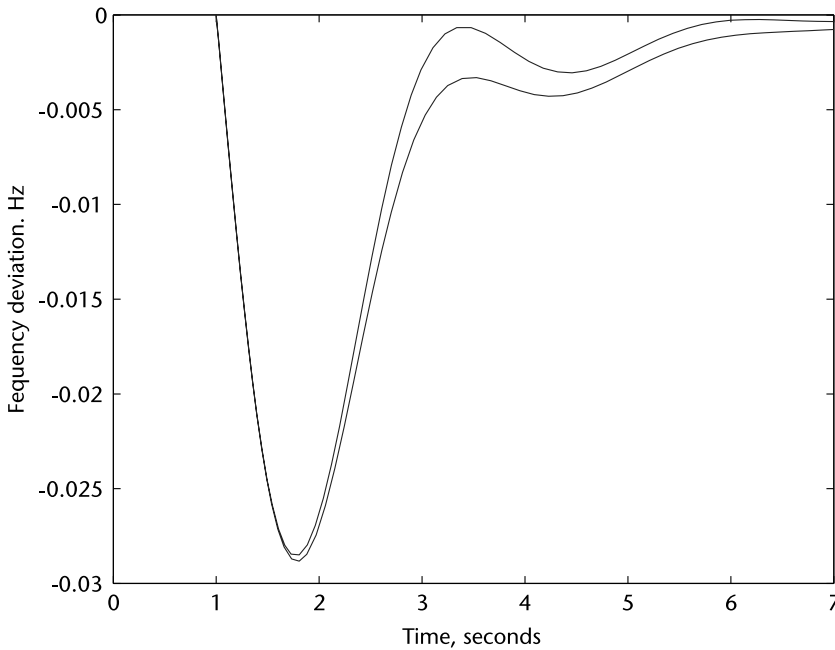
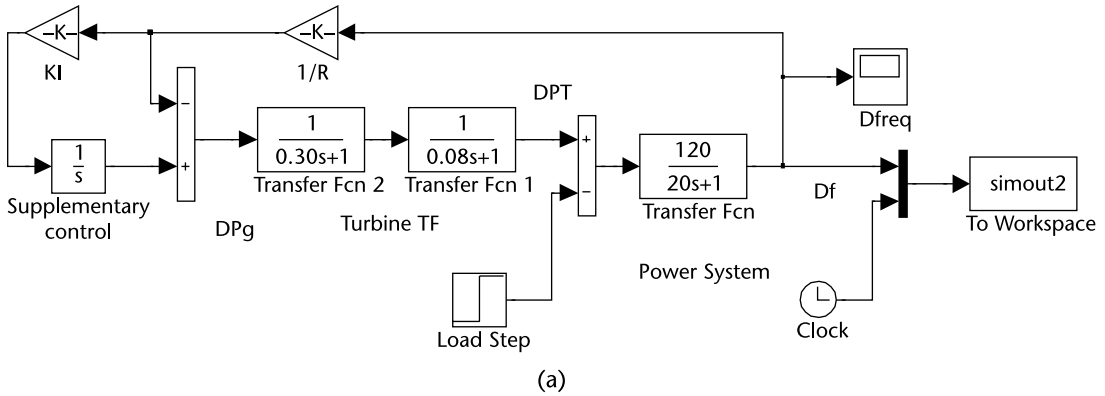


Figure 8.22 Supplementary control loop to bring back frequency deviation to zero.

8.7 Incremental Power Model to Include a VSC-STATCOM

AC load flow solutions for power networks include models for all the main components: transmission lines, on load tap changer power transformers, and new control devices. The new arrangements are usually based on power electronics whose characteristics make very useful and versatile controls fast acting and dependable with promising possibilities for the better use of transmission assets and better system control. To include various arrangements might pose a problem if new devices need to be incorporated into the traditional analysis tools as the power flow studies. In

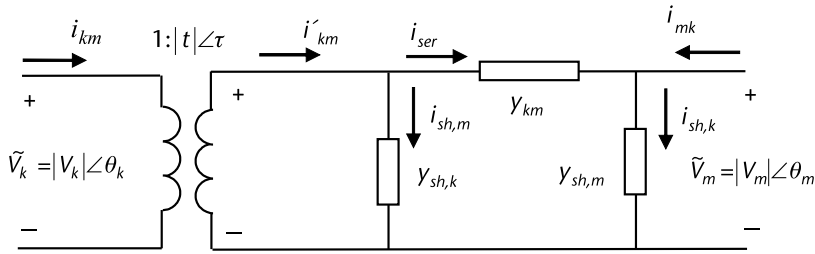


Figure 8.23 Ideal Complex power transformer and a π circuit.

this section, we develop a versatile model to incorporate new devices based on the concept of incremental real and reactive power in conjunction with nodal power balance. The resulting system of equations, when solved, includes nodal analysis and for the nonlinear case the incremental model is the accepted expression for Newton’s iterative process.

8.7.1 Power Flows in a Complex Transformer and a Transmission Line

The concept of a complex power transformer is useful in representing a device that can control both the real and reactive power flows as well as the voltage at terminals; an extension to this control problem might be a congestion problem or the voltage control at a given node. This functionality can be realized by power electronics [4] whose purpose is to render a flexible and diverse control and to be readily available within an already stressed power system.

8.7.1.1 Complex Power Transformer

The circuit in Figure 8.24 allows us to visualize the angle shift and phasor magnitudes from primary to secondary in a complex power transformer.

To include winding losses, a series conductance component is added to the ideal complex transformer. A shunt branch can be connected, as shown in Figure 8.23.

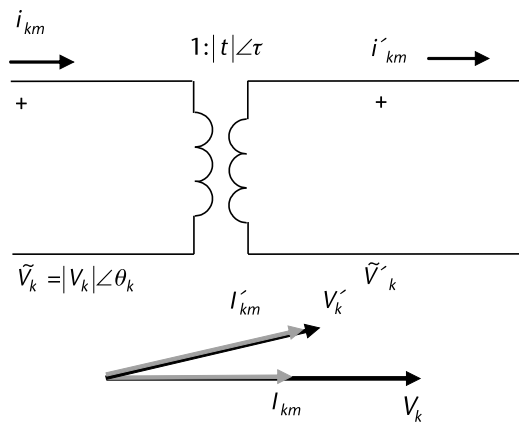


Figure 8.24 Ideal complex power transformer.

8.7.1.2 On Load Tap Changer (OLTC)

In this case, shunt admittances are zero as well as the phase shift angle τ :

$$\begin{aligned} y_{sb,k} &= y_{sb,m} = 0 \\ \tau &= 0 \end{aligned} \quad (8.52)$$

8.7.1.3 Transmission Line

The π representation of a positive sequence circuit will be obtained if we make:

$$\begin{aligned} y_{sb,k} &= y_{sb,m} = y_{sb2} \\ |t| &= 1, \tau = 0 \end{aligned} \quad (8.53)$$

8.7.2 Expressions for Incremental Power Flow

The first term of a Taylor's series expansion for p_{km} and q_{km} includes the change of the series susceptance b_{km} .

$$\begin{aligned} \Delta p_{km} &= \frac{\partial p_{km}}{\partial \theta_k} \Delta \theta_k + \frac{\partial p_{km}}{\partial \theta_m} \Delta \theta_m + \frac{\partial p_{km}}{\partial \tau} \Delta \tau + \frac{\partial p_{km}}{\partial |V_k|} |V_k| \frac{\Delta |V_k|}{|V_k|} \\ &\quad + \frac{\partial p_{km}}{\partial |V_m|} |V_m| \frac{\Delta |V_m|}{|V_m|} + \frac{\partial p_{km}}{\partial |t|} |t| \frac{\Delta |t|}{|t|} + \frac{\partial p_{km}}{\partial b_{km}} b_{km} \frac{\Delta b_{km}}{b_{km}} \end{aligned} \quad (8.54)$$

$$\begin{aligned} \Delta q_{km} &= \frac{\partial q_{km}}{\partial \theta_k} \Delta \theta_k + \frac{\partial q_{km}}{\partial \theta_m} \Delta \theta_m + \frac{\partial q_{km}}{\partial \tau} \Delta \tau + \frac{\partial q_{km}}{\partial |V_k|} |V_k| \frac{\Delta |V_k|}{|V_k|} \\ &\quad + \frac{\partial q_{km}}{\partial |V_m|} |V_m| \frac{\Delta |V_m|}{|V_m|} + \frac{\partial q_{km}}{\partial |t|} |t| \frac{\Delta |t|}{|t|} + \frac{\partial q_{km}}{\partial b_{km}} b_{km} \frac{\Delta b_{km}}{b_{km}} \end{aligned} \quad (8.55)$$

Similar equations can be written for Δp_{mk} and Δq_{mk} . In (8.54) and (8.55), various terms can be identified as state variables, like nodal angles and voltage magnitudes, but the incremental changes of phase shifting angle τ , tap magnitude, and increase/decrease of the susceptance b_{km} are also identified as control variables. Due to transmission losses and the nature of series inductance, there will be a different amount of power from m to k ; this requires that we write the incremental equations from node m to k .

$$\begin{aligned} \Delta p_{mk} &= \frac{\partial p_{mk}}{\partial \theta_m} \Delta \theta_m + \frac{\partial p_{mk}}{\partial \theta_k} \Delta \theta_k + \frac{\partial p_{mk}}{\partial \tau} \Delta \tau + \frac{\partial p_{mk}}{\partial |V_m|} |V_m| \frac{\Delta |V_m|}{|V_m|} \\ &\quad + \frac{\partial p_{mk}}{\partial |V_k|} |V_k| \frac{\Delta |V_k|}{|V_k|} + \frac{\partial p_{mk}}{\partial |t|} |t| \frac{\Delta |t|}{|t|} + \frac{\partial p_{mk}}{\partial b_{km}} b_{km} \frac{\Delta b_{km}}{b_{km}} \end{aligned} \quad (8.56)$$

$$\Delta q_{mk} = \frac{\partial q_{mk}}{\partial \theta_m} \Delta \theta_m + \frac{\partial q_{mk}}{\partial \theta_k} \Delta \theta_k + \frac{\partial q_{mk}}{\partial \tau} \Delta \tau + \frac{\partial q_{mk}}{\partial |V_m|} |V_m| \frac{\Delta |V_m|}{|V_m|} + \frac{\partial q_{mk}}{\partial |V_k|} |V_k| \frac{\Delta |V_k|}{|V_k|} + \frac{\partial q_{mk}}{\partial |t|} |t| \frac{\Delta |t|}{|t|} + \frac{\partial q_{mk}}{\partial b_{km}} b_{km} \frac{\Delta b_{km}}{b_{km}} \quad (8.57)$$

$$\begin{bmatrix} -1 & 0 & \frac{\partial p_{km}}{\partial \theta_k} & \frac{\partial p_{km}}{\partial \theta_m} & 0 & 0 & \frac{\partial p_{km}}{\partial V_k} V_k & \frac{\partial p_{km}}{\partial V_m} V_m \\ 0 & -1 & \frac{\partial p_{mk}}{\partial \theta_k} & \frac{\partial p_{mk}}{\partial \theta_m} & 0 & 0 & \frac{\partial p_{mk}}{\partial V_k} V_k & \frac{\partial p_{mk}}{\partial V_m} V_m \\ +1 & 0 & 0 & 0 & 0 & 0 & 0 & 0 \\ 0 & +1 & 0 & 0 & 0 & 0 & 0 & 0 \\ 0 & 0 & \frac{\partial q_{km}}{\partial \theta_k} & \frac{\partial q_{km}}{\partial \theta_m} & -1 & 0 & \frac{\partial q_{km}}{\partial V_k} V_k & \frac{\partial q_{km}}{\partial V_m} V_m \\ 0 & 0 & \frac{\partial q_{mk}}{\partial \theta_k} & \frac{\partial q_{mk}}{\partial \theta_m} & 0 & -1 & \frac{\partial q_{mk}}{\partial V_k} V_k & \frac{\partial q_{mk}}{\partial V_m} V_m \\ 0 & 0 & 0 & 0 & +1 & 0 & 0 & 0 \\ 0 & 0 & 0 & 0 & 0 & +1 & 0 & 0 \end{bmatrix} \begin{bmatrix} \Delta p_{km} \\ \Delta p_{mk} \\ \Delta \theta_m \\ \Delta q_{km} \\ \Delta q_{mk} \\ \frac{\Delta V_k}{V_k} \\ \frac{\Delta V_m}{V_m} \end{bmatrix} = \begin{bmatrix} -\frac{\partial p_{km}}{\partial \tau} \Delta \tau - \frac{\partial p_{km}}{\partial |t|} |t| \frac{\Delta |t|}{|t|} - \frac{\partial p_{km}}{\partial b_{km}} b_{km} \frac{\Delta b_{km}}{b_{km}} \\ -\frac{\partial p_{mk}}{\partial \tau} \Delta \tau - \frac{\partial p_{mk}}{\partial |t|} |t| \frac{\Delta |t|}{|t|} - \frac{\partial p_{mk}}{\partial b_{km}} b_{km} \frac{\Delta b_{km}}{b_{km}} \\ \Delta P_k \\ \Delta P_m \\ -\frac{\partial q_{km}}{\partial \tau} \Delta \tau - \frac{\partial q_{km}}{\partial |t|} |t| \frac{\Delta |t|}{|t|} - \frac{\partial q_{km}}{\partial b_{km}} b_{km} \frac{\Delta b_{km}}{b_{km}} \\ -\frac{\partial q_{mk}}{\partial \tau} \Delta \tau - \frac{\partial q_{mk}}{\partial |t|} |t| \frac{\Delta |t|}{|t|} - \frac{\partial q_{mk}}{\partial b_{km}} b_{km} \frac{\Delta b_{km}}{b_{km}} \\ \Delta Q_k \\ \Delta Q_m \end{bmatrix} \quad (8.58)$$

Equations (8.54)–(8.58) represent individual elements, transmission lines, or power transformers. The nodal power balance expresses the connectivity in the network. These types of incremental relations are the basis for the Newton's iterative method—the one that is used to solve the general load flow problem.

8.7.2.1 Partial Derivatives, Incremental Power Flow

Numerical values for the partial derivatives in (8.58) can be obtained from a given set of nodal voltages and the calculated real and reactive power from k to m and from m to k . Formulas for partial derivatives were presented in Chapter 6.

8.7.2.2 Load Flow Solution by Newton's Method

For an AC power network, a solution for complex nodal voltages is to be determined, starting with an assumed set of values. With these voltages, the element's power flows are determined, nodal power balances are calculated, and the nodal *power mismatches* are obtained. As the initial voltages might not be the network's solution, the maximum absolute value of the power mismatch would not be smaller than a prescribed small tolerance. An iterative process that requires building the incremental set (8.58) is used. The coefficient matrix is known as *Jacobian*; its pattern is highly sparse and there will be a need to use special techniques in order to efficiently solve large networks. Usually, in the right hand side of (8.58) we find the control variables that are assumed fixed, so we are left with real and reactive power mismatches and the need to solve for correction $\Delta \theta$'s and $\Delta V/V$ to the state variables.

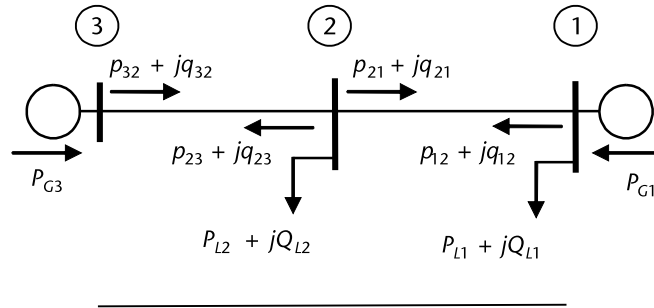


Figure 8.25 Three-node system to illustrate the incremental equations.

Example 8.10

Solution for a three-node system (see Figure 8.25):

The regular load flow problem is solved by Newton's method using (8.58) with no reactive compensation at node 3, assuming transmission lines only. The solution is shown in Figure 8.26.

Data for elements

Nelem = 2 Nnod = 3

Elem	Nsal	Nlleg	r	x	ykm		ysh	
1	2	1	0.0500	0.1000	4.0000+j	-8.0000	0.0000+j	0.0000
2	2	3	0.0100	0.1000	0.9901+j	-9.9010	0.0000+j	0.0000
3	1	2	0.0500	0.1000	4.0000+j	-8.0000	0.0000+j	0.0000
4	3	2	0.0100	0.1000	0.9901+j	-9.9010	0.0000+j	0.0000

Data for nodes

Nodo	tipo	V	angle	PG	QG	PL	QL
1	0	1.0000	0.0000	0.0000	0.0000	0.0000	0.0000
2	-1	1.0000	0.0000	0.0000	0.0000	0.2500	0.2000
3	1	1.1338	0.0000	0.0000	0.0000	0.0200	0.0000

Flows through elements

Elem	Nsal	Nlleg	skm	
1	2	1	0.0000+j	0.0000
2	2	3	-0.1325+j	-1.3248
3	1	2	0.0000+j	0.0000
4	3	2	0.1502+j	1.5020

Iteration = 0 max Mismatch = 1.124752e+000

Iteration = 1 max Mismatch = 8.044233e-002

Iteration = 2 max Mismatch = 3.069485e-004

Iteration = 3 max Mismatch = 4.592218e-009

Nodal results

Node	type	Voltage	angle	PG	QG	PL	QL
1	0	1.0000	-0.0000	0.3016	-0.6328	0.0000	0.0000
2	-1	1.0500	-3.3742	-0.0000	-0.0000	0.2500	0.2000
3	1	1.1338	-3.9289	0.0000	0.9525	0.0200	0.0000

Load flow results

Elem	type	Nsal	Nlleg	pkm	qkm
------	------	------	-------	-----	-----

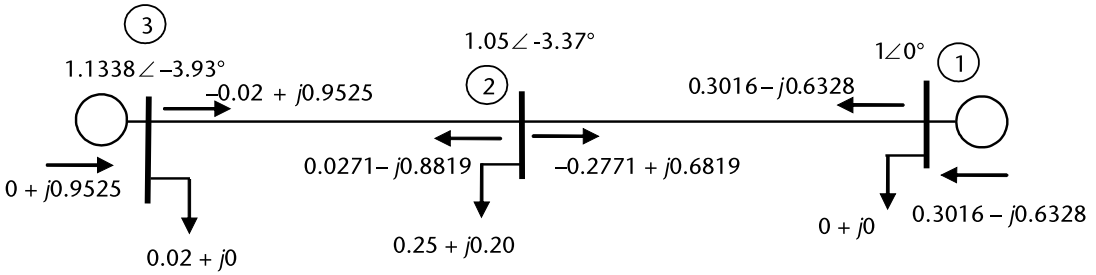


Figure 8.26 System for load flow studies.

1	0	2	1	-0.2771	0.6819
2	0	2	3	0.0271	-0.8819
3	0	1	2	0.3016	-0.6328
4	0	3	2	-0.0200	0.9525

8.8 Voltage Source Converter (VSC) and STATCOM

An equivalent circuit is used to represent the VSC with a complex power transformer a series and a shunt admittance, as in Figure 8.27. The tap magnitude $|t|$ will represent the amplitude modulation index m'_a . The phase shifting angle τ can be adjusted so that the current is in phase with the voltage and no reactive power is required; this concept is used to identify this portion of the circuit as of DC type. Relations (8.59) are recognized for a two-level, three-phase VSC, and operated in the linear range of modulation. $E_{n,DC}$ is analogous to a DC voltage with value $\sqrt{2}$. To characterize a STATCOM, a series OLTC transformer is needed and is connected from node n to node k (see Figure 8.27). The following values (8.59) do not

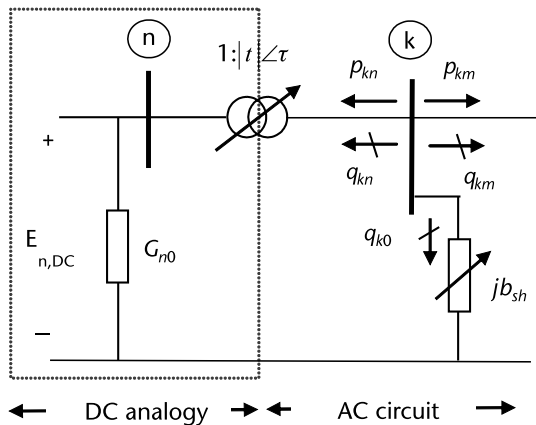


Figure 8.27 Equivalent circuit for a VSC, DC analogy, and AC circuit with a complex transformer.

consider overmodulation, which with proper handling of harmonics would increase the usage of the DC link with no distortion on currents and line to line voltages.

$$|t| = m'_a = \frac{\sqrt{3}}{2m_a} \quad 0 < m_a < 1 \quad \tau = \phi \tag{8.59}$$

8.8.1 Incremental Model for the VSC

We present the main components of the VSC.

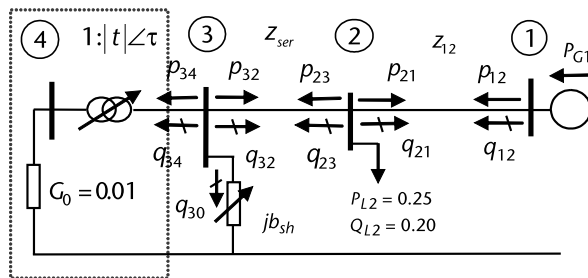
From Figure 8.28 and prior to the solution process, it is recognized that an ideal complex transformer is connected from node 3 to 4. At this point, the result for voltage and current in an ideal complex transformer is applied. The conductance G_0 connected at node 4 requires only real power; the reactive power due to b_{sb} is calculated using (8.60).

$$q_{30} = -|V_3|^2 b_{sb} \tag{8.60}$$

The solution should be such that the voltage magnitude at node 2 is controlled to a fixed value. The unknowns are nodal angles: θ_2, θ_3 , voltage magnitude for V_3 , and the value of b_{sb} ; this susceptance element is required to keep the voltage at node 2 at the requested value. The real and reactive nodal balances are a set of nonlinear equations (8.62). When the iterative process converges, the vales for $\tau = \theta_3$ and $|t|$ are calculated by (8.61).

$$|\tilde{V}_4||t|\angle\tau = |\tilde{V}_3|\angle\theta_3 \tag{8.61}$$

$$\left[\begin{array}{l} +\Delta p_{21} + \Delta p_{23} = \Delta P_2 \\ +\Delta p_{32} + \Delta p_{34} = +\Delta p_{32} = \Delta P_3 \text{ as } p_{34} = cte. \\ +\Delta q_{21} + \Delta q_{23} = \Delta Q_2 \\ +\Delta q_{32} + \Delta q_{34} + \Delta q_{30} = +\Delta q_{32} + \Delta q_{30} = \Delta Q_3 \text{ as } q_{34} = 0 \end{array} \right] \tag{8.62}$$



$$z_{12} = 0.05 + j0.10 \text{ puvalues}$$

$$z_{ser} = 0.01 + j0.10$$

Figure 8.28 VSC system configuration.

The incremental model is a Newton's algorithm that is used to solve for corrections to the state variables: nodal angles, voltage magnitude, and compensating susceptance. The incremental set (8.62) requires partial derivatives for q_{30} and ΔP 's values. The solution starts with initial values for variables θ_2 , θ_3 , $|V_3|$, and b_{sb} .

$$\Delta q_{30} = \frac{\partial q_{30}}{\partial |V_3|} |V_3| \frac{\Delta |V_3|}{|V_3|} + \frac{\partial q_{30}}{\partial b_{sb}} \Delta b_{sb} \quad (8.63)$$

$$\frac{\partial q_{30}}{\partial |V_3|} |V_3| = -2|V_3|^2 b_{sb} \quad (8.64)$$

$$\frac{\partial q_{30}}{\partial b_{sb}} = -|V_3|^2 \quad (8.65)$$

After three iterations, the maximum mismatch is $5.46e-009$. The voltage at node 2 is kept at a value of 1.05 pu and the shunt capacitive susceptance required is $b_{sb} = 0.7408$ pu. The voltage for node 3 is 1.1338 and the angle is -3.93 degrees; the tap value in the complex transformer is $1.1338/1.4142 = 0.8017$ and the phase shifting angle is -3.93 degrees. Losses of 2% are represented by the shunt conductance at node 4. One additional possibility is to include a resistive shunt branch at node 3; its value might be determined by an open circuit test for the VSC configuration.

Data for elements

Nelem = 2 Nnod = 3

Elem	Nsal	Nlleg	r	x	yk	ym	ysh	ysm
1	2	1	0.0500	0.1000	4.0000+j	-8.0000	0.0000+j	0.0000
2	2	3	0.0100	0.1000	0.9901+j	-9.9010	0.0000+j	0.0000
3	1	2	0.0500	0.1000	4.0000+j	-8.0000	0.0000+j	0.0000
4	3	2	0.0100	0.1000	0.9901+j	-9.9010	0.0000+j	0.0000

Data for nodes

Node	type	V	angle	PG	QG	PL	QL
1	0	1.0000	0.0000	0.0000	0.0000	0.0000	0.0000
2	1	1.0500	0.0000	0.0000	0.0000	0.2500	0.2000
3	-1	1.0000	0.0000	0.0000	0.0000	0.0200	0.0000

Data for bshunt

Nodes = 3 bshunt0 = 0.5000

Flows through elements

Elem	Nsal	Nlleg	sk	sm
1	2	1	0.2100+j	0.4200
2	2	3	0.0520+j	0.5198
3	1	2	-0.2000+j	-0.4000
4	3	2	-0.0495+j	-0.4950

Iteration = 0 max mismatch = 1.139802e+000

Iteration = 1 max mismatch = 1.307479e-001

Iteration = 2 max mismatch = 6.236311e-004
 Iteration = 3 max mismatch = 5.463104e-009

Nodal results

Node	type	Voltage	angle	PG	QG	PL	QL
1	0	1.0000	-0.0000	0.3016	-0.6326	0.0000	0.0000
2	1	1.0500	-3.3738	0.0000	0.0000	0.2500	0.2000
3	-1	1.1338	-3.9284	-0.0000	0.9523	0.0200	0.0000

Load flow results

Elem	type	Nsal	Nlleg	pkm	qkm
1	0	2	1	-0.2771	0.6817
2	0	2	3	0.0271	-0.8817
3	0	1	2	0.3016	-0.6326
4	0	3	2	-0.0200	0.9523

Results for the VSC

bshunt = 0.7408 (>0 capacitive) power q to the node = -0.9523
 maprim = 0.8017 tao = -3.9284 ma = 0.9257

8.9 Extensions to the Model

The incremental model can be applied to various practical power network configurations.

8.9.1 Reactive Power and Voltage Control

Example 8.11

With a variable shunt susceptance at node 3 in the configuration shown in Figure 8.29, voltage control on node 2 and the real power to be supplied to node 4 as 0.005 pu, the reactive power flow into the system can be controlled according to the operational needs in the power system. Assuming that the voltage for node 2 should be fixed at 0.95 pu, the iterative process shows convergence at three iterations with a mismatch of $9.841\text{e-}12$. The inductive compensation required is 0.1682 pu,

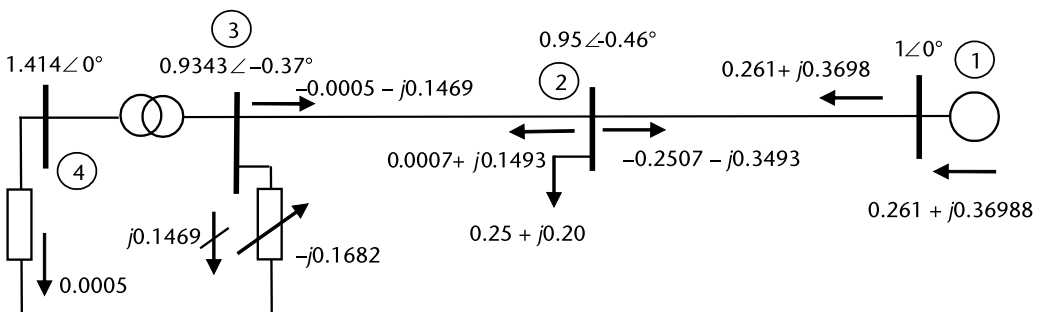


Figure 8.29 VSC system configuration for voltage control.

and it is noted that the current flowing through the VSC has a low value; internal losses are quite small, 0.05%.

Data for elements

Nelem =	2	Nnod =	3						
Elem	Nsal	Nlleg	r	x	ykm		ysh		
1	2	1	0.0500	0.1000	4.0000+j	-8.0000	0.0000+j	0.0000	
2	2	3	0.0100	0.1000	0.9901+j	-9.9010	0.0000+j	0.0000	
3	1	2	0.0500	0.1000	4.0000+j	-8.0000	0.0000+j	0.0000	
4	3	2	0.0100	0.1000	0.9901+j	-9.9010	0.0000+j	0.0000	

Data for nodes

Node	type	V	angle	PG	QG	PL	QL
1	0	1.0000	0.0000	0.0000	0.0000	0.0000	0.0000
2	1	0.9500	0.0000	0.0000	0.0000	0.2500	0.2000
3	-1	1.0000	0.0000	0.0000	0.0000	0.0005	0.0000

Bshunt Data

Node =	3	bshunt0 =	0.5000
--------	---	-----------	--------

Flows through elements

Elem	Nsal	Nlleg	skm	
1	2	1	-0.1900+j	-0.3800
2	2	3	-0.0470+j	-0.4703
3	1	2	0.2000+j	0.4000
4	3	2	0.0495+j	0.4950

Iteration =	0	max mismatch =	6.502970e-001
Iteration =	1	max mismatch =	3.886674e-002
Iteration =	2	max mismatch =	1.790303e-005
Iteration =	3	max mismatch =	9.841572e-012

Nodal Results

Node	type	Voltage	angle	PG	QG	PL	QL
1	0	1.0000	-0.0000	0.2610	0.3698	0.0000	0.0000
2	1	0.9500	-0.4589	0.0000	0.0000	0.2500	0.2000
3	-1	0.9343	-0.3673	0.0000	-0.1469	0.0005	0.0000

Flow results

Elem	type	Nsal	Nlleg	pkm	qkm
1	0	2	1	-0.2507	-0.3493
2	0	2	3	0.0007	0.1493
3	0	1	2	0.2610	0.3698
4	0	3	2	-0.0005	-0.1469

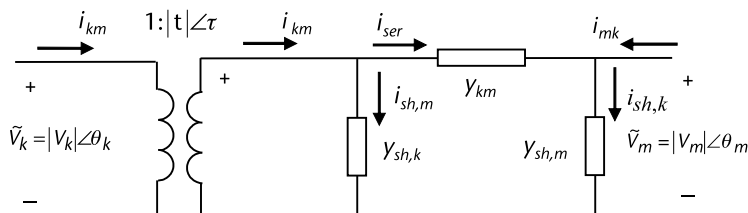


Figure 8.30 VSC system configuration for voltage control.

Results for the VSC

```
bshunt = -0.1682 (>0 capacitive) power q into node = 0.1469
maprim = 0.6606 tao = -0.3673 ma = 0.7628
```

8.9.2 DC Load

Example 8.12

It is interesting to extend the case so that DC load is supplied at node 4; this is a common situation in a practical configuration. It is like a back-to-back arrangement that interconnects two AC power systems with the same or with different frequencies. For a DC load of 0.5318 pu, corresponding $G_0 = 0.2659$ pu. The mismatch is $3.004e-07$ in three iterations.

```
Iteration = 3 Max mismatch = 3.004665e-007
```

Nodal results

Node	type	Voltage	angle	PG	QG	PL	QL
1	0	1.0000	-0.0000	0.8723	-0.8554	0.0000	0.0000
2	1	1.0500	-7.1120	-0.0000	-0.0000	0.2500	0.2000
3	-1	1.1613	-10.2532	0.0000	1.3635	0.5318	0.0000

Flow results

Elem	type	Nsa1	Nlleg	pkm	qkm
1	0	2	1	-0.7977	1.0046
2	0	2	3	0.5477	-1.2046
3	0	1	2	0.8723	-0.8554
4	0	3	2	-0.5318	1.3635

Results for the VSC

```
bshunt = 1.0111 (>0 capacitive) power q into node = -1.3635
maprim = 0.8211 tao = -10.2532 ma = 0.9482 G0= 0.2659 pu
```

8.10 STATCOM Model

To have a representation for the STATCOM, a load tap changing transformer (OLTC) is needed in series to the VSC circuit from Section 8.8.1.

8.10.1 OLTC's Real and Reactive Power Flows

Let us assume a balanced configuration so the positive sequence of a transformer with a tap changing under load, as shown in Figure 8.31, will be part of the STATCOM. Power flow equations and the partial derivatives for the incremental model use $\tau = 0$, $y_{sb,k} = y_{sb,m} = 0$ and $|t|$ within bounds (see Figure 8.30).

Example 8.12

A modified network to represent an STATCOM includes an OLTC, the model uses $|t| = 1.1335$, constrained to be within bounds $0.8 < |t| < 1.2$, series impedance $r_T = 0.01$ and $x_T = 0.10$ in pu. The voltage at node 2 will be fixed to 1.05 pu. Convergence shows a mismatch of $4.334e-007$ in 3 iterations (see Figure 8.31).

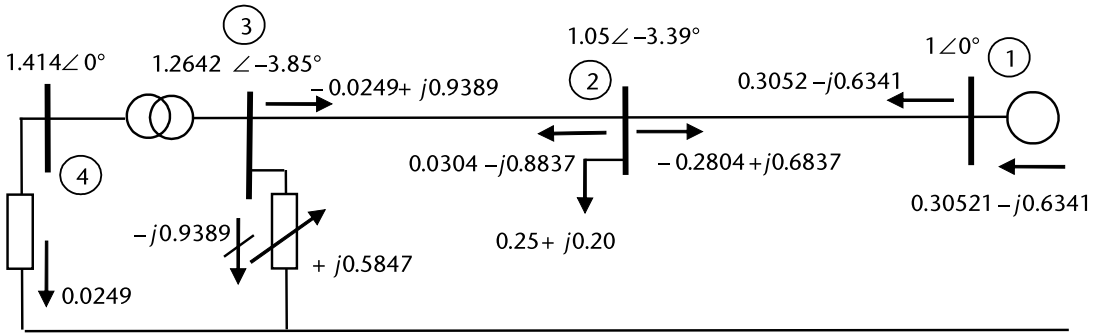


Figure 8.31 Complex power transformer for OLTC configuration.

Data for elements

Nelem = 2 Nnod = 3

Elem	Nsal	Nlleg	r	x	yk	ym	ysh	ysl
1	2	1	0.0500	0.1000	4.0000+j	-8.0000	0.0000+j	0.0000
2	2	3	0.0100	0.1000	0.9901+j	-9.9010	1.1335+j	0.0000
3	1	2	0.0500	0.1000	4.0000+j	-8.0000	0.0000+j	0.0000
4	3	2	0.0100	0.1000	0.9901+j	-9.9010	1.1335+j	0.0000

Data for nodes

Node	type	V	angle	PG	QG	PL	QL
1	0	1.0000	0.0000	0.0000	0.0000	0.0000	0.0000
2	1	1.0500	0.0000	0.0000	0.0000	0.2500	0.2000
3	-1	1.0000	0.0000	0.0000	0.0000	0.0249	0.0000

Data for the bshunt

Node = 3 bshunt0 = 0.5000

Flows in elements

Elem	Nsal	Nlleg	skm	qkm
1	2	1	0.2100+j	0.4200
2	2	3	0.2241+j	2.2410
3	1	2	-0.2000+j	-0.4000
4	3	2	-0.1883+j	-1.8829

Iteration = 0 Max mismatch = 2.861005e+000

Iteration = 1 Max mismatch = 9.628746e-001

Iteration = 2 Max mismatch = 5.902866e-003

Iteration = 3 Max mismatch = 4.334714e-007

Nodal results

Node	type	Voltage	angle	PG	QG	PL	QL
1	0	1.0000	-0.0000	0.3052	-0.6341	0.0000	0.0000
2	1	1.0500	-3.3975	-0.0000	0.0000	0.2500	0.2000
3	-1	1.2642	-3.8498	-0.0000	0.9389	0.0249	0.0000

Load flow results

Elem	type	Nsal	Nlleg	pkm	qkm
1	0	2	1	-0.2804	0.6837
2	1	2	3	0.0304	-0.8837
3	0	1	2	0.3052	-0.6341
4	1	3	2	-0.0249	0.9389

Results for the VSC

bshunt = 0.5874 (>0 capacitive) power q into node = -0.9389
 maprim = 0.8939 tao = -3.8498 ma = 1.0322 G0= 0.01245 pu

Next, the STATCOM (see Figure 8.32) is connected at node 9 of a 14-node system (see Figure 8.33); it will replace the capacitor compensation for the base case. The

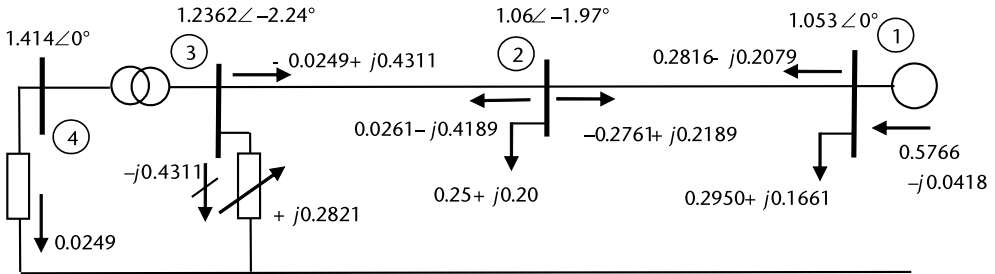
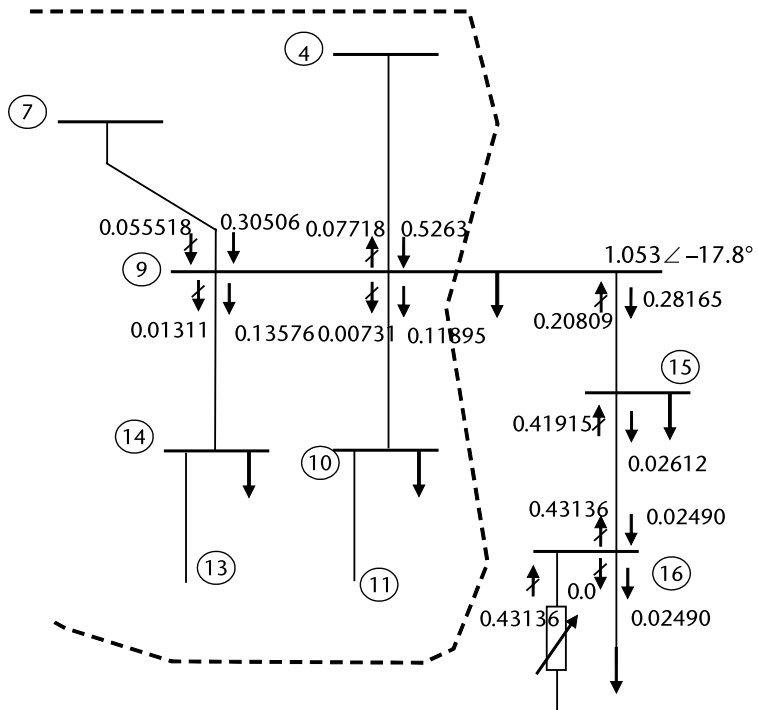


Figure 8.32 STATCOM configuration for voltage control.



Node	Voltage	Angle	Load
4	1.0106	-12.05	
7	1.0593	-16.07	
9	1.0530	-17.80	0.2950+i0.1660
10	1.0488	-19.64	0.0900+i0.0580
14	1.0338	-19.64	
15	1.06	-19.78	0.2500+i0.2000
16	1.2362	-20.04	0.0249+i0.0000

Figure 8.33 STATCOM voltage control and reactive power injection at node 9.

STATCOM is connected at node 9. Two additional nodes are required, 15 and 16, and the iterative process shows good convergence.

8.11 Chapter Summary

The material in this chapter covers real power control and reactive power, first with a static model, which is valid for small changes around the operating point. We introduced modeling and analysis for simple circuit arrangements in order to approach step-by-step the problem of *optimal control coordination*. This can be done for real power flows and existing control, as well as for reactive power and voltage related control problems. The discussion cannot be complete unless turbine response and its controls are included. This is done by working with the reasonable assumption that the relation between *rotor speed*, frequency and real power as supplied by the turbine and the power required by the load in the system. More should be said about the control problem, and the models with which we include turbine, governor, droop, and other extensions into the realm of interarea assistance during disturbances in neighboring areas.

In the last part of this chapter, rotor dynamics were given. It should be noted that an *error frequency* is present. This points to the need of additional feedback control to be included so that the system's frequency error will eventually be reduced to zero through an integral control action. We included (without much discussion) transfer functions and the SIMULINK® environment; this was done in order to have a glimpse about the type of dynamic response and to have an idea about the *time constant* for this kind of processes, VSC and STATCOM models were discussed using a complex transformer model.

References

- [1] Stagg, G., and A. El-Abiad, *Computer Methods in Power System Analysis*, New York: McGraw-Hill, 1968.
- [2] Brown, H. E., *Solution of Large Networks by Matrix Methods*, New York: John Wiley & Sons, 1975.
- [3] Shipley, R. B., *Introduction to Matrices and Power Systems*, New York: John Wiley & Sons, 1976.
- [4] Miller, T. J. E., *Reactive Power Control in Electric Systems*, New York: John Wiley & Sons, 1982.

General Fault Studies in Electrical Power Systems

9.1 Introduction

Fault studies in electrical systems are required to find out the values of the electrical currents that flow when undesired circuit connections are present. The estimation of the high value currents that flow under fault conditions allows the protection engineer to establish the setting for the protective equipment, select circuit breaker capabilities, and to make an assessment on how the fault condition affects the whole system. Various types of faults might occur; these might include several phases and ground. A general fault equation can be very useful, and such equation can treat various shunt or series fault connections that make up the undesired electrical connection. There are various frames of reference that can be used (i.e., *abc* phase coordinates or symmetrical components, just to name the most frequently used).

9.2 Fault Equation in Phase Coordinates *abc*

In order to write the calculation procedure, let us assume that a network equivalent (Thévenin) is available for the left side, as shown in Figure 9.1. For the right side, we can draw and write a nodal admittance fault. Shown in Figure 9.1 are the boundary conditions for nodal voltages and currents into the system and into the fault, (9.1) and (9.2).

When the electric fault is present at the connection point *F*, the three-phase nodal voltages and currents *abc* must comply with the boundary conditions expressed as:

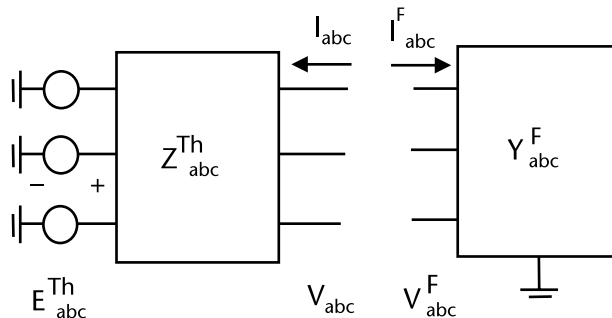


Figure 9.1 System's Thévenin equivalent and admittance fault connection Y_{abc}^F .

$$V_{abc} = V_{abc}^F \quad (9.1)$$

$$I_{abc} = -I_{abc}^F \quad (9.2)$$

Thévenin's network equivalent and the fault connection equations are:

$$V_{abc} = V_{abc}^F = E_{abc}^{Th} + Z_{abc}^{Th} I_{abc} \quad (9.3)$$

$$Y_{abc}^F V_{abc}^F = I_{abc}^F \quad (9.4)$$

To calculate the fault current, various forms can be obtained; one by substitution of (9.3) on the left of (9.4). Recognizing that voltages at the boundary are equal, U is a unit matrix.

$$Y_{abc}^F (E_{abc}^{Th} - Z_{abc}^{Th} I_{abc}^F) = I_{abc}^F \quad (9.5)$$

$$I_{abc}^F = (U + Y_{abc}^F Z_{abc}^{Th})^{-1} Y_{abc}^F E_{abc}^{Th} \quad (9.6)$$

A different expression can be derived if the fault impedance matrix Z_{abc}^F is written.

$$V_{abc} = E_{abc}^{Th} + Z_{abc}^{Th} I_{abc} \quad (9.7)$$

$$V_{abc}^F = Z_{abc}^F I_{abc}^F \quad (9.8)$$

$$E_{abc}^{Th} - Z_{abc}^{Th} I_{abc}^F = Z_{abc}^F I_{abc}^F \quad (9.9)$$

$$I_{abc}^F = (Z_{abc}^F + Z_{abc}^{Th})^{-1} E_{abc}^{Th} \quad (9.10)$$

The fault current is I_{abc}^F by (9.5) or (9.10). We apply the fault current value back to the network, into the left in Figure 9.1. With this step, we find out what the nodal voltages are when the fault current is engaged.

9.3 Fault Equation in Coordinates 012

Symmetrical components, or coordinates 012, are widely used by power system engineers to represent a three-phase, symmetrically balanced power system. The fault circuit itself might impose an unbalanced condition, and we assume that the symmetrical component representation for the fault connection is available.

In the 012 symmetrical components reference, Thévenin's system equivalent and the fault circuit equation are:

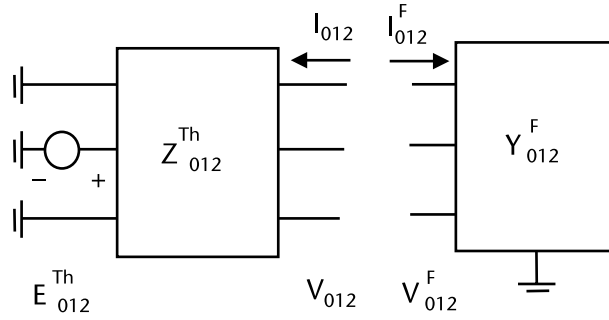


Figure 9.2 System's Thévenin equivalents and a fault matrix connection Y_{012}^F .

$$V_{012} = E_{012}^{Th} + Z_{012}^{Th} I_{012} \tag{9.11}$$

$$Y_{012}^F V_{012}^F = I_{012}^F \tag{9.12}$$

Recognizing that at the electrical boundary $V_{012} = V_{012}^F$, then:

$$I_{012}^F = (U + Y_{012}^F Z_{012}^{Th})^{-1} Y_{012}^F E_{012}^{Th} \tag{9.13}$$

An alternative is to use the fault impedance matrix in the symmetrical components reference Z_{012}^F .

$$I_{012}^F = (Z_{012}^{Th} + Z_{012}^F)^{-1} E_{012}^{Th} \tag{9.14}$$

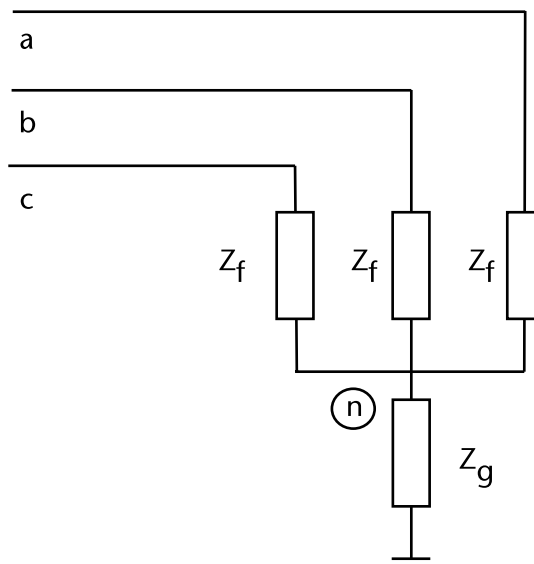


Figure 9.3 Three-phase fault connections.

9.3.1 Three-Phase Fault

To illustrate the step in a general solution, let us assume the following three-phase fault configuration:

The nodal impedance matrix in the abc reference for this type of fault and its symmetrical 012 components are shown as (9.15) and (9.16) (see Figure 9.3).

$$Z_{abc}^F = \begin{bmatrix} z_f + z_g & z_g & z_g \\ z_g & z_f + z_g & z_g \\ z_g & z_g & z_f + z_g \end{bmatrix} \quad (9.15)$$

$$Z_{012}^F = T_S^{-1} Z_{abc}^F T_S = \begin{bmatrix} z_f + 3z_g & 0 & 0 \\ 0 & z_f & 0 \\ 0 & 0 & z_f \end{bmatrix} \quad (9.16)$$

Where $\alpha = 1\angle 120^\circ$, $\alpha^2 = 1\angle 240^\circ$

$$T_S = \begin{bmatrix} 1 & 1 & 1 \\ 1 & \alpha^2 & \alpha \\ 1 & \alpha & \alpha^2 \end{bmatrix} \quad T_S^{-1} = \frac{1}{3} \begin{bmatrix} 1 & 1 & 1 \\ 1 & \alpha & \alpha^2 \\ 1 & \alpha^2 & \alpha \end{bmatrix} \quad (9.17)$$

We use (9.6) to calculate the abc fault current information or (9.10) to find the 012 fault current.

Example 9.1

Assume a Thévenin's equivalent for a balanced three-phase system as in Figure 9.2 and a fault impedance matrix abc as shown in Figure 9.3. Let us find the fault current and the abc voltages at the connecting node. Values are in pu.

$$I_{abc}^F = (Z_{abc}^{Th} + Z_{abc}^F)^{-1} E_{abc}^{Th} = \left(\begin{bmatrix} z & m & m \\ m & z & m \\ m & m & z \end{bmatrix} + \begin{bmatrix} z_f + z_g & z_g & z_g \\ z_g & z_f + z_g & z_g \\ z_g & z_g & z_f + z_g \end{bmatrix} \right)^{-1} \begin{bmatrix} E_a^{Th} \\ E_b^{Th} \\ E_c^{Th} \end{bmatrix} \quad (9.18)$$

Thevenin's Equivalent matrix, abc

Zthabc =

$$\begin{bmatrix} 0.0100 + 0.1000i & 0 - 0.0500i & 0 - 0.0500i \\ 0 - 0.0500i & 0.0100 + 0.1000i & 0 - 0.0500i \\ 0 - 0.0500i & 0 - 0.0500i & 0.0100 + 0.1000i \end{bmatrix}$$

Fault impedances $z_f = 0.01000 + j 0.10000$ $z_g = 0.00000 + j 0.01000$

ZFabc =

$$\begin{bmatrix} 0.0100 + 0.1100i & 0 + 0.0100i & 0 + 0.0100i \\ 0 + 0.0100i & 0.0100 + 0.1100i & 0 + 0.0100i \\ 0 + 0.0100i & 0 + 0.0100i & 0.0100 + 0.1100i \end{bmatrix}$$

Thevenin's Voltage, abc
 Voltage Etha = 1.00000 +0.00
 Voltage Ethb = 1.00000 -120.00
 Voltage Ethc = 1.00000 +120.00

Fault current, abc
 Current IFa = 3.98726 -85.43
 Current IFb = 3.98726 +154.57
 Current IFc = 3.98726 +34.57

Voltage at fault node, abc
 Voltage VFa = 0.40071 -1.14
 Voltage VFb = 0.40071 -121.14
 Voltage VFc = 0.40071 +118.86

Phasors results are shown in Figure 9.4, as are the magnitude and angle for Thévenin's voltages and fault currents. Note that the fault current magnitude is close to 4 pu and lags the voltage by an angle close to 90°.

To solve the fault current problems, power system engineers routinely use symmetrical components. The information required is the fault impedance or admittance and the system's sequence impedances, as well as the positive sequence of Thévenin's voltage source.

$$I_{012}^F = (Z_{012}^{Tb} + Z_{012}^F)^{-1} E_{012}^{Tb} = \left(\begin{bmatrix} Z_0^{Tb} & 0 & 0 \\ 0 & Z_1^{Tb} & 0 \\ 0 & 0 & Z_2^{Tb} \end{bmatrix} + \begin{bmatrix} Z_0^F & 0 & 0 \\ 0 & Z_1^F & 0 \\ 0 & 0 & Z_2^F \end{bmatrix} \right)^{-1} \begin{bmatrix} 0 \\ E_1^{Tb} \\ 0 \end{bmatrix} \quad (9.19)$$

$$I_{012}^F = \begin{bmatrix} I_0^F \\ I_1^F \\ I_2^F \end{bmatrix} = \begin{bmatrix} 0 \\ \frac{E_1^{Tb}}{Z_1^{Tb} + Z_1^F} \\ 0 \end{bmatrix} \quad (9.20)$$

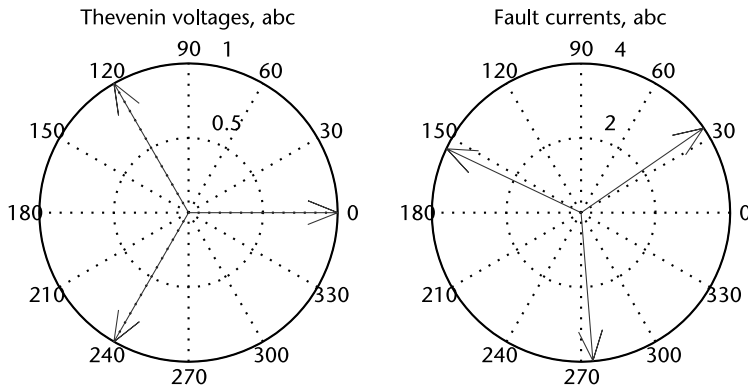


Figure 9.4 Thévenin's voltages and fault current in abc reference.

A particular case is a solid three-phase fault with $Z_1^F = 0$. In this case (see Figure 9.5):

$$I_{012}^F = \begin{bmatrix} I_0^F \\ I_1^F \\ I_2^F \end{bmatrix} = \begin{bmatrix} 0 \\ \frac{E_1^{Tb}}{Z_1^{Tb}} \\ 0 \end{bmatrix} \tag{9.21}$$

Thevenin's Equivalent matrix, 012

Zth012 =

0.0100	0.0000 + 0.0000i	0.0000 - 0.0000i
-0.0000	0.0100 + 0.1500i	0.0000 + 0.0000i
0 + 0.0000i	0.0000 - 0.0000i	0.0100 + 0.1500i

Fault impedances z_f = 0.01000+j 0.10000 z_g = 0.00000+j 0.01000

ZF012 =

0.0100 + 0.1300i	-0.0000 + 0.0000i	-0.0000 - 0.0000i
-0.0000 - 0.0000i	0.0100 + 0.1000i	0.0000 + 0.0000i
0 + 0.0000i	0.0000 - 0.0000i	0.0100 + 0.1000i

Thevenin's Voltage, 012

Voltage Eth0 = 0.00000	+0.00
Voltage Eth1 = 1.00000	-0.00
Voltage Eth2 = 0.00000	+90.00

Fault current, 012

Current IF0 = 0.00000	-92.38
Current IF1 = 3.98726	-85.43
Current IF2 = 0.00000	+0.46

Voltage at fault node, 012

Voltage VF0 = 0.00000	+15.58
Voltage VF1 = 0.40071	-1.14
Voltage VF2 = 0.00000	+87.14

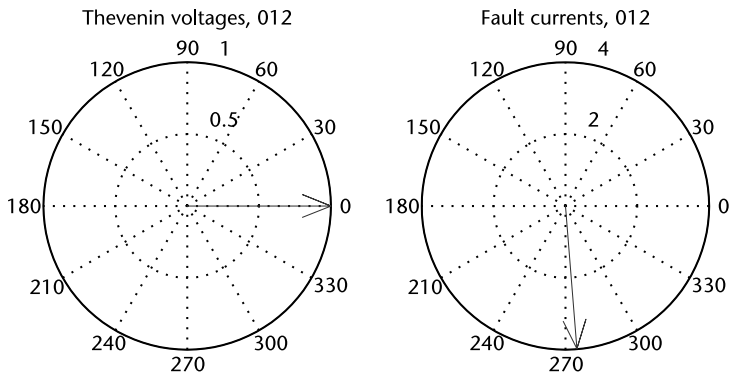


Figure 9.5 Thévenin's voltages and fault current, in the 012 references.

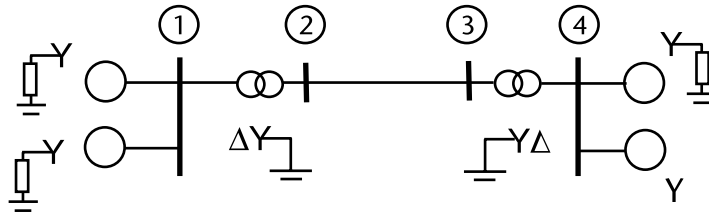


Figure 9.6 One-line diagrams for a three-phase power network.

The values calculated using the sequence domain 012 can be transformed into the original *abc* frame of reference using the inverse transformation. The results are the same as the ones obtained if we work directly in the *abc* phases.

Example 9.2

With values in pu, the calculation of fault currents for a power network is simplified using the Thévenin’s equivalent, as seen from the faulted node. Let us illustrate the procedure for a fault at bus 3 using Figure 9.6. The data shown in Table 9.1. To study fault currents in a power system, we start with a list of elements and how they are connected. Special care is required in order to properly represent transformer’s connections; for example, in delta connections there is a infinite impedance to the zero sequence current. One artifice that allows us to have the same network structure for both the positive and the zero sequence networks is through the inclusion of a *fictitious node*. Using this auxiliary node, we split both the positive and the zero sequence impedances for the transformer. In Figure 9.7, nodes 5 and 6 are

Table 9.1 Sequence Data for Elements in Figure 9.6 (values in pu)

Element	$x(+)$	$x(-)$	$x(0)$	Neutral
Generator 1	0.1512	0.10	0.050	0.30
Generator 2	0.1457	0.09	0.045	0.15
Transformer 1	0.08	0.08	0.08	0.0
Transformer 2	0.15	0.15	0.15	0.0
Motor 1	0.25	0.20	0.07	0.30
Motor 2	0.50	0.42	0.10	∞
T. Line 1	0.17	0.17	0.51	

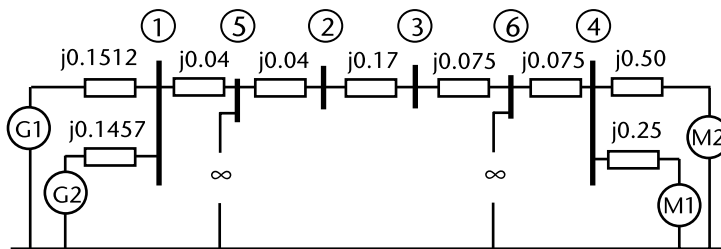


Figure 9.7 Positive sequence connection, impedance values in pu.

not actual system nodes; using these auxiliary nodes it helps us to have the same number of nodes for the positive, the negative (see Figure 9.8), and the zero sequence (see Figure 9.9) networks.

Positive sequence Zbus

Element	from	to	z(pu)	
1	1	5	0.0000+j	0.0400
2	5	2	0.0000+j	0.0400
3	2	3	0.0000+j	0.1700
4	3	6	0.0000+j	0.0750
5	6	4	0.0000+j	0.0750

Shunt	at node	z(pu)	
1	1	0.0000+j	0.1512
2	1	0.0000+j	0.1457
3	5	Inf+j	0.0000
4	6	Inf+j	0.0000
5	4	0.0000+j	0.5000
6	4	0.0000+j	0.2500

Z(+) = Columns 1 through 6

0 + 0.0656i	0 + 0.0563i	0 + 0.0367i	0 + 0.0193i	0 + 0.0610i	0 + 0.0280i
0 + 0.0563i	0 + 0.1171i	0 + 0.0762i	0 + 0.0401i	0 + 0.0867i	0 + 0.0581i
0 + 0.0367i	0 + 0.0762i	0 + 0.1602i	0 + 0.0843i	0 + 0.0564i	0 + 0.1223i
0 + 0.0193i	0 + 0.0401i	0 + 0.0843i	0 + 0.1233i	0 + 0.0297i	0 + 0.1038i
0 + 0.0610i	0 + 0.0867i	0 + 0.0564i	0 + 0.0297i	0 + 0.0938i	0 + 0.0431i
0 + 0.0280i	0 + 0.0581i	0 + 0.1223i	0 + 0.1038i	0 + 0.0431i	0 + 0.1505i

To calculate the fault current at node 3 we need information of the Thévenin’s equivalent impedance for the network as seen at this node. For generator’s positive sequence impedance will have a value that depends on the time at which the fault current is calculated; for a physical explanation see Section 9.7. For a fault calculated within two to four cycles, the subtransient reactance x'' must be included. For a fault current calculation at five to eight cycles, we need to consider the transient reactance x' , and for longer periods, the synchronous reactance x_s . Rotating machines might have positive and negative sequence reactance with a slightly different value.

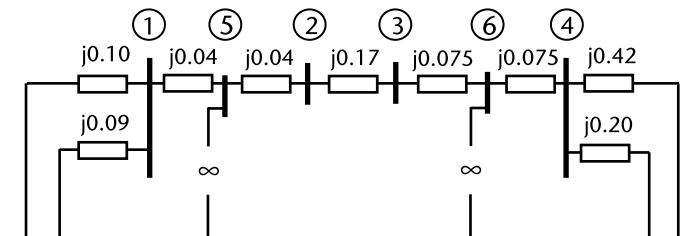


Figure 9.8 Negative sequence connections.

Negative sequence Zbus

Element	from	to	z(pu)	
1	1	5	0.0000+j	0.0400
2	5	2	0.0000+j	0.0400
3	2	3	0.0000+j	0.1700
4	3	6	0.0000+j	0.0750
5	6	4	0.0000+j	0.0750

Shunt	at node	z(pu)	
1	1	0.0000+j	0.1000
2	1	0.0000+j	0.0900
3	5	Inf+j	0.0000
4	6	Inf+j	0.0000
5	4	0.0000+j	0.4200
6	4	0.0000+j	0.2000

Z(-) = Columns 1 through 6

0 + 0.0435i	0 + 0.0370i	0 + 0.0232i	0 + 0.0110i	0 + 0.0403i	0 + 0.0171i
0 + 0.0370i	0 + 0.0995i	0 + 0.0624i	0 + 0.0296i	0 + 0.0683i	0 + 0.0460i
0 + 0.0232i	0 + 0.0624i	0 + 0.1457i	0 + 0.0691i	0 + 0.0428i	0 + 0.1074i
0 + 0.0110i	0 + 0.0296i	0 + 0.0691i	0 + 0.1040i	0 + 0.0203i	0 + 0.0866i
0 + 0.0403i	0 + 0.0683i	0 + 0.0428i	0 + 0.0203i	0 + 0.0743i	0 + 0.0316i
0 + 0.0171i	0 + 0.0460i	0 + 0.1074i	0 + 0.0866i	0 + 0.0316i	0 + 0.1345i

Zero sequence Zbus

Element	from	to	z(pu)	
1	1	5	Inf+j	0.0000
2	5	2	0.0000+j	0.0400
3	2	3	0.0000+j	0.5100
4	3	6	0.0000+j	0.0750
5	6	4	Inf+j	0.0000

Shunt	at node	z(pu)	
1	1	0.0000+j	0.9500
2	1	0.0000+j	0.4950
3	5	0.0000+j	0.0400
4	6	0.0000+j	0.0750
5	4	Inf+j	0.1000
6	4	0.0000+j	0.9700

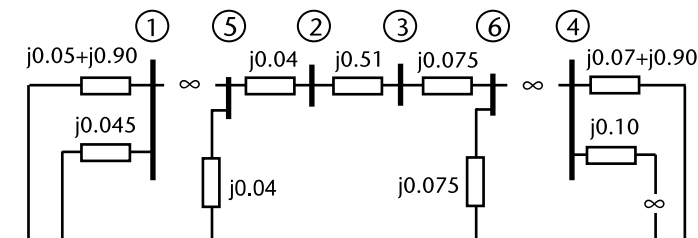


Figure 9.9 Zero sequence network.

Z(zero) = Columns 1 through 6

0 + 0.3254i	0	0	0	0	0
0	0 + 0.0714i	0 + 0.0162i	0	0 + 0.0357i	0 + 0.0081i
0	0 + 0.0162i	0 + 0.1196i	0	0 + 0.0081i	0 + 0.0598i
0	0	0	0 + 0.9700i	0	0
0	0 + 0.0357i	0 + 0.0081i	0	0 + 0.0378i	0 + 0.0041i
0	0 + 0.0081i	0 + 0.0598i	0	0 + 0.0041i	0 + 0.0674i

Consider a *three-phase fault* at node 3 with fault impedance *abc* as in (9.15); in case of an open connection, the impedance will be infinite or with zero admittance value. Usually, load currents are small when compared to the larger fault currents; therefore, load currents are neglected. Let us use the following pu values to calculate a three-phase fault where $Z_f = j0.0$, $Z_g = j0.05$, $Z_3^{Tb0} = j0.1196$, $Z_3^{Tb+} = j0.1602$ and $Z_3^{Tb-} = j0.1457$.

Thevenin's Equivalent matrix, 012

ZTh012 =

0 + 0.1196i	0	0
0	0 + 0.1602i	0
0	0	0 + 0.1457i

Fault impedances $z_f = 0.0000 + j 0.0000$ $z_g = 0.0000 + j 0.0500$

ZF012 =

0.0000 + 0.1500i	-0.0000	-0.0000 - 0.0000i
-0.0000 - 0.0000i	0.0000 - 0.0000i	0.0000 - 0.0000i
-0.0000 - 0.0000i	0.0000 - 0.0000i	0.0000 - 0.0000i

Thevenin's voltage source, 012

Voltage ETh0 =	0.0000	0.00
Voltage ETh1 =	1.0000	0.00
Voltage ETh2 =	0.0000	0.00

Fault current, 012

Current IF0 =	0.0000	-180.00
Current IF1 =	6.2422	-90.00
Current IF2 =	0.0000	-39.70

Voltage at faulted node, 012

Voltage VF0 =	0.0000	90.00
Voltage VF1 =	0.0000	-90.00
Voltage VF2 =	0.0000	-129.70

Thevenin's voltage source, abc

Voltage ETha =	1.0000	0.00
Voltage EThb =	1.0000	-120.00
Voltage EThc =	1.0000	120.00

Fault current, abc

Current IFa =	6.2422	-90.00
Current IFb =	6.2422	150.00
Current IFc =	6.2422	30.00

Voltage at faulted node, abc
 Current VFa = 0.0000 90.00
 Current VFb = 0.0000 90.00
 Current VFc = 0.0000 90.00

A well-known result for three-phase faults gives previous results in the frame of reference 012.

$$I_{012}^F = \begin{bmatrix} I_0^F \\ I_1^F \\ I_2^F \end{bmatrix} = \begin{bmatrix} 0 \\ 1 \angle 0^\circ \\ j0.1602 \\ 0 \end{bmatrix} = \begin{bmatrix} 0 \\ 6.2422 \angle -90^\circ \\ 0 \end{bmatrix} \quad (9.22)$$

Once the fault current is calculated, a negative value of the fault current is injected into node 3 in the original network for each sequence (in this case, zero and negative currents are zero). The effect from this current injection is a change in nodal voltages; these changes added to the voltage values before the fault condition will give the new voltage values when the fault is present.

Magnitude of Nodal voltages with fault present, node 3
 Vnew =
 0.7711
 0.5244
 0.0000
 0.4737
 0.6478
 0.2369

9.3.2 Other Types of Shunt Faults

Sections 9.2 and 9.3.1 discussed the general but basic formulation in abc and 012 sequence frame of reference as a particular case for the three-phase fault. Other fault configurations might include two lines and Earth or single-phase. In general, unbalanced faults might not include Earth, as is the case of a fault between two phases with no connection to ground. Equations (9.13) and (9.6) can solve the problem; the advantage of (9.13) is that in some fault connections the 012 admittances are not directly obtained, but the fault admittance in reference *abc* can be written and then transformed into the domain 012 so that the formula can be applied.

Example 9.3

Write the fault admittance matrix 012 for Figure 9.10. For this fault connection, find the fault current at node 3 in Example 9.2. Use the following per unit values: $z_f = 0.0 + 0.1j$; $z_g = 0.05j$.

First, we write the fault admittance matrix *abc*. We then calculate the 012 matrix; the result has a nondiagonal form, which implies that the sequence networks are interconnected due to the fault.

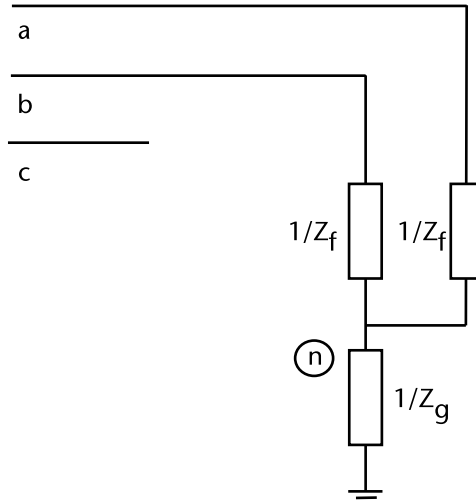


Figure 9.10 Unbalanced fault connections.

$$I_{012}^F = (U + Y_{012}^F Z_{012}^{Tb})^{-1} Y_{012}^F E_{012}^{Tb} \tag{9.23}$$

YFabcn =
 0 -10.0000i 0 0 0 +10.0000i
 0 0 -10.0000i 0 0 +10.0000i
 0 0 0 0
 0 +10.0000i 0 +10.0000i 0 0 -40.0000i

YFabc =
 0 - 7.5000i 0 + 2.5000i 0
 0 + 2.5000i 0 - 7.5000i 0
 0 0 0 0

Thevenin's Equivalent matrix, 012

ZTh012 =
 0 + 0.1196i 0 0
 0 0 + 0.1602i 0
 0 0 0 + 0.1457i

Fault impedances zf = 0.0000+ j 0.1000 zg = 0.0000+ j 0.0500

YF012 =
 -0.0000 - 3.3333i -1.4434 - 0.8333i 1.4434 - 0.8333i
 1.4434 - 0.8333i 0.0000 - 5.8333i -3.6084 - 2.0833i
 -1.4434 - 0.8333i 3.6084 - 2.0833i -0.0000 - 5.8333i

Thevenin's voltage source, 012

Voltage ETh0 = 0.0000 0.00
 Voltage ETh1 = 1.0000 0.00

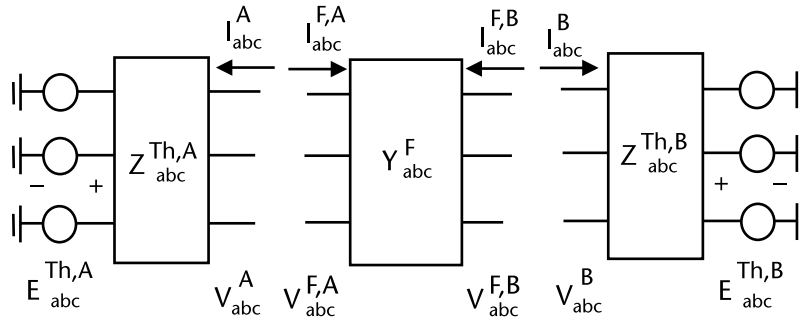


Figure 9.11 Series fault connections in the reference frame *abc*.

```

Voltage ETh2 = 0.0000      0.00
Fault current, 012
Current IF0 = 0.9792      -150.00
Current IF1 = 2.4523      -90.00
Current IF2 = 1.4730      -30.00
    
```

```

Voltage at faulted node, 012
Voltage VF0 = 0.1171      120.00
Voltage VF1 = 0.6071      -0.00
Voltage VF2 = 0.2146      -120.00
    
```

```

Thevenin's voltage source, abc
Voltage ETha = 1.0000      0.00
Voltage EThb = 1.0000     -120.00
Voltage EThc = 1.0000      120.00
    
```

```

Fault current, abc
Current IFa = 3.7032      -83.37
Current IFb = 3.7032      143.37
Current IFc = 0.0000      126.87
    
```

```

Voltage at faulted node, abc
Current VFa = 0.4493      -10.83
Current VFb = 0.4493     -109.17
Current VFc = 0.9389      120.00
    
```

9.4 Series Faults

Sections 9.2 and 9.3 have used the general and basic formulation in either the *abc* or the 012 frame of reference for shunt type of faults. Those faults are connected to the ground, but there are some variations in electrical connections during a fault wherein the ground is not involved; this other type of fault is a series connection where the matrix can be written in admittance or impedance form. To have a

general discussion, let us start with Thévenin's equivalent circuits to the left and to the right of a series configuration, as shown in Figure 9.11. Assume that the fault matrix is written in admittance form in coordinates abc .

The boundary conditions that must be met for voltages at the fault and fault currents; Thévenin equivalents for the left and the right hand side allow us to write the model.

$$\begin{aligned} V_{abc}^A &= V_{abc}^{F,A} & \text{and} & & V_{abc}^B &= V_{abc}^{F,B} \\ I_{abc}^A &= -I_{abc}^{F,A} & & & I_{abc}^B &= -I_{abc}^{F,B} \end{aligned} \quad (9.24)$$

$$\begin{aligned} Y_{abc}^F (V_{abc}^{F,A} - V_{abc}^{F,B}) &= I_{abc}^{F,A} \\ Y_{abc}^F (V_{abc}^{F,B} - V_{abc}^{F,A}) &= I_{abc}^{F,B} \end{aligned} \quad (9.25)$$

Here, superscripts A and B are for the system at the left and the system to the right, respectively. The superscript F , A and F , B relate to the fault condition for the system to the left and for the system to the right, respectively. Our aim is to calculate the fault current that flows into each system when the fault admittance is connected.

$$V_{abc}^A = E_{abc}^{Th,A} + Z_{abc}^{Th,A} I_{abc}^A = E_{abc}^{Th,A} - Z_{abc}^{Th,A} I_{abc}^{F,A} \quad (9.26)$$

$$V_{abc}^B = E_{abc}^{Th,B} + Z_{abc}^{Th,B} I_{abc}^B = E_{abc}^{Th,B} - Z_{abc}^{Th,B} I_{abc}^{F,B} \quad (9.27)$$

From (9.24)

$$\begin{bmatrix} Y_{abc}^F & -Y_{abc}^F \\ -Y_{abc}^F & Y_{abc}^F \end{bmatrix} \begin{bmatrix} V_{abc}^{F,A} \\ V_{abc}^{F,B} \end{bmatrix} = \begin{bmatrix} I_{abc}^{F,A} \\ I_{abc}^{F,B} \end{bmatrix} \quad (9.28)$$

$$\begin{bmatrix} Y_{abc}^F & -Y_{abc}^F \\ -Y_{abc}^F & Y_{abc}^F \end{bmatrix} \left(\begin{bmatrix} E_{abc}^{Th,A} \\ E_{abc}^{Th,B} \end{bmatrix} - \begin{bmatrix} Z_{abc}^{Th,A} & 0 \\ 0 & Z_{abc}^{Th,B} \end{bmatrix} \begin{bmatrix} I_{abc}^{F,A} \\ I_{abc}^{F,B} \end{bmatrix} \right) = \begin{bmatrix} I_{abc}^{F,A} \\ I_{abc}^{F,B} \end{bmatrix} \quad (9.29)$$

$$\begin{bmatrix} I_{abc}^{F,A} \\ I_{abc}^{F,B} \end{bmatrix} = \left(\begin{bmatrix} U & 0 \\ 0 & U \end{bmatrix} + \begin{bmatrix} Y_{abc}^F & -Y_{abc}^F \\ -Y_{abc}^F & Y_{abc}^F \end{bmatrix} \begin{bmatrix} Z_{abc}^{Th,A} & 0 \\ 0 & Z_{abc}^{Th,B} \end{bmatrix} \right)^{-1} \begin{bmatrix} Y_{abc}^F & -Y_{abc}^F \\ -Y_{abc}^F & Y_{abc}^F \end{bmatrix} \begin{bmatrix} E_{abc}^{Th,A} \\ E_{abc}^{Th,B} \end{bmatrix} \quad (9.30)$$

In matrix notation, we find a solution similar to (9.9), but now as applied to the series fault connection. The 012-fault equation can be deduced from the abc domain with a similar structure; only the notation abc is changed to 012.

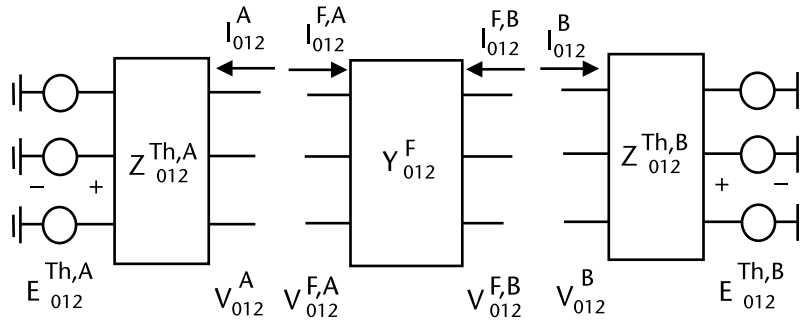


Figure 9.12 Series fault connections frame of reference 012.

Example 9.4

For the connection given in Figure 9.12, let us use Thévenin equivalents *A* and *B* and the fault admittance matrix in symmetrical components 012. Find the currents that flow when the fault series admittance matrix is inserted (see Figure 9.13).

Thevenin's Equivalent matrix, 012

ZTh012A =

$$\begin{bmatrix} 0 + 0.3000i & 0 & 0 \\ 0 & 0 + 0.1000i & 0 \\ 0 & 0 & 0 + 0.1000i \end{bmatrix}$$

ZTh012B =

$$\begin{bmatrix} 0 + 0.1500i & 0 & 0 \\ 0 & 0 + 0.0500i & 0 \\ 0 & 0 & 0 + 0.0500i \end{bmatrix}$$

Fault impedances $z_f = 0.0000 + j 0.1000$ $z_m = 0.0000 + j 0.0100$

YF012 =

$$\begin{bmatrix} -0.0000 - 8.3333i & 0 - 0.0000i & 0.0000 + 0.0000i \\ 0.0000 - 0.0000i & 0.0000 - 11.1111i & -0.0000 - 0.0000i \\ -0.0000 & 0.0000 - 0.0000i & 0.0000 - 11.1111i \end{bmatrix}$$

Thevenin's voltage source A, 012

Voltage ETh0 = 0.0000 0.00

Voltage ETh1 = 1.0000 0.00

Voltage ETh2 = 0.0000 0.00

Thevenin's voltage source B, 012

Voltage ETh0 = 0.0000 0.00

Voltage ETh1 = 0.9000 0.00

Voltage ETh2 = 0.0000 0.00

Fault current, 012

Current IF0A = 0.0000 -90.00

Current IF1A = 0.4167 -90.00

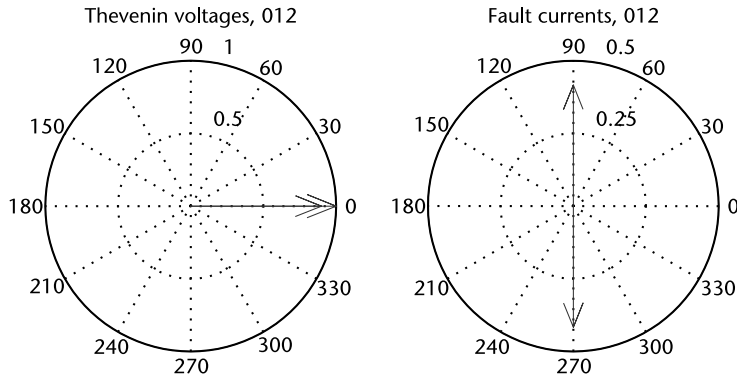


Figure 9.13 Sequence Phasors, voltages, and *fault currents*.

Current IF2A	=	0.0000	-56.31
Current IF0B	=	0.0000	90.00
Current IF1B	=	0.4167	90.00
Current IF2B	=	0.0000	123.69
IabcA, abc			
Current IFa	=	0.4167	-90.00
Current IFb	=	0.4167	150.00
Current IFc	=	0.4167	30.00
IabcB, abc			
Current IFa	=	0.4167	90.00
Current IFb	=	0.4167	-30.00
Current IFc	=	0.4167	-150.00

9.5 Useful Circuit Interpretation for Fault Connections

So far, we have presented and used formulas that are general procedures for fault calculations. They work well for fault currents and voltage values calculations when shunt or series faults are present. Sometimes, a circuit interpretation for a particular fault condition helps the engineer to understand and visualize applications of how to solve and identify problems; such procedure follows.

9.5.1 Single-Phase Fault

In a three-phase balanced network when an unexpected connection of phase *a* to the ground (as shown in Figure 9.14), we find that the three sequence currents are equal; this condition comes from (9.31). The sequence circuits 012 should be connected in series so that the currents are equal.

$$\begin{bmatrix} I_0 \\ I_1 \\ I_2 \end{bmatrix} = T_S^{-1} \begin{bmatrix} I_a \\ I_b \\ I_c \end{bmatrix} = \frac{1}{3} \begin{bmatrix} 1 & 1 & 1 \\ 1 & \alpha & \alpha^2 \\ 1 & \alpha^2 & \alpha \end{bmatrix} \begin{bmatrix} I_a \\ 0 \\ 0 \end{bmatrix} = \frac{1}{3} \begin{bmatrix} I_a \\ I_a \\ I_a \end{bmatrix} \quad (9.31)$$

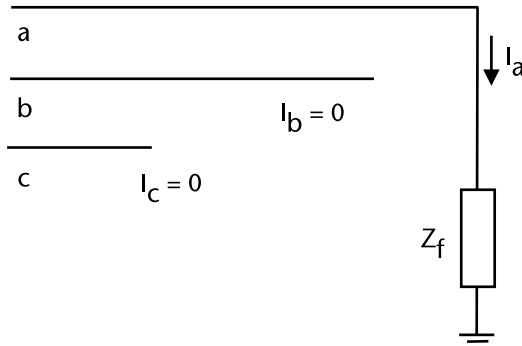


Figure 9.14 One-phase to ground fault connection, *abc* reference.

The voltage V_a at the fault is given as follows:

$$\begin{bmatrix} V_a \\ V_b \\ V_c \end{bmatrix} = \begin{bmatrix} 1 & 1 & 1 \\ 1 & \alpha^2 & \alpha \\ 1 & \alpha & \alpha^2 \end{bmatrix} \begin{bmatrix} V_0 \\ V_1 \\ V_2 \end{bmatrix} = \begin{bmatrix} V_0 + V_1 + V_2 \\ \\ \end{bmatrix} \quad (9.32)$$

$$V_a = V_0 + V_1 + V_2 = I_a z_F = 3I_1 z_F \quad (9.33)$$

A circuit interpretation for (9.33) is shown in Figure 9.15, where $I_1 = 1/3 I_a$ from (9.31). The positive sequence fault current I_1 is calculated in the series configuration, as in (9.34).

$$I_1 = \frac{E_{Th}}{Z_1^{Tb} + Z_2^{Tb} + Z_0^{Tb} + 3z_F} \quad (9.34)$$

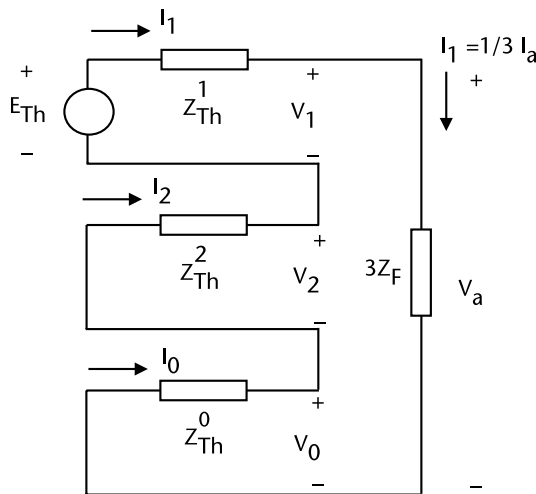


Figure 9.15 Sequence circuits connection for a single-phase fault.

Once I_1 is calculated, $I_2 = I_0 = I_1$ so the phase currents abc and voltages are calculated by (9.26).

$$\begin{bmatrix} I_a \\ I_b \\ I_c \end{bmatrix} = \begin{bmatrix} 1 & 1 & 1 \\ 1 & \alpha^2 & \alpha \\ 1 & \alpha & \alpha^2 \end{bmatrix} \begin{bmatrix} I_0 \\ I_1 \\ I_2 \end{bmatrix} = \begin{bmatrix} I_0 + I_1 + I_2 \\ 0 \\ 0 \end{bmatrix} = \begin{bmatrix} 3I_1 \\ 0 \\ 0 \end{bmatrix} \quad (9.35)$$

$$\begin{bmatrix} V_0 \\ V_1 \\ V_2 \end{bmatrix} = \begin{bmatrix} 0 \\ E_{Tb} \\ 0 \end{bmatrix} - \begin{bmatrix} Z_0^{Tb} & 0 & 0 \\ 0 & Z_1^{Tb} & 0 \\ 0 & 0 & Z_2^{Tb} \end{bmatrix} \begin{bmatrix} I_0 \\ I_1 \\ I_2 \end{bmatrix} \quad (9.36)$$

$$\begin{bmatrix} v_a \\ v_b \\ v_c \end{bmatrix} = \begin{bmatrix} 1 & 1 & 1 \\ 1 & \alpha^2 & \alpha \\ 1 & \alpha & \alpha^2 \end{bmatrix} \begin{bmatrix} V_0 \\ V_1 \\ V_2 \end{bmatrix} \quad (9.37)$$

9.5.2 Fault Between Two Phases, No Ground

For a three-phase balanced network with an unintended connection of two phases: b and c and no connection to the ground (as shown in Figure 9.16) imposes the following boundary conditions.

$$I_a = 0 \quad I_b = -I_c \quad V_b - V_c = I_b z_f \quad (9.38)$$

Zero sequence current is zero. The positive and negative sequence currents are related through:

$$\begin{bmatrix} I_0 \\ I_1 \\ I_2 \end{bmatrix} = T_S^{-1} \begin{bmatrix} I_a \\ I_b \\ I_c \end{bmatrix} = \frac{1}{3} \begin{bmatrix} 1 & 1 & 1 \\ 1 & \alpha & \alpha^2 \\ 1 & \alpha^2 & \alpha \end{bmatrix} \begin{bmatrix} 0 \\ I_b \\ -I_b \end{bmatrix} = \frac{1}{3} \begin{bmatrix} 0 \\ a - a^2 \\ -(a - a^2) \end{bmatrix} I_b \quad (9.39)$$

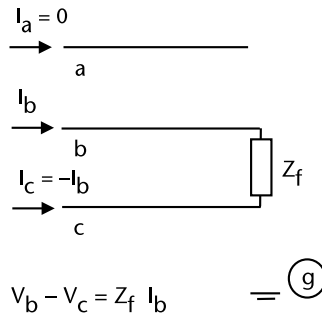


Figure 9.16 Two phases fault, no ground connection in the abc domain.

$$I_1 = \frac{1}{3}(\alpha - \alpha^2)I_b = -I_2 \quad (9.40)$$

Phase voltages and sequence quantities are:

$$\begin{bmatrix} V_a \\ V_b \\ V_c \end{bmatrix} = \begin{bmatrix} 1 & 1 & 1 \\ 1 & \alpha^2 & \alpha \\ 1 & \alpha & \alpha^2 \end{bmatrix} \begin{bmatrix} V_0 \\ V_1 \\ V_2 \end{bmatrix} \quad (9.41)$$

$$V_b = V_0 + \alpha^2 V_1 + \alpha V_2 \quad (9.42)$$

$$V_c = V_0 + \alpha V_1 + \alpha^2 V_2$$

$$V_b - V_c = (\alpha^2 - \alpha)V_1 + (\alpha - \alpha^2)V_2 = (\alpha^2 - \alpha)(V_1 - V_2) = z_F I_b \quad (9.43)$$

$$(V_1 - V_2) = \frac{z_F I_b}{(\alpha^2 - \alpha)} = \frac{z_F 3I_1}{-(\alpha^2 - \alpha)^2} = z_F I_1 \quad (9.44)$$

$$V_1 = V_2 + z_F I_1 \quad (9.45)$$

Using (9.45), an equivalent circuit is drawn; it relates a connection of the positive and the negative sequence networks for this type of fault (see Figure 9.17).

The fault current calculation can be done from the circuit connection, sequence currents 012 and sequence voltages are determined. Those values are then transformed to the abc domain in order to find the line current flowing during the fault.

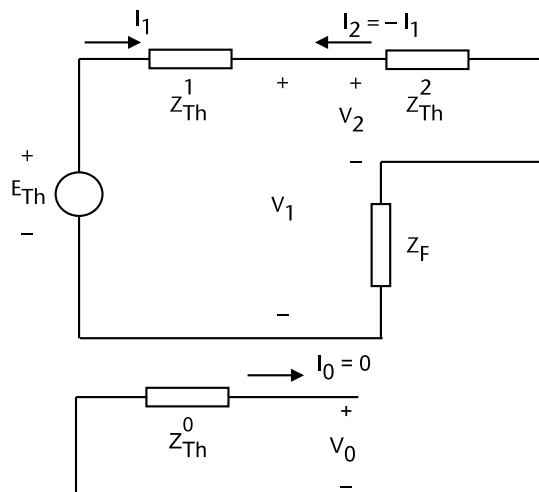


Figure 9.17 Fault on two phases, no ground connection in the abc domain.

$$I_1 = \frac{E_{Tb}}{Z_1^{Tb} + Z_2^{Tb} + z_F} \quad (9.46)$$

9.5.3 Fault Between Two Phases and Ground

For a three-phase balanced network a connection of two phases: b , c , and ground as shown in Figure 9.18 has the following boundary conditions in phase voltages. For currents: zero sequence is zero, (9.47) give the positive and negative sequence values.

$$\begin{aligned} V_b &= z_F I_b + z_g (I_b + I_c) \\ V_c &= z_F I_c + z_g (I_b + I_c) \end{aligned} \quad (9.47)$$

$$\begin{bmatrix} I_a \\ I_b \\ I_c \end{bmatrix} = T_S \begin{bmatrix} I_0 \\ I_1 \\ I_2 \end{bmatrix} = \begin{bmatrix} 1 & 1 & 1 \\ 1 & \alpha^2 & \alpha \\ 1 & \alpha & \alpha^2 \end{bmatrix} \begin{bmatrix} I_0 \\ I_1 \\ I_2 \end{bmatrix} \quad (9.48)$$

$$\begin{aligned} I_a &= 0 = I_0 + I_1 + I_2 \\ I_b &= I_0 + \alpha^2 I_1 + \alpha I_2 \\ I_c &= I_0 + \alpha I_1 + \alpha^2 I_2 \end{aligned} \quad (9.49)$$

Voltage and current relations (see Figure 9.19):

$$\begin{aligned} I_b - I_c &= (\alpha^2 - \alpha)(I_1 - I_2) \\ V_b - V_c &= z_F (I_b - I_c) = (\alpha^2 - \alpha)(V_1 - V_2) = z_F (\alpha^2 - \alpha)(I_1 - I_2) \\ (V_1 - V_2) &= z_F (I_1 - I_2) \end{aligned} \quad (9.50)$$

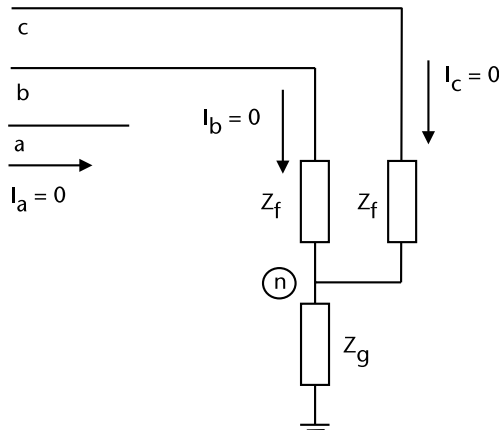


Figure 9.18 Unbalanced fault connection.

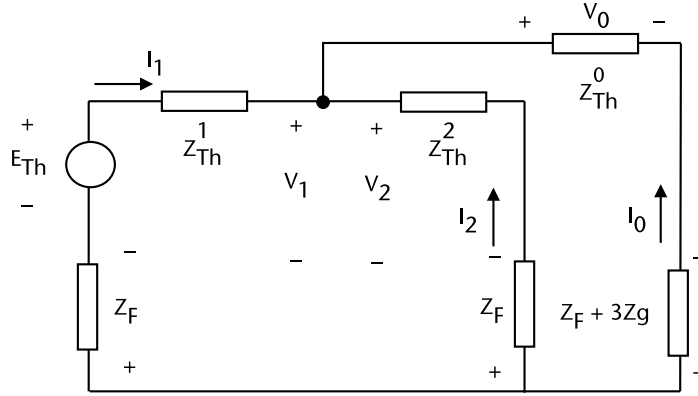


Figure 9.19 Sequence network connections, two phases and ground.

$$I_b + I_c = 2I_0 + (\alpha^2 - \alpha)(I_1 + I_2) = 2I_0 - (I_1 + I_2) \tag{9.51}$$

$$V_b + V_c = (z_F + 2z_g)(I_b + I_c) = (z_F + 2z_g)[2I_0 - (I_1 + I_2)] = 3I_0(z_F + 2z_g)$$

$$V_b + V_c = 2V_0 - (V_1 + V_2) = 3I_0(z_F + 2z_g) \tag{9.52}$$

$$2V_0 - V_1 - V_2 + z_F I_1 - z_F I_2 = 3I_0(z_F + 2z_g)$$

$$2V_0 - 2V_1 + z_F I_1 - z_F(-I_0 - I_1) = 3I_0(z_F + 2z_g) \tag{9.53}$$

$$2V_0 - 2V_1 + 2z_F I_1 - 2z_F I_0 - 6I_0 z_g = 0$$

$$V_0 - I_0(z_F + 3z_g) = V_1 - z_F I_1 = V_2 - z_F I_2 \tag{9.54}$$

Equations (9.49) and (9.54) require that the sequence networks should be in parallel.

9.6 Alternative Equation for Fault Current Calculation

Some useful¹ matrix results from (9.4) and (9.10) are:

$$I_{012}^F = (Z_{012}^F + Z_{012}^{Tb})^{-1} E_{012}^{Tb} \tag{9.55}$$

$$I_{012}^F = (U + Y_{012}^F Z_{012}^{Tb})^{-1} Y_{012}^F E_{012}^{Tb} \tag{9.56}$$

1 . Lemma $(AB)^{-1} = B^{-1}A^{-1}$

With U as the unity matrix, $(AB)^{-1}(AB) = U$. We then multiply by the right with B^{-1} and then by A^{-1}

Then

$$\begin{aligned} (Z_{012}^F + Z_{012}^{Th})^{-1} &= \left(Z_{012}^F (Y_{012}^F Z_{012}^F + Y_{012}^F Z_{012}^{Th}) \right)^{-1} \\ &= \left(Z_{012}^F (U + Y_{012}^F Z_{012}^{Th}) \right)^{-1} = (U + Y_{012}^F Z_{012}^{Th})^{-1} Y_{012}^F \end{aligned} \quad (9.57)$$

9.7 Transient and Subtransient Impedances in Magnetic Circuits

When a sudden change in operating conditions happens to magnetically coupled circuits, the immediate response from circuit currents is to maintain the magnetic flux values; this is the principle of *constant flux linkages*. This type of response is a transient that lasts accordingly to the *time constants* for the magnetic circuits involved.

9.7.1 Transient Response in a Magnetic Circuit

The flux linkages for magnetic coupled circuits (see Figure 9.20):

$$\begin{bmatrix} L_d & \sqrt{\frac{3}{2}} M_f \\ \sqrt{\frac{3}{2}} M_f & L_{ff} \end{bmatrix} \begin{bmatrix} \Delta i_d \\ \Delta i_f \end{bmatrix} = \begin{bmatrix} \Delta \lambda_d \\ \Delta \lambda_f = 0 \end{bmatrix} \quad (9.58)$$

Using the *partial inversion* in (9.58) to exchange the zero into the left-hand side, we get (9.59). The flux linkage to current relation is a *reduced transient inductance*; (9.59). Such is the nature of the transient response in coupled circuits: in a synchronous machine it is the field winding and the phase windings interacting in the *d*-axis of the synchronous machine.

$$\begin{bmatrix} L_d - \frac{3 M_f^2}{2 L_{ff}} & -\frac{\sqrt{\frac{3}{2}} M_f}{L_{ff}} \\ -\frac{\sqrt{\frac{3}{2}} M_f}{L_{ff}} & -\frac{1}{L_{ff}} \end{bmatrix} \begin{bmatrix} \Delta i_d \\ 0 \end{bmatrix} = \begin{bmatrix} \Delta \lambda_d \\ \Delta i_f \end{bmatrix} \quad (9.59)$$

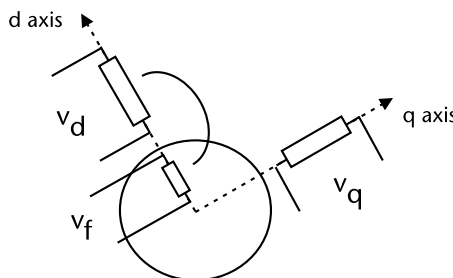


Figure 9.20 Magnetic coupled circuits, *d*-axis.

$$\Delta\lambda_d = \left(L_d - \frac{3}{2} \frac{M_f^2}{L_{ff}} \right) \Delta i_d \tag{9.60}$$

9.7.2 Subtransient Response

As seen in Figure 9.21, the flux linkages along the *d*-axis will tend to be constant in the field circuit, the direct axis, and in the damper circuit *kd*. A similar effect holds true for the coupled circuit in the *q*-axis, the quadrature winding, and the damper *kq*. After *partial inversion* steps to exchange the zero values from the right hand side in (9.61) to the left-hand side, we have a reduced coefficient that will be the *subtransient inductance* in the *d*-axis. In the *q*-axis, we will have a transient.

$$\begin{bmatrix} L_d & \sqrt{\frac{3}{2}}M_f & \sqrt{\frac{3}{2}}M_D \\ \sqrt{\frac{3}{2}}M_f & L_{ff} & M_r \\ \sqrt{\frac{3}{2}}M_D & M_r & L_D \end{bmatrix} \begin{bmatrix} \Delta i_d \\ \Delta i_f \\ \Delta i_{kd} \end{bmatrix} = \begin{bmatrix} \Delta\lambda_d \\ \Delta\lambda_f = 0 \\ \Delta\lambda_{kd} = 0 \end{bmatrix} \tag{9.61}$$

$$\Delta\lambda_d = \left(L_d - \begin{bmatrix} \sqrt{\frac{3}{2}}M_f & \sqrt{\frac{3}{2}}M_D \end{bmatrix} \begin{bmatrix} L_{ff} & M_r \\ M_r & L_D \end{bmatrix}^{-1} \begin{bmatrix} \sqrt{\frac{3}{2}}M_f \\ \sqrt{\frac{3}{2}}M_D \end{bmatrix} \right) \Delta i_d \tag{9.62}$$

$$\Delta\lambda_d = L_d'' \Delta i_d \tag{9.63}$$

From the results outlined, we observe the following relation for the subtransient reactance, transient, and synchronous reactance values.

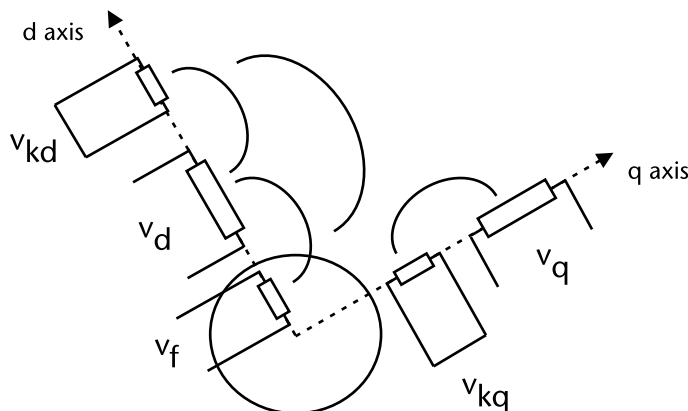


Figure 9.21 Magnetic coupled circuits, *d*-axis and *q*-axis.

$$L_d'' \ll L_d' \ll L_d \quad (9.64)$$

The transient phenomena will always be present in a synchronous machine due to the field winding and the magnetic coupling with the d -axis equivalent stator windings. The subtransient behavior is due to the existence of the damper circuit beside the field winding in the d -axis. The time constants of the field and the damper windings are very different, considering the high resistance value in the short-circuited damper winding.

Typically, the subtransient phenomena dies out in about three to four cycles, and the transient will last for about eight to ten cycles. This reasoning justifies the use of subtransient reactance for fault current determination up to four cycles and the transient reactance in the range of eight cycles in the Thévenin's equivalent circuit of the synchronous generators.

References

- [1] Stevenson, W. D., *Elements of Power System Analysis, Second Edition*, New York: McGraw-Hill Book Company, 1962.
- [2] Stagg, G. W., and A. H. El-Abiad, *Computer Methods in Power System Analysis*, Tokyo, Japan: McGraw-Hill Book Company, 1968.
- [3] Elgerd, O. I., *Electric Energy Systems Theory: An Introduction, Second Edition*, New York: McGraw-Hill Book Company, 1982.
- [4] Gross, C. A., *Power Systems Analysis*, New York: John Wiley & Sons 1979.

Contingency Analysis

10.1 Introduction

Electrical power systems are designed years in advanced by engineering planning departments, considering load growth and energy requirements, using load forecasting and other relevant socioeconomic information, and projecting the information by forecasting tools various years into the future. Available energy sources such as oil fuels, hydropower, nuclear, wind, solar, and other renewables will be considered as power plants of the appropriate technology that will be chosen with optimal criteria in mind and to be considered in the planning scenarios. The available technology also plays a role in selecting AC or DC transmission, voltage level of operation, and transmission capacity. Together with technical and economical requirements, they will be compared and the right projects will be selected for system reinforcements and expansion.

The shipment of large amounts of energy from the power generating sites to the load centers requires high capacity transmission lines and transformers to step up to voltage transmission levels, and at the receiving end, step down the voltages so that energy can reach effectively from the source site to load locations. The time into the future is classified broadly as short, medium, and long-term; these are measured conveniently in years. Short term might be up to 5 years, medium from 5 to 10 years, and long-term could be anywhere from 10 to 30 years in advance. These ranges are practically defined by the time it takes to develop different type of projects; for example, a large hydro project might take about 10 years for environmental and land flood assessment, dam construction, machinery installation, and substation-transmission line building and commissioning. For a new combined cycle power plant, it may take 3 to 4 years, and transmission line projects ranging from 3 to 6 years are standard.

Planning usually assumes a three-phase balanced AC system. It is considered that the impedance sequence parameters are available for generators, transformers, and transmission lines, that network configuration and load values are known; with this information, we solve the *base case load flow*. Planning studies are assessment tasks used to establish the efficiency, security, and reliability of the existing and the future power system. Steady state, transient, and dynamic responses are evaluated among other required technical assessments.

Efficiency studies relate to what type, what size, and how many generating units need to be selected, and what are the most appropriate technologies and primary energy resources available (i.e., gas, coal, fossil fuels, nuclear, hydro, wind, solar). Heat rate curves, water usage, and the energy available from wind and solar would

be needed in order to solve the energy coordination usage. An optimal formulation solves the problem written for each stage in the planning horizon.

Reliability of a power system relates to studies aimed at estimating if the system will be able to supply its load; this is also known as *adequacy*, given that generators might trip and might not be available to supply power to the system. Together with transmission lines being unavailable due to faults, the uncertainty needs to be put into a proper model to process the *rate of failure* of generators transformers and transmission lines. The result at each study period is the expected value to supply the required load. Statistics and information about the generator's and transformer's availability, as well as the line rate of failure, are a key piece of information to build an appropriate probabilistic model.

Security assessment is a study of how well a system's voltages, frequency, and lines without overloads are maintained in the system, at steady state, and during contingencies. Contingencies are caused by faults in the system and line or generator's tripping. The question to be answered is: as generators and transmission lines trip, is the system robust and able to maintain synchronism between all connected generators? The loss of elements comprises the contingency studies.

Contingency analysis is a study that poses the question: what happens to the system's variables (voltages and power flows) when a generator or a power plant trips? What are the changes to the system's variables when a transmission or a transformer trips due to an electrical fault or as a consequence of switching phenomena? How would a system's topology changes affect neighboring transmission elements? How can we be prepared for power overloads or high/low voltage related problems? What happens in the case of multiple contingency situations? Results are evaluated first assuming that a new steady state is reached from the base case to the postcontingency situation; in this case, the transient process in how electric energy is going to be reassigned following a process with damped oscillations is not considered.

In a short time horizon, as in operation planning and close to *real time*, for fast network solutions and network analysis, some approximations similar to the ones derived for the *fast decoupled load flow* might be introduced. Central to network studies of this kind of applications establish a steady state converged solution or *base case*, and multiple practical applications are derived for the operation or for the planning process from this condition.

One requirement in conducting a contingency analysis is to have a fast calculation of adjusted values for the system's state variables: new values for node voltages and nodal angles, as well as the new power flows. Network models are derived according to the required application and can range from DC analogous approximations to full AC Newton's formulation, especially in those cases that are critical in terms of large nodal angle separation (heavy load or large changes in the system), or voltage problems with reduced margin to the voltage collapse point.

A more complete steady state formulation could be a solution by optimal power flows and control for some selected cases. The fast study of contingency analysis might show results that need extended analysis through various dynamic. In order to study generators and swing response to include inertia, generating units regulation characteristics or to include complete transient stability studies. If nondecaying oscillations are detected in the dynamic studies, this could lead into dynamic

response analysis so that control settings, control modeling, and control tuning can be evaluated.

10.2 General System Incremental Linear Network

To establish fast studies, linear models can be devised and used. At this point, we can make reference to models developed in Chapter 6 to conduct real power flow approximation, as (6.91) that is written here as (10.1) for completeness.

$$-x_{km} \frac{\Delta p_{km}}{|V_k|} + \Delta\theta_k - \Delta\theta_m = -\Delta\tau \tag{10.1}$$

- x_{km} Series reactance of element from node k to node m
- Δp_{km} Incremental real power flow from node k to node m
- $\Delta\theta_k$ Incremental nodal angle node k
- $\Delta\theta_m$ Incremental nodal angle node m
- $|V_k|$ Nodal voltage magnitude at node k
- $\Delta\tau$ Incremental phase shifting angle, control at element km

From (10.1) the incremental equivalent circuit is shown in Figure 10.1.

Expression (10.1) will be used for each element in our network. To complete the set of equations, an analogue to KCL is written for the incremental nodal power balance. By constructing a general incremental-hybrid equation for all elements and the set of nodal power balances by KCL, it will give a *primitive* circuit type of equation.

$$\begin{bmatrix} -X & A \\ A^t & 0 \end{bmatrix} \begin{bmatrix} \frac{\Delta p}{V} \\ \Delta\theta \end{bmatrix} = \begin{bmatrix} -\Delta\tau \\ \frac{\Delta P}{V} \end{bmatrix} \tag{10.2}$$

Where

- X Diagonal matrix of element’s reactance
- $\Delta\theta$ Incremental nodal angles
- $\Delta p/V$ Incremental power through elements

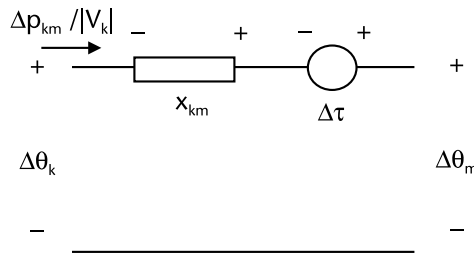


Figure 10.1 Linearized model for incremental real power flow.

$\Delta P/V$ Incremental nodal power injection

By *partial inversion* over all of the elements, gives a reduced equivalent matrix as seen from the system's nodes. The numerical step renders a susceptance matrix B_{bus} , which is Norton's equivalent matrix (10.3). The right hand side will have the incremental changes to real power flows through transmission elements and the nodal incremental power injections.

$$\begin{bmatrix} B & BA \\ A^t B & A^t BA \end{bmatrix} \begin{bmatrix} \Delta\tau \\ \Delta\theta \end{bmatrix} = \begin{bmatrix} \frac{\Delta p}{V} \\ \frac{\Delta P}{V} \end{bmatrix} \quad (10.3)$$

Where

$$B = X^{-1} \quad \text{Diagonal matrix when there are no mutual couplings}$$

$$B_{\text{bus}} = A^t BA \quad \text{Nodal susceptance matrix}$$

From the second row of the matrix equation (10.3), we write:

$$B_{\text{bus}} \Delta\theta = \frac{\Delta P}{V} - A^t B \Delta\tau \quad (10.4)$$

In this case, the incremental nodal angles $\Delta\theta$ in (10.4) are the state variables. Provided that one node angle is taken as reference and solving by *partial inversion* or matrix inversion algorithms, we calculate $\Delta\theta$.

$$\Delta\theta = X_{\text{bus}} \left(\frac{\Delta P}{V} - A^t B \Delta\tau \right) \quad (10.5)$$

Where

$$X_{\text{bus}} = B_{\text{bus}}^{-1}$$

Once the vector $\Delta\theta$ is calculated, the element's incremental power $\Delta p/V$ is found through the first row in the matrix equation (10.3).

$$\frac{\Delta p}{V} = B(A\Delta\theta + \Delta\tau) \quad (10.6)$$

The steps for a network's solution are:

- From network connectivity information, write the A matrix, which is an element-node connection matrix. Form the diagonal matrix X .
 $A(km, Nsal) = +1$ element km out from node $Nsal$
 $A(km, Nlleg) = -1$ element km to node $Nlleg$
- From the information of nodal injections by current sources, j_{km} .
 $I_{\text{bus}}(Nlleg) = I_{\text{bus}}(Nlleg) + j_{km}$ source km injects current into node $Nlleg$

- $$I_{bus}(Nsal) = I_{bus}(Nsal) - j_{km} \quad \text{source } km \text{ extracts current from node } Nsal$$
- Calculate $B_{bus} = A^tBA$ and the vector of powers $-A^tB\Delta\tau$.
 - Find X_{bus} and solve $\Delta\theta = X_{bus}(\Delta P/V - A^tB\Delta\tau)$.
 - Calculate $\Delta p/V = B(A\Delta\theta + \Delta\tau)$.
 - Nodal angle difference at each element terminals by $A\Delta\theta$.

The described calculations can be conducted using *sparse techniques*, especially as matrices A , X , and B_{bus} will be highly sparse. The nodal reactance matrix X_{bus} (which is the inverse of B_{bus}) is calculated by columns, as in many cases, the application requires only a few elements of the inverse matrix.

Example 10.1

Consider a network and solve for θ_{bus} , and the real power flows p_{km} . Assume node voltage magnitudes as 1.0 pu, complex tap values as $1.0\angle 0$. The parameters are shown in Table 10.1. This will give the *base case* from which several concepts will be derived. Using reactance values only, follow steps from a) to f) listed in the previous algorithm and solve for unknown nodal angles θ_2 , θ_3 , and θ_4 . The constraints to be satisfied are the nodal power balances for real power.

$$|t| \angle \tau = t_\alpha + jt_\beta = 1.0\angle 0^\circ$$

Base case solution
Real power flows, Base Case

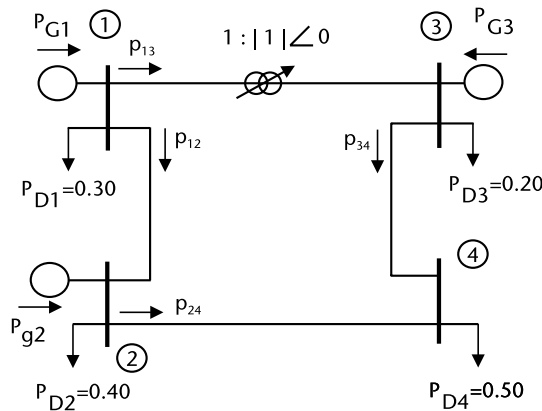


Figure 10.2 Circuit to study real power flows only.

Table 10.1 Connectivity and Parameter Values from Figure 10.2

Element	$Nsal - k$	$Nlleg - m$	x_{km}	tap	$y b_{sh/2}$
1	1	2	0.099	-1	0
2	1	3	0.099	$1+j0$	0
3	3	4	0.066	-1	0
4	2	4	0.0495	-1	0

```

Nelem =      4   Nnod =      4   Nref =      1

Element      Nfrom      Nto      x Value      essage
   1          1         2      0.0990      0.0000
   2          1         3      0.0990      0.0000
   3          3         4      0.0660      0.0000
   4          2         4      0.0495      0.0000
    
```

Nodal conditions, Base Case

```

Node Num      Type Nod      Nodal angle      PGen      Pload
   1          +0         0.00         0.0000         0.6000
   2          +1         0.00         0.4200         0.8000
   3          +1         0.00         0.6400         0.4000
   4          -1         0.00         0.0000         1.0000
    
```

Slack type 0, Gen type 1, Load type -1

A =

```

   1      -1       0       0
   1       0      -1       0
   0       0       1      -1
   0       1       0      -1
    
```

Ybus =

```

 20.2000  -10.1000  -10.1000         0
-10.1000   30.3000         0  -20.2000
-10.1000         0   25.2500  -15.1500
         0  -20.2000  -15.1500   35.3500
    
```

Xbus =

```

 0.0000   0.0000   0.0000   0.0000
 0.0000   0.0677   0.0313   0.0521
 0.0000   0.0313   0.0677   0.0469
 0.0000   0.0521   0.0469   0.0782
    
```

Real power flows, Base Case

```

Element      Nfrom      Nto      p Value
   1          1         2      0.7105
   2          1         3      0.4295
   3          3         4      0.6695
   4          2         4      0.3305
    
```

Nodal solution, Base Case

```

Node Num      Type Nod      Nod_angle deg      PGen      Pload
   1          +0         -0.0000         1.7400         0.6000
   2          +1         -4.0307         0.4200         0.8000
   3          +1         -2.4363         0.6400         0.4000
   4          -1         -4.9682         0.0000         1.0000
    
```

Note that the row and column for the reference node are zero in the bus reactance matrix.

10.3 Sensitivity Matrix for a Linear Circuit

The algorithm described in Section 10.2 takes advantage of a natural partition of information for elements and for the network's nodes; this is used to solve the problem. An interesting alternate interpretation is useful if a whole *partial inversion* process is conducted on (10.3), provided that one node is referenced. The results show that the inverse matrix is a *sensitivity matrix* that relates by means of the coefficients changes of the *control variables* over the *dependent variables*. For this formulation, the dependent variables are the increment to nodal angles and the increments on power flows through elements.

$$\begin{bmatrix} \frac{\Delta p}{V} \\ \Delta \theta \end{bmatrix} = \begin{bmatrix} S_{br,\tau} & S_{br,\Delta P} \\ S_{bus,\tau} & S_{bus,\Delta P} \end{bmatrix} \begin{bmatrix} -\Delta \tau \\ \frac{\Delta P}{V} \end{bmatrix} \quad (10.7)$$

Control variables $\Delta \tau$ and $\Delta P/V$

Dependent variables $\Delta p/V$ and $\Delta \theta$

Example 10.2

Consider the linear network from Example 10.1. Write the general circuit form as given by (10.3). Solve for real power flows Δp_{km} and $\Delta \theta_{bus}$. Show the hybrid matrix (here called W) and its inverse W^{-1} (sensitivity matrix).

Real power flows, Base Case

Element	Nfrom	Nto	x Value	esource
1	1	2	0.0990	0.0000
2	1	3	0.0990	0.0000
3	3	4	0.0660	0.0000
4	2	4	0.0495	0.0000

Nodal conditions, Base Case

Node Num	Type	Nod	Nodal angle	PGen	Pload
1	+0		0.00	0.0000	0.6000
2	+1		0.00	0.4200	0.8000
3	+1		0.00	0.6400	0.4000
4	-1		0.00	0.0000	1.0000

Slack type 0, Gen type 1, Load type -1

$W =$

-0.0990	0	0	0	1.0000	-1.0000	0	0
0	-0.0990	0	0	1.0000	0	-1.0000	0
0	0	-0.0660	0	0	0	1.0000	-1.0000
0	0	0	-0.0495	0	1.0000	0	-1.0000
1.0000	1.0000	0	0	0	0	0	0
-1.0000	0	0	1.0000	0	0	0	0
0	-1.0000	1.0000	0	0	0	0	0
0	0	-1.0000	-1.0000	0	0	0	0

Sensitivity matrix

W1 =

-3.1895	3.1895	3.1895	-3.1895	0	-0.6842	-0.3158	-0.5263
3.1895	-3.1895	-3.1895	3.1895	0	-0.3158	-0.6842	-0.4737
3.1895	-3.1895	-3.1895	3.1895	0	-0.3158	0.3158	-0.4737
-3.1895	3.1895	3.1895	-3.1895	0	0.3158	-0.3158	-0.5263
0	0	0	0	0.0000	0.0000	0.0000	0.0000
-0.6842	-0.3158	-0.3158	0.3158	0.0000	0.0677	0.0313	0.0521
-0.3158	-0.6842	0.3158	-0.3158	0.0000	0.0313	0.0677	0.0469
-0.5263	-0.4737	-0.4737	-0.5263	0.0000	0.0521	0.0469	0.0782

Real power flows, Base Case

Element	Nfrom	Nto	p Value
1	1	2	0.7105
2	1	3	0.4295
3	3	4	0.6695
4	2	4	0.3305

Nodal solution, Base Case

Node Num	Type	Nod	Nod_angle deg	PGen	Pload
1	+0	-0.0000		1.7400	0.6000
2	+1	-4.0307		0.4200	0.8000
3	+1	-2.4363		0.6400	0.4000
4	-1	-4.9682		0.0000	1.0000

10.3.1 Sensitivity Matrix for Incremental Control Changes

The inverse matrix $W1$ shown in Example 10.2 is a sensitivity matrix as (10.7). From a control point of view, when *phase shifters* $\Delta\tau$ are available, changes can be studied to calculate their influence and effects. The effects can be quantified by looking into the column of the inverse matrix $W1$ that corresponds to the element where the phase shifter is located. Similarly, the same can be said about control changes by nodal injections $\Delta P/V$; the coefficients in the column of the inverse matrix $W1$ will show how much the power flows, and nodal angles will change given the new condition of a nodal injection $\Delta P/V$. First, let us assume that a *phase shifter* is located at element 1-3. An incremental change $\Delta\tau_{13} = 0.05$ radians (2.86°), will cause changes to power flows and nodal angles. Calculation follows the use of the second column of $W1$. Results include the angle difference through transmission elements; this will allow a look into the *steady state stability margin*, which, according to engineering practice for high voltage transmission lines, should not go above 30° .

Dt = 0.0500

Real power flows, control change Dt13 = 0.05 rad

Element	Nfrom	Nto	p Value	Angle qkm
1	1	2	0.5511	3.13
2	1	3	0.5889	0.48
3	3	4	0.8289	3.13
4	2	4	0.1711	0.49

Nodal solution, control change Dt13 = 0.05 rad

Node Num	Type	Nod	Nod_angle deg	PGen	Pload
----------	------	-----	---------------	------	-------

1	+0	-0.0000	1.7400	0.6000
2	+1	-3.1260	0.4200	0.8000
3	+1	-0.4762	0.6400	0.4000
4	-1	-3.6112	0.0000	1.0000

For a change of nodal injection, we will assume an increase in the load at node 4 by 0.5 pu. Show the new values for power flows and nodal angles. The calculated values are changes to the base case from Example 10.2. The nodal angle differences on a transmission element are shown again to keep track of the stability margin.

Real power flows, control change DP/V =0.5 pu (load)						
Element	Nfrom	Nto	p Value	Angle qkm		
1	1	2	0.9737	5.52		
2	1	3	0.6663	3.78		
3	3	4	0.9063	3.43		
4	2	4	0.5937	1.68		
Nodal solution, control change DP/V =0.5 pu (load)						
Node Num	Type	Nod	Nod_angle deg	PGen	Pload	
1	+0		-0.0000	2.2400	0.6000	
2	+1		-5.5236	0.4200	0.8000	
3	+1		-3.7799	0.6400	0.4000	
4	-1		-7.2075	0.0000	1.5000	

This model will solve for control actions and their effects on power flows and nodal angles with reference to values from the base case. An interesting extension can be addressed when a transmission element line or transformer is *tripped* due to a fault clearing procedure, and we need the new values of power flows and nodal angles. The new values for power flows will show if any transmission element is overloaded. This is discussed in Section 10.4.

10.4 Single Contingency Model

We are interested in the new operating state after a transmission line or a transformer is suddenly disconnected from the network due to a fault and after the protective scheme has performed its duties. The attention is focused on the new steady state and no dynamic is modeled for the transition period. In control centers for electric systems, extensive evaluation of network conditions, power flows through each element, and nodal values for the network are analyzed; this is done for every credible contingency. Fast results are required in an operational environment; operators in the control room need to know ahead of time that if certain contingencies occur, the system's vulnerabilities, and how to make appropriate remedial preparations. Calculation speed can be accomplished by linear network approximations, as the ones presented in Section 10.3 for real power flow and nodal angles. A refinement must be worked out because the element on outage will not be part of the system. Let us work the concept through Thévenin's equivalent.

10.4.1 Thévenin's Equivalent

We now recall how the Thévenin's equivalent, as seen from two nodes to which the tripped element is connected, can be defined and how the node voltages make the Thévenin's voltage sources. Connecting the negative series admittance of the original element to the Thévenin's nodes will help us find the currents that flow to the newly connected admittance. As in the fault analysis presented in Chapter 9, we inject the currents back into the network equivalent to calculate the nodal angles changes, once we have the value of the current through the new admittance. All of this is a result of connecting the negative value of the admittance between nodes k and m . We work the steps to solve this problem using voltage and current notation; the results can then be applied in an analogous form to a particular incremental real power flow or to the incremental reactive power problem. Therefore, we use the analogy of current to power flow and voltage to the nodal angle.

For the outage of an element y_{km} connected between nodes k and m , as shown in Figure 10.3, let us use Thévenin's equivalent from the network's impedance matrix that already includes y_{km} . Then connect, from node k to node m , the admittance $-y_{km}$. When the new negative admittance is connected, the boundary conditions of nodal voltages and nodal currents must be met. The net effect should be that no admittance is connected from k to m . As a result, this will represent the outage of element from node k to node m . By solving the set of equations, we determine currents I_k and I_m . The negative of these currents needs to be injected back into node k and m , respectively. By completing this step, we find changes to the system's nodal voltages. With updated nodal voltages, the current that flows through each network element can be found.

The equations presented so far are similar to the ones used in the general fault analysis in Chapter 9; only that in this case we upgrade our notation and the electrical conditions for the contingency case. We start with Thévenin's equation looking from nodes k and m into the network as (10.8), then we write the nodal voltage equation (10.9) for the portion of the admittances to be connected at nodes k and m ; this will give us the nodal admittance matrix for connecting the admittance $-y_{km}$. Boundary conditions for voltages and currents are written in (10.10).

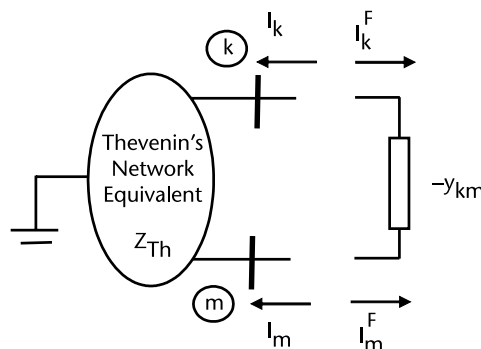


Figure 10.3 Equivalent circuit to study outage admittance y_{km} .

$$\begin{bmatrix} V_k \\ V_m \end{bmatrix} = \begin{bmatrix} E_k \\ E_m \end{bmatrix} + \begin{bmatrix} Z_{kk} & Z_{km} \\ Z_{mk} & Z_{mm} \end{bmatrix} \begin{bmatrix} I_k \\ I_m \end{bmatrix} \quad (10.8)$$

$$\begin{bmatrix} -y_{km} & y_{km} \\ y_{mk} & -y_{mm} \end{bmatrix} \begin{bmatrix} V_k \\ V_m \end{bmatrix} = \begin{bmatrix} I_k^F \\ I_m^F \end{bmatrix} \quad (10.9)$$

$$\begin{bmatrix} I_k \\ I_m \end{bmatrix} = - \begin{bmatrix} I_k^F \\ I_m^F \end{bmatrix} \quad \begin{bmatrix} V_k \\ V_m \end{bmatrix} = \begin{bmatrix} V_k^F \\ V_m^F \end{bmatrix} \quad (10.10)$$

Where:

- E_k Thévenin's voltage, node k
- E_m Thévenin's voltage, node m
- I_k Nodal current k
- I_m Nodal current m
- V_k Nodal voltage k
- V_m Nodal voltage m
- V_k^F Nodal voltage k new connection
- V_m^F Nodal voltage m new connection
- I_k^F Nodal current into node k new connection
- I_m^F Nodal current into node m new connection

Substitution of (10.8) into (10.9) gives us the explicit equation to calculate nodal currents into the newly added admittance element $-y_{km}$.

$$\begin{bmatrix} -y_{km} & y_{km} \\ y_{mk} & -y_{mm} \end{bmatrix} \left(\begin{bmatrix} E_k \\ E_m \end{bmatrix} - \begin{bmatrix} Z_{kk} & Z_{km} \\ Z_{mk} & Z_{mm} \end{bmatrix} \begin{bmatrix} I_k^F \\ I_m^F \end{bmatrix} \right) = \begin{bmatrix} I_k^F \\ I_m^F \end{bmatrix} \quad (10.11)$$

$$\begin{bmatrix} I_k^F \\ I_m^F \end{bmatrix} = \left(\begin{bmatrix} 1 & 0 \\ 0 & 1 \end{bmatrix} + \begin{bmatrix} -y_{km} & y_{km} \\ y_{mk} & -y_{mm} \end{bmatrix} \begin{bmatrix} Z_{kk} & Z_{km} \\ Z_{mk} & Z_{mm} \end{bmatrix} \right)^{-1} \begin{bmatrix} -y_{km} & y_{km} \\ y_{mk} & -y_{mm} \end{bmatrix} \begin{bmatrix} E_k \\ E_m \end{bmatrix} \quad (10.12)$$

Once nodal currents are determined, these currents are injected into the corresponding nodes k and m in the system of equations (10.13). Assuming that this is the only change of nodal injections, the incremental changes to all nodal voltages are calculated, with only two currents considered as I_k and I_m . In this case, (10.14) will only require column k and column m in order to calculate the incremental changes ΔV to nodal voltages.

$$[\Delta V] = [S_{\text{bus},\Delta I}] [\Delta I] \quad (10.13)$$

$$\begin{bmatrix} \Delta V_1 \\ \Delta V_2 \\ \vdots \\ \Delta V_n \end{bmatrix} = \begin{bmatrix} S_{1,k} & S_{1,m} \\ \vdots & \vdots \\ S_{n,k} & S_{n,m} \end{bmatrix} \begin{bmatrix} \vdots \\ \Delta I_k \\ \vdots \\ \Delta I_m \\ \vdots \end{bmatrix} \quad (10.14)$$

The new nodal voltages are calculated adding ΔV to the voltages V^0 from the base case solution.

$$V^{\text{new}} = V^0 + \Delta V \quad (10.15)$$

The currents that now flow through elements are updated by (10.16) with a value of zero for the admittance of element km in $[z]^{-1}$. Voltage source e might be zero if there is no series voltage source in elements.

$$i^{\text{new}} = [z]^{-1}(A^t V^{\text{new}} - e) \quad (10.16)$$

Example 10.3

For the network in Example 10.1, there is a line connecting node 3 to node 4. Consider that this line *trips*, and that we are interested in the new power flows and nodal angles under this contingency. Use the results in this section, using Thévenin's equivalent with an analogy of current as real power and voltages as nodal angles. Update the base case solution for the contingency with steps described by (10.9)–(10.16).

$$Z_{\text{Th}} = \begin{bmatrix} 0.0677 & 0.0469 \\ 0.0469 & 0.0782 \end{bmatrix}$$

$$y_{34} = -15.1500$$

$$E_{\text{Th}} = \begin{bmatrix} -0.0425 \\ -0.0867 \end{bmatrix}$$

$$I_{\text{Fall}a} = \begin{bmatrix} -3.1800 \\ 3.1800 \end{bmatrix}$$

Real power flows, Contingency Case

Element	Nfrom	Nto	p Value	Angle θ_{km}
1	1	2	1.3800	7.83
2	1	3	-0.2400	-1.36
3	3	4	0.0000	12.03
4	2	4	1.0000	2.84

Nodal solution, Contingency Case					
Node Num	Type	Nod	Nod_angle deg	PGen	Pload
1	+0		-0.0000	1.7400	0.6000
2	+1		-7.8285	0.4200	0.8000
3	+1		1.3615	0.6400	0.4000
4	-1		-10.6650	0.0000	1.0000

Nodal angles and power flows in elements are updated to reflect the loss of the transmission element *km*. The calculation of angle differences between nodes to which an element is connected can be used as an indication of the *stability margin* for that element. The angle difference changes as load through the element increases; this can be the result of the outage of the transmission element *km*. Not having connected this *km* line causes the power flows to be redirected and the nodal angles will adjust to the new power flows condition.

Example 10.4

For a network with structure, as seen in Figure 10.2, consider the outage of one line at a time; this is the $(N - 1)$ criteria used in power systems security evaluation. Show the nodal angle difference across each transmission line at the output results. The line with the outage condition shows an angle difference, but it has no meaning because the line is in a *tripped condition*.

Real power flows, Base Case					
Nelem =	4	Nnod =	4	Nref =	1
Element	Nfrom	Nto	x Value	esource	
1	1	2	0.0990	0.0000	
2	1	3	0.0990	0.0000	
3	3	4	0.0660	0.0000	
4	2	4	0.0495	0.0000	
Nodal conditions, Base Case					
Node Num	Type	Nod	Nodal angle	PGen	Pload
1	+0		0.00	0.0000	0.9000
2	+1		0.00	0.4200	1.2000
3	+1		0.00	0.6400	0.6000
4	-1		0.00	0.0000	1.5000
Slack type 0, Gen type 1, Load type -1					
Xbus =					
0.0000	0.0000	0.0000	0.0000		
0.0000	0.0677	0.0313	0.0521		
0.0000	0.0313	0.0677	0.0469		
0.0000	0.0521	0.0469	0.0782		
Base case solution					
Line	Nsal	Nlleg	pkm	Diff_angle	
1	1	2	1.3105	7.4344	
2	1	3	0.9295	5.2728	
3	3	4	0.9695	3.6665	
4	2	4	0.5305	1.5048	

Node	angle	PG	PL
1	-0.00	3.1400	0.9000
2	-7.43	0.4200	1.2000
3	-5.27	0.6400	0.6000
4	-8.94	0.0000	1.5000

Solution for contingency, line 1 out, k = 1 m = 2

Line	Nsal	Nlleg	pkm	Diff_angle
1	1	2	-0.0000	23.5423
2	1	3	2.2400	12.7072
3	3	4	2.2800	8.6227
4	2	4	-0.7800	-2.2124

Node	angle	PG	PL
1	-0.00	3.1400	0.9000
2	-23.54	0.4200	1.2000
3	-12.71	0.6400	0.6000
4	-21.33	0.0000	1.5000

Solution for contingency, line 2 out, k = 1 m = 3

Line	Nsal	Nlleg	pkm	Diff_angle
1	1	2	2.2400	12.7072
2	1	3	-0.0000	16.6971
3	3	4	0.0400	0.1513
4	2	4	1.4600	4.1412

Node	angle	PG	PL
1	-0.00	3.1400	0.9000
2	-12.71	0.4200	1.2000
3	-16.70	0.6400	0.6000
4	-16.85	0.0000	1.5000

Solution for contingency, line 3 out, k = 3 m = 4

Line	Nsal	Nlleg	pkm	Diff_angle
1	1	2	2.2800	12.9341
2	1	3	-0.0400	-0.2269
3	3	4	-0.0000	17.4156
4	2	4	1.5000	4.2546

Node	angle	PG	PL
1	-0.00	3.1400	0.9000
2	-12.93	0.4200	1.2000
3	0.23	0.6400	0.6000
4	-17.19	0.0000	1.5000

Solution for contingency, line 4 out, k = 2 m = 4

Line	Nsal	Nlleg	pkm	Diff_angle
1	1	2	0.7800	4.4248
2	1	3	1.4600	8.2824

3	3	4	1.5000	5.6728
4	2	4	-0.0000	9.5304
Node	angle	PG	PL	
1	-0.00	3.1400	0.9000	
2	-4.42	0.4200	1.2000	
3	-8.28	0.6400	0.6000	
4	-13.96	0.0000	1.5000	

Results show that nodal angles change to new values; the power flows are adjusted to comply with the power condition imposed by the contingency. Angles increase across both the transmission lines and its power flows. For this small system, the $(N - 1)$ condition (one line out at a time) does not lead the system into difficulties in terms of large nodal angles (close to 30°). From the security point of view, the system is secure under the criteria $(N - 1)$. We have already mentioned that the line outage will cause a power oscillatory problem; we therefore assume that it is a well-damped phenomena, so in a reasonable time (few seconds) we will reach a new steady state that will be the one calculated through the contingency analysis.

10.4.2 Voltage and Reactive Power Under Contingencies

As the real power model used in Section 6.6, in Chapter 6, we had an incremental reactive power model for transmission elements connected from node k to node m . Reasonable approximations were made for high voltage systems. According to Figure 10.4, we will write two equations: incremental series flows (10.17) and nodal balances of reactive power for node k and for node m (10.18) and (10.19), respectively.

The circuit model for the transmission line includes the line-charging susceptance. It might also include shunt reactive power-compensating devices. For the transmission line, no tap is available so $\Delta|t| = 0$. For each element km , (10.17) is applied and nodal balance equations for node k and for node m as in (10.18).

$$-x_{km} \frac{\Delta q_{km}}{|V_k|} + \Delta|V_k| - \Delta|V_m| = -\Delta|t| \tag{10.17}$$

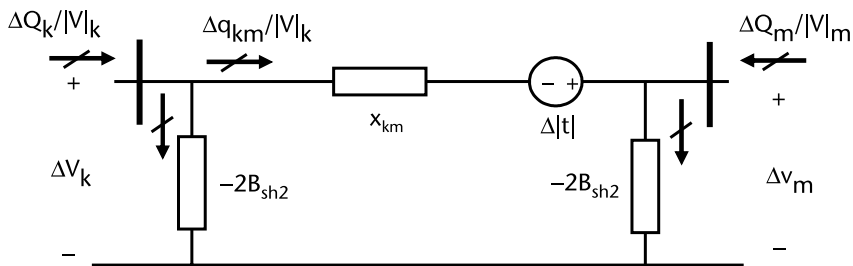


Figure 10.4 Incremental circuit to model voltages and reactive power flow through element km .

$$\frac{\Delta Q_k}{|V_k|} = \frac{\Delta q_{km}}{|V_k|} - ((2B_{sb2})\Delta|V_k|) \quad (10.18)$$

$$\frac{\Delta Q_m}{|V_m|} = -\frac{\Delta q_{km}}{|V_m|} - ((2B_{sb2})\Delta|V_m|) \quad (10.19)$$

x_{km}	Series reactance of element from node k to node m
Δq_{km}	Incremental reactive power flow from node k to node m
$\Delta V_k $	Incremental nodal voltage, node k
$\Delta V_m $	Incremental nodal voltage, node m
$ V_k , V_m $	Nodal voltage magnitude at node k and at node m
$\Delta t $	Incremental tap, control at element km
B_{sb2}	Susceptance in π equivalent for element km

Example 10.4

For a four-node system, write the incremental model for voltages and reactive power flows. We use (10.17) for elements and (10.18)–(10.19) for nodal reactive power balances.

$$\left[\begin{array}{l} (1) \quad -x_{12} \frac{\Delta q_{12}}{|V_1|} + \Delta|V_1| - \Delta|V_2| = -\Delta|t| \\ (2) \quad -x_{13} \frac{\Delta q_{13}}{|V_1|} + \Delta|V_1| - \Delta|V_3| = 0 \\ (3) \quad -x_{34} \frac{\Delta q_{34}}{|V_3|} + \Delta|V_3| - \Delta|V_4| = 0 \\ (4) \quad -x_{24} \frac{\Delta q_{24}}{|V_2|} + \Delta|V_2| - \Delta|V_4| = 0 \\ \text{Node 1} \quad + \frac{\Delta q_{12}}{|V_1|} - (2B_{sb2_{12}} \Delta|V_1|) + \frac{\Delta q_{13}}{|V_1|} - (2B_{sb2_{13}} \Delta|V_1|) = \frac{\Delta Q_{G1}}{|V_1|} - \frac{\Delta Q_{D1}}{|V_1|} \\ \text{Node 2} \quad - \frac{\Delta q_{12}}{|V_1|} - (2B_{sb2_{12}} \Delta|V_2|) + \frac{\Delta q_{24}}{|V_2|} - (2B_{sb2_{24}} \Delta|V_2|) = \frac{\Delta Q_{G2}}{|V_2|} - \frac{\Delta Q_{D2}}{|V_2|} \\ \text{Node 3} \quad - \frac{\Delta q_{13}}{|V_1|} - (2B_{sb2_{13}} \Delta|V_3|) + \frac{\Delta q_{34}}{|V_3|} - (2B_{sb2_{34}} \Delta|V_3|) = \frac{\Delta Q_{G3}}{|V_3|} - \frac{\Delta Q_{D3}}{|V_3|} \\ \text{Node 4} \quad - \frac{\Delta q_{24}}{|V_2|} - (2B_{sb2_{24}} \Delta|V_4|) - \frac{\Delta q_{34}}{|V_3|} - (2B_{sb2_{34}} \Delta|V_4|) = \frac{\Delta Q_{G4}}{|V_4|} - \frac{\Delta Q_{D4}}{|V_4|} \end{array} \right] \quad (10.20)$$

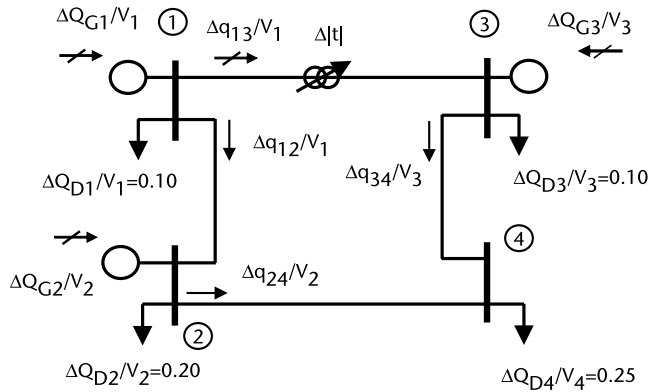


Figure 10.5 Incremental circuit to model voltages and reactive power flow.

For the circuit in Figure 10.5, the hybrid matrix expression is shown by (10.21); note that line from node 1 to node 3 does not have a shunt capacitive connection.

$$\begin{bmatrix}
 -x_{12} & 0 & 0 & 0 & +1 & -1 & 0 & 0 \\
 0 & -x_{13} & 0 & 0 & +1 & 0 & -1 & 0 \\
 0 & 0 & -x_{34} & 0 & 0 & 0 & +1 & -1 \\
 0 & 0 & 0 & -x_{24} & 0 & +1 & 0 & -1 \\
 +1 & +1 & 0 & 0 & -2B_{sb2}^{12} & 0 & 0 & 0 \\
 -1 & 0 & 0 & +1 & 0 & -2(B_{sb2}^{12} + B_{sb2}^{24}) & 0 & 0 \\
 0 & -1 & +1 & 0 & 0 & 0 & -2B_{sb2}^{34} & 0 \\
 0 & 0 & -1 & -1 & 0 & 0 & 0 & -2(B_{sb2}^{24} + B_{sb2}^{34})
 \end{bmatrix}
 \begin{bmatrix}
 \frac{\Delta q_{12}}{|V_1|} \\
 \frac{\Delta q_{13}}{|V_1|} \\
 \frac{\Delta q_{34}}{|V_3|} \\
 \frac{\Delta q_{24}}{|V_2|} \\
 \Delta |V_1| \\
 \Delta |V_2| \\
 \Delta |V_3| \\
 \Delta |V_4|
 \end{bmatrix}
 =
 \begin{bmatrix}
 -\Delta |t| \\
 0 \\
 0 \\
 0 \\
 \frac{\Delta Q_1}{|V_1|} \\
 \frac{\Delta Q_2}{|V_2|} \\
 \frac{\Delta Q_3}{|V_3|} \\
 \frac{\Delta Q_4}{|V_4|}
 \end{bmatrix}
 \tag{10.21}$$

Assuming that a transmission line *trips*, this will cause changes to nodal voltages and reactive power flows through elements; it is required to calculate the changes. We use the electric current analogy in Figure 10.6; we use voltages and currents.

Nodal equations are used as (10.8) and (10.10). Equation (10.22) represents the nodal matrix for the connecting element, including its shunt susceptances (see Figure 10.6).

$$\begin{bmatrix}
 -y_{km} + 2B_{sb2} & y_{km} \\
 y_{mk} & -y_{mm} + 2B_{sb2}
 \end{bmatrix}
 \begin{bmatrix}
 V_k \\
 V_m
 \end{bmatrix}
 =
 \begin{bmatrix}
 I_k^F \\
 I_m^F
 \end{bmatrix}
 \tag{10.22}$$

Now, the nodal currents into the connecting admittances (10.22) are represented in (10.23).

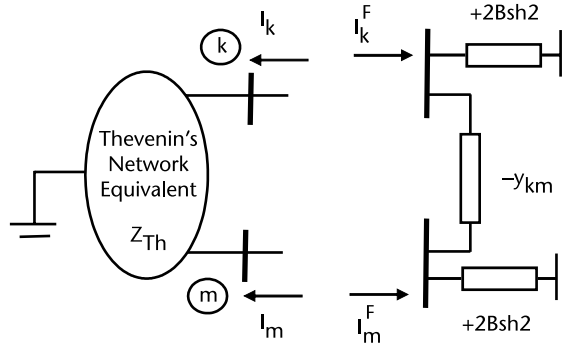


Figure 10.6 Incremental current model to solve for nodal voltages and reactive power flows.

$$\begin{bmatrix} I_k^F \\ I_m^F \end{bmatrix} = \left(\begin{bmatrix} 1 & 0 \\ 0 & 1 \end{bmatrix} + \begin{bmatrix} -y_{km} + 2B_{sh2} & y_{km} \\ y_{mk} & -y_{mm} + 2B_{sh2} \end{bmatrix} \begin{bmatrix} Z_{kk} & Z_{km} \\ Z_{mk} & Z_{mm} \end{bmatrix} \right)^{-1} \begin{bmatrix} -y_{km} & y_{km} \\ y_{mk} & -y_{mm} \end{bmatrix} \begin{bmatrix} E_k \\ E_m \end{bmatrix} \quad (10.23)$$

Currents calculated from (10.23) are injected back into the network at node k and m . Incremental nodal voltages ΔV by (10.13)–(10.14) will update the nodal voltages from the base case V^0 as in (10.15).

$$\begin{aligned} \Delta I_k &= -I_k^F \\ \Delta I_m &= -I_m^F \end{aligned} \quad (10.24)$$

Currents flowing through elements are updated by (10.16) (which is repeated below). It should be noted that the series admittance for element y_{km} is zero; this is considered before inverting the diagonal matrix $[z]^{-1}$.

$$i^{\text{new}} = [z]^{-1}(A^t V^{\text{new}} - e) \quad (10.16)$$

Example 10.5

For the circuit in Figure 10.2, the base case is a load flow solution only for the reactive power. A fast *decoupled* load flows converges in two iterations for the B' part and two iterations for the B'' part of the problem. All values in pu.

- Show the sensitivity matrix for the reactive power incremental model.
- For the reactive power model, solve for changes in reactive power flows and nodal voltages after the line connected from node 3 to node 4 is tripped. Use as starting point the base case solution.

Data for the small network in Figure 10.5 is listed below. The solution appears in Figure 10.7.

Number of nodes =		4		Number of elements =		4	
Element	Nsal	Nlleg	r	x	bsh2		
1	1	2	0.0000	0.2000	0.0400		
2	1	3	0.0000	0.3000	0.0600		
3	3	4	0.0000	0.2500	0.0200		
4	2	4	0.0000	0.2000	0.0300		
Node	Ntype	Voltage	Angle	PG	QG	PL	QL
1	0	1.00000	0.0000	0.0000	0.0000	0.0000	0.0000
2	1	1.00000	0.0000	0.0000	0.0000	0.0000	0.1000
3	1	1.00000	0.0000	0.0000	0.0000	0.0000	0.1000
4	-1	1.00000	0.0000	0.0000	0.0000	0.0000	0.3000
IterationP =		0.0		MaxDP =		0.000000e+000	
IterationQ =		0.0		MaxDQ =		3.500000e-001	
IterationP =		2.0		MaxDP =		0.000000e+000	
IterationQ =		2.0		MaxDQ =		6.647207e-007	

Load flows in elements

Element	Nsal	Nlleg	p	q
1	1	2	0.0000	0.0400
	2	1	0.0000	0.0400
2	1	3	0.0000	0.0600
	3	1	0.0000	0.0600
3	3	4	0.0000	0.1794
	4	3	0.0000	-0.1353
4	2	4	0.0000	0.2292
	4	2	0.0000	-0.1647

Nodal Solution

Node	Ntype	Voltage	Angle	PG	QG	PL	QL
1	0	1.00000	0.00	0.0000	0.1000	0.0000	0.0000

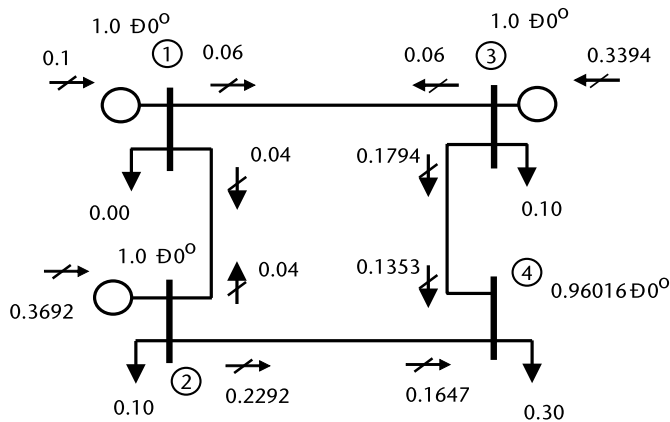


Figure 10.7 Circuit solution, only voltages and reactive power flows.

2	1	1.00000	0.00	0.0000	0.3692	0.0000	0.1000
3	1	1.00000	0.00	0.0000	0.3394	0.0000	0.1000
4	-1	0.96016	0.00	0.0000	0.0000	0.0000	0.3000
Total Generation		PG =	0.0000	QG =	0.8085		
Total Load		PL =	0.0000	QL =	0.5000		
Losses		P =	0.0000	Q =	0.3085 (> TL requirement)		

The sensitivity matrix for the reactive power incremental model is listed as W1

W1 =

-5.0000	0.0000	0.0000	-0.0000	0.0000	-0.0000	0.0000	-0.0000
0.0000	-3.3333	-0.0000	0.0000	0.0000	0.0000	-0.0000	-0.0000
0.0000	-0.0000	-2.2022	2.2472	-0.0000	-0.0000	0.0000	-0.4494
-0.0000	0.0000	2.2472	-2.1910	0.0000	0.0000	-0.0000	-0.5618
0.0000	0.0000	-0.0000	0.0000	0.0000	0.0000	0.0000	0.0000
-0.0000	0.0000	-0.0000	0.0000	0.0000	0.0000	0.0000	0.0000
0.0000	-0.0000	0.0000	-0.0000	0.0000	0.0000	0.0000	0.0000
-0.0000	-0.0000	-0.4494	-0.5618	0.0000	0.0000	0.0000	0.1124

Notice that various rows and columns are zero, due to the fact that nodes 1, 2, and 3 are voltage-controlled nodes and their voltage value remains constant (increments are zero).

Results for a single contingency: line 3–4 out.

Solution to single contingency
line on outage 3, 4
Thevenin and Fault equivalent

	ZTh		YF		ETh	IF
0.0000	0.0000	-3.9600	4.0000	1.0000	-0.2795	
0.0000	0.1124	4.0000	-3.9600	0.9602	0.3563	

Updated

Flows	Voltages	Exact values(from load flow solution)	
0.0400	1.0000	0.0400	1.0000
0.0600	1.0000	0.0600	1.0000
0.0000	1.0000	0.0000	1.0000
0.4294	0.9201	0.3784	0.9302

10.5 Participation Factors from System's Lines

Consider a connected line that is carrying a flow p_{km} from node k to node m . If that line is no longer in service, the amount of power it was carrying will be taken by the remaining lines in the system, assuming that no changes are made to system's load and generation. For system security analysis, it is of great importance to know the amount that each remaining line will take and if the new amount of power will get near any transmission limit.

To calculate the amount of power to be shared, let us use Figure 10.8. The transmission line from node k to m , carrying power Δp_{km} , is assumed to be tripped and the amount of power $\Delta P_k = \Delta p_{km}$ will be injected into node k and $\Delta P_m = -\Delta p_{km}$ into node m . The numerical response of the network to this condition will provide changes to line flows and nodal angles. We calculate the normalized power flow changes with respect to ΔP_k ; we will find the power sharing factor when line km is not connected because of its contingency.

$$\frac{\Delta p_{rs}}{\Delta P_k} \tag{10.25}$$

Example 10.6

For the circuit in Figure 10.2, the base case is a load flow solution solving for real power only. Line (1) from node 1 to node 2 has a power flow of 1.3105. A contingency occurs and the line is tripped; the solution is given by the steps developed in Section 10.4. Now one step further is to normalize the incremental changes in power flows by the power injected into node k . All values are in pu.

Base case solution

Line	Nsal	Nlleg	pkm	Diff_angle
1	1	2	1.3105	7.4344
2	1	3	0.9295	5.2728
3	3	4	0.9695	3.6665
4	2	4	0.5305	1.5048

Node	angle	PG	PL
1	-0.00	3.1400	0.9000
2	-7.43	0.4200	1.2000
3	-5.27	0.6400	0.6000
4	-8.94	0.0000	1.5000

Incremental solution =

- 0.0000
- 1.3105
- 1.3105
- 1.3105
- 0
- 0.2811
- 0.1298
- 0.2163

Solution for Line Outage FACTOR, line 1 out, k = 1 m = 2

Line	Nsal	Nlleg	pk/DP
1	1	2	-0.0000
2	1	3	1.0000
3	3	4	1.0000
4	2	4	-1.0000

xtotal =

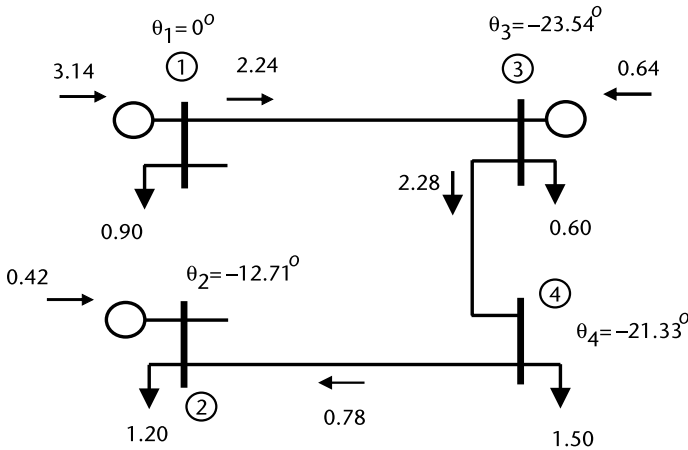


Figure 10.8 Circuit solution only real power flows, line 1 to 2 tripped.

- 0
- 2.2400
- 2.2800
- 0.7800
- 0.0000
- 0.4109
- 0.2218
- 0.3723

10.6 Summary

Contingency analysis is a very important task that must be conducted mainly in the control centers in order to assess the security of the electric power system. In order to conduct this task, fast calculating tools are required to evaluate what happens to the system’s variables when a generator trips and important generation is lost, as well as to find out what would likely occur if a transmission line is disconnected due to an overload condition, a fault, or erroneous action of a tripping device. Linear models are mainly used to provide the fastest solution possible and to get a broad picture of what to expect with respect to real power flows and nodal angles. A linear model that relays in material from Chapters 6 and 9 is used in the realm $P - \theta$ with an analogy through voltage current modeling; a similar analogy is applied to the reactive power—voltage model.

For large power networks as they exist today, with many nodes and transmission elements, the efficient handling of network connectivity information must be done through sparse techniques. Sparsity techniques work only on nonzero values from the models used through ingenious programming of Gaussian elimination to solve the system of equations. We did not delve into those techniques, but rather concentrated our attention on the basics and principles in order to have a solid foundation to tackle more advanced problems and applications.

State Estimation in Electrical Power Systems

11.1 Introduction

Electrical power systems are an ensemble of multiple components: generating units in power plants, power transformers, transmission lines, and a wide variety of loads to be supplied. Operating and planning conditions must be able to handle uncertain conditions and random events, such as units that trip, overloading of transformers, transmission line outages, and random components as part of the electrical load. In the operating environment, power engineers need to know as close as possible, and in reliable form, the true nature of the state variables for the power system. For the electric network, the state variables are node voltage magnitudes and nodal angles. Once the complex voltages for all nodes in the system are known, all derived quantities (i.e., power flows and losses, quality indices) can be calculated, assuming that transmission lines and transformers impedances (admittances) values are known. The calculated values are needed by personnel in the control center so that the monitoring and the *wellbeing* of the system can be assessed. If some deterioration ensues, control actions will follow. Some control actions depend on automatic equipment, their set points, and control laws implemented. For some slow-developing phenomena, human intervention might be required; full awareness of how conditions evolve in the power system is required.

The ideal assumptions under which the power system is planned include components and a load-power generation balance that can drastically differ during real time operation due to switching actions or automatic protection schemes. Modern control centers rely on measured quantities: real and reactive power, voltage magnitudes, currents, and circuit breakers status. This information is collected periodically at remote terminal units (RTU) and sent through communication channels to feed fast digital processing computers located at the control center. Raw information includes meter and transmission errors that are collected and assumed to be synchronously taken. Filtered information that blocks high-frequency noise and nonfundamental 60 Hz components is fed into digital processing algorithms that use redundant information so that, statistically, the *best state estimation* can be obtained. Redundancy is a key concept in applying statistical properties to the estimated quantities that are based on the nature of the measuring error component. A statistical test over the measured quantities can be applied to accept or reject a measurement that is suspected to be spurious.

This chapter presents probability models and assumptions regarding the measurements of a power system's quantities, the quality of measuring devices, and an optimal procedure that works with redundant information to find the best estimate for state variables and derived quantities that can be attained.

11.1.1 Centralized Data Acquisition System

The evolution of monitoring and control of modern power systems is rooted in black-out events in the last fifty years. In the late 1960s, digital computers, hardware for measuring electric variables at substations, and communication media converged and were used to implement applications to monitor and control the power systems with the main objective of avoiding blackouts. One main assumption is that the electrical system is in a quasi-steady state, and that voltage magnitudes, real and reactive power flows, as well as the system's frequency, were almost constant. Therefore, data gathering into a central processing computer at a control center from RTUs, as shown in Figure 11.1, was considered to be simultaneously taken from various substations in the system. Processed measurements and breaker status information were used with transmission lines and transformer parameters to obtain a best estimate for the *state of the system*. Voltage magnitudes, nodal angles, and other results for AC system quantities, such as real and reactive power flows, are derived, and the system health can be monitored from the state estimation.

Figure 11.1 shows the main components of data gathering by means of RTUs. A scan of information is periodically collected by the control center from all the RTUs that are strategically deployed on the power system. Various digital applications are part of the package of application in the control center central processing units (CPUs); for our explanation only the state estimation is depicted. The development of power systems continued to grow in complexity and wide interconnections were

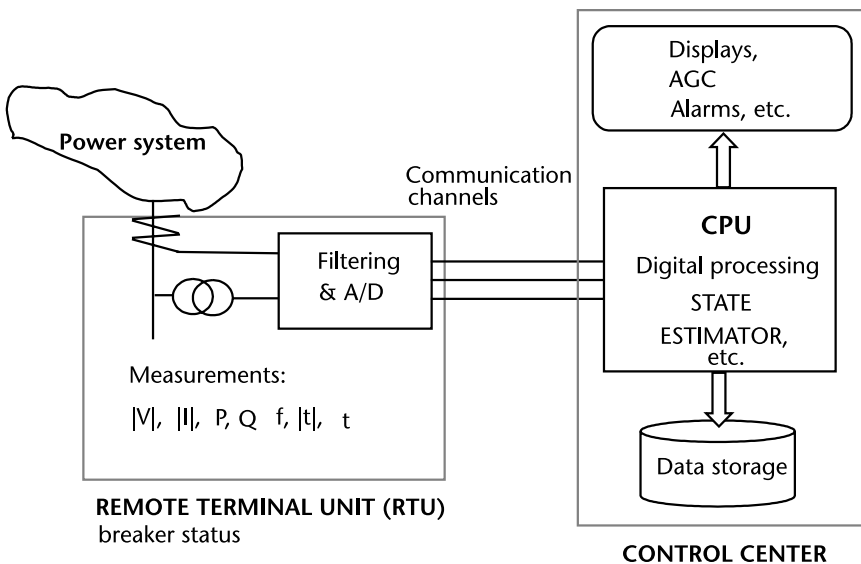


Figure 11.1 Power system, measurements in RTU, and control center.

implemented in the last thirty years. The control centers and their monitoring tools were not capable and not fast enough to prevent blackouts in North America, Japan, Europe, and other regions in the last 10 years. New developments in technology, computing processing power, and communications through fiber optics opened new concepts, such as phasor measurement units (PMUs) with the capacity to synchronize into a very accurate time the measurements and to conduct the processing at a faster rate than compared to the old RTU's equipment. We will visit the basic ideas behind the concept.

11.2 Least Squares, Linear Model

One way to approach the problem is based on the assumption that the measurement error ε follows a Normal probability distribution with expected value $\mu = 0$ and with variance σ^2 . This is a reasonable assumption, as the presence of several random variables in the process will tend to add and to behave as a Normal probability distribution $N(\mu, \sigma^2)$. Assuming a continuous random variable ε , the Normal probability distribution ($\mu = 0, \sigma^2 = 1$) has a bell-shaped form, as shown in Figure 11.2

$$\text{PDF}(\varepsilon) = \frac{1}{\sigma\sqrt{2\pi}} e^{-\frac{(\varepsilon-\mu)^2}{2\sigma^2}} \quad (11.1)$$

The area under the $\text{PDF}(\varepsilon)$ is the probability of variable $a \leq \varepsilon < b$.

$$p(a \leq \varepsilon < b) = \int_a^b \text{PDF}(\varepsilon) d\varepsilon \quad (11.2)$$

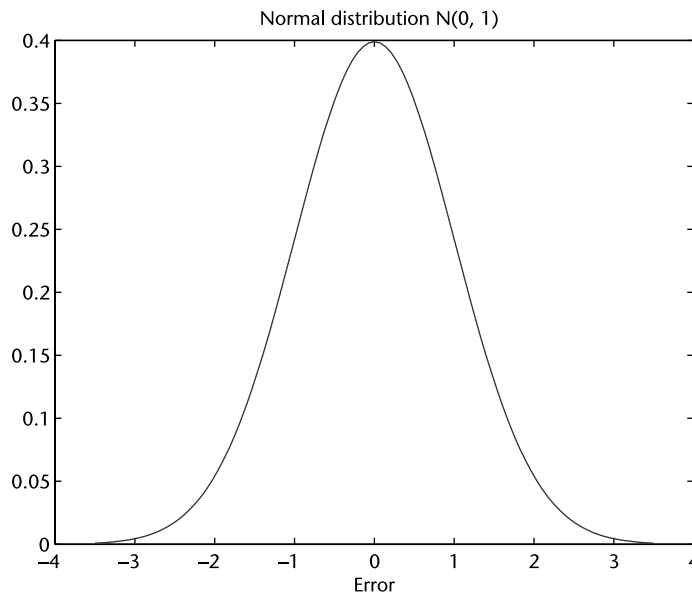


Figure 11.2 Normal probability distribution $N(\mu = 0, \sigma^2 = 1)$.

To start, let us assume that in a scatter diagram for measured values y^m at x values resemble a linear shape. Then the model suggested is $y = a_1x + a_0$, where a set of n measurements gives the linear equation:

$$y_k^{\text{meas}} = a_1x_k + a_0 + \varepsilon_k$$

$$\begin{bmatrix} y_1^{\text{meas}} \\ y_2^{\text{meas}} \\ \vdots \\ y_n^{\text{meas}} \end{bmatrix} = \begin{bmatrix} x_1 & 1 \\ x_2 & 1 \\ \vdots & \vdots \\ x_n & 1 \end{bmatrix} \begin{bmatrix} a_1 \\ a_0 \end{bmatrix} + \begin{bmatrix} \varepsilon_1 \\ \varepsilon_2 \\ \vdots \\ \varepsilon_n \end{bmatrix} \quad (11.3)$$

The so-called *measurement error* ε_k for each measured value is identified in Figure 11.3.

y_k^{meas} Measured value for y_k
 y_k^{th} y_k from model

The summation of squared errors (SS) after the linear model is substituted gives a way to estimate coefficients a_1 and a_0 . A sound criterion is to minimize the summation of the squared errors; optimal values for a_1 and a_0 are derived from the gradient of the SS values.

$$SS = \sum_{k=1}^m \varepsilon_k^2 = \sum_{k=1}^m (y_k^{\text{meas}} - a_1x_k - a_0)^2 \quad (11.4)$$

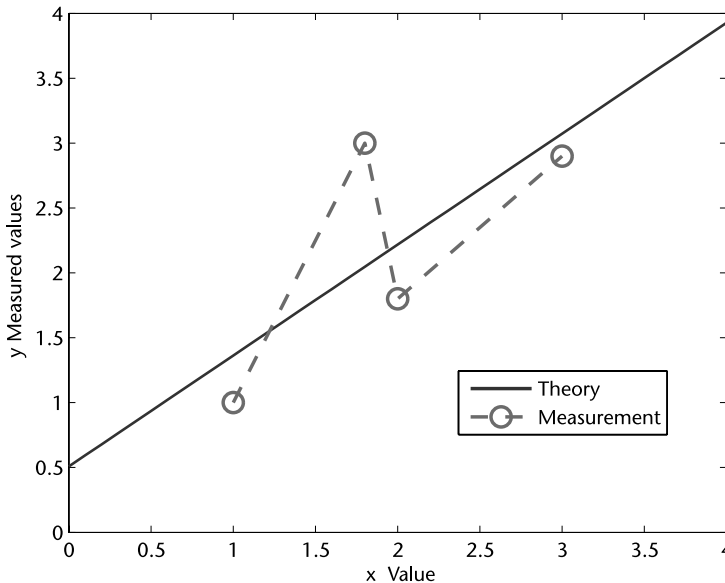


Figure 11.3 Scatter diagram for measured values and a linear model assumption.

$$\nabla SS = \begin{bmatrix} \frac{\partial SS}{\partial a_1} \\ \frac{\partial SS}{\partial a_0} \end{bmatrix} = \begin{bmatrix} 0 \\ 0 \end{bmatrix} \quad (11.5)$$

$$\begin{bmatrix} \frac{\partial SS}{\partial a_1} \\ \frac{\partial SS}{\partial a_0} \end{bmatrix} = \begin{bmatrix} 2 \sum_{k=1}^m (y_k^{\text{meas}} - a_1 x_k - a_0)(-x_k) \\ 2 \sum_{k=1}^m (y_k^{\text{meas}} - a_1 x_k - a_0)(-1) \end{bmatrix} \quad (11.6)$$

Expressions in (11.6) can be arranged. To illustrate this concept, let us consider that four different measurements are available; when transpose matrix properties are applied we get (11.10) as the least squares solution.

$$\left[(y_1^{\text{meas}} - a_1 x_1 - a_0)(y_2^{\text{meas}} - a_1 x_2 - a_0)(y_3^{\text{meas}} - a_1 x_3 - a_0)(y_4^{\text{meas}} - a_1 x_4 - a_0) \right] \begin{bmatrix} x_1 & 1 \\ x_2 & 1 \\ x_3 & 1 \\ x_4 & 1 \end{bmatrix} = \begin{bmatrix} 0 & 0 \end{bmatrix} \quad (11.7)$$

$$\left[\begin{array}{cccc} x_1 & x_2 & x_3 & x_4 \\ 1 & 1 & 1 & 1 \end{array} \right] \left\{ \begin{array}{l} \left[\begin{array}{l} y_1^{\text{meas}} \\ y_2^{\text{meas}} \\ y_3^{\text{meas}} \\ y_4^{\text{meas}} \end{array} \right] - \left[\begin{array}{l} x_1 & 1 \\ x_2 & 1 \\ x_3 & 1 \\ x_4 & 1 \end{array} \right] \left[\begin{array}{l} a_1 \\ a_0 \end{array} \right] \end{array} \right\} = \begin{bmatrix} 0 \\ 0 \end{bmatrix} \quad (11.8)$$

$$A^t A \begin{bmatrix} a_1 \\ a_0 \end{bmatrix} = A^t y^{\text{meas}} \quad (11.9)$$

$$\begin{bmatrix} a_1 \\ a_0 \end{bmatrix} = (A^t A)^{-1} A^t y^{\text{meas}} \quad (11.10)$$

A matrix whose elements are determined by the selected model; in our case, a linear form.

$$y_k^{\text{meas}} - y_k^{\text{theory}} = y_k^{\text{meas}} - a_1 x_k - a_0 = y_k^{\text{meas}} - \begin{bmatrix} x_k & 1 \end{bmatrix} \begin{bmatrix} a_1 \\ a_0 \end{bmatrix} \quad (11.11)$$

Table 11.1 Data Measurements for Example 11.1

x_i	y_i
1.0	1.0
1.8	3.0
2.0	1.8
3.0	2.9

Example 11.1

Assume a set of measured y 's and the corresponding x values. Form the A matrix and $A_1 = (A^t A)^{-1}$ that is the covariance matrix.

$$\begin{aligned}
 A &= \begin{matrix} 1.0000 & 1.0000 \\ 1.8000 & 1.0000 \\ 2.0000 & 1.0000 \\ 3.0000 & 1.0000 \end{matrix} \\
 A_1 &= \begin{matrix} 0.4926 & -0.9606 \\ -0.9606 & 2.1232 \end{matrix} \\
 x_{sol} &= \begin{matrix} 0.8547 \\ 0.5084 \end{matrix}
 \end{aligned}$$

The linear model whose parameters were obtained by solving the least squares criteria and the set of errors or residuals are shown. The mean residual value and its variance are calculated for $y = a_1 x + a_0 = 0.8547x + 0.5084$.

$$\begin{aligned}
 \text{epsilon (residuals)} &= \begin{matrix} -0.3631 \\ 0.9532 \\ -0.4177 \\ -0.1724 \end{matrix} \\
 \text{e-mean} &= 8.3267\text{e-}016 \\
 \text{e-var} &= 0.4149
 \end{aligned}$$

11.2.1 Power System's Linear State Estimation

To directly apply the linear model presented by (11.10), we can use an all-real power network. The procedure requires a given network structure where topology is already determined (i.e., no network topology analysis is conducted); network topology would require breaker status information. As a first step, we solve an ideal condition assuming no errors in the information and we get a base case solution. For the second step, we identify the linear model when line power flows are the available measured quantities and the information set is redundant; there are more measurements than parameters to be estimated. The third step includes measurements of

real power injections, which might be the case when load information or power generation is available.

Example 11.2

Let us apply the *least squares* criteria to find an estimate of the state for a real power-only network. First, let us solve the base case using a power flow solution, and then we use line real power flow measurements that include errors (see Figure 11.4). Finally, we will consider expanding the initial set of line measurements to include nodal power injections coming from generators or loads as shown in Figure 11.5.

Use the power flow equation for each element (11.12) and the nodal power balance for all the nodes, considering the net power injection as the difference generated power minus load required: $P_{GK} - P_{LK}$.

$$-x_{km} p_{km} + \theta_k - \theta_m = 0 \quad (11.12)$$

For the base case as a load flow solution, it requires lines/transformers connectivity, reactance values, and nodal power conditions. For this case, voltage magnitude is assumed 1.0 pu for all nodes, and the state variables are the nodal voltage angles.

Real power flows, base case			
Line data	Nsal	Nlleg	x(pu)
1	1	2	0.1000
2	2	3	0.2000
3	5	3	0.1000
4	4	5	0.1500
5	4	1	0.1500

Initial Nodal conditions			
Node	angle	PG(pu)	PL(pu)
1	0.0000	0.0000	0.5000
2	0.0000	1.5000	0.0000
3	0.0000	0.0000	1.0000
4	0.0000	0.0000	0.8000
5	0.0000	0.0000	0.0000

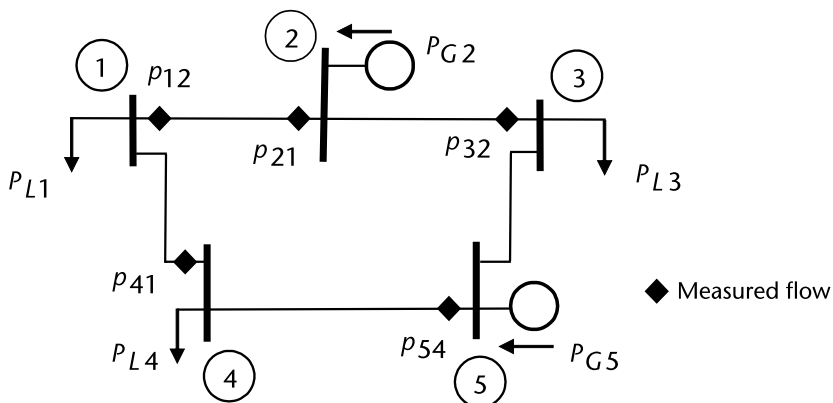


Figure 11.4 Small real power network, flow measurements shown.

Line flows solution, Base case

Line	Nsal	Nlleg	flow(pu)
1	1	2	-0.8857
2	2	3	+0.6143
3	5	3	+0.3857
4	4	5	-0.4143
5	4	1	-0.3857

Nodal solution, Base case

Node	angle(deg)	PG(pu)	PL(pu)
1	-0.2456	0.0000	0.5000
2	+4.8292	1.5000	0.0000
3	-2.2100	0.0000	1.0000
4	-3.5605	0.0000	0.8000
5	-0.0000	0.8000	0.0000

Now, we write the set of measurements flows shown in Figure 11.4 in terms of unknown nodal angles for each real power flow measured as follows:

$$\begin{bmatrix}
 -x_{12}p_{12} + \theta_1 - \theta_2 = 0 \\
 -x_{21}p_{21} + \theta_2 - \theta_1 = 0 \\
 -x_{41}p_{41} + \theta_4 - \theta_1 = 0 \\
 -x_{54}p_{54} + \theta_5 - \theta_4 = 0 \\
 -x_{32}p_{32} + \theta_3 - \theta_2 = 0
 \end{bmatrix} \tag{11.13}$$

In matrix form, the information allows to us to visualize the *A* matrix, which we call the *measurement matrix* as in (11.10). In compact matrix notation, (11.16) shows the information and matrix operations to find matrix *A*.

$$\begin{bmatrix}
 -x_{12} & 0 & 0 & 0 & 0 \\
 0 & -x_{21} & 0 & 0 & 0 \\
 0 & 0 & -x_{41} & 0 & 0 \\
 0 & 0 & 0 & -x_{54} & 0 \\
 0 & 0 & 0 & 0 & -x_{32}
 \end{bmatrix}
 \begin{bmatrix}
 p_{12} \\
 p_{21} \\
 p_{41} \\
 p_{54} \\
 p_{32}
 \end{bmatrix}^{\text{meas}}
 +
 \begin{bmatrix}
 +1 & -1 & 0 & 0 & 0 \\
 -1 & +1 & 0 & 0 & 0 \\
 -1 & 0 & 0 & +1 & 0 \\
 0 & 0 & 0 & -1 & +1 \\
 0 & -1 & +1 & 0 & 0
 \end{bmatrix}
 \begin{bmatrix}
 \theta_1 \\
 \theta_2 \\
 \theta_3 \\
 \theta_4 \\
 \theta_5
 \end{bmatrix}
 =
 \begin{bmatrix}
 0 \\
 0 \\
 0 \\
 0 \\
 0
 \end{bmatrix} \tag{11.14}$$

$$-[X]p^{\text{meas}} + [M][\theta] = [0] \tag{11.15}$$

$$p^{\text{meas}} = [X]^{-1}[M][\theta] = [A][\theta] \tag{11.16}$$

- [X] Diagonal matrix of elements reactance values, according to power flow measurement
- [M] Matrix with node connectivity information of the measured element
- p^{meas} Set of measured line power flows

- A Matrix for the set of measurements in terms of state variables
 θ State variables for the electrical circuit

$$[A] = [X]^{-1}[M] \quad (11.17)$$

The solution by least squares is reached once a reference angle is assigned for the *slack bus*.

$$[\theta] = (A^t A)^{-1} A^t p^{\text{meas}} \quad (11.18)$$

With the estimated values for nodal angles θ , the residuals ε are calculated.

$$\varepsilon = p^{\text{meas}} - [A][\theta] = p^{\text{meas}} - p^{\text{calc}} \quad (11.19)$$

Real power flows, measurements

Line data	Ns1	Nlleg	x(pu)	pmeasured
1	1	2	0.1000	-0.9000
2	2	1	0.1000	+0.8500
3	4	1	0.1500	-0.4000
4	5	4	0.1500	+0.4000
5	3	2	0.2000	-0.6100

Nodal angle estimation, slack is node 5

Node	angle(deg)
1	+0.0000
2	+5.0134
3	-1.9767
4	-3.4377
5	+0.0000

Estimation of network Line flows

Line	Ns1	Nlleg	estimated flow
1	1	2	-0.8750
2	2	3	+0.6100
3	5	3	+0.3450
4	4	5	-0.4000
5	4	1	-0.4000

Nodal net power estimation, slack is node 5

Node	Pnet(pu)
1	-0.4750
2	+1.4850
3	-0.9550
4	-0.8000
5	+0.7450

Flows calculation and residuals

Line	Ns1	Nlleg	pmeasured	pcalc	residuals
1	1	2	-0.9000	-0.8750	-0.0250
2	2	1	+0.8500	+0.8750	-0.0250

3	4	1	-0.4000	-0.4000	-0.0000
4	5	4	+0.4000	+0.4000	+0.0000
5	3	2	-0.6100	-0.6100	+0.0000

Matrix A in (11.17) must include equations that relate every available measurement to the state variables. Now let us extend the basic model considering that, in Figure 11.4, some nodal power injections are measured; this is depicted in Figure 11.5. The measured nodal powers must also be expressed in terms of the state variables of our problem (i.e., nodal angles). To relate nodal power measurements and state variables, we use elements from the nodal susceptance matrix to be multiplied by the state variables. The original A matrix in (11.14) will be expanded to include information about the nodal measurements. From Figure 11.5, the nodal measured power P is expressed as:

$$\begin{bmatrix} -P_{L1} \\ -P_{L3} \\ -P_{L4} \end{bmatrix} = \begin{bmatrix} B_{11}\theta_1 + B_{12}\theta_2 + B_{14}\theta_4 \\ B_{32}\theta_2 + B_{33}\theta_3 + B_{35}\theta_5 \\ B_{41}\theta_1 + B_{44}\theta_4 + B_{45}\theta_5 \end{bmatrix} \tag{11.20}$$

$$\begin{bmatrix} -P_{L1} \\ -P_{L3} \\ -P_{L4} \end{bmatrix} = \begin{bmatrix} B_{11} & B_{12} & 0 & B_{14} & 0 \\ 0 & B_{32} & B_{33} & 0 & B_{35} \\ B_{41} & 0 & 0 & B_{44} & B_{45} \end{bmatrix} \begin{bmatrix} \theta_1 \\ \theta_2 \\ \theta_3 \\ \theta_4 \\ \theta_5 \end{bmatrix} \tag{11.21}$$

$$\begin{bmatrix} p^{\text{meas}} \\ p^{\text{meas}} \end{bmatrix} = \begin{bmatrix} A \\ B \end{bmatrix} [\theta] = [A_{\text{mod}}][\theta] \tag{11.22}$$

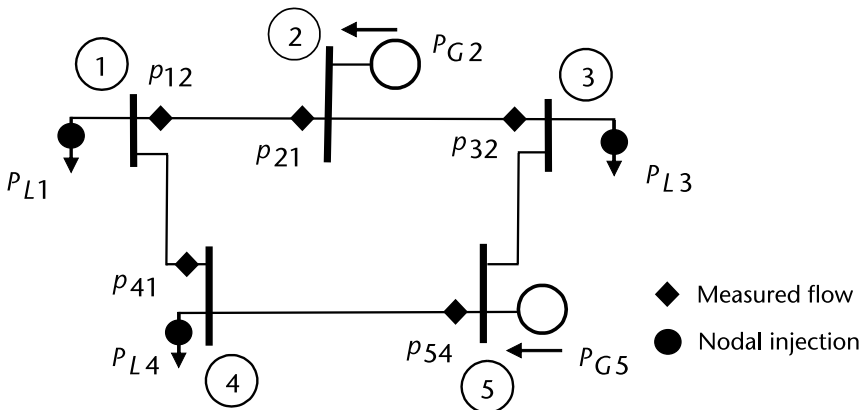


Figure 11.5 Small real power-only network, line flows, and nodal measurements are shown.

Submatrix B in (11.22) is a part of the nodal susceptance matrix for the network, and it is that portion that relates net measured nodal power to nodal angles. The submatrix B is appended to the initial A matrix to form the new *measurement matrix* A_{mod} . The least squares solution is used now to solve for the state variables.

$$[\theta] = (A_{\text{mod}}^t A_{\text{mod}})^{-1} A_{\text{mod}}^t \begin{bmatrix} p^{\text{meas}} \\ P_{\text{meas}} \end{bmatrix} \quad (11.23)$$

Net nodal power measurements

Node	Pnet_measured
1	-0.4800
3	-1.0800
4	-0.7900

Nodal angle estimation, slack is node 5

Node	angle(deg)
1	-0.1930
2	+4.7868
3	-2.4971
4	-3.5102
5	-0.0000

Estimation of network Line flows

Line	Nsal	Nlleg	estimated flow
1	1	2	-0.8691
2	2	3	+0.6356
3	5	3	+0.4358
4	4	5	-0.4084
5	4	1	-0.3860

Nodal net power estimation, slack is node 5

Node	Pnet(pu)
1	-0.4832
2	+1.5048
3	-1.0715
4	-0.7944
5	+0.8442

Flows estimation and residuals

Line	Nsal	Nlleg	pmeasured	pcalc	residuals
1	1	2	-0.9000	-0.8691	-0.0309
2	2	1	+0.8500	+0.8691	-0.0191
3	4	1	-0.4000	-0.3860	-0.0140
4	5	4	+0.4000	+0.4084	-0.0084
5	3	2	-0.6100	-0.6356	+0.0256

Nodal power estimation and residuals

Node	Pmeasured	Pcalculated	residuals
1	-0.4800	-0.4832	+0.0032
3	-1.0800	-1.0715	-0.0085
4	-0.7900	-0.7944	+0.0044

11.3 Maximum Likelihood and Weighted Least Squares

To approach the idea of parameter estimation using a set of measurements that are taken from various devices with different quality and performance in their output, let us assume that a random variable x with a Normal probability density function (11.1) has two samples x_1 and x_2 .

$$\text{PDF}(x_1) = \frac{1}{\sigma_1\sqrt{2\pi}} e^{-\frac{(x_1-\mu)^2}{2\sigma_1^2}} \quad (11.24)$$

$$\text{PDF}(x_2) = \frac{1}{\sigma_2\sqrt{2\pi}} e^{-\frac{(x_2-\mu)^2}{2\sigma_2^2}} \quad (11.25)$$

The estimation of μ will be a value that maximizes the probability of getting the sample values x_1 and x_2 . The joint probability density is:

$$\xi = \text{PDF}(x_1)\text{PDF}(x_2) = \frac{1}{\sigma_1\sqrt{2\pi}} e^{-\frac{(x_1-\mu)^2}{2\sigma_1^2}} \frac{1}{\sigma_2\sqrt{2\pi}} e^{-\frac{(x_2-\mu)^2}{2\sigma_2^2}} \quad (11.26)$$

$$\xi = \frac{1}{\sigma_1\sigma_2(\sqrt{2\pi})^2} e^{-\frac{(x_1-\mu)^2}{2\sigma_1^2} - \frac{(x_2-\mu)^2}{2\sigma_2^2}} \quad (11.27)$$

To maximize the function ξ , it is convenient to transform the exponential (11.27), and then find the solution for the gradient equal to zero.

$$\text{Ln}\xi(\mu) = -\text{Ln}\sigma_1\sigma_2(\sqrt{2\pi})^2 - \frac{(x_1-\mu)^2}{2\sigma_1^2} - \frac{(x_2-\mu)^2}{2\sigma_2^2} \quad (11.28)$$

$$\frac{d}{d\mu}(\text{Ln}\xi) = \frac{(x_1-\mu)}{\sigma_1^2} - \frac{(x_2-\mu)}{\sigma_2^2} = 0 \quad (11.29)$$

$$\left(\frac{1}{\sigma_1^2} + \frac{1}{\sigma_2^2}\right)\mu = \frac{x_1}{\sigma_1^2} + \frac{x_2}{\sigma_2^2} \quad (11.30)$$

In matrix form, (11.30) can be written in general terms for A , the *observation matrix* and a *weight matrix* R . This interpretation will be very useful in cases where more measurements are available.

$$\begin{bmatrix} 1 & 1 \end{bmatrix} \begin{bmatrix} \frac{1}{\sigma_1^2} & 0 \\ 0 & \frac{1}{\sigma_2^2} \end{bmatrix} \begin{bmatrix} 1 \\ 1 \end{bmatrix} \mu = \begin{bmatrix} 1 & 1 \end{bmatrix} \begin{bmatrix} \frac{1}{\sigma_1^2} & 0 \\ 0 & \frac{1}{\sigma_2^2} \end{bmatrix} \begin{bmatrix} x_1 \\ x_2 \end{bmatrix} \quad (11.31)$$

$$A = \begin{bmatrix} 1 \\ 1 \end{bmatrix} \quad R = \begin{bmatrix} \frac{1}{\sigma_1^2} & 0 \\ 0 & \frac{1}{\sigma_2^2} \end{bmatrix} \quad (11.32)$$

It is readily recognized that (11.31) has the general form of *minimum weighted squares* with the solution as (11.34). This result can be generalized in order to solve the state estimation problem for power networks that have measuring devices of various qualities and whose individual measurement variances σ_k^2 are known.

$$A^t R A \mu = A^t R x^{\text{meas}} \quad (11.33)$$

$$\mu = (A^t R A)^{-1} A^t R x^{\text{meas}} \quad (11.34)$$

Example 11.3

A simple case (see Figure 11.6) will illustrate the derivation of the A , measurement matrix and of the weight matrix R , when various measuring devices of different quality are used. Assume that three power-measuring devices are used with its variance values as listed.

Three measurements for the real power flow p_{12} are:

$$\begin{bmatrix} p_{12}^{m,1} = 1.95 & \sigma_1^2 = 1.5 \\ p_{12}^{m,2} = 2.01 & \sigma_2^2 = 0.5 \\ p_{12}^{m,3} = 1.92 & \sigma_3^2 = 0.8 \end{bmatrix} \quad (11.35)$$

The model for power flow measurement in terms of state variables and then matrices A and R can be deduced.

$$x_{12} p_{12}^{m,k} = \theta_1 - \theta_2 \quad (11.36)$$

$$\begin{bmatrix} x_{12} & 0 & 0 \\ 0 & x_{12} & 0 \\ 0 & 0 & x_{12} \end{bmatrix} \begin{bmatrix} p_{12}^{m,1} \\ p_{12}^{m,2} \\ p_{12}^{m,3} \end{bmatrix} = \begin{bmatrix} 1 & -1 \\ 1 & -1 \\ 1 & -1 \end{bmatrix} \begin{bmatrix} \theta_1 \\ \theta_2 \end{bmatrix} \quad (11.37)$$

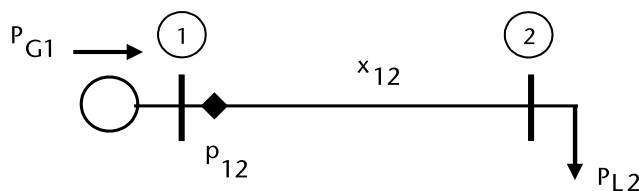


Figure 11.6 Flow measurements with different quality devices.

$$\begin{bmatrix} p_{12}^{m,1} \\ p_{12}^{m,2} \\ p_{12}^{m,3} \end{bmatrix} = \begin{bmatrix} x_{12} & 0 & 0 \\ 0 & x_{12} & 0 \\ 0 & 0 & x_{12} \end{bmatrix}^{-1} \begin{bmatrix} 1 & -1 \\ 1 & -1 \\ 1 & -1 \end{bmatrix} \begin{bmatrix} \theta_1 \\ \theta_2 \end{bmatrix} \quad (11.38)$$

$$A = \begin{bmatrix} x_{12} & 0 & 0 \\ 0 & x_{12} & 0 \\ 0 & 0 & x_{12} \end{bmatrix}^{-1} \begin{bmatrix} 1 & -1 \\ 1 & -1 \\ 1 & -1 \end{bmatrix} \quad R = \begin{bmatrix} \frac{1}{\sigma_1^2} & 0 & 0 \\ 0 & \frac{1}{\sigma_2^2} & 0 \\ 0 & 0 & \frac{1}{\sigma_3^2} \end{bmatrix} \quad (11.39)$$

The state estimation procedure to find θ_1 and θ_2 (one nodal angle is reference) using (11.34):

$$A^t R A \begin{bmatrix} \theta_1 \\ \theta_2 \end{bmatrix} = A^t R \begin{bmatrix} p_{12}^{m,1} \\ p_{12}^{m,2} \\ p_{12}^{m,3} \end{bmatrix} \quad (11.40)$$

```

Real power flows, base case
Line data  Nsal  Nlleg  x(pu)
  1         1     2     0.1000
Initial Nodal conditions
Node      angle  PG(pu)  PL(pu)
  1       0.0000  0.0000  0.0000
  2       0.0000  0.0000  2.0000
Line flows solution, Base case
Line      Nsal  Nlleg  flow(pu)
  1         1     2     +2.0000
Nodal solution, Base case
Node      angle(deg)  PG(pu)  PL(pu)
  1      -0.0000    2.0000  0.0000
  2     -11.4592    0.0000  2.0000
Real power flows, measurements
Line data  Nsal  Nlleg  x(pu)  pmeasured  sigma^2
  1         1     2     0.1000  +1.9500    +0.0010
  2         1     2     0.1000  +2.0100    +0.0010
  3         1     2     0.1000  +1.9200    +0.0010
Nodal angle estimation, slack is node  1
Node      angle(deg)
  1       +0.0000
  2      -11.2300

```

Estimation of network Line flows

Line	Nsal	Nlleg	estimated flow
1	1	2	+1.9600

Nodal net power estimation, slack is node 1

Node	Pnet(pu)
1	+1.9600
2	-1.9600

Flows calculation and residuals

Line	Nsal	Nlleg	pmeasured	pestim	residuals
1	1	2	+1.9500	+1.9600	-0.0100
2	1	2	+2.0100	+1.9600	+0.0500
3	1	2	+1.9200	+1.9600	-0.0400

11.3.1 Bad Data Detection

Residues are the result of the difference between measured quantities and the calculated value for the same quantity once the state variables are estimated. We have stressed the need of redundancy, which is the concept of having more measurements than the number of state variables to be determined. This concept makes statistical sense when the question of *bad data* needs to be addressed and resolved. We will briefly present the statistical properties that help us to identify, through a hypothesis test, whether a measurement or a set of measurements must be rejected because of reasonable doubt about belonging to the statistical process and should therefore be considered as *bad measurements*.

For a DC type of network with n total nodes, p power line flows, n nodal voltages, and n nodal power injections, the maximum possible redundancy will be the index obtained from the ratio of available measurements to the number of state variables; in this case, n nodal voltages are the state variables.

$$\text{Redundancy}_{\text{DC}} = \frac{2p + V_n + P_n^{\text{net}}}{n - 1} \quad (11.41)$$

- p Number of power line flows, from node k to node m
- V_n Number of node voltage magnitudes, n nodes
- P_n^{net} Net power injected at n nodes
- n Total nodes in the network

For AC networks, the state estimation has several measurements that might include: real and reactive power flow in transmission elements (sending and receiving end), real and reactive power injections into a node, and nodal voltage magnitudes. Consider a network with np real power flow, nq reactive power flows, n nodes (including voltage magnitude, net real power, and net reactive power) and then the total number of measurements that might be available with respect to the number of nodal voltages and angles as state variables, where one nodal angle is a reference:

$$\text{Redundancy}_{AC} = \frac{2np + 2nq + 3n}{2n - 1} \quad (11.42)$$

The redundancy index is an indication of how the number of measurements relate to the number of state variables, but does not address the problem of *observability* on the network; observability is a property of being able to determine all state variables from the set of redundant measurements, which requires them to be set strategically given the network topology. A close problem to the observability question is how to appropriately locate meters throughout the network and deploy them in such a way that no portions of the network are left out (unobservable) at the estimation process.

In general, the residue ε_k is normalized with respect to the standard deviation, as in (11.43). The difference between the measured quantity and the predicted value by the theoretical model is divided by the standard deviation of the meter; this quantity is tied to the meter's quality.

$$\varepsilon_k = \frac{y_k^{\text{meas}} - y_k^{\text{th}}}{\sigma_k} \quad (11.43)$$

Assuming that most variables y_k are to be measured from the power system and follow a Normal probability distribution, the summation of squared normalized errors follows a Chi-square χ_{df}^2 probability distribution that is characterized by its degrees of freedom df (see Figure 11.7).

$$f(x) = K_{df} x^{(df-2)/2} e^{-x/2} \quad (11.44)$$

$$K_{df} = \frac{1}{2^{df/2}} \Gamma\left(\frac{df}{2}\right) \quad (11.45)$$

Where

K_{df} Constant that depends on the degrees of freedom, df

$\Gamma(df/2)$ Gamma function

To identify which measurements have gross errors, the χ_{df}^2 Chi-square distribution provides the basis for a hypothesis test. Recognizing that the area under the probability distribution is 1.0, we would like to find a value of $x(\alpha) = c$ such that the calculated value of $\chi_{df,\alpha}^2$ has a high probability to yield a reliable state estimation.

$$\chi_{df,\alpha}^2 \leq c \quad (11.46)$$

If the calculated value is less than c in (11.46), we can accept the hypothesis that all measurements are within the range of its reasonable variability and accept that the set of measurements is a *good batch*. We can then conclude that the data is useful for the estimation process. On the contrary, if the Chi-squared value calculated is larger

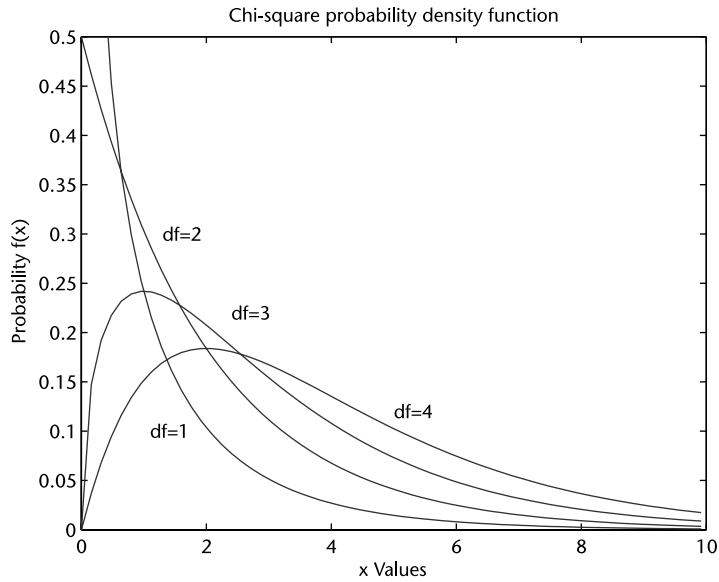


Figure 11.7 Chi-square probability distribution, χ^2_{df} with df degrees of freedom.

than c , then identification and discarding process for the high value of normalized residual should be conducted. In summary, the *bad data* identification steps are:

1. The measurement batch is used for the estimation process through a linear or a nonlinear model, depending on the relation for measured quantity and state variables.
2. Using the estimation results, normalized residuals are used in (11.47).

$$\chi^2_{df} = \sum_k \frac{(y_k^{\text{meas}} - y_k^{\text{tb}})^2}{\sigma_k^2} \quad (11.47)$$

3. A probability value of significance α is selected to conduct the hypothesis test, which is to accept or reject the set of measurements. Values for α of 0.95 or 0.99 are commonly used. From tables, such as the short Table 11.2 for illustrative purposes, depending on α and the degrees of freedom df , the c value in (11.46) is identified.
4. If the calculated value (11.47) is less than the value c from the Table 11.2, then the measurements are accepted as appropriate. If the calculated value

Table 11.2 Values for c in (11.46) Chi-square distribution with df (degrees of freedom) α .

Chi-square $\chi^2_{df,\alpha}$	$\alpha = 0.95$	$\alpha = 0.99$
$df = 3$	7.815	11.35
$df = 4$	9.49	13.28

(11.47) is larger than c , then some measurements are candidates to be rejected. When redundancy is high, discarding some *bad measurements* would pose no problem to the process. If the data to be discarded affects the redundancy index, then an average of observed values might replace the *bad data*; some other reasonable criteria can be used to replace the bad data.

When some data is discarded, a new estimation process is conducted using the reduced set of measurements. Next, the calculation of Chi-squared for Example 11.3 shows a Chi-squared = 4.2.

```
Flows calculation and residuals
Line      Nsal      Nlleg  pmeasured  pestim      residuals
  1         1         2    +1.9500    +1.9600    -0.0100
  2         1         2    +2.0100    +1.9600    +0.0500
  3         1         2    +1.9200    +1.9600    -0.0400
Chi2 = 4.2000
```

The calculated value is compared to the value in Table 11.2 with number of degrees of freedom $df = 2$ and $\alpha = 0.95$: $\chi^2_{3-1,0.95} = 5.99$. The calculated value of 4.2 suggests that the measurements are within reasonable error and no data needs to be discarded.

Example 11.4

Consider in Example 11.3 that one measurement fails to reflect a proper value. Consider that the second measurement is given as 1.0. Calculation for the Chi-squared value is 583.3, suggesting the existence of *bad data*.

```
Real power flows, measurements
Line data  Nsal      Nlleg  x(pu)      pmeasured  sigma^2
  1         1         2    0.1000    +1.9500    +0.0010
  2         1         2    0.1000    +1.0000    +0.0010
  3         1         2    0.1000    +1.9200    +0.0010

Nodal angle estimation, slack is node  1
Node   angle(deg)
  1     +0.0000
  2     -9.3010

Estimation of network Line flows
Line      Nsal      Nlleg  estimated flow
  1         1         2    +1.6233

Nodal net power estimation, slack is node  1
Node      Pnet(pu)
  1       +1.6233
  2       -1.6233

Flows calculation and residuals
Line      Nsal      Nlleg  pmeasured  pestim      residuals
  1         1         2    +1.9500    +1.6233    +0.3267
  2         1         2    +1.0000    +1.6233    -0.6233
  3         1         2    +1.9200    +1.6233    +0.2967
Chi2 = 583.2667
```

To identify suspicious data with high errors, we use the value of the normalized residual (11.43). The value of the second residual points into this measurement as a candidate to be analyzed.

Normalized residuals squared

1	+106.7111
2	+388.5444
3	+88.0111

11.4 Nonlinear Minimum Squares

When the measured variables, such as the real and reactive power flows in an electric network, are related by nonlinear relations to the state variables (i.e., for transmission elements from node k to node m), we recall that the real and the reactive power are:

$$p_{km} = |V_k|^2 g_{km} - |V_k||V_m| g_{km} \cos \theta_{km} - |V_k||V_m| b_{km} \sin \theta_{km} \quad (11.48)$$

$$q_{km} = -|V_k|^2 (b_{km} + B_{sb/2}) - |V_k||V_m| g_{km} \sin \theta_{km} + |V_k||V_m| b_{km} \cos \theta_{km} \quad (11.49)$$

Where

$V_k = V_k \angle \theta_k$	Nodal voltage for sending end, node k
$V_m = V_m \angle \theta_m$	Nodal voltage for receiving end, node m
$y_{km} = g_{km} - jb_{km}$	Series admittance for the transmission element
$B_{sb/2}$	Capacitive susceptance for the transmission element

If g_{km} and $B_{sb/2}$ are zero, the real and reactive power flow equations from node k to node m are simplified, but still remain nonlinear expressions in nodal voltage magnitudes and nodal angles, which are identified as state variables.

$$p_{km} = -|V_k||V_m| b_{km} \sin \theta_{km} \quad (11.50)$$

$$q_{km} = -|V_k|^2 b_{km} + |V_k||V_m| b_{km} \cos \theta_{km} \quad (11.51)$$

The residue ε_p for real power in a line is (11.52), where $p_{km} = f(|V_k|, |V_m|, \theta_k, \theta_m)$ is given by (11.50) and its incremental form as (11.53).

$$\varepsilon_p = p_{km}^{\text{meas}} - p_{km} \quad (11.52)$$

$$\Delta f = \frac{\partial f}{\partial \theta_k} \Delta \theta_k + \frac{\partial f}{\partial \theta_m} \Delta \theta_m + \frac{\partial f}{\partial |V_k|} |V_k| \frac{\Delta |V_k|}{|V_k|} + \frac{\partial f}{\partial |V_m|} |V_m| \frac{\Delta |V_m|}{|V_m|} \quad (11.53)$$

Partial derivatives in (11.53) were presented in Chapter 6, and they will be part of the linearized matrix A that is needed to solve the nonlinear AC least square estimation problem. The nonlinear estimation is conducted through an iterative process and starts with reasonable values for the state variables; an update is then obtained. In this process, we also calculate the new values for the partial derivatives. The calculated increments are used to update the values of the state variables.

Example 11.5

We solve a nonlinear state estimation case.

Parameter values and measurements are listed. They include power flows, nodal power injection, and nodal voltages. The information about the quality of each measured quantity goes into the R matrix. When the iterative process converges, a final result shows the state estimation and residuals with respect to the measured values. An index is calculated so that a test with the Chi-square distribution can be conducted. In this case, five measurements are proposed in order to estimate three state variables: two voltage magnitudes and one nodal angle.

General network information and load flow, base case

Number of elements = 1 Number of nodes = 2
 Element Nfrom Nto z bsh/2
 1 1 2 0.0100 +j 0.1000 0.0000

Shunt elements = 1

Element Node zshunt
 1 2 0.0000 +j 2.5000

Node data information

Node	type	Voltage	angle(rad)	PG	QG	PL	QL
1	0	1.0500	+0.0000	0.0000	0.0000	0.0000	0.0000
2	-1	1.0000	+0.0000	0.0000	0.0000	0.5000	0.2000

Load flow convergence

Iteration = 0 Dmax = 4.504950e-001
 Iteration = 1 Dmax = 1.057711e-002
 Iteration = 2 Dmax = 1.518130e-005
 Iteration = 3 Dmax = 3.037523e-011

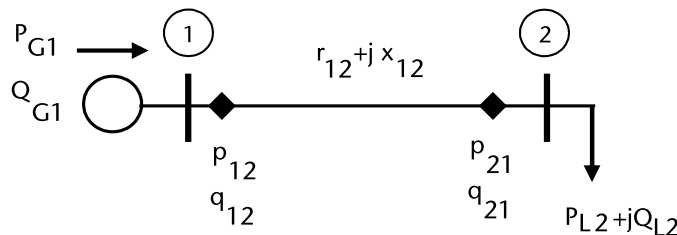


Figure 11.8 Power flows, nodal voltages, and nodal power measurements with devices of different quality.

Line	Nsal	Nlleg	pkm	qkm
1	1	2	+0.5061	+0.6490
1	2	1	-0.5000	-0.5875
Shunt	Nsal	pkm	qkm	
1	2	+0.0000	+0.3875	

Node	Voltage	angle(rad)	PG	QG	PL	QL
1	1.0500	-0.0000	+0.5061	+0.6490	+0.0000	+0.0000
2	0.9843	-2.4470	+0.0000	+0.0000	+0.5000	+0.2000

Power summary

SGtot = +0.5061 j +0.6490
 SLtot = +0.5000 j +0.2000
 SLoss = +0.0061 j +0.4490 (Q>0 required by reactive elements)

State Estimation Measurements from network variables

Number of line flows = 2

Element	Nfrom	Nto	z	bsh/2	meas	(1=p,0=q)	s^2
1	1	2	0.0100 +j	0.1000	0.5000	1	2.00e-003
2	1	2	0.0100 +j	0.1000	0.6000	0	4.00e-003

Nodal powers = 1

Injection	Node	meas	(1=P,0=Q)	s^2
1	2	-0.2100	0	1.00e-003

Nodal voltage = 2

Measur	Node	meas	s^2
1	1	1.0400	1.00e-003
2	2	0.9900	1.00e-003

Initial values for state variables

Node	Vmag	angle(rad)
1	1.0000	0.0000
2	1.0000	0.0000

Iteration = 1 Maxdesv = 4.738539e-002

Iteration = 2 Maxdesv = 4.430767e-003

Iteration = 3 Maxdesv = 7.984505e-006

Final values for state variables

Node	Vmag	angle(rad)	degrees
1	1.0437	-0.0000	-0.0000
2	0.9775	-0.0415	-2.3805

k	measurement	residue
1	+0.5000	+0.0021
2	+0.6000	-0.0414
3	-0.2100	-0.0120
4	+1.0400	-0.0037
5	+0.9900	+0.0116

Index for chi^2-test = 0.7239 degrees of freedom = 2

With results shown for the index Chi-square as 0.7239, 2 degrees of freedom and selecting α we should check if the measurements pass the hypothesis test of not having bad measurements.

11.5 Thévenin's Equivalent and Parameter Estimation

An interesting problem is related to parameter estimation. Let us pose a problem about the need of a Thévenin's equivalent as seen from a given network node. Assume that the voltage, current, and power are measured at node 2 in Figure 11.9.

To build the model, let us write the equation with voltages and power. From the model, we can deduce the measurement expression.

$$f(V_2) = V_2^2 - V_1 V_2 + r_{Th} P_2 = 0 \quad (11.54)$$

$$+E_{Th} V_2 - r_{Th} P_2 = V_2^2 \quad (11.55)$$

With paired values of measurements V_2 and P_2 (assumed to be simultaneous), we write the measurement equation in the form (11.3). A least squares solution will find the best estimates for E_{Th} and r_{Th} . The A matrix is identified in (11.56) as (11.58).

$$\begin{bmatrix} (V_2^{(1)})^2 \\ (V_2^{(2)})^2 \\ \vdots \\ (V_2^{(n)})^2 \end{bmatrix} = \begin{bmatrix} V_2^{(1)} & -P_2^{(1)} \\ V_2^{(2)} & -P_2^{(2)} \\ \vdots & \vdots \\ V_2^{(n)} & -P_2^{(n)} \end{bmatrix} \begin{bmatrix} E_{Th} \\ r_{Th} \end{bmatrix} + \begin{bmatrix} \varepsilon_1 \\ \varepsilon_2 \\ \vdots \\ \varepsilon_n \end{bmatrix} \quad (11.56)$$

$$\begin{bmatrix} E_{Th} \\ r_{Th} \end{bmatrix} = (A^t A)^{-1} A^t \left[(V_2^{\text{meas}})^2 \right] \quad (11.57)$$

$$A = \begin{bmatrix} V_2^{(1)} & -P_2^{(1)} \\ V_2^{(2)} & -P_2^{(2)} \\ \vdots & \vdots \\ V_2^{(n)} & -P_2^{(n)} \end{bmatrix} \quad (11.58)$$

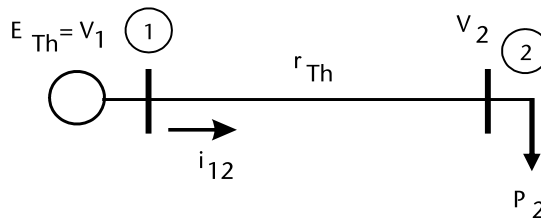


Figure 11.9 Simple network to estimate parameters in a network model.

Once the estimated values of Thévenin's equivalent are done, we estimate the maximum power that can be transferred by the line and ask what the *voltage collapse margin* is.

$$P_2^{\max} = \frac{E_{Th}^2}{4r_{Th}} \tag{11.59}$$

Example 11.6

Assume an equivalent network (as in Figure 11.9) whose voltage E_{Th} and equivalent resistance r_{Th} change due to network topology variations as $r_{Th} = 0.05, 0.10, 0.15$ and $E_{Th} = 1.0$. We collect various pairs of measurements at node 2 as voltage and power. With (11.57), the Thévenin's equivalent is estimated and then we find the margin to *voltage collapse*.

k	rTh	Pmax
1	0.0500	5.0000
2	0.1000	2.5000
3	0.1500	1.6667

With the use of four pairs of *measurements* available at a given time, find an estimate for components E_{Th} and r_{Th} of the Thévenin's equivalent. Calculate the limit for power transfer and the so-called *power margin* for each of the measured power values.

Data from measurements

k	Voltage	Power P
1	0.9762	0.4639
2	0.8545	2.4860
3	0.9259	1.3718
4	0.8122	3.0500

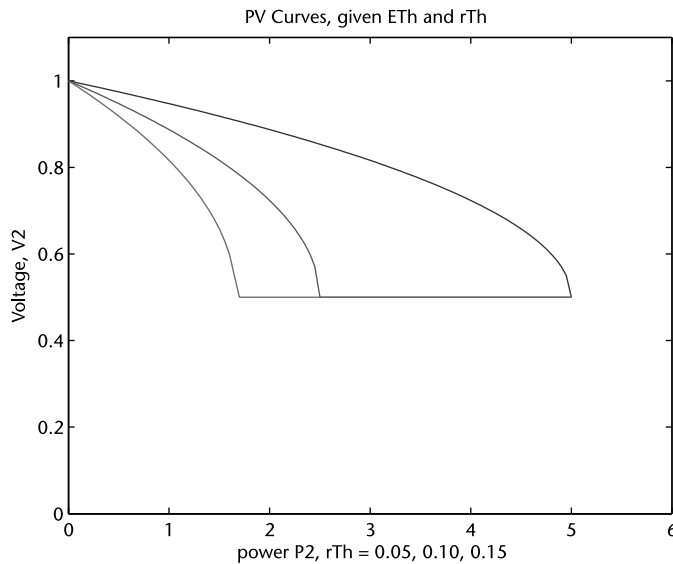


Figure 11.10 PV curves for circuit in Figure 11.9, $E_{Th} = 1.0$.

Estimation				
ETh =	1.0000	rTh =	0.0500	Pmax = 4.9996
k	Voltage	Power	Residual	Pmargin
1	0.9762	0.4639	-7.5322e-006	4.5357
2	0.8545	2.4860	-1.2247e-006	2.5136
3	0.9259	1.3718	+1.3160e-005	3.6278
4	0.8122	3.0500	-5.1933e-006	1.9496

The procedure to estimate the Thévenin equivalent continues as sets of new measurements arrive at the processing facility. To monitor the estimation process, it is advisable to implement a performance index so that changes in the equivalent can be detected. The changes can be the result of lines switching or power generators being in or out of service. These changes have a more pronounced effect in *weak systems*, where it is highly recommended to implement the scheme described as a *regular control function*. The procedure is quasistatic and assumes that the set of measurements belong to a homogeneous operating condition.

11.6 Phasor Estimation and Related Problems

An important and relevant application is the one related to rms phasor estimation (i.e., magnitude and angle of a phasor with respect to a reference). This application is sure to gain more attention as its use becomes more widespread in the electric system's monitoring and control. In a given bus of a three-phase balanced system, operating in steady state, a system's frequency might be considered constant at the nominal value of 60 Hz. Voltage measurement is done through power transformers where the high voltage value is reduced to a standard value of 69.9 V and the high current measurement is reduced to 5 A by a current transformer, using the appropriate transformer ratios. Analog signals are filtered in order to block high frequency signals and noise in general; ideally, the sampled values are from a pure 60 Hz sinusoidal signal except for a fault current condition where an aperiodic (DC) component might be present.

From the filtered 60 Hz signals for voltage and current, sampling is conducted at a convenient rate (i.e., twelve samples per cycle or a faster rate). With the sampled values v_k and i_k at time t_k , the magnitudes $|V_k|$, $|I_k|$, and angles θ_{kV} , θ_{kI} are estimated using the 12 samples available or a reduced *window* where three or more samples can be used. This depends on the properties that we want from the window of observation. Example 11.7 and Figure 11.10 show uniform sampling for an rms phasor, magnitude $120/\sqrt{3}$ V, and a phase angle of 45° .

Example 11.7

Uniform 12 sampled values (see Figure 11.11) for a voltage signal $v(t) = 97.98 \cos(2\pi ft + \pi/4)$ V.

Sample	time(s)	voltage(V)
Time samples of voltage, V		

1	0.000000	69.2820
2	0.001389	25.3590
3	0.002778	-25.3590
4	0.004167	-69.2820
5	0.005556	-94.6410
6	0.006944	-94.6410
7	0.008333	-69.2820
8	0.009722	-25.3590
9	0.011111	25.3590
10	0.012500	69.2820
11	0.013889	94.6410
12	0.015278	94.6410

The task of monitoring and evaluating of the electrical system's health can be organized with an adequate set of phasor measurement units (PMUs) at various electrical nodes. A complete wide-area measurement network can be designed using synchro phasors with adequate resolution and synchronized in time. This system's information will help monitor and closely control a modern power system in real time. The techniques used to estimate the actual value of phasors are related to the least square fitting applications, some take advantage of the Fourier's formulation or Kalman's filter recurrent calculations, especially as applied to sampling at appropriate rate. Ingenious and straightforward forms are also available. We do not delve into variations, just some examples to capture the flavor of the applications into the measurements with the aim of monitoring or for power system's protection, which is an interesting world in itself.

Example 11.8

Assume that a sampling point in a balanced three-phase network has a Thévenin equivalent and a three-phase fault is ensued along a transmission line (see Figure 11.12).

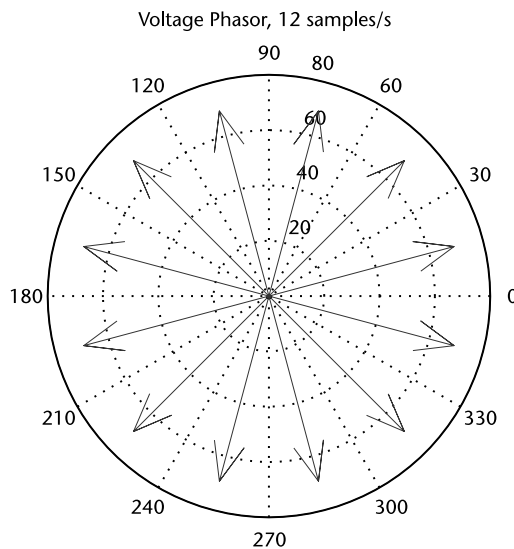


Figure 11.11 RMS phasor voltage, 12 samples per cycle. $V_{rms} = 69.28$ V, $\phi = 45^\circ$.

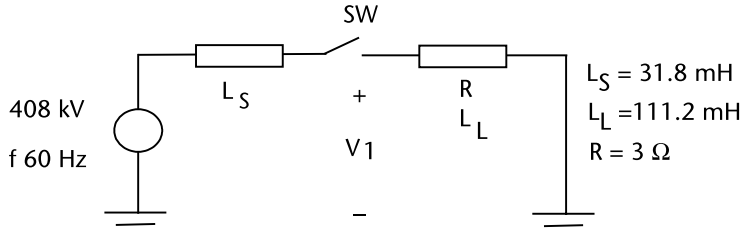


Figure 11.12 Three-phase balanced fault for an AC network equivalent.

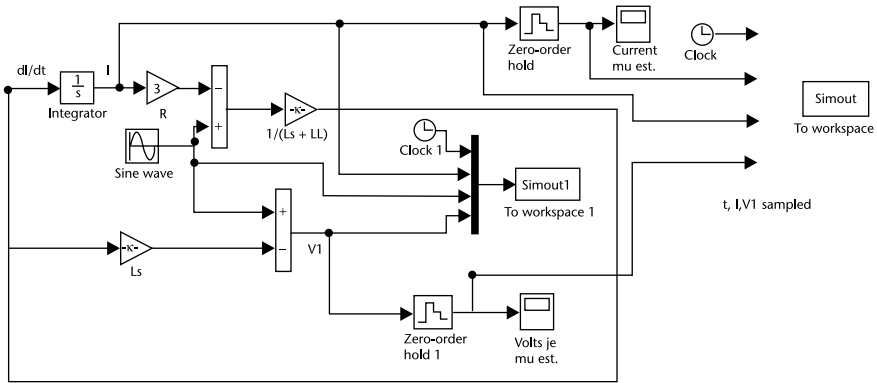


Figure 11.13 Simulink diagram for a three-phase fault. Source voltage V_1 at the switch SW and fault current. The sampling rate is twelve samples per cycle.

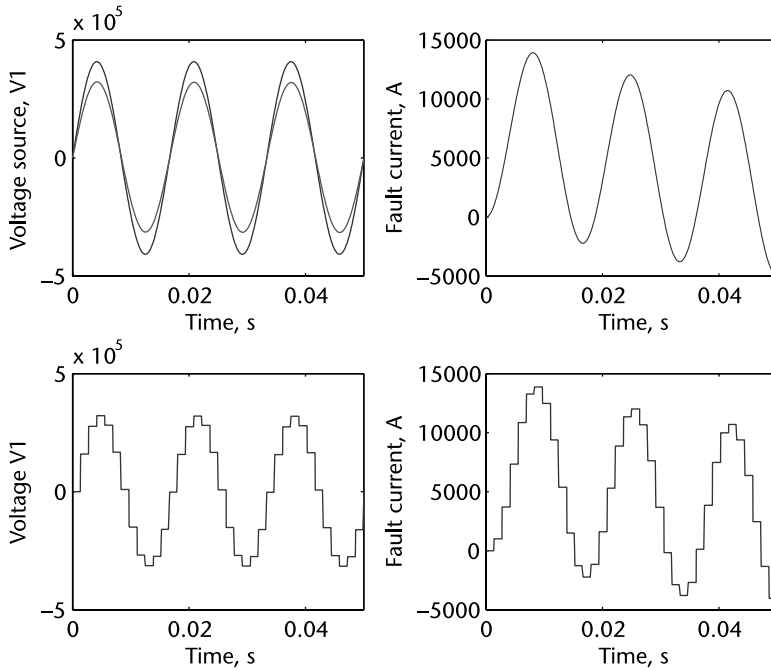


Figure 11.14 Voltage at source at V_1 , sampling of voltage at SW and fault current; twelve samples per cycle.

Consider that load current—previous to the fault condition—is negligible and simulate the fault by closing switch SW when the voltage source is crossing at zero.

The case in Example 11.8 shows an ideal situation without noise components; only the DC current offset is present, use is made of simulation by Figure 11.13 and results in Figure 11.14. To estimate the voltage phasor, let us use four samples according to one of many variations that can be used. With 12 samples/cycle $\Delta t = 1/(12f) = 1/720$ seconds, considering a constant frequency of 60 Hz. For a cosine voltage with angle ϕ_V , at every sample time t_k , (11.61) shows elements to form the *measurement matrix A* in order to apply the *squared minimum* estimation.

$$V(t) = V_m \cos(\omega t + \phi_V) \quad (11.60)$$

$$V_k = V_m (\cos(\omega t_k) \cos \phi_V - \sin(\omega t_k) \sin \phi_V) = \cos(\omega t_k) V_a - \sin(\omega t_k) V_b \quad (11.61)$$

With four samples, we estimate components V_a and V_b , and then the magnitude V_m and angle ϕ_V .

$$\begin{bmatrix} V_k \\ V_{k+1} \\ V_{k+2} \\ V_{k+3} \end{bmatrix} = \begin{bmatrix} \cos \omega t_k & -\sin \omega t_k \\ \cos \omega t_{k+1} & -\sin \omega t_{k+1} \\ \cos \omega t_{k+2} & -\sin \omega t_{k+2} \\ \cos \omega t_{k+3} & -\sin \omega t_{k+3} \end{bmatrix} \begin{bmatrix} V_a \\ V_b \end{bmatrix} + \begin{bmatrix} \varepsilon_k \\ \varepsilon_{k+1} \\ \varepsilon_{k+2} \\ \varepsilon_{k+3} \end{bmatrix} \quad (11.62)$$

$$V_a = V_m \cos \phi_V \quad V_b = V_m \sin \phi_V \quad (11.63)$$

$$V_m = \sqrt{V_a^2 + V_b^2} \quad \phi_V = \tan^{-1} \left(\frac{V_b}{V_a} \right) \quad (11.64)$$

The rms voltage phasor is estimated by:

$$V = \frac{V_m}{\sqrt{2}} \angle \phi_V \quad (11.65)$$

RMS Phasor estimation			
frequency	Samples/cycle	Sampling time(s)	Sampling (degrees)
60	12	1.3889e-003	30.00

Sample	Voltage, V
1	+0.0000e+000
2	+2.0400e+005
3	+3.5334e+005
4	+4.0800e+005
5	+3.5334e+005
6	+2.0400e+005

```

7      +2.3115e-010
8      -2.0400e+005
9      -3.5334e+005
10     -4.0800e+005
11     -3.5334e+005
12     -2.0400e+005
A matrix      measurements, V
1.000000     -0.000000     +0.0000e+000
0.866025     -0.500000     +2.0400e+005
0.500000     -0.866025     +3.5334e+005
0.000000     -1.000000     +4.0800e+005

Va = -1.4552e-011      Vb = -4.0800e+005
Vm = +4.0800e+005      Vrms = +2.8850e+005      angle = +90.00

```

Example 11.9

For Example 11.7, we notice that the fault current might have a DC or *asymmetrical component* (in this case, the rms phasor for the current might not be directly estimated). One possible solution is to first estimate R and L_L components for the circuit; this can be an opportunity to extend our minimum square estimation process.

First, let us write the differential equation that describes the voltage and current in the time domain. Then, by discrete integration using the trapezoidal rule from sample values for voltage and current at times t_k and t_{k+1} , we have a sampled form that can be used to estimate the unknowns R and L_L .

$$v_1(t) = Ri(t) + L_L \frac{di}{dt} \quad (11.66)$$

$$\int_{t_k}^{t_{k+1}} v_1(t) dt = R \int_{t_k}^{t_{k+1}} i(t) dt + L_L \int_{t_k}^{t_{k+1}} di \quad (11.67)$$

$$[v_1(t_k) + v_1(t_{k+1})] \frac{\Delta t}{2} = R[i(t_k) + i(t_{k+1})] \frac{\Delta t}{2} + L_L [i(t_{k+1}) - i(t_k)] \quad (11.68)$$

Using three samples, the model from (11.68) is:

$$\begin{bmatrix} [i(t_k) + i(t_{k+1})] \frac{\Delta t}{2} & [i(t_{k+1}) - i(t_k)] \\ [i(t_{k+1}) + i(t_{k+2})] \frac{\Delta t}{2} & [i(t_{k+2}) - i(t_{k+1})] \\ [i(t_{k+2}) + i(t_{k+3})] \frac{\Delta t}{2} & [i(t_{k+3}) - i(t_{k+2})] \end{bmatrix} \begin{bmatrix} R \\ L_L \end{bmatrix} = \begin{bmatrix} [v_1(t_k) + v_1(t_{k+1})] \frac{\Delta t}{2} \\ [v_1(t_{k+1}) + v_1(t_{k+2})] \frac{\Delta t}{2} \\ [v_1(t_{k+2}) + v_1(t_{k+3})] \frac{\Delta t}{2} \end{bmatrix} \quad (11.69)$$

```

R and LL estimation
Nsamples =          5

```

Samples	Current	Voltage
1	0.0000e+000	0.0000e+000
2	1.0041e+003	1.5930e+005
3	3.7088e+003	2.7724e+005
4	7.3328e+003	3.2216e+005
5	1.0850e+004	2.8200e+005
R =	3.0049 Ohms	LL = 0.1085 H

The estimated values for R and L_L compare well to the *true* values for the resistance of $R = 3$ ohms and inductance $L_L = 111.2$ H. With the estimated values, the nonperiodic component in the current can be removed and the rms phasor current estimated. In some applications, like in protective relaying, the parameter estimation for R and L_L will allow distance estimation to the fault location so that it can be situated within an expected distance with a tolerance; the tolerance is a result of various uncertainties imbedded within the measurements and the sampling. Errors in measurements come mainly from current transformers (CTs), the fault impedance and possible interference as noise.

11.6.1 Wide Area Measurements

Phasor estimation and its applications is a fertile and rapidly evolving field. It is aimed at closely monitoring the *quality* of electrical processes that a power system is experiencing and a set of indicators to evaluate what can be considered the system's *health*. Voltage and reactive power flows, frequency, power flows, oscillations, and damping characteristics are several of the main variables to monitor to ensure secure system's operation.

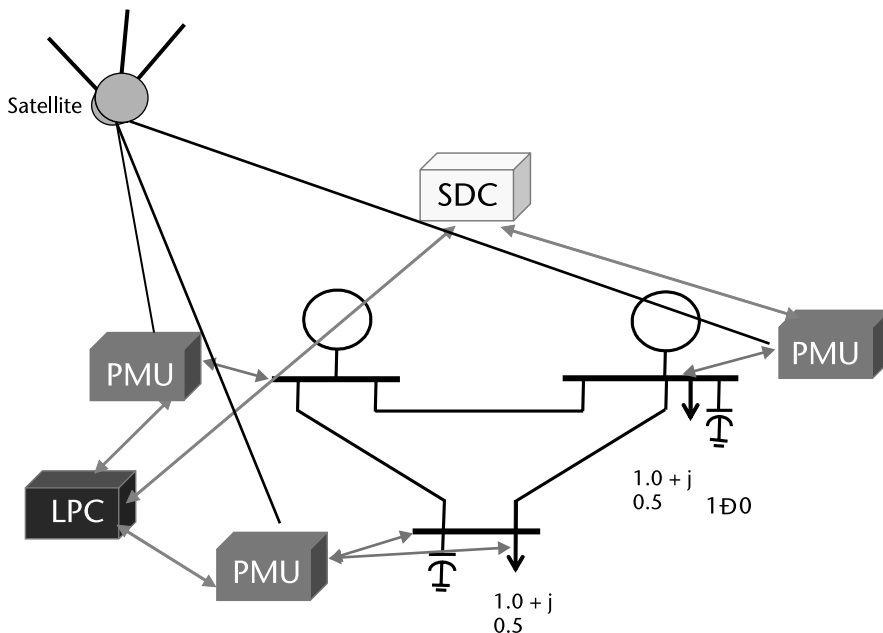


Figure 11.15 Wide area measurements, PMUs, LPCs, and SDCs.

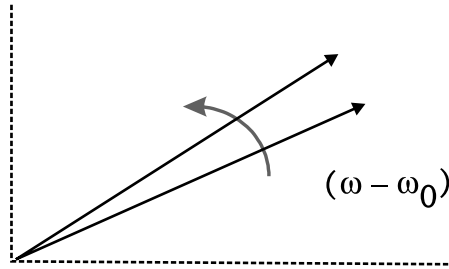


Figure 11.16 Phasor in a changing frequency condition.

Voltage magnitude monitoring and estimation of the *power margin* were just touched upon in this chapter; frequency deviation from the rated system's frequency is also a concern when phasor estimation is conducted. These problems can be tackled by what is now known as wide area measurement (WAM) (see Figure 11.15), which is a carefully designed system of data gathering by PMUs, local phasor concentrators (LPCs) that gather selected information from PMUs, and the system data concentrators (SDCs).

Applications for power system's security need to evaluate its performance under a frequency changing condition (see Figure 11.16). The question of how a change in frequency affects the phase of phasors or the calculation of symmetrical components must be included in the estimation process. Frequency measurement is also an issue, as well as the question of how unbalanced the system condition is. Transient phenomena related to electromechanical oscillations, the transient response of current and potential transformers, and the filter response when used for signal conditioning are some of the interesting concepts that are being studied right now for monitoring and control in electrical power systems.

11.7 Observability

One interesting problem is that of analyzing how much redundancy is needed for a good estimation process. This has technical and economic implications. We would like to have a good level of redundancy, observability at the best cost. A related issue is what set of values should be measured? What is a set that allows us to have *observability* over the state variables in the system? This situation is important in bad data detection and we must be able to discard measurements that statistically

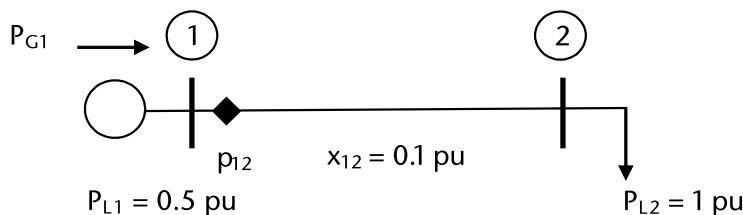


Figure 11.17 Flow measurement and measurement equation.

are unreliable or are suspected of not belonging to the set of measurements that allow the best estimation for the state condition of the power system.

Example 11.10

Let us follow what happens when we have just one measurement for power flow p_{12} and we like to estimate the state variable θ_2 (see Figure 11.17). The real power model is used and the A measurement matrix is written.

$$-p_{12}x_{12} + \theta_1 - \theta_2 = 0 \quad (11.70)$$

$$\begin{bmatrix} 1 & -1 \end{bmatrix} \begin{bmatrix} \theta_1 \\ \theta_2 \end{bmatrix} = [-x_{12}] [p_{12}] \quad A = \begin{bmatrix} 1 & -1 \end{bmatrix} \quad (11.71)$$

To solve for minimum squares:

$$\begin{bmatrix} \theta_1 \\ \theta_2 \end{bmatrix} = (A^t A)^{-1} A^t [-x_{12}] [p_{12}] \quad (11.72)$$

We can take a closer look into the matrix $A^t A$.

$$(A^t A) = \begin{bmatrix} +1 \\ -1 \end{bmatrix} \begin{bmatrix} +1 & -1 \end{bmatrix} = \begin{bmatrix} +1 & -1 \\ -1 & +1 \end{bmatrix} \quad (11.73)$$

In (11.73), we have a singular matrix that cannot be inverted, and we must solve for the state variables. We can say that the state variables cannot be estimated. If we take one node as reference, the process can continue, but with only one measurement to determine one state variable, results are adjusted to meet the measured value. We can appreciate that we really need more measurements to conduct a good estimation process.

Real power flows, base case

Line data	Nsal	Nlleg	x(pu)
1	1	2	0.1000

Initial Nodal conditions

Node	angle	PG(pu)	PL(pu)
1	0.0000	0.0000	0.5000
2	0.0000	0.0000	1.0000

Line flows solution, Base case

Line	Nsal	Nlleg	flow(pu)
1	1	2	+1.0000

Nodal solution, Base case

Node	angle(deg)	PG(pu)	PL(pu)
1	-0.0000	1.5000	0.5000
2	-5.7296	0.0000	1.0000

```

Real power flows, measurements
Line data   Nsal   Nlleg   x(pu)   pmeasured
   1         1       2       0.1000  +0.9500
ans =
   0.0000   0.0000
   0.0000   0.0100

Nodal angle estimation, slack is node   1
Node      angle(deg)
   1      +0.0000
   2      -5.4431

Estimation of network Line flows
Line      Nsal   Nlleg   estimated flow
   1         1       2       +0.9500

Nodal net power estimation, slack is node   1
Node      Pnet(pu)
   1      +0.9500
   2      -0.9500

Flows calculation and residuals
Line      Nsal   Nlleg   pmeasured   pestim   residuals
   1         1       2       +0.9500    +0.9500  +0.0000

```

References

- [1] Stevenson, W. D., *Elements of Power System Analysis, Second Edition*, New York: McGraw-Hill Book Company, 1962.
- [2] Stagg, G., and A. E. El-Abaid, *Computer Methods in Power System Analysis*, Tokyo, Japan: McGraw-Hill Book Company, 1968.
- [3] Elgerd, O. I., *Electric Energy Systems Theory: An Introduction, Second Edition*, New York: McGraw-Hill Book Company, 1982.
- [4] Wood, A. J., B. F. Wollenberg, and G. B. Sheble, *Power Generation, Operation and Control*, Hoboken, NJ: IEEE Wiley 2014.
- [5] Phadke, A. G., and J. S. Thorp, *Synchronized Phasor Measurements and their Applications*, New York: Springer, 2008

About the Author

Dr. Acha holds a Ph.D. in power systems from the University of Texas at Arlington. He spent a postdoctoral year at the Energy System Research Center, University of Texas at Arlington, and also holds an M.Sc. in power engineering from Seccion de Graduados ESIME-IPN, México City.

His main interests are modeling and analysis of AC-DC electric power systems, network planning, power system operation security and reliability, monitoring, and control in the context of wide area measurements and protection measures for large electrical power systems. He is a promoter of HVDC ties between countries and electric regions as a means to fully take advantage of energy exchanges for economic and system reliability reasons.

Dr. Acha has been involved for several years in specialized training for utility engineers in Mexico and Central and South America; he firmly believes in training to advance utility personnel into a deeper and wider understanding of the fundamental principles that govern the action of electrical power systems.

Dr. Acha has experience in power system operation and has worked at the National Control Center for a large utility in Mexico. He has been involved with various Mexican universities, directing and conducting applied research in the planning and operation of electric utilities. He taught undergraduate and graduate courses in the EE power curricula for several years and has published several research papers in the areas of interest.

Index

A

- ABCD* constants, 146–51
 - equivalent for series connection, 148
 - nodal admittance matrix from, 148–51
 - power flow calculations with, 151–54
 - series connection of two models, 148
 - shunt admittance and, 147
 - for two-port network, 147
- Admittance matrix
 - fault, 307, 311
 - nodal, 35, 53, 83, 200
 - shunt, 121
 - three-phase, 202
- Asymmetrical component, 370
- Autotransformer
 - connections, 88
 - defined, 85
 - equivalent for, 86, 87
 - equivalent values for, 88
 - single-phase, 86
 - See also* Transformer models
- Axial conductors, 102–5

B

- Backward substitution, 40
- Backward waves, 157, 158
- Bad data detection, 357–61
- Bad measurements, 357, 360
- Balanced complexors, 18
- Base case load flow, 321
- Best state estimation, 343
- Branches, 38
- Bundled conductors, 105–7, 136

C

- Cables
 - calculation of parameters, 122
 - cross section, 123
 - horizontal underground arrangement, 125

- one-phase armored, 127
- series impedance, 123–26
- series impedance matrix, 125–26
- shunt capacitance, 126–27
- spacing for neutral and phase conductor, 124
- tape shielded, 126
- three-phase, 127–32
- See also* Transmission lines
- Capacitance
 - Gauss' law and, 117–22
 - mutual, 129
 - phasor representation for, 11
 - shunt, 126–27
 - three-phase cables, 128
- Capacitance matrix, 120
- Capacitors
 - defined, 10
 - electric charge storage, 31
 - phasor model for, 10
 - voltage and current through, 9
 - voltage-current characteristics, 32
- Carson's equations, 112, 113, 114, 122
- Characteristic impedances
 - boundary conditions at point of connection, 160
 - configuration of elements and, 165
 - defined, 158
 - element transition point, 159
- Charges, potential at midpoint between, 119
- Chi-square probability distribution, 358, 359
- Circle diagrams
 - at receiving end, 152
 - at sending in, 154
 - use of, 153
- Circuits
 - AC, power and energy in, 6–11
 - AC, voltage and current in, 6
 - branches and links, 38

- Circuits (*Cont.*)
 DC, 4–6
 with lumped elements, 32–33
 magnetic, 318–20
 mathematical, 42
 number required to transport electric power, 139–40
 series *RLC*, 66
 Thévenin's equivalent, 42, 43
 work and energy in, 4–18
See also Equivalent circuits
- Clarke's transformation, 62
- Compensating current, 54
- Complex numbers, 23–25
- Complexors
 balanced, 18
 cosine time function, 6
 defined, 6
 rotating, 8
- Complex plane
 defined, 23
 illustrated, 24
- Complex power, 200
- Complex transformers
 with complex tap, 250
 ideal, 283
 incremental reactive power flow in, 179–80
 incremental real power flow in, 176–79
 for OLTC configuration, 293
 overview, xvi
 power flows in, 283
- Conductors
 axial, 102–5
 bundled, 105–7, 136
 four-strand, 133
 geometric distances of, 114
 parallel, 102, 104, 105, 107
 parallel, over ideal plane, 120
 parallel to ideal equipotential plane, 119
 retained, 136
 round, 101
 single, 100–102
 three-strand, 132
 transmission arrangement and geometry, 107
- Congestion
 minimum control effort and, 262
 problem, 262
- Constant flux linkages, 318
- Contingencies
 cause of, 322
 reactive power under, 335–40
 voltage under, 335–40
- Contingency analysis
 defined, 322
 general system incremental linear network, 323–27
 introduction to, 321–23
 participation factors, 340–42
 sensitivity matrix, 327–29
 single contingency model, 329–40
 summary, 342
- Control actions, 198–200
- Cost
 equal incremental solution, 212
 incremental, 214, 216, 218, 239
 marginal, 212
 real power marginal, 226
 short-term marginal, 208, 235
 thermal, 239
See also Minimum operating cost
- Cost criterion, 207
- Cost function
 establishing, 208
 in minimum control effort, 265
 optimal problem, 218
 surface and equality constraint, 210, 214
 surface illustration, 209
 value, 211
- Cramer's rule, 42
- Currents
 AC circuits, 6
 compensating, 54
 continuity of, 162, 163
 nodal, 21, 36
 three-phase unbalanced, 65
 through resistance, 8
 traveling, 160, 161
- D**
- DC circuits, 4–6
- DC current transmission element, 194
- DC load, 292
- DC network power flow solutions
 incremental power flow equations, 194–98
 overview, 193–94
- Decoupled optimal power flow solution, 229
- Decoupled power flow calculation, 193
- Decoupled sequence matrix, 117
- Decoupling
 defined, 59
 of state equations, 64–67

- $\Delta\Delta$ connection
 - current information, 76
 - illustrated, 75
 - partial inversion, 76
 - symmetrical components transformation, 76
 - three-phase bank, 74–77
- E**
- Earth return, 112–17
- Eigenvalue problem, 60
- Eigenvalues, 61
- Eigenvectors, 61
- Electrical length, 28
- Energy
 - in AC circuits, 6–11
 - average use per capita, 2
 - consumption, USA, 3
 - in electric circuits, 4–18
 - kinetic, 276–77
 - main sources of, 2
 - systems, 1–18
 - total, 275
 - by type of source, 3
 - work and, 273–82
- Equal incremental costs
 - penalty factor and, 218
 - solution, 211–12, 218
- Equality constraint
 - cost function surface and, 210, 214
 - hydrothermal coordination, 234–35
- Equivalent circuits
 - incremental reactive power flow, 188
 - incremental real power flow, 186–87, 251
 - long transmission lines, 144–46
 - outage admittance, 330
 - single-phase transformer model, 69
 - Thévenin's, 167
 - three windings transformer, 90
 - voltage source converter (VSC), 287
- Equivalent depth, 112
- Equivalent height, 133–34
- Equivalent incremental cost, 239
- Equivalent resistance, 31
- Error frequency, 295
- F**
- Faraday's law, 30, 99
- Fast decoupled load flow, 189, 191, 322, 338
- Fault admittance matrix, 307, 311
- Fault connections
 - circuit interpretation for, 312–17
 - matrix, 299
 - negative sequence, 304
 - one-phase to ground, 313
 - series, 309, 311
 - three-phase, 299
 - unbalanced, 308, 316
- Fault currents, 312
- Fault equation
 - in coordinates 012, 298
 - in phase coordinates *abc*, 297–98
 - Thévenin's equivalent and, 298
- Faults
 - contingencies and, 322
 - current calculation, 317–18
 - introduction to, 297
 - series, 309–12
 - shunt, 307–9
 - single-phase, 312–14
 - studies of, 297–320
 - three-phase, 300–307, 368
 - between two phases, no ground, 314–16
 - between two phases and ground, 316–17
- Fictitious node, 303
- Flexible AC transmission system (FACTS), 249
- Flow measurements, 355, 372
- Flux linkages, 103
- Force
 - defined, 274
 - distance and, 273–74
 - rotating torque, 275
 - vector, 274
- Forward waves, 157, 158
- Four-node system load flows, 231
- G**
- Gaussian elimination, xv, 27, 41
 - large scale network equivalents, 48
 - linear equations and, 40–44
- Gauss' law, 117–22
- Geometric inductance, 112
- Geometric inductance matrix, 103
- Geometric mean radius (GMR), 103, 132–33
- Ground wires
 - boundary conditions for, 108
 - inclusion, 107–9
 - partial inversion, 109
- H**
- Hessian matrix, 237
- Hydrothermal coordination
 - cascaded case, 241

- Hydrothermal coordination (*Cont.*)
 defined, 233
 demand requirement, 236
 equality constraint, 234–35
 generation blocks, 239
 generation to supply demand and losses,
 241
 illustrated, 235
 incremental costs, 235–36
 incremental water flow, 235
 load demand for time changing values,
 239
 objective function and constraints, 234–42
 of power system, 233–342
 solution, 238
 steps, 233–34
 variations, 242
- I**
- Image method, 121
- Impedance
 mutual, 129, 130
 from Ohm's law, 34
 self, 130
 sequence, 111–12
 series, 113
 surge, 143–44
 three windings transformer, 89
 transformation, 111
- Impedance matrix
 reduced, 116
 series, 112
 transposed transmission line, 110
 values, 53
- Implicit method, 205
- Incremental costs
 equal, 218
 equivalent, 239
 hydrothermal coordination, 235–36
 optimal gradient, 214
 penalized, 216
- Incremental DC power flow equations,
 194–98
- Incremental power, 194–95
- Incremental power flows
 complex power transformer, 175–80
 control actions and, 198–200
 expressions for, 284–87
 partial derivatives, 285
 three-node system, 201
 three-node system illustration, 198
 transmission lines, 180–82
- Incremental power model, 282–87
 DC load, 292
 extensions to, 290–92
 reactive power and voltage control, 290–92
- Incremental reactive power flows
 equivalent circuit, 188
 linearized model, 323
 model, 258
 with partial derivatives, 187, 188
 series and shunt components, 259
 in transformer, 179–80
 transmission line, 181–82
- Incremental real power flows
 equivalent circuit, 187, 251
 with partial derivatives, 188
 in transformer, 176–79
 transmission line, 181, 182
- Incremental torque, 277
- Incremental water flow, 235
- Inductance
 geometric, 112
 Ohm's law and, 31
 reduced transient, 318
 series, 99–112
 subtransient, 319
- Inductive compensation, 290–91
- Inductors
 circuit representation, 31
 defined, 9
- Inequality constraints, 213–16
- Inertia constant, 278
- Instantaneous power, 11–13, 274
- Inverse Laplace transform, 157, 158
- J**
- Jacobian matrix, 199, 200
- Jules, 274
- K**
- Kinetic energy, 276–77
- Kirchhoff's current law (KCL), 27, 33–35
 circuit configuration and, 33
 in circuit solution, 18
 current summation, 20
 in matrix form, 34
- Kirchhoff's voltage law (KVL), 38–39
- Kron's reduction, 44
- Kuhn-Tucker multiplier, 214, 271

L

- Lagging power factor, 16
- Lagrange function, 218–19, 222
- Lagrange multipliers, 208, 219, 237
- Lagrangian equation and gradients, 212
- Laplace transform, 279
- Laplace transformed equations, 156
- Lattice diagrams, 165–66
- Leading power factor, 16
- Least squares
 - criteria, applying, 349
 - principle, xviii
 - solution, 353
 - weighted, 354–61
- Linear circuits, 327–29
- Linear equations, 40–44
- Linear models
 - for fast studies, 323
 - for incremental real power flow, 323
 - least squares, 345–53
 - sparse techniques, 325
 - steps for network solution, 324–25
- Linear state estimation, 348–53
- Line transposition, 109–10
- Links, 38
- Load center, generation site remote from, 140
- Load convention
 - for power flows, 13–18
 - using, 33
- Load flows
 - AC solutions, 282
 - base case, 321
 - equations, 183
 - fast decoupled, 189, 191, 322, 338
 - four-node system, 231
 - incremental AC formulation, 198
 - for minimum loss solution, 225, 230
 - problem, 182
 - results, 185
 - small DC solution, 198
 - solution by Newton's method, 285–87
 - solution diagram, 191
 - three-phase, 202, 203
- Load intervention, 153
- Local phasor concentrators (LPCs), 372
- Longitudinal networks
 - defined, 255
 - real power flow control, 255–58
 - sparse patterns for matrix, 256
- Long transmission lines
 - equivalent circuit, 145–46
 - flat line concept, 143
 - incremental distance in, 141
 - no-load line, 144
 - nominal π and equivalent circuit, 144–45
 - propagation velocity, 143–44
 - surge impedance, 143–44
 - $V(x)$ and $I(x)$ equations in, 141–46
 - wave length, 143–44
 - See also* Transmission lines
- Loop-element connection matrix, 39
- Losses
 - hydro and thermal generation, 241
 - minimum, 218–22
 - no, optimal dispatch with, 211–16
 - penalized incremental, 219
 - real power, 216–18, 233
 - transmission, 222–23
- Lumped elements, circuits with, 32–33

M

- Magnetic circuits
 - illustrated, 318, 319
 - subtransient response, 319–20
 - transient response, 318–19
- Marginal cost, 212
- Mathematical circuits, 42
- Matrix inversion
 - defined, 44
 - lemma, 56–57
- Matrix of potentials, 120
- Matrix transformation, 62–64
- Measurement error, 346
- Measurement matrix, xviii, 351, 372
- Measurements
 - bad, 357, 360
 - in estimation process, 373–74
 - flow, 355, 372
 - good batch, 358
 - nodal power, 362
 - in RTU, 344
 - voltage, 366
 - wide area, 371–72
- Mesh equations, 28
- Minimum control effort
 - congestion and, 262–73
 - cost function, 265
 - defined, 262
 - optimal coordinated control, 270–73

- Minimum control effort (*Cont.*)
 - reactive power flow control, 268–70
 - real power flow control, 250, 265–68
 - sensitivity coefficients, 262–64
 - three-node system, 266, 268
- Minimum effort, 198
- Minimum losses, 218–22
- Minimum operating cost
 - power flow formulation, 225–33
 - power systems, 207–8
 - three-node system load flows for, 225, 230
- Minimum squares estimation, xviii
- Minimum weighted squares, 355
- Mutual capacitance, 129
- Mutual impedance, 129, 130

- N**
- Negative sequence connections, 304
- Network analysis
 - circuits with lumped elements, 32–33
 - diakoptical approach, 54–56
 - introduction to, 27–29
 - Kirchhoff's current law (KCL), 33–35
 - Kirchhoff's voltage law (KVL), 38–39
 - large scale network equivalents, 48–54
 - linear equations and Gaussian elimination, 40–44
 - matrix inversion lemma, 56–57
 - nodal formulation, 35–38
 - Norton's and Thévenin's equivalents, 47–48
 - Ohm's law, 29–32
 - Y_{BUS} and Z_{BUS} matrix elements, 44–47
- Network equivalents
 - illustrated, 51, 52
 - large scale, 48–54
 - partitioned, 49–54
 - See also* Norton's equivalent; Thévenin's equivalent
- Newton-Raphson iterative method, 169
- Newton's incremental form, 216–17
- Newton's iterative process, 172–73, 220, 226, 237
- Newton's power flow solution, 174–75, 182–85, 285–87
- Nodal admittance matrix, 53, 83, 200
 - from $ABCD$ constants, 148–51
 - defined, 36
- Nodal current equations, 34
- Nodal currents, 21, 36
- Nodal equations, 28
- Nodal formulation, 35–38
- Nodal method, 35, 36
- Nodal voltages, 12, 200, 331
- Node currents
 - three-phase complex transformer, 75, 78, 80
 - three phase transformer, 92, 93
- Node elimination
 - circuit illustration, 41
 - Norton's equivalent after, 40
- Node equation, 33
- Node voltages, 27
- Nonlinear equations
 - DC real power flow problems and, 172
 - low voltage solution, 173
 - Newton's iterative process, 172–73
 - solution of, 169–73
- Nonlinear minimum squares, 361–64
- Normal probability distribution, 345, 354, 358
- Norton's equivalent, 47–48
 - after node elimination, 40
 - after node one elimination, 48
 - defined, 27
 - for synchronous generator, 201

- O**
- Observability, 358, 372–74
- Observation matrix, 354
- Ohm's law, 20, 28, 29–32
 - admittance form, 35
 - compact matrix equation, 74–75
 - inductance and, 31
 - model, 188
- One-phase to ground fault connection, 313
- on load tap changer (OLTC), 284
 - complex power transformer, 293
 - real and reactive power flows, 292–95
- Open circuit coefficients, 27
- Open conductor, 200
- Optimal control coordination, 295
- Optimal coordinated control efforts, 270–73
 - defined, 270
 - load flow solution, 273
 - sensitivity coefficients, 271
 - tap chance, 271
 - voltage magnitudes, 273
- Optimal operation of power systems, 207–48
 - hydrothermal coordination, 233–42
 - introduction to, 207
 - minimum losses, 218–22

- minimum operating cost, 207–8
 - nonlinear optimization, 207–11
 - optimal dispatch with no losses, 211–16
 - real power losses, 216–18
 - second-order derivatives, 242–48
 - transmission losses included, 222–33
 - Optimal reactive power flow control, 268–70
 - Optimal real power flow control, 265–68
 - Organization, this book, xv–xviii
 - Outage admittance, 330
- P**
- Parallel conductors
 - bundle, 105
 - interpretation of equivalent impedance, 107
 - over ideal plane, 120
 - set of three, 102, 104
 - Parameter estimation
 - simple network for, 364
 - Thévenin's equivalent and, 364–66
 - Partial derivatives
 - calculation, 196
 - incremental power, 194–95
 - incremental power flows, 285
 - reactive power, 244
 - of second-order, 246–48
 - Partial inversion, xv, 27, 42–44
 - algorithm, 97–98
 - bundled conductors, 106
 - ground wire inclusion, 109
 - large scale network equivalents, 48
 - lemma, 54
 - procedure, 43–44
 - rules, 43
 - single-phase transformer model, 68, 72
 - three-phase $\Delta\Delta$ bank, 76
 - three-phase $Y\Delta$ bank, 78
 - Partial matrix inversion, 36, 72
 - Participation factors, 340–42
 - Partitioned networks, 49–54
 - Passive elements, 28
 - Phase shifters, 187, 328
 - Phasor measurement units (PMUs), 345, 367
 - Phasors, 7–11
 - capacitance representation, 11
 - in changing frequency condition, 372
 - estimation, 366–72
 - inductance representation, 10
 - in resistance, 9
 - voltage and current, 9, 14
 - Piecewise networks, 55
 - Power
 - in AC circuits, 6–11
 - complex, 200
 - in DC circuits, 4–6
 - incremental, 194–95
 - instantaneous, 11–13, 274
 - mismatches, 285
 - nominal, 278
 - reactive, 12–13, 141, 151, 244, 246–48, 335–40
 - real, 12–13, 151
 - for three-phase circuit, 18–23
 - time versus, 275
 - triangles, 14
 - turbine's, 277–79
 - Power balance, 278
 - Power factor
 - effect on voltage, 19
 - lagging, 16
 - leading, 16
 - table, 18
 - Power flow calculations
 - with *ABCD* constants, 151–54
 - circle diagram, 152, 153, 154
 - decoupled, 193
 - Power flow equations, 175–82
 - Power flows, 169–205
 - approximations, 186–93
 - in complex transformer, 283
 - DC network solutions, 193–98
 - incremental, 175–82
 - introduction to, 169
 - lagging power factor, 16
 - leading power factor, 16
 - load, base case, 270
 - load convention for, 13–18
 - minimum cost formulation, 225–33
 - Newton's solution, 174–75, 182
 - PV curve, 170
 - real, control of, 250–58
 - solution of nonlinear equations, 169–73
 - for three-phase circuit, 19
 - in transmission line, 284
 - unbalanced three-phase, 200–205
 - Power margin, 365, 371
 - Power mismatch equation, 184
 - Power systems
 - fault studies, 297–320
 - health, 371

- Power systems (*Cont.*)
- hydrothermal coordination, 233–42
 - linear state estimation, 348–53
 - measurements in RTU, and control center, 344
 - minimum losses, 218–22
 - minimum operating cost, 207–8
 - nonlinear optimization, 207–11
 - optimal dispatch with no losses, 211–16
 - optimal operation, transmission losses included, 222–33
 - optimal operation of, 207–48
 - rate of failure, 322
 - real power losses, 216–18
 - reliability, 322
 - second-order derivatives, 242–48
 - security, 372
 - state estimation in, 343–74
 - wellbeing, 343
- Power-voltage relation, 170
- Primary loop control
- dynamic frequency response, 280
 - frequency, 279–82
 - frequency response, 281
 - illustrated, 279
 - supplementary control loop, 282
- Proportionality constants, 32
- PV curve
- characteristics, 172
 - circuit for, 171
 - multiple solutions to power flow, 170
 - for resistive load, 171
- R**
- Rate of failure, 322
- Reactance, in series inductance, 99
- Reactance matrix, 104
- Reactive power, 12–13
- compensation, 17
 - under contingencies, 335–40
 - incremental power model and, 290–92
 - obtaining from terminal relations, 151
 - partial derivatives, 244
 - partial second-order derivatives, 246–48
 - transmission line requirement, 141
- Reactive power flow
- circuit solution, 339
 - incremental circuit to model, 335, 337
 - incremental current model, 338
 - sensitivity matrix, 340
- Reactive power flow control, 258–62
- base case, 269
 - circuit to study, 259, 268
 - matrix equation, 260–61
 - minimum control effort, 268–70
 - network for, 262
 - optimal, 268–70
 - tap change, 261
 - three-node system, 268
 - voltage condition, 261
- Reactive VARs, 249
- Real power, 12–13
- flows, 325
 - losses, 216–18, 233
 - marginal costs, 226
 - obtaining from terminal relations, 151
- Real power flow control, 250–55
- base case, 265–66
 - incremental model, 263–64
 - longitudinal networks, 255–58
 - minimum actions, 250
 - minimum control effort, 265–68
 - network for, 251
 - optimal, 265–68
 - options, 255
 - sensitivity factors, 253
 - sparse nature of the matrix, 253, 254
 - three-node system, 263
 - three-node system base case, 266
- Reduced gradient, 208
- Reduced transient inductance, 318
- Redundancy, 343
- Reference angle, 200
- Reflection coefficients, 159, 163, 166
- Reflexion coefficients, 158–59
- Refraction coefficients, 159, 163, 166
- Regular control function, 366
- Remote terminal units (RTUs), 343, 344
- Resistance
- connectivity elements, 52
 - defined, 7, 29
 - equivalent, 31
 - in series inductance, 99
 - voltage and current phasors through, 9
 - voltage and current through, 8
- Resistors
- voltage-current characteristics, 29, 30
 - voltage-current relation, 30
- Retained conductors, 136
- Right of ways, 140

RMS phasor, 7, 9, 367, 369–70
 Rotating speed, 276
 Rotating torque, 275
 Rotor speed, 295
 Round conductor, 101

S

Sag estimation, 134
 Scatter diagrams, 346
 Second-order derivatives, 242–48
 Self impedance, 130
 Sensitivity coefficients, 262–64, 265, 271
 Sensitivity matrix
 defined, 272, 327
 for incremental control changes, 328–29
 for linear circuit, 327–29
 reactive power incremental model, 340
 Sequence impedances, 111–12
 Series fault connections, 309, 311
 Series impedance
 cables, 123–26
 transmission line arrangement for
 calculation, 113
 two-port element in, 146
 Series inductance, 99–112
 axial conductors, 102–5
 bundled conductors, 105–7
 ground wire inclusion, 107–9
 line transposition, 109–10
 reactance, 99
 resistance, 99
 sequence impedances, 111–12
 single conductor, 100–102
 Series *RLC* circuit, 66
 Shielded wires, 135
 Short-term marginal costs, 208, 235
 Shunt admittance, 147
 Shunt admittance matrix, 121
 Shunt capacitance, 126–27
 Shunt faults, 307–9
 Shunt reactive compensation, 259
 Shunt susceptances, 337
 SIMULINK® environment, 295
 Single contingency model
 overview, 329
 Thévenin's equivalent, 330–35
 See also Contingency analysis
 Single-phase fault, 312–14
 Single-phase transformer model, 67–74
 alternative circuit, 95–97
 base quantities selection steps, 70
 equivalent circuit, 69
 equivalent circuit, grounded neutrals,
 69
 illustrated, 67
 mutually coupled circuits and pu values,
 72
 partial inversion, 68, 72
 per unit values, 69–74
 pu base value determination, 69–70
 solution for, 73
 voltage, current, and impedance, 71
 voltage relations, 68
 voltages and currents, 70
 Sinusoidal voltage, 6, 8, 10
 Slack bus, 351
 Source participation factors, 64
 Sparse techniques, 325, 342
 Squared errors, 346
 Stability margin, 333
 Stability's angle limit, 154
 STATCOM
 characterization, 287
 configuration for voltage control, 294
 model, 292–95
 modified network, 292
 voltage control and reactive power injection,
 294
 State estimation
 best, 343
 centralized data acquisition system,
 344–45
 defined, 344
 introduction to, 343–45
 least squares, linear model, 345–53
 nonlinear minimum squares, 361–64
 observability, 358, 372–74
 parameter estimation, 364–66
 phasor estimation, 366–72
 weighted least squares, 354–61
 Static VAR compensators (SVCs), 249
 Steady state stability margin, 328
 Subtransient inductance, 319
 Subtransient response, 319–20
 Surge impedance, 143–44
 Symmetrical components transformation,
 62–64
 sequence impedances, 111
 three-phase $\Delta\Delta$ bank, 76
 System data concentrators (SDCs), 372

T

- Tape shielded cable, 126
- Taylor's series expansion, 284
- Thermal cost, 239
- Thermal limit, 154
- Thévenin's equivalent, 47–48, 168
 - in 012 references, 302
 - in *abc* reference, 301
 - circuit, 42, 43, 167
 - defined, 48
 - fault connection equations and, 298
 - fault matrix connection and, 299
 - parameter estimation and, 364–66
 - single contingency model, 330–35
 - for synchronous generator, 201
 - three-phase fault, 300
 - voltage source, 48
- Three-phase balanced network, 314, 366
- Three-phase bank transformer
 - model, 74–85
 - node currents, 75, 78, 80
 - overview, 74
 - three-phase $\Delta\Delta$ bank, 74–77
 - three-phase $Y\Delta$ bank, 77–79
 - three-phase YY bank, 79–85
 - See also* Transformer models
- Three-phase cables
 - capacitances, 128
 - center coordinates, 128
 - mutual capacitance, 129
 - phases, 127
 - pipe type, 129–32
 - pipe type cradle arrangement, 128
 - self impedance, 130
 - susceptance values, 129
 - See also* Cables
- Three-phase circuit, 18–23
- Three-phase fault, 300–307
 - for AC network equivalent, 368
 - connections, 299
 - fictitious node, 303
 - impedance *abc*, 306
 - one-line diagrams, 303
 - results, 307
 - Simulink diagram, 368
 - Thévenin's equivalent, 300
- Three phase transformer
 - defined, 92
 - example, 93–95
 - node currents, 92, 93
 - See also* Transformer models
- Three-phase unbalanced currents, 65
- Three windings transformer
 - circuit representation, 89
 - core and windings, 92
 - currents and voltage for, 91
 - defined, 89
 - delta equivalent, 91
 - equivalent circuit, 90
 - impedances, 89
 - tertiary winding, 91
 - See also* Transformer models
- Time constants, 318
- Torque
 - incremental, 277
 - rotating, 275
- Total energy, 275
- Transfer functions, 295
- Transformation matrix, 61, 63
- Transformer models
 - autotransformer, 85–88
 - decoupling of state equations, 64–67
 - introduction to, 59
 - single-phase, 67–74
 - symmetrical components transformation, 62–64
 - three-phase, 92–95
 - three-phase bank, 85
 - three windings transformer, 89–92
- Transient response, 318–19
- Transmission limits
 - stability's angle limit, 154
 - thermal limit, 154
 - from voltage drop, 155–56
- Transmission line loadability
 - ABCD* constants, 146–51
 - approximate real power handling and losses, 137–41
 - compensation requirements, 150, 151
 - introduction to, 137
 - plots for stability limit, 150
 - power flow calculations, 151–54
 - transmission limits, 154–56
 - $V(x)$ and $I(x)$ equations in, 141–46
 - wave equation and time expressions, 156–68
- Transmission line modeling
 - cable parameters, 122–32
 - Earth return, 112–17
 - equivalent height, 133–34

- Gauss' law and capacitance, 117–22
 - geometric mean radius (GMR), 132–33
 - illustrated, 137
 - introduction to, 99
 - lines in parallel, 135
 - series inductance, 99–112
 - Transmission lines
 - axial conductors, 102–5
 - bundled conductors, 105–7
 - high voltage, approximations, 138
 - incremental power flows for, 180–82
 - incremental reactive power flow for, 181–82
 - incremental real power flow for, 181, 182
 - long, 141–46
 - number of circuits required, 139–40
 - in parallel, 135–36
 - parameter values, 138
 - power flows in, 284
 - reactive power requirement, 141
 - round conductor, 101
 - sag estimation, 134
 - single conductor, 100–102
 - transposition, 109–10
 - Transmission losses
 - minimum cost power flow formulation, 225–33
 - nodal power balance, 222
 - optimal operation, 222–33
 - overview, 222–25
 - Transposed transmission lines, 109–10
 - Traveling currents, 160, 161
 - Traveling voltages, 157, 161
 - Traveling waves
 - backward, 157, 158
 - defined, 157
 - forward, 157, 158
 - Tripped condition, 329, 333
 - Trips, line, 332, 337
 - Turbine's power, 277–79
- U**
- Unbalanced fault connections, 308, 316
 - Unbalanced three-phase power flow, 200–205
 - incremental concepts, 201
 - iterative process, 202
- V**
- Vector force, 274
 - Voltage and current
 - AC circuits, 6
 - lagging power factor, 16
 - Laplace transformed equations, 156
 - leading power factor, 16
 - phasors, 14
 - phasors in resistance, 9
 - single-phase transformer model, 70
 - for three-phase circuit, 19
 - through inductance, 9
 - through resistance, 8
 - through series R, L C circuit, 11
 - Voltage collapse margin, 365
 - Voltage control
 - STATCOM, 294
 - voltage source converter (VSC), 290, 291
 - Voltage drop
 - limit from, 155–56
 - in terms of nodal voltages, 35
 - total power at receiving end and, 155
 - Voltages
 - under contingencies, 335–40
 - continuity of, 162, 163
 - measurement, 366
 - nodal, 12, 200, 331
 - node, 27
 - phase, 315
 - reflected, 167
 - sinusoidal, 6, 8, 10
 - traveling, 157, 161
 - Voltage source converter (VSC)
 - equivalent circuit for, 287
 - incremental model for, 288–90
 - system configuration, 288
 - system configuration for voltage control, 290, 291
- W**
- Weak systems, 366
 - Weighted least squares, 354–61
 - Weight matrix, 354
 - Wide area measurements, 371–72
 - Work
 - energy and, 273–82
 - force and distance, 273–74
- Y**
- Y_{BUS} matrix, 56–57
 - $Y\Delta$ connection, 77–79
 - YY connection
 - illustrated, 79
 - nodal admittance matrix, 83

YY connection (Cont.)

- nodal matrix in sequence quantities, 84
- node current relations, 82
- product matrices, 84
- three-phase bank, 79–85
- voltage across elements, 81

Z

- $Z_{\text{BUS matrix}}$, 44–47
- Zero sequence current, 314
- Zero sequence network, 305